

1. Report No. FHWA-SC-13-04		2. Government Accession No.		3. Recipient's Catalog No.	
4. Title and Subtitle Precast Alternative for Flat Slab Bridges				5. Report Date October 2013	
				6. Performing Organization Code	
7. Author(s) H. Sheng , B.G. Nielson, W. Pang, S. D. Schiff				8. Performing Organization Report No.	
9. Performing Organization Name and Address Clemson University, Glenn Department of Civil Engineering 306 S. Palmetto Blvd. Clemson, SC 29634-0911				10. Work Unit No. (TRAIS)	
				11. Contract or Grant No.	
12. Sponsoring Agency Name and Address South Carolina Department of Transportation Office of Materials and Research 1406 Shop Road Columbia, South Carolina 29201				13. Type of Report and Period Covered Final Report August 2009 – October 2013	
				14. Sponsoring Agency Code SPR 682	
15. Supplementary Notes Prepared for the SCDOT in cooperation with the Federal Highway Administration					
16. Abstract <p>The cast-in-place (CIP) concrete slab bridge and the hollow core flat slab bridge are two very common bridge types utilized by the South Carolina Department of Transportation (SCDOT). The CIP bridge is durable but has a long construction time while the hollow-core bridge has a short construction time but produces durability concerns. Trying to balance the speed of construction for hollow-core and the durability of CIP, the SCDOT commissioned this study to provide a recommendation for an alternative bridge type that could: 1) eliminate or minimize longitudinal cracking, 2) have a shorter erection time than the CIP flat slab system, and 3) have no restriction on ADTT and can be used on the National Highway System.</p> <p>There were two distinct phases in this research. In Phase 1, a thorough online survey and telephone interviews were conducted to investigate the pros and cons of existing short-span bridge systems used by other state departments of transportation. In addition, feedback from contractors and precast element fabricators in the Southeast region was also solicited. Based on this work, a precast bridge system known as the NEXT-D (Northeast Extreme Tee) beam was selected by the SCDOT for further testing and validation. The experimental and analytical validation along with the design of a 6 ft. wide section (NEXT-6) and an 8 ft. wide section (NEXT-8), with span lengths from 22 ft. to 40 ft., was the focus of Phase 2.</p> <p>The results of the experimental study indicated that U-shaped reinforcing bars and poly-vinyl alcohol (PVA) fiber reinforced ultra-high performance concrete (UHPC) were an effective combination when used for the shear key located between precast NEXT elements. These results were also used to calibrate analytical models which were used to better understand and quantify the load demands associated with this beam type. Using this new understanding, a set of new design guidelines for the new NEXT-6 and NEXT-8 bridge systems was developed. For the beam design, the AASHTO live load distribution factors for tee beams are recommended to be used. For the deck design, the AASTHO strip method is recommended with some modification. A simplified four-step procedure was developed to assist bridge engineers in determining the design demands (positive and negative moments) on a one-foot strip of deck for Strength I and Service I limit states.</p> <p>The results of this study, field experience with existing cast-in-place and precast bridges and sound engineering judgment allow the investigators to believe with a reasonable degree of confidence that the construction of a bridge using the provided recommendations and new system will lead to durable bridges that are cost effective and can be constructed using an accelerated schedule. One of the immediate needs is to now share the results of this study with neighboring states, so that the investment of needed steel forms by precasters can result in similar precast pieces sold to multiple states.</p>					
17. Key Words Precast bridge joint, hollow-core bridge, NEXT D bridge, bridge construction, prestressed concrete bridge			18. Distribution Statement No restrictions.		
19. Security Classif. (of this report) Unclassified		20. Security Classif. (of this page) Unclassified		21. No. Of Pages 588	22. Price

Total Printing Cost	\$421.50
Number of Units	25 copies
Cost per Unit	\$16.86

South Carolina Department of Transportation
Research Project No. 682:
Precast Alternative for Flat Slab Bridges

Final Report for
the South Carolina
Department of Transportation

Clemson University
October 26th, 2013

Bryant G. Nielson, PhD, SE
Senior Lecturer

Scott D. Schiff, PhD
Professor

Weichiang Pang, PhD
Assistant Professor

Huan Sheng
Graduate Student

This page intentionally left blank.

Table of Contents

1	Introduction	1
1.1	Problem Description	1
1.2	Objective and Scope of Research	2
1.3	Outline of Report	3
2	Background	5
2.1	Department of Transportation Website Search	5
2.2	Accelerated Bridge Construction Literature Search	9
2.3	Adjacent Beam Bridge Literature Search	15
3	Performance Perceptions of Adjacent Box Girder Bridges	41
3.1	Department of Transportation Web Survey	41
3.2	Target State Phone Survey	44
3.3	Contractor & Fabricator Interviews	49
4	Field Verification of Core Box Bridge Performance	55
4.1	Objectives	55
4.2	Bridge Detail	55
4.3	Instrumentation	58
4.4	Load	60
4.5	Loading Setup	61
4.6	Procedure	63
4.7	Test Results Interpretation	68
4.8	Conclusions	73
5	Bridge Type Selection	75
5.1	Department of Transportation Web Search	75
5.2	Advanced Systems	75
5.3	Hollow Core and Box Beam Study	76
5.4	Survey & Interview Results	77
5.5	Suck Creek Bridge Testing	78
5.6	Summary of Findings	79
5.7	Mini-Workshop Summary	82
6	Performance Assessment of NEXT-D Shear Key	95
6.1	The Big Picture	95
6.2	Introduction	97
6.3	Experimental Setup	98
6.4	Primary Shear Key Material Selection	103
6.5	Primary Verification of Reinforcing Details	107
6.6	Experiment Matrix Development	109

6.7	Shear Key Casting and Material Properties	112
6.8	Specimen Testing	119
6.9	Analysis of Results - Performance at Strength Level	125
6.10	Result Analysis—Performance at Service Level	141
6.11	Simulation Validation	145
6.12	Shear Key Material Determination	147
6.13	Closure	149
7	Demand Quantification for NEXT-D Beam	151
7.1	Scope and Objectives	151
7.2	Bridge Modeling	152
7.3	Shear Key Modeling	155
7.4	Solid FEM	157
7.5	Shell FEM	161
7.6	Bridge Live loads	166
7.7	Shell FEM vs Solid FEM	168
7.8	Strip Width Determination for AASHTO Live Loads	173
7.9	Design Tandem vs Design Truck	175
7.10	Calibration of Shear Key Finite Element Model	177
7.11	Closure	192
8	NEXT-D Bridge Design	195
8.1	Parapet and overhang design	195
8.2	Beam analysis and design	196
8.3	Live load distribution factor	197
8.4	Beam design	201
8.5	Deck analysis and design	204
8.6	Sensitivity study	217
8.7	Deck design	219
8.8	Closure	222
9	Summary and Conclusions	225
9.1	Summary	225
9.2	Conclusions	225
	Appendices	235
A	Department of Transportation Web Survey	237
B	Phone Interview Transcripts	249
B.1	Phone Interview with Thomas Domagalski	249
B.2	Phone Interview with Julius Volgyi	250
B.3	Phone Interview with Suresh Patel	251
B.4	Phone Interview with Tim Keller	253
B.5	Phone Interview with Terry Frake and Steve Beck	255
B.6	Phone Interview with John Holt	257
B.7	Phone Interview with Paul Chung	259
B.8	Phone Interview with Benjamin Tang	260
B.9	Phone Interview with Jugesh Kapur	261
B.10	Phone Interview with George Christian	263
B.11	Phone Interview with Paul Liles	265
B.12	Notes on Phone Interview with Ed Wasserman	267

B.13	Notes on Phone Interview with Rita Seraderian	267
C	Contractor and Fabricator Interview Transcripts	269
C.1	Email Interview with Troy M. Jenkins, PE (New York Fabricator)	269
C.2	Phone Interview with Mark D. Losee (New York Fabricator)	270
C.3	Phone Interview with JR Parimuha (North Carolina Fabricator)	272
C.4	Phone Interview with Gary Fisher (Texas Fabricator)	274
C.5	Email Interview with Chuck Prussack, PE (Washington Fabricator)	277
C.6	Email Interview with Bill Heston (North Carolina Contractor)	278
C.7	Phone Interview with Sandy Tesch (Texas Contractor)	280
D	Mini-Workshop Questionnaires	283
E	Letter from PCINE	293
F	Parapet and Deck Design for NEXT-D Beam	295
G	Shear Key Modeling	375
H	Load Distribution Calculations	377
I	Sample Bridge Calculations for NEXT-8 40 ft.	391
J	Bridge Drawings	417
K	CONSPAN Input and Output	433
K.1	NEXT-6 40 ft. - Input	433
K.2	NEXT-6 40 ft. - Exterior Beam Output	451
K.3	NEXT-6 40 ft. - Interior Beam Output	478
K.4	NEXT-8 40 ft. - Input	505
K.5	NEXT-8 40 ft. - Exterior Beam Output	521
K.6	NEXT-8 40 ft. - Interior Beam Output	548

This page intentionally left blank.

List of Tables

2.1	States without details available online	5
2.2	States with rapid construction superstructure details	6
2.3	Stabilizing TPT force to limit differential strain in adjacent members (Fu and Jeong, 2009).	35
3.1	State usage of adjacent beam bridges	42
3.2	Reflective cracking survey responses	43
3.3	Alternative bridge types used.	43
4.1	Dump Truck Weight	61
4.2	Values obtained from the first test for the first setup	64
4.3	Values obtained from the first test for the second setup	66
6.1	Grout and PVA fiber ratios considered	105
6.2	Average compressive and tensile strengths of concrete and grout materials	106
6.3	Test results of GF12 cylinder ($3in \times 6in$)	106
6.4	Test results of concrete cylinder ($4in \times 8in$)	106
6.5	Experiment matrix for static tests	112
6.6	Mixture proportions of shear key material	113
6.7	Typical proportions of UHPC (per yd^3 of UHPC) (Graybeal, 2006)	114
6.8	Cylinder test results	117
6.9	Compressive strengths during tests	118
6.10	Specimen casting date and testing date	121
6.11	Fatigue load determination on shear key based on shear key stiffness	125
6.12	Fatigue load applied in the test	125
6.13	Specimen capacity summary	129
6.14	Specimen ductility index	139
6.15	Relationship between ductility index and maximum moment	140
7.1	Properties of concrete used in the NEXT-D models	158
7.2	Parapet section properties	162
7.3	Stem section properties	164
7.4	Rigid link section properties	164
7.5	Demand per foot for the NEXT-6 bridge based on recommended strip widths	177
7.6	Demand per foot for the NEXT-8 bridge based on recommended strip widths	177
7.7	Material properties in the shear key FEM	180
7.8	Parameter summary in the shear key FEM	185
7.9	Correlation coefficients	191
8.1	Load distribution factors for NEXT-8	200
8.2	Load distribution factors for NEXT-6	201
8.3	Factored moment demand caused by dead load	214

8.4	NEXT-8 — Design demands provided by the formula vs demands from the bridge FEM (shown in parentheses) for the strength I limit state	215
8.5	NEXT-8 — Design demands provided by the formula vs demands from the bridge FEM (shown in parentheses) for the service I limit state	216
8.6	NEXT-6 — Design demands provided by the formula vs demands from the bridge FEM (shown in parentheses) for the strength I limit state	216
8.7	NEXT-6 — Design demands provided by the formula vs demands from the bridge FEM (shown in parentheses) for the service I limit state	216
8.8	Reinforcing bar configuration capacities	222
8.9	NEXT-8 — Final design capacity vs demand	222
8.10	NEXT-6 — Final design capacity vs demand	223

List of Figures

1.1	Hollow-core beam section currently used by the SCDOT (SCDOT, 2010)	2
2.1	Texas box beams (TxDOT, 2010)	6
2.2	Texas decked slab beam (TxDOT, 2010)	7
2.3	New York continuity detail (NYSDOT, 2010a)	8
2.4	Ohio continuity detail (ODOT, 2010))	8
2.5	Texas continuity detail (TxDOT, 2010)	9
2.6	Modified precast beam in slab system (Konda et al., 2007)	10
2.7	Poutre Dalle system (Ralls et al., 2005)	11
2.8	Dalle Preflex system (Culmo, 2009)	11
2.9	MNDOT system (Culmo, 2009)	12
2.10	Grout filled splice sleeve (ERICO, 2010)	12
2.11	First system (Badie and Tadros, 2008)	13
2.12	Second system (Badie and Tadros, 2008)	13
2.13	Third system (Badie and Tadros, 2008)	14
2.14	Two lane modular bridge (Roscoe-Bridge, 2010)	14
2.15	Typical shear key	16
2.16	Typical shear key	16
2.17	Temperature effects (Miller et al., 1999)	17
2.18	Japanese box beams (El-Remaily et al., 1996)	18
2.19	Japanese box beam post tensioning (El-Remaily et al., 1996)	18
2.20	New York full depth shear key (NYSDOT, 2010a)	19
2.21	Miller shear key test member (Miller et al., 1999)	20
2.22	Korean shear key placement study (Kim et al., 2008)	21
2.23	Laterally post tensioned multibeam bridge (Badwan and Liang, 2007)	21
2.24	Lakeview Drive collapse (PennDOT, 2006)	24
2.25	Lakeview Drive box beam section (PennDOT, 2006)	24
2.26	Formation of positive restraint moments (Saadeghvaziri et al., 2006)	28
2.27	MoDOT engineering policy guide continuity detail (MoDOT, 2010)	29
2.28	Grout filled splices used in continuity connections (Jansson, 2008)	30
2.29	Minimum number of transverse diaphragms for 48" boxes (Grace and Jensen, 2008)	33
2.30	Minimum number of transverse diaphragms for 36" boxes (Grace and Jensen, 2008)	33
2.31	Minimum TPT force per diaphragm (Grace and Jensen, 2008)	34
2.32	Comparison of TPT force used by states nationwide (Russell, 2009)	36
2.33	NYSDOT plan shown with five TPT locations (NYSDOT, 2010b)	38
2.34	Texas TPT detail (TXDOT, 2009)	39
2.35	TXDOT plan shown with TPT locations (TXDOT, 2009)	40
3.1	Robust shear key detail (Texas) (TxDOT, 2010)	45
3.2	Decked slab beam section (Texas) (TxDOT, 2010)	46
3.3	Deck bulb-T bridge girder (Washington) (WSDOT, 2010)	46

3.4	Inverset system unit (New York) (Culmo, 2009)	47
3.5	NEXT F beam (PCINE, 2010)	48
3.6	NEXT D beam (PCINE, 2010)	48
4.1	Cross section of Suck Creek bridge	56
4.2	Plan view of Suck Creek bridge	56
4.3	Details for 50 ft. and 40 ft. span interior sections	57
4.4	Shear key details of Suck Creek bridge	57
4.5	View of LVDT	58
4.6	View of (a) LVDT arrangement, (b) relative displacements LVDT setup, and (c) global vertical displacements LVDT setup	59
4.7	View of first test setup	59
4.8	LVDT locations for first test setup	60
4.9	View of second test setup	60
4.10	LVDT locations for second test setup	61
4.11	Truck dimensions	62
4.12	Loading setup for the first instrument setup	62
4.13	Loading setup for the second instrument setup	63
4.14	Truck position for the first test for first instrument setup	64
4.15	Truck position for the second test for first instrument set	65
4.16	Truck position for the third test for first instrument set	65
4.17	Truck position for the ninth test for first instrument set	66
4.18	Truck position for the first test for second instrument set	67
4.19	Truck position for the second test for second instrument set	67
4.20	Truck position for the seventh test for second instrument set	68
4.21	Displacements for first test for the first setup	68
4.22	Displacements for second test for the first setup	69
4.23	Displacements for third test for the first setup	69
4.24	Displacements for fourth test for the first setup	69
4.25	Displacements for fifth test for the first setup	70
4.26	Displacements for sixth test for the first setup	70
4.27	Displacements for seventh test for the first setup	70
4.28	Displacements for eighth test for the first setup	70
4.29	Displacements for ninth test for the first setup	71
4.30	Displacements for first test for the second setup	71
4.31	Displacements for second test for the second setup	71
4.32	Displacements for third test for the second setup	71
4.33	Displacements for fourth test for the second setup	72
4.34	Displacements for fifth test for the second setup	72
4.35	Displacements for sixth test for the second setup	72
4.36	Displacements for seventh test for the second setup	72
5.1	Inverted-Tee beam	82
5.2	NEXT-D beam	82
5.3	Variation on the NEXT-D beam	83
5.4	Possible sections requiring feedback	88
5.5	Longitudinal joint options	88
5.6	NEXT-D geometry requested by the SCDOT	92
5.7	Modified NEXT-D joint configuration	92
5.8	NEXT-6 possible wheel path	93
5.9	NEXT-8 possible wheel path	93

6.1	Performance assessment procedure	96
6.2	Modified NEXT-D examined in this study	97
6.3	Original NEXT-D configuration with headed reinforcement	97
6.4	Reaction frame	99
6.5	Original shear key configuration	100
6.6	Strain gauge distribution on headed bar	101
6.7	Initial sensor layout (part 1)	102
6.8	Initial sensor layout (part 2)	102
6.9	Loading configuration	103
6.10	Cylinder tests	107
6.11	Results from direct tension test	108
6.12	Proposed detail for NEXT-D bridge joint - part 1	109
6.13	Proposed detail for NEXT-D bridge joint - part 2	110
6.14	Details for specimen to be tested	111
6.15	Slab casting at Metromont	113
6.16	Preparation before specimen casting and shear key material mixing	115
6.17	Workability of UHPC	115
6.18	Specimen before and after casting	116
6.19	Bond test	117
6.20	Cylinder compressive strengths during specimen tests	118
6.21	Cylinder failure modes in bond tests	119
6.22	Pull-off test results for the UHPC with PVA combination	120
6.23	Restraining effect of UHPC	120
6.24	Final sensor layout (part 1)	122
6.25	Final sensor layout (part 2)	122
6.26	Typical loading protocol for static test	123
6.27	Typical loading protocol for fatigue test	124
6.28	Cracks due to shrinkage before tests	126
6.29	Cracking pattern after strength test-bottom view (STA-04)	127
6.30	Cracking pattern after strength test-side view	127
6.31	Multiple cracks under load strip	129
6.32	Shear moment interaction diagram: Blue represents grout with PVA group; green UHPC with steel group; red UHPC with PVA (high moment); and black UHPC with PVA (high shear. Square and circle represent static tests, others monotonic tests.	132
6.33	Rotational stiffness degradation of shear key	134
6.34	Translational stiffness degradation under load strip	135
6.35	Stiffening effect of concrete on embedded bar (Adapted from (Hsu, 1993))	139
6.36	Interface cracking based on BDI readings	142
6.37	Stiffness degradation during fatigue test	144
6.38	Rebar strain at the maximum fatigue load level	146
7.1	Dimensions for the 40 ft. span NEXT-6 bridge model	152
7.2	Dimensions for the 40 ft. span NEXT-8 bridge model	153
7.3	Frame to solid connection in SAP2000 using rigid links	154
7.4	Frame element stiffness matrix for a six-inch section of shear key	155
7.5	Shear key local axis	156
7.6	Element stiffness matrix for beam elements with inclusion of shear deformations	156
7.7	Shear key stiffness verification model	157
7.8	Shear key connection in solid model	158
7.9	Parapet dimensions (SCDOT 2008)	159
7.10	Solid modeling layout for NEXT-8	159

7.11	Solid modeling layout for NEXT-6	160
7.12	Restraints for solid model	160
7.13	Shear key connection in shell model	161
7.14	Parapet in section designer	162
7.15	Stem dimension	163
7.16	Stem modeling in section designer	163
7.17	Restraints for shell model	165
7.18	SAP2000 NEXT-8 shell model	165
7.19	Shell modeling layout for NEXT-8	166
7.20	Shell modeling layout for NEXT-6	166
7.21	AASHTO design truck (AASHTO, 2012)	167
7.22	AASHTO design tandem (AASHTO, 2012)	167
7.23	Design tandem moving transversely	168
7.24	Shear influence line for the shear keys in the NEXT-6 bridge under a design tandem loading at mid-span	169
7.25	Moment influence line for the left side of the shear keys in the NEXT-6 bridge under a design tandem loading at mid-span	169
7.26	Shear influence line for the shear keys in the NEXT-8 bridge under a design tandem loading at mid-span	170
7.27	Moment influence line for the left side of the shear keys in the NEXT-8 bridge under a design tandem loading at mid-span	170
7.28	Shear influence line for the shear keys in the NEXT-6 bridge without parapets under a design tandem loading at mid-span	171
7.29	Moment influence line for the left side of the shear keys in the NEXT-6 bridge without parapets under a design tandem loading at mid-span	171
7.30	Shear influence line for the shear keys in the NEXT-8 bridge without parapets under a design tandem loading at mid-span	172
7.31	Moment influence line for the left side of the shear keys in the NEXT-8 bridge with no parapets bridge under a design tandem loading at mid-span	172
7.32	Design tandem longitudinal load placement	173
7.33	Shear in each shear key element of Key 5 along the length of an 8 ft. section NEXT-D bridge with load at the critical shear location	174
7.34	Moment in each shear key element of Key 4 along the length of an 8 ft. section NEXT-D bridge with load at the critical positive moment location	174
7.35	Moment in each shear key element of Key 5 along the length of an 8 ft. section NEXT-D bridge with load at the critical negative moment location	175
7.36	Design tandem strip width determination	176
7.37	Single 32 kip axle strip width determination	176
7.38	Two 32 kip axle strip width determination	176
7.39	Shear key stiffness matrix	178
7.40	Shear key local axis	178
7.41	Shear key configuration	179
7.42	Shear key FEM geometry	179
7.43	Material model	181
7.44	Mode I debonding model	183
7.45	Rebar behavior under pull-off test (Tastani and Pantazopoulou, 2002)	184
7.46	Volume division for mesh using brick elements	185
7.47	Shear key FEM after mesh	186
7.48	Boundary conditions and displacements for FEM-Rz	187
7.49	Boundary conditions and displacements for FEM-X	187
7.50	Boundary conditions and displacements for FEM-Y	188

7.51	Boundary conditions and displacements for FEM-Z	188
7.52	Data acquisition in FEM-Rz	189
7.53	Converted moment-rotation	190
7.54	Calibration of pre-cracking behavior	191
7.55	Calibrated moment-rotation curve	192
7.56	Load-displacement curve for stiffness determination	193
7.57	Shear key stiffness based on the 4 in. FEM in units of kips and in.	193
8.1	Stiffness matrix for shear key frame element in the bridge FEM in units of kips and inches	198
8.2	Critical load position for the 40 ft. span in beam line analysis	199
8.3	Critical load position for the 30 ft. span in beam line analysis	199
8.4	Model geometry of NEXT 8 in CONSPAN	202
8.5	Model geometry of NEXT 6 in CONSPAN	203
8.6	Section cuts in the bridge FEM	205
8.7	Transverse demand distribution for NEXT-8 in the bridge FEM	205
8.8	Design normalized demands for NEXT-8	205
8.9	Local axis for a shell element in the bridge FEM	206
8.10	AASHTO model of NEXT-8 using SAP2000	207
8.11	Output convention for frame element in SAP2000	208
8.12	Transverse demand distribution for NEXT-8 in the AASHTO model	209
8.13	Live load transverse demand envelope in bridge FEM	210
8.14	Critical demand ratios of bridge FEM result over AASHTO method result	211
8.15	Deck demand formula development	212
8.16	Factored dead load effect for NEXT-8	213
8.17	Factored dead load effect for NEXT-6	213
8.18	Comparison between dead load effect of 3D FEM and AASHTO 1D FEM in Strength I limit state	215
8.19	Comparison between dead load effect of 3D FEM and AASHTO 1D FEM in Service I limit state	216
8.20	Sensitivity of transverse demand envelope to shear key stiffness	218
8.21	Sensitivity of transverse demand envelope to stem depth	219
8.22	Sensitivity of transverse demand envelope to concrete Young's modulus	220
8.23	Demand vs capacity provided by various rebar configurations	221
J.1	NEXT-6 22 ft. deck and beam detail	418
J.2	NEXT-6 30 ft. deck and beam detail	419
J.3	NEXT-6 40 ft. deck and beam detail	420
J.4	NEXT-8 20 ft. deck and beam detail	421
J.5	NEXT-8 30 ft. deck and beam detail	422
J.6	NEXT-8 40 ft. deck and beam detail	423
J.7	NEXT-6 22 ft. deck and beam cross-section detail	424
J.8	NEXT-6 30 ft. deck and beam cross-section detail	424
J.9	NEXT-6 40 ft. deck and beam cross-section detail	425
J.10	NEXT-8 22 ft. deck and beam cross-section detail	425
J.11	NEXT-8 30 ft. deck and beam cross-section detail	426
J.12	NEXT-8 40 ft. deck and beam cross-section detail	427
J.13	NEXT-6 notes and bar details	428
J.14	NEXT-8 notes	428
J.15	NEXT-8 22 ft. bar details	429
J.16	NEXT-8 30 ft. bar details	430

J.17 NEXT-8 40 ft. bar details 431

Chapter 1

Introduction

1.1 Problem Description

The cast-in-place flat slab bridges have been widely used in the State of South Carolina for short span bridges. These bridges have historically performed very well including a noticeable durability and has no restrictions on the level of traffic they are allowed to carry. This past positive performance is in large part the reason for its prolific use in the State today. However, the use of such a system comes at the cost of a lengthy construction time. The flat slab bridge requires a significant amount of on-site labor compared with other bridge systems available. Not only does this increase cost associated with the direct construction of the bridge but it also often requires a lengthy and costly disruption of traffic flow in the area. Many state Departments of Transportation (DOTs) have been desirous to address the issue of construction time by exploring and developing a field of Accelerated Bridge Construction (ABC). Under the umbrella of ABC, the use of pre-cast concrete systems has proven invaluable.

The South Carolina Department of Transportation (SCDOT) uses adjacent precast hollow core slab bridges, shown in Figure 1.1, on low volume secondary roads as an alternative to the robust cast-in-place concrete flat slab bridge. These sections are used on twenty to seventy foot spans. They are low cost, easy and relatively quick to install. However, there are some drawbacks. Longitudinal reflective cracks tend to form in the asphalt overlay along the joints between adjacent sections. Transverse cracks also develop at the abutments and bents where no continuity is provided between adjacent spans. These cracks are problematic because they allow water to seep between the members and corrode the prestressing and post tensioning steel. The longitudinal cracks also signify the possible break down of the load transferring capability of the shear key. Since the hollow core beams are designed to take only a fraction of the wheel line load, premature failure of the beam is possible without the load sharing action.

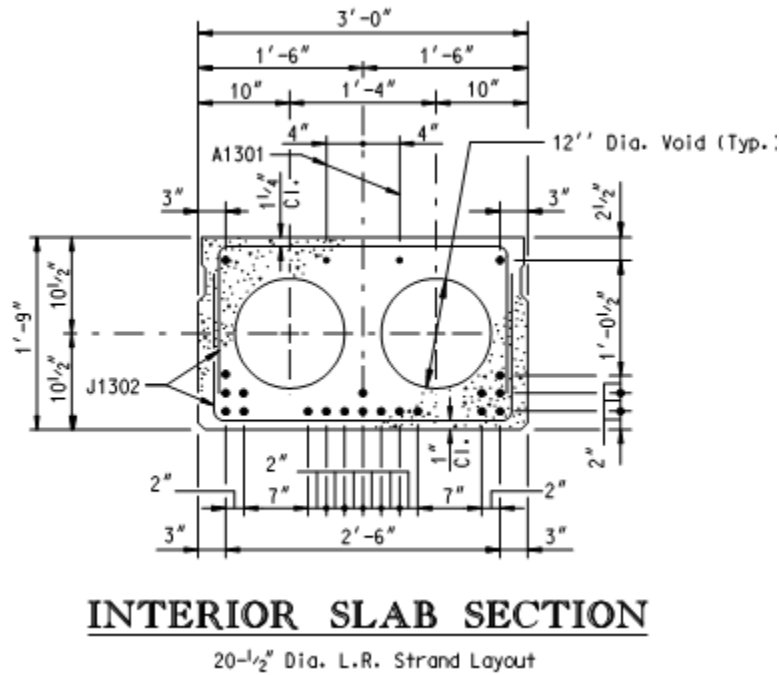


Figure 1.1: Hollow-core beam section currently used by the SCDOT (SCDOT, 2010)

1.2 Objective and Scope of Research

Since the precast hollow-core bridge system has limitations on its use. The SCDOT is seeking an alternative to the flat slab bridges which has a faster erection time but does not have the same short-comings as the hollow-core bridge system exhibits. Thus the overall objective of this research is to identify an improved system to meet their needs. The goals associated with this objective are to find a system that will:

- Eliminate or minimize longitudinal and transverse cracking
- Lower, if possible, the initial price and maintenance costs
- Have a shorter erection time than cast-in-place (CIP) slabs
- Provide a longer service life than the current precast hollow-core slabs
- Be available for use on all routes (no Annual Daily Traffic (ADT) or National Highway System (NHS) restriction)
- Be designed so it does not need an asphalt or concrete overlay

The effort to identify a system, which would provide the rapid construction of the hollow-core system but the durability of the cast-in-place system, consisted of two main phases. The first phase was to do a mostly paper study to identify short comings in the currently used bridge types,

glean information of other State Departments of Transportation, solicit feedback from contractors and fabricators and then assist the SCDOT in identifying a promising bridge alternative to further investigate. The second phase dealt directly with using the selected bridge system – NEXT-D. This included an experimental component, an analytical component and a design component. This report presents the work which was performed, along with providing results and conclusions, relative to the identification of an adequate alternative to the widely used cast-in-place flat slab bridge.

1.3 Outline of Report

This report is organized into nine chapters with the following contents:

1.3.1 Phase 1 – Bridge System Identification

Chapter 2 provides background information relative to the hollow-core bridge and also other currently used bridge types considered to use accelerated construction. This includes the results of an in-depth search of DOT webpages and a search of the literature to identify candidate bridge systems along with known advantages and disadvantages.

Chapter 3 presents feedback obtained from select state DOTs regarding potential bridge candidates for a suitable alternative. This information was collected using a web-based survey and also targeted phone and email based interviews. It also presents the collection and distillation of information pertaining to alternate bridge systems. Bridge contractors and bridge beam fabricators across the United States were interviewed regarding their experiences with different bridge types.

Chapter 4 reports on an in-field verification study of a hollow-core bridge performance. This experimental work examined the behavior of bridge at the interface (shear key) between the adjacent beams.

Chapter 5 provides a summary of the findings of the work in previous chapters. It also discusses findings from a mini-workshop held to solicit feedback from local contractors and fabricators. The selection of the NEXT-D bridge system is also identified.

1.3.2 Phase 2 – NEXT-D Bridge System Evaluation

Chapter 6 begins an explicit evaluation of the NEXT-D bridge system. Specifically it reports on an experimental program which was conducted to evaluate and refine the shear key configuration and construction associated with this bridge type.

Chapter 7 presents a set of analytical studies, used in conjunction with the experimental program, designed to evaluate the behavior of the proposed bridge system – including the way loads are distributed within the bridge.

Chapter 8 deals with the design of the NEXT-D bridge type. In addition to providing some typical design details for the bridge, recommendations are provided pertaining to design approaches for the system.

Chapter 9 provides a brief description of overall findings, recommendations and future work.

This page intentionally left blank

Chapter 2

Background

2.1 Department of Transportation Website Search

The first task performed as part of this research was a thorough search of all fifty states Department of Transportation websites. These websites were searched for available online bridge details and accelerated bridge construction types. The available online details were examined for bridge types that could be used in rapid construction for short span bridges. These details were gathered and the estimated economy, speed, and feasibility of each system were assessed in a cursory manner.

2.1.1 Overall Findings

Thirty-seven of the fifty states provide bridge construction details online. The remaining thirteen that did not provide details are listed in Table 2.1. Utah was the only state that had a separate accelerated bridge construction site with ABC standards, manuals, and workshop notes. The standards include details for precast girders, precast deck panels, precast abutments, and precast footings. The standards also have details for self-propelled modular transports (SPMTs), which Utah has used to successfully replace large bridges. These standards are not feasible for use in this research because the superstructure details available are for long spans and the use of SPMTs is beyond the scope of this project.

The states found with rapid construction details are listed in Table 2.2. Most of these details, such as the channel slabs, box beams and prestressed slab members, are similar to the hollow core

Table 2.1: States without details available online

Alaska	Arizona	Arkansas	Connecticut
Delaware	Georgia	Hawaii	Mississippi
Nebraska	New Mexico	Rhode Island	Vermont
	Wyoming		

Table 2.2: States with rapid construction superstructure details

Alabama	Precast Concrete Channel Slabs
California	Hollow Core and Box Beams
Florida	U – Beam and Slab Members
Idaho	Box Girders and Prestressed Slabs
Illinois	Precast Prestressed Deck Beams
Kansas	Inverted Tee
Kentucky	Precast Prestressed Box Beams
Massachusetts	Precast Box Beams and Precast Deck Beams
Michigan	Prestressed Box Beams
New York	Prestressed Adjacent Beams
North Carolina	Box Beams and Cored Slabs
Ohio	Box Beams
Oregon	Precast Prestressed Box and Precast Prestressed Slab
Pennsylvania ¹	Box Beams
Texas	Box Beams and Prestressed Decked Slab Beams
Virginia	Box Beams and Voided Slabs
Washington	Precast Prestressed Slabs and SIP Trapezoidal Tub Girders
Wisconsin	Prestressed Slab and Box Girders

¹Due to recent degradation issues, PennDOT is no longer using Adjacent Box Beam construction.

sections. The U – beams and trapezoidal tub girders are very deep members that still require a cast-in-place concrete deck, so these details were not of much interest. The inverted tee of Kansas was also deep and required a concrete deck.

2.1.2 Sections of Interest

Texas has some of the more unique sections. Their box beams had much larger shear keys than the traditional sections seen in other states (Figure 2.1). The decked slab beams from Texas are a box beam with flanges (Figure 2.2a). What is unique about this section is that the shear connection is a weld instead of a grouted post-tensioned shear key (Figure 2.2b).

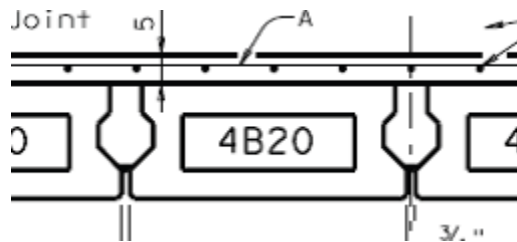


Figure 2.1: Texas box beams (TxDOT, 2010)

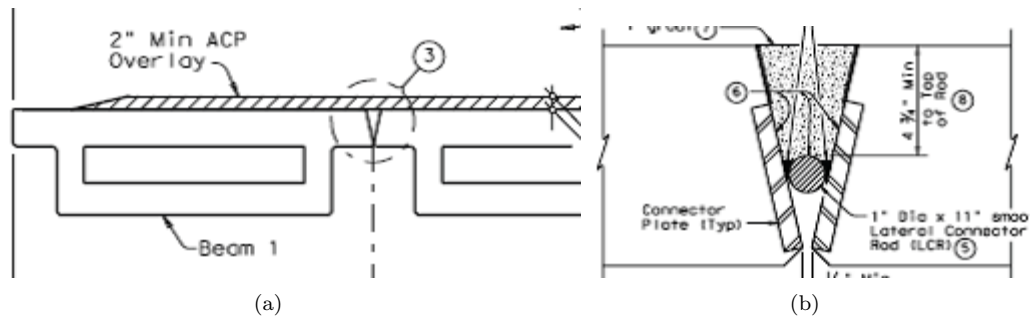


Figure 2.2: Texas decked slab beam (TxDOT, 2010)

2.1.3 Adjacent Beam Restrictions

States that had hollow core details available were studied in depth to find their route restrictions and overlay requirements. Massachusetts, New York, and Washington all required at least a five-inch reinforced concrete overlay on all their adjacent beam bridges. North Carolina and Oregon both require a reinforced concrete overlay on National Highway System routes, or routes with a specific ADT or Annual Daily Truck Traffic (ADTT). Other websites did not have this information available.

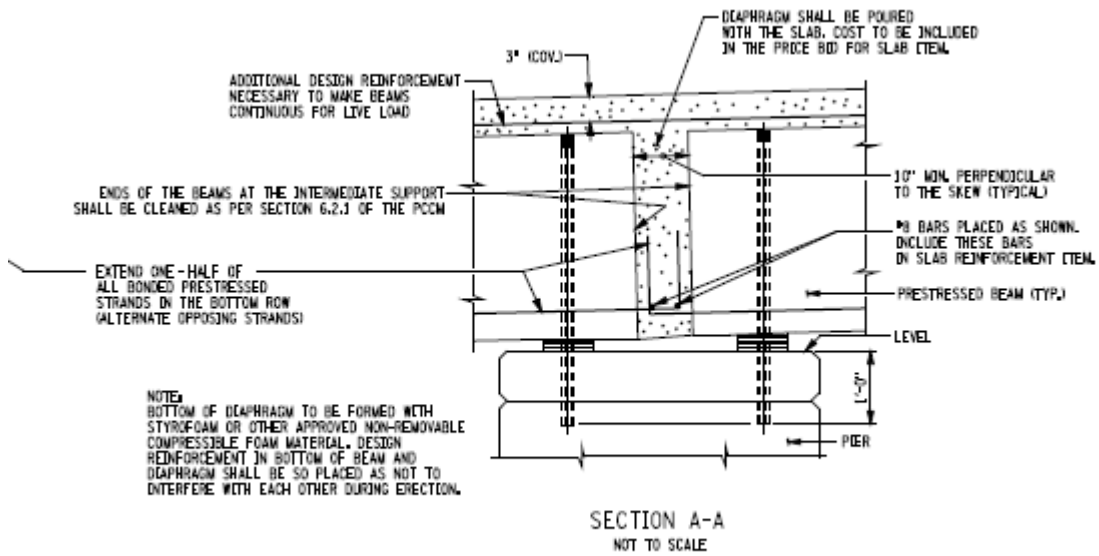
2.1.4 Continuity Details

Another consideration when examining these bridge details was the problem of transverse cracking over the bents. The standards were searched for any detail that would provide continuity or minimize cracking over the bents in the adjacent beam bridges. New York and Ohio both provide details for continuity diaphragms between spans of adjacent box beams (Figure 2.3 and Figure 2.4 respectively). Texas provides a detail which only includes the notch in the precast members to make way for a small pour that connects the top reinforcement in the two beams (Figure 2.5). This detail may not provide moment restraint, but it may help reduce the cracking at the bents.

2.1.5 Closure

Very few states had online evidence of new accelerated short-span systems. Texas had intriguing shallow member details such as the large shear key in their adjacent box beams and their decked slab beams. Therefore, Texas should be targeted for further investigation in later portions of this research.

Other states using adjacent beam systems usually require a concrete overlay when using the bridge on high ADT or NHS routes. Other states have been questioned on their use of concrete overlays and whether they find them effective on high truck traffic routes in the state DOT survey portion of this report. Literature has been studied to determine if there is a proven design theory for using these overlays and is summarized in the Adjacent Beam Bridge Literature Search section.



CONTINUOUS FOR LIVE LOAD CONNECTIONS

Figure 2.3: New York continuity detail (NYSDOT, 2010a)

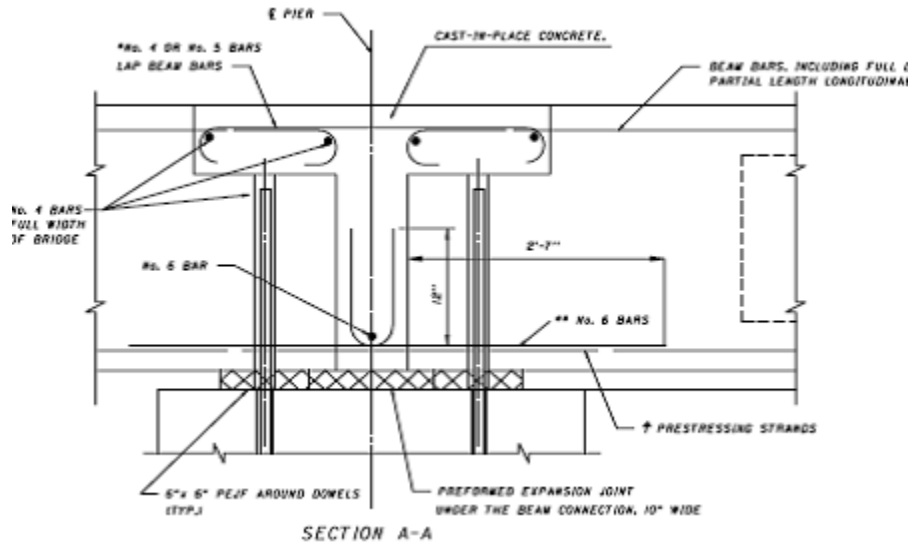


Figure 2.4: Ohio continuity detail (ODOT, 2010))

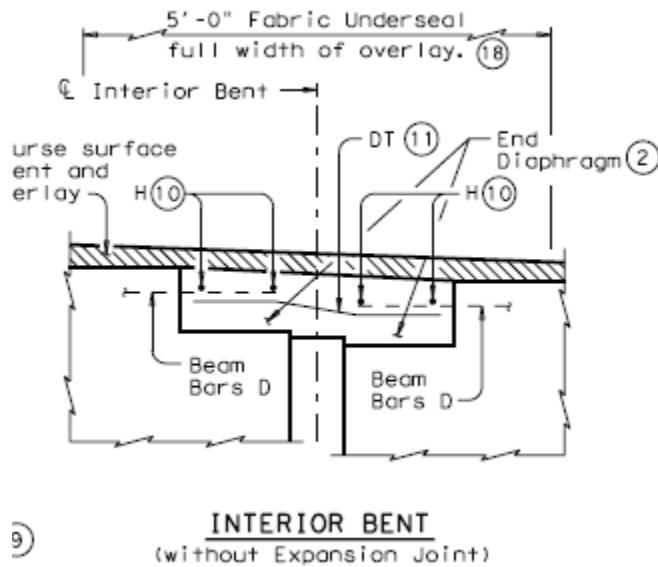


Figure 2.5: Texas continuity detail (TxDOT, 2010)

New York, Ohio, and Texas had continuity details available on their websites. The details from New York and Ohio are full continuity diaphragms, where Texas' detail is not a full diaphragm. These states should be targeted and questioned about the effectiveness of these systems.

2.2 Accelerated Bridge Construction Literature Search

To learn of the recent research in bridge design, a search of publications relating to accelerated bridge construction techniques and designs was conducted. Several publications were found relating to new systems, new materials, and new construction practices to reduce the erection time of bridges.

2.2.1 Beam-in-Slab

A few papers detail different beam-in-slab systems. The most recent system consists of rolled wide flange sections precast in concrete with transverse arching (see Figure 2.6) (Konda et al., 2007). This system was designed to target bridge spans of 40 to 80 feet and designed to serve on low volume roads. Research and testing would be needed to determine if this system or similar systems could be used on high ADT roads for shorter spans. A drawback of this system is the need for large cast in place concrete pours between precast sections.

2.2.2 FHWA International Study

In the Federal Highway Administrations 2005 survey of Japanese and European prefabricated bridge systems, France was discovered to have a few short span solutions (Ralls et al., 2005).

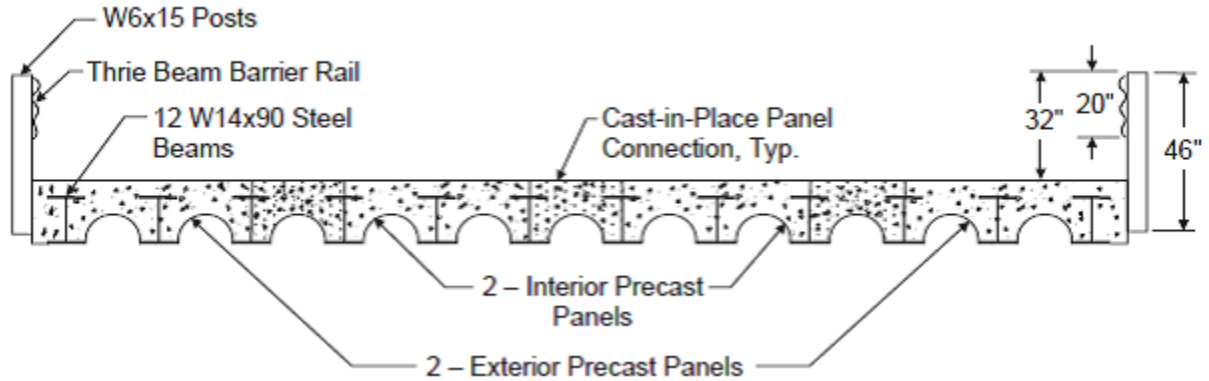


Figure 2.6: Modified precast beam in slab system (Konda et al., 2007)

The first is called the Poutre Dalle system and consists of a shallow precast inverted tee beam which serves as the stay in place formwork for the bridge (see Figure 2.7). The members are placed adjacently and a cast in place concrete deck is then poured over them. This system is typically used for span lengths of 20 to 82 ft. This system retains the clearance ability of the South Carolina hollow core slabs and decreases the occurrence of cracking because of the elimination of a cold-joint through the depth of the slab. The second system is called the Dalle Preflex system and is very similar to the Poutre Dalle system. The system consists of steel wide flange sections with their bottom flanges precast in concrete (see Figure 2.8). Just as in the Poutre Dalle system, the units are placed adjacently and covered with cast-in-place concrete. The Minnesota Department of Transportation has created their own modified version of the Poutre Dalle system and has implemented it successfully on several of their bridges (see Figure 2.9) (Culmo, 2009). However, The Poutre Dalle system has the same deficiency as the beam-in-slab system, where large cast-in-place concrete pours are needed.

2.2.3 Grout Filled Splice Sleeves

The Michigan Department of Transportation has conducted a research study on the use of grout filled splice sleeves used in precast construction (Jansson, 2008). These sleeves are proprietary products manufactured by Lenton. The sleeves come in different sizes for specific rebar (see Figure 2.10). These sleeves can be placed in members during precasting and rebar jutting out from an adjoining member can be fitted into the sleeve during erection. These sleeves are listed in ACI 550.1R-09 as acceptable means of emulating cast-in-place concrete details (ACI, 2009). These sleeves are mainly used in vertical connections such as connecting piers to pier caps and beams because of the difficulty of grouting normal connections in these situations. There is not much information on using these to make horizontal connections such as adjoining adjacent beams. The tolerances would need to be controlled well to ensure match up when erecting the beams. However, if these systems could be implemented successfully in adjacent construction, the load sharing ability could be enhanced between members.



Figure 2.7: Poutre Dalle system (Ralls et al., 2005)

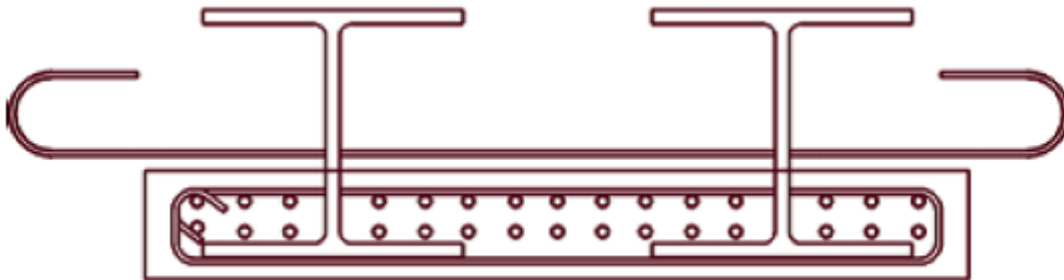


Figure 2.8: Dalle Preflex system (Culmo, 2009)

2.2.4 Full Depth Precast Concrete Bridge Deck Panel System

In a National Cooperative Highway Research Program (NCHRP) report, non-proprietary splice sleeves similar to the ones discussed previously were made of small slices of hollow structural steel (HSS) tube and implemented in full-depth precast deck panels (Badie and Tadros, 2008). The target of this research was to create a precast deck panel system that did not require post tensioning. Three different configurations for connecting adjacent deck panels were considered. The first was an emulation of the grouted splice sleeves where the rebar jutting from one deck panel was slid into a sleeve through a hole in the side of the adjacent panel. Using small holes in the top of the splice panel, the sleeve was filled with grout (see Figure 2.11). In the second configuration, a splice was included in each of the panels and the space above the splices was kept free of concrete to allow a small length of rebar to be dropped in (see Figure 2.12). The pocket was then filled with grout.



Figure 2.9: MNDOT system (Culmo, 2009)

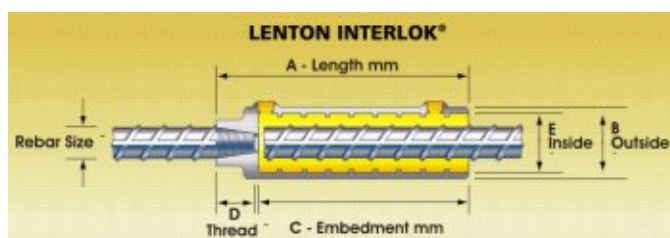


Figure 2.10: Grout filled splice sleeve (ERICO, 2010)

In the third configuration, the HSS piece serves as a physical connection for two threaded rods by using hex nuts (see Figure 2.13). Also, as in the second configuration, the pocket is filled with grout after the connection. Several specimens were constructed and tested. The test results showed that the first and second configurations were effective in connecting the deck panels. By implementing these types of connections in adjacent beam construction, it may be possible to eliminate post tensioning from the design. However, cracking along the joints may not be eliminated. Research and experimentation would be needed to conclude such results.

2.2.5 Modular Bridges

A short span bridge option that has become popular in the midwest is the use of modular steel bridges. These bridges are made in strips of steel grid that can be placed and fastened together using bolted diaphragms (see Figure 2.14). These bridges are mainly used for very low volume

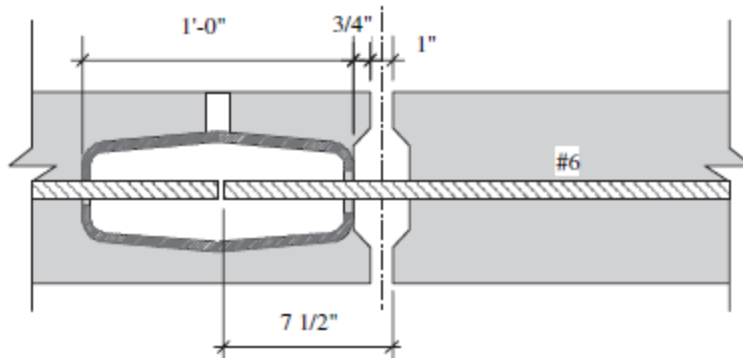


Figure 2.11: First system (Badie and Tadros, 2008)

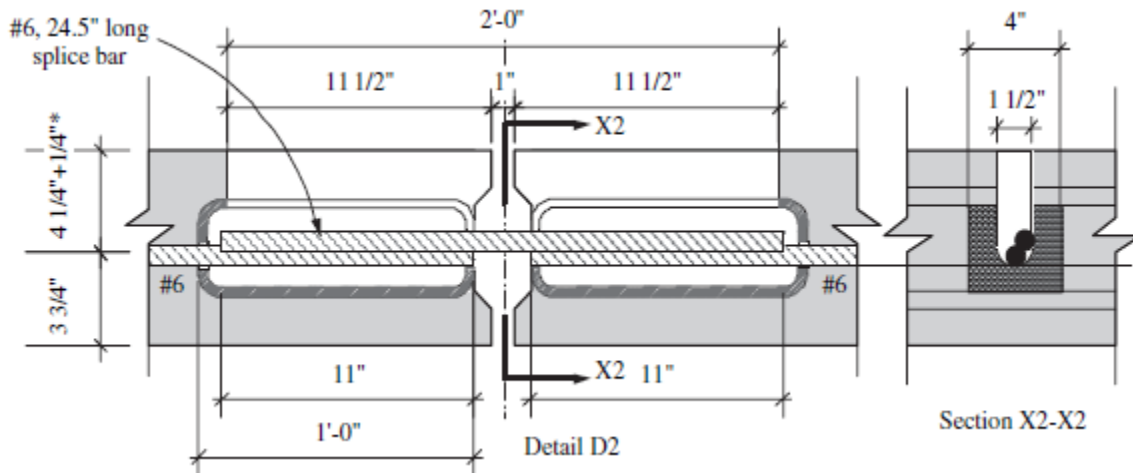


Figure 2.12: Second system (Badie and Tadros, 2008)

roads or temporary purposes, but can be fitted with precast deck panels to make them permanent vehicular bridges. Big R Bridge (Big-R-Bridge, 2010) and Roscoe Bridge (Roscoe-Bridge, 2010) manufacture these types of modular structures. If this system could be tested and authorized for high ADT routes, this may be a high speed alternative for short span bridges with the use of precast deck panels.

2.2.6 Rapid Hardening Concrete

An article from Construction and Building Materials describes a practical case of using rapid hardening concrete on a short span bridge (Cangiano et al., 2009). The experiment was conducted in Italy using precast elements as stay-in-place forms for the early age strength concrete. The concrete was self-compacting and achieved a compressive strength of about 80 MPa (11.6 ksi) within twenty-four hours. Although one of the targets of this research is to eliminate topping when constructing these short spans, cast-in-place concrete may be required in a desirable design. The use of this rapid

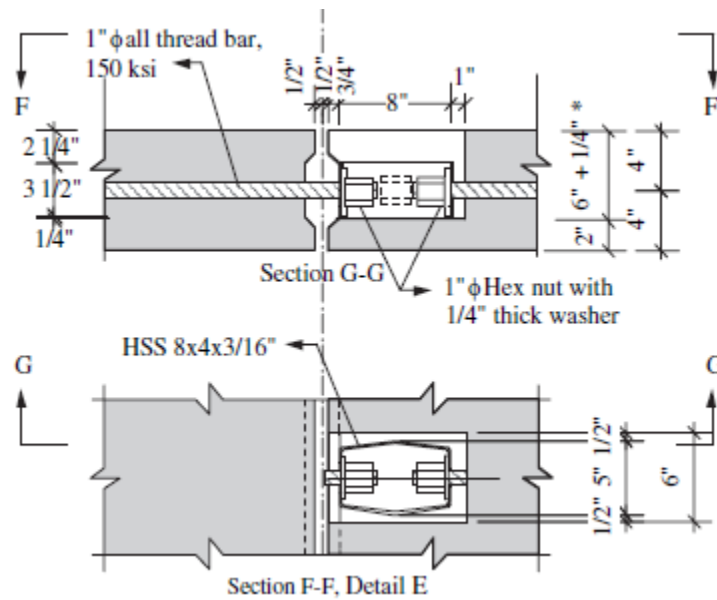


Figure 2.13: Third system (Badie and Tadros, 2008)

28'-32' travel way, four-module unit

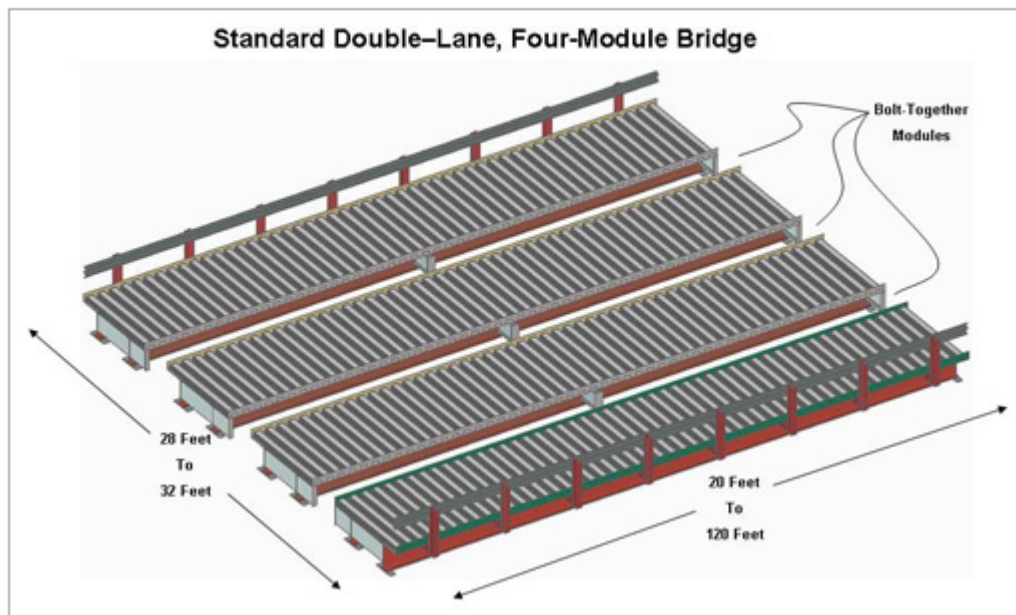


Figure 2.14: Two lane modular bridge (Roscoe-Bridge, 2010)

hardening concrete could be used to shorten the construction time greatly and should be taken into consideration.

2.2.7 Self-Propelled Modular Transports

Articles were found promoting the use of self-propelled modular transports (SPMTs) and barges as an accelerated construction technique (Bergeron, 2008; Cho, 2007). Large, full-width sections of bridges are built nearby and rolled or floated into place using the SPMTs. This technique is excellent in reducing road closure time and reducing construction time and costs. However, given the terrain in South Carolina and the short spans this research deals with, these solutions do not appear to be a feasible way to achieve this project’s objectives.

2.2.8 Closure

This journal search discovered a few systems that could be feasible in providing the improvements sought after in this research. The Poutre Dalle and Minnesota DOT systems could greatly improve the performance of the bridge (i.e. reduce cracks) by possibly only increasing the construction time by a small amount. Grout filled splice sleeves may have a practical application in this research, however more research is needed to determine if they are effective means of shear transfer between beams. Since these grout filled splice sleeves may be costly, using the “homemade” systems proposed for the full-depth precast concrete bridge deck panel systems may be more feasible. Modular bridges are very rapid, however they have only been used on very low traffic bridges thus far and more research would be needed to determine their long-term performance on high ADT roads. Rapid hardening concrete is a beneficial solution to the problem of accelerated bridge construction and should be considered if cast-in-place concrete is needed in the final design.

2.3 Adjacent Beam Bridge Literature Search

2.3.1 Shear Key

Precast concrete bridges are a very important facet in accelerated bridge construction and have the potential to expedite the replacement of older, structurally deficient bridges in the United States. Precast adjacent beam bridges are popular for shorter spans because of their speed of erection and low clearance abilities. Different states use different variations of these types of bridges; such as hollow core slabs, deck beams, and the larger box beams. Box beams are used in about two-thirds of the fifty states (Russell, 2009).

The major weakness of these bridges is the shear transfer mechanism between the adjacent beams. The most common shear transfer mechanism used is a shear key (see Figure 2.15). The most common problem reported for these bridges is cracking through the grout–beam interface along the longitudinal joint (Russell, 2009). This behavior seems unrelated to maximum span or skew of the bridge, but can be correlated to amount of heavy truck traffic crossing the bridge (Russell, 2009; Lall et al., 1998). Many states have restrictions against using these bridge types on roads with high ADT

or on the NHS because of the cracking tendencies (Culmo, 2009). These cracks can be a concern when one considers the possible loss of load sharing between the adjacent beams. Further concerns include the detrimental effects of water and deicing salts leaking between the beams and corroding prestressing strands and transverse ties (Huckelbridge Jr. et al., 1995).

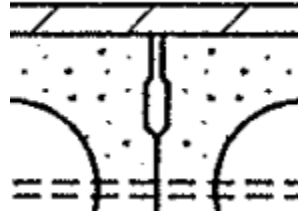


Figure 2.15: Typical shear key

The AASHTO Load and Resistance Factor Design (LRFD) Specifications provide no design parameters for the common method of shear transfer of using the combination of grouted shear keys and lateral ties (Culmo, 2009). Therefore, the size and type of shear key and amount of post-tensioning has evolved by trial and error and varies widely between State departments of transportation (DOTs) (Culmo, 2009). The most common mitigation strategy for cracks along the shear key, which many state DOTs implement, is to require five to six inches of reinforced concrete overlay on the beams. In addition to the overlay requirement, some state DOTs also increase the amount of transverse post-tensioning force. However, approximately sixty-five percent of all states still see reflective cracking through the concrete overlay (Russell, 2009).

2.3.1.1 Common Details

The most common shear key placement is at the top flange of the beam and they are usually very small keyways (see Figure 2.16). Due to the narrowness of the keyway it can be very difficult to place the grout correctly. The West Virginia DOT investigated several high volume bridges and concluded the shear key failures were due to inadequate grouting procedures during construction (El-Remaily et al., 1996).

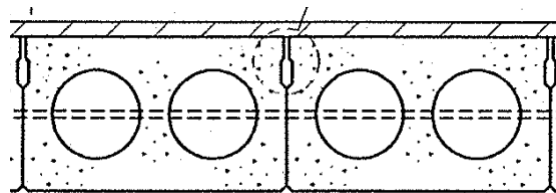


Figure 2.16: Typical shear key

The moment transferred between the beams creates a hinging action about the shear key and can possibly lead to opening and closing of the grout at the top face of the beams (Lall et al.,

1998; Miller et al., 1999). Furthermore, the application of post-tensioning force at mid-depth after the curing of a partial-depth shear key may create moment and opening of the grout at the top of the beams (Russell, 2009). To improve the performance and durability of the shear keys, tensile moment action at the shear key face needs to be reduced.

2.3.1.2 Temperature Effects

It has been noted by some researchers that these longitudinal cracks appear very quickly after construction of the bridge (Russell, 2009; Miller et al., 1999; Hlavacs et al., 1996). The warming of the wearing surface due to the sun creates a camber in the members and causes the adjacent beams to pull apart or put significant tension force on the grout (Miller et al., 1999). This pulling apart is caused by the adjacent beam axes not being perfectly parallel (see Figure 2.17). Miller et al. (1999) found that the cyclic loading of the adjacent beams propagated the cracks created by temperature strain, but did not create any new cracks from the live load alone (Miller et al., 1999; Hlavacs et al., 1996).

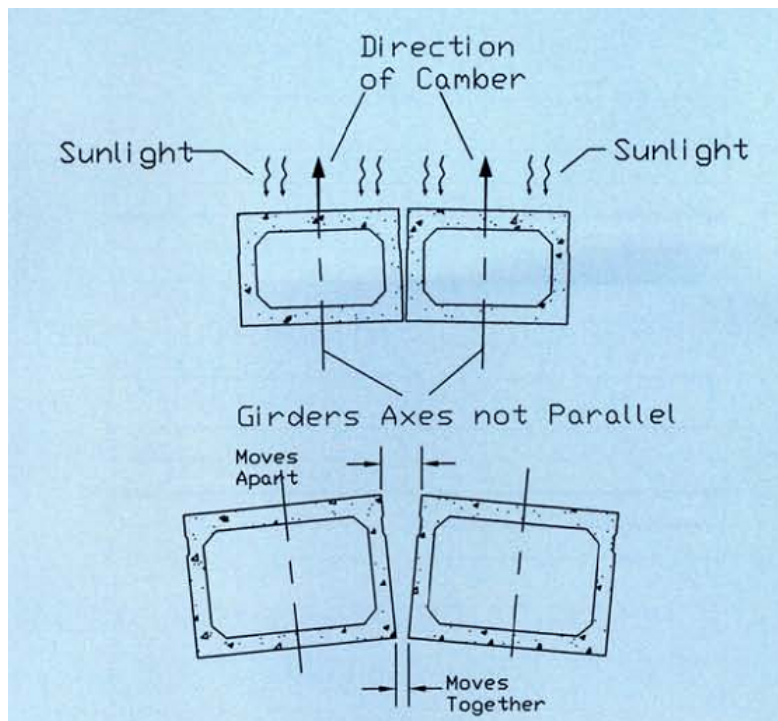


Figure 2.17: Temperature effects (Miller et al., 1999)

Miller et al. (1999) also conducted tests on the same box beam with different shear key locations and materials. Tests using a mid-depth shear key instead of an upper flange shear key encountered much less temperature cracking when the grout was not extended to the top of the beam.

When Miller et al. (1999) tested epoxy grout in the shear keys instead of non-shrink grout, it was found to have greater bond strength to the beams. However, it also has a coefficient of thermal expansion that is three times that of normal non-shrink grout. This would make it more susceptible to thermal cracking during large temperature changes.

It should also be noted that different temperature ranges during a time period can “heal” the longitudinal cracks (i.e. cause the gap of the temperature cracks to close), making them difficult to detect (Hlavacs et al., 1996). Therefore, more longitudinal cracks can be present on a bridge than is apparent. A totally different set of cracks could be detectable during a different time of the day, or a different time of the year.

2.3.1.3 High Performance Details

According to the FHWA 2005 survey of the bridge systems in Japan and some European countries (Ralls et al., 2005), Japanese box beam details experience little-to-no longitudinal cracking. Unlike the typical small partial-depth shear keys used in the United States, the Japanese shear key is full-depth and very wide (see Figure 2.18) (El-Remaily et al., 1996). The keyways are filled with cast-in-place concrete instead of non-shrink grout. The Japanese bridge systems use considerably more post-tensioning by using more diaphragms and having two layers of lateral ties (see Figure 2.19). The two layers of lateral ties help prevent the rotating moment about the shear keys that is a common cause of cracking along the longitudinal joints. Rather than specifying a constant post-tensioning force for all box beam bridges, the Japanese standards require a detailed analysis of each bridge to determine the amount and location of post-tensioning (El-Remaily et al., 1996). Although this system may perform much better than the American system, it also requires form work for the cast-in-place shear keys, more analysis and more field work to apply post-tensioning.



Figure 2.18: Japanese box beams (El-Remaily et al., 1996)

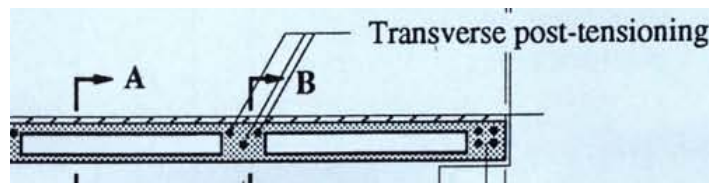


Figure 2.19: Japanese box beam post tensioning (El-Remaily et al., 1996)

In 1990, the New York Department of Transportation conducted a study to determine the cause of reflective cracking through the five-inch concrete topping observed in the box beam bridges

(Lall et al., 1998). From the results of the inspections on existing bridges they decided to make some changes to their standard box beam detail. The shear keys were increased from partial-depth to full-depth (see Figure 2.20) and more post-tensioning ties were added to all spans. These new standards were implemented in 1992, and in 1996 a follow-up study was performed on the new bridges. Only twenty-three percent of the new bridges exhibited longitudinal cracking along the shear keys as opposed to fifty-four percent cracked in 1990 (Lall et al., 1998). According to the inspection personnel, these cracked bridges had ADTs of 5000 or more.

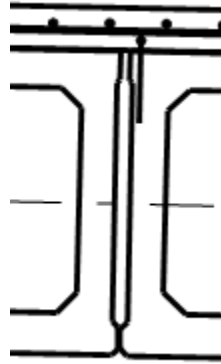


Figure 2.20: New York full depth shear key (NYSDOT, 2010a)

2.3.1.4 Experimental Studies

Miller et al. (1999) conducted an experimental study comparing the performance of upper shear keys with mid-depth shear keys (Figure 2.21), and comparing the use of non-shrink grout with the use of epoxy grout. Three different tests were performed: non-shrink grout in an upper shear key, non-shrink grout in a mid-depth shear key, and epoxy grout in the upper shear key.

The mid-depth shear key was only grouted to the top of the shear key, and not all the way to the top face of the beams. The mid-depth shear key performed much better than the upper shear key and also transferred more load after cracking (Miller et al., 1999). An advantage of the mid-depth shear key is that the empty throat area above the shear key can be filled with a sealant to help prevent leaking. The epoxy grout did not fail throughout the testing, however it is noted that when the epoxy grouted beams do fail, it is through the concrete of the beam, which could be an undesirable mode of failure (Miller et al., 1999). Epoxy grout is also more expensive and more difficult to work with during construction.

Huckelbridge et al. (1995) tested the relative deflection of five box beam bridges in Ohio, in 1995. The two bridges discussed in this journal (STA 30-23.02 in East Canton, Ohio and SUM224-12.50 in Akron, Ohio) had been in service since the mid-seventies. The displacements were measured using relative displacement transducers. All of the test structures showed relative displacements in some joints that would be an indication of shear key failure (> 1 mil or 0.001 inch). It was noticed

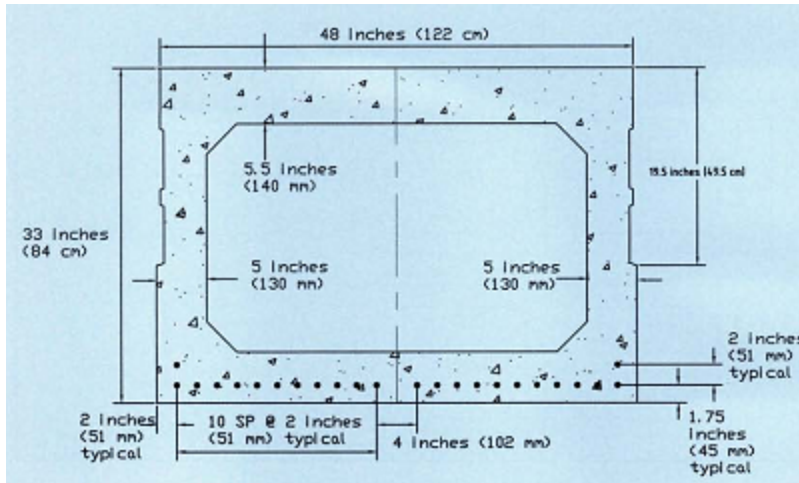


Figure 2.21: Miller shear key test member (Miller et al., 1999)

that not all of the joints with large relative displacements showed signs of distress that are visible from the outside. This suggests that there may be a lag time between shear key failure and exterior cracks. Most of the shear keys that showed signs of fracture still transferred a fair amount of load. The failure typically occurred along the bond line between the grout and the box beams, and therefore there was still mechanical friction to transfer load. It was also observed in this study that the current tie bars used for transverse connectivity had almost no effect on how the shear keys performed (Huckelbridge Jr. et al., 1995).

2.3.1.5 Numerical Studies

South Korea is a relatively recent user of prestressed box beams. To determine the best place for the shear key in their box beams, they used a finite element model using four different configurations (see Figure 2.22) (Kim et al., 2008). Their shear keys are modeled similar to the Japanese system with a partial shear key notch within the larger shear key (see Figure 2.22). They also use cast-in-place concrete for their key filler material.

From the study, the relative vertical displacements were found for each model. The model without a shear key performed the worst, with relative deflections 30 to 60% greater than that of the mid depth shear key. The bottom shear key had relative deflections 4 to 6% greater than that of the mid depth shear key. The mid depth shear key and top shear key performed very similarly. The top shear key only had relative deflections 0.2 to 0.6% greater than the mid depth shear key.

Badwan and Liang (2007) created a finite element model for a two span continuous laterally post tensioned multi-beam bridge (see Figure 2.23). The bridge included a full depth shear key between members.

The model was calibrated using field measurements of flexural strain in the bottom of the members. After analyzing the model, it was found that the effective grout stiffness did not have an effect on the bridges response to truck loads. It was also found that, if no cracks develop in the

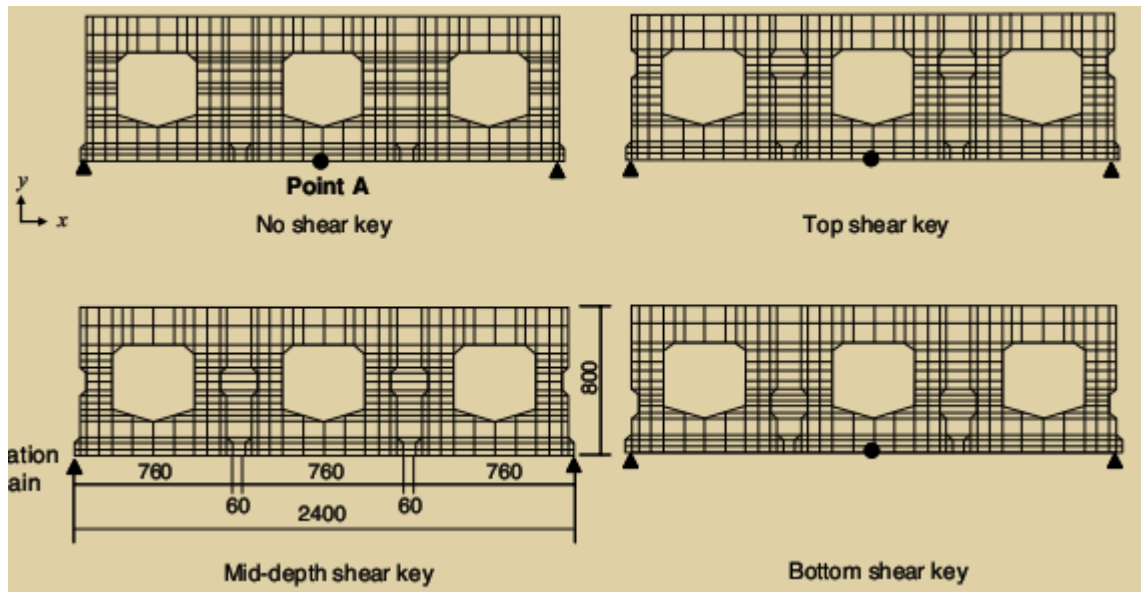


Figure 2.22: Korean shear key placement study (Kim et al., 2008)

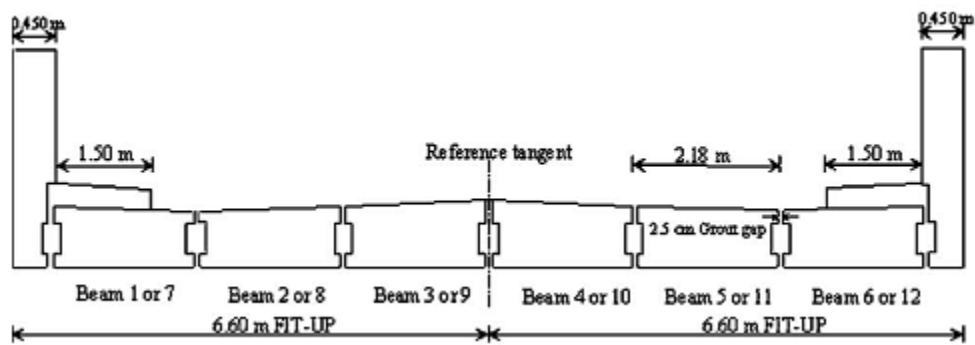


Figure 2.23: Laterally post tensioned multibeam bridge (Badwan and Liang, 2007)

grouted shear keys, the removal of post tensioning force has no noticeable effect on how the bridge distributes live loads.

2.3.1.6 Published Recommendations

The following provides a summary of recommendations for dealing with reflective cracking in longitudinal shear keys. These recommendations have been shown to decrease the amount of cracking, but not eliminate the cracking completely.

- Move the shear key to the neutral axis of the member (Miller et al., 1999).
- Use a full depth shear key that can be grouted easily (Russell, 2009; El-Remaily et al., 1996; Miller et al., 1999).
- Provide post-tensioning in the top and bottom of the beam (Lall et al., 1998; El-Remaily et al., 1996).
- Sandblast the keyways before shipping and clean with compressed air before erection (Russell, 2009).
- Transversely post-tension after grouting the keys if it will not cause moment about the shear key (Russell, 2009).
- Use a grout material with high bond strength (Russell, 2009; Miller et al., 1999).

2.3.1.7 Closure

A number of key findings related to the performance of the shear key are as follows:

- States often use a reinforced concrete overlay in order to use this bridge type on high ADT roads, however, it has been shown through studies that the overlay does not completely eliminate the longitudinal cracking.
- Applying mid-depth post-tensioning with a top flange shear key after grouting can lead to cracking at the top of the member along the joint.
- The effects of temperature on the girders may initiate cracks in the longitudinal joints without any load being applied to the bridge.
- Cyclic loads do not necessarily make new cracks along the joints, but they do propagate cracks created by temperature effects.
- Larger and deeper shear keys improve the ability to grout effectively and decrease the amount of rotation about the shear key of the member, therefore decreasing tensile opening at the top of the key.
- Many failed shear keys (i.e. having full-depth cracks) still transfer load through friction.
- Transverse tie bars do not contribute significantly to shear transfer.

- Mid-depth shear keys display the best relative vertical displacement performance in comparison to other shear key locations.

2.3.2 Durability

One problem common to these adjacent beam bridge types with voids is over time the prestressing steel strands tend to corrode and without proper maintenance can lead to catastrophic failure or collapse of the bridges before the structure is even known to be structurally deficient through visual bridge inspection. Water and deicing salts leaking through open joints can infiltrate the boxes and over time corrode the prestressing steel in the sections. The decreased area of steel leads to loss of strength and without maintenance can eventually lead to failure and collapse of the structure. Cardboard forms used in the voids can deteriorate over time and clog the drain holes in the box beams, trapping the water and salts in the section leading to further corrosion issues. According to FHWA's Connection Details for Prefabricated Bridge Elements and Systems, these adjacent beam bridges are very durable and many have been in service for over 50 years without significant deterioration (Culmo, 2009). However, this is not always the case since many of the strand deterioration issues are undetectable with simple visual inspection and therefore are missed. Improved inspection techniques are in the works nationally as universities such as Lehigh and Toledo have undergone research in order to evaluate various nondestructive tests that may be able to be used in the field to inspect these bridges for hidden strand corrosion (Nims and Devabahktuni, 2011).

2.3.2.1 Pennsylvania Lakeview Drive Bridge Collapse

One such case of undetected strand deterioration and unexpected failure of a bridge is seen in the collapse of SR 1014 over I-70 (Lakeview Drive bridge) in Pennsylvania on December 27, 2005. The bridge was a non-composite prestressed concrete adjacent box beam bridge. The fascia beam located on span three collapsed onto I-70 eastbound lane at approximately 6 pm on December 27, 2005 (see Figure 2.24). There were no serious injuries reported. The bridge had a bituminous wearing surface with no waterproofing. The box beams were connected with 1 in. steel tie rods and non-shrink grout in the shear keys.

The box beams were 48" x 42" with 60 prestressing strands each. A concrete barrier was attached directly to the fascia beam. After the grout in the shear key failed the fascia beam acted as a single unit which it was never designed to do. This change in behavior was a major contributor to the subsequent failure (see cross-section shown in Figure 2.25).

The bridge was not considered structurally deficient before collapse. However, at the time of its last inspection, the bridge girders were found to have numerous scrapes and spalls due to truck impacts and the prestressing strands were exposed on the soon-to-be failed beam. The bridge had a low clearance of 14'-5" which resulted in the multiple impacts. Having been built in the 1960s, the bridge was about 45 years old and thus possessed outdated reinforcement detailing standards. The voids in the box beams were formed with cardboard, not commonly used today, and the strands were very small with questionable quality control and reinforcement cover (PennDOT, 2006). Despite all



Figure 2.24: Lakeview Drive collapse (PennDOT, 2006)

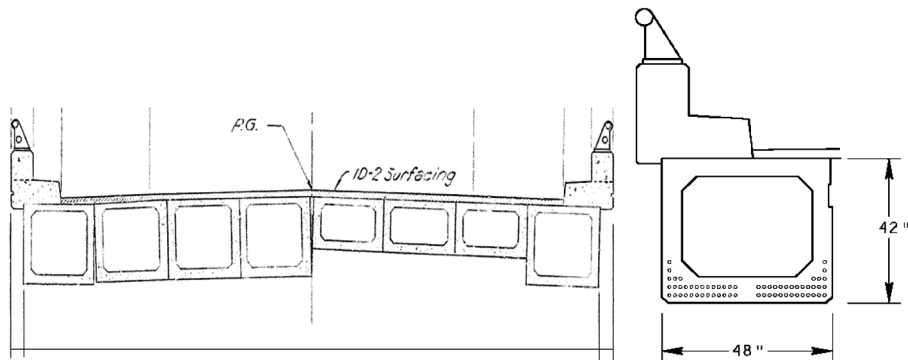


Figure 2.25: Lakeview Drive box beam section (PennDOT, 2006)

of these issues, inspections did not deem the bridge structurally deficient largely because only 20 of the 39 failed strands (out of 60 total strands in the section) could be visually inspected.

The largest factor contributing to the failure of the bridge was the corrosion of the hidden strands. The material properties of the bridge were tested in a forensic study performed by Lehigh University and Michael Baker Corporation. The measured concrete compressive strength and the strand yield strength were found to be greater than the specified design values which clearly indicates that material strength degradation was not the issue (Hartle, 2009). Contrary to the conventional wisdom at the time which assumed that reinforcement encased in concrete doesn't corrode, strand losses extended past what inspectors could visually assess. In this case, a lab assessment of the girder showed that 39 of the 60 strands (65% of the total strands in the section) had failed which is 95% more than that determined in the original field inspection a year before the bridge collapsed (PennDOT, 2006). The corrosion was due to an open joint at the barrier that allowed deck leakage through the joint and allowed water and years of salt spray to infiltrate into the sections. One should be reminded that these box beams used cardboard forms, which have been found to soak up water and eventually slip and clog up drain holes in the box beams, thus allowing water and salts to reside in the voids and corrode the steel. Water intrusion and corrosion was the main cause for the collapse in this instance. Many of the issues this bridge had (i.e. cardboard forms, small strands, and poor cover) are largely avoided in today's practice. Furthermore, this failure was directly linked to poor maintenance of the bridge and also construction techniques that today are known to be outdated (PennDOT, 2006). Other factors contributing to the failure include: loss of load transfer through the shear key (shear key grout failed thus it lost the transfer mechanism), truck collision damage, and original fabrication quality control (PennDOT, 2006).

2.3.2.2 Aftermath

As a result of this event, Pennsylvania surveyed surrounding states and found at least six states with similar problems/failures with these bridge types (Jones, 2010). Within two months of this bridge failure PennDOT proceeded to re-inspect all adjacent box beams that were deemed structurally deficient. The remaining 700+ adjacent box bridges were inspected within eight months of the collapse. New rating guidelines were implemented with stricter inspection conditions to downgrade bridges with any visual problems. These new rating guidelines incorporated recommended assumptions for additional strand losses and fascia beams acting as single units. The number of structurally deficient bridges more than doubled in the state with the new rating guidelines. There were no proven methods at the time to determine deterioration of hidden strands and no cost effective rehabilitation and repair schemes have been identified for these initial low cost bridges as they near the end of their useful life. Therefore, Pennsylvania issued a moratorium on non-composite adjacent box beam bridges as a result of the collapse (PennDOT, 2006).

Other states have taken notice as well and Raymond A. Hartle, PE of Michael Baker Corporation has given presentations at numerous bridge conferences across the country on the forensic study done for this collapsed beam (Hartle, 2009). Hartle mentions seven key inspection requirements that are imperative when inspecting these non-composite adjacent box beam bridges: document ex-

posed strands, document cracking patterns, define strand corrosion, measure camber, investigate independent beam action, evaluate barrier and barrier connection, and clear clogged drain holes. Hartle has given this presentation and given exercises to various bridge conferences by presenting pictures of a bridge and having the members of the conference rate the bridge accordingly.

2.3.2.3 Non-Destructive Testing of Strand Corrosion

At the time of the Lakeview Drive collapse, there were no proven methods to determine deterioration of hidden strands and therefore plenty of research has begun in order to identify a non-destructive test to track the corrosion in hidden strands in prestressed adjacent box beam bridges. Dr. Nims of the University of Toledo has begun a project titled “Magnetic Sensor for Nondestructive Evaluation of Deteriorated Prestressing Strand” in which they are attempting to use magnets to evaluate the corrosion of hidden strands in prestressed beams (Nims and Devabahktuni, 2011). The research began in 2009 and at that time, despite national studies, no effective nondestructive sensor technology had been identified (Nims and Devabahktuni, 2011).

Dr. Naito at Lehigh University has been working on a project with PennDOT since December 2007 titled “Inspection Methods and Techniques to Determine Non-visible Corrosion of Prestressing Strands in Concrete Bridge Components” (Jones, 2010). In 2010 they completed their destructive evaluation tests, all nondestructive evaluation vendor reports have been studied, and an extension was granted so that three NDT technologies can be studied more in-depth. Lehigh is designing a concrete test-slab so that two different magnetic NDT technologies can be used to attempt to detect various reinforcement damages. Lehigh is also analyzing 3D Laser Scanning methods for feasibility and practicality in field use. Lehigh has also recommended a new bridge rating method for use in hopes of improving current inspection practices and improving structure life and safety. In total six NDE vendors visited Lehigh to inspect the box beams and the results of the inspections were compared to the results of the destructive evaluation in order to compare the NDE inspections to the actual conditions of the strands. A questionnaire was sent out to all involved inspection groups to gather data on costs and feasibility of the methods. The draft version of the NDT report was submitted to PennDOT in early December of 2009 (Jones, 2010).

2.3.2.4 Conclusions

The largest factor contributing to the failure of the Lakeview Drive Bridge was the corrosion of the hidden strands. No other similar adjacent box beam failures have been identified through literature searching. A nondestructive test that can determine the corrosion in hidden strands will surely improve the quality of inspections and maintenance on these bridges and extend their useful life and improve the safety of the systems. Dr. Nims notes that “new higher strength less permeable concretes and improved casting procedures are making boxes much better than those from the 60’s and 70’s” so these durability issues will only improve as these bridge types are used in future designs (Nims and Devabahktuni, 2011). However caution must be taken when inspecting the bridges that were built 40 to 50 years ago. This should also be considered when working on the new designs of

these bridges and therefore maintenance procedures of these new designs must be accounted for in order to protect the bridges and ensure a long service life and safety as well.

2.3.3 Continuity

The spans of prestressed concrete bridges are commonly made continuous in order to improve the structural efficiency by reducing the maximum positive moment in the spans of the bridge. Continuous-span bridges are also advantageous since they reduce deflections and result in a better riding surface. This type of design is also beneficial from a maintenance point of view compared to a simply supported design since it eliminates open joints at intermediate supports. Eliminating these open joints helps to minimize water drainage onto the substructure that can cause rebar corrosion and concrete spalling and delaminating issues. Many states construct bridges with continuity diaphragms, but for design calculation purposes, the spans are considered as simply supported, thus not taking advantage of the reduced positive moment but still benefiting from the lack of open joints (Saadeghvaziri et al., 2006).

Existing continuity connections have their own shortcomings, however, including the development of positive restraint moments. Other shortcomings include diaphragm cracking at the internal pier, due to time dependent effects that affect bridge durability and aesthetics, and time consuming and expensive joint construction due to reinforcement congestion (Saadeghvaziri et al., 2006). These shortcomings must be addressed in order to justify the use of continuous spans.

The use of continuous designs with rapid construction bridge projects can be advantageous for the previously stated reasons but can also slow-down the construction process thus hindering the goal of a rapid construction solution. The benefits of accelerated bridge construction include minimized traffic disruption, improved work zone safety and minimized environmental impact due to less time on the job site. Prefabricating the bridge components in order to speed-up the construction can also improve constructability, increase quality, and lower life-cycle costs. The use of continuous spans and the continuity diaphragm detail for rapid-construction adjacent box girder bridges must be accounted for in the design in order to maximize the efficiency of the structure while permitting rapid construction.

2.3.3.1 Common details

Bridges composed of simple-span precast prestressed concrete girders made continuous through cast-in-place decks and diaphragms have been used by most states since the 1960's. These bridges are typically made continuous for live loads and super-imposed dead loads but are designed as simply supported for deck and girder weight. The continuous nature of this design causes positive restraint moments to develop over the internal supports due to time dependent properties such as creep and shrinkage (see Figure 2.26).

These moments occur since the girders tend to camber upward due to creep of the concrete and continuity keeps the girder ends from rotating, which results in positive restraint moments in the girders over the interior bents. Because of this positive moment, cracks usually develop at the

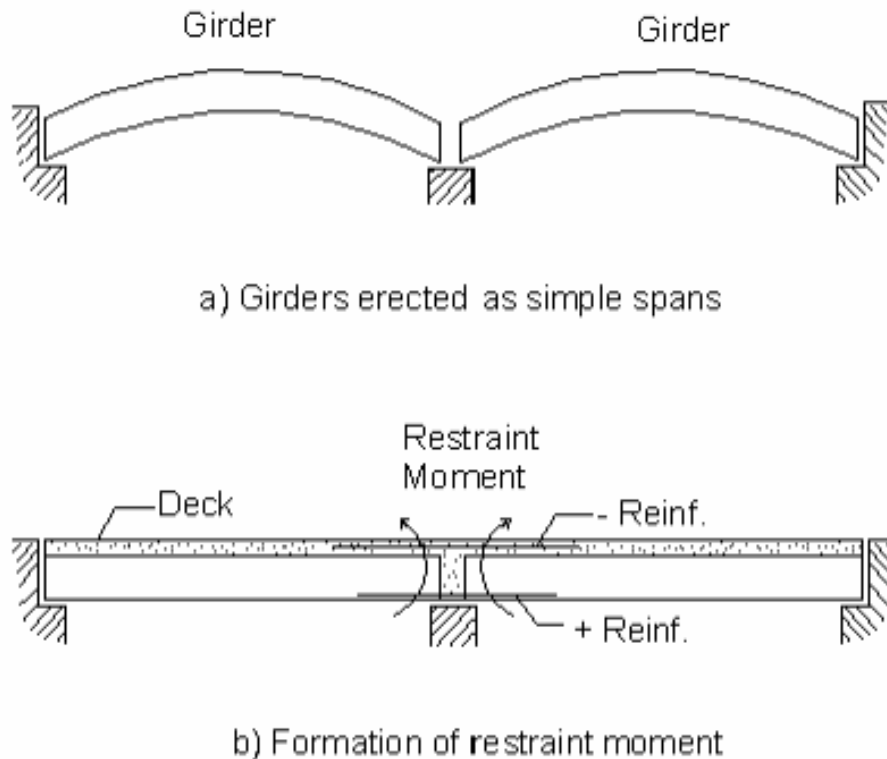


Figure 2.26: Formation of positive restraint moments (Saadeghvaziri et al., 2006)

bottom of the diaphragms, which can cause corrosion of the reinforcement in the diaphragms as well as simply damaging the bridge aesthetics (Saadeghvaziri et al., 2006).

These effects are accounted for in the continuity diaphragm with either mild steel reinforcement or prestressed strands (AASHTO, 2007). The continuity diaphragm is typically concrete cast-in-place after the precast prestressed girders have been placed. The mild reinforcement or prestressed strands, used to account for the positive restraint moments, typically continue from the bottom flanges of the precast girders into the diaphragm. Some state DOTs provide their continuity details on their websites, including Missouri, one of the few states that consistently uses continuous spans for their adjacent box girder bridges (see Figure 2.27).

2.3.3.2 Exploratory details

The problems with continuous spans such as the development of positive moments and diaphragm cracking at the internal pier, as well as reinforcement congestion at joints, are common to various design details used by many states (Saadeghvaziri et al., 2006). One new mitigation strategy being considered involves using Carbon Fiber Reinforced Polymer (CFRP) sheets, instead of mild steel or prestressed strands, which will address these problems at the continuity connection while

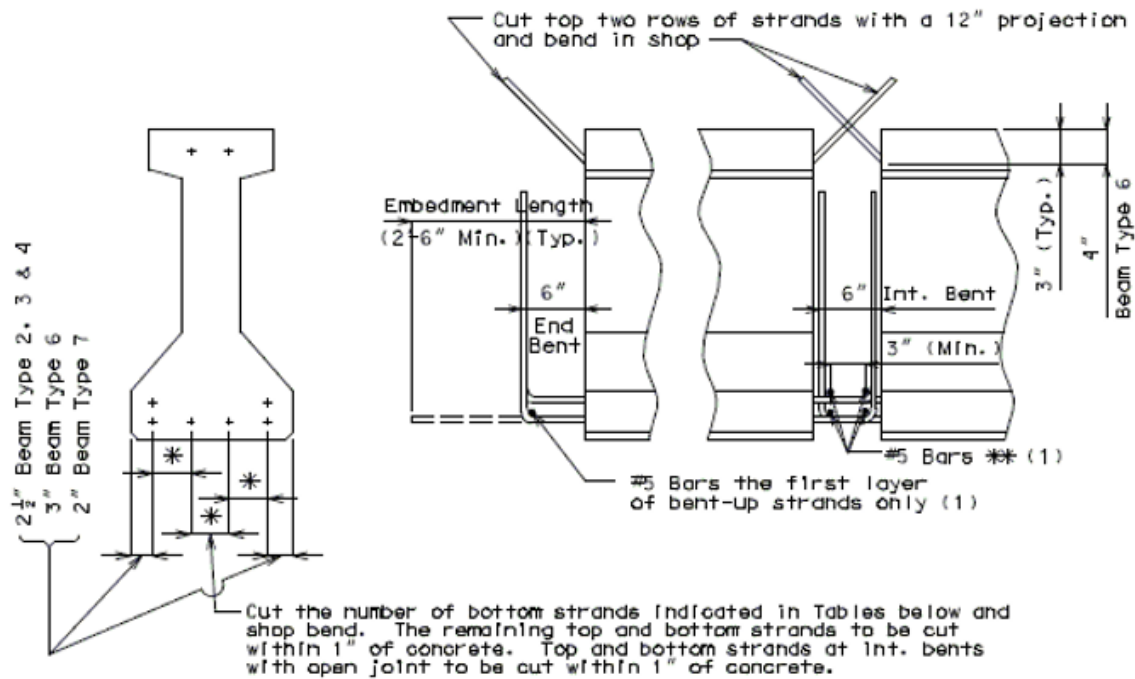


Figure 2.27: MoDOT engineering policy guide continuity detail (MoDOT, 2010)

further enhancing structural effectiveness. To provide continuity, CFRP reinforcement is attached to the top of the girders over the cast in place diaphragm. The negative moment over the supports caused by the deck weight balances the positive restraint moment caused by creep in the prestressed girders. The proposed design eliminates positive moment cracking while increasing structural efficiency. Furthermore, there is no need for positive moment reinforcement in the diaphragm under gravity loads, thus, reducing reinforcement congestion and facilitating construction. Laboratory tests and Finite Element Analyses were carried out and support the notion that the CFRP sheet is an ideal material for continuity connections (Saadeghvaziri et al., 2006). However, CFRP sheets are typically more expensive in dollars per square foot than conventional mild reinforcing bars and their use has been minimal in continuity diaphragms thus far.

Another detail worth examining are mechanical splice sleeves, which have been used in some cases to provide continuity over joints (Jansson, 2008). This report evaluates two proprietary grout-filled mechanical reinforcement splices, the Lenton Interlok and the NMB Splice Sleeve, for suitability in connecting precast concrete structural elements. One of the concerns that commonly arises with the use of prefabricated elements is how to develop quality connections while maintaining structural integrity through precast sections. The objective when it comes to designing connections for precast elements can be considered as emulating cast-in-place construction. Lapped bars, welded splices, and mechanical splices can be used in the connections, and more specifically grout filled mechanical splices can be used. These are unique in their ability to connect precast elements together. Grout

filled splices can provide continuity of the reinforcement between precast elements and properly emulate cast in place construction. As seen in Figure 2.28, grout filled splices can be used to create live load continuity as negative moment reinforcement over a pier. This detail was used for the North Street Bridge in Medford, Massachusetts. The negative moment reinforcement was cast into the top of the precast prestressed deck-beams and connected with splices over each pier joint (Jansson, 2008).

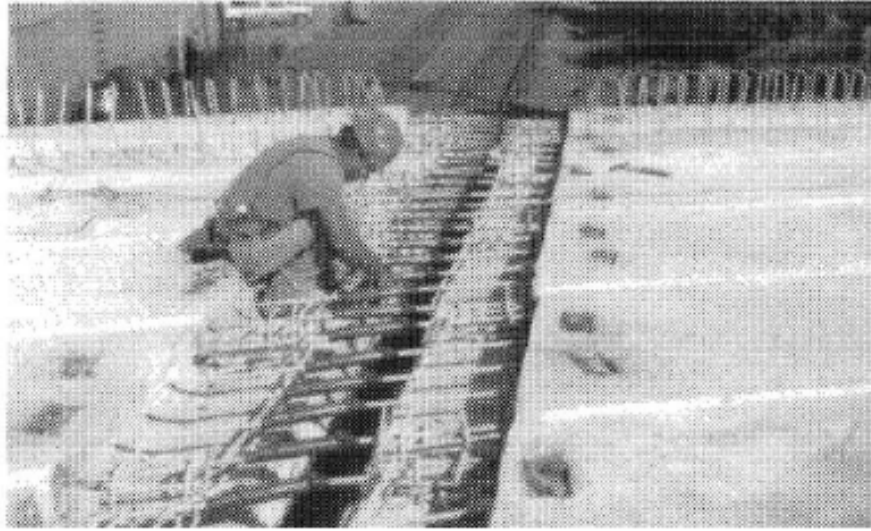


Figure 2.28: Grout filled splices used in continuity connections (Jansson, 2008)

The testing, led by Peter O. Jansson, P.E., included slip, fatigue, ultimate load and creep tests. Both splices met the AASHTO LRFD provisions for slip and fatigue and neither showed susceptibility to significant creep displacements. The ultimate load of the two splices demonstrated that they are capable of exceeding 125 percent of the reinforcing bar's yield strength and in most cases 150 percent. The limited data did suggest that epoxy coating might lower the ultimate load capacity after sustained loading (Jansson, 2008). Despite this, these grout filled splices may have potential as options for longitudinal continuity in the adjacent beam bridges.

2.3.3.3 Performance

Studies and field experience indicate that waiting to establish continuity until girders are at least 90 days old will significantly reduce or eliminate the development of positive restraint moments at the internal piers (AASHTO, 2007). Positive restraint moments can be ignored using the simplified approach, the design approach used if the girder age is at least 90 days when continuity is established. The girders perform much better (less positive restraint moment cracking) at this age; therefore the restraint moments can be ignored. Depending on the ability of the fabricator to stockpile, this age could be accounted for off-site in the precast yards, thus not impacting the

construction time. However, experience of the SCDOT with local fabricators indicates that most have limited space to stock pile beams for this purpose.

2.3.3.4 Published Recommendations

In AASHTO's design example for BIII-48 adjacent box girder bridges, designs were performed assuming continuity established at 7, 28, and 90 days. If the girder age is at least 90 days, restraint moments can be neglected, and this is the "simplified approach". The "general approach" considers the effects of restraint moments and must be used if the girder age is under 90 days when continuity is established (AASHTO, 2007).

2.3.3.5 Challenges

One challenge in continuous-span bridge construction is to minimize the positive moment cracks occurring at the interior bents, while still avoiding an open joint but still having the benefits of reduced positive moments in the spans due to the continuity. The creep of concrete that causes these cracks is difficult to minimize, and some studies have shown the magnitude of the positive restraint moments are independent of the amount of reinforcement placed at the interior supports (Saadeghvaziri et al., 2006).

Another challenge is to ensure rapid-construction while also properly designing and constructing continuous girder spans. The cast-in-place continuity diaphragm, even with quick setting and consolidating concrete, cannot keep up with the construction pace of the rest of the prestressed, precast bridge components. It is advantageous to pour the continuity diaphragm once the girder age is at least 90 days, since AASHTO permits positive restraint moments due to creep to be ignored at this age, however this may slow down the construction process if the girders are not at least 90 days old at the time they are brought to the construction site. In order to use the "simplified approach", per AASHTO, and neglect the positive restraint moments in the design, the girders must cure for most of that 90-day time period prior to reaching the jobsite in order to facilitate rapid construction. This is not uncommon, as long as the fabricator yard has the capacity for storing the girders prior to time of construction which has proven to be a challenge due to the limited storage space of fabricators local to South Carolina.

2.3.4 Transverse Post Tensioning

The longitudinal reflective cracks that are appearing above the shear keys between adjacent beam are a major concern with these bridges. The cracks can cause secondary distresses associated with limited transverse load distribution and can also cause debonding, delamination, and corrosion of the steel reinforcement. The use of transverse post-tensioning (TPT) has been considered a viable solution to minimize the development of the longitudinal cracks in the box-beam bridges (Grace and Jensen, 2008). Transverse ties, grouted or ungrouted, vary from a limited number of nontensioned, threaded rods to several high-strength strands post-tensioned in multiple stages (Russell, 2009). The amount of TPT can be varied by the number of transverse diaphragms, the number of strands at each diaphragm, and the amount of TPT force applied at each strand. Recently, some experimental

and numerical studies have addressed these issues in order to produce some recommendations for design since AASHTO's recommendation of 250 psi applied over a keyway depth of 7" is rarely met by states since it is very conservative and difficult to reach (Russell, 2009).

2.3.4.1 Lawrence Technological University and Michigan DOT

Lawrence Technological University worked with the Michigan DOT in 2008 on a project dealing with unbonded carbon fiber composite cables (CFCC) for TPT of side-by-side box-beam bridges. Experimental and numerical research projects were developed to address the effect of the level of TPT and the number of transverse diaphragms on the performance of side-by-side box-beam bridges using unbonded CFCC. The experimental project included constructing and testing a half-scaled 30 degree skewed bridge model and conducting transverse strain and load distribution tests. The distribution of transverse strain developed at the top surface of the deck slab and the deflection across the width of the bridge were examined for three, four, and five transverse diaphragms and for 20, 40, and 80 kips of TPT force in the experimental project. After load distribution tests, the bridge model was loaded until failure to evaluate the response of the CFCC used for TPT strands and to check the load-carrying capacity of the model. The numerical project included performing finite element analysis using ABAQUS and investigating longitudinal cracking for a wide range of side-by-side box-beam bridges with different spans and widths. Different loading cases were evaluated to establish the adequate number of diaphragms and appropriate TPT forces in order to prevent the development of longitudinal deck cracks (Grace and Jensen, 2008).

The experimental results demonstrated that increased TPT significantly improved load distribution among the side-by-side box-beams. In this research, the case of five diaphragms resulted in better load distribution than the case of three diaphragms. It was also found that different arrangements of the TPT forces had insignificant influence on the transverse strains that developed between the diaphragms. Regardless of the number of transverse diaphragms and levels of TPT forces experienced in the model, the resulting transverse strain did not satisfy the transverse stresses limit of 250 psi in the deck slab recommended by AASHTO (2007). When the level of TPT force was increased from 0 to 20 kips per diaphragm the bridge model's behavior improved accordingly. However, at levels of TPT above 40 kips, the improvement in the behavior of the bridge model was minimal. Therefore, applying a TPT force of 40 kips was adequate to hold the adjacent beams together to act as a one unit when the bridge model was subjected to the vertical load although it did not satisfy the AASHTO limit of 250 psi.

The numerical study revealed that both live load and the positive temperature gradient lead to the development of longitudinal reflective cracks between the adjacent beams. The number of adequate diaphragms was found to be a function of span length and the bridge width. Providing an adequate combination of diaphragms and TPT force was found to delay the development of longitudinal cracks. The study found that the AASHTO recommendation of 250 psi as minimum transverse prestress required throughout longitudinal joints in side-by-side box-beam bridges is impractical and unreachable with the current layout of the TPT arrangements within the box-beams in side-by-side box-beam bridges. This prescribed stress level can be attained at the diaphragms

but not between the diaphragms. The minimum number of diaphragms needed to delay longitudinal reflective cracking is provided for 48" and 36" wide beams in Figure 2.29 and Figure 2.30, respectively.

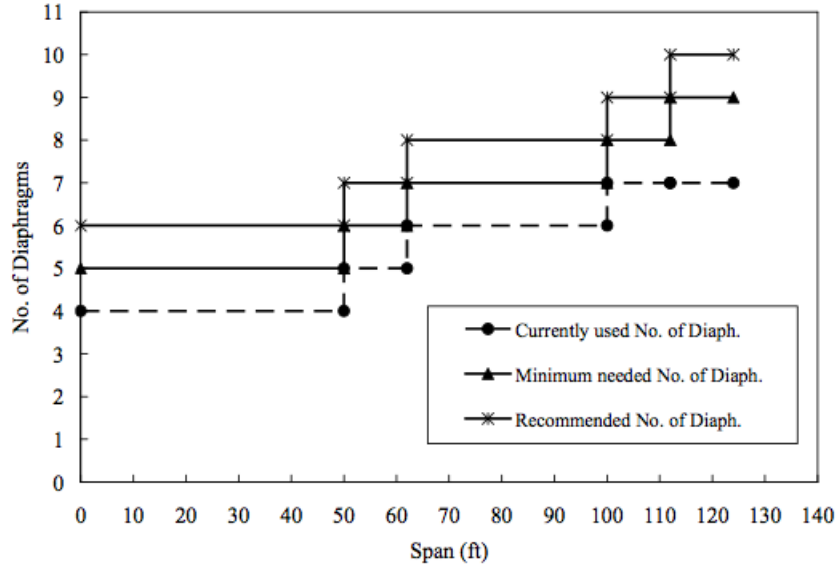


Figure 2.29: Minimum number of transverse diaphragms for 48" boxes (Grace and Jensen, 2008)

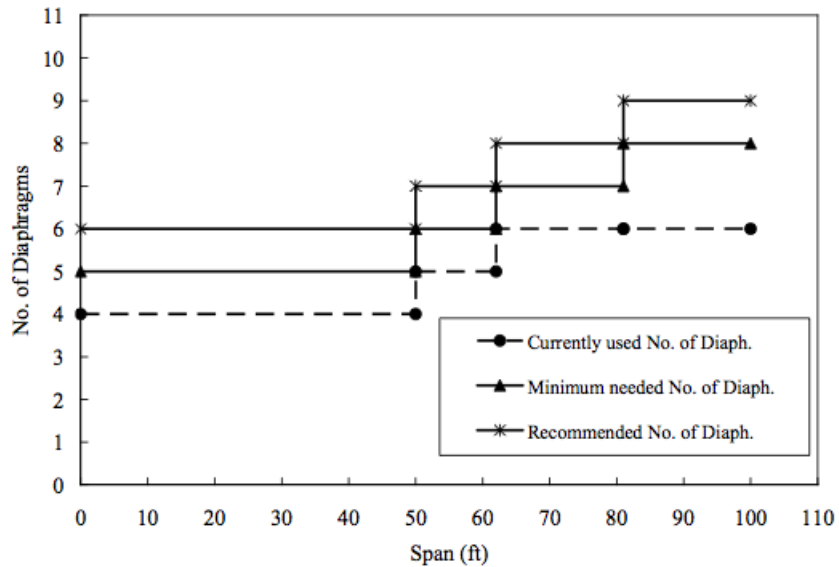


Figure 2.30: Minimum number of transverse diaphragms for 36" boxes (Grace and Jensen, 2008)

The appropriate level of the TPT force increases when increasing the bridge width and slightly decreases when increasing the concrete strength of the deck slab. This phenomenon is illustrated in Figure 2.31.

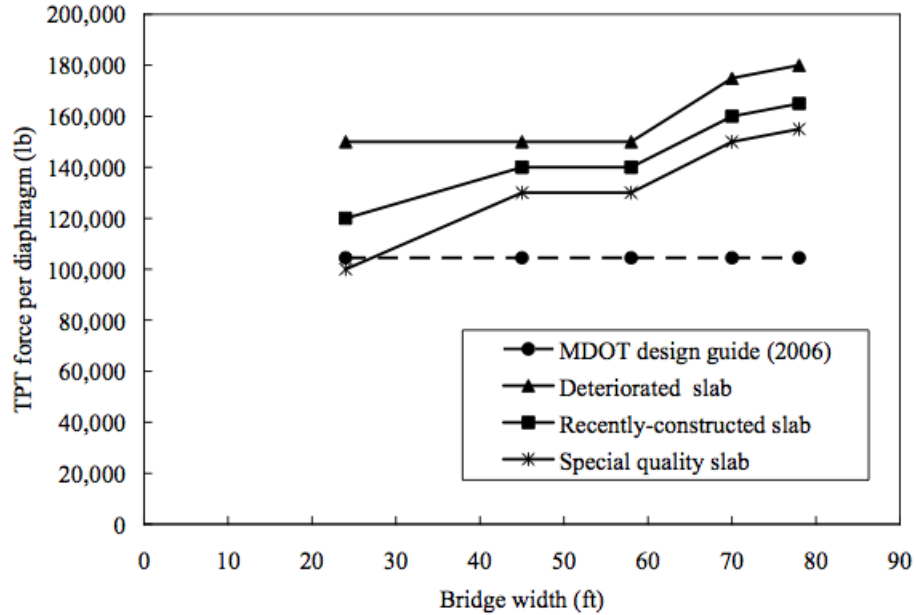


Figure 2.31: Minimum TPT force per diaphragm (Grace and Jensen, 2008)

This project found that the current Michigan DOT specifications for both number of diaphragms and amount of TPT were insufficient to delay the development of longitudinal reflective cracks, thus their results were recommended to the Michigan DOT for future projects.

2.3.4.2 University of Maryland and Maryland State Highway Administration

The University of Maryland teamed with the Maryland DOT and the Maryland State Highway Administration in 2009 to test the DOT's new transverse post-tensioning requirements which involved replacing tie rods with new high strength rods with higher post-tensioning to provide a more tightly integrated modular slab bridge system. The project first entailed field test data of the newly constructed Wallace Creek Bridge to validate the modification of Maryland's design with higher post-tensioning forces. The Wallace Bridge testing was implemented to observe short-term live load deck behaviors under different transverse post-tensioning forces, 30 kip and 80 kip at each diaphragm location (2 for this bridge). Strain gages were also used to measure strain under the two different TPT forces. The project also included a finite element bridge model analysis using ANSYS that was subjected to the same post-tensioning sets as the Wallace Bridge in order to compare the two tests and further justify the results (Fu and Jeong, 2009).

The key in this research was to provide confidence to the Maryland DOT in using the new design with a higher post-tensioning force. The maximum field test data was very close to the

Table 2.3: Stabilizing TPT force to limit differential strain in adjacent members (Fu and Jeong, 2009).

Span Length (ft)	Approx. Stabilizing TPT Force (kip)
35	60
40	70
45	80
50	80
55	90

ANSYS model data and both showed the same trends, thus the model was considered reliable. The two projects both showed that a tightly integrated modular slab bridge system with higher post-tensioning forces provided better structural integrity. It was found that the effects of transverse bars before cracking of the shear key were insignificant. Once the shear key is cracked, however, the rod is brought into a vital role in preventing the structure from undergoing more deterioration and ensuring the structure behaves monolithically. In the project’s parametric study using a finite element model analysis, it was found for a 35 ft. span that the microstrain under post-tension in the beams was not stabilized until 35 kips, and Maryland had only been using 30 kips for TPT. Therefore, Maryland’s post-tensioning force recommendation was not sufficient to relieve displacement of the bridge that leads to the development of longitudinal reflective cracks. Further parametric studies dealing with various span lengths produced the following recommendations, presented in Table 2.3 (Fu and Jeong, 2009).

Through both the FEA model testing with a HS25 truck, the test truck on the Wallace Bridge, and the finite element parametric study, the current code of practice in Maryland was recommended to be modified to increase the post-tensioning force to a higher level based on span length so that the shear key is strengthened and less cracks are produced at the section. The researchers also mentioned that more in depth study and projects were necessary in order to verify these results and finalize recommendations for the Maryland DOT (Fu and Jeong, 2009).

2.3.4.3 NCHRP Synthesis 393: Adjacent Precast Concrete Box Beam Bridges: Connection Details

Henry Russell, the consultant selected by the National Cooperative Highway Research Program (NCHRP), performed a survey nationwide to examine the current details and construction practices associated with adjacent precast, prestressed concrete box beams. This survey included information on transverse post-tensioning details and construction practices for the bridges based on the responses of 35 states, five Canadian provincial transportation agencies, three railroads, and thirteen U.S. counties. Among the TPT results from the survey include:

- The most common transverse tie consists of unbonded post-tensioned strands or bars

- Approximately half the states grout the keyway before post-tensioning and approximately half the states grout the keyway after post-tensioning
- There is no consensus about the number of transverse ties and the magnitude of post-tensioning force
- In single-stage construction, all beams are generally connected transversely at one time
- In two-stage construction, a variety of sequences is used

Many states were found to define TPT in different ways: force per bar or strand, force per duct, or torque on a threaded bar. The number of transverse diaphragms used by states varied from one to five, generally based on span length. These diaphragm locations were at the ends, midspan, quarter points, and third points, depending on the number of ties that were needed for the specific bridge span. This survey verified that if tie rods remain snug, they contribute significantly to load distribution among the beams (Russell, 2009).

Surprisingly, 81 percent of the states that responded to the survey indicated that they did not make any design calculations to determine the number of ties necessary. However, the states did provide the TPT force used for each tie and spacing of ties they used. Normalized data in force per unit length was generated to compare the amount each state uses (See Figure 2.32).

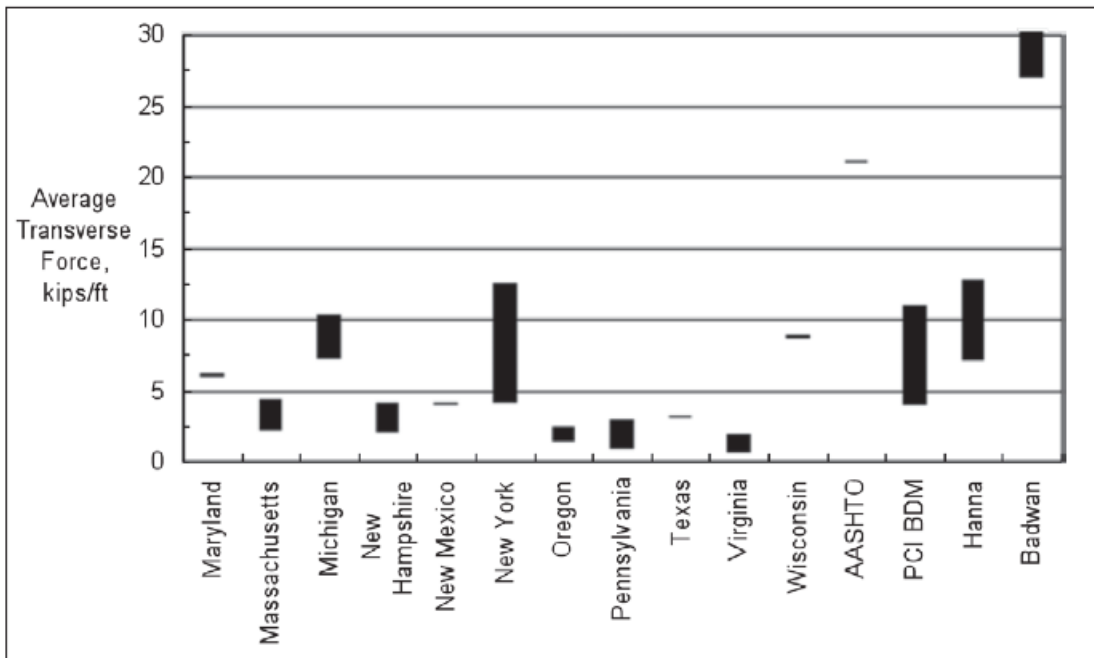


Figure 2.32: Comparison of TPT force used by states nationwide (Russell, 2009)

In addition to the eleven states shown in the Figure 2.32, four other values were plotted for comparison. The AASHTO value is based on a compressive stress of 250 psi applied over a keyway

depth of 7 in. The 2004 PCI Bridge Design Manual (BDM) value was based off a design chart to determine the required effective TPT force. The Hanna values are based on a best-fit equation rooted in grid analysis and the Badwan values are based on using a grillage analogy. The Badwan value appears very high because it was reported as required TPT compressive stresses, thus these stresses were assumed to act over the full depth of the section used in their analyses, but this was not certain. Some states appear to have a range since they use a set value of TPT regardless of the span length (Russell, 2009).

Figure 2.32 illustrates that not only is the AASHTO recommended value higher than that of other research groups (except Badwan, due to assumptions), but it is also higher than every value reported by surveyed states. AASHTO LRFD Articles 5.14.4.3.3c and 5.14.4.3.3d require a minimum transverse prestress of 250 psi on a compressed depth of at least 7 inches, which is the recommended depth of the shear key (AASHTO, 2007). This is equivalent to a TPT force of 21 kip/ft, which would require 1.5-inch diameter, 270-ksi low-relaxation strands stressed to 189 ksi after losses at 16.5-in. centers. If based on a 5-in. depth as stated in Commentary C5.14.4.3.3d, the TPT force would be 15 kip/ft. However, Commentary C5.14.4.3.3c states that the economy of these sections is sacrificed once duct spacing is less than 4 feet. Also, Commentary C5.14.4.3.3d states that the post-tensioning tendons should be located at the centerline of the key, whereas 68 percent of the respondents to Russell's survey reported that ties were placed at mid-depth of the section. The survey therefore indicates that states do not necessarily follow AASHTO's recommendations for TPT and it also indicates that the AASHTO recommendation for TPT is uneconomical and extremely difficult to reach (Russell, 2009).

2.3.4.4 Common Details

Two of the details of interest are the New York adjacent box beams with full depth shear keys and the Texas adjacent box beams with robust, full depth shear keys. Both of these states' standards and bridge design manuals include their TPT recommendations, and these states are satisfied with their current details.

Section 9.2.6 of the NYSDOT Bridge Manual states that transverse tendons must be placed parallel to the skew of the unit and as close to the mid-depth of the section as possible. Each tendon is composed of three 1/2" diameter low relaxation strands tensioned to 28 kip per strand and these are tensioned after the shear keys have been grouted. For span lengths less than 50 ft., three TPT force locations are required: one group is located at each end of the unit approximately 7 in. from the centerline of bearings and another group is located at the centerline of the span. For span lengths greater than 50 ft., five TPT force locations are required: one group is located at each end of the unit approximately 7 in. from the centerline of bearings, one group is located at the centerline of the span, and one group is located midway between each end group and centerline of the span (NYSDOT, 2010b). The NYSDOT detail for a span greater than or equal to 50 ft. is shown in Figure 2.33.

These TPT requirements have been consistent since 1992, when New York revised their TPT recommendations. At the time, transverse ties were not used in adjacent box beam bridges

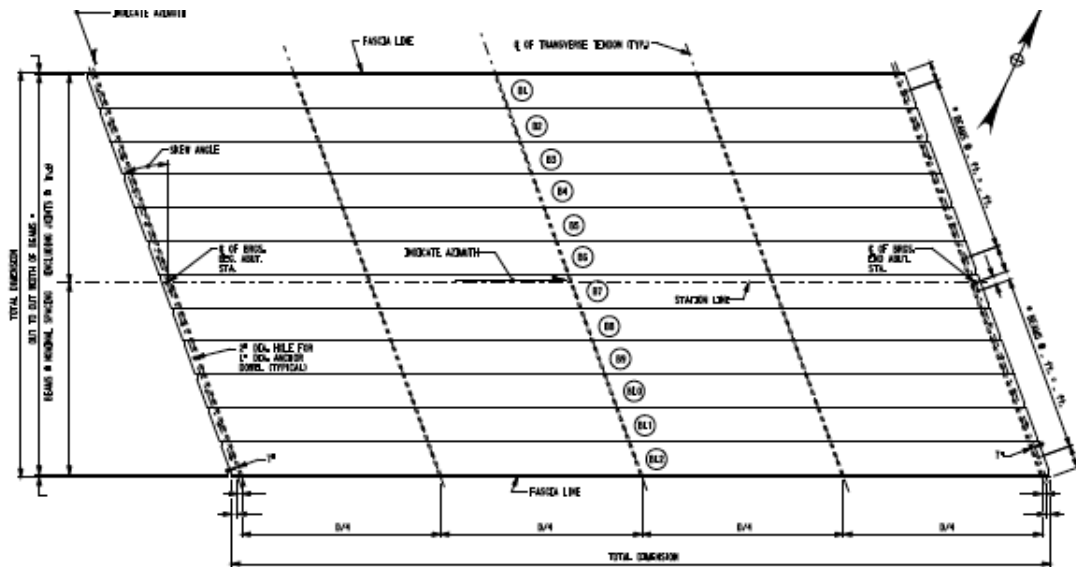


Figure 2.33: NYSDOT plan shown with five TPT locations (NYSDOT, 2010b)

with spans up to 50 ft. in New York. For spans of 50 to 75 ft. one transverse tendon was used at the center and for spans longer than 75 ft. tendons were used at the quarter points. All of the tendons at that time were stressed to a force of 30 kips. At the time, New York was experiencing heavy longitudinal cracking issues and increased the TPT requirements and changed their shear key, which led to the details they still use today (Russell, 2009).

Chapter 3, Section 9 of the Texas DOT Bridge Design Manual states that TPT is required for all box beam bridges topped with an asphalt concrete pavement (ACP) overlay applied directly to the top of beams. The majority of the time, Texas uses a 5 in. concrete overlay instead of using ACP and post-tensioning, however this section of the manual gives some recommendations on post-tensioning for those cases where it is required. The tendons are limited to a maximum spacing of 10 ft. and the first tendons are set 10 ft. from the centerlines of the bents. Through phone interviews with the Texas DOT, it was discovered that Texas does not have a target post-tensioning force, however over the years the force has been increasing and is currently around 30 kip, which is higher than ever before (TXDOT, 2009). The Texas detail for a prestressed concrete box beam with ACP overlay and post-tensioning is shown in Figure 2.34.

The Texas standard details call for 1.5" diameter hole through the interior and exterior beam diaphragms and a 3" diameter hole through webs and voids for interior beams. A 1" PVC pipe sleeve is used with either 1/2" monostrand Grade 270 tendons or 5/8" threaded Grade 150 bars (TXDOT, 2009). As seen in Figure 2.34, the tendons are located at about the mid-depth of the shear keys. The plan view of the Texas DOT span with TPT is given in Figure 2.35.

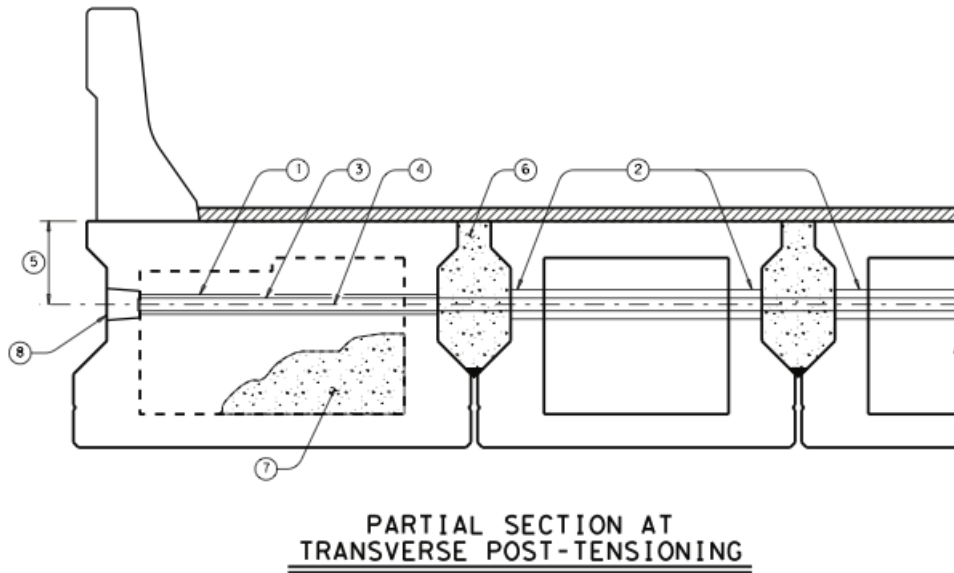


Figure 2.34: Texas TPT detail (TXDOT, 2009)

2.3.4.5 Conclusions

The following conclusions are made based on the transverse post-tensioning research and current details used by targeted states:

- There is no consensus among states about the number of transverse ties and the magnitude of the TPT force, and many states do not even specify a target force.
- The current AASHTO LRFD Specifications recommend 250 psi of TPT stress applied over a keyway depth of 7 in., which is more than any state recommends that was surveyed by Russell (2009). This amount is not possible between diaphragms with the current configurations of diaphragms and tendons (Grace and Jensen, 2008).
- According to the Lawrence Tech research, applying a TPT force of 40 kips is adequate to hold the adjacent beams to act as a one unit when subjected to a vertical load (Grace and Jensen, 2008).
- The recommended number of diaphragms is a function of bridge span and these recommendations are given in Figure 2.29 and Figure 2.30. The recommended amount of TPT force is a function of bridge width and relevant recommendations are given in Figure 2.31 (Grace and Jensen, 2008). The approximate stabilizing force that ensures similar strains between adjacent members is given in Table 2.3. This force increases as the bridge span increases. For span lengths of 35 to 55 ft., the TPT force varies from 60 to 90 kips.
- New York currently uses three to five transverse diaphragms with three 28 kip tendons at each location.

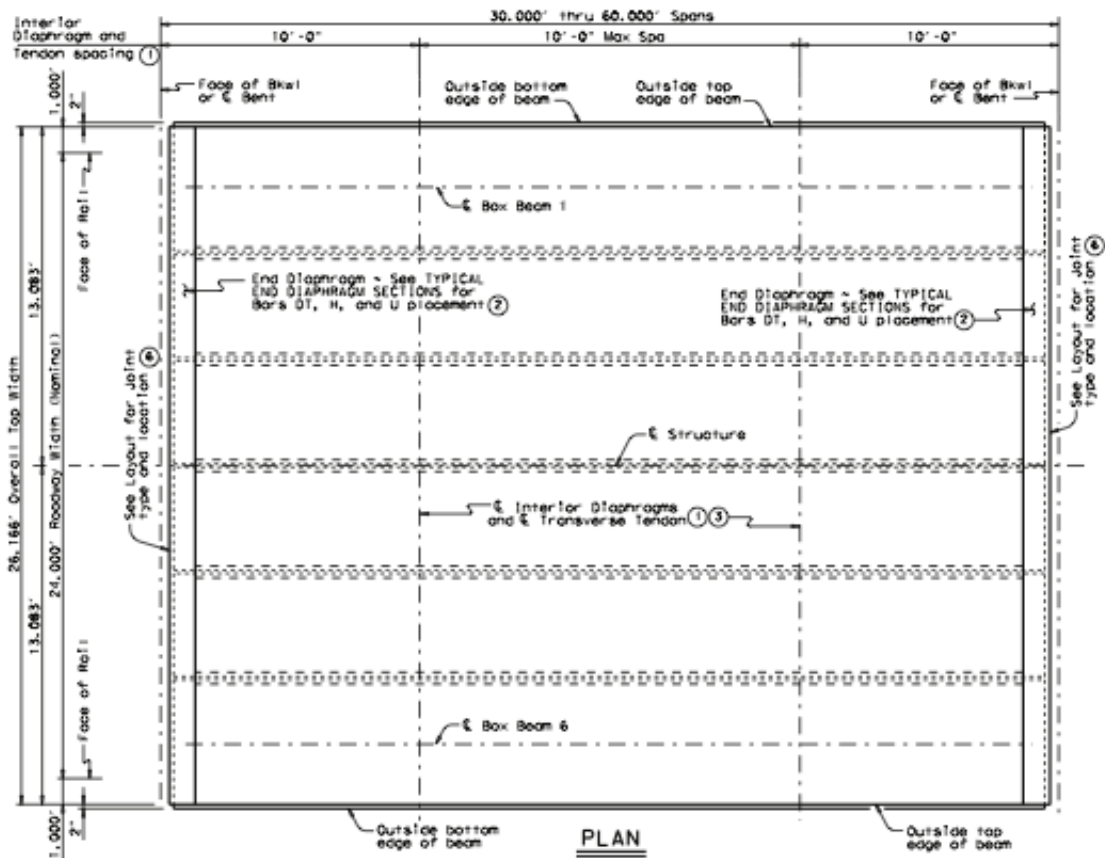


Figure 2.35: TXDOT plan shown with TPT locations (TXDOT, 2009)

- Texas currently limits their tendon spacing to 10 ft. but only uses TPT when an ACP overlay is used, which is not often. Texas does not have a target post-tensioning force in their standards but is currently using around 30 kips.

Chapter 3

Performance Perceptions of Adjacent Box Girder Bridges

Having completed a thorough literature and web review of specifics pertaining to the adjacent box girder bridges, a targeted approach was taken to solicit view points from those involved in building and maintaining such bridges. This solicitation consisted of both web-based and phone-based surveys of State DOTs in addition to interviews of contractors and fabricators who have experience with this bridge type.

3.1 Department of Transportation Web Survey

To learn about the practices and performance of bridges similar to the hollow core system and to learn if another DOT has more advanced alternatives to the hollow core system, the DOTs across the country were surveyed. The web survey was created using SurveyMonkey (See Appendix A) and was sent out in late February 2010 through the SCDOT to all other DOTs nationally and the states were given a few weeks to respond. The survey included “Low Profile” and “High Profile” portions which both included general, construction, post-tensioning, shear key, continuity, and bridge alternative sections of questions. Twenty-two different DOTs submitted complete responses to the survey which helped to form a more targeted follow-up phone-based survey to selected DOTs. This also helped to identify some practices used by other states which had not been noted before.

3.1.1 DOT Responses

There were over 33 entries registered through SurveyMonkey for the survey after a few weeks, however, only 22 of these entries qualified as “complete” responses since many were unfinished, inconsistent, duplicates, or filled in without state identification. These responses were sorted based on the types of bridges used by the states (see Table 3.1).

Two states that were targeted initially after the DOT website search portion of the project were Florida and Tennessee, mainly for geographic reasons. However, neither of these states claimed

Table 3.1: State usage of adjacent beam bridges

Types Used	States
Low Profile	AL, ME, MS, WA
High Profile	IN
Both	CA, IL, MA, MO, NM, OH, OR, TX, UT, VA
Neither	FL, KS, MT, ND, OK, PA, TN

to use adjacent beam bridges therefore they were both removed from the targeted states list and were not contacted in the phone survey portion of the project.

3.1.2 Longitudinal Reflective Cracking

Many of the responses gathered indicated that less than 20% of the states' bridges experience longitudinal reflective cracking. Only one state, Ohio, selected the highest cracking category on the survey, indicating that 81-100% of their adjacent beam bridges experience this cracking. Most states did indicate that they were very concerned with these cracks, leading to the assumption that they are aware of them and have been putting forth some effort to try and prevent them. Since this problem is widely believed to be rooted at the shear key detail, the shear key responses and post-tensioning responses are included in Table 3.2 along with the reported percentage of bridges that experience this longitudinal cracking. Studies have shown that full depth shear keys or partial depth shear keys at the mid depth of the member minimize the cracking compared to partial depth shear keys at the top or bottom face of the member. In general, research shows it is best to use a full depth shear key.

3.1.3 Continuity

The only states that indicated in their survey responses that they make these adjacent beam bridges longitudinally continuous for multi-spans were California, Massachusetts, Missouri, Ohio, and Washington. All of these states indicated they account for positive restraint moments when designing the continuity diaphragm in order to minimize cracking and potential bridge durability and aesthetic issues. California, Missouri, and Washington indicated their girder age must be between 25-90 days when it is placed, Massachusetts calls for a girder age of 8-24 days and Ohio does not specify.

3.1.4 Alternatives

A few states listed alternatives to adjacent beam bridges at the end of the survey and these responses are summarized in Table 3.3. Not many of these were rapid-construction short span alternatives. However, more intriguing alternatives were discovered in the follow-up phone conversations later on in the research.

Table 3.2: Reflective cracking survey responses

State	Bridges	Shear Key			Post Tensioning	
	Longitudinal Cracking (%)	Depth	Location	Grout	Before/After Key Grout	Strands or Rods
Alabama	0-20%	Partial	Top Face	CIP	Before	Rods
California	0-20%	Partial	Centroid	Non-shrink	After	Both
Illinois	21-40%	Partial	Top Face	Non-shrink	Before	Rods
Indiana	No Reply	No Reply	No Reply	No Reply	No Reply	No Reply
Maine	No Reply	Full	Full	Non-shrink	No Reply	Strands
Massachusetts	41-60%	Full	Full	Epoxy	After	Strands
Mississippi	0-20%	Partial	Top Face	Non-shrink	After	Rods
Missouri	0-20%	Partial	Top Face	Non-shrink	After	Rods
New Mexico	0-20%	Partial	Top Face	Non-shrink	Before	Rods
Ohio	81-100%	Partial	Top Face	Non-shrink	After	Rods
Oregon	0-20%	Partial	Top Face	Non-shrink	No Reply	No Reply
Texas	No Reply	Partial	Centroid	CIP	After	Both
Utah	41-60%	Partial	Top Face	Non-shrink	Before	Both
Virginia	21-40%	Both	Top Face	Non-shrink	Before	Both
Washington	0-20%	Partial	Top Face	CIP	Before	Strands

Table 3.3: Alternative bridge types used.

State	Alternative Bridge Types Used
Alabama	Precast Concrete Deck Channels
California	Spliced Precast Girder Systems
Tennessee	CONSPAN Arch, Single T Girder
Washington	Deck Bulb T, Precast Concrete Deck Form Panels

3.1.5 Closure

Many states consider longitudinal cracking along the joints of their adjacent beam bridges an issue. Due to the many differences in practices and crack prevalence, it is difficult to determine which methods best remedy the longitudinal cracking problem. Also, there is not a consensus on what girder age to use when creating continuity between the box beams. This shows that the use of continuity depends on the individual DOT's common practice and not a universally accepted superior detail.

3.2 Target State Phone Survey

To gain more detail on the practices and performance of bridges similar to the hollow core system, learn more about alternative systems, and to follow-up on the survey responses, phone calls were made to target DOTs across the country that either filled out the survey or were a state of interest based on the website search. Unique targeted questions were created for each state that was contacted based on the website searching and web survey responses. The phone conversations were recorded, with permission of the DOTs, and the interview transcripts can be found in Appendix B.

3.2.1 Targeted States

Twelve states were targeted and contacted based on the website search and web survey responses received. The states and target reasons are listed below.

- California – low cracking, use hollow core, use box beams, mid-depth key
- Georgia – geographically close
- Illinois – minimum 5 in. reinforced concrete overlay required, made key wider and deeper
- Michigan – use splice sleeves to provide continuity over piers
- Missouri – minimal cracks, continuity with composite concrete deck, overlay required
- New York – box beams, slab beams, full depth key
- North Carolina – cored slabs, upper key, geographically close
- Ohio – minimum 3 in. asphalt overlay with waterproofing required, large amounts of cracks
- Oregon – minimal cracks, 5 in. reinforced concrete overlay required with higher ADTs
- Tennessee – geographically close, recently stopped constructing adjacent beam bridges
- Texas – built many, robust shear key, alternative option – decked slab beams
- Virginia – use voided slab, top key – switched to full depth key within last 10 years
- Washington – voided slab, top key, recently began using 5 in. reinforced concrete topping

3.2.2 Practices Affecting Bridge Performance

Practices that were confirmed to improve bridge performance based on these conversations included: full-depth shear keys, larger shear keys (see Texas detail, Figure 3.1), reinforced concrete topping, post-tensioning after grouting the shear key, and more post-tensioning/higher post-tensioning stress.

Factors that were confirmed to degrade bridge performance based on these conversations included: reinforcing steel corrosion, partial depth shear keys, little/no post-tensioning, and post-tensioning before grouting the shear key. The NYSDOT mentioned that corrosion of steel in these

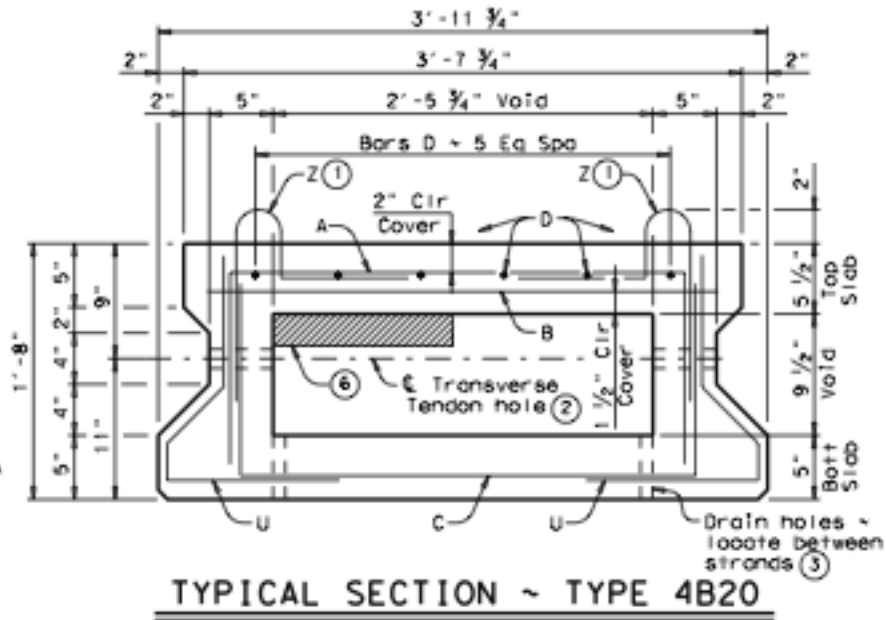


Figure 3.1: Robust shear key detail (Texas) (TxDOT, 2010)

bridges was one of the main reasons their state had limited the usage of box beams recently. The cracking issues undoubtedly led to water interacting with the steel and thus causing the corrosion problems. As evidenced in the durability section of the report, this is a very serious problem that led to the collapse of the Lakeview Drive Bridge in Pennsylvania and has led to a number of research projects across the country in an effort to improve inspection techniques to minimize the steel corrosion in these bridges. This is one of the main reasons the cracks are troublesome for these bridges, in addition to serviceability and load sharing issues.

3.2.3 Alternatives

Alternatives that were discovered to be of interest in these conversations include Decked Slab Beam Bridges (Texas), Deck Bulb-T Bridges (Washington), NEXT Beam (Precast/Prestressed Concrete Institute Northeast) and also the Inverset System (New York). The Decked Slab Beams for the same depth usually span farther, use fewer beam lines to haul out to a jobsite, and install quicker since there is really no field placed concrete to complete the superstructure, it's just grout and some welding. They are used so far primarily on low-volume roads where Texas wanted to replace a bridge very quickly. Texas has built some in a week or less, but warns that they are fairly new. Their shear key detail is different from the common details seen across the country since they use welded connector plates in a "V" like detail (see Figure 3.2). One concern with this detail is fatigue, since welds are more susceptible to stress risers and fatigue problems. The details have

not been used long enough for sufficient study on this to occur, but this is definitely something to consider when using this detail. They have not noticed much reflective cracking, and although they have only been used for a short period, no sign of reflective cracking as of 2010 is still a good sign (see Decked Slab Beam detail, Figure 3.2a and Figure 3.2b).

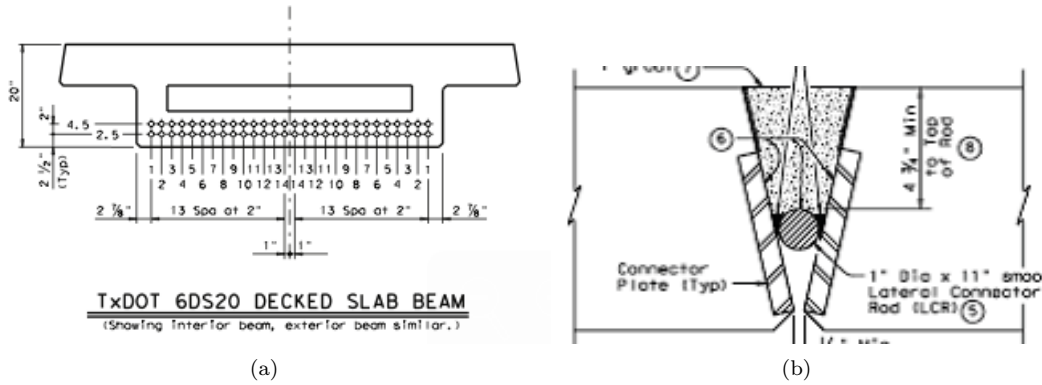


Figure 3.2: Decked slab beam section (Texas) (TxDOT, 2010)

The Deck Bulb-T Bridges use a reinforced concrete topping but the Washington DOT states they provide for faster construction than the adjacent beam bridges and thus are used when faster construction is needed (See Figure 3.3).

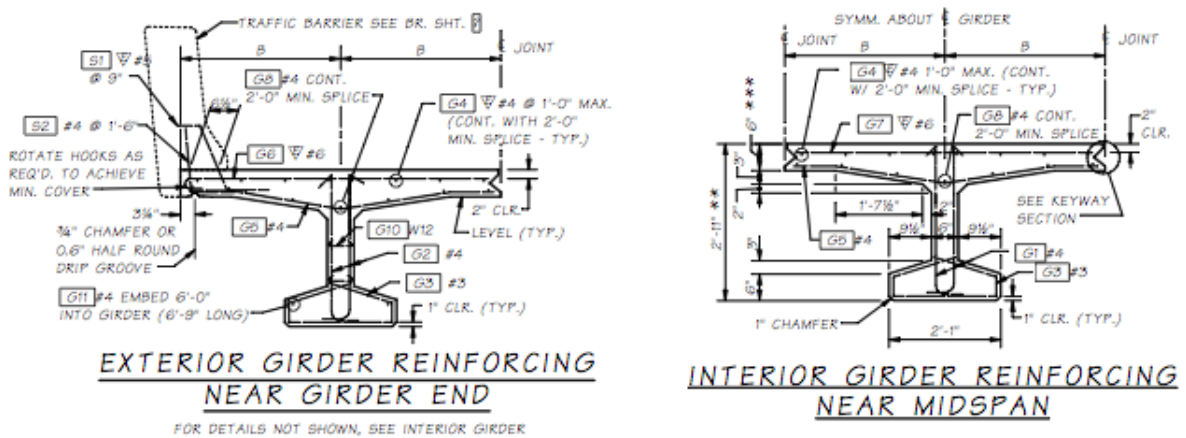


Figure 3.3: Deck bulb-T bridge girder (Washington) (WSDOT, 2010)

The invert system, which was developed in Oklahoma in the 1980's, is used frequently by the NYSDOT. This system is essentially a double tee unit that can be transported to the bridge site and erected quickly. The system consists of two steel stringers supporting a composite concrete deck (see Figure 3.4). The main connection to adjacent units is accomplished using bolted diaphragm plates. The overhangs of the units are normally kept small so that the connection at the deck level

is essentially a shear connection that requires only a grouted keyway. The New York DOT has used this system at length to replace aging bridge superstructures and to increase vertical clearance at highway overpasses.



Figure 3.4: Inverset system unit (New York) (Culmo, 2009)

The Precast Concrete Institute Northeast has been working on a replacement system for adjacent box beams. It is called the Northeast Extreme Tee beam (PCINE, 2010). This section is a squat double tee beam that ranges from 28 to 46 inches in depth. Two different versions of this beam are provided: the NEXT F, which requires an 8 in. cast-in-place overlay (Figure 3.5), and the NEXT D, which requires an 8 in. wide shear key between adjacent sections (Figure 3.6). These sections can be up to ten feet wide, therefore reducing the number of sections required and amount of joints that must be filled. The NEXT F provides stay-in-place forms, but does not require the same amount of rebar work needed for the Minnesota Inverse Tee beam. The shear key for the NEXT D system has been tested for two million cycles and still exhibits the ability to prevent water seepage through the joint. These sections are also much easier to inspect as compared to the box beams and hollow core beams. More information may be found at http://www.pcine.org/index.cfm/resources/bridge/Northeast_Extreme_Tee_Beam. Rita Seraderian of PCI Northeast stated in 2010 that Pennsylvania DOT had recently adopted this system to replace their adjacent box beam bridges (See Appendix B).

Another detail of interest is the cored slab bridges in North Carolina, which appear to be performing well and are pretty similar to the South Carolina details, except that the NCDOT details include transverse post-tensioning instead of tie rods. The environment is similar in the two states and many of the same contractors and fabricators could be used, so this was a detail of interest. In the phone conversations with the North Carolina DOT, it was also discovered they have used cored slab bridges without any topping, although they did mention that on high ADT and NHS roads an overlay is required. They have only done about a half dozen of these and when they are used they add a few inches to the cored slab unit itself for grinding. They mentioned they are pleased with them, but have not been using them for long so there have not been many performance reviews on

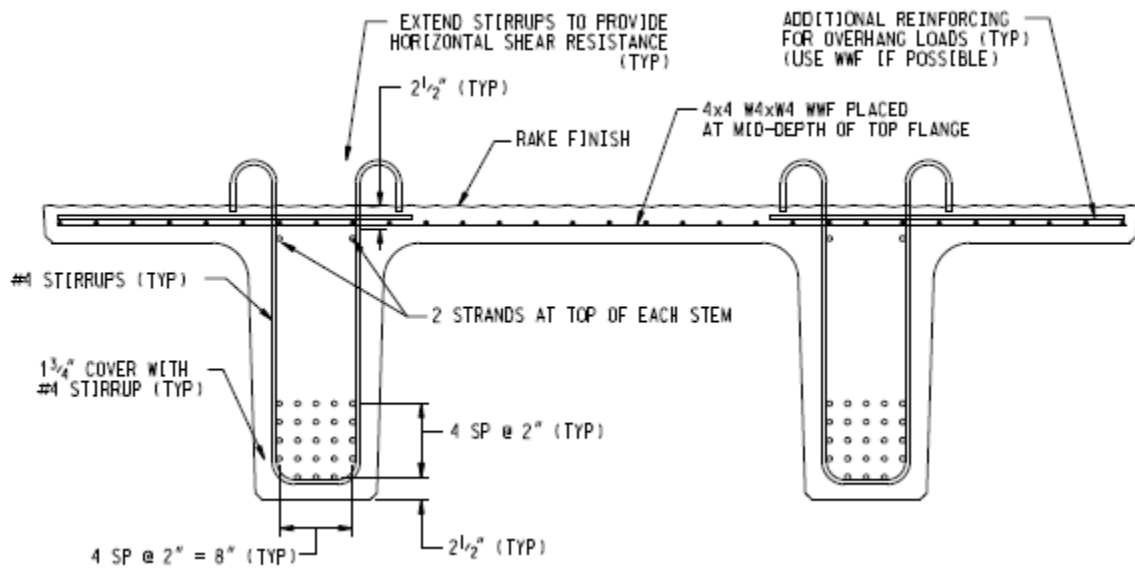


Figure 3.5: NEXT F beam (PCINE, 2010)

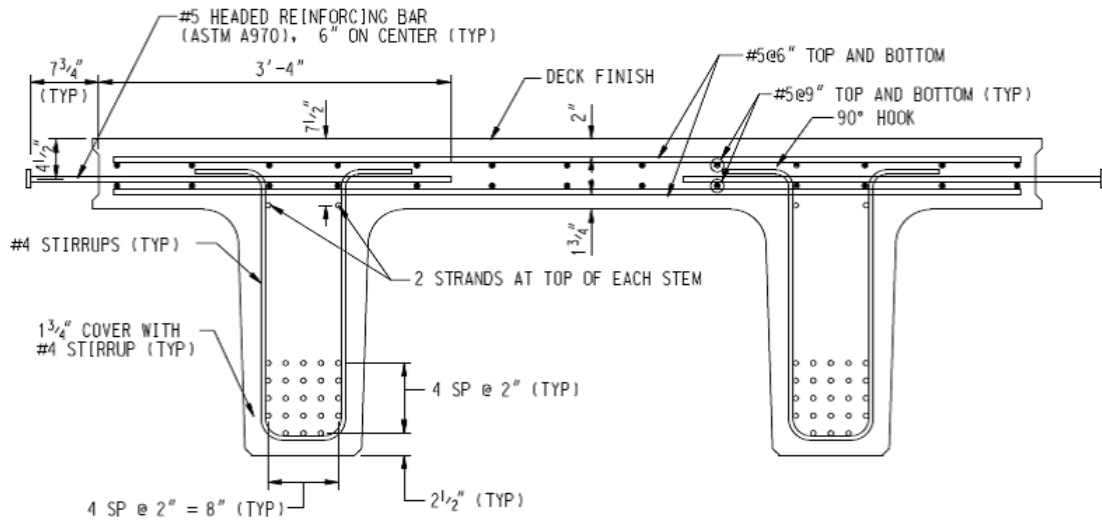


Figure 3.6: NEXT D beam (PCINE, 2010)

the bridges. One such project without an overlay was the Ocracoke project, which was built by Carolina Bridge Company and produced by Florence Concrete Products and Bayshore Products. These fabricators and contractors were contacted to follow-up on their perspective on the system (see Chapter 4).

3.2.4 Closure

Systems that could be potential solutions or could lead to a better detail (targets for fabricator and contractor contacts) include:

- New York – Box Beams, Slab Beams, Inverset System
- North Carolina – Box Beams, Cored Slabs (with and without topping)
- Oregon – Box Beams, Slab Beams
- Texas – Box Beams with robust shear key, Slab Beams, Decked Slab Beams
- Washington – Slab Beams, Deck Bulb-T
- PCI Northeast – NEXT beam system

Through conversations with the DOTs these systems seem to minimize the reflective cracking issues, ensure rapid construction, and in some cases allow for longitudinal continuity. These states, for the most part, are very pleased with the performance of these systems. These states have been followed-up with and asked for contractor and fabricator contact information in order to get more perspective on the use of these different bridge types.

3.3 Contractor & Fabricator Interviews

To gain more detail on the practices and performance of bridges similar to the hollow core system, learn more about alternative systems, and to follow-up on the phone conversations with the DOTs, contractors and fabricators provided by target DOTs across the country were contacted by phone and email. Unique targeted questions were created for each contractor and fabricator provided by each state in order to learn more about the specific projects those contractors and producers work on. The phone and email interview transcripts can be found in Appendix C.

3.3.1 New York Fabricators

Two different fabricators from New York were reached and asked about the adjacent box beam and slab beam bridges they work on and were asked to compare these projects to alternatives they work on. Troy M. Jenkins, the Chief Engineer for Northeast Precast Products, and Mark Losee, the Pre-Stress Manager for Jefferson Concrete were interviewed.

Neither fabricator noted much difference or preference between working on adjacent or spread box beams. Neither mentioned that shear keys were difficult to deal with or that they had

much preference in the type of key or type of transverse post-tensioning used. Both fabricators indicated that they are willing to roughen the shear key surface when it is called for in a project. Jenkins did note that it is difficult to avoid joints between adjacent beams since many times the beams are not perfectly straight. One issue Losee mentioned specifically was that New York had begun to curve tendons and run them up to the top of the sections in some projects. This detail allows moisture to go enter the duct from the top surface and cause problems. He is concerned about the use of these curved tendons. According to Losee, after the first tendon is in place, the subsequent strands may get wrapped around the first one and may result in lost compression or rip out near the top. Both fabricators did mention they were satisfied overall with the details for these bridges for single and also multi-span continuous designs. Neither one indicated any issues with having to wait for a particular girder age. According to Losee, the state requires 60 days of waiting period on continuous multi-span bridge projects and normally the contractor is the one accounting for this waiting period between beam pours and deck pours. He did mention that he would normally hold them for the contractor for about a month thus shortening the site storage of the girders significantly.

Losee did confirm that the NYSDOT has been using fewer adjacent box beams recently and that they have begun to search for alternatives, mainly due to the corrosion issues older bridges have been exhibiting recently. He noted that New York has explored the use of the double bulb-T sections, but the double bulb-T bridges are heavy that many people are not very pleased with them. In addition, unlike the adjacent box beams, the design is not smooth underneath the double bulb-T sections, so things can get caught underneath them. This is one advantage of keeping the adjacent box beams. The state is looking into using the New England bulb-T, but Losee does not think the new design will be a viable solution. He is not worried about the adjacent box beams being replaced by other systems.

In response to the questions about durability in these bridges, Jenkins felt that many of the bridges experiencing corrosion problems today were designed many years ago with different standards and the newer designs cannot accurately be compared to those older bridges in terms of susceptibility to corrosion. Losee agreed that the state is having problems with the older adjacent box beam bridges but cited this as a maintenance issue. This tends to support the current research and opinions nationwide about the durability of these bridges – i.e. most of the issues are due to poor maintenance and also poor standards and practices when they were built 40-50 years ago.

3.3.2 North Carolina Fabricators

One fabricator from North Carolina was reached and asked about the adjacent box beam and cored slab beam bridges they work on and was asked to compare these projects to alternatives they work on. JR Parimuha of Florence Concrete Products of Sumter, SC was interviewed since they worked on one of the few untopped cored slab bridges North Carolina has built thus far.

Parimuha mentioned that they prefer cored slab bridges and adjacent box beam bridges and that he feels they are a great way to construct a bridge. He mentioned they have produced beams for bridges with both an asphalt and concrete overlay and he also thinks the bridges without

overlays are good systems. One concern he had with the untopped sections was that the grout used to patch the hold-down locations can chip out when the contractor grinds the top. Other than that, Parimuha could not think of any disadvantages of using the untopped sections. Parimuha noted that North Carolina uses double ducts occasionally to get more post-tensioning and that these systems are not difficult for the fabricators to produce and that this is something they could do in South Carolina as well in order to get more post-tensioning.

Parimuha noted that he was aware of durability issues in bridges up North but that it was no reason to abandon the use of these bridges. He was not aware of any durability issues in this region with these bridges and noted that if void drains or other changes were necessary in order to minimize durability issues that they would be willing to make changes in the beams they produce. Parimuha has not worked on an adjacent beam that was continuous for multi-spans.

He mentioned that these bridges have been around awhile and are well-liked by fabricators, but if they need to change some details they are willing to do so. He mentioned he is aware that the bridges were designed to be easy to construct and produce and knows that improvements may need to be made and he is willing to adjust their work to accommodate the changes. Overall, he was happy with the current details but would be willing to adjust them if necessary.

3.3.3 Texas Fabricators

The main fabricator used for decked slab beams and adjacent beam bridges in Texas is Flexicore, the producer that played a large role in coming up with the decked slab beam detail. Gary Fisher of Flexicore was reached over the phone and asked some questions about the decked slab beams, adjacent box beams, and other bridge types they produce.

Fisher mentioned they do not really prefer one to the other when producing deck slabs or box beams. As for advantages, there are fewer deck slab beams than box beams, but the deck slabs are heavier and cost more, so they require bigger cranes for contractors and are more freight. This is a key disadvantage with using deck slabs, if large equipment is not possible these bridges may not be possible. According to Fisher, for a single span structure, both types can probably be assembled in about a half-day. In short, there does not appear to be much time difference between the two systems.

Fisher did not have many details that he would like to change; he seemed to be satisfied with the details in general. For disadvantages, Fisher just mentioned making sure the void doesn't float up, for both deck slab beams and adjacent boxes. He also stated that putting the plates in the deck slabs can be a little bit difficult; more or less like the double Ts he produces, due to the reinforcement congestion in a small area. Fisher did not mention any difficulty in manufacturing the robust Texas shear key and did not notice a problem with making the bridges continuous and the fabricators needing to hold on to beams for a long time in order to ensure the girder age is high enough once the deck is poured. Fisher said they have been using deck slab beams since around 2006 or 2007, so when asked about potential fatigue issues with the welded plates in the shear keys, he mentioned that they probably had not been around long enough to notice this yet, if it was

a problematic detail. The fatigue issue is definitely something to be tracked, however, with these bridges as they begin to age in the next ten to twenty years.

Overall, Fisher is happy with the details and does not see any causes for concern with the current deck slab beam and adjacent box beam details that are being used in Texas. He thinks the contractors like the adjacent box beams because they can put them down right up against each other and have an area to work on. The contractors get their jobs done sooner and can do more jobs, since they do not have to wait around to either weld in metal deck or put deck panels on top like what is required for a girder project.

3.3.4 Washington Fabricators

The main fabricator used for deck bulb-T and adjacent beam bridges in Washington, which was provided by the Washington DOT, is Central-Premix. Chuck Prussack was reached through email and asked some questions pertaining to the Washington details. Prussack is very happy with the adjacent beam bridges and has built thousands of them over 50 years with excellent service life. Central-Premix participated in the generation of the details used in Washington and they are very happy with them. Prussack did note that most of the bridges Central-Premix have done are not for the DOT but for cities, counties, US Forest Service (USFS), etc.

They usually have a full-length grouted keyway, weld ties at about 5 ft. on-center, and no overlay but they have produced bridges that use asphalt and cast-in-place concrete overlays as well. In Washington they use weld ties at 5 ft. on-center for slab bridges as well, as opposed to transverse high-strength rods. Prussack believes whether weld ties or rods are used, they should be about 5' on-center maximum to provide a tensile tie across the keyway with the grout providing the shear capacity in order to minimize differential movement that causes reflective cracking. He stated that he does not like transverse rods because they normally end up too far apart and contribute to the reflective cracking. This was an interesting take and possibly something to consider, that post-tensioning rods are spaced too far apart and if used should be moved closer together in the new South Carolina details.

3.3.5 North Carolina Contractors

The North Carolina DOT provided a list of contractors they have used for cored slab beam and adjacent box beam projects. One of the contractors contacted was Balfour Beatty, and Bill Heston answered some questions regarding his perspective on these bridges through email.

Heston mentioned that cored slab bridges are well suited where span lengths can be short and the top-down construction method is preferred/required. He noted that the details for this bridge type work well for the application and result in a relatively inexpensive solution. Surprisingly, Heston mentioned that a normal 2-lane cored slab bridge with shoulders, built using the top-down method, takes about six weeks to construct a full cycle for a 50 ft. span. This seems to be slower than other estimates from other contractors. He also mentioned that the shear keys can be difficult to work with on these beams. He believes the key width is too narrow, causing significant quantities of grout to be wasted and too much time to ensure they are properly filled. Heston believes the keys could

be twice as wide and use about the same amount of grout and they would make filling faster and quality more consistent. Other bridge types he works on typically do not use grouted keys. Heston noted that they have seen bridges with asphalt, concrete, or no overlay, and of these concrete is the most expensive and least preferred. He also noted that on a cubic yard basis, a concrete wearing surface on a cored slab bridge is much more expensive than a CIP deck on a prestressed girder bridge. Overall, however, Heston was satisfied with the current details and did not point out anything else he would like to change.

3.3.6 Texas Contractors

The Texas DOT provided a list of contractors they have used for deck slab beam and adjacent box beam projects. Sandy Tesch of ConStar Construction was contacted by phone and answered some questions regarding his perspective on decked slab beams and adjacent box beams in Texas.

ConStar constructed two of the first three or so decked slab beams ever constructed. They noted that the voids in the beams are a huge advantage since they can make the beams about 20% lighter and the erection time is minimal. It is quite possible to install a deck-slab member in one day, and then the grout could be completed in one more day.

One particular challenge associated with the decked slab beams is the size of the crane required. Primarily this is a source of significant expense. The cost for utilizing a crane for one day, mainly mobilization cost, was \$15,000. However, for this one span bridge all of the beams were set in two to three hours. The actual placement of the deck slabs is minimal compared to the move-in and move-out of the crane and girders. After the placement of the deck slabs, a certified welder is required to work on the welded plates in the shear key. The plates are welded every six or seven feet, and then the rod is placed in and welded on both sides. Tesch said it probably took one to two days to weld all the rods and then it just becomes a matter of grout placement. The whole process takes roughly one week.

According to Tesch, the most difficult aspect of working on these bridges is making sure the open space of the work area is adequate, since the crane will be large and will need to spin around and move in that area. The shear key detail is pretty simple but it does require a certified bridge welder, which is not always available. He mentioned that Texas normally seems to use these bridges for single and double span projects and he has never worked on a bridge that was made longitudinally continuous for multi-spans, but knows they are out there.

3.3.7 Closure

As evidenced by all of the interviews with fabricators and contractors thus far, all of the targeted bridge types are acceptable to DOTs, contractors, and producers. Most of the issues that have caused problems thus far are either minor details or details that were worked out over time with more experience. Most producers seem to not prefer one adjacent type to the other, but they all tend to like the adjacent beams as a whole. The favoritism is mainly due to the construction speed, which the contractors obviously like as well. Durability is still a concern in these bridges, but the

fabricators interviewed strongly believe that it is a maintenance issue and an issue due to outdated methods more than anything in the 40 to 50 year-old structures that are currently experiencing durability problems. Some details, like the Texas deck slab beams, need more time in order to prove their durability and performance over their intended life but so far seem to be producing good results.

Chapter 4

Field Verification of Core Box Bridge Performance

To better understand the load-sharing behavior of a bridge's members when subjected to different loadings, an in-situ test was conducted on an existing bridge on March 15th, 2010. The bridge that was identified by the SCDOT for testing is located on S-241 over Suck Creek in Cherokee County, South Carolina. The deformations of the bridges were measured using linear variable differential transformers (LVDTs). Through controlled loading and positioning, it was possible to observe movement of several members of the hollow core bridge. This chapter presents an overview of the preliminary results of the tests performed on the Suck Creek bridge.

4.1 Objectives

The objectives of the field testing are as follows:

- Monitor relative and global displacements for hollow core slab bridge at Suck Creek.
- Understand behavior of hollow core slab bridge under controlled loading.
- Use the data from displacement monitoring to explain why cracks form on the wearing surface of the Suck Creek bridge.

4.2 Bridge Detail

The Suck Creek bridge is a two-span hollow cored slab bridge built in 2009. Its spans are 40 ft. and 50 ft. in length. It is 36 ft. wide and composed of twelve (12) hollow core beams. Each beam has a width of 3 ft. and a height of 21 in. and two, 12 in. diameter cylindrical voids along its length. All internal boundaries of the beams incorporate a grout shear key. This shear key is omitted on the external face of the outer beams. Figure 4.1 through Figure 4.4 illustrate the details of the bridge and its components.

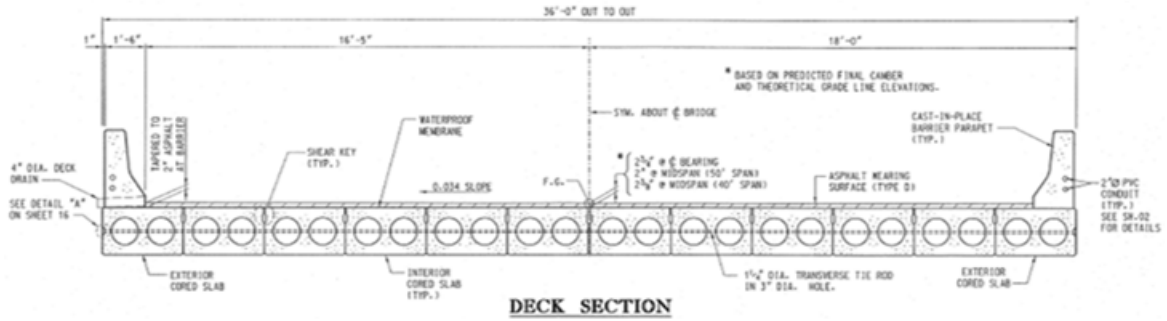


Figure 4.1: Cross section of Suck Creek bridge

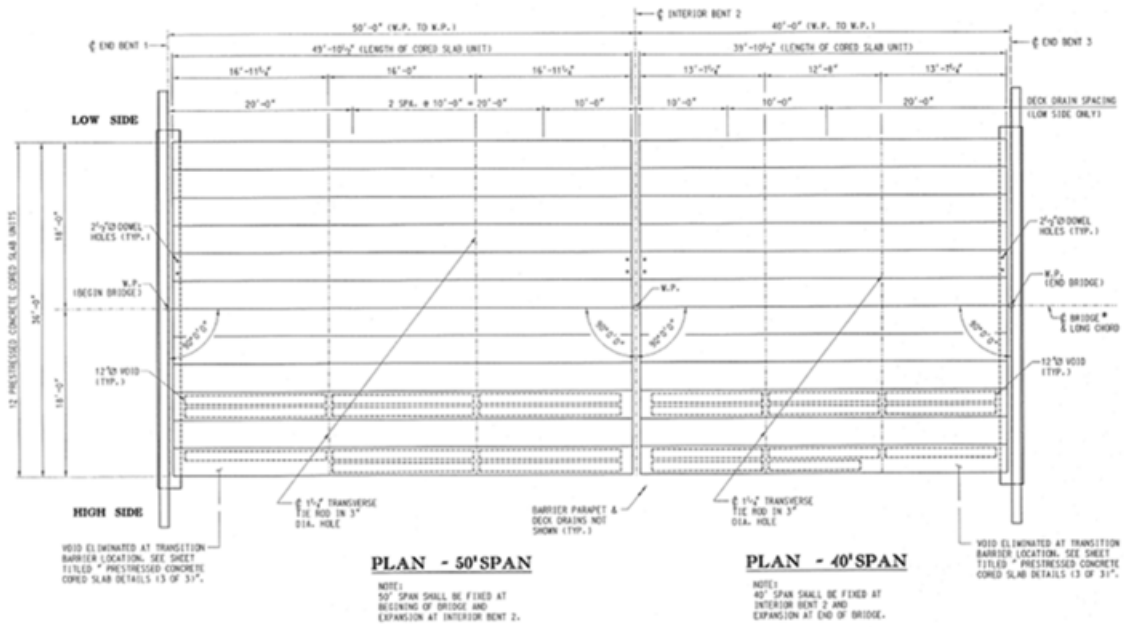


Figure 4.2: Plan view of Suck Creek bridge

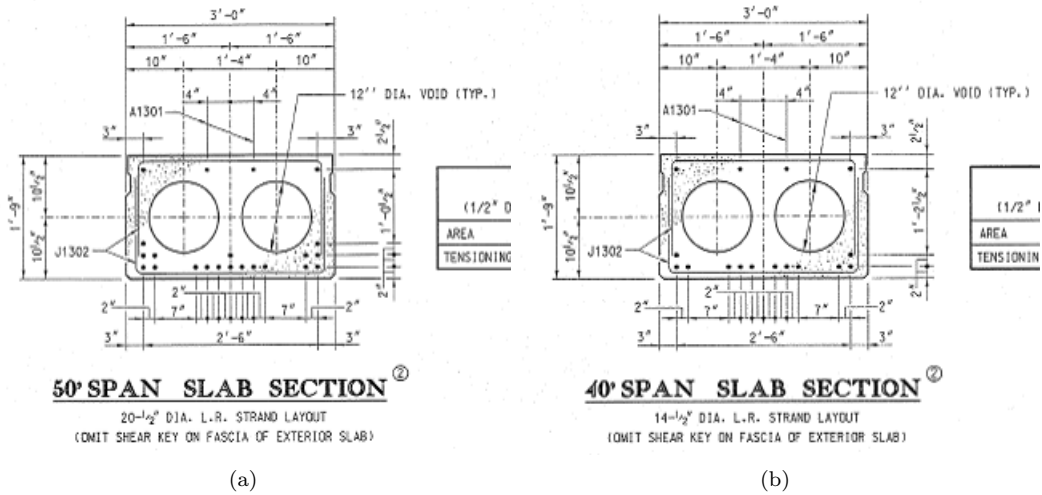
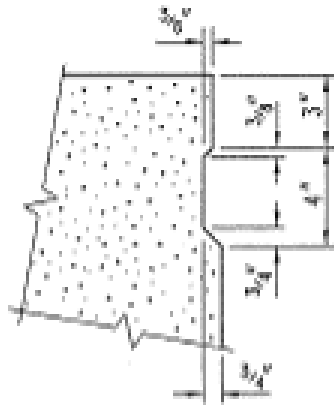


Figure 4.3: Details for 50 ft. and 40 ft. span interior sections



SHEAR KEY DETAIL

NOTE:
 OMIT SHEAR KEY ON OUTSIDE FACE
 OF EXTERIOR CORED SLABS.

Figure 4.4: Shear key details of Suck Creek bridge

4.3 Instrumentation

The instruments used in the test were linear variable differential transformers (LVDTs), a type of electrical transformer that measures linear displacement. The LVDTs were fixed on plexiglass which was attached on an aluminum bracket secured to the bridge beams. Two LVDTs at each beam interface were used to measure relative horizontal displacements. These LVDTs were placed at a fixed distance from each other in order to facilitate the measurement of relative rotation between the beams. One LVDT was used to measure relative vertical displacement – i.e. deformation in the shear key. Additionally, LVDTs were installed between the river bed and the bridge to monitor global displacements of the bridge mid-span. Figure 4.5 shows a typical LVDT used in this test. Figure 4.6 illustrates a diagram of the LVDT arrangement as well as a view of the LVDTs as setup for the bridge test.

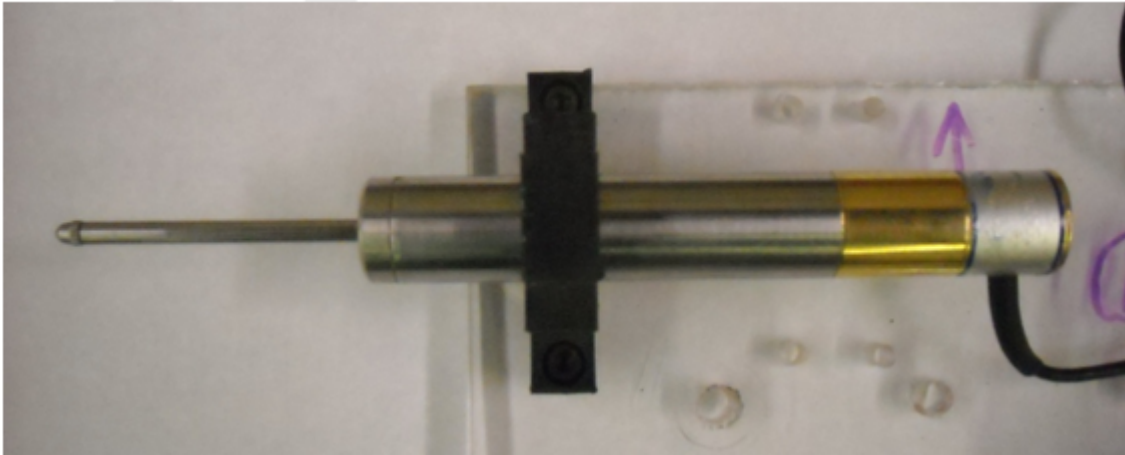


Figure 4.5: View of LVDT

The arrangement of the linear variable differential transformers used for the test consisted of four instruments per location. The two LVDTs used to measure relative horizontal displacement were secured on one plexiglass section on one beam and adjusted to measure the rotation of another plexiglass section secured to the adjacent beam. The center-to-center distance between the LVDTs was 5.375 in. Another LVDT was secured to the second plexiglass section and installed to measure relative vertical displacement between the two beams. An additional LVDT was installed on the river bed to monitor global vertical displacement.

This arrangement was used for four adjacent beams on each test. On the first test setup, instruments were setup on the joints between the first and second, second and third, third and fourth, and fourth and fifth beams. Figure 4.7 shows the location of the LVDTs the setup for the first test. Figure 4.8 illustrates the setup for the first test setup.

For the second test setup, the instruments were relocated to monitor the displacements between the third and fourth, fourth and fifth, fifth and sixth, and sixth and seventh beams. Figure

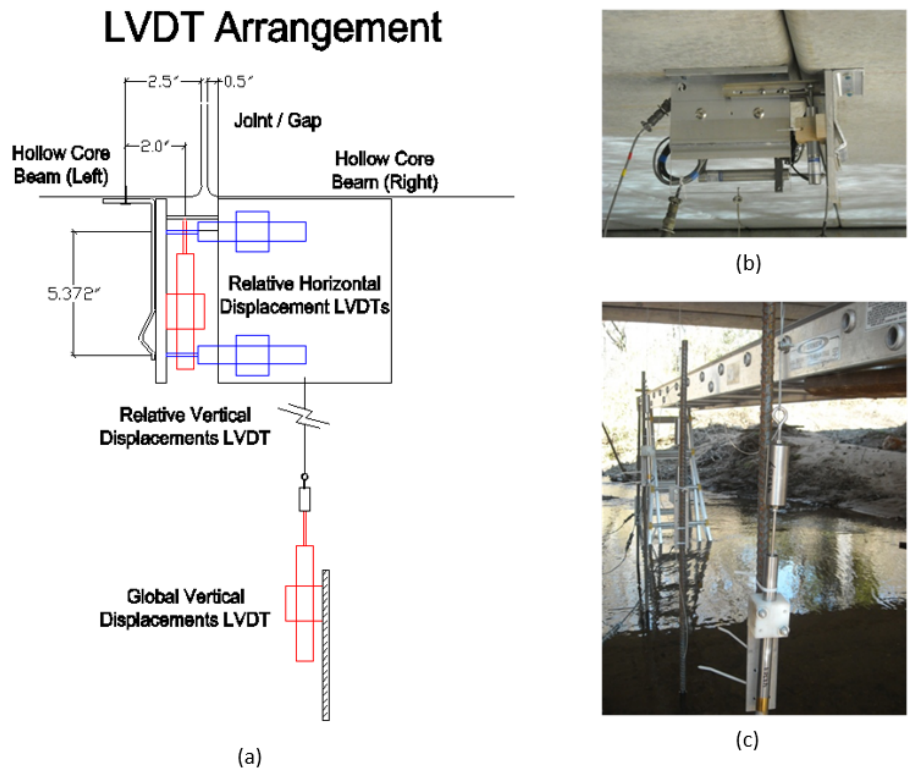


Figure 4.6: View of (a) LVDT arrangement, (b) relative displacements LVDT setup, and (c) global vertical displacements LVDT setup



Figure 4.7: View of first test setup

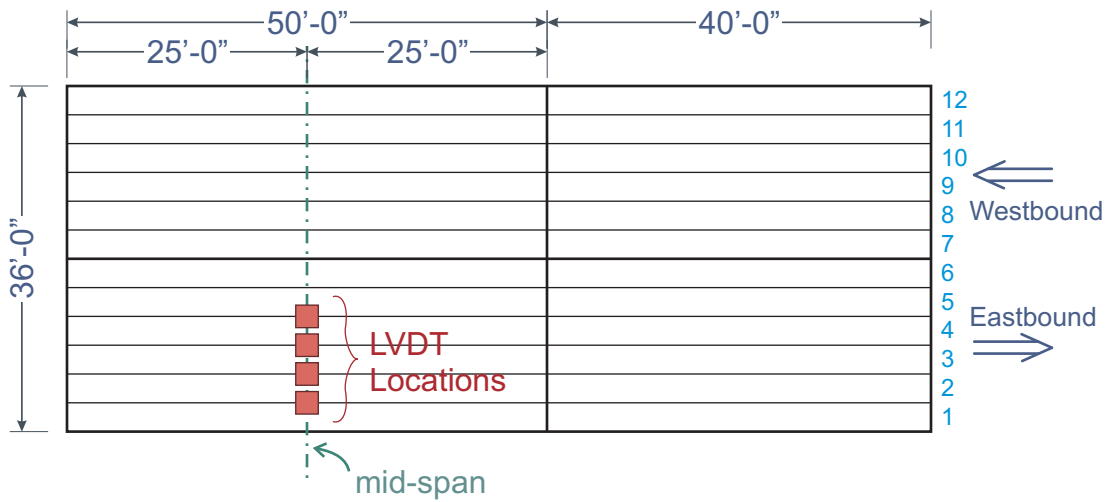


Figure 4.8: LVDT locations for first test setup

4.9 illustrates the setup for the second test. Figure 4.10 shows the location of the LVDTs for the second test setup.



Figure 4.9: View of second test setup

4.4 Load

The loading for the test was a dual rear axle dump truck provided by the South Carolina Department of Transportation. Prior to the test, the truck was weighed at the Certified Automated

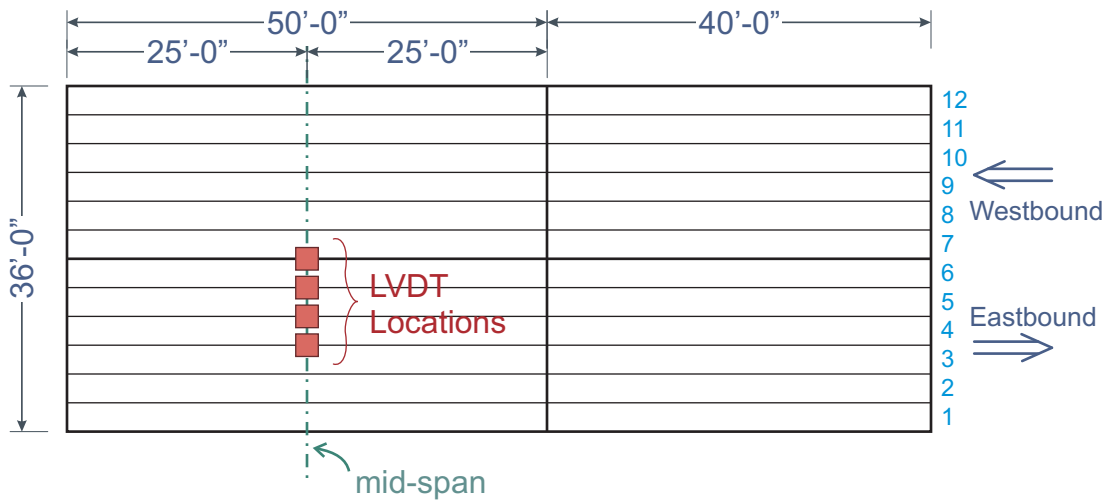


Figure 4.10: LVDT locations for second test setup

Table 4.1: Dump Truck Weight

Axle	Weight in lbs.
Steer Axle	10,000
Middle Axle (front drive axle)	28,720
Gross Weight	38,720

Truck Scale. The results of this weigh are provided in Table 4.1. The dimensions of the truck footprint used are shown in Figure 4.11.

4.5 Loading Setup

The controlled loading setup used for the test was based on the positioning of the truck across the 50 ft. bridge span. On the first test for the first instrument setup, the steer axle of the truck was applied with the right tire just above the joint between the second and third beam. For the second test of this same setup, the front drive axle was positioned at this same spot. All following tests had this same loading setup where each subsequent test relocated the truck to an adjacent shear key. The position for the load was marked on the bridge’s wearing surface to make directions to truck driver easier and positioning more precise. Figure 4.12 and Figure 4.13 illustrate the loading position for each performed test, original truck position is represented by a sketch of the vehicle and all tire positions are shown as ‘x’.

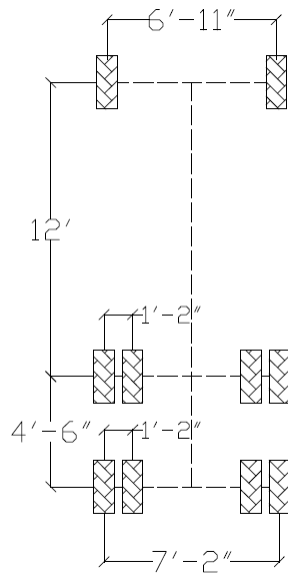


Figure 4.11: Truck dimensions

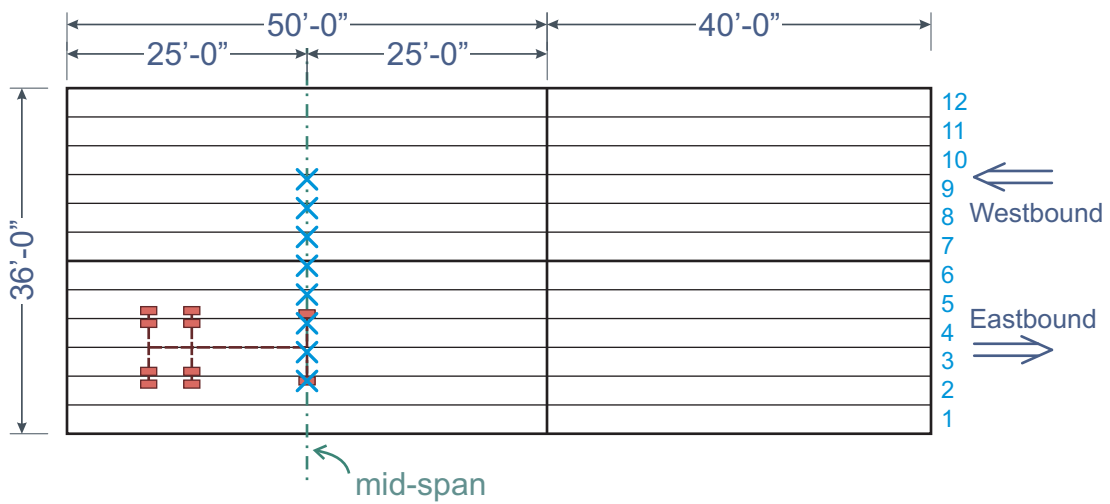


Figure 4.12: Loading setup for the first instrument setup

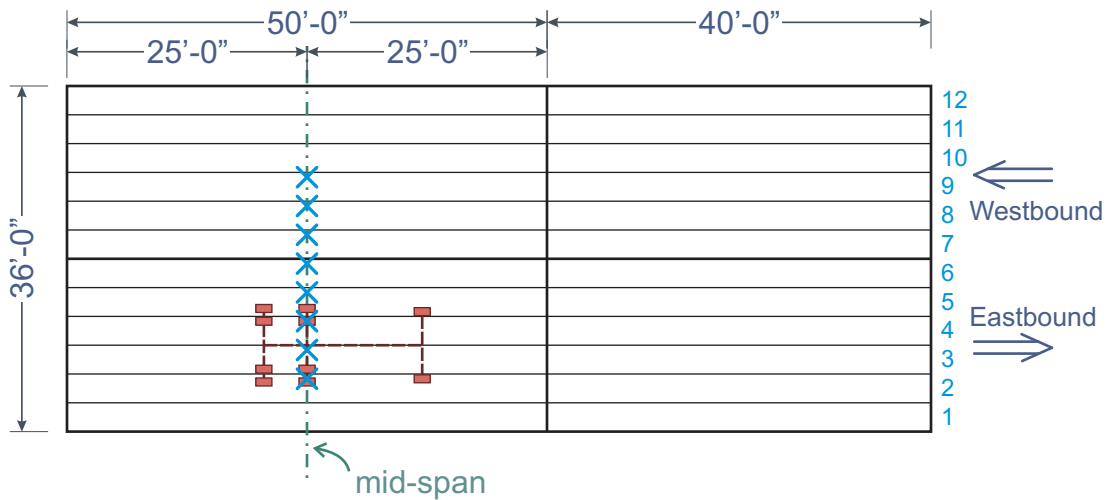


Figure 4.13: Loading setup for the second instrument setup

4.6 Procedure

The procedure followed through the test is as follows. First, the brackets used to hold the plexiglass were installed along the mid span of the 50 ft. span on both sides of the joints between the first seven beams. Additionally, rebar was positioned just below the first four joints on the river bed to hold the LVDTs intended to measure global vertical displacements.

After installing the brackets, the plexiglass holding the LVDTs was secured to each bracket and the global displacement LVDTs were secured on the rebar for the first four joints. For each LVDT (four on each joint) calibration was performed taking zero values and using control displacement blocks.

When all LVDTs had been calibrated, the loading of the bridge was executed. The controlled load for the first test for the first setup was positioning the truck's steer axle on the mid span with the right tire six feet away from the edge of the bridge (just above the joint between the second and third beam) on the east bound lane, as shown in Figure 4.12. When the truck's steer axle was in position, readings were taken for the mean (μ) and coefficient of variation (COV) of the displacement over a period of one minute for each LVDT. Table 4.2 presents the values obtained for μ and COV of the displacement for the first test for the first setup for each LVDT.

After values were recorded for each LVDT, the truck was relocated for the second test. The position for the second test was having the front right tire of the drive axle take the original position of the right steer tire, thus applying a larger direct load on the joint between the beams. Again, readings were taken for the μ and COV of the displacement for each LVDT. For the third test, the truck position was shifted along the mid span line 3 ft. towards the center line of the bridge, therefore acting directly on the joint between the third and fourth beams. All readings were taken and the truck was moved to its next position. Positions 4 to 9 for the first setup consisted of moving the drive axle of the truck transversely along the mid span in 3-ft increments, consequently acting

Table 4.2: Values obtained from the first test for the first setup

Joint	LVDT	Mean (in.)	COV of Displacement
Relative Displacement Measurements			
1	Relative Vertical	-0.0171	0.010
	Horizontal Top	0.0032	0.019
	Horizontal Bottom	0.0037	0.010
2	Relative Vertical	-0.0004	0.003
	Horizontal Top	0.0064	0.013
	Horizontal Bottom	0.0079	0.006
3	Relative Vertical	-0.0004	0.021
	Horizontal Top	-0.0002	0.210
	Horizontal Bottom	-0.0003	0.030
4	Relative Vertical	0.0050	0.005
	Horizontal Top	0.0056	0.010
	Horizontal Bottom	0.0058	0.016
Global Displacement Measurements			
1	Global Vertical	-0.063	0.032
2	Global Vertical	-0.071	0.003
3	Global Vertical	-0.067	0.006
4	Global Vertical	-0.063	0.001

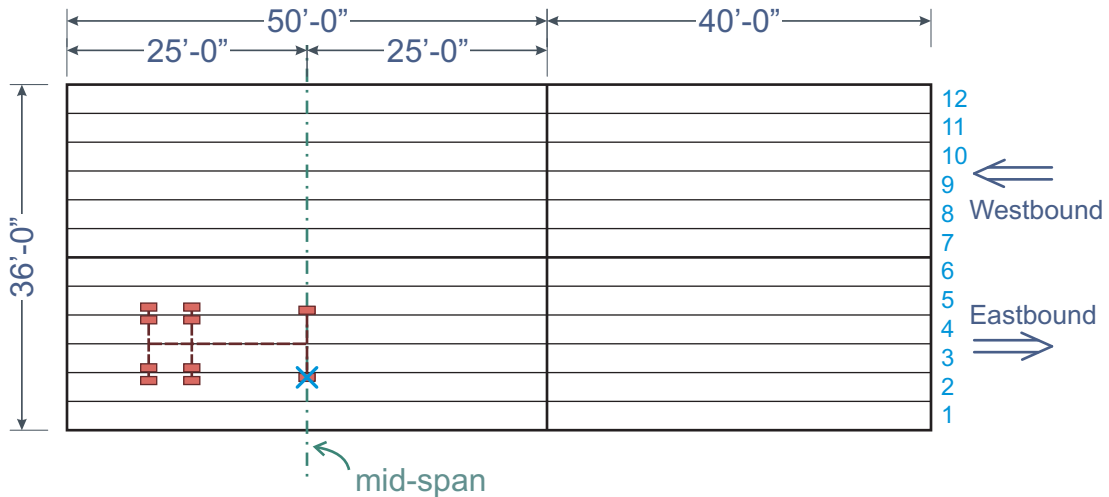


Figure 4.14: Truck position for the first test for first instrument setup

directly on the joints between the beams. The truck positions for the first instrument setup are shown in Figures 4.14 through 4.17.

For the second setup, all instrumentation for the first joint (between the first and second beams) was moved to the fifth joint (between the fifth and sixth beams) and the instrumentation for the second joint (between the second and third beams) was moved to the sixth joint (between the sixth and seventh beams). As mentioned in the Loading Setup section, the first test for the second

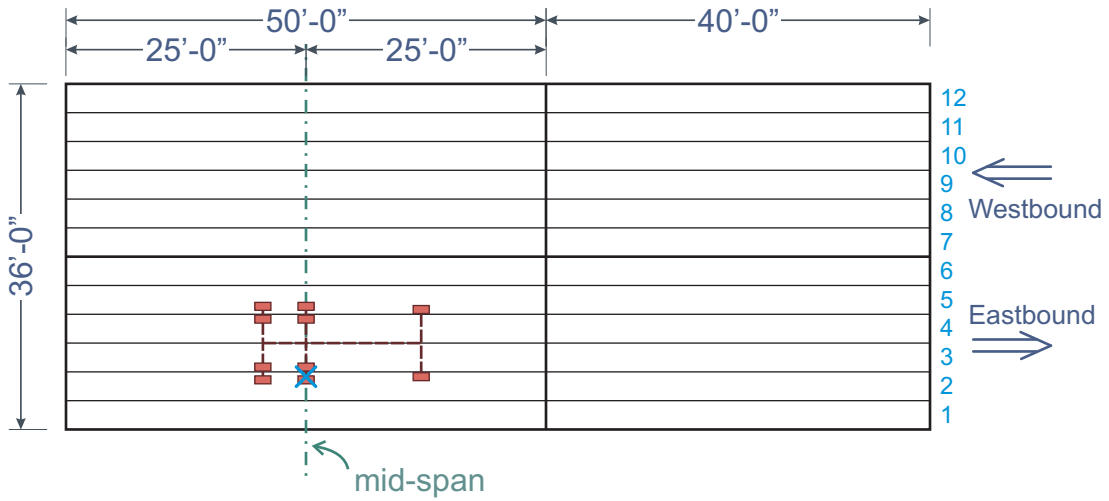


Figure 4.15: Truck position for the second test for first instrument set

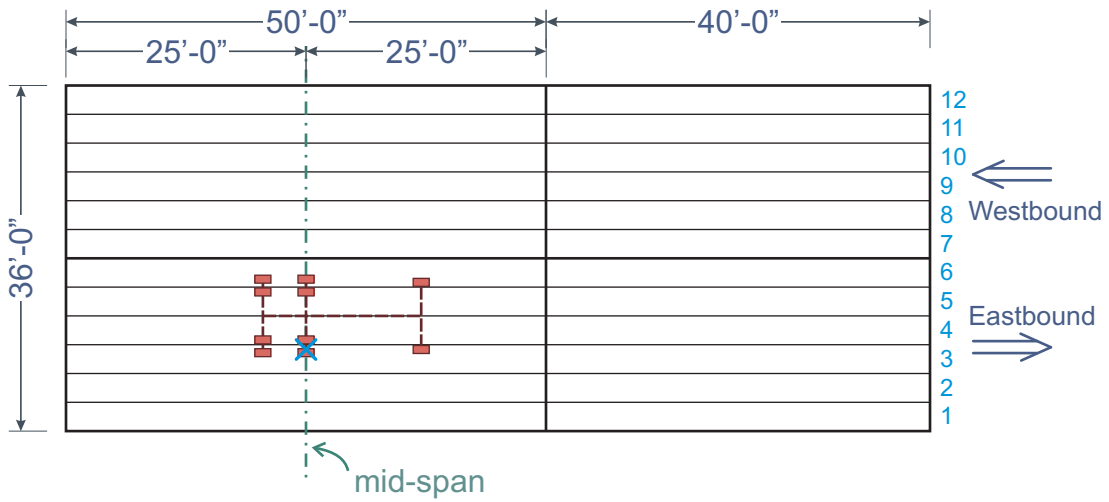


Figure 4.16: Truck position for the third test for first instrument set

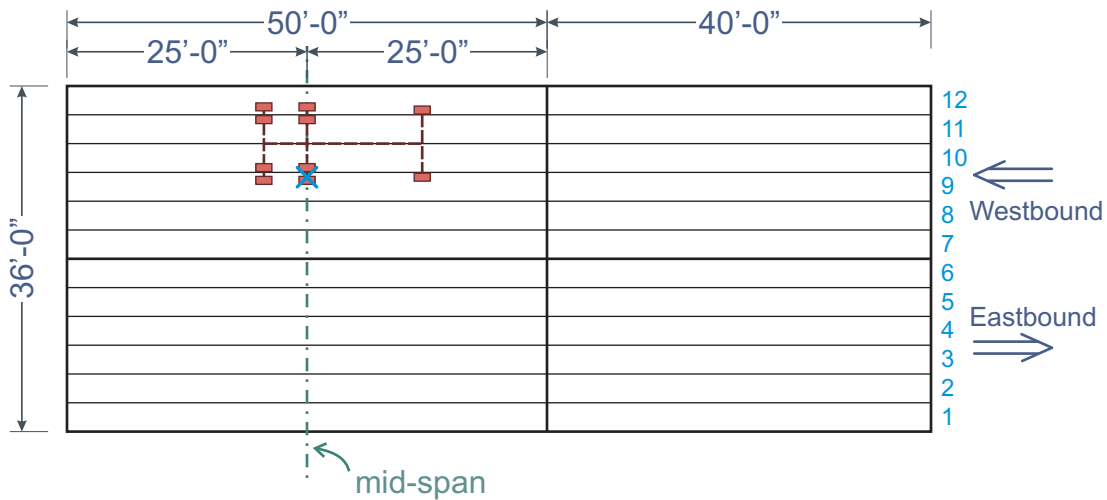


Figure 4.17: Truck position for the ninth test for first instrument set

Table 4.3: Values obtained from the first test for the second setup

Joint	LVDT	μ (inches)	COV
Relative Displacement Measurements			
3	Relative Vertical	0.0032	0.017
	Horizontal Top	-0.0010	0.008
	Horizontal Bottom	-0.0013	0.008
4	Relative Vertical	0.0082	0.008
	Horizontal Top	-0.0017	0.013
	Horizontal Bottom	-0.0020	0.093
5	Relative Vertical	-0.0033	0.012
	Horizontal Top	0.0043	0.012
	Horizontal Bottom	0.0052	0.024
6	Relative Vertical	0.0076	0.002
	Horizontal Top	0.0038	0.017
	Horizontal Bottom	0.0032	0.007
Global Displacement Measurements			
3	Global Vertical	-0.068	0.032
4	Global Vertical	-0.051	0.003
5	Global Vertical	-0.091	0.006
6	Global Vertical	-0.081	0.001

instrumentation setup was performed with the right tire of the truck's steer axle positioned over the first joint (position of the truck during the second test for the first instrument setup). Once more, readings were recorded. Table 4.3 presents the values obtained for μ and COV of the displacement for the first test for the second setup for each LVDT.

After values were recorded for each LVDT, the truck was relocated for the second test. The position for the second test was accomplished by shifting the right tire of the truck's drive axle along

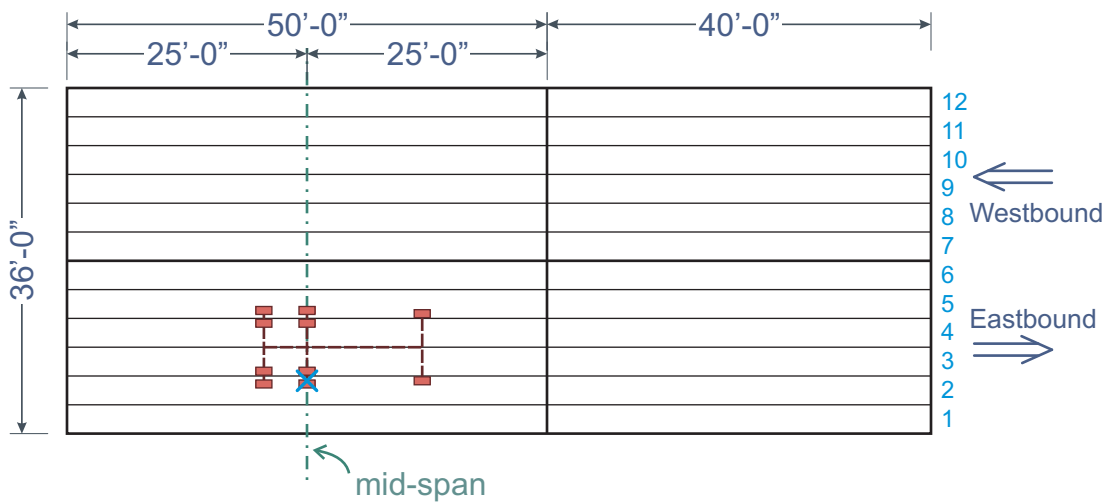


Figure 4.18: Truck position for the first test for second instrument set

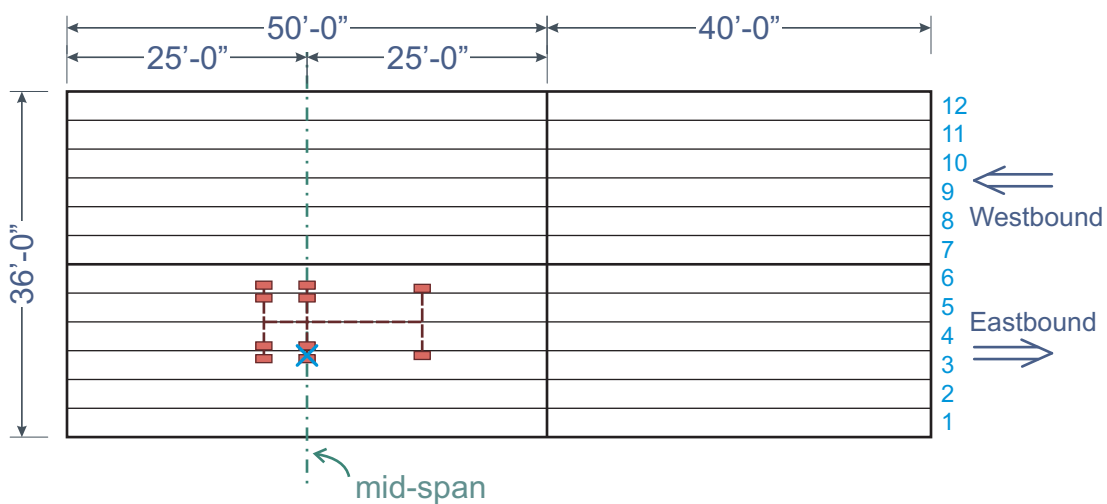


Figure 4.19: Truck position for the second test for second instrument set

the mid span line 3 ft. towards the center line of the bridge, therefore acting directly on the joint between the third and fourth beam. Positions 3 to 7 for the second setup consisted of moving the drive axle of the truck along the mid span in 3 ft. intervals, consequently acting directly on the joints between the beams. Figure 4.18 through Figure 4.20 show the position of the truck for the first, second, and seventh test in the second setup.

Using all the recorded data, calculations were performed to assess the behavior of each beam for each load scenario. To obtain the relative angular displacement between beams at the measured joints, data from both horizontally set LVDTs was used. Likewise, the vertically set LVDTs were used to calculate relative and global vertical displacements where relative vertical displacements are indicative of shear key deformation. Figure 4.21 through Figure 4.36 illustrate the obtained

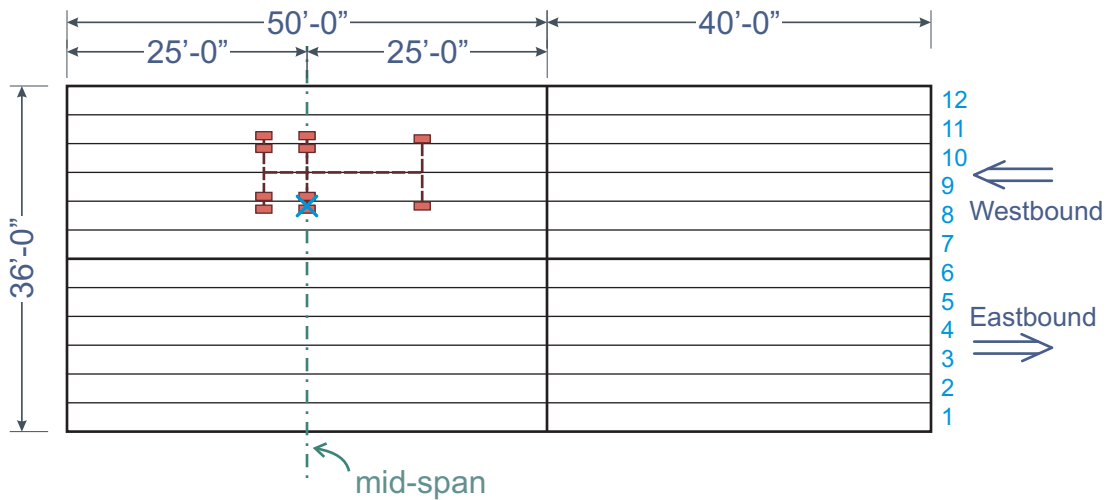


Figure 4.20: Truck position for the seventh test for second instrument set

displacements of the beams for all tests and setups. It should be noted that the shaded beam sections shown in Figure 4.21 to Figure 4.36 were not instrumented.

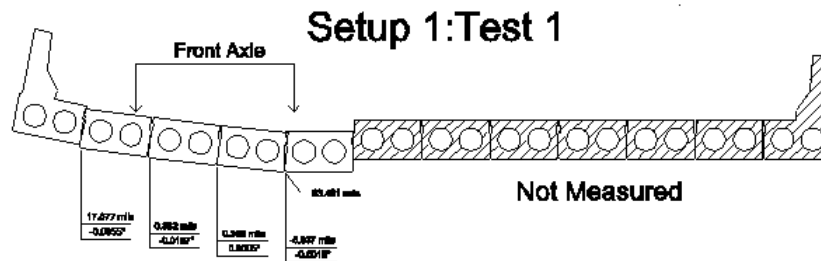


Figure 4.21: Displacements for first test for the first setup

4.7 Test Results Interpretation

It can be observed from the test results that load transfer occurs from beam to beam by use of the shear key. This load transfer affects the bridge by causing global vertical displacements, as well as relative rotation and vertical displacements between bridge members.

The largest deformation between any two of the bridge members was consistently registered between the outer-most beam and the adjacent beam. One may note that there exists a significant difference in stiffness of the outermost beam and the beam adjacent to it. Not only is the moment of inertia different, but the section becomes an irregular shape once the parapet has been added. This will likely cause temperature based cracks to develop prematurely at this joint. The relatively large deformation at the outermost joint can also be confirmed by examining the bridge's rolling surface

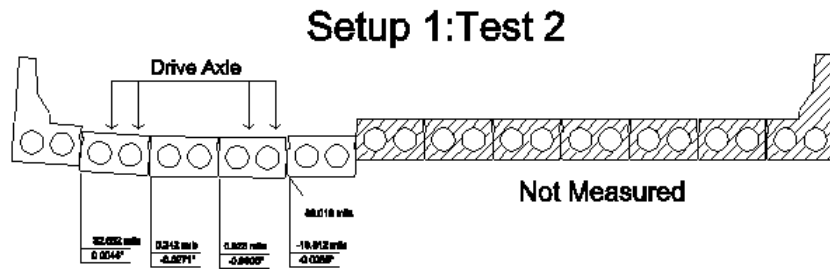


Figure 4.22: Displacements for second test for the first setup

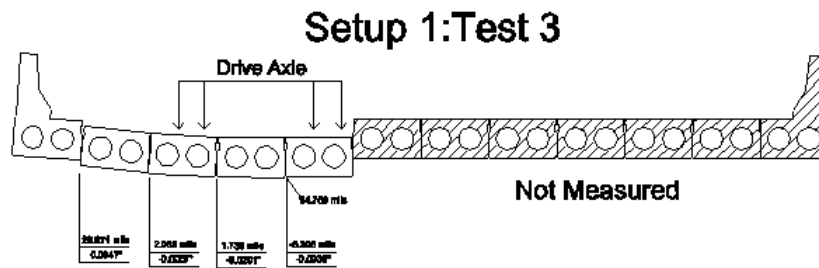


Figure 4.23: Displacements for third test for the first setup

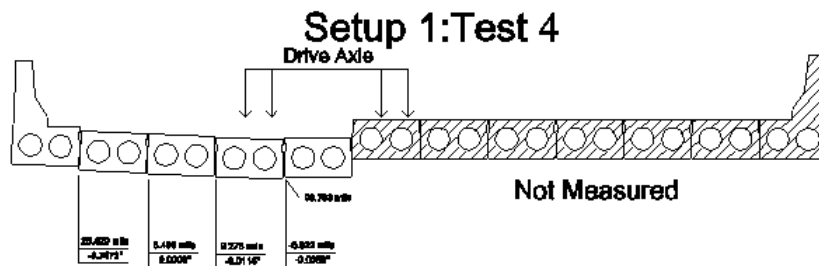


Figure 4.24: Displacements for fourth test for the first setup

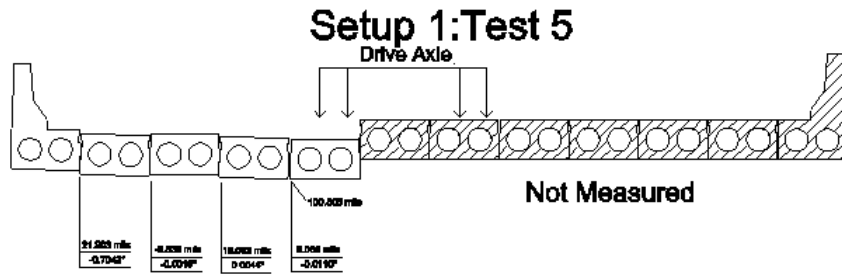


Figure 4.25: Displacements for fifth test for the first setup

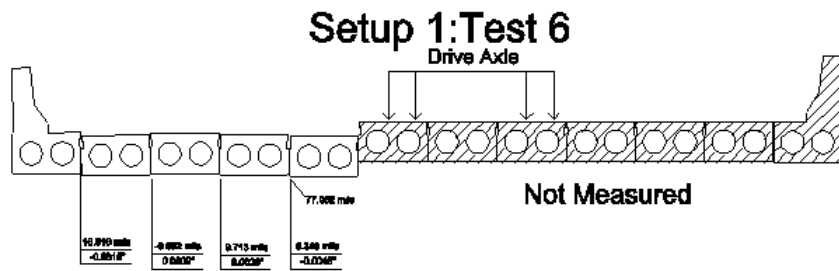


Figure 4.26: Displacements for sixth test for the first setup

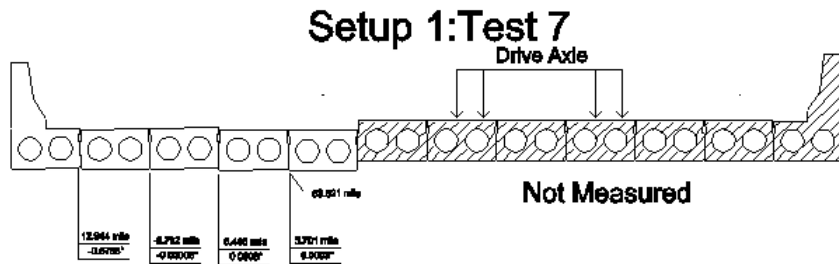


Figure 4.27: Displacements for seventh test for the first setup

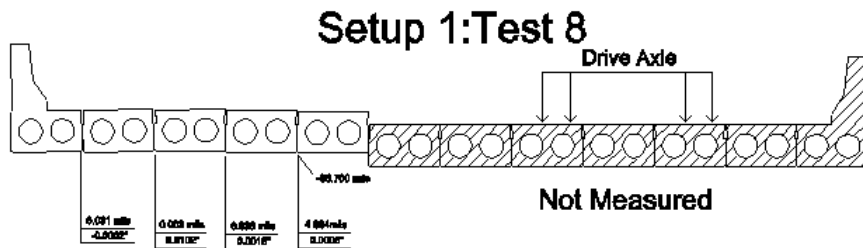


Figure 4.28: Displacements for eighth test for the first setup

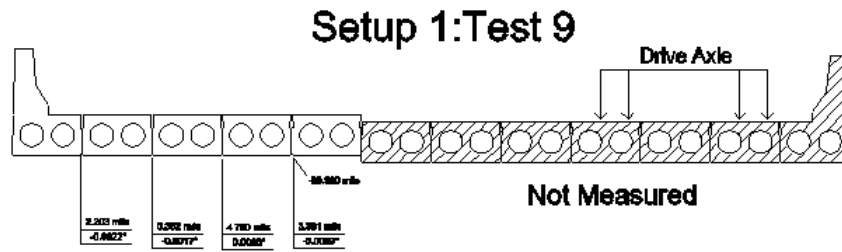


Figure 4.29: Displacements for ninth test for the first setup

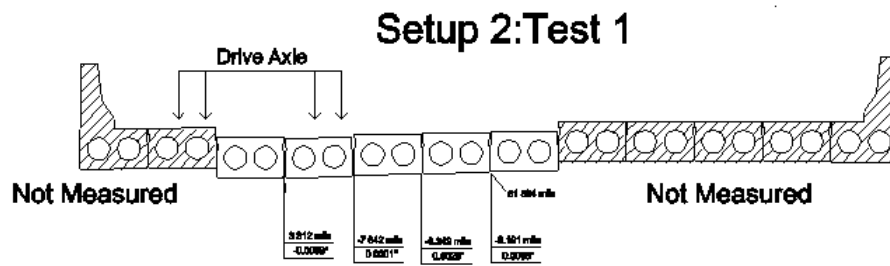


Figure 4.30: Displacements for first test for the second setup

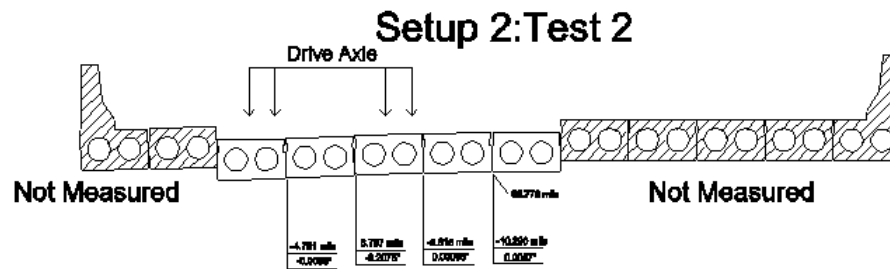


Figure 4.31: Displacements for second test for the second setup

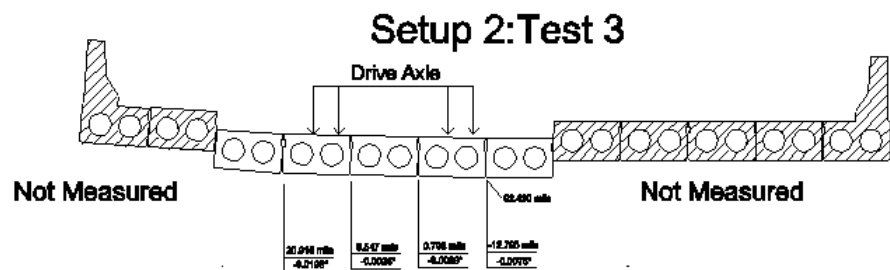


Figure 4.32: Displacements for third test for the second setup

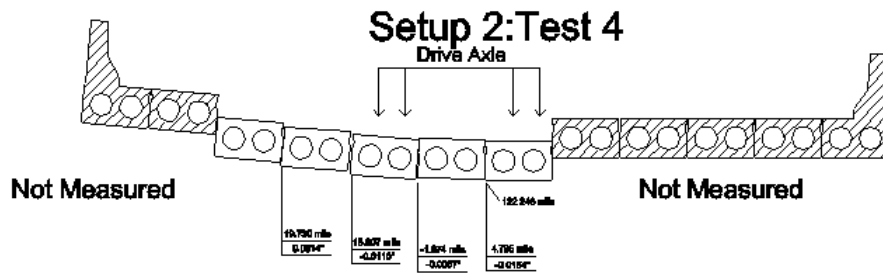


Figure 4.33: Displacements for fourth test for the second setup

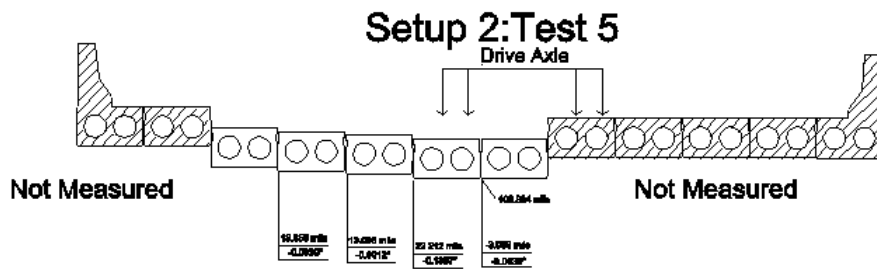


Figure 4.34: Displacements for fifth test for the second setup

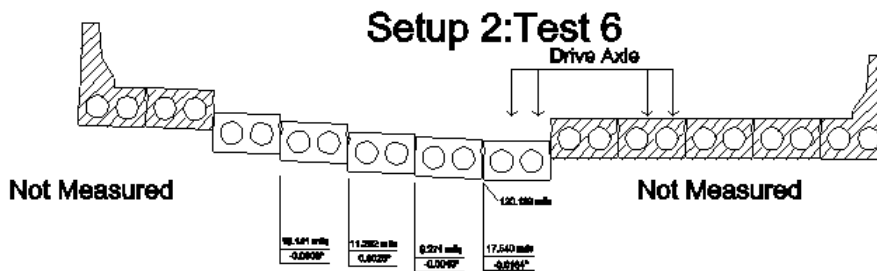


Figure 4.35: Displacements for sixth test for the second setup

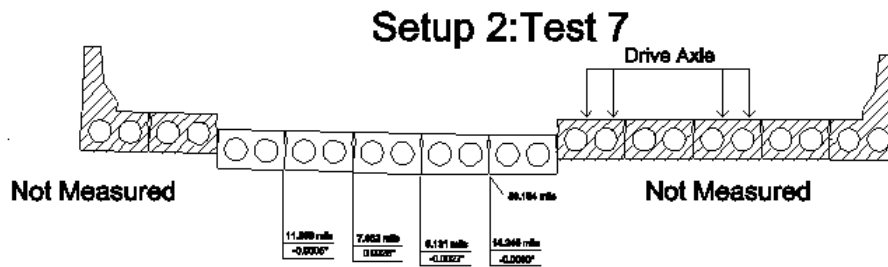


Figure 4.36: Displacements for seventh test for the second setup

where the most significant cracking can be visually detected in the wearing surface along the position of this joint throughout the length of the span. At this joint, the test registered relative vertical displacements of up to 0.033 inches and relative rotation of up to 0.747 degrees. This reinforces the findings in the literature review which state that applying a mid-depth transverse tie rod with a top flange shear key can lead to rotation about the tie rod and cracking at the top of the member along the joint (Russell, 2009).

Taking into account the age of the Suck Creek Bridge, the measured deformations and observed cracking are considered very significant. Although an appreciable amount of transfer ability still exists in the shear keys, further degradation and weakening of the joint is to be expected. A more robust shear key than was used in this bridge is clearly justified.

4.8 Conclusions

A number of significant conclusions may be drawn from the results of this field verification. They are as follows:

- As expected, beams in a hollow core slab bridge transmit stresses from one to the other by means of the shear key, creating relative rotational and vertical displacements.
- The observed relative deformations are significant for a bridge that is only a year old.
- Cracks on the bridge's wearing surface are a consequence of the relative angular and vertical displacements between the beams in the hollow cored slab bridge.
- These cracks may lead to the reduction of the shear key's strength.
- The largest deformation was recorded between the outer-most beam and the adjacent beam.
- The location of the largest deformation may be a consequence of the stiffness differential of the outer-most beam and its adjacent beam due to the bridge's parapet.
- The maximum recorded vertical displacement between members was 0.033 in. and the maximum relative rotation was 0.747 degrees.

This page intentionally left blank

Chapter 5

Bridge Type Selection

All of the literature searches, surveys and interviews were conducted to identify feasible options for meeting the objectives of this project. The SCDOT steering committee, assigned to oversee this work, was tasked with selecting the desired bridge section to further pursue. However, this selection was made only after a summary of findings, recommendations and feedback from local contractors and fabricators were obtained.

This Chapter presents a summary of the findings from the background work. It then gives the initial recommendations of the research team to the steering committee. This set the framework for a mini-workshop to be held with local contractors and fabricators. The mini-workshop was used as a mechanism to solicit feedback relative to desirable and undesirable details. This Chapter further presents the rationale the SCDOT steering committee used in the selection of the NEXT-D bridge section along with the outstanding research needs associated with this section.

5.1 Department of Transportation Web Search

Very few states had online evidence of new accelerated short-span systems. Texas had intriguing shallow member details such as the large shear key in their adjacent box beams and their decked slab beams. Therefore, Texas was targeted for further investigation in later portions of this research. Other states using adjacent beam systems seem to always require a concrete overlay when using the bridge on high ADT or NHS routes. New York, Ohio, and Texas had continuity details available on their websites. The details from New York and Ohio are full continuity diaphragms, where Texas' detail is not a full diaphragm.

5.2 Advanced Systems

This journal search discovered a few systems that could be feasible in providing the improvements sought after in this research. The Poutre Dalle and Minnesota DOT systems could greatly improve the performance of the bridge by possibly increasing the construction time by a

small amount. Proprietary grout filled splice sleeves are available and may have a practical application in this research, however more research is needed to determine if they are effective means of shear transfer between beams. Since these proprietary grout filled splice sleeves may be costly, using the non-proprietary systems proposed for the full-depth precast concrete bridge deck panel systems may be more feasible. Modular bridges are very rapid, however they have only been used on very low traffic bridges thus far and more research would be needed to determine their suitability for high ADT routes. Rapid hardening concrete is a beneficial solution to the problem of accelerated bridge construction and should be considered if cast-in-place concrete is needed in the final design.

5.3 Hollow Core and Box Beam Study

- States often use a reinforced concrete overlay in order to use this bridge type on high ADT roads, however, it has been shown through studies that the overlay does not completely eliminate the longitudinal cracking.
- Applying mid-depth post-tensioning with a top flange shear key after grouting can lead to cracking at the top of the member along the joint.
- The effects of temperature on the girders create cracks in the longitudinal joints without any load being applied to the bridge.
- Cyclic loads do not necessarily make new cracks along the joints, but they do propagate cracks created by temperature effects.
- Larger and deeper shear keys improve grouting techniques and decrease the amount of rotation about the shear key of the member, therefore decreasing tensile opening at the top of the key.
- Many failed shear keys still transfer load through friction.
- Transverse tie bars do not contribute significantly to shear transfer.
- Mid-depth shear keys display the best relative displacement performance in comparison to other shear key locations.

The following suggestions have been shown through studies to improve the performance of the longitudinal joints and reduce the appearance of cracks. However, these suggestions have not proven solutions in completely suppressing the problem in all cases:

- Move the shear key to the neutral axis of the member (Miller et al., 1999).
- Use a full depth shear key that can be grouted easily (Russell, 2009; El-Remaily et al., 1996; Miller et al., 1999).
- Provide post-tensioning in the top and bottom of the beam (Lall et al., 1998; El-Remaily et al., 1996).

- Sandblast the keyways before shipping and clean with compressed air before erection (Russell, 2009).
- Transversely post-tension after grouting the keys if it will not cause moment about the shear key (Russell, 2009).
- Use a grout material with high bond strength (Russell, 2009; Miller et al., 1999).

Reinforcing steel corrosion due to deicing salts and water infiltrating into and staying clogged in the voids in these systems was been a major concern with these bridges and led to a major failure in Pennsylvania with the Lakeview Drive Bridge collapse. A nondestructive test that can determine the corrosion in hidden strands will surely improve the quality of inspections and maintenance on these bridges and extend their useful life and improve the safety of the systems. Due to newer forms, larger strands, more concrete cover, and other factors, durability issues will only improve as these bridge types are used in future designs and more expertise is available in this field. However, caution still must be taken when inspecting the bridges that were built 40 to 50 years ago. This should also be considered when working on the new designs of these bridges and therefore maintenance procedures of these new designs must be accounted for in order to protect the bridges and ensure a long service life and safety as well.

One challenge in creating continuity at the bents is to minimize the positive moment cracks occurring at the interior bents, while still avoiding an open joint but still having the benefits of reduced positive moments in the spans due to the continuity. Another challenge is to ensure rapid-construction while also properly designing and constructing continuous girder spans. The cast-in-place continuity diaphragm, even with quick setting and consolidating concrete, cannot keep up with the construction pace of the rest of the prestressed, precast bridge components.

5.4 Survey & Interview Results

Many states consider longitudinal cracking along the joints of their adjacent beam bridges an issue. Due to the many differences in practices and crack prevalence, it is difficult to determine which methods best remedy the longitudinal cracking problem. Also, there is not a consensus on what girder age to use when creating continuity between the box beams. This shows that the use of continuity depends on the individual DOT's common practice and not a universally accepted superior detail.

Practices that were confirmed to improve bridge performance based on phone conversations included:

- full-depth shear keys
- larger shear keys
- reinforced concrete topping
- post-tensioning before grouting the shear key

- more post-tensioning/higher post-tensioning stress

Factors that were confirmed to degrade bridge performance based on these conversations included:

- reinforcing steel corrosion
- partial depth shear keys
- little/no post-tensioning
- post-tensioning after grouting which applies an eccentric load to the key

Systems that could be potential solutions or could lead to a better detail (targets for fabricator and contractor contacts) include:

- New York - Box Beams, Slab Beams, Inverset System
- North Carolina - Box Beams, Cored Slabs
- Oregon - Box Beams, Slab Beams
- Texas - Box Beams with robust shear key, Slab Beams, Decked Slab Beams
- Washington - Slab Beams, Deck Bulb-T
- PCI Northeast - NEXT beam system

Based on conversations with the DOTs these systems seem to minimize the reflective cracking issues, ensure rapid construction, and in some cases allow for longitudinal continuity and these states are very pleased with the performance of these systems. Conversations with fabricators and contractors have supported these systems as bridges that are not difficult to work with and ensure a rapid construction job that is favorable to all parties: DOTs, producers, and contractors.

5.5 Suck Creek Bridge Testing

- As expected, beams in a hollow core slab bridge transmit stresses from one to the other by means of the shear key, creating relative rotational and vertical displacements.
- The observed relative deformations are significant for a bridge that is only a year old.
- Cracks on the bridge's rolling surface are a consequence of the relative angular and vertical displacements between the beams in the hollow cored slab bridge.
- These cracks may lead to the reduction of the shear key's strength.
- The largest deformation was recorded between the outer-most beam and the adjacent beam.
- The location of the largest deformation may be a consequence of the stiffness differential of the outer-most beam and its adjacent beam due to the bridge's parapet.
- The maximum recorded vertical displacement between members was 0.033 in. and the maximum relative rotation was 0.747 degrees.

5.6 Summary of Findings

Both published literature and personal communications with DOTs show that common problems in adjacent beam bridge systems are the longitudinal cracking along the joints and water drainage through these joints, especially in the presence of de-icing salts. The web and phone surveys with the DOTs only uncovered a few more feasible alternative systems than were discovered in the website search: Inverset System and Deck Bulb-T. Contact with the Texas DOT confirmed the feasibility of the modified box beam and decked slab members as good alternative short-span systems.

Testing of the Suck Creek Bridge, which possesses no notable TPT, confirms that rotation does occur about the shear key and that distress in the shear key can occur at a fairly young age of the bridge. Suggestions from literature say using a full depth shear key instead of a partial depth shear key or using post-tensioning would help decrease this rotational movement and therefore decrease the reflective cracking at the joints.

Most sources state that adding a reinforced concrete overlay, requiring more post-tensioning and having full depth shear keys help decrease the severity of longitudinal cracking along the joints. However, as seen from publications and interviews with the state DOTs, these remedies do not seem to fully solve the problem. Thus, most states use these bridges only when necessary for clearance on high ADT routes. This suggests that a better performing solution will be found in a system unlike that of a conventional adjacent beam bridge. The following is a summary of the key bridge sections explored as part of this study.

5.6.1 Texas/New York Robust Shear Key with Target Post-Tensioning Force (Fig.2.34)

Pros:

- Can be applied to South Carolina hollow core details or entire section can be copied
- Large full-depth shear key that helps prevent rotation and reduces cracks and stress in shear key
- Construction speed similar to hollow core sections
- Use of target post-tensioning force improves beam interaction
- Can be modified to be used without an overlay

Cons:

- No proven method to eliminate longitudinal cracks on high volume roads
- Requires post-tensioning to reduce cracking
- Larger amount of grout or cast-in-place concrete required for shear keys
- Still includes voids which are difficult to inspect

5.6.2 Modified Beam-In-Slab System (Fig.2.6)

Pros:

- No longitudinal cracks
- Larger sections use less sections per span and less connections
- No voids which facilitate easier inspection
- No post-tensioning required
- No overlay required

Cons:

- Large amount of cast-in-place concrete for connection
- Research specifies this system for low volume roads

5.6.3 MNDot Inverted Tee System (Fig.2.7)

Pros:

- Elimination of transverse and longitudinal joints and joint cracks
- No falsework required
- No post-tensioning required
- Can be used with rapid hardening concrete

Cons:

- Required onsite rebar placement
- Large cast-in-place concrete overlay required

5.6.4 Grout Filled Splice Sleeves (Fig.2.11 and Fig.2.12)

Pros:

- Eliminates post-tensioning
- Can easily be implemented in hollow core sections
- May help continuity over bents

Cons:

- May not prevent rotation and joint cracks
- Large amounts of proprietary splices or grout pockets required

5.6.5 Texas Decked Slab Beams and Washington Decked Bulb Tee (Fig.3.2 and Fig.3.3)

Pros:

- Welded shear connections reduce amount of grouting required for connecting adjacent beams
- Can be used without concrete or asphalt overlay
- Washington section can be easily inspected
- Less members to be transported and erected

Cons:

- Requires employment of a welder
- Concerns with fatigue of welds on high volume roads
- Sections do not resist rotation between members
- Requires a larger crane

5.6.6 Inverset System (Fig.3.4)

Pros:

- Structural integrity relies on bolted connections, not grouted shear keys
- Does not require concrete curing
- Easy to inspect; no water retaining areas

Cons:

- Steel requires painting and is possibly more expensive
- Large amount of bolted connections requires more onsite labor
- Bolted connections require working under the bridge, therefore does not lend itself to top-down construction

5.6.7 NEXT Beam (Fig.3.5 and Fig.3.6)

Pros:

- No formwork required on NEXT-F beam
- No overlay required on NEXT-D beam
- No post tensioning required

- Less sections needed

Cons:

- Requires cast-in-place concrete
- Larger crane needed

5.7 Mini-Workshop Summary

Following a discussion with the SCDOT steering committee, three bridge sections were selected to further investigation. These three beam sections are the inverted-Tee, the NEXT-D, and a variation on the NEXT-D. These sections are shown in Fig.5.1 through Fig.5.3.

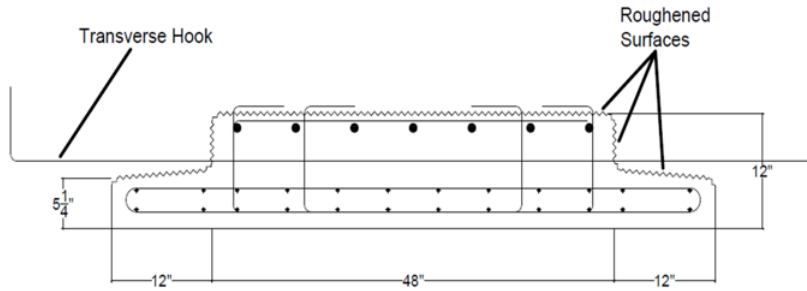


Figure 5.1: Inverted-Tee beam

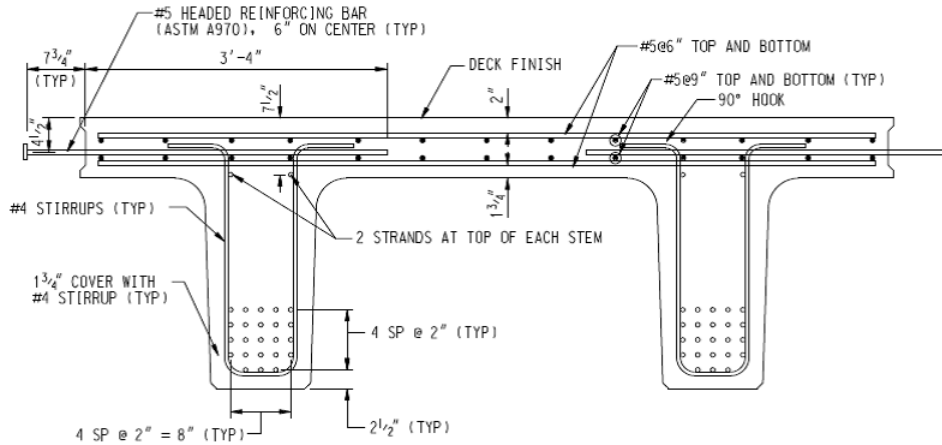


Figure 5.2: NEXT-D beam

Feedback on issues related to these three section - both from the contractor and fabricator perspective - was desired before making a final selection of the beam type the SCDOT would like to use. On August 3, 2010 a mini-workshop was held in Columbia, SC at the SCDOT headquarters.

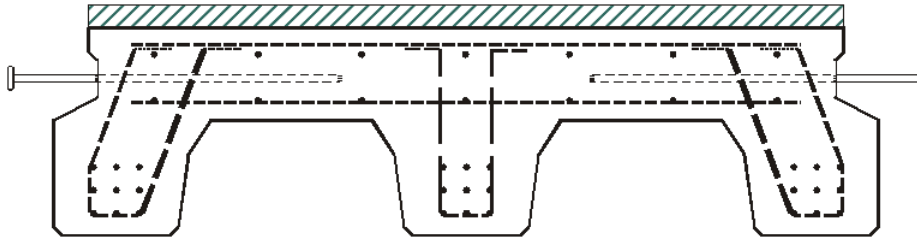


Figure 5.3: Variation on the NEXT-D beam

Fabricators and contractors from region were invited to attend and provide feedback regarding the three sections which were being considered as an alternative to the hollow-core slab. After receiving some background - including the objectives involved in selecting a new beam section - each group (contractors and fabricators) was asked to complete a questionnaire with respect to each proposed section. The complete questionnaires may be found in Appendix D. A summary of the comments and findings from these questionnaires follows here but a full context of some of the responses will require a review of the questions and details posed to the participants - see Appendix D.

5.7.1 Fabricator/Contractor Response Summary

All questions were set in the context of a 48' wide x 40' single span bridge. The summary is given in question and answer form.

General Contractor Question: What is the maximum section weight which is reasonable to set without taking extraordinary measures?

Max Section Weight is 30,000 pounds but ideal is 22,000 pounds.

5.7.1.1 Inverted-Tee:

1. Fabrication difficulty compared to cored-slab (1 being easier, 5 being more difficult):

5

2. What is the relative time, compared to hollow-core bridges, to construct one span (i.e. set beams, place reinforcement and any concrete/grout)?

More than 50% longer to construct compared to hollow core

3. What is the relative erection cost, compared to hollow-core bridges, to construct one span (i.e. set beams, place reinforcement and any concrete/grout, crane capacity)?

More than 50% more expensive compared to hollow core due to crane size

4. What details of the proposed section are friendly?

- Bottom flange can be used as a form (Contractor)
- Knowing the key is filled (Contractor)
- Concrete is better than grout for keys (Contractor)
- Expansion coefficient of section and key material are the same (Contractor)

- No Post-Tensioning (Contractor)
- Strands are low (Fabricator)
- Low center of gravity (Fabricator)

5. What details of the proposed section are unfriendly?

- Transverse Hook - section must be slid under adjacent sections (Contractor)
- Transverse hook may be a safety issue (Contractor)
- 90 degree hook must be capped for OSHA (Contractor)
- Multiple Span Set-up (Contractor)
- Projected steel complicates fabrication (Fabricator)
- Not top-down construction friendly (Fabricator)
- Bottom horizontal stirrup too tight (Fabricator)
- Raked finish difficult on sides (Fabricator)
- Removal of side forms may be difficult (Fabricator)
- Hard to screed (Fabricator)
- Clearance to the bottom flange (Fabricator)

6. What modifications would you propose to ease construction difficulties and cost or fabrication and transport difficulties and cost?

- Eliminate transverse hook with headed bar, also try a drop-in cage (Contractor)
- Non-composite design to support crane for top-down construction (Contractor)
- Roughening of the surface should be done with water-blasting (Fabricator)
- Draft sides (Fabricator)
- Cast sides smooth and get bond with rebar (Fabricator)

7. Would light-weight concrete make a big difference in construction time and/or cost or have an impact on fabrication cost?

- No advantage to light-weight concrete (Contractor)
- It would reduce shipping cost if more than one element can be shipped on truck (Fabricator)
- Higher material cost (Fabricator)
- Possibly on shorter widths or shorter sections (Fabricator)

5.7.1.2 NEXT-D Beam:

1. Fabrication difficulty compared to cored-slab (1 being easier, 5 being more difficult):

4

2. What is the relative time, compared to hollow-core bridges, to construct one span (i.e. set beams, place reinforcement and any concrete/grout)?

Relatively same time to construct as hollow core

3. What is the relative erection cost, compared to hollow-core bridges, to construct one span (i.e. set beams, place reinforcement and any concrete/grout, crane capacity)?

Between 5% and 25% more expensive compared to hollow core (would require 100 ton crane)

4. What details of the proposed section are friendly?

- Deck in Place (Contractor)
- Key Details (Contractor)
- Difficulty similar to hollow core (Fabricator)
- Forms would allow F or D (Fabricator)
- Quite versatile, would allow producer to invest in forms (Fabricator)
- For cross-slope, sloping of the cap would be allowed (It is not preferred in hollow core) (Fabricator)
- Side forms can be reused for multiple depths and/or widths (Fabricator)
- No voids (DOT)
- Clean (Fabricator)

5. What details of the proposed section are unfriendly?

- Weight (Contractor)
- Studs must be off-set at plant correctly (Contractor)
- Possible broken corners (Contractor)
- Grinding - camber between sections (Contractor)
- Vertical and sag vertical curves would be difficult (Contractor)
- Projected steel is too frequent (Fabricator)
- New forms (Fabricator)

6. What modifications would you propose to ease construction difficulties and cost or fabrication and transport difficulties and cost?

- Use stay-in-place-forms for key detail (Contractor)

- Add 2" cover for grinding (2" min cover must be maintained after grinding) (Contractor)
- Reduce depth to 18" (Fabricator)
- Use of sleeves or another alternative to studs (Fabricator)
- Section should not be 12 ft. wide because of the need of a permit to transport it (Fabricator)
- Removable heads (Fabricator)
- 4" development length for welded wire fabric, D31 wire #5 bars and would likely be cheaper (Fabricator)
- Make joint at center wider to slope crown at center (Fabricator)
- Possibly using threaded couplers to eliminate bolts (DOT)

7. Would light-weight concrete make a big difference in construction time and/or cost or have an impact on fabrication cost?

- Could drop crane size one class (Contractor)
- Could make erection easier (Contractor)
- It would reduce shipping cost if more than one element can be shipped on truck (Fabricator)
- Higher material cost (Fabricator)

5.7.1.3 Clemson Adaptation:

1. Fabrication difficulty compared to cored-slab (1 being easier, 5 being more difficult):

4

2. What is the relative time, compared to hollow-core bridges, to construct one span (i.e. set beams, place reinforcement and any concrete/grout)?

Relatively same time to construct as hollow core (Contractor)

3. What is the relative erection cost, compared to hollow-core bridges, to construct one span (i.e. set beams, place reinforcement and any concrete/grout, crane capacity)?

Between 5% and 25% more expensive to construct as hollow core (Contractor)

4. What details of the proposed section are friendly?

- Good width (Contractor)
- Fewer joints to grout (Contractor)
- No use of formwork (Contractor)
- Minimal rebar use (Contractor)
- Crane movement for multiple spans (Contractor)

- Not quite as flexible with width adjustment (Fabricator)
- No voids (Fabricator)

5. What details of the proposed section are unfriendly?

- Headed rebar projections (Contractor)
- Headed rebar offset (Contractor)
- Projected steel for side forms (More difficult than NEXT D because of shape) (Fabricator)
- Stirrup placement would be difficult (Fabricator)
- Not as friendly, width difficult to adjust (Fabricator)
- Stirrups (Fabricator)

6. What modifications would you propose to ease construction difficulties and cost or fabrication and transport difficulties and cost?

- Reduce rebar projection length in order to avoid setting conflict (Contractor)
- Grinding vs. grooving (Contractor)
- Dowel details projection from cap. Drill and epoxy (Contractor)
- Stud splice (Fabricator)
- Welded wire fabric (Fabricator)
- Change stirrups to rectangular shape

7. Would light-weight concrete make a big difference in construction time and/or cost or have an impact on fabrication cost?

- It would reduce erection cost (Contractor)
- It would reduce crane size (Contractor)
- The use of lightweight might be an issue for the shear key (Contractor)

8. Please rank in order the section most fabricator and contractor friendly.

9. Please identify the shear key detail which is most fabricator and contractor friendly.

Section	Rank		Comments (if any)
	Contractors	Fabricators	
Option A	3rd	4th	Elliptical hollows may be a safety issue (Fabricator)
Option B	2nd	2nd	
Option C	4th	1st	Simplest (DOT)
Option D	1st	3rd	Elliptical hollows may be a safety issue (Fabricator)

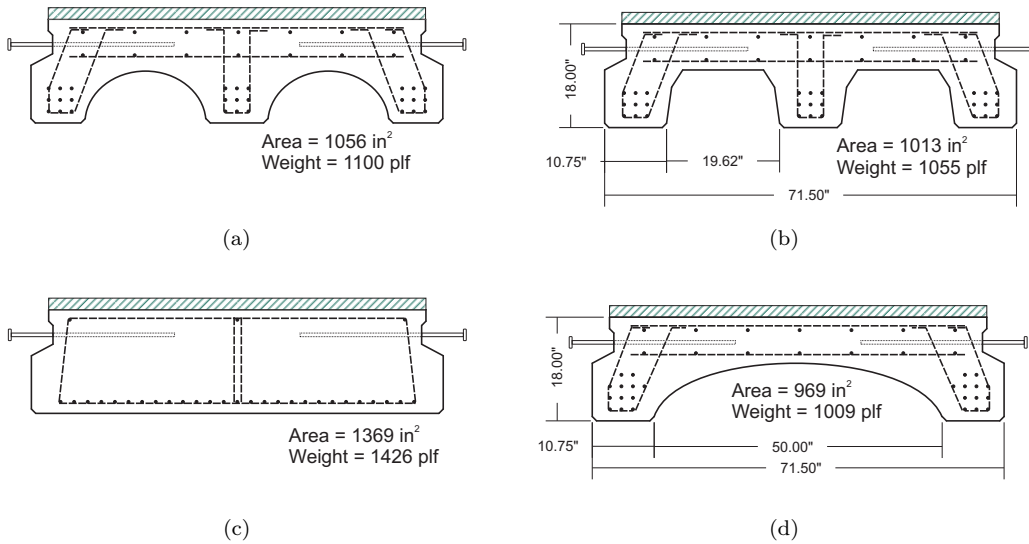


Figure 5.4: Possible sections requiring feedback

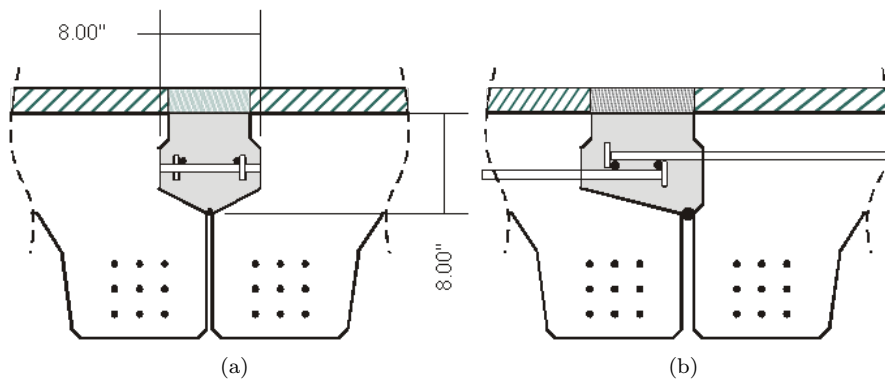


Figure 5.5: Longitudinal joint options

Section	Rank		Comments (if any)
	Contractors	Fabricators	
Option A	1st	1st	Vertically offset studs (Fabricator)
Option B	2nd	2nd	Makes bed directional (Fabricator) Makes vertical offset good for fabrication in either section (Fabricator)

5.7.1.4 Continuity - Headed Option:

1. What aspects of the proposed details are friendly?

- Pier B intermediate (Contractor)
- Abutment detail supports multiple construction sequence (Contractor)
- Pier A intermediate, length of product would affect tolerances (Fabricator)

2. What aspects of the proposed details are unfriendly?

- Potential rebar conflict (Contractor)
- Keyway in-cap (Contractor)
- Preferred (Contractor)
- Sensitive tolerance on length (1.5" joint) (Fabricator)
- Not quite flexible, especially for side form (Fabricator)
- Longitudinal direction location specific, no turn around (Fabricator)

3. What modifications would you propose to ease construction difficulties and cost or fabrication and transport difficulties and cost?

- Allow straight drop (Contractor)
- Allow symmetry placement (Contractor)
- Hook overlap for bar placement (Contractor)
- Design allowed for crane to move across for multiple spans (Contractor)
- 6' panel preferred (Contractor)
- Product symmetry would be easier (Fabricator)

4. Is the fact that the profile at each end of a section is not identical overlay problematic?

- No (Contractor)
- Yes, it is too easy to place sections backwards (Contractor)
- Yes (Fabricator)

5.7.1.5 Continuity - Hooked Option

1. What aspects of the proposed details are friendly?

- Preferred over headed option (Contractor)
- Runs concrete amount up and makes pouring joints out of truck reasonable (Contractor)
- Helps being able to have time between pouring approach slab and setting members (Contractor)
- Ends are the same (Fabricator)
- Seems pretty clean (Fabricator)

2. What aspects of the proposed details are unfriendly?

- Projecting rebar (Fabricator)
- Requires holes in formwork
- Hooks would reduce shear resistance (Fabricator)
- Headers made need to be slotted (Fabricator)

3. What modifications would you propose to ease construction difficulties and cost or fabrication and transport difficulties and cost?

- Increase space to put rods in (Contractor)
- Change hook to L-shape (Fabricator)
- Hooked bars placed at top (Fabricator)
- Preferably bend bars after fabricated (Fabricator)
- Rebar projecting from cap into hole cast in slab (Fabricator)

5.7.1.6 Wrap-up Meeting Notes

To close the mini-workshop a wrap-up meeting was held. The following is a list of significant comments coming from the meeting is provided below.

- Considering changing NEXT-D to 18" deep which would take around 10,000 pounds out of member. There are still concerns about whether this is enough to help contractors since 2" need to be added to the section for grinding so that added weight may cancel out the weight lost from making the section 18" deep.
- Thoughts on whether precasters can cast such that grinding is not necessary, since grinders are not well-liked by contractors: however fabricators do not want to be responsible for the rideability issues associated with camber problems in the members
 - Grinding and additional 2" overlay is about same price, and contractors do not like grinder being the controlling person on job site
- Forms startup cost issue: could lead to one fabricator having a leg up on other fabricators if they take a risk on buying the forms and then the bridge type is chosen. For the next bid they would be much lower than a competing producer that must include the form cost in their bid
- Could buy NEXT-D beams from out-of-state producers to try out the bridge so that fabricators do not have to commit to the bridge type prior to a bridge being built and tested in SC.

5.7.1.7 Workshop Observation

Many of the participants in the workshop were desirous to stay with the hollow-core bridge section. They expressed that they were comfortable with the fabrication and erection of such section and would prefer not to deviate from this. However, when pressed, the overall inclination was to favor the NEXT-D section. The SCDOT steering committee came to the same conclusion and as such elected to work to implement the NEXT-D bridge beam (communicated via email on August 26, 2010). One specific change that the SCDOT steering committee requested was to modify the cross-section of the NEXT-D beam so that it may be used in widths of 6 - 8 ft. and not 8 - 10 ft. as originally proposed by the PCINE. This had some very distinct implications on the cross-section of the beam. Fig.5.6 shows the original geometry proposed by the PCINE and also the modified section requested by the SCDOT. Fig.5.7 shows the joint geometry associated with the modified section while Fig.5.8 and Fig.5.9 show some typical lane layouts (wheel paths) using the typical widths of the modified sections.

5.7.2 Implementation of the NEXT-D beam

Based on outcomes of the workshop, the NEXT-D beam was deemed the most viable candidate by the SCDOT steering committee. The investigation of issues specific to this beam type was conducted. Part of this effort was to identify all of the research done on this particular beam type to-date. The research which is the basis for this beam type (shear key type) is work done out of the

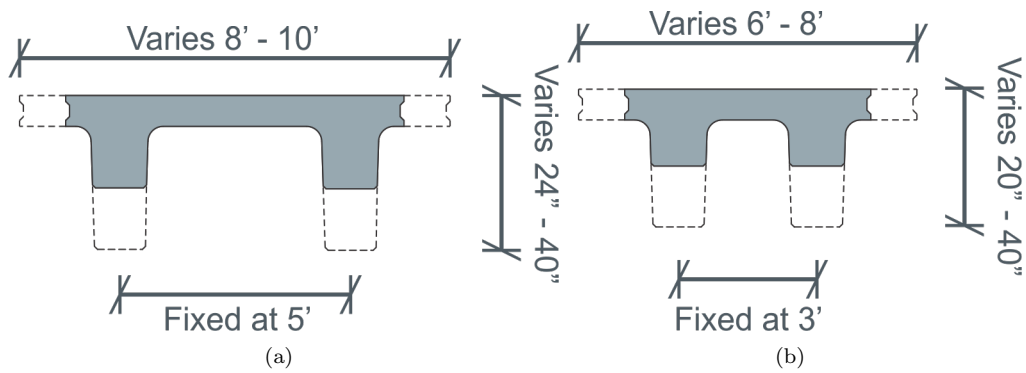


Figure 5.6: NEXT-D geometry requested by the SCDOT

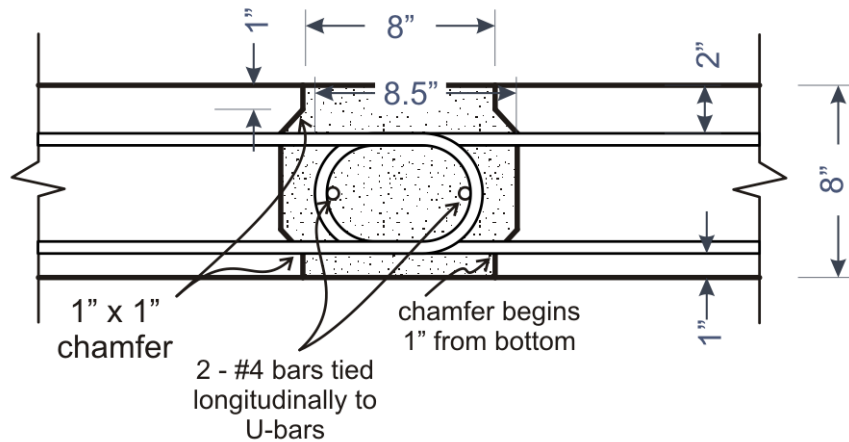


Figure 5.7: Modified NEXT-D joint configuration

University of Tennessee, Knoxville as part of an NCHRP project (12-69) (Oesterle and Elremaily, 2009). This project focused on the experimental analysis of a 6 in. deep diamond shape shear key which uses #5 headed bars in a staggered configuration. Other related work by the FHWA has explored the use of ultra-high performance concrete in similar type shear keys (Graybeal, 2010b,a). This showed much improved performance as compared with traditional non-shrink grouts. Research results are very positive and as such inspired the NEXT-D development team (PCINE) to adopt the concept in their “new” system. Basic engineering judgment was used to extrapolate the NCHRP 12-69 findings to the NEXT-D beam application.

As a follow-up, the lead developers of the NEXT-D beam, Mr. Mike Culmo of CME Associates, Inc. and Ms. Rita Seraderian of PCI Northeast, were contacted on September 1, 2010 to further explore any perceived issues which might prevent the implementation of the NEXT-D beam. During the course of the conversation a couple significant issues were raised (see Appendix E for letter from Mr. Culmo). Among these issues are that the performance of the shear key in its cur-

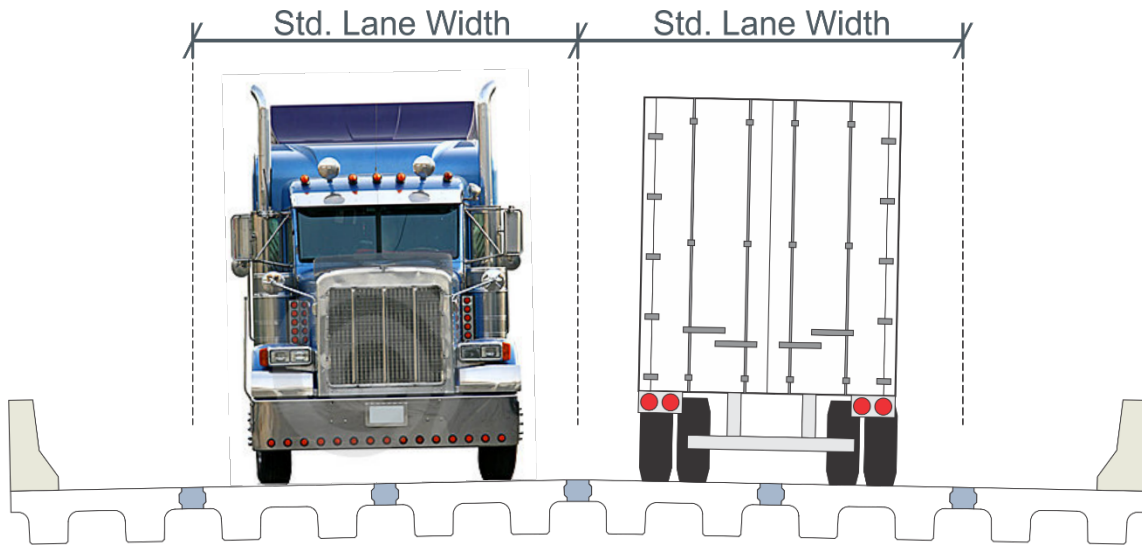


Figure 5.8: NEXT-6 possible wheel path

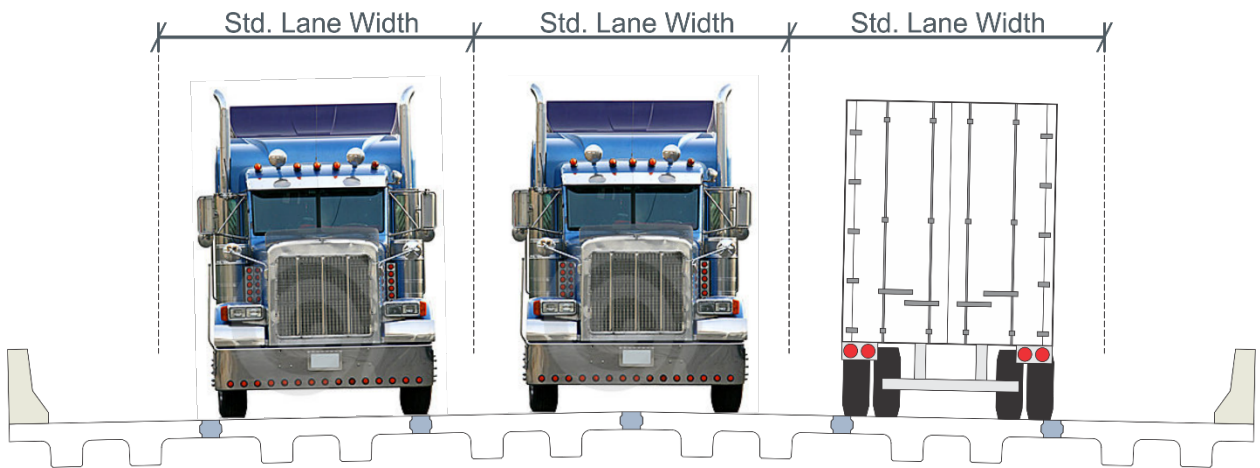


Figure 5.9: NEXT-8 possible wheel path

rently proposed configuration (i.e. shape and reinforcement placement) had not been experimentally verified yet. The previous tests focused on determining the moment capacity of the shear key (Baur et al., 2010) while the shear behavior was not fully investigated. In addition, the actual shear and moment demands on the shear key were not well understood. Several questions were raised with respect to this: Does the AASHTO LRFD strip method apply to this beam type when performing slab design? Are the shear forces and design moments in AASHTO conservative or un-conservative when some of the slab spans are very short while adjacent spans are longer (up to two times)?

At the time the decision was made to move forward with the NEXT-D beam was made, it showed extensive promise in the area of accelerated bridge construction. However, it had not yet been built since the concept was only released early in the year of 2010. Its actual performance was still uncertain and as such was not recommended for high-volume roads. Interestingly enough, it is the belief of the NEXT-D development team that this bridge type is ideal for high-volume roads (Culmo and Seraderian, 2010). However, the development team could not confidently recommend it for that use until the aforementioned key issues were addressed.

As a result of the research gaps associated with the NEXT-D beam, an experimental and analytical program was developed to specifically address these gaps. Specifically, an experimental phase was initiated to explore the capacity and performance of the proposed shear key configuration. An analytical phase was initiated to examine the demand that is placed on the NEXT-D beam components including the deck, the shear key and the beam itself. The next couple of chapters present these studies and then present the proposed bridge design to be used in South Carolina as a feasible alternative to flat slab cast-in-place bridges on high volume roads.

Chapter 6

Performance Assessment of NEXT-D Shear Key

6.1 The Big Picture

The next three chapters (including the experiment, demand evaluation, and bridge design) are interdependent because of the shear key associated with the NEXT-D bridge. Indeed, the shear key influences, not only the behavior and performance of the bridge, but also the load demand placed on the bridge components and their subsequent designs. Thus it is difficult to discuss the performance assessment of the shear key without knowing the implications relative to analytical modeling. The specific link between the chapters is the stiffness matrix associated with the shear key. Information related to this matrix and the resulting performance prevents a linear presentation of the research which was conducted. To make the flow of this interaction more clear for the reader, an overview of the big picture is provided here.

The experiments of Chapter 6 aim at fully understanding the performance of the shear key with respect to stiffness and strength in the static sense and durability under fatigue. One of the unknowns is the magnitude of the fatigue load, which in the case studied is determined using a 3D finite element model of the NEXT-D bridge. However, this model required knowledge of the shear key stiffness which was provided by the static test results. To evaluate whether the fatigue load exerted is conservative or not, the stiffness obtained from the fatigue test will be compared with the stiffness from the static test. Refer to Figure 6.1 for a visual illustration of the performance assessment procedure. As far as the final design is concerned, the 3D bridge finite element model is used to determine both the transverse (deck) and longitudinal (beam) demands, which will provide a reference for further simplification of the beam design and deck design. In order to get a reasonable demand distribution, the shear key stiffness again is the key. This stiffness matrix will be determined based on the experimentally calibrated shear key finite element model. Therefore, this chapter will occasionally refer to the work presented in Chapters 7 and 8 while those chapters will refer to the work presented in Chapter 6.

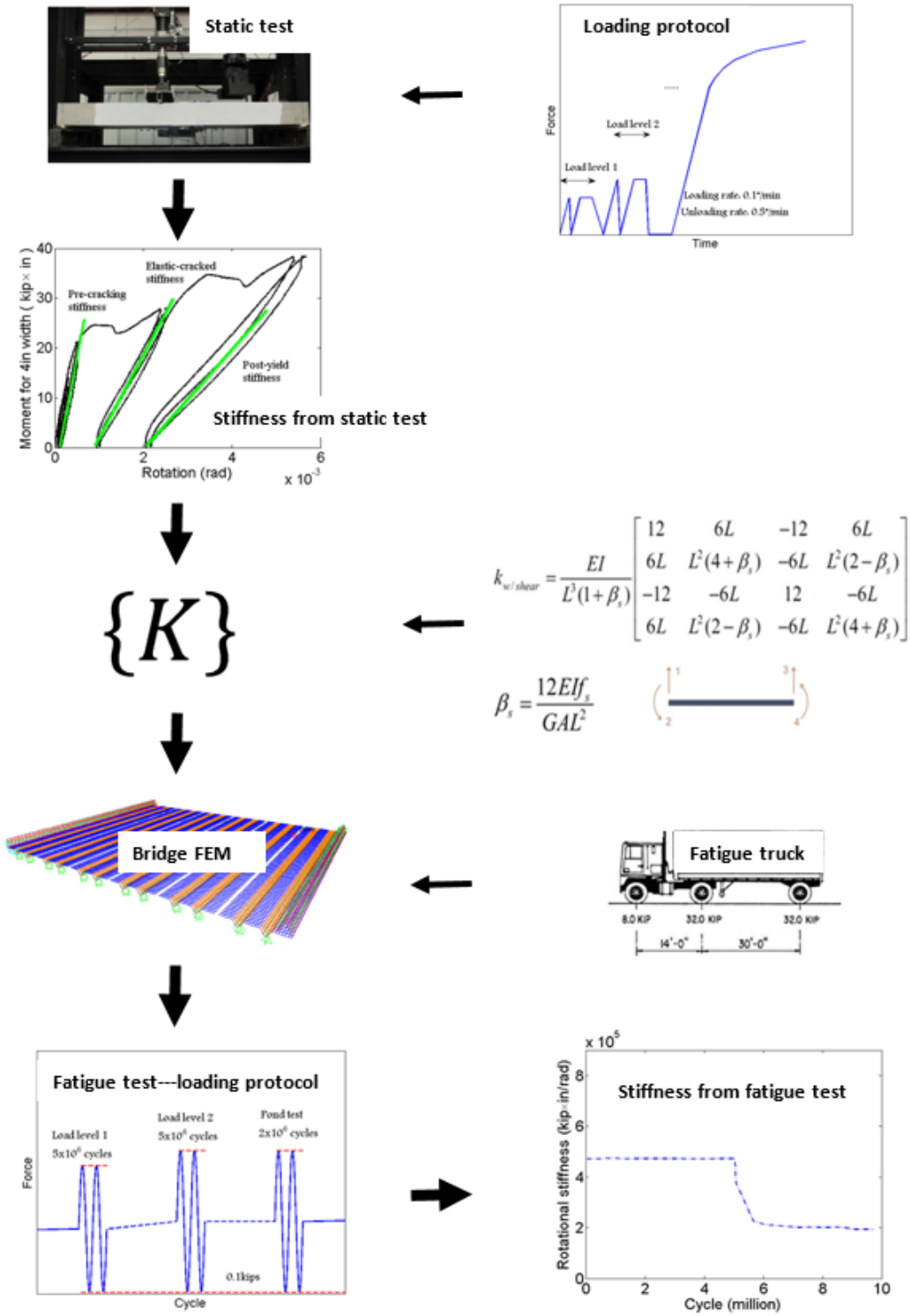


Figure 6.1: Performance assessment procedure

6.2 Introduction

The durability of transverse joints associated with adjacent precast concrete beams/slabs is a serious concern for state highway departments. The movement towards accelerated bridge construction (ABC) will only increase the number of precast concrete bridges built as existing bridges are replaced and new bridges are needed as the transportation routes are expanded. In South Carolina (SC) as well as most other states, the durability of longitudinal joints between adjacent prestressed hollow core concrete slabs compelled the South Carolina Department of Transportation (SCDOT) to look for alternative designs for short-span bridges on low volume roads and to see whether this bridge design is also suitable for use on high ADT roads in-place of cast-in-place concrete bridges or precast concrete bridges with a structural topping. According to an earlier investigation (Deery, 2010) - see also Chapter 5, the NEXT-D system developed by the Northeast Region of the Prestressed Concrete Institute (PCINE) was identified to be a promising alternative. This NEXT-D beam system is essentially a precast concrete double-tee beam (see Figure 6.2) with U-bars extending from the edges of the flanges into field cast shear keys. The original configuration used headed bars (see Figure 6.3) but was changed so that the shear key reinforcement could better control cracking.

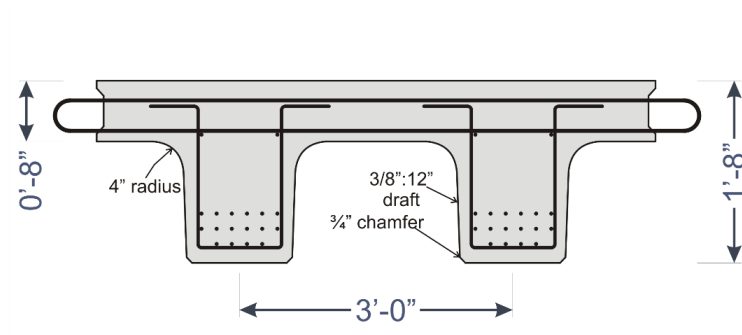


Figure 6.2: Modified NEXT-D examined in this study

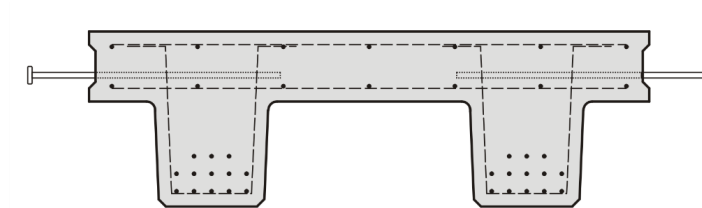


Figure 6.3: Original NEXT-D configuration with headed reinforcement

The detail of the shear key provides the required continuity between units and eliminates the need for additional transverse post-tensioning or structural topping over the precast concrete units. The NEXT-D beam system can be used to facilitate accelerated bridge construction and is

believed to be suitable for high ADT roads (Baur et al., 2010). However, before the NEXT-D beam system can be constructed, especially on the high ADT routes, several key issues still need to be resolved.

Additional testing to investigate the strength and stiffness of the shear key in the current configuration (i.e. shape and reinforcing details) needs to be conducted considering a number of different load demand scenarios. Previous tests on similar connections have focused on the behavior of shear key under high moments. For the NEXT-D beam studied, one must recognize that large shear forces and relatively small bending moments may exist and this aspect has not been investigated. Graybeal (2010b) performed some studies on diamond-shaped shear keys using UHPC as the shear key grout material to investigate long-term fatigue damage. However, the shear key shape and reinforcing details in those studies do not directly reflect those under current consideration (see Figure 6.2).

While the literature suggests that the NEXT-D beam system appears ready for implementation, there are a few issues, such as fatigue issues, that need to be addressed before bridge engineers can have confidence in specifying this bridge system on high volume roads. An experimental research program was undertaken to study the structural behavior of the longitudinal shear key and its influence on the design of the bridge system. Experiments focus on both the capacity and load-deformation behavior of the shear key under static loading and also the reduction in strength and stiffness after an accumulation of many cycles of low level loading to address fatigue.

Given that the shear key is intended to create transverse continuity and that the shear key demand is a function of the stiffness of the shear key, a series of tests were proposed to look at different ratios of bending moment to shear force in the key. In order to understand the actual fatigue demand on the shear key, the shear key stiffness in the static test was considered in the demand determination for the fatigue tests. Subsequently, the shear key stiffness in the fatigue tests can be used to validate the demand determination procedure. Two different commercially available cementitious premixes were used. One of the premixes was QUIKRETE Non-Shrink Precision Grout #1585 along with the addition of PVA fibers to control the formation of micro cracks. The other premix was Lafarge Ductal with the addition of either steel or PVA fibers and a high-range water reducer (super plasticizer). The results of the shear key testing along with additional analytical studies were used to determine an appropriate transverse distribution of applied loading and to validate the design of the shear key to meet desired performance with respect to both strength and serviceability (see Figure 6.1).

This Chapter addresses the following aspects: experimental setup, shear key material selection, verification of shear key reinforcing details, and recommendation for the shear key design based upon the performance of the shear key during the tests.

6.3 Experimental Setup

The experimental setup includes the use of an existing steel reaction frame - modified for the testing of shear key specimens, static and fatigue load actuators, the control system, the design of a shear key specimen and data sensors deployed on each specimen and the data collection system.



Figure 6.4: Reaction frame

6.3.1 Steel reaction frame

The steel reaction frame shown in Figure 6.4 was originally built to test wall systems under both in-plane and out-of-plane loads. This frame was also designed to be self-reacting to eliminate any attachment to a foundation. Since the shear key specimens would be tested in a horizontal position a new support system was designed and fabricated and attached to the four vertical columns of the reaction frame. The upper beams were also modified to allow the large hydraulic actuators to hang from them. In Figure 6.4, the smaller 35-kip fatigue actuator is shown in proper position to apply a load to the shear key specimen. When a static test is conducted, both actuators are shifted to the left until the larger 160-kip actuator is in proper position to apply a load to a shear key specimen.

The actuators are connected to a feedback control system that allows for either a displacement- or load-controlled system to be conducted. The static tests were run using a displacement-controlled protocol, and the fatigue tests were run using a load-controlled protocol. However, the system was also setup to monitor abrupt changes in stiffness so that the onset of possible failure could be detected and shut the system down. While the investigators were interested in the ultimate capacity of the specimen, there was no benefit to destroying the specimen and risk damage to sensors, actuators or reaction frame and more importantly the safety of the personnel conducting the tests.

6.3.2 Specimen dimensions and shear key configuration

The original shear key specimen was designed to be 92 in. in length, 48 in. in width and 8 in. in thickness with the shear key centered between two pieces of precast concrete. The shear key

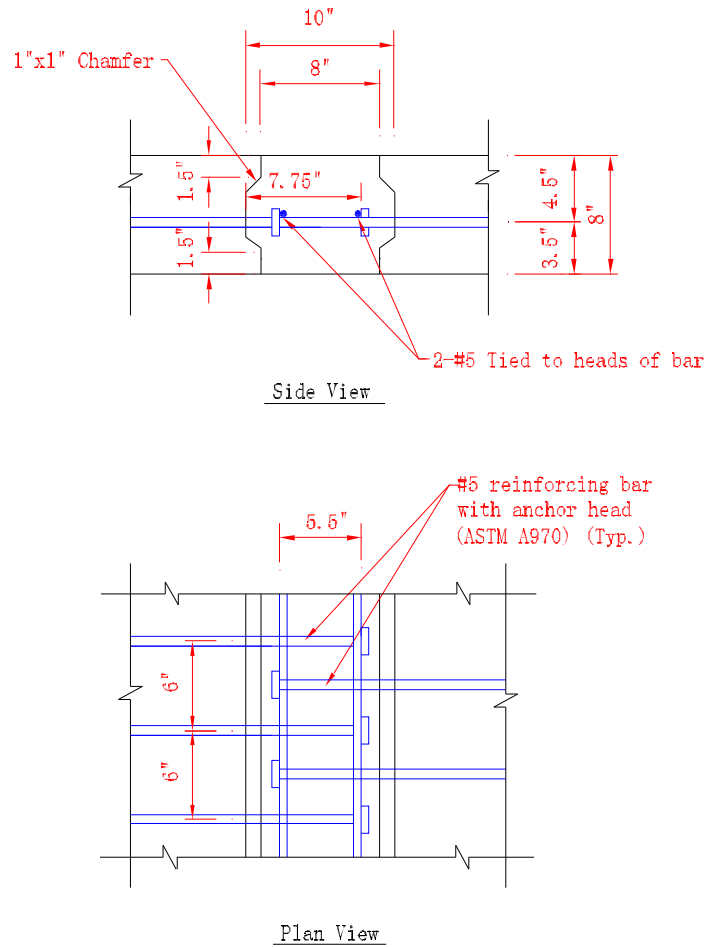


Figure 6.5: Original shear key configuration

configuration as proposed by PCINE uses a single layer of headed bar extending from each precast piece into the shear key as illustrated in Figure 6.5. Since the #5 headed bars were on staggered spacing, two #5 bars were tied to these headed bars to help facilitate tension load transfer from the headed bars in one piece to the headed bars in the other piece. In addition, five #4 bars were tied to the headed bars in each piece to serve as shrinkage and temperature steel and also hold the headed bars in proper position during casting of the specimens. The precast concrete had a 28-day design compressive strength of 6000 psi.

6.3.3 Sensor layout

Sensors were selected based upon the data that was needed to understand and quantify the behavior of the shear key specimen under either static or fatigue loading. The key information desired was the strain distribution through the thickness of the shear key, the deflection of the specimen and

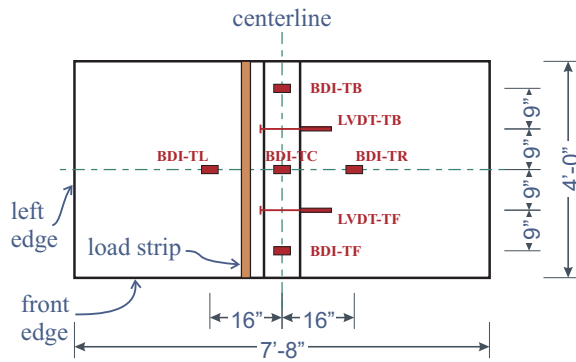


Figure 6.6: Strain gauge distribution on headed bar

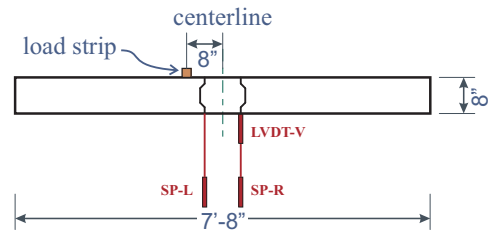
the relative rotation of the shear key with respect to the precast pieces and the possible opening of the interfaces between the shear key and precast concrete pieces. This data along with the applied loading of the specimen was collected at a regular interval during the testing of the specimen. Strain transducers were attached to the top and bottom surfaces of the specimen to measure bending strains, strain gages were adhered to selected bars extending into the shear keys (see Figure 6.6), LVDTs and string pots were used to measure vertical deflection of the specimen, relative rotations of the shear key and the opening of interfaces between each piece of precast and the shear key. The complete instrumentation diagram along with the chosen name for each sensor is shown in Figure 6.7 and Figure 6.8.

6.3.4 Loading configuration

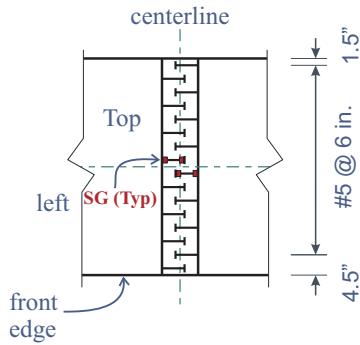
With the aim of exploring the shear key behavior under different moment to shear ratios, it was proposed that four ratios be tried including 43, 32, 22 and 12. The two extreme ratios would be tested first and the other two intermediate ratios would only be tested if deemed necessary – they were not necessary. The different moment to shear ratios are realized by only changing the position of the right support, which is 43 in. away from the center of the shear key in the high moment test (HM) and 12 in. in the high shear test (HS) (see Figure 6.9). The applied loading was placed 8 in. off-center so that the shear key had a constant shear from face-to-face of the key. The bending span for the high moment configuration was set to 86 in. to ensure that there was not a bearing failure. The high shear configuration required the specimen to be cantilevered beyond the right support so that the strength of the reinforcing steel could be fully developed. This movement of the right



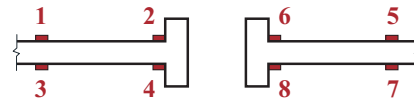
BDI and LVDT Layout - Top View



String Pot and LVDT Layout - Side View

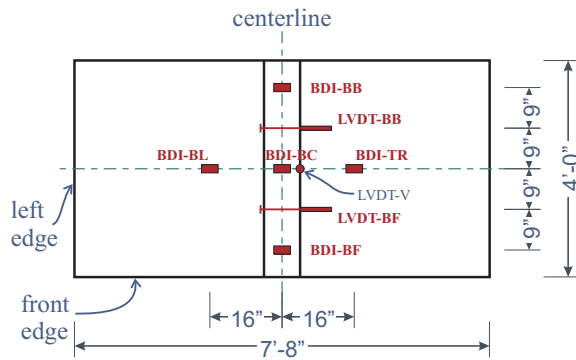


Strain Gauge Layout - Top View



Strain Gauge Layout - Front View

Figure 6.7: Initial sensor layout (part 1)



BDI and LVDT Layout - Bottom View

Nomenclature:

1: Top BDIs (same for bottom BDIs):

- BDI-TB: BDI top back
- BDI-TC: BDI top center
- BDI-TF: BDI top front
- BDI-TL: BDI top left
- BDI-TR: BDI top right

2: LVDTs:

- LVDT-TF: LVDT top front
- LVDT-TB: LVDT top back
- LVDT-BF: LVDT bottom front
- LVDT-BB: LVDT bottom back
- LVDT-V: LVDT vertical

Figure 6.8: Initial sensor layout (part 2)

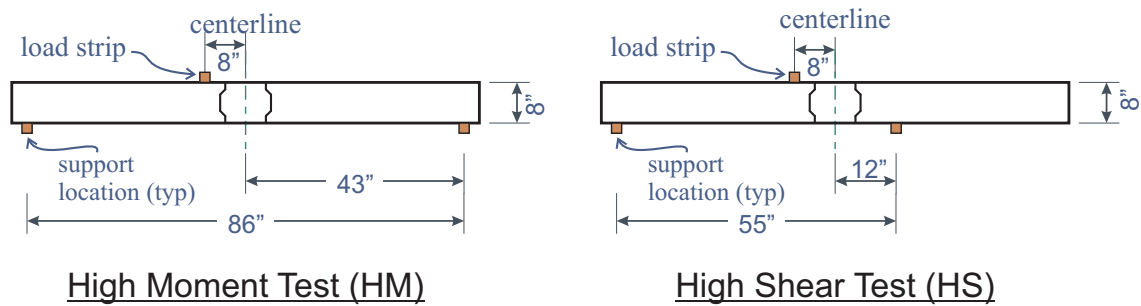


Figure 6.9: Loading configuration

support allowed all specimens to have identical fabrication and provided more versatility in making adjustments to the experimental program as results from each test were analyzed.

6.4 Primary Shear Key Material Selection

6.4.1 Selection criteria

When selecting shear key materials, four aspects are of primary concern.

1. A shear key material with high early strength is desired to facilitate accelerated bridge construction.
2. The durability of the shear key material should be exceptional and have the ability to bond to the precast concrete and create a bond strength that exceeds the tensile capacity of the weaker precast concrete.
3. The shear key material is expected to possess required workability so that long shear keys can be formed in a single pour and eliminate cold joints with the shear key material.
4. The cost of the shear key material including placement costs should be tolerable. The impact of a higher unit cost of high performing shear key material compared to typical concretes is offset by the relatively small amount of shear key material needed to construct a bridge. In fact, the size of the shear key will likely get smaller as the strength parameters of the shear key material increases.

Nowadays, high early strength with good workability is no longer a problem by the use of water reducing admixtures in the shear key material mix design. The biggest concern is the durability of the shear key material during service, which combined with a best possible shear key profile, plays a significant role in improving the durability of the shear key. This durability issue is initiated by cracking at the bond or within the key, which leads to rebar corrosion when exposed to water and deicing salts. This corrosion reduces the performance of the shear key over time. Hence, when choosing a shear key material, the critical issue is to control the crack propagation at the

bond and in the shear key itself. To realize this, a material that possesses high bonding properties, toughness, and dimensional stability is desired. Considering the fact that all cementitious materials are brittle and prone to crack, it is necessary to add supplementary reinforcement like fibers in the shear key material to control the crack propagation within the shear key itself.

6.4.2 Primary material selection

Based on the previous successful examples of similar studies (Graybeal, 2010a), the original plan for the shear key material was to use Lafarge Ductal, an ultra-high performance concrete (UHPC) with micro fibers. Typically the specification calls for the use of steel fibers in structural applications and PVA fibers in architectural (non-structural) applications. The reason for this selection of Ductal is that it is well known that the use of standard non-shrink grouts has not traditionally performed well in the proposed shear key application. Based on work performed by FHWA researchers, this UHPC shows extreme promise for meeting both strength and serviceability requirements of the shear key. Furthermore, the original objective of this research was to develop a complete design of a bridge and neither the budget nor schedule allowed for much development of shear key materials. Instead, the researchers needed to pick from existing materials with the possibility of minimal modifications. Ductal was believed to have all of the desired attributes and would likely be an acceptable shear key material and lower the risk of this research project not developing a plausible solution.

Although the South Carolina Department of Transportation (SCDOT) was concerned about the cost of Ductal, the bigger issues were the specification of a proprietary product for the shear key material and that the steel fibers supplied by Lafarge for the Ductal mix design were manufactured from steel wire drawn outside of the United States. The “Buy American” provision of the 1982 Surface transportation Assistance Act limits the amount of foreign produced steel that can be used in the construction of a bridge. The amount of steel fiber in the shear key material would typically exceed the Buy American limits and thus would require a waiver for each bridge constructed by the SCDOT. Since the SCDOT did not want to be in a position to continually request waivers, alternate mix designs were investigated – namely a typical non-shrink grout with PVA fibers added to the mix and a UHPC using PVA fibers instead of steel fibers.

A material study using an “off-the-shelf” non-shrink precision grout was considered for an alternative. Quikrete Non-Shrink Precision Grout with high strength and non-shrink properties was selected for this purpose. The Nycon-PVA-RFS400 micro fiber was selected for this investigation because it has dimensions (0.006 inches in diameter by 0.6875 inches in length), which are similar to the steel fibers dimensions (0.008 inches in diameter by 0.5 inches in length) used in Ductal. The Nycon-PVA-RFS400 micro fibers are touted to possess superior crack control properties and excellent tensile and molecular bond strength. The micro fibers are not intended to increase overall strength of the grout but rather control the micro cracking.

A control mix without fibers and three different fiber-to-grout ratios were explored using standard ASTM compression and split cylinder tests using 3 in. x 6 in. cylinders (ASTM, 2010, 2011). The four mixes are outlined in Table 6.1. The GF0.5 and GF2 mix designs represent a typical

Table 6.1: Grout and PVA fiber ratios considered

ID	Description	Volume Percentage, %
G	Grout without fibers	0.000
GF0.5	Grout with fibers (0.5 ounces / 50-lb bag)	0.085
GF2	Grout with fibers (2 ounces / 50-lb bag)	0.340
GF12	Grout with fibers (12 ounces / 50-lb bag)	2.000

range of fiber content as indicated by the fiber manufacturer (i.e. 1 to 8 lbs/yd³ of mix). The fourth mix represents a volumetric ratio that is identical to the ratio used in the Ductal material (i.e. 243 pounds of steel fiber/yd³ of mix and 45 pounds of PVA fiber/yd³ of mix). The water volume recommended for a 50-lb bag of Quikrete Non-shrink Precision Grout ranges from 3 to 6 quarts depending on the flowability needed and recognizing that the addition of more water lowers the compressive strength of the mix. Based on some experimentation, five quarts of water per 50-bag was selected so as to achieve a workable mix while obtaining a desired compressive strength.

To ensure that fibers were distributed uniformly in the grout, for GF12 cylinders, a drill mounted paint/grout paddle mixer and a bucket were used instead of a drum mixer, which was used for the other three groups of cylinders. After an approximate five-minute mixing process, the mix was scooped into the molds, rodded and tapped according to ASTM C192 (ASTM, 2007a). They were then put into the curing room immediately. Considering the fast application requirement of the shear key, the cylinders were water cured in the curing room for either two or three days with only the first day in molds. After curing, the cylinders were stored at room temperature until tested.

Cylinder tests included a compression test, a splitting tension test, and a direct tension test. The first two tests (see Figure 6.10) were performed according to ASTM C39 and ASTM C496, respectively. Table 6.2 provides a summary of the average strength values obtained from each test where each test has a sample size of three to six specimens. A few basic trends can be identified from the results. For example, the curing duration did have a notable effect on the compressive strength of the grout. The compressive strength is also adversely affected by the addition of fiber on the order of 6 to 10 percent, while the splitting tensile strength is not affected greatly until large volume ratios of fibers were used. The two percent by volume (GF12) mix design demonstrated a 13.6 percent increase in splitting tensile strength over the unreinforced grout. The individual specimen values for the GF12 and concrete are given in Table 6.3 and Table 6.4.

For the direct tension test, steel fixtures were epoxied to both ends of a cylinder. After curing of the epoxy, the cylinder was tested using a universal testing machine (UTM) by applying a tensile force to the cylinder through the steel end fixtures. A loading rate ranging between 0.020 in/min - 0.026 in/min was applied to keep the stress level application rate within acceptable limits. Although this direct tension test is theoretically applicable, it was difficult to align/level the end plates to produce a pure tensile force in the cylinder. These tests did provide an indication of the benefit of high dosage of fiber reinforcement. The ductility of each mix design under direct tension was explored and is demonstrated in Figure 6.11. Since mitigating crack propagation under fatigue

Table 6.2: Average compressive and tensile strengths of concrete and grout materials

ID	Compressive Strength(psi) ASTM C39	Splitting Tensile Strength(psi) ASTM C496	Curing(days)
Concrete-28 day	6930		
G-14 day	10340	1210	2
GF0.5-14 day	9380	1120	2
GF2.0-14 day	9560	1280	2
G-14 day	10960	1360	3
GF12.0-14 day	10230	1545	3

Table 6.3: Test results of GF12 cylinder ($3in \times 6in$)

Cylinder	Compressive Strength(psi)			Splitting Tensile Strength (psi)			f'_c (14-day)
	3-day	7-day	14-day	3-day	7-day	14-day	
1 ²	7060	9410	10200	1170	1450	1565	
2	7480	9000	10430	1200	1355	1510	
3	7630	8570	9130	1095	1300	1635	
4	7250	8710	10370	1205	1245	1485	
5	6850	9680	10760	1185	1185	1610	
6	7530	9680	10480	1205	1245	1455	
Mean f'_{cr}	7300	9180	10230	1175	1300	1545	8500
Note	1. The design compression strength f'_c is calculated using $f'_{cr} = 1.10f'_c + 700(psi)$ in accordance with ACI 318 – 11Table 5.3.2.2(ACI, 2011) 2. Cylinders 1-3 belong to a different batch from cylinders 4-6						

Table 6.4: Test results of concrete cylinder ($4in \times 8in$)

Cylinder	Compressive Strength (psi)				f'_c (28 day)
	3 day	7 day	14 day	28 day	
1	5360	5930	6180	6390	
2	5460	6080	6250	7060	
3	6090	6160	6520	7350	
Mean f'_{cr}	5640	6060	6320	6930	5500

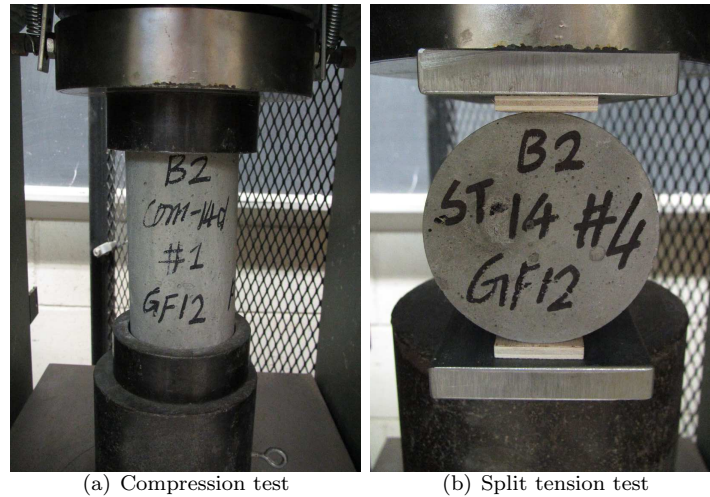


Figure 6.10: Cylinder tests

loadings is the purpose of the fibers, post-crack behavior (i.e. ductility) is a preliminary screening tool for the different mix designs. Ductility is taken as the ratio of the specimen extension divided by the specimen extension at ultimate load. As seen in Figure 6.11, the highly reinforced material (GF12) is the only material that exhibited the ability to sustain any load beyond the ultimate region. While fatigue testing is going to be required to identify if the crack control is met, these static results indicate that only one material mix should be investigated further.

In addition to the tests mentioned above, a bond strength test between concrete and GF0.5 was also performed using the same direct tension method with the purpose of getting a better understanding about the bond strength at the interface between the shear key and the slab. Bond test results suggest the bond may be more sensitive to tension than the concrete itself is.

Later a smaller diameter and shorter length PVA fiber Nycon-PVA-RECS15 (0.001496 in. in diameter x 0.375 in. in length) was selected for testing. This smaller fiber was selected to be able to get more fibers to cross any given crack for the same volumetric ratio of fiber. Like the Nycon-PVA-RFS400, the Nycon-PVA-RECS15 can also improve the ductility when the same volume percentage is used. Because the fiber is smaller, the mix would contain more fibers per unit volume and thus more uniform distribution in the new mix design, more water was added to account for the increasing surface area of the new fibers. Therefore the new mix design was 50 pounds of Quikrete Non-Shrink Precision Grout, 12 ounces of Nycon-PVA-RECS15 and 6 quarts of water.

6.5 Primary Verification of Reinforcing Details

After determining the materials to be used, the deck was then checked according to AASHTO LRFD Bridge Design Specifications for moment capacity (ϕM_n), interface shear transfer (shear friction), cracking control under service loads and minimum reinforcement requirements. This was verified with a single full-scale test of the system. In the original design detail proposed by PCINE,

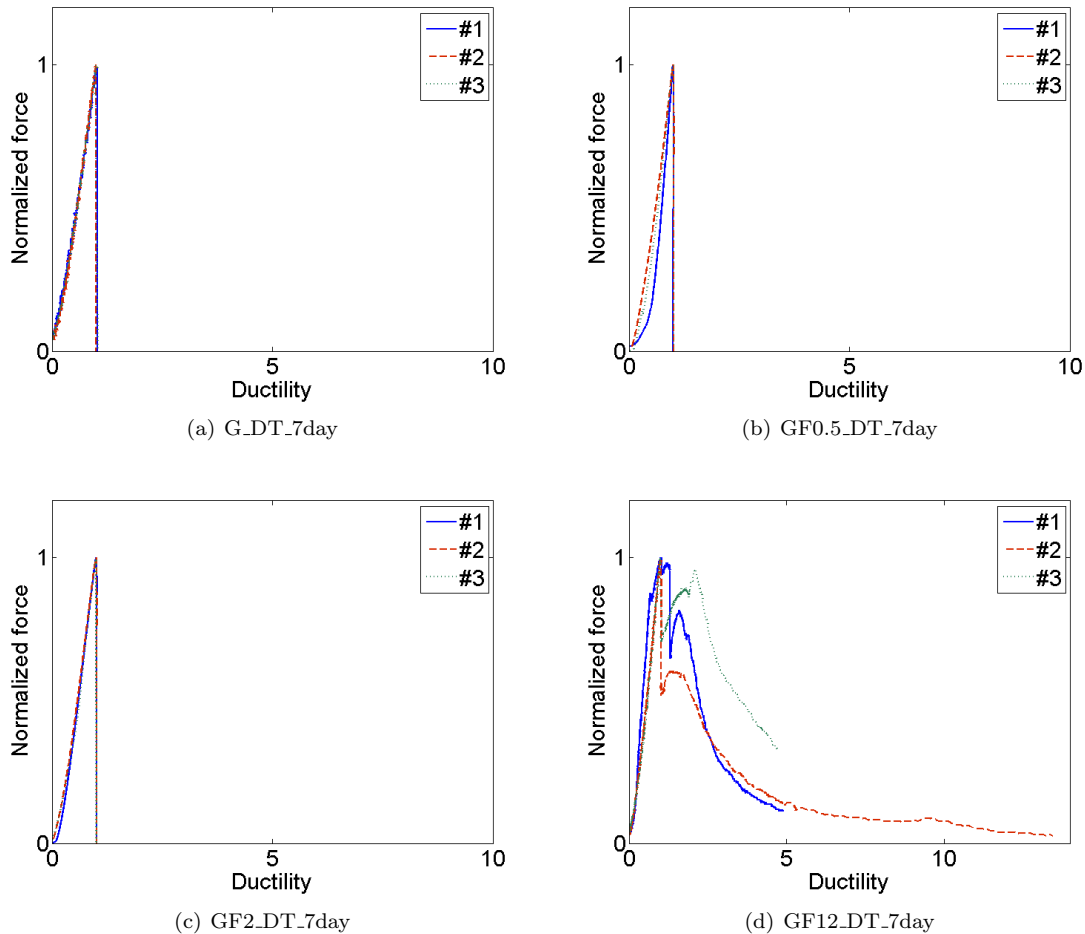


Figure 6.11: Results from direct tension test

the position of the headed rebar ($\#5@6$ in. o.c. in one layer) failed to satisfy the cracking requirement (AASHTO 5.7.3.4-1) under service loads. Since crack control is of great importance for this study, especially at the interface, a modification was proposed to use two layers of reinforcing steel instead of one. This change will allow the steel to be placed more closely to the free surfaces and thus become more effective in the control of crack width. Because of this, it was proposed that a switch from headed bars to a U-bar be considered. The U-bar allows for the centroid of the bar to be placed closer to the free-surfaces while maintaining the requisite cover as opposed to the headed bar.

Considering both the strength and serviceability requirements, a small range of reinforcement arrangements was examined. The use of $\#5$ bars does not satisfy the minimum bend radius requirement, and therefore $\#4$ bars were considered. It was decided to use a reinforcement schedule of $\#4$ U-shaped bars at 8 in. o.c. (shown in Figure 6.12 and Figure 6.14) for further testing under both static and fatigue loads.

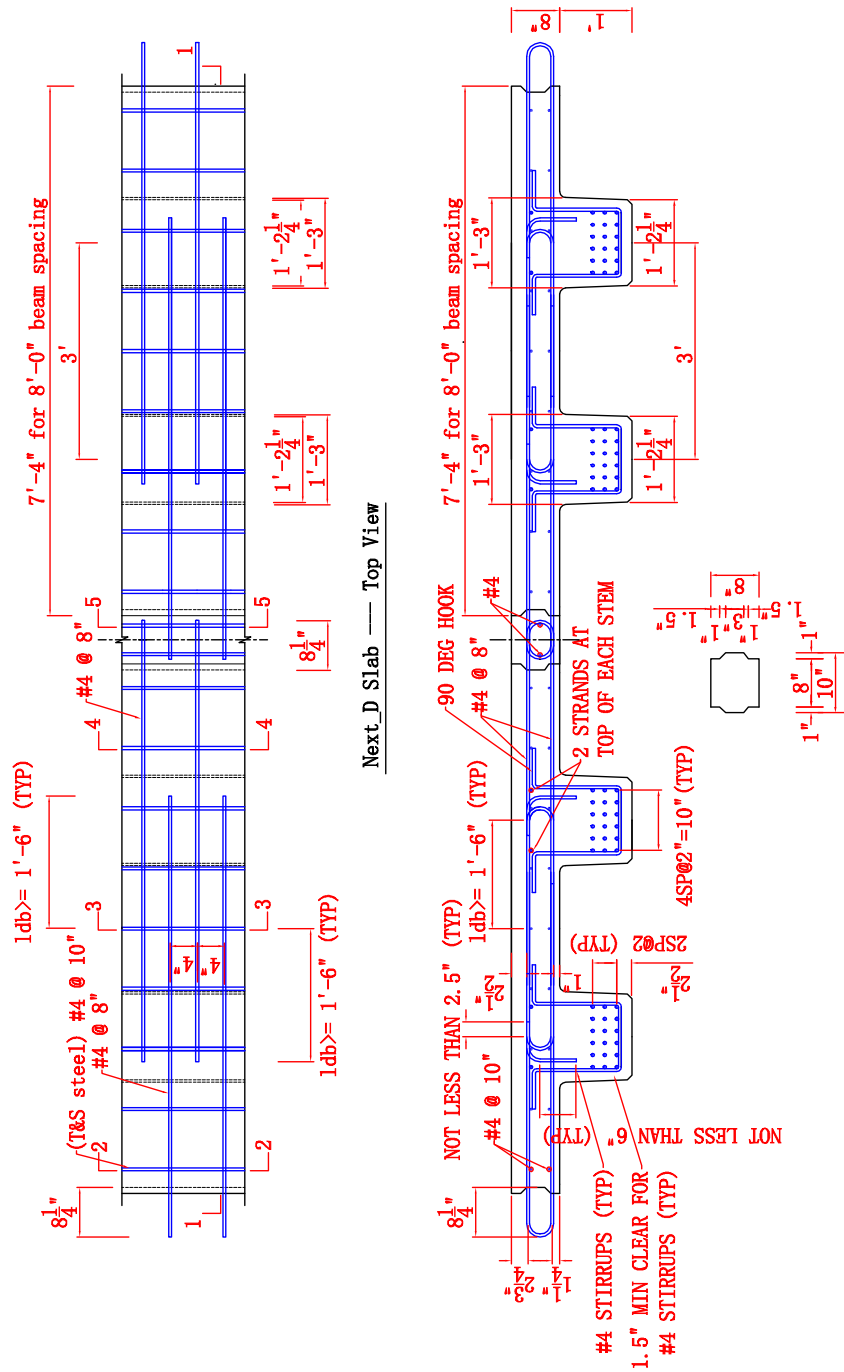
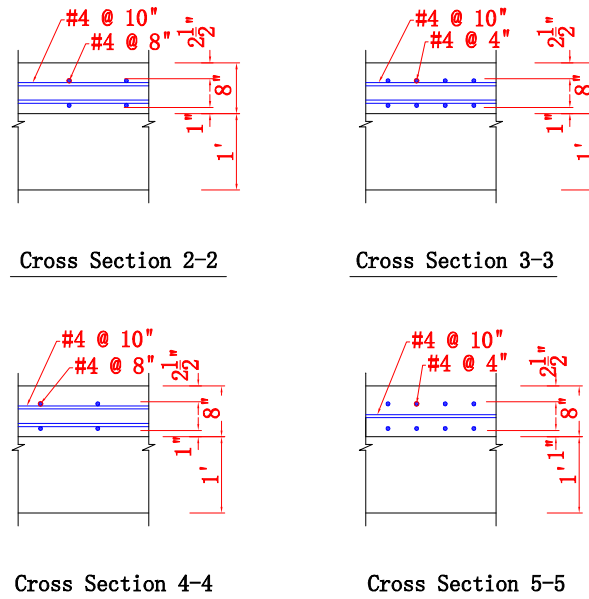


Figure 6.12: Proposed detail for NEXT-D bridge joint - part 1

6.6 Experiment Matrix Development

After the shear key material and reinforcing details were determined, the first group of specimen tests using the Quikrete Non-Shrink Precision Grout and PVA fiber mix as the shear



Note: Up to 2 inches of additional concrete may be added on top of the slab to accommodate any requisite grinding.

Figure 6.13: Proposed detail for NEXT-D bridge joint - part 2

key material was carried out. First, a static test was conducted to determine the stiffness of the specimen and the results were used to determine the magnitude of the fatigue load in a subsequent test. Due to the additional one quart of water added in the mix design for workability, the shear key material compressive strength was about 7500 psi during the day of static testing, which was quite similar with that of the concrete. The first crack in the static test happened at the interface when the bending moment across the width of the specimen reached 121 kip-in. The fatigue test showed cracks at the shear key interface after about 5000 cycles under a fatigue load level of 8.7 kips (equals 180 k-in of internal moment). A pond test conducted after 10 million fatigue load cycles showed an immediate seepage through the shear key interfaces. This fatigue load level used was later found to be higher than that required – the process is explained later in this chapter – and another fatigue test was later performed at a load of 5.3 kips (110 k-in of internal moment). As a consequence of the elevated fatigue load, the results of the fatigue test and pond test may not have direct application, but the early cracking at the interface in the static test did cause some concern in this preliminary test. The direct tensile bond test also showed bond failure. It was observed that the fiber did help control the crack propagation of the shear key, but as expected did not help improve the bond at the interface.

Due to the concerns of using Quikrete Non-Shrink Precision Grout, the next set of tests focused on using Lafarge’s Ductal with a steel fiber in the mix (JS1000) to see if there would be an improvement in the shear key performance. The test results using Ductal with steel fibers showed a

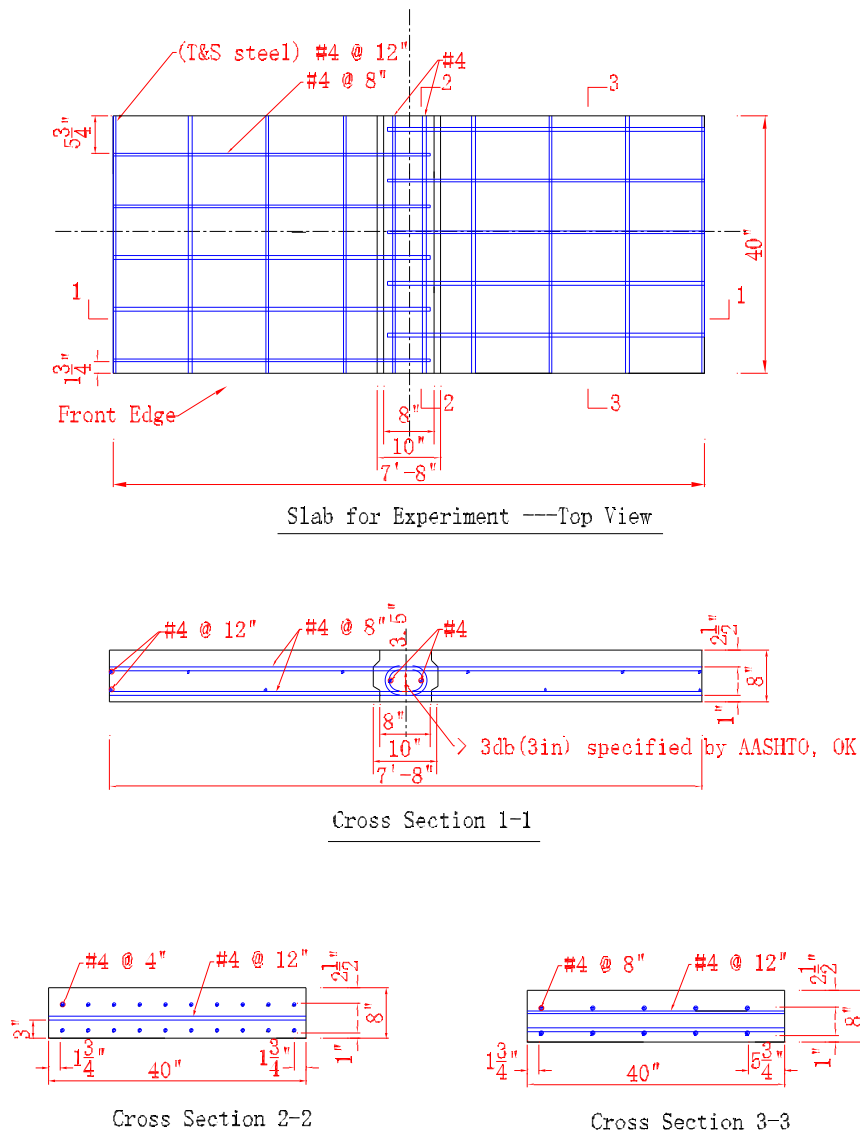


Figure 6.14: Details for specimen to be tested

significant improvement in bond cracking strength, which was 277 kip-in, 129 percent higher than that of the Quikrete mix hereafter just referred to as grout. After 10 million cycles of fatigue load which was also higher than that required, although there were slight cracks in one of the precast concrete pieces, there was no cracking along the interfaces. The subsequent 2 million cycles of loading during the ponding test showed no seepage through the interfaces. This performance clearly satisfied the design criteria.

Despite the superior performance of the UHPC with steel fibers compared to traditional non-shrink grout with PVA fibers, a mix design using UHPC with PVA fibers was tested to avoid

Table 6.5: Experiment matrix for static tests

Shear Key Mixture	Moment to Shear Ratio	Specimen ID
Quikrete Non-Shrink Precision Grout + Nycon-PVA-RECS15	43 (HM)	STA-01
		MONO-01
		MONO-01(redo)
Lafarge UHPC + steel fiber	43 (HM)	STA-02
		MONO-02
Lafarge UHPC + Kuraray PVA	43 (HM)	STA-03
		STA-04
		MONO-03
Lafarge UHPC + Kuraray PVA	12 (HS)	STA-05
		STA-06
		MONO-04

the previously mentioned concern of using steel fibers in the mix. Since the UHPC mix with steel fibers exceeded the level of performance required, it was believed that a mix design using Ductal with PVA fibers (JS2000) would provide a lower, but acceptable, level of performance. Therefore another six specimens were fabricated using Ductal with PVA fibers as the shear key material. Three specimens were tested using a high moment demand in the shear key – two static and one fatigue. The fatigue tests are also labeled as mono because following each fatigue test a monotonic static test was performed on each specimen. The remaining three specimens were tested using a high shear demand in the shear key – two static and one fatigue.

Described above is the chronological history of shear key material selection. This experiment matrix is illustrated in Table 6.5. Next detailed information from specimen casting to testing will be presented both horizontally between different groups of specimens, and vertically from static test to fatigue test within each group.

6.7 Shear Key Casting and Material Properties

The casting and curing of the precast concrete pieces was provided by Metromont located in Greenville, SC (see Figure 6.15). The specified 28-day design compressive strength of concrete was 6 ksi. After delivery of the precast concrete pieces to Clemson, the shear keys were cast at the Wind and Structural Engineering Research Facility. The next section of this report will focus on the following aspects: mixture proportions of shear key material, casting and curing of shear key and cylinders, and material properties. Specimen testing will be discussed in the next subsection.

6.7.1 Mixture proportion

The material proportions for each shear key material combination are listed in Table 6.6. For the group of Quikrete with PVA specimens, the water amount was determined through some



Figure 6.15: Slab casting at Metromont

Table 6.6: Mixture proportions of shear key material

ID	Material Combination	Fiber Dimension (in.) (diameter \times length)	Mix Design Ratio by Weight (Pre-mix:Water:Fiber:HRWR)
1	Grout with PVA fiber	0.001496 \times 0.375	50.00 : 12.52 : 0.75 : 0.00
2	UHPC with steel fiber	0.00800 \times 0.500	50.00 : 2.96 : 3.55 : 0.68
3	UHPC with PVA fiber	0.007874 \times 0.750	50.00 : 3.53 : 0.87 : 0.68

experiments as mentioned before so that a balance can be achieved between workability and compressive strength. For the two groups of UHPC mixes, the material proportions were provided by Lafarge. An extremely low water to cement ratio was possible by using a high range water reducer (HRWR). A typical UHPC mixture proportion is listed in Table 6.7 (Graybeal, 2006). In the mixture, the largest granular particle is fine sand with a dimension between 150 and 600 μm . The second largest particle is Portland cement with an average diameter of 15 μm , followed by crushed quartz, which has an average diameter of 10 μm . The smallest particle is silica fume. The large quantity of fine sand can help reduce the quantity of cement. Dimensionally speaking, steel fiber is the largest material in the matrix. The dimension and quantity of steel fibers are determined in a way so that the steel fibers can effectively control cracking, and increase the tensile capacity and toughness of the material (Graybeal and Hartmann, 2003). In this typical mixture, two percent by weight of steel fibers with a diameter of 0.008 in. and a length of 0.5 in. are used.

6.7.2 Preparation and shear key material mixing

Within a couple of days of casting, the shear key interface of the precast concrete pieces were sand blasted at the casting yard to roughen the surface for improved bond between the shear key material and the precast concrete. Prior to placing the shear key, the interface was washed to

Table 6.7: Typical proportions of UHPC (per yd³ of UHPC) (Graybeal, 2006)

Material	Amount (lb.)	Percent by Weight
Portland Cement	1200.0	28.5
Fine Sand	1720.0	40.8
Silica Fume	390.0	9.3
Ground Quartz	355.0	8.4
Super plasticizer	51.8	1.2
Accelerator	50.5	1.2
Steel Fibers	263.0	6.2
Water	184.0	4.4

clean the surface as shown in Figure 6.16a. Also prior to the casting, strain gauges were attached to the rebar and the lead wires were carefully routed through the side faces of the shear key (see Figure 6.16b). A couple of hours before shear key casting, shear key interfaces were rinsed with water using a sprayer and kept wet before casting to control the absorption of water from the shear key material into the precast during the casting of the shear key. The mixing of grout with PVA fibers was quite conventional, and took about five minutes to mix and maintain workability for about ten minutes. Compared to conventional concrete, mixing UHPC requires increased energy input. Therefore a high-energy mixer was used to mix the Ductal (see Figure 6.16c). On mixing days with elevated ambient air temperatures, ice was used rather than water to keep the mix cool during mixing.

6.7.3 Workability

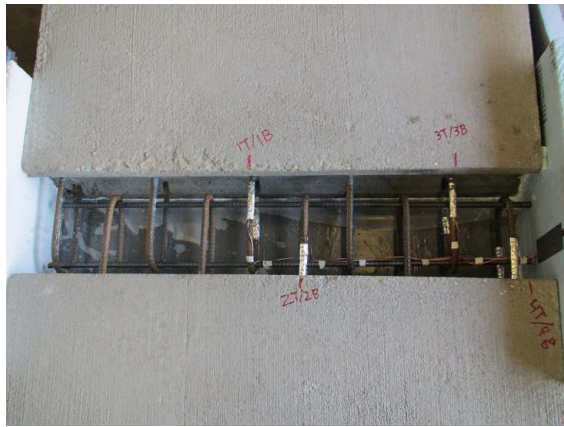
In the two UHPC mixes, one reason for the high compressive strength is a very low water to premix ratio. To create acceptable workability and flow, a high range water reducer is added to the mix. This can impact the compressive strength along with the workability. Therefore an optimum amount of HRWR needs to be used for good workability. There are several distinct phase changes in the UHPC material during the mixing. Shown in Figure 6.17a is the UHPC material near the completion of the mixing. At this point in time, the material is very sticky, but flows when placed into the formwork. To measure the flowability of the mix, a flow table test similar to that described in ASTM C1437 was used to measure the rheological properties of the UHPC (see Figure 6.17b) (ASTM, 2007b). When casting the shear key, there was no need to vibrate or even rod the material during after individual lifts.

6.7.4 Curing

Curing is very important for enhancing material properties for cementitious materials. Since UHPC has a very low water to cement ratio, it is very important to seal the top surface of the uncured UHPC with an impermeable layer immediately after casting to avoid evaporation of the water from the surface layer. If sealing is delayed too long, the surface layer will not have enough water for hydration, which will lead to self-desiccation, and subsequent autogenous shrinking, cracking, and



(a) Shearkey interface after sandblasting



(b) Strain gauge preparation



(c) Mixing of UHPC material



(d) Mixing of Quikrete material

Figure 6.16: Preparation before specimen casting and shear key material mixing



(a) UHPC at end of mix cycle



(b) Flow table test

Figure 6.17: Workability of UHPC

poor long-term durability. In the case studied, immediately after casting, specimens were sealed using a plastic film for three days (see Figure 6.18). Similar to the specimens, cylinders were cured in molds which were sealed for three days and then cured out of the molds until testing of the cylinders.

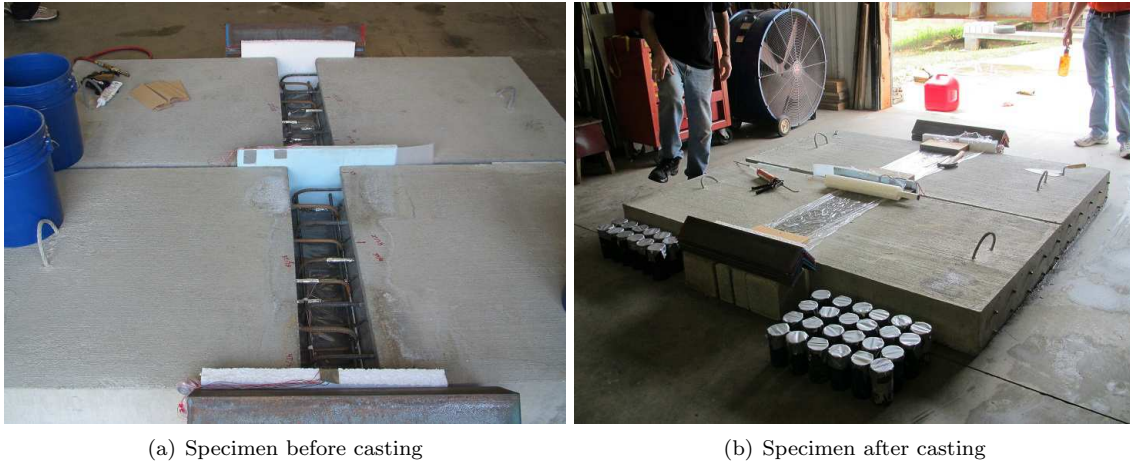


Figure 6.18: Specimen before and after casting

6.7.5 Cylinder tests

Based on the properties desired, the shear key materials were tested for compressive strength (ASTM C39), split tensile strength (ASTM C496), and bond performance. In the bond tests, the cylinders with a flat bond surface were subjected to direct tension, and the cylinders with a sloped bond surface were subjected to compression (slant shear test). For each test, the cylinders were tested at certain ages like 4-day, 7-day, 14-day, 28-day, and also on the initiation of either a static or fatigue test of a shear key specimen. Since UHPC has a very high compressive strength, testing a 6 in. by 12 in. cylinder would require a very high capacity test machine. According to Graybeal (2006) and Graybeal and Davis (2008), a decreased cylinder size of 3 in. by 6 in., and an increased loading rate of 150 psi/sec are acceptable. In this research, only 3 in. by 6 in. cylinders were used. Considering there were not many cylinders to be tested and it would be better to keep the loading rate the same for both the UHPC mix and the grout mix, the loading rate was kept within the range specified by ASTM C39, which is 200 lbs./sec to 300 lbs./sec for a 3 in. x 6 in. cylinder.

In the direct tensile bond test (see Figure 6.19), the ends of the cylinders were epoxied to steel end plates that could be attached to the base platen and crosshead of a UTM machine. A displacement rate of 0.026 in./min was applied to keep the strain rate within the acceptable range. Knowing that there are many drawbacks with the direct tensile test like the alignment issue and the epoxy issue, this test is mainly for a bonding performance (failure modes) study. In addition to the tests mentioned above, pull-off tests according to ASTM C1583 were performed at the same

Table 6.8: Cylinder test results

Mixture ID	Compressive Strength (psi)		Splitting Tensile Strength (psi)	
	4-day	28-day	4-day	28-day
UHPC with steel	16290	26970	2665	N/A
UHPC with PVA	13820	21070	1735	N/A
Grout with PVA	N/A	7400	N/A	1270

ages to test the bond between the UHPC with PVA mix with the precast concrete (see Figure 6.19) (ASTM, 2004).

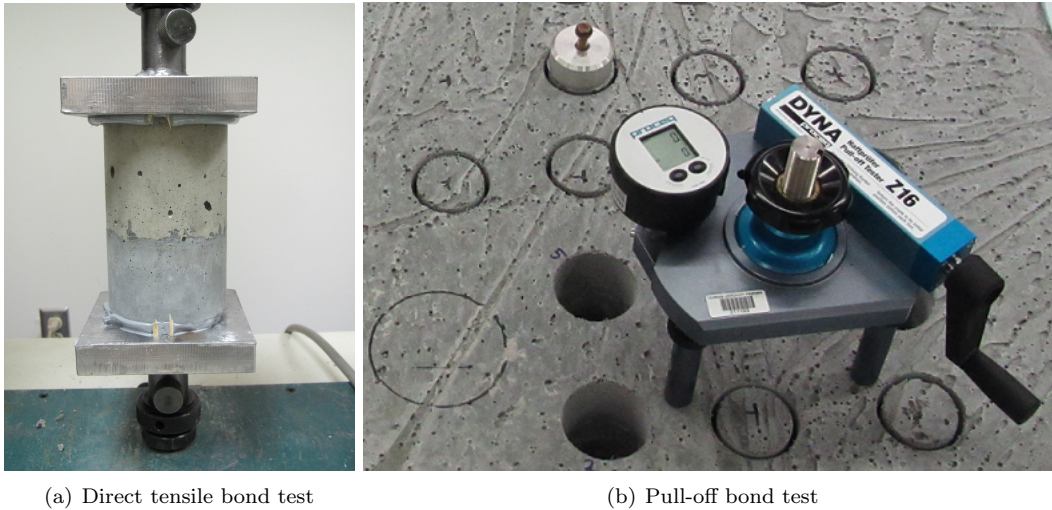


Figure 6.19: Bond test

6.7.6 Cylinder test results

The compressive strengths from cylinder tests, as illustrated in Figure 6.20, show that the UHPC with steel group had the highest compressive strength at the same cylinder age, followed by the UHPC with PVA group, and then the grout group. This relationship is mainly influenced by the water to premix ratio. The 4-day and 28-day compressive strengths and splitting tensile strengths for each material combination are listed in Table 6.8. Cylinder compressive strengths during the static and fatigue tests are listed in Table 6.9 and will be later referenced in the subsection of experimental result analysis.

For the UHPC groups, all the bond tests including direct tensile test, slant shear test, and pull-off test show that most of the specimens failed in the concrete (see Figure 6.21a and Figure 6.21b). A typical failure mode from pull-off tests is shown in Figure 6.22. For the grout group,

Table 6.9: Compressive strengths during tests

Specimen ID	Precast (psi)	Shear Key (psi)
STA-01	7500	7500
STA-02	8280	25490
STA-03	9530	15190
STA-04	9680	18510
STA-05 and 06	8730	22330
MONO-02	8070	26970
MONO-03	6530	21070
MONO-04	6570	N/A
MONO-01(redo)	6280	7670

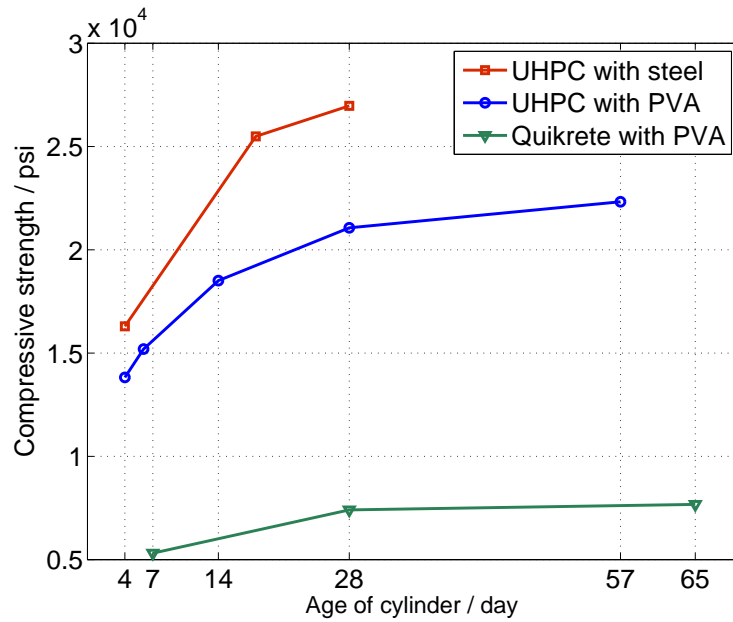


Figure 6.20: Cylinder compressive strengths during specimen tests

the typical failure is at the bond in both the direct tensile test and slant shear test (see Figure 6.21c and Figure 6.21d). For the UHPC groups, the slant shear test results indicate that although the cylinders failed in the concrete, their strengths are slightly higher compared with those of pure concrete (see Figure 6.23), which may result from the restraint of the UHPC material.



Figure 6.21: Cylinder failure modes in bond tests

6.8 Specimen Testing

For each group of specimens in the experiment matrix mentioned in Table 6.5, both static tests and fatigue tests were conducted. For each specimen, the concrete casting date, shear key casting date, and specimen testing date are summarized in Table 6.10 for later reference. The results from the static test are not only used in the fatigue load determination, but also used in the calibration of the shear key finite element model. The results from a fatigue test can highlight the performance of the shear key joint durability, and also validate the fatigue load exerted on it.

The slab is simply supported on two steel rods covered by a dense plastic tube that are aligned parallel to the shear key. In the high moment test, the slab has a span of 86 in., with the



Figure 6.22: Pull-off test results for the UHPC with PVA combination

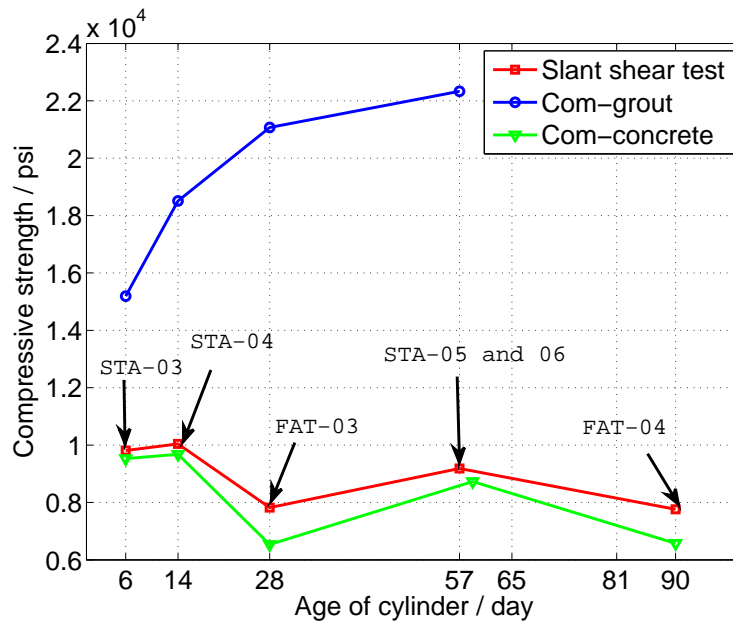


Figure 6.23: Restraining effect of UHPC

Table 6.10: Specimen casting date and testing date

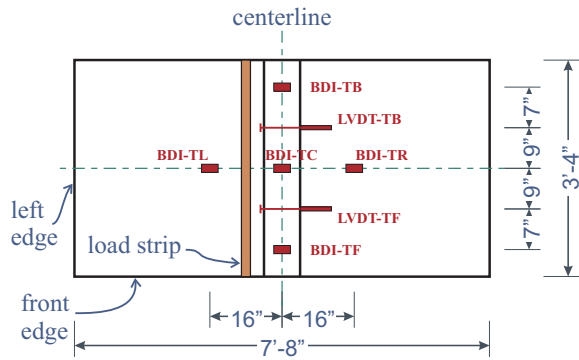
Specimen ID	Precast	Shear Key	Specimen Testing Day
STA-01	01/25/12	01/31/12	02/17/12
FAT-01	01/25/12	01/31/12	03/01 – 03/26/12
STA-02	04/11/12	04/27/12	05/15/12
FAT-02	04/11/12	04/27/12	05/23 – 06/16/12
STA-03	03/29/12	07/26/12	08/01/12
STA-04	03/29/12	07/26/12	08/09/12
STA-05	04/16/12	07/26/12	09/21/12
STA-06	04/16/12	07/26/12	09/27/12
FAT-03	06/12/12	07/26/12	08/17 – 09/10/12
FAT-04	06/12/12	07/26/12	10/11 – 11/02/12
FAT-01(redo)	09/17/12	10/16/12	11/17 – 12/11/12

right support located 43 in. from the centerline of the shear key. In the high shear test, the slab span is 55 in., with the right support located 12 in. from the shear key centerline. The load strip is a square steel tube that runs the full width of the specimen and is located 8 in. left of the centerline of the shear key. A 160-kip actuator was used for static tests and a 35-kip actuator was used for the fatigue tests. Both the static and fatigue tests were controlled using software provided by MTS. Data from all the specimen sensors, including strain transducers, strain gauges, string pots and LVDTs were acquired using LabVIEW 8.2.

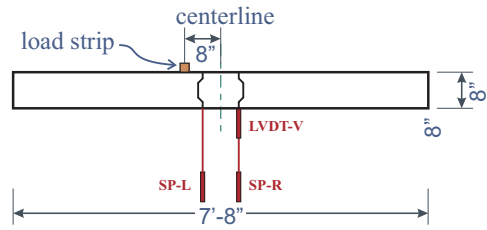
Before specimen testing, all the sensors were calibrated. The typical sensor layout is shown in Figure 6.24 and Figure 6.25. The scale factor obtained for each sensor would later be applied to the experimental data. After sensor calibration, for each group of specimens, the static test was conducted first, the results of which were processed for the shear key rotational stiffness and vertical stiffness needed in the later fatigue demand determination procedure. Before each fatigue test, the fatigue actuator was tuned to ensure the feedback signal reflect accurately the command signal. The details of the tests will be discussed in the following paragraphs.

6.8.1 Static test

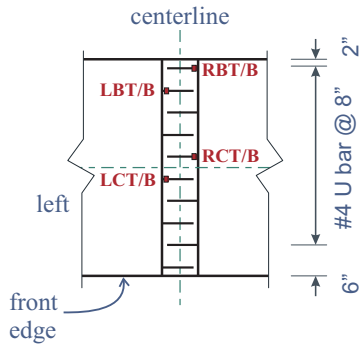
About two hours were required to complete a high moment test and 4.5 hours to complete a high shear test. The static tests are composed of several load levels. At each level, the specimen was loaded and unloaded twice until the final load level. In the second cycle at each load level, before unloading, the load was held at the specified load level, during which time crack developments were marked. There could be a drop of about 0.2 kips to 0.3 kips during the holding phase. To keep the load strip in contact with the slab, the bottom load limit is set to be 0.1 kips, rather than a complete unloading of the specimen. The test was stopped when a large deformation happened under a small load increment. The test was under displacement control, with a displacement rate of 0.1 in/min, and the unloading rate of 0.5 in/min. The rate is determined in a way such that



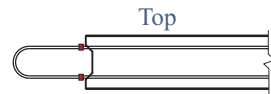
BDI and LVDT Layout - Top View



String Pot and LVDT Layout - Side View

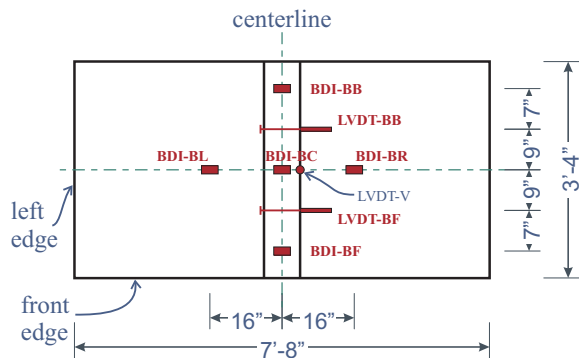


Strain Gauge Layout - Top View



Strain Gauge Layout - Front View

Figure 6.24: Final sensor layout (part 1)



BDI and LVDT Layout - Bottom View

Nomenclature - strain gauges:

- SG-LBT/B: SG-left back top/bottom
- SG-LCT/B: SG-left center top/bottom
- SG-RCT/B: SG-right center top/bottom
- SG-RBT/B: SG-right back top/bottom

Figure 6.25: Final sensor layout (part 2)

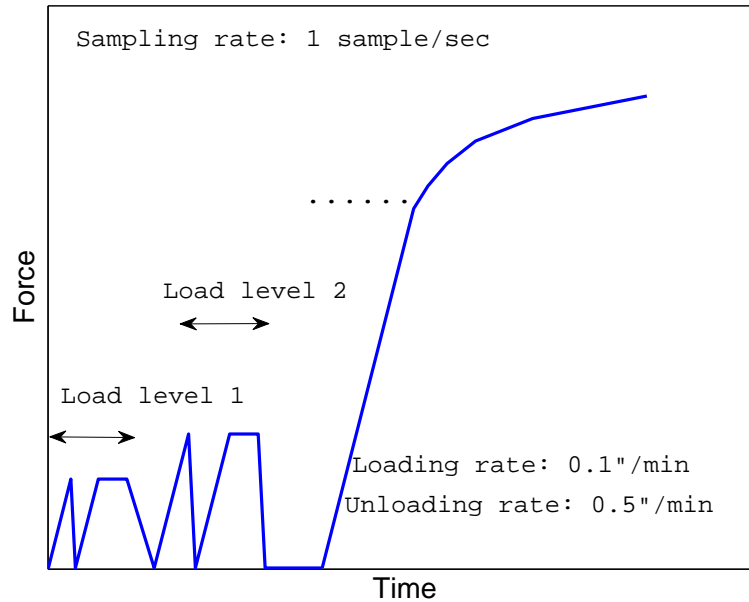


Figure 6.26: Typical loading protocol for static test

the strain rate is acceptable and the test can be finished within a reasonable time frame. Data was acquired throughout the whole process. The sampling rate was specified to provide enough data to capture the response without being overwhelmed with large data files. Refer to Figure 6.26 for a typical loading protocol.

6.8.2 Fatigue test

In order to capture the performance of the shear key during its expected service life, the fatigue test was determined to need 10 million cycles. The specimen was tested under a sine-wave load, the frequency of which was determined considering both the system response and the time available. For the high moment test, the frequency applied was 5 Hz, and for the high shear test, it was found that 6 Hz could be used. Generally a fatigue test took 22 to 25 days to complete the 10 million cycles. After building a water pond reservoir above the shear key and the surrounding area, another 2 million cycles of load were applied to the specimen. During these 2 million cycles the shear key was monitored for leakage through the shear key and the interface. After the pond test, the specimen was loaded monotonically until a large deformation was observed under a small load increment. The whole process of applying the monotonic loading only took a few minutes. The monotonic test was similar to the static test with respect to loading rate and data sampling rate. Different from the static test and monotonic test, the fatigue test was under load control. The MTS software was configured to acquire data (actuator load and actuator extension) at a rate of 10 samples / cycle for a consecutive 2 seconds after every 5000 cycles. The data from the other sensors

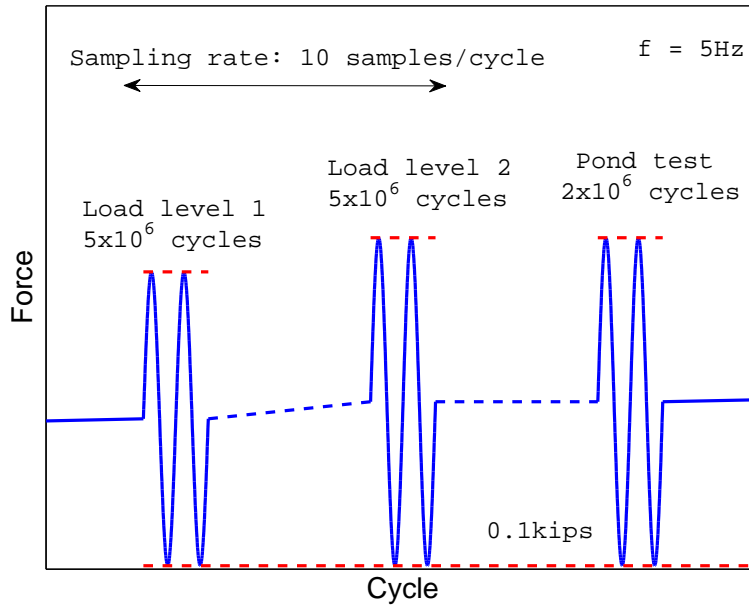


Figure 6.27: Typical loading protocol for fatigue test

were sampled at approximately the same rate in LabVIEW but roughly on a daily base for a short period of time. Refer to Figure 6.27 for a typical loading protocol.

The elastic-cracked shear key rotational stiffness and translational stiffness from the static tests were used to determine the shear key stiffness matrix in the bridge finite element model. The fatigue load was determined by exerting the design truck specified in LRFD Art. 3.6.1.2.2, (AASHTO, 2012) but with a constant spacing of 30 ft. between the two 32 kip axles. The load was exerted between the inner face of the parapet in order to obtain the critical demands in the shear key. The critical positive moment demand was then used to calculate the unfactored external force in the high moment test, and the critical shear demand was used to determine the unfactored external force in the high shear test. Two load levels were used in the fatigue test (see Figure 6.27). The final load was then calculated by multiplying a load factor of 0.75 for the fatigue II limit state, and an impact factor of 1.33 for the first load level, and 1.75 for the second load level. The impact factor used for each load level was determined based on the following reasons. According to AASHTO LRFD Table 3.6.2.1-1, for deck joints, the impact factor is 1.75 for all the limit states. It is understood that the intent of this provision is to address the impact upon transverse expansion joints. However, in the case studied, the shear key is a joint that is longitudinal to the bridge centerline and will not likely experience the same impact that a transverse joint will. Therefore, the 1.75 factor is checked and considered to be a conservative upper limit. This factor was used for the second load level. For all other components, AASHTO LRFD Table 3.6.2.1-1 specifies an impact factor of 1.15 for the fatigue limit state. Again, consider that the shear key is a joint, the impact factor should be higher than 1.15. Therefore to be conservative, an impact factor of 1.33 was applied for the first load level. The

Table 6.11: Fatigue load determination on shear key based on shear key stiffness

ID	Stiffness from Static Test		Stiffness in FEM		Fatigue Load	
	K_t (k/in)	K_r (k-in/rad)	K_t (k/in)	K_r (k-in/rad)	$IM = 1.33$	$IM = 1.75$
FAT-01	376.5	83879.0	56.5	12581.9	5.20	6.85
FAT-02	575.9	581473.5	86.4	87221.0	7.07	9.31
FAT-03	420.0	100000.0	63.0	15000.0	5.49	7.23
FAT-04	550.0	117890.0	82.5	17683.5	7.94	10.45

Table 6.12: Fatigue load applied in the test

Specimen ID	Load level Applied (Cycle/million)					
FAT-01	8.7(10.6)					
FAT-02	8.7(5.9)	9.7(4.1)				
FAT-03	4.9(1.8)	6.5(0.4)	5.4(0.4)	5.6(4.2)	7.3(3.3)	
FAT-04	8.1(5.0)	10.6(5.0)				
FAT-01(redo)	5.3(5.0)	7.0(5.0)				

required load levels for each specimen are listed in Table 6.11, and the applied load levels are listed in Table 6.12.

6.9 Analysis of Results - Performance at Strength Level

This section will focus on the analysis of the results from the performance at strength level (static test and monotonic test). Analyzed specimen performances at the strength level include crack propagation, failure mechanism and final capacity, stiffness degradation, and ductility, of which, failure mechanism and final capacity are specially discussed in detail.

6.9.1 Cracking propagation during strength test

6.9.1.1 Before test

Before any live load was exerted, cracks were observed on the top and at the bottom of the shear key, and sometimes along the interfaces of the shear keys (Figure 6.28). This phenomenon happened for all the shear key material combinations except for the UHPC with steel fiber combination. The cracks are deemed to result from drying shrinkage and the curing procedure applied. Cracks within the shear key were usually transversal (orthogonal to the load strip), indicating that there is

tension longitudinally, and this tension is possibly due to the volume reduction in the longitudinal direction.

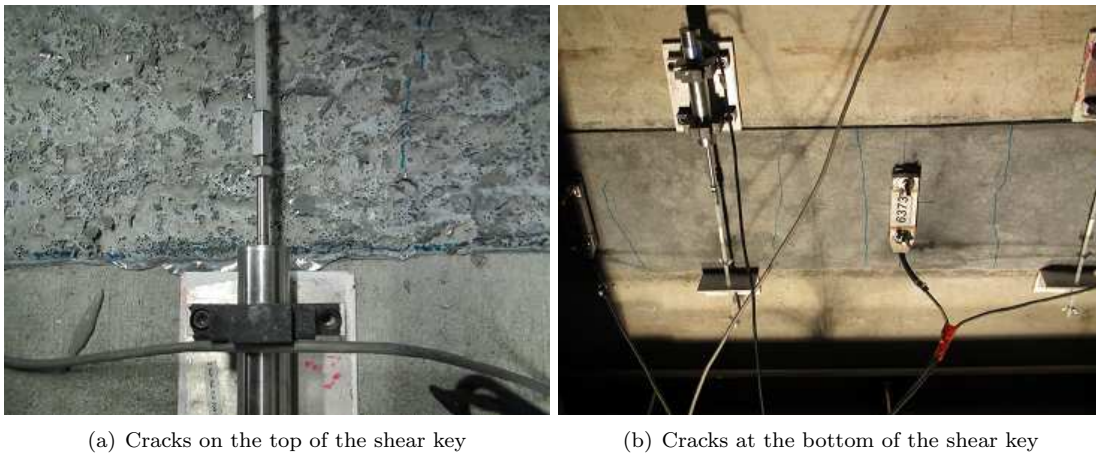


Figure 6.28: Cracks due to shrinkage before tests

6.9.1.2 Bottom view

Since the load was uniformly distributed along the width of the shear key specimen, the specimen behaved like a one-way slab during the strength tests. In the static tests, the first crack usually occurred in the precast close to the load strip where maximum moment existed. The first crack occurred under a load level between 8 and 12 kips, or under a maximum moment between 166 and 250 kip-in. for the high moment tests. For high shear tests, this load level is between 12 and 16 kips, or a maximum moment between 153 and 204 kip-in. At the beginning, the direction of the crack is longitudinal, which is orthogonal to the direction of flexural tension. As the load level increased, the cracking zone spread. New cracks formed alongside the first crack, and old cracks propagated. When the load level was high enough, transverse cracks were formed under the U-bars, which were spaced 8 in. on-center. A grid-like pattern in the precast was formed in this way for most of the strength tests (see Figure 6.29). The longitudinal cracks resulted from flexural tension, while the transverse cracks directly under the U-bar were formed due to bond splitting. Such cracks did not appear during fatigue tests because the service loads were not big enough to result in high bond stress. There was no regular cracking pattern in the shear key, which was possibly due to the existence of fibers. Since the direction of fibers can make a big difference in tensile strength of the specimen, it can also influence the direction of cracks. There was no visible crack in the shear key made of UHPC and steel fiber at any stage during the monotonic test.

6.9.1.3 Side view

On the side of the slab, a typical cracking propagation in the precast is first the cracks grew vertically due to flexural tension and then they changed direction towards the load strip due

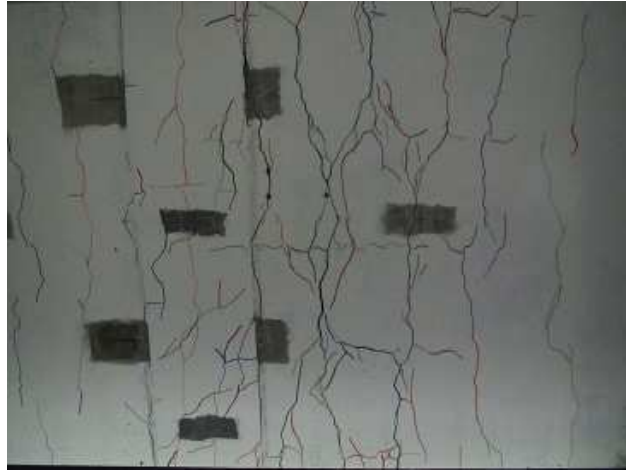
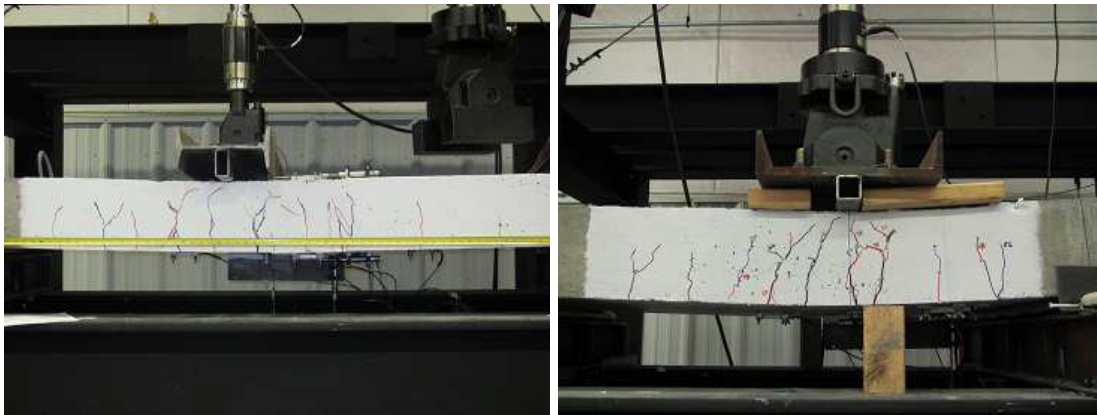


Figure 6.29: Cracking pattern after strength test-bottom view (STA-04)

to shear as they approached the top edge of the slab (see Figure 6.30). This type of crack is referred to as flexural shear crack. The inclined crack is fairly pronounced in the high shear tests. Within the shear key, due to its special geometry and the existence of fibers, cracks sometimes propagated along the interface of the key. The cracks also sometimes started from the bond and then switched their direction either towards the key or the precast while sometimes the cracks grew into the bond from elsewhere. Again due to the influence of fibers, there was no regular pattern in the shear key.



(a) High moment test (STA-04)

(b) High shear test (STA-05)

Figure 6.30: Cracking pattern after strength test-side view

6.9.1.4 Bond crack

During the static tests, the first interface crack happened at the left bond at a moment about 121 kip-in., 277 kip-in., 183 kip-in., 247 kip-in., 285 kip-in., and 285 kip-in. for specimens STA-01 to STA-06, respectively (see Table 6.5 for test specimen designations). These cracking moments

were obtained from the moment-curvature curves based on LVDT readings and will be discussed later in this chapter. It can be observed that the cracking moments for STA-02, STA-04, STA-05, and STA-06 are quite close. Although with the same shear key material combination, STA-03 has a much lower bond cracking strength than STA-04 mainly due to the fact that it was tested 6 days after the shear key was cast while STA-04 was tested 14 days after that. The shear key cylinders tested the day during the tests showed a compressive strength of 15.2 ksi for STA-03, and 18.5 ksi for STA-04. Although STA-03 has a shear key compressive strength about 82 percent of that of STA-04, its bond cracking strength is only 74 percent of that of STA-04.

6.9.2 Failure mechanism and final capacity

6.9.2.1 Failure mechanism

For all the specimens tested, the final failure mode was ductile regardless of whether it is high moment test or high shear test. The failure mode is a flexural failure for the high moment test, while for the high shear test, it is considered to be a mixture of a flexural failure and a shear failure. This conclusion is made by observing the cracks from the high shear tests, in which the cracks due to shear were quite wide and close to the top of the slab. Failure is caused by the widening of cracks especially under the load strip and at the left bond, which led to increasing strain of rebar until they all yielded, at which time, large deflection occurred when the load nearly stopped increasing.

6.9.2.2 Critical cross section identification

In order to determine the final moment and shear capacity, it is important to identify the critical section. For the current test configuration, there are two possible critical cross sections, one of which is under the load strip which has the largest moment, and the other at the left shear key interface. Two reasons can explain why the left shear key interface can be critical. First, depending on the strength and interface properties of concrete slab, the properties of shear key material, the age of the shear key when tested, and the shrinkage of the shear key, the bond can be the weakest part in the whole system. Detailed influences on the bond property of the factors mentioned above will be discussed in the following paragraph. Second, in contrast to the multiple cracks formed under the load strip, there was only one crack at the interface once it was formed (see Figure 6.31). Since multiple cracks dissipate energy much better than a single crack does, with the same amount of energy, a single crack can get much wider than multiple cracks. A wider crack can lead to larger strain in the reinforcing steel; therefore the bond is a critical cross section. It should be noted that in no case was the shear key weaker than the bond, which can also be seen the cylinder bond test in direct tension. Hence the possibility that there may be a critical cross section in the shear key is excluded. Based on direct observation and rebar strain, it is concluded that the specimens with the grout material combination, and the specimens in the high shear tests failed at the left bond, and others failed in the precast close to the load strip (refer to Table 6.13 for details). Keep in mind that all specimens were loaded past the design loads up to failure. This simply describes the mode of failure and is not indicative of insufficient capacities.



Figure 6.31: Multiple cracks under load strip

Table 6.13: Specimen capacity summary

Shear Key Mixture and Loading Condition	Specimen ID	Critical Cross Section	Max. Moment kip-in	Max. Shear kip
Grout with PVA (HM)	STA-01	Left bond	763.5	15.6
	MONO-01	Left bond	690.6	14.0
	MONO-01(redo)	Left bond	674.8	13.7
UHPC with steel (HM)	STA-02	Under load strip	742.5	20.7
	MONO-02	Under load strip	745.4	20.8
UHPC with PVA (HM)	STA-03	Under load strip	736.7	20.7
	STA-04	Under load strip	738.0	20.7
	MONO-03	Under load strip	727.0	20.4
UHPC with PVA (HS)	STA-05	Left bond	650.0	40.9
	STA-06	Left bond	634.1	40.2
	MONO-04	Left bond	543.8	34.6

6.9.2.3 Influencing factors on bond property

One of the factors that can significantly influence bond performance between old concrete and new materials is the surface property of concrete interface. A strong saturated rougher concrete surface can significantly improve the bond performance by providing better particle interlock and reducing water loss from the shear key material which has a very low water to cementitious material ratio. The most influencing factor is the property of the shear key material. Compared with the grout, the UHPC material provides a bond that is stronger than concrete by taking advantage of its high quantity of pozzolans like fly ash and silica fume. Pozzolan improves the bond property mainly through two mechanisms: filler effect and pozzolanic activity. On the one hand, it acts as fillers to fill in the voids of the concrete interface, and on the other hand, it reacts with calcium hydroxide (CH) in the concrete with the presence of moisture to form C-S-H gel, which is much stronger than CH. The shear key age when tested can also influence the bond to some degree, which is evident from the fact that STA-03 with a 6-day old shear key cracked at the bond at a lower load level than STA-04 which had a 14-day old shear key. Another factor that should be paid attention to is the effect of shrinkage of shear key material on the bond property, which under the constraint of the concrete slab can lead to cracks along the bond and in the key. The shrinkage effect can be reduced by the restraint of fibers. Compared with steel fibers, PVA fibers provide much less restraint. This is why shrinkage cracks were observed from the UHPC with PVA, and grout with PVA combinations, but not from the UHPC with steel combination.

6.9.2.4 Capacity determination

After determining the critical cross section, the moment and shear capacities at the cross section were calculated, accounting for the dead load of the concrete slab, which was assumed to have a uniform density of 150 lb/ft³. It should be noted that for most of the specimens, final capacities were not achieved, which can be observed from the load-displacement curve. Tests were stopped when large deformation occurred with only a small increase of load. The maximum capacities of all the slabs at the corresponding critical cross sections are tabulated in Table 6.13. The capacities of all the 11 slabs determined from experiments will later be compared with the shear-moment interaction diagram based on modified compression field theory (Collins and Mitchell, 2001).

6.9.2.5 Shear-moment interaction diagram

The shear- moment interaction diagram for a cross section in the concrete slab is determined based on the modified compression field theory by Collins and Mitchell (Collins and Mitchell, 2001), which can be applied to beam-like elements that conform to the assumption that plane section remains plane after loading (AASHTO LRFD 5.8.1). Compared with the classical compression field theory, the modified theory takes into account of the concrete principle tensile stress after cracking, which is deemed to be more realistic when explaining the shear failure mechanism. In order to calculate the shear capacity of a cross section, combined equilibrium, compatibility, and constitutive models need to be applied. Due to the complexity involved in the calculation, design aids were provided by Collins and Mitchell to reduce the effort. And these aids are available in AASHTO

LRFD Appendix B5. According to this theory, for a slab cross section without either transverse reinforcement or prestressed reinforcement, the shear capacity of a cross section is provided only by the nominal shear strength of the concrete. And the procedure to determine this capacity can be stated as follows:

Step 1: Determine the crack spacing parameter S_{xe} using the formula:

$$S_{xe} = S_x \frac{1.38}{a_g + 0.63} \leq 80 \text{ in} \quad (6.1)$$

where a_g is the maximum aggregate size (in.), and 0.75 in. is used in this case, S_x is the minimum of the effective shear depth and the maximum distance between layers of longitudinal crack control reinforcement, which in this case is 4 in. The reinforcement area in each layer should not be less than $0.003d_v S_x$. The minimum shear depth d_v is defined as the distance, measured perpendicular to the neutral axis, between the resultants of the tensile and compressive forces due to flexure, but it needs not be taken less than the greater of $0.9d_e$ or $0.72h$, where d_e is the distance from the extreme compressive fiber to the centroid of the tensile force in the tension reinforcement (4.75 in. in this case), and h is the height of the specimen (8 in. in this case). Therefore d_v is calculated to be 5.76 in., S_x is taken to be 4 in., and S_{xe} is determined to be 4 in..

Step 2: Select a range of longitudinal strain ϵ_x , for instance from 0 to 2000 microstrain and go to AASHTO LRFD Table B5.2 – 2. With the S_{xe} determined in step 1, a range of θ and β can be calculated corresponding to the values of S_{xe} selected, where θ is the angle of inclination of diagonal compressive stresses, and β is a factor indicating ability of diagonally cracked concrete to transmit tension and shear.

Step 3: The nominal shear capacity V_n of the cross section can be calculated according to AASHTO LRFD 5.8.3.3:

$$V_n = 0.036\beta\sqrt{f'_c}b_v d_v \quad (6.2)$$

where f'_c is the specified compressive strength of concrete (ksi) (6 ksi in this case), and b_v is the effective web width taken as the minimum web width within the depth d_v (40 in in this case).

Step 4: With several shear capacity values being determined, the corresponding moment capacity can also be calculated according to AASHTO LRFD Table B5.2 – 2:

$$\epsilon_x = \frac{\frac{M_u}{d_v} + 0.5|V_u| \cot \theta}{E_s A_s} \quad (6.3)$$

where M_u is the factored moment and should not be less than $V_u d_v$, V_u is the factored shear force, E_s is the Young's modulus of nonprestressed steel, ϵ_x is the normal strain and A_s is the area of nonprestressed steel on the flexural tension side of the member at the section under consideration. The resistance factor is chosen to be unity. Several combinations of M_u and V_u calculated following the above procedure can give a shear failure line.

Step 5: The yielding of longitudinal reinforcement before failure can reduce the shear capacity of the slab. Therefore when determining the moment failure line, the minimum longitudinal reinforcement requirement should be considered. The formula according to AASHTO LRFD 5.8.3.5 – 1 is simplified for the case studied as:

$$A_s f_y = \frac{M_n}{d_v} + V_n \cot \theta \quad (6.4)$$

With other parameters all known, M_n can be plotted against V_n . Since there is no transverse or prestressed reinforcement, the shear capacity is zero at pure moment. In this way a moment failure line is generated (see Figure 6.32).

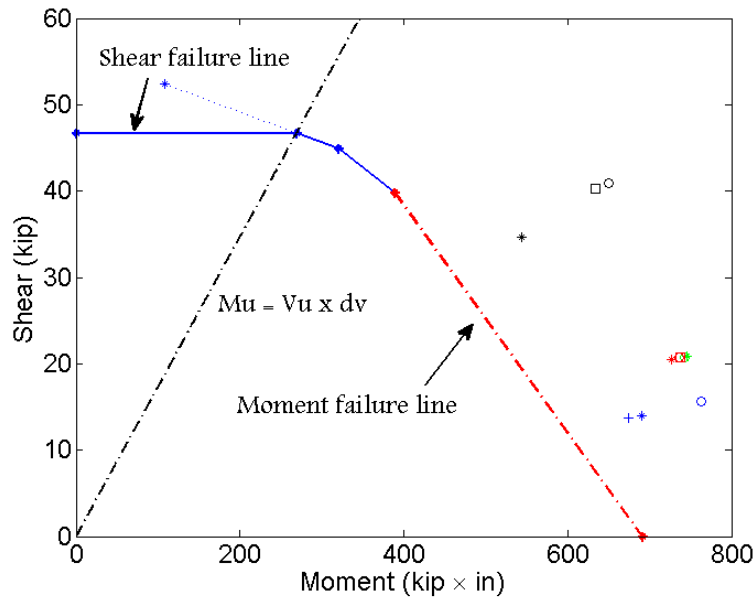


Figure 6.32: Shear moment interaction diagram: Blue represents grout with PVA group; green UHPC with steel group; red UHPC with PVA (high moment); and black UHPC with PVA (high shear). Square and circle represent static tests, others monotonic tests.

It should be noted that the maximum moment calculated from the modified compression field theory is much larger than that calculated according to AASHTO LRFD 5.7.3.2 due to different moment arms d_v being used. Although d_v is defined as the distance between the resultant tensile force and the resultant compressive force, it has a minimum limit according to AASHTO LRFD 5.8.2.9, which explains why the moment capacity calculated is larger. When using the formula from AASHTO, the resistance factor is unity, so that it gives the maximum resistance. Moreover, this shear-moment diagram is obtained for the concrete, not for the bond. For some of the slabs that failed at the bond, a diagram with less resistance is supposed to be obtained. This can be justified by the fact that if the bond is stronger than the concrete, the slab cannot fail at the bond under the

same demand, not to mention that the bond had a smaller demand than the concrete during the test.

6.9.2.6 Discussion

For the eleven slabs tested, the maximum shear and moment capacities (considering dead load) they subjected to during the experiments all exceeded what are predicted from the shear moment diagram (Figure 6.32). Even after 10 million cycles, there is still a large reserve capacity. It should be noted that these specimens were tested under lab environment. In real case, the rebar may become corroded during service, which can reduce the ductility and also the capacity of the slab. By comparison, all the specimens show positive capacity performances. The specimens that failed close to the load strip have pretty close maximum capacities. For the specimens failed at the left bond, compared with the grout with PVA group, the UHPC with PVA—high shear group shows a significant bond. The specimen capacity variation within each group is related to the strength variation of the precast and the shear key material. For instance, the compressive strengths of both concrete and shear key material of MONO-04 during the test day were lower than those of STA-05 and STA-06, which led to a lower bond strength of the former than the latter two. For the specimens in the high moment tests, the specimens with UHPC material combinations which failed in the precast, generally gave higher capacities than those of the specimens with grout material combinations which failed at the bond. This is due to the fact that the precast concrete tensile strengths in the specimens were generally stronger than the bond between the grout and the precast, whereas, this was not the case for the bond between the UHPC and the precast.

6.9.3 Stiffness degradation at the strength level

6.9.3.1 Significance

A stiffness comparison between static tests and the corresponding monotonic test is provided in Figure 6.33 and Figure 6.34, which includes the rotational stiffness of the shear key and the vertical stiffness under the load strip. A comparison like this can directly tell the stiffness changes from static test to monotonic test. From the stiffness change at the fatigue load level, a rough estimate can be made about the conservativeness of the fatigue load applied. The comparison can also tell the property variation from specimen to specimen. Additionally, we can also get some ideas about the influence of the fatigue test on the specimen performance in the later monotonic test.

6.9.3.2 Determination

In Figure 6.33, the rotational stiffness comparison between the static tests and the corresponding monotonic test is presented by plotting the moment at the center of shear key against the rotation of the shear key. This rotation is calculated based on LVDT data by subtracting the top LVDT reading (in compression) from the corresponding bottom LVDT reading (in tension), the result of which is divided by the vertical distance between these two LVDTs. The vertical stiffness

under the load strip is presented in Figure 6.34 by plotting the load exerted by the load cell against the distance measured from the left string pot, which is close to the load strip.

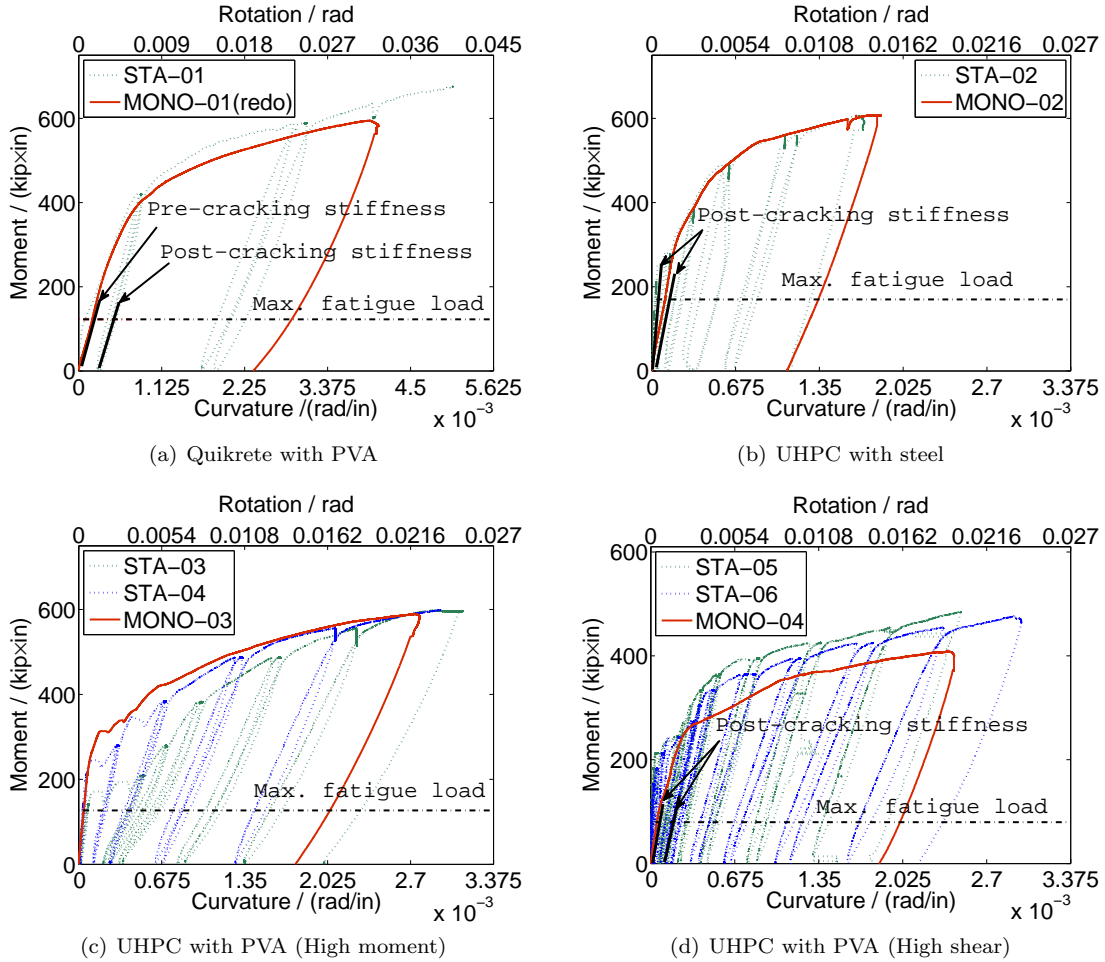


Figure 6.33: Rotational stiffness degradation of shear key

6.9.3.3 Moment-rotation curve

Generally speaking, the moment-rotation curve in the post-fatigue monotonic test generally agrees well with the corresponding curves in the static tests, especially for the combinations of UHPC with steel fiber and UHPC with PVA fiber in the high moment test. A significant difference between the curves in the static test with that in the monotonic test is that the static specimens, since they were in a virgin state at the beginning of the test, underwent a large deformation when the bond cracked (i.e. a sudden horizontal shift in the moment-rotation curve), while the monotonic specimens, after the fatigue test, usually did not exhibit this phenomenon. As far as stiffness is concerned, except for the UHPC with PVA combination in the high moment test, we can see a clear drop of rotational stiffness within the fatigue load level for other material combinations. The high

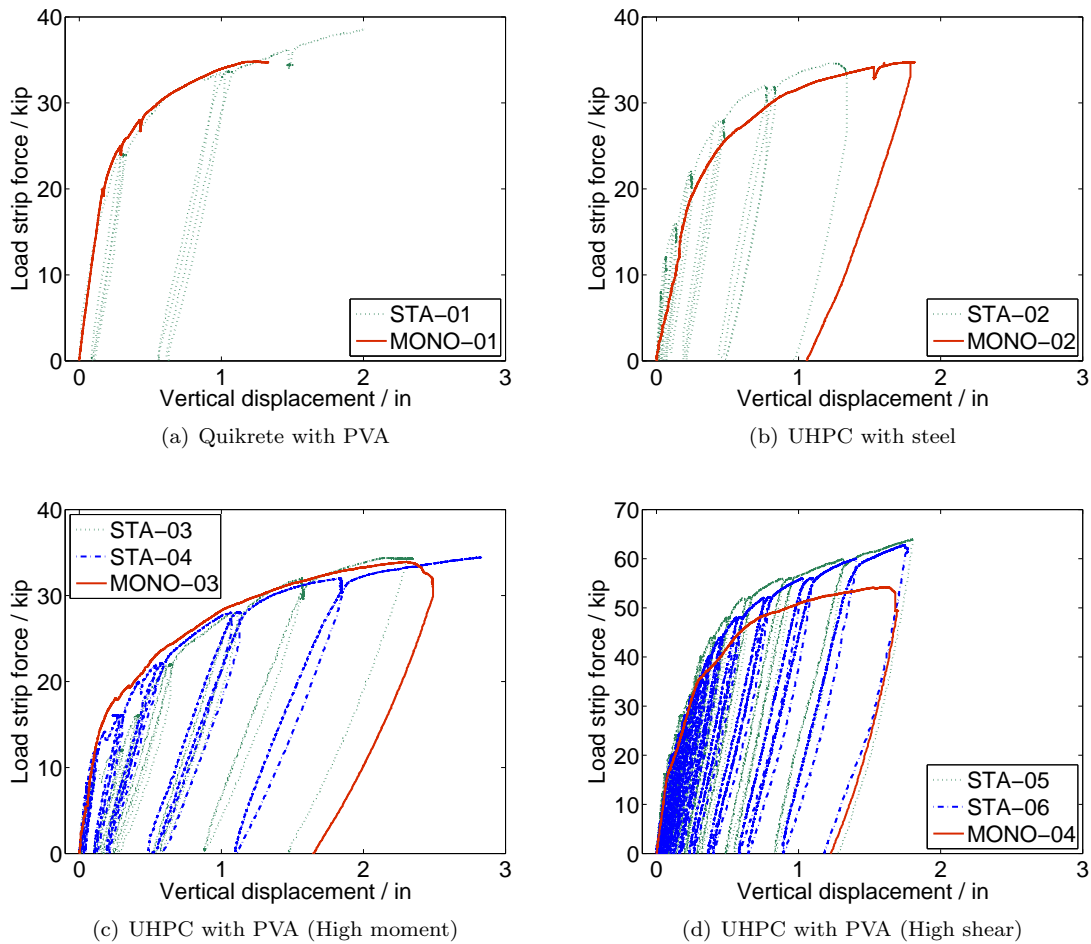


Figure 6.34: Translational stiffness degradation under load strip

rotational stiffness of MONO-03 within the fatigue load level seems to indicate that the fatigue load exerted for MONO-03 was not conservative. However, the same specimen, at a load level about 310 kip-in., shows a large increase in rotation, which is an indication of interface cracking. This cracking was not visible though. Since the stiffness used when determining the fatigue load is the stiffness after material cracking, the high initial stiffness for MONO-03 before bond cracking does not necessarily mean that the fatigue load is not conservative. Other specimens under monotonic tests do not have this indication of bond cracking. Later analysis showed that the shear key interfaces for MONO-02 and MONO-04 already cracked during the fatigue tests. For these two specimens, their stiffness after bond cracking within the fatigue load level is compared with that in the corresponding static tests. It can be observed from the comparison that MONO-02 has a much lower post-cracking stiffness than that in STA-02, and MONO-04 did not show much difference between the two stiffness values. Later analysis shows that there is no interface cracking for MONO-01(redo) after the fatigue test, and

its stiffness before bond cracking is pretty close to the post-cracking stiffness in the corresponding static test.

From what has been discussed above, it can be inferred that the fatigue loads exerted tend to be conservative for FAT-02, and close to the requested demand for FAT-04. For FAT-03 and FAT-01(redo), the loads exerted were not big enough to crack the bond, and a conclusion cannot be made about the conservativeness of the fatigue load applied for FAT-03. In order to get a better understanding of the stiffness change, an analysis of stiffness degradation during the fatigue test is carried out.

6.9.3.4 Force-displacement curve

The vertical stiffness under the load strip, as will be discussed later, is mainly determined by the effective moment of inertia of concrete. The change of the effective moment of inertia of concrete has a lot to do with the crack development in the concrete, and therefore the compressive strength of concrete and fatigue load magnitude during the fatigue test. The shear key rotation, on the other hand, restrains the deflection increment for the slab with UHPC material combinations. This restraining effect is deemed to be greatly influenced by the strength of the shear key material. After the fatigue test, there was a significant drop of effective moment of inertia in the precast of MONO-02, which resulted in a significant increase in vertical deflection and therefore stiffness degradation especially in the first half of the curve (Figure 6.34b). The stiffness in the latter half of the curve generally agreed between the two curves due to the fact that there was not much change of concrete compressive strength and shear key compressive strength from STA-02 to MONO-02. For MONO-03, the monotonic curve agrees pretty well with the static curves. This is due to the fact that on the one hand, there were only a few cracks in the slab after fatigue test, and on the other hand, there was a big improvement of shear key compressive strength from 15190 psi in STA-03, and 18510 psi in STA-04 to 21070 psi in MONO-03, which led to a higher restraining effect of the shear key. The vertical stiffness degradation resulted from a reduction of effective moment of inertia and is therefore compensated by the restraining effect of the shear key. For MONO-04, there were very few cracks developed after the fatigue test, but since there was a drop of concrete strength (from 8730 to 6575 psi) and shear key strength (from 22330 to 18370 psi) from the static tests to the monotonic test, the stiffness kept degrading compared with those in the static tests.

6.9.3.5 Variation from specimen to specimen

There are a lot of sources for variation in the properties from one specimen to another. The main sources in the case studied include the strength of concrete and the strength of shear key, which also influence bond properties. The most typical example is the force-deformation curves of STA-03 and STA-04. For these two specimens, both the precast and the shear key were cast the same day. The only difference between these two specimens is STA-03 was tested 6 days after the shear key was cast, and STA-04 14 days after the shear key was cast. The concrete compressive strengths were close between these two specimens, while there was a 22 percent increase of shear key material strength from STA-03 to STA-04, which resulted in a 35 percent increase in bond cracking strength

from the former to the latter. For STA-05 and STA-06, their precast elements were cast the same day and their shear keys were cast on the same day. The former was tested 57 days after the shear key was cast, and the later 63 days after that. The strengths of concrete and shear key between these two specimens during the test days were similar. Therefore there is not much variation in the force-deformation curves of these two specimens.

6.9.4 Ductility

6.9.4.1 Significance

For a certain material, ductility is closely related to toughness or the work of fracture, which is a measure of the material's capacity to resist crack propagation (Gordon, 1991). A low grade reinforcing steel is very ductile, and its work of fracture is very high. A brittle material, like concrete, has a tensile stress-strain curve that encompasses only a small area, and so its work of fracture is fairly small compared with that of reinforcing steel. This explains why concrete is so sensitive to cracks and steel is not and why it is necessary to put ductile materials in concrete to provide safety. The significance of ductility in a structural system can be reflected from the fact that large deformations can happen due to ductility before the structure collapse. For an indeterminate structure, sufficient ductility leads to demand redistribution and permits the formation of several plastic hinges, and therefore increases the capacity of the structure. Hence the larger the ductility, the more safety margin there is.

6.9.4.2 Quantification

Ductility can be quantified by a ductility index, which is the ratio of the ultimate deformation to the yield deformation. The common deformation used for quantifying ductility includes curvature and displacement. For a typical moment-curvature plot which shows the formation of a plastic hinge, the yield curvature ψ_y and ultimate curvature ψ_u can be used to calculate the ductility index. This is calculated as:

$$\mu = \frac{\psi_u}{\psi_y} \quad (6.5)$$

Similarly, the index based on displacement can be determined as:

$$\mu = \frac{D_u}{D_y} \quad (6.6)$$

where D_u is the ultimate displacement, and D_y the yield displacement.

Since only the rotation at the bond was monitored, the experimental moment-curvature relationship is only available for the specimens that failed at the bond. Thus for these specimens, the ductility index can be calculated using the quotient of curvatures. For specimens that failed close to the load strip, the ductility can be determined by the quotient of displacements under the load strip. The curvature is determined by subtracting the top LVDT reading (compression) from the corresponding bottom LVDT reading (tension), the result of which is divided by the distance between the two LVDTs (10.25 in.) and the width of the shear key (8 in.). Simply put, the

curvature is calculated by dividing the rotation of shear key by the width of the shear key. Strictly speaking, the curvature calculated this way is not the curvature at the failed bond, but an averaged curvature over the width of the shear key. However, considering that during the strength test, the left interface cracked much more seriously than the shear key - especially after rebar yielded - and that the curvature is mainly attributed to big cracks, the left bond must take a major weight in the yield curvature ψ_y and ultimate curvature ψ_u . In this sense the curvature calculated based on the LVDT measurements is considered sufficient to represent the curvature at the left bond.

The moment-curvature relationship mentioned above is typically composed of three phases: before bond cracking, after bond cracking but before rebar yielding, and after rebar yielding (see Figure 6.33). In the first phase, the moment-curvature curve is close to linear. In the second phase, non-linearity becomes obvious due to bond cracking, and the slope of the curve becomes flatter than that in the first phase. During the last phase, the curve was approaching a flat line due to rebar yielding. Note that it is not a flat line like that in an idealized stress-strain curve of a bare bar when yielding happens. Rather it is similar to the average stress-strain curve of an embedded bar (see Figure 6.35), the strain of which should be monitored over a distance that covers at least several cracks. The increasing mean stress after mean yielding strain is due to the tension stiffening effect of concrete. Since the LVDT monitored the whole width of the shear key, within which several cracks were covered, the shape of the moment-curvature curve should be similar to the stress-strain curve of an embedded bar.

The yield curvature can be determined by identifying the yield moment, which is the moment that causes the first rebar to yield. In the case studied, since not all of the rebar at the left bond were monitored, the smallest moment that cause yielding of the rebar monitored is taken as the yield moment. The ductility index calculated using this value therefore tends to be conservative. The ultimate curvature is determined as largest curvature in the moment-curvature curve. Since most of the specimens did not achieve its ultimate capacity as discussed before, the ductility index calculated is representative of demand ductility and not capacity ductility. Remember that demand ductility is always less than capacity ductility and can serve as a conservative estimate of the capacity ductility. Similar to ψ_y and ψ_u , D_y and D_u can be determined correspondingly for specimens that failed at a cross section close to the load strip. Since the yield moments at the corresponding failed cross sections are not available from any sensors, the yield moments based on rebar strain gauge readings were used.

The ductility indices calculated are listed in Table 6.14 for all the specimens. It can be seen that for the high moment group, the ductility index generally varies from 5.5 to 8 except for MONO-02, which has the minimum ductility index of 2.78. This low value results from the high yield displacement used in the calculation, which is possibly due to a high yield moment was chosen based on strain gauge readings. The ductility index in the high group varies between 8.8 and 11.7. A general trend is observed: the ductility dropped from the static tests to the corresponding monotonic test. Rearranging these specimens, as shown in Table 6.15, shows that this drop is caused by the increase of ψ_y or D_y , which implies the compression zone dimension in the monotonic test is larger than that in the static test(s). A larger compression block dimension means a weaker cementitious material at the critical cross section and therefore a lower strength at this cross section. This is

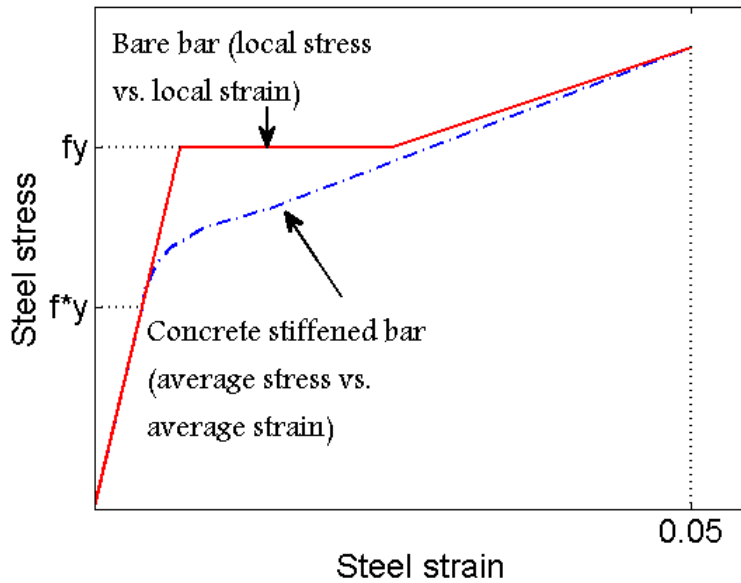


Figure 6.35: Stiffening effect of concrete on embedded bar (Adapted from (Hsu, 1993))

Table 6.14: Specimen ductility index

Shear Key Mixture and Loading Condition	Specimen ID	ψ_y (or D_y)	ψ_u (or D_u)	μ
Grout with PVA (HM)	STA-01	0.6498×10^{-3}	0.0051	7.81
	MONO-01	<i>N/A</i>	<i>N/A</i>	<i>N/A</i>
	MONO-01(redo)	0.7301×10^{-3}	0.0041	5.57
UHPC with steel (HM)	STA-02	0.2436	1.3475	5.53
	MONO-02	0.6519	1.8141	2.78
UHPC with PVA (HM)	STA-03	0.4036	2.3437	5.81
	STA-04	0.3549	2.8291	7.97
	MONO-03	0.4346	2.4899	5.73
UHPC with PVA (HS)	STA-05	0.2256×10^{-3}	0.0025	11.06
	STA-06	0.2553×10^{-3}	0.0030	11.67
	MONO-04	0.2763×10^{-3}	0.0024	8.83

confirmed by the maximum moment or shear from the strength test. Therefore, this low ductility is deemed more likely to result from the low strength of the cementitious materials during the test day, rather than the influence of the fatigue tests.

Table 6.15: Relationship between ductility index and maximum moment

Shear Key Mixture and Loading Condition	Specimen ID	ψ_y (or D_y)	μ	Max. Moment (kip-in)
Grout with PVA (HM)	STA-01	0.6498×10^{-3}	7.81	763.5
	MONO-01(redo)	0.7301×10^{-3}	5.57	674.8
UHPC with steel (HM)	STA-02	0.2436	5.53	742.5
	MONO-02	0.6519	2.78	745.4
UHPC with PVA (HM)	STA-04	0.3549	7.97	738.0
	STA-03	0.4036	5.81	736.7
	MONO-03	0.4346	5.73	727.0
UHPC with PVA (HS)	STA-05	0.2256×10^{-3}	11.06	650.0
	STA-06	0.2553×10^{-3}	11.67	634.1
	MONO-04	0.2763×10^{-3}	8.83	543.8

A suggested improvement to the calculation of ductility is to calculate the rotational capacity of a member at a plastic hinge (Skogman et al., 1988). This rotational capacity is calculated as:

$$\theta_p = \psi_u d = \epsilon_{cu} \frac{d}{c} \quad (6.7)$$

in which d is the effective depth at each moment concentration, c the distance from the extreme compression fiber to the neutral axis, and ϵ_{cu} the limit strain at the extreme compression fiber. It should be noted that

$$\psi_u = \frac{\epsilon_{cu}}{c} \quad (6.8)$$

where d is recommended to be the total spreading length of the plastic hinge at each moment concentration (Sawyer, 1964). The minimum ductility calculated in this way is assured in older versions of AASHTO LFRD (prior to 2005) by limiting the maximum value of $\frac{c}{d_e}$ to be less than 0.42, in which d_e is the effective depth from the extreme compression fiber to the centroid of the tensile force in the tensile reinforcement. In the versions after that, however, this limit is eliminated and replaced by reducing the factored resistance of prestressed and nonprestressed sections if the tensile steel quantity increases under the condition that the net strain in the extreme tensile steel is less than 0.005 (AASHTO LRFD 5.5.4.2.1). Only when there is also a corresponding increase in compression steel, can the factored resistance of the section be increased. This new specification accounts for the decreasing ductility due to the increasing over-strength. For the slab tested, at ultimate flexural capacity, the tensile strain in the extreme steel fiber is 0.023, much larger than 0.005, if the design 28-day compressive strength of concrete 6 ksi is used. Therefore ductility in this respect is satisfied and there should be no reduction of factored flexural resistance of the section.

6.10 Result Analysis—Performance at Service Level

At the service level, the stiffness degradation is the focus of the discussion. Also discussed are bond performance, reserve capacity and fatigue life, and crack propagation.

6.10.1 Bond performance

6.10.1.1 Leakage-based

The leakage of water along the shear key interface during a pond test is a direct evidence of interface cracking both on the top and at the bottom of the interface. During the pond test, there was leakage along the shear key interfaces of FAT-01. However, since a larger than required fatigue load was applied on FAT-01, it is not prudent to say the bond is unsound from this evidence. Later a make-up specimen FAT-01(redo) showed no leakage after 2 million cycles of the pond test. In addition, having no leakage during the pond test only indicates that there are no interconnected channels to help convey the water from the top to the bottom. Therefore pond test itself is not sufficient to determine if there are any top or bottom interfacial cracks.

6.10.1.2 Sensor information-based

To further detect the existence of any bond cracks, the strain transducer readings are needed. The bottom shear key interface is under flexural tension, and therefore much more sensitive to cracks compared to the top interface. If there is any crack along the bottom edge of the bond, there will be a drop of the corresponding bottom strain transducer reading of the strain due. This is because a bond failure at the bottom fiber results in a stress relief in the shear key material. Such evidence would be sufficient to prove the interface cracking unless the cracks form in the shear key adjacent to the strain transducer but not in between the measurement points of the transducer. This would relieve the strain but the transducer wouldn't be able to detect it directly. It should also be noted that any cracks that happened between the measurement points of the strain transducer during a test could increase the strain, which may overcome the drop of the strain due to interface cracking. Therefore if interface cracking and in-between strain transducer cracking happened during the same data acquisition interval, identifying interface cracking would not be easy. Fortunately no such situation happened in the test.

6.10.1.3 Discussion

With the aid of strain transducer data, it was found that there is no interface cracking for FAT-03 and the make-up specimen FAT-01(redo), while a sudden localized drop of strain transducer readings, although not serious, happened in FAT-02 and FAT-04 at the beginning of the higher load level (see Figure 6.36). For FAT-02, there was also gradual drop of strain transducer readings during the first load level, which indicates that the bond was degrading slowly during that period. Therefore although there was no leakage for FAT-02 and FAT-04, there was a slight cracking at the bottom edge of the bond.

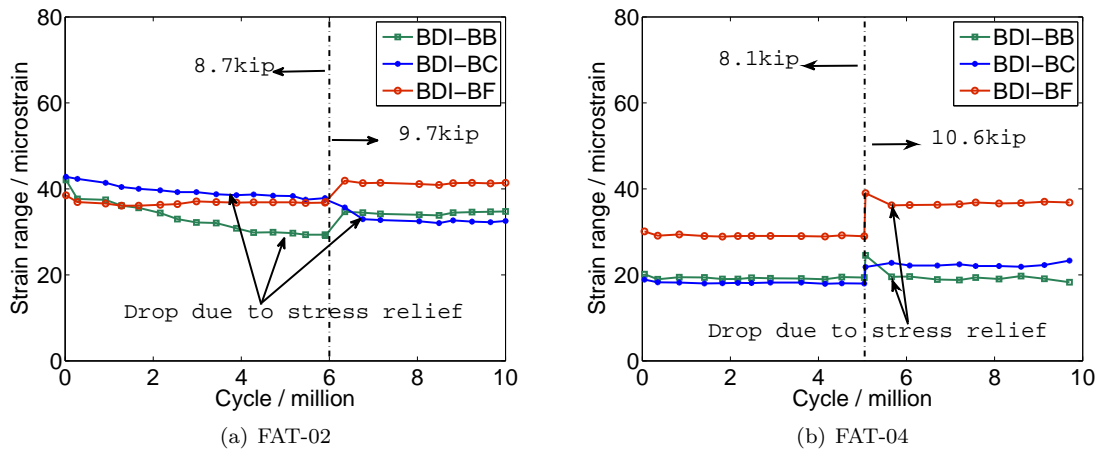


Figure 6.36: Interface cracking based on BDI readings

6.10.2 Stiffness degradation

6.10.2.1 Relations with the big picture

The rotational stiffness and vertical stiffness of the shear key from the static tests were used as important parameters in the bridge model to determine the fatigue load that is exerted on the shear key. The stiffness degradation from the fatigue test therefore needs to be examined to validate the simulation prediction so that the conservativeness of the fatigue load can be known.

6.10.2.2 Significance

Relative stiffness of a certain component is closely related to the load demand it experiences. During the service life of a bridge, all the materials will deteriorate gradually, which can cause subsequent stiffness degradation. Since the stiffness degradation differs from component to component, a relative stiffness change will occur, resulting in demand redistribution. In the case of NEXT-D Beam Bridge, the precast stem and the cast-in-place shear key can be much stiffer than the precast slab, and therefore can attract much higher loads and greater demand. During service, the prestressed stem is assumed to not crack in tension, therefore its stiffness will remain at a constant level, while the stiffness of the shear key may drop due to material cracking. Therefore the relative stiffness of the shear key decreases, so does the demand proportion on it. It can be imagined that as the relative stiffness of the shear key decreases, the demand proportion on the stem would increase.

6.10.2.3 Stiffness calculation

From the fatigue test, the shear key rotational stiffness was calculated by dividing the moment in the center of the shear key by the average shear key rotation from LVDT readings, which is consistent with the way that stiffness was calculated in the static test. The vertical stiffness of shear key was not calculated due to the fact that the displacement measured by vertical LVDT was

so small during the fatigue test that the resolution of the sensor accounts for a large percent of it, and therefore the data from the sensor was not reliable. Instead, the vertical stiffness under the load strip was calculated by dividing the applied load by the global displacement readings from the left string pot. Although the left string pot is not directly under the load strip, the distance between them is so small that the displacement it measured is considered to be similar enough to the actual displacement under the load strip. In all of the stiffness calculations for the fatigue test, it is the range of displacement and range of load that were used rather than the absolute value. When dealing with the data, the range of each cycle was calculated, added together, and then averaged over the number of cycles. In this way the effect of extreme data can be reduced. Except for FAT-01 which had no LVDTs on top of the slab, the rotational stiffness degradation for each specimen was plotted against each other.

6.10.2.4 General trend

Shown in the stiffness degradation plots (see Figure 6.37), of all the specimens, FAT-02 has the highest initial rotational stiffness of about 8.99×10^5 kip-in/rad. During the first load level of 8.7 kips from 0 to about 6 million cycles, its stiffness continued dropping. After that, a higher load level of 9.7 kips was exerted, accompanied by a big drop of the rotational stiffness, which stabilized at about 3.18×10^5 kip-in/rad from 6.7 million cycles to 10 million cycles. Compared with that of FAT-02, the stiffness of FAT-04 was quite stable (4.72×10^5 kip-in/rad) during the first load level of 8.1 kips from 0 to 5 million cycles. At the beginning of the second load level of 10.6 kips, its stiffness dropped and stabilized at about 2.02×10^5 kip-in/rad from 6 million cycles to the end. Compared with the two specimens mentioned above, FAT-03 did not have much change in its rotational stiffness. The biggest drop (from 6.06×10^5 kip-in/rad to 4.73×10^5 kip-in/rad) happened at the beginning of the second load level at the end of 2 million cycles, when the load was increased from 4.9 to 6.5 kips. During the third and fourth load levels (from 2.4 to 6.9 million cycles), the stiffness got stabilized at a value of about 4.41×10^5 kip-in/rad. At the beginning of the final load level of 7.3 kips, the stiffness dropped and stabilized at the value of about 4.38×10^5 kip-in/rad until about 9.5 million cycles, where the stiffness dropped again to the value of 4.24×10^5 kip-in/rad due to a longitudinal crack in the shear key. With the smallest initial stiffness of 1.06×10^5 kip-in/rad, FAT-01(redo) had a very little change in its rotational stiffness throughout the test except at the beginning of the sixth million cycles when the load was increased from 5.3 to 7 kips. Its final stabilized stiffness is 0.77×10^5 kip-in/rad.

The initial rotational stiffness for the shear keys made with UHPC material combinations (FAT-02 to FAT-04) varies from 4.7×10^5 to 9.0×10^5 kip-in/rad. The combination of UHPC with steel fiber gave the highest initial rotational shear key stiffness as that showed in the static tests. For FAT-03 and FAT-04, although they had the same shear key material combination, the initial stiffness of FAT-04 (4.72×10^5 kip-in/rad) is 71.9 percent of that of FAT-03 (6.06×10^5 kip-in/rad). Since the precast strengths of the two specimens during the test day were pretty close, their effects on the stiffness through influencing the soundness of the bond can be neglected. The interface of concrete slab can also be neglected. The remaining major factors include the strength and shrinkage

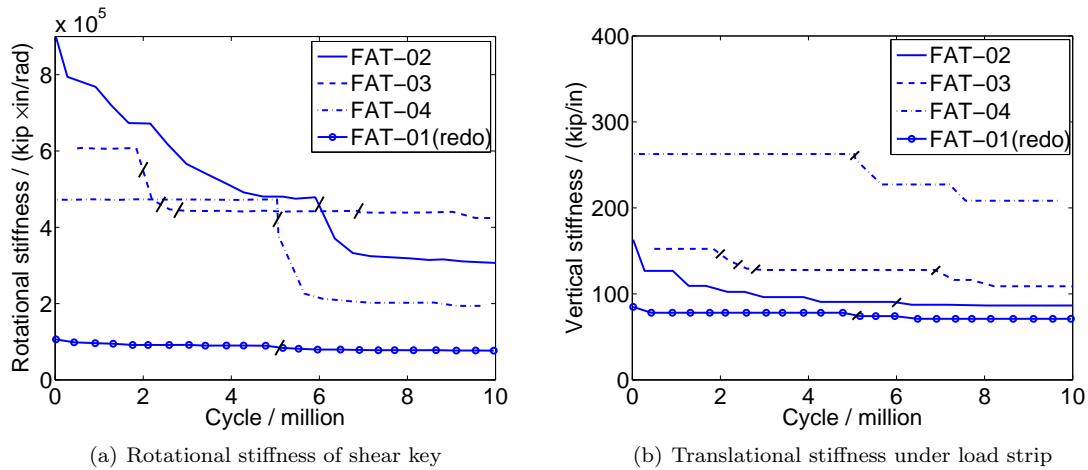


Figure 6.37: Stiffness degradation during fatigue test

of the shear key material, and the age at which the specimen was tested. The shear key cylinder tests during the corresponding test day showed that the average compressive strength for FAT-04 was 18370 psi, 87.2 percent of that for FAT-03 (21070 psi). Remember the same situation happened for STA-03 and STA-04, where STA-03 had a shear key compressive strength about 82 percent of that of STA-04, its bond cracking strength was only 74 percent of that of STA-04. The influence of the other two factors can be combined together. Since FAT-03 and FAT-04 were tested 22 and 77 days, respectively, after the shear key was cast, the shear key material property of FAT-04 can be influenced more by creep and shrinkage than that of FAT-03. For instance, due to the increase in strain caused by creep, Young's modulus of shear key is reduced under long-term repetitive loads (Barker and Puckett, 2007). Young's modulus is believed to be closely related to stiffness. Detailed effects of creep and shrinkage on material properties will also be discussed later.

As far as vertical stiffness degradation (see Figure 6.37) is concerned, the high shear test, due to its different support condition experiences a displacement under the load strip which is smaller than those in the high moment tests. This explains its higher stiffness compared with the specimens in the high moment tests. For the three specimens subjected to a high moment-to-shear ratio (FAT-02, FAT-03, and FAT-01(redo)), the general trends of vertical stiffness degradation are similar to those of rotational stiffness degradation. Although the highest stiffness still came from FAT-02, the difference between it and that of FAT-03 is not as pronounced as that in shear key rotational stiffness. This is because there are different degradation mechanisms for these two kinds of stiffness.

Finally, due to the resolution of sensors, the stiffness values used above and in the plots do not represent the exact value, and the real stiffness degradation plots should be much smoother than what are presented. However, compared with the displacements measured, the resolutions of sensors account for only a small percent. Generally speaking, the stiffness values presented are within a tolerable range and the general trends of stiffness degradation are considered reliable.

6.11 Simulation Validation

For FAT-02 and FAT-03, the corresponding rotational stiffness stabilized after interface cracking from the fatigue tests were 3.1×10^5 kip-in/rad and 4.4×10^5 kip-in/rad (see Figure 6.37). This is equivalent to about 53.3 and 440 percent of the values used to predict the demand. The rotational stiffness value used in this sense is conservative for FAT-02. The higher stiffness for FAT-03 is due to the fact that there was no bond cracking during the fatigue test. Similar to FAT-03, there was no bond cracking for FAT-01(redo), but it had a low rotational stiffness of 0.77×10^5 kip-in/rad, which is about 92 percent of that applied in demand determination and therefore the value applied is pretty conservative.

6.11.1 Reserve capacity and fatigue life

6.11.1.1 Significance

Reserve capacity after a fatigue test is an indicator of the remaining fatigue life of a certain component of a structure. For a reinforced concrete structure, the reserve capacity of rebar may not determine the remaining life of the whole structure since the system is usually indeterminate, but it is closely related to the remaining life of a certain component. The strain of rebar selected should be at a critical cross section where the strain is the maximum. For a reinforced concrete member without cracks, the strain of rebar varies from section to section according to the external loads. After cracking, the strain at the crack is much larger than that protected by concrete due to tension stiffening effect of concrete (Hsu, 1993). This effect is especially obvious at low strains, which is what happened during the fatigue test. Therefore when determining the reserve capacity or fatigue life of rebar, sensors should be installed in sections that have critical strains. In the case studied, strain gauges were installed in the shear key close to the bond which is very sensitive to cracks from past experience. Therefore the remaining life of the shear key can be known if we think that the shear key has lost its bond.

6.11.1.2 Reserve capacity

Following 10 million cycles of the fatigue test and 2 million cycles of the pond test, the specimen was loaded monotonically until failure. From the monotonic test, rebar strains were plotted against the applied monotonic load at a level that is a little bit larger than the corresponding fatigue load in order to show the maximum rebar strain at the maximum fatigue load, marked by a horizontal line (see Figure 6.38). It is evident in the plots that UHPC with PVA combination (FAT-03 and FAT-04) gave smaller maximum strains at the final fatigue load level compared with other material combinations. The smallest strain (85 microstrain) is from FAT-03, which is 4.1 percent of the yield strain (2070 microstrain) of the reinforcing steel. Compared with FAT-04, this low strain of FAT-03 is due to the fact that there is no bond cracking in the fatigue test. The grout combination FAT-01(redo) gave the largest maximum strain (550 microstrain), which is about 26.6 percent of the yield strain of rebar. This is possibly because a very conservative load was applied. The UHPC with steel fiber combination (FAT-02) gave a maximum strain close to FAT-04 due to the fact that they

all had bond cracked during the fatigue tests. Even so, their maximum rebar strains are still smaller than that of FAT-01(redo), which indicates a much higher Young's modulus of UHPC materials than that of the grout material. This also explains why UHPC material combinations attract more demands than grout material combination.

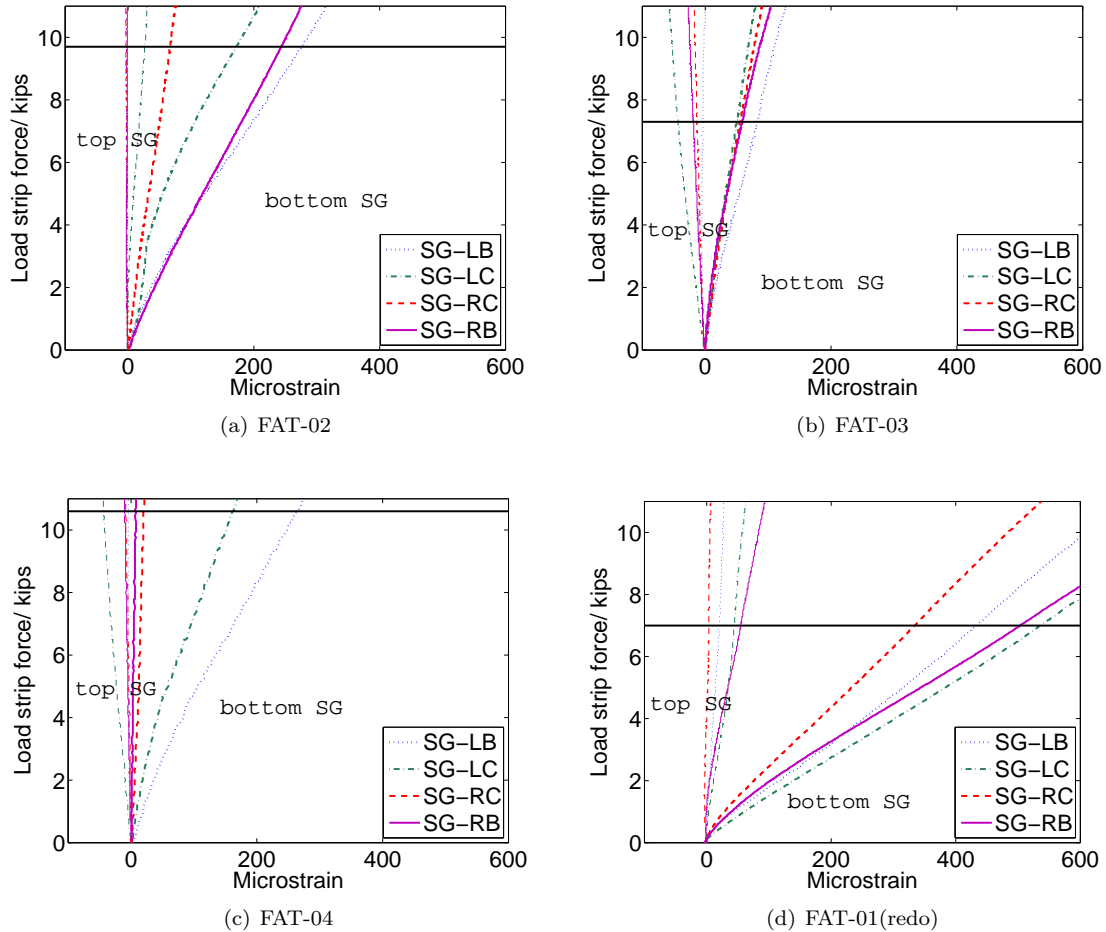


Figure 6.38: Rebar strain at the maximum fatigue load level

6.11.1.3 Fatigue life

Bridge slabs in AASHTO are not designed for fatigue limit states. According to ACI Committee 215 (ACI, 1974), beams subjected to repetitive loads under the service state should be checked for the possibility of fatigue distress so that adequate performance under service can be assured. Fatigue tests of reinforcing steel below 10 million cycles seem to indicate that reinforcing steel has a stress endurance limit below which its fatigue life is infinite. Of all the factors that can influence the fatigue life of steel, the stress range, which is the difference between the maximum stress and the minimum stress, is deemed to be the most critical one. In AASHTO [A5.5.3.2], the fatigue threshold

for straight reinforcement without a cross weld in the high-stress region is taken as:

$$(\Delta F)_{TH} = 24 - 0.33f_{min} \quad (6.9)$$

where f_{min} is the minimum stress. The units used for stress are all ksi. In the slabs tested, the minimum load level is 0.1 *kips*, which is small enough to consider f_{min} to be equal to zero. Then the final limit range would be 24 ksi. The maximum stress ranges during the fatigue tests are 8.1 ksi, 2.4 ksi, 7.9 ksi, and 15.9 ksi for FAT-02, FAT-03, FAT-04, and FAT-01(redo), respectively. It can be seen that under 10 million cycles of fatigue load, FAT-02, FAT-03, and FAT-04 are still far from getting distressed from fatigue. However, this does not represent the final conclusion until the conservativeness of the fatigue load for each specimen is known.

It should be noted however, the strain of the rebar at the critical bond may not be the controlling strain for the fatigue life of the rebar. Other possible critical locations include the bends within the shear key, and the critical section in the concrete slab considering the shear key and the bond may be much stronger than the concrete. For the slab tested, the rebar strain under the load strip, where the plastic hinge may form, can control the fatigue life. For the bridge, this controlling strain could be within the concrete that is adjacent to the joint due to the large demand attracted to it by the shear key. However as far as bond performance is concerned, the stress range of rebar close to the bond is good enough as an indicator.

6.12 Shear Key Material Determination

As mentioned in 6.4.1, when selecting shear key materials, it is important that the shear key material possesses high early strength with good workability to satisfy the needs of accelerated bridge construction, high durability both at the bond and within the key itself to solve the joint durability issue, and reasonable cost. The durability requires that the material should possess high toughness to control crack propagation both at the bond and within the material. Also the material should have good dimensional stability. Considering that in a 40 ft. span bridge, considerable shrinkage in the longitudinal direction could happen - thus giving rise to cracks and reducing the long-term durability. Based on the previous discussion from specimen casting to testing, an evaluation of the performance of each shear key material combination is summarized as follows:

6.12.1 Early strength

Shown in the cylinder tests, the UHPC combinations all had 4-day strength above 13000 psi. Due to the addition of HRWR, the UHPC groups had very good workability that it can compact itself when casting specimens. For the grout with PVA combination, the 7-day compressive strength is 5310 psi, and the 28-day compressive strength is 7405 psi. There are some trade-offs between workability, toughness, and compressive strength. The addition of fiber although can increase the toughness, it requires a higher amount of water to improve workability, which decreases compressive strength.

6.12.2 Stiffness-demand

As far as the stiffness-demand relationship is concerned, the UHPC combination, due to its high stiffness, attracted a corresponding large demand on it and also the precast adjacent to it. The grout group by comparison attracted a smaller demand which resulted in only a few cracks in the adjacent precast. The UHPC with PVA group, with a stiffness in-between those of the above two groups, attracted a moderate internal moment that caused a few cracks in the precast. Nevertheless, it does not mean the lower the shear key stiffness the better. Think about this in another perspective, the low shear key stiffness could cause large demands in the precast close to the stem. Obviously a balance needs to be achieved.

6.12.3 Durability

During the fatigue tests, generally all the bonds performed pretty well. For the UHPC groups, cylinder bond tests showed a typical failure in the concrete. For the grout with PVA group, although there was no bond cracking in the fatigue test, bond failure happened in the cylinder bond tests. At the end of the fatigue test, there was no crack within the shear key for the UHPC group, and a few cracks in other groups with a width barely observable with the naked eye.

6.12.4 Dimensional stability

Shrinkage cracks were found both on the top and at the bottom of the shear key for the UHPC with PVA and grout with PVA groups. The shrinkage crack is considered to result from the curing method applied and less internal restraint from the PVA fiber. Larfarge indicates that no indication of such cracks has been seen for the in-field use of UHPC with PVA (JS2000).

6.12.5 Rebar stress

After 10 million cycles, the rebar in the UHPC groups are far from getting distressed, even in the case of FAT-02 and FAT-04, which had a slight interface cracking. For the grout with PVA group, due to the low Young's modulus of the shear key material, although there was no bond cracking, the stress range of rebar at the fatigue load level is the largest compared with other material combinations.

6.12.6 Strength

All the material combinations showed higher strengths than the capacities predicted in the shear-moment interaction diagram.

6.12.7 Cost

Among the three combinations, the grout with PVA is the most economical, and the UHPC combination is most expensive with a cost that can be four times as high as the grout. These relative

costs are purely for the base material. However, if the full-advantage of UHPC is realized then the shear key details may be optimized - thus reducing overall costs.

6.13 Closure

The experimental phase of this research provided important information needed in determining the expected demand in a shear key of a constructed bridge. The data from the static testing was used to validate the magnitude of the load applied during the fatigue testing and it was also used to calibrate a finite element model of the shear key model used to estimate the transverse distribution of load and demand within the shear keys across a bridge deck. Through the experimental studies, the performance of individual shear keys constructed with different materials could be evaluated to help specify the design criteria for the shear key. Nevertheless, there are still some questions that need to be answered. For instance, what was the conservativeness of the fatigue load that was applied to the specimens? How sensitive is the transverse distribution to the performance of the shear key? Could the reinforcement extending into the shear key be two straight bars instead of a U-bar. Some of these questions may be answered after the model is calibrated and further analytical studies are conducted and other will need further experimental research.

From what has been discussed above, the UHPC with PVA fiber reinforcement is recommended as the most appropriate shear key material for the NEXT-D beam bridge. Basically it satisfies all the requirements for the application studied. The cost is a deterrent but considering the relatively small amount of material, it is feasible within the context of an entire bridge project.

In the subsequent chapters, it is necessary to determine the demand distribution factor of the NEXT-D beam bridge using finite element analysis, which requires the input of stiffness matrix from the shear key finite element model. Before that, the model needs to be calibrated first using the experimental data, which will be discussed in the next chapter.

This page intentionally left blank

Chapter 7

Demand Quantification for NEXT-D Beam

7.1 Scope and Objectives

As far as the NEXT-D bridge design is concerned, the load distribution formulas of LRFD for beam design, as they are given in the AASHTO Bridge Design Specifications (AASHTO, 2012), do not directly apply as the beam has a stem spacing of 3 ft. Furthermore, the AASHTO strip method for calculating demands placed on the deck does not consider the varying deck spans which are typical to the NEXT-D bridge. Therefore, the refined analysis method as described in LRFD Article 4.6.3 is required in order to determine the appropriate load distribution factors and deck demands for the NEXT-D bridges. In this study, a three dimensional finite element modeling (3D FEM) of the NEXT-D bridges is carried out using the commercial analysis package SAP2000 (CSI, 2011c). Base models are built for NEXT-D bridges with a span length of 40 ft., and a beam spacing of either 6 ft. (NEXT-6) or 8 ft. (NEXT-8).

In this Chapter, the following topics are covered including the modeling details of the base model and the basic findings relative to bridge behavior and the associated load demands. Since the finite element model is sensitive to the modeling assumptions, an initial study was performed to assess the requisite level of accuracy within the model. Two types of model were created, one using frame and shell elements while the other used solid elements. This screening study provided modeling guidance for the other analytical bridge models used in this research.

Since the AASHTO strip width formulas do not apply to the NEXT-D bridges with varying deck spans, appropriate strip widths for the live loads are determined for the NEXT-D bridges. In the bridge FEM, the modeling of the shear key is specifically addressed. This required experimental data to be collected (see Chapter 6) and also a detailed shear key model which is discussed later in this chapter. In the shear key finite element model, the shear key stiffness is calibrated based on experimental data. This model aims at determining a stiffness matrix for the shear key, which will be fed into the bridge finite element model. The primary objective of this study is to provide reliable

finite element models for short-span NEXT-D bridges (between 22 ft. and 40 ft.) to facilitate the later bridge design discussed in the next chapter.

7.2 Bridge Modeling

7.2.1 Bridge Geometry

As per the request of the SCDOT, this project is to focus on bridge spans of 22 to 40 ft. The use of a six-foot wide NEXT-D section and an eight-foot wide NEXT-D section were investigated because these widths represent the range for which the SCDOT has specific interest. For the base model, only the 40 ft. span bridges for NEXT-6 and NEXT-8 were constructed initially. The bridge model is supported six inches in from each end which is considered to be the center of bearing. For both NEXT-6 and NEXT-8, the width of the bridge is 47 ft. and 4 in. The NEXT-6 bridge model consists of eight NEXT-D beams and seven shear keys, and the NEXT-8 bridge model consists of six NEXT-D beams and five shear keys. Refer to Figure 7.1 and Figure 7.2 for geometry details of base bridge models.

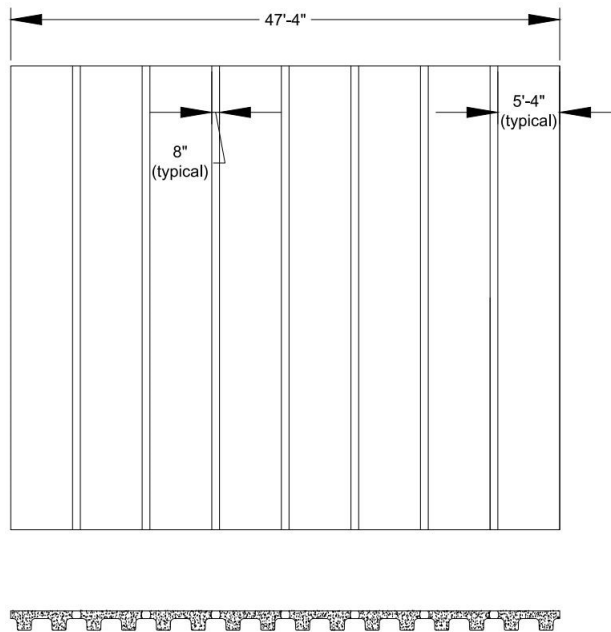


Figure 7.1: Dimensions for the 40 ft. span NEXT-6 bridge model

7.2.2 Modeling Approach

The Federal Highway Administration (FHWA) provides guidelines for the refined analysis of deck slabs. They state that plate, shell, or solid elements may be used to model a bridge deck for refined deck analysis. However, plates cannot be used as part of 3D models that include decks

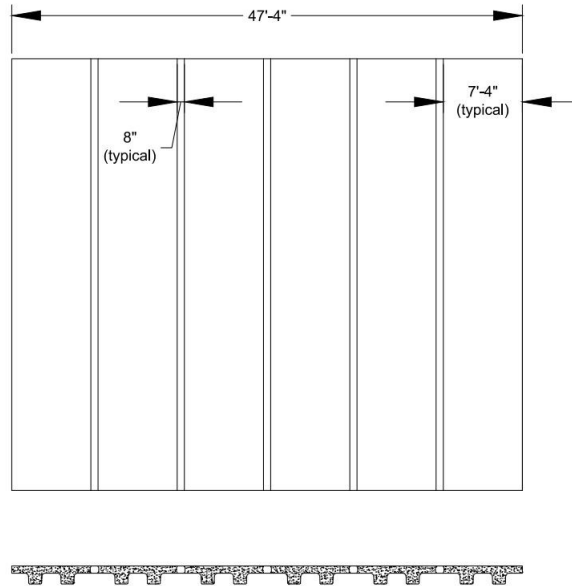


Figure 7.2: Dimensions for the 40 ft. span NEXT-8 bridge model

and girders because they do not account for in plane forces in the deck. Shell and solid elements are both acceptable methods of modeling bridge decks, of which, shell elements are easier to work with because of the simplicity of getting output from the software (FHWA, 2011).

Finite element modeling is sensitive to the model inputs, so it is important to establish certain criteria in order to obtain reasonable results. For this project, two types of finite element models were built using SAP2000 (CSI, 2011c) for the same bridge. One model used eight-node solid elements for the NEXT-D sections and parapets and the other model used four-node shell elements for the bridge deck and frame elements for the stems and parapets. In the shell model, the slab was connected to the stems and the parapets using rigid links. In both models, the shear key was represented by a frame element, the input of which is to be determined based on the calibrated shear key finite element model talked about later.

7.2.3 Solid Modeling

For the solid model, solid elements were used to represent the entire NEXT-D section along with the parapets. “The solid element is an eight-node element that is based on an isoparametric formulation that includes nine optional incompatible bending modes” (CSI, 2011a). It is very important to ensure that the incompatible bending modes option is turned on to achieve accurate results. This feature is selected during the definition of a solid section. The material is also specified in the solid element definition. Material properties include modulus of elasticity (E), shear modulus (G), Poisson’s ratio (ν), coefficient of thermal expansion (α), and mass density (m) or weight density (w). E , G , ν , and α can all be defined as direction specific (CSI, 2011a). However, because concrete is assumed to be isotropic, this option was not utilized for the solid model used in the study. SAP2000

has built in material properties for different concrete mixes of various strengths, so these predefined materials were utilized to define the material for the solid elements used in the model.

One of the problems with modeling the bridge using solid elements arises from the fact that the solid elements in SAP2000 only have translational degrees of freedom at the nodes (CSI, 2011a). For this model, it was necessary to connect a frame element – used to model the shear key – to the nodes of solid elements and obtain internal forces and moments. When a frame element is connected to a node on a solid element, no moment or torsion is transferred. This problem is solved by the use of rigid links as shown in Figure 7.3, in which the rigid link (vertical member) connects the frame element (horizontal member) to the node shared by the four solid elements. A rigid link is a member that is defined to be extremely rigid so it does not contribute to any additional deformation to a structure.

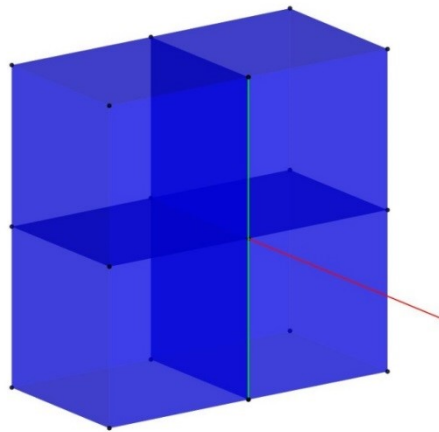


Figure 7.3: Frame to solid connection in SAP2000 using rigid links

7.2.4 Shell Modeling

In the formulation of the shell model, shell elements were used to represent the integrated bridge deck, and frame elements were used to represent the beam stems and the parapets. “The shell element is a three- or four-node formulation that combines membrane and plate-bending behavior” (CSI, 2011a)). In order to ensure accurate results, it is important to keep the aspect ratio of a rectangular shell element (the ratio of the longest side to the shortest side) as close to unity as possible. One should try to keep the ratio less than four, and most certainly never greater than ten. A shell element in SAP2000 has all six degrees of freedom at each node - three translational and three rotational (CSI, 2011a).

There are two shell formulations, one of which is the thick-plate formulation, which includes the effects of transverse shear deformation, and the other the thin-plate formulation, which ignores the contributions of shear deformation. In general, the thick-plate formulation is more accurate, but it is more sensitive to large aspect ratios and can result in inaccurate results in such cases. In this study, the thin-plate formulation was used, the results of which were compared to those from the

solid model in order to determine whether this thin-plate formulation is adequate. Here, the solid element is assumed to provide the most realistic results (CSI, 2011b) and taken as the reference model.

The main problem that arises with the use of shell elements for modeling a 3D bridge is accurately modeling the geometry of the different members in relation to each other. This problem was solved through the use of rigid links. When a shell member is drawn in SAP2000, it is depicted as a plane, and when a frame member is drawn, it is depicted as a line. In reality, the shell and the frame actually possess three dimensional geometries. For example, for a NEXT-D bridge, the centroid of the bridge slab and the bridge stem are separated. In order to model this geometric relationship, members are drawn at their centroid, and then connected using rigid links.

7.3 Shear Key Modeling

The appropriate modeling of the shear key with a correct stiffness plays a significant role in demand determination of the NEXT-D bridges. In the base model, the shear key frame element is spaced 6 in. apart to provide adequate connectivity between the beams while trying to control the overall size and runtime of the model. This element spacing also allows for the investigation of shear key demand distribution in the longitudinal direction. The stiffness of the shear key frame element was obtained based on an original study by Flores Duron (Flores-Duron, 2011) before any experiment was carried out. The stiffness matrix is displayed in Figure 7.4, in which 1-3 denote translational degrees of freedom and 4-6 denote rotational degrees of freedom. Refer to Figure 7.5 for shear key local axes.

$$\begin{array}{c}
 \mathbf{1} \quad \mathbf{2} \quad \mathbf{3} \quad \mathbf{4} \quad \mathbf{5} \quad \mathbf{6} \\
 \left(\begin{array}{cccccc}
 1201 \text{ kip/in} & 0 & 0 & 0 & 0 & 0 \\
 & 220 \text{ kip/in} & 0 & 0 & 0 & 513 \text{ kip/rad} \\
 & & 817 \text{ kip/in} & 0 & 1905 \text{ kip/rad} & 0 \\
 & & & 381 \text{ (kip-in)/rad} & 0 & 0 \\
 & \text{(Symmetric)} & & & 21929 \text{ (kip-in)/rad} & 0 \\
 & & & & & 5905 \text{ (kip-in)/rad}
 \end{array} \right)
 \end{array}$$

Figure 7.4: Frame element stiffness matrix for a six-inch section of shear key

In order to achieve the requisite stiffness matrix of Figure 7.4, the stiffness matrix formulation considering shear deformations for a 2D beam was utilized (Figure 7.6) to identify the parameter input of the shear key frame element. In the formulation matrix shown in Figure 7.6, E stands for modulus of elasticity, I stands for moment of inertia, f_s is the shape factor, G is the shear modulus, A is the cross sectional area, and L is the length of the element. It should be noted that axial stiffness is equal to $\frac{AE}{L}$ and torsional stiffness is equal to $\frac{JG}{L}$ where J is the torsional constant. In the

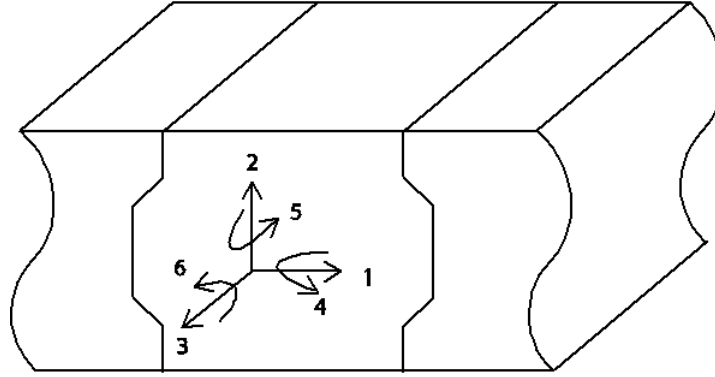


Figure 7.5: Shear key local axis

matrix, the shear modulus G is obtained based on the predefined Young's modulus E and Poisson's ratio, leaving I , f_s , A , and L the only unknown parameters. This 2D formulation matrix can be applied to the 3D problem by considering cross section properties in the orthogonal directions.

$$k_{w/shear} = \frac{EI}{L^3(1 + \beta_s)} \begin{bmatrix} 12 & 6L & -12 & 6L \\ 6L & L^2(4 + \beta_s) & -6L & L^2(2 - \beta_s) \\ -12 & -6L & 12 & -6L \\ 6L & L^2(2 - \beta_s) & -6L & L^2(4 + \beta_s) \end{bmatrix}$$

$$\beta_s = \frac{12EIf_s}{GAL^2}$$

Figure 7.6: Element stiffness matrix for beam elements with inclusion of shear deformations

Based on the formulation, the length of the shear key frame element was determined to be 4.66 in. ($\frac{2 \times 513 \text{ kip/rad}}{220 \text{ kip/in}} = 4.66 \text{ in.}$), which does not necessarily fit well in the 8 in. gap left in the model for the shear key. This problem was solved through the use of equal constraints, i.e., one end of the shear key frame element was attached to the shell(or solid) element in one beam, and the other end was constrained to the shell/solid element in the adjacent beam using equal constraints for all the degree of freedoms.

The section properties of the shear key frame element determined this way include cross sectional area (A), torsional constant (J), moment of inertia about both axes (I_2 , I_3), and shear

area in both directions. The reliability of this method was checked by creating a very simple model of a 4.66 in. long frame element that was fixed at one end and free at the other (Figure 7.7). The free end was constrained with a fixed node that was 3.44 in. away from it using equal constraints, therefore creating an 8 in. spacing between the fixed nodes. Unit displacements and rotations were applied to both the fixed end of the frame and the fixed node, and the reactions show that all the desired stiffness terms are obtained.

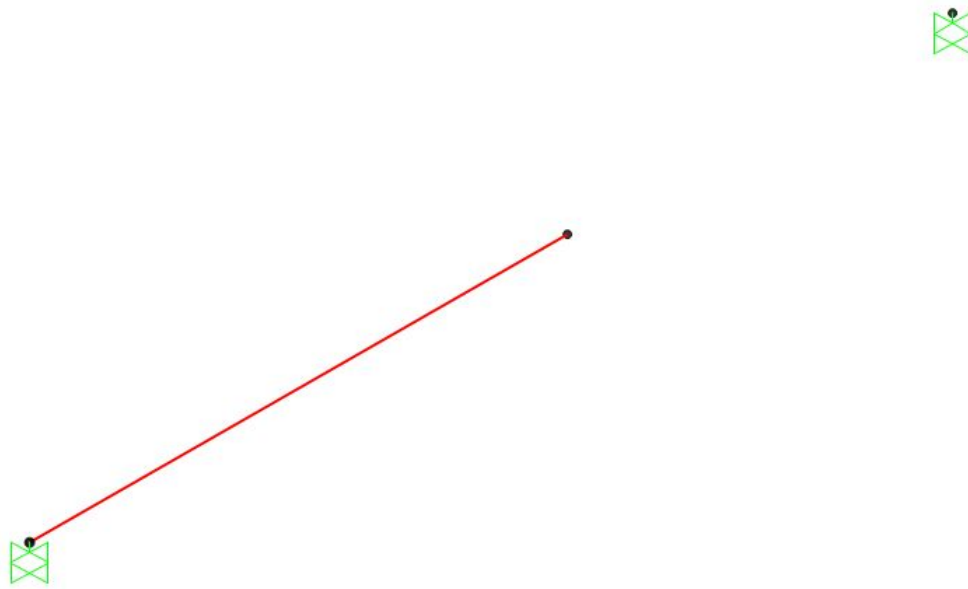


Figure 7.7: Shear key stiffness verification model

7.4 Solid FEM

7.4.1 Shear Key

The shear key frame element is connected to the adjacent solid element as illustrated in Figure 7.8, where the dots represent the equal constraints for the shear key, and the vertical lines on the face of the solid elements represent the rigid links.

7.4.2 Beams and Parapets

In the solid model, both the beam cross section and the parapets are represented by solid elements. The concrete material properties are shown in Table 7.1.

The incompatible bending modes option was turned on for all solid elements in order to ensure the most accurate results. The solid elements were given a longitudinal dimension of 6 in. so that the nodes would match up with the nodes of the shear keys. The solid elements in the bridge deck were divided in the transverse direction into sections between 3.25 and 3.75 in. wide so that

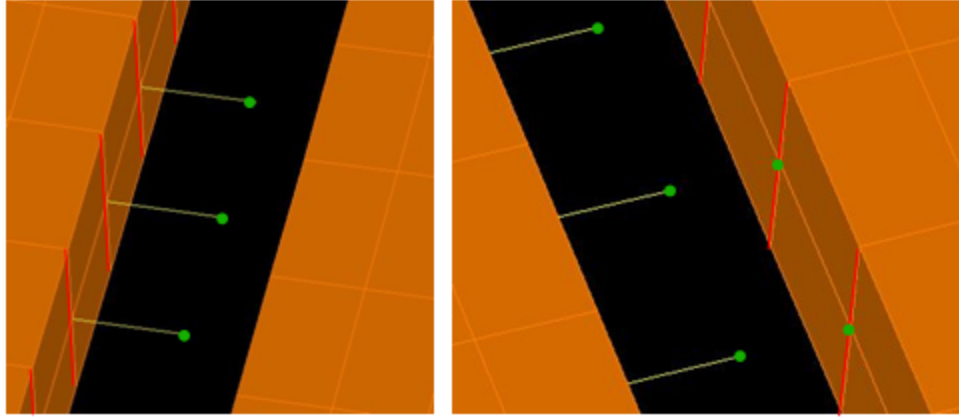


Figure 7.8: Shear key connection in solid model

Table 7.1: Properties of concrete used in the NEXT-D models

Property	Value	Units
Compressive Strength	6.0	ksi
Weight per Unit Volume	150.0	$\frac{lb}{ft^3}$
Modulus of Elasticity	4415.2	ksi
Poisson's Ratio	0.2	-
Shear Modulus	1839.7	ksi

wheel loads could be applied at various locations along the bridge. The deck is composed of two layers of 4 in. high solid elements vertically. The stem was divided into four solid elements transversely and three solid elements vertically. The fillet between the deck and the stem was modeled using two six-node triangular solid elements. It is important to keep the aspect ratio of the longest side to the shortest side of a solid element as close to unity as possible in order to achieve accurate results (CSI, 2011a). In the model the largest aspect ratio is $\frac{6}{3.25} = 1.85$ for the rectangular solids and $\frac{6}{1.58} = 3.80$ for the triangular solids. The parapet was also broken up into smaller solid elements in order to match the nodes up with the nodes of the bridge deck. The parapet was modeled with the dimensions given in Figure 7.9. The modeled cross sections of the exterior beams for both NEXT-8 and NEXT-6 are displayed in Figure 7.10 and Figure 7.11 respectively.

7.4.3 Restraints

In order to ensure a symmetric response and avoid Poisson effect induced stresses at the supports for the bridge, special attention was paid to the restraints placed on the bridge. In the model, at the location of the support, which is 6 in. from the end, all of the nodes at the bottom of the stems are restrained in the z (vertical) direction. At one end of the bridge, the node on the far

7.5 Shell FEM

7.5.1 Shear Key

The shear key frame element is connected to adjacent shell elements as described before. The shear key to deck connection in the shell model is shown in Figure 7.13. The dots show the equal constraints for the shear keys.

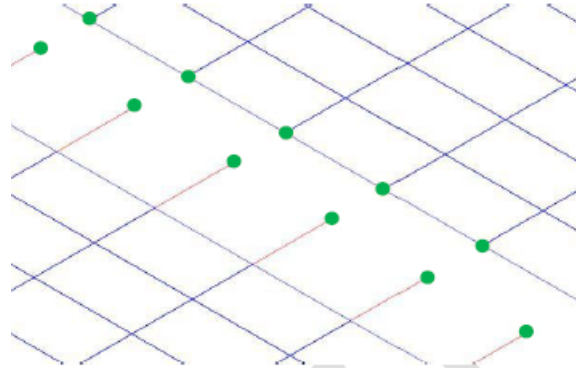


Figure 7.13: Shear key connection in shell model

7.5.2 Deck

The deck for the shell model was modeled using thin shells, which were assigned a thickness of 8 in. representing the thickness of the deck. The shear key frame elements were spaced along the span length of the bridge at 6 in. from center to center. The dimensions of the shell element were set to be 6 in. along the span length of the beam in order to match up with the location of the shear keys' nodes. The shells were divided in the transverse direction into sections between 3.25 and 3.75 in. so that wheel loads could be applied at various locations along the bridge. It is important to keep the aspect ratio of the longest side to the shortest side of a rectangular shell element below four to achieve accurate results (CSI, 2011a). The largest aspect ratio for the shells in the model is $\frac{6}{3.25} = 1.85$. The shells over the stems of the bridge were assigned a modifier for bending due to the fact that in a real NEXT-D beam, the deck and the stems are integral, and the deck would have the stiffness of the entire depth of the section in these locations. This was accomplished by applying a stiffness modifier of 15.625 for the bending in the transverse direction because the entire depth of the deck and stem is 20 in., while the depth of the slab is 8 in., and $I = \frac{(bh^3)}{12}$. Therefore, $I_{total} = \frac{(6in \times (20in)^3)}{12} = 4000in^4$ and $I_{deck} = \frac{(6in \times (8in)^3)}{12} = 256in^4$ and $\frac{(4000in^4)}{(256in^4)} = 15.625$.

7.5.3 Parapet

The parapet was modeled as a frame element using the section designer feature of SAP2000. A screen capture of the parapet shown in the section designer feature is shown in Figure 7.14. The compressive strength of the parapet was preliminarily assigned to be 6 ksi for this initial study

Table 7.2: Parapet section properties

Property	Value	Units
Cross Sectional Area:	425	in ²
Torsional Constant:	15459	in ⁴
Moment of Inertia about 3-axis:	41324	in ⁴
Moment of Inertia about 2-axis:	7962	in ⁴
Shear Area in 2-direction:	311	in ²
Shear Area in 3-direction:	392	in ²

but all final analyses were done using the SCDOT recommended 4ksi. These section properties are shown in Table 7.2.

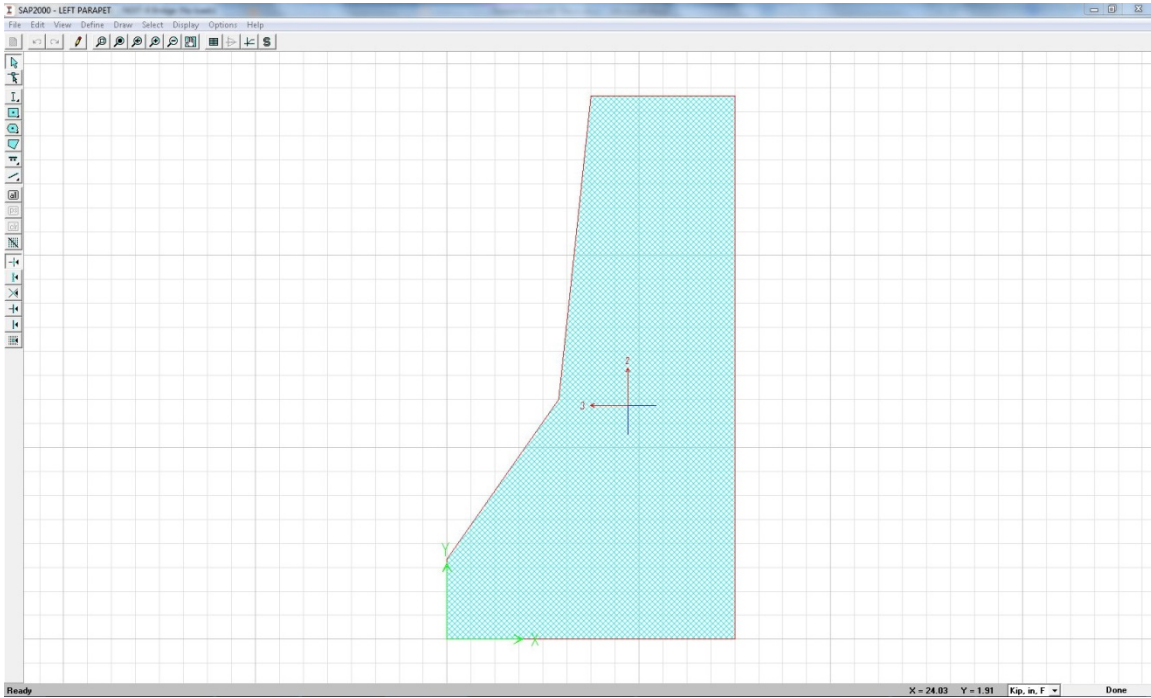


Figure 7.14: Parapet in section designer

The parapet is connected to the deck using rigid links. The links allow the centroid of the parapet to be located properly in space relative to the rest of the bridge. Each parapet frame element is 6 in. long in order to correspond with the shear key spacing.

7.5.4 Stem

The stem of the bridge was also modeled as a frame element using section designer. The stem was taken to be the entire section of concrete below the eight-inch bridge deck. The stem

geometry in the real case is shown in Figure 7.15. A screen capture of the stem section in section designer is shown in Figure 7.16. The compressive strength of the stem was assigned to be 6 ksi, and the section properties of the stem are shown in Table 7.3.

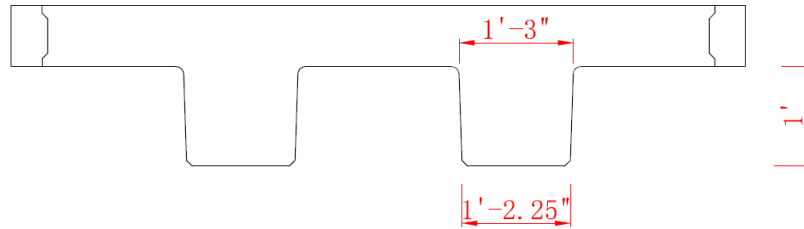


Figure 7.15: Stem dimension

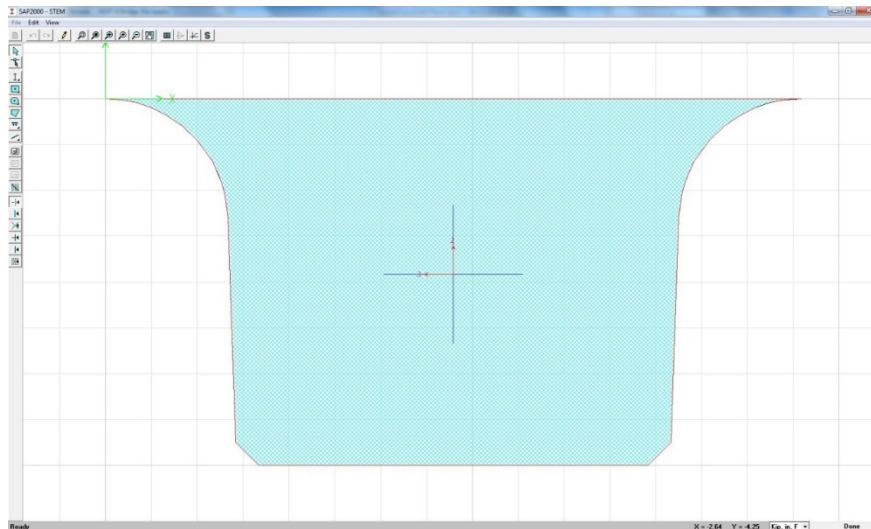


Figure 7.16: Stem modeling in section designer

The stems are also connected to the slab using rigid links so that the geometry of the bridge could accurately be represented in three dimensional space. Each stem frame element is 6 in. long in order to correspond with the shear key spacing.

7.5.5 Rigid Links

The rigid links are created to connect the various elements of the bridge so that their relative geometry could accurately be represented in a 3D model. The parapets and stems are connected to the deck at their centroids. The links were assigned properties to prevent any additional deflection to the bridge. If elements in a model have properties that are too stiff, SAP2000 will generate an ill-conditioned stiffness matrix, so the analysis details were monitored to be sure that this was not

Table 7.3: Stem section properties

Property	Value	Units
Cross Sectional Area:	116	in ²
Torsional Constant:	2763	in ⁴
Moment of Inertia about 3-axis:	1444	in ⁴
Moment of Inertia about 2-axis:	2279	in ⁴
Shear Area in 2-direction:	96	in ²
Shear Area in 3-direction:	100	in ²

Table 7.4: Rigid link section properties

Property	Value	Units
Cross Sectional Area:	1000000	in ²
Torsional Constant:	1000000	in ⁴
Moment of Inertia about 3-axis:	1000000	in ⁴
Moment of Inertia about 2-axis:	1000000	in ⁴
Shear Area in 2-direction:	0	in ²
Shear Area in 3-direction:	0	in ²

the case. The shear area of the rigid links was assigned to be zero because this causes SAP2000 to ignore the contributions of shear deformation. The properties of the rigid links are shown in Table 7.4.

7.5.6 Restraints

The shell model was restrained the same way as the solid model. The only difference was that for the shell model, there was only one node at the bottom of the stem, which is where the rigid links and the longitudinal stem frame member come together. All of the stems at the support location were restrained in the z (vertical) direction. On one end of the bridge, the stem closest to the side of the bridge was restrained for translation in all three directions. On the diagonally opposite corner of the bridge, one node was restrained for translation in the y (transverse) direction in order to keep the bridge from rotating. All of the supported nodes were unrestrained for rotation. Refer to Figure 7.17 for support details.

The final shell model for the eight-foot NEXT-D section is illustrated in Figure 7.18. The modeled cross sections of the exterior beams for both NEXT-8 and NEXT-6 are displayed in Figure 7.19 and Figure 7.20 respectively.

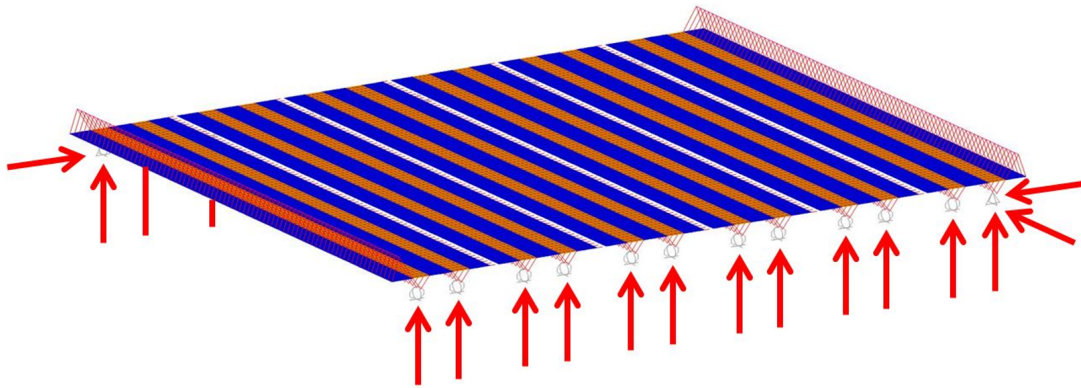


Figure 7.17: Restraints for shell model

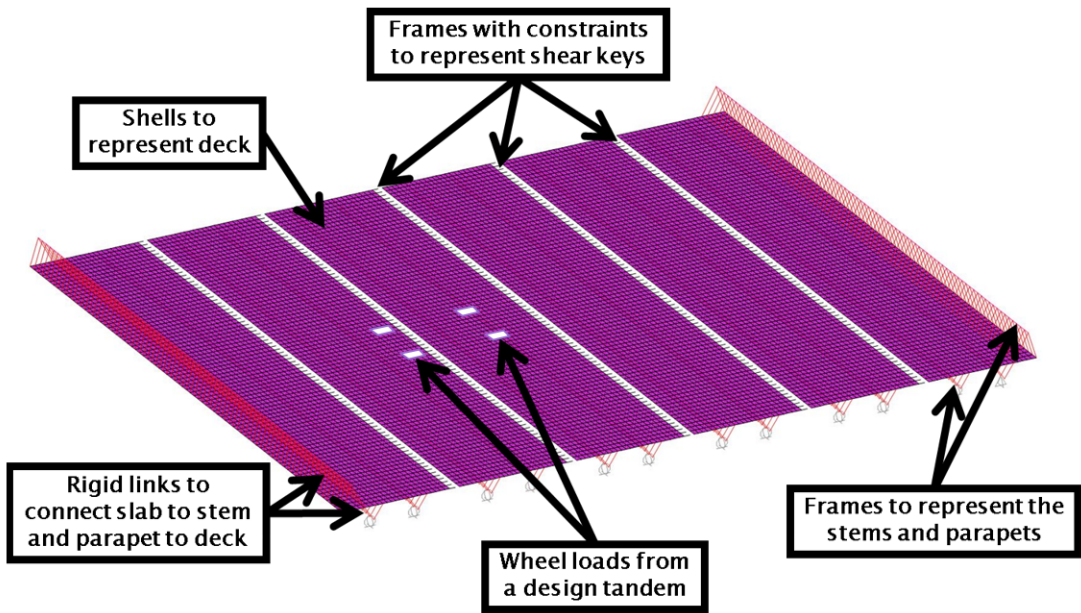


Figure 7.18: SAP2000 NEXT-8 shell model

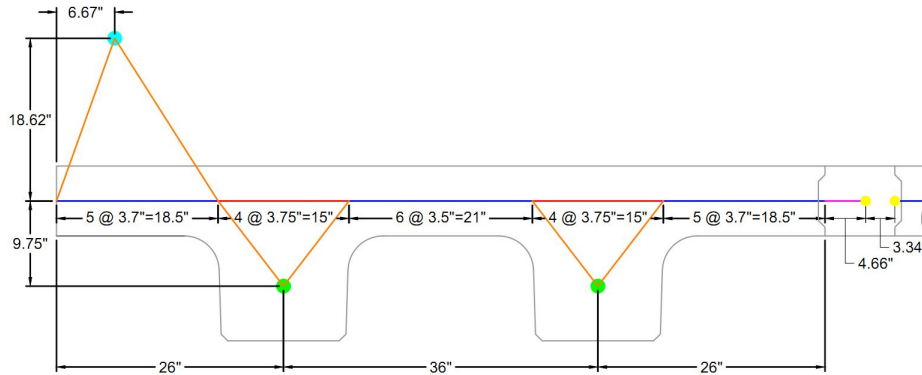


Figure 7.19: Shell modeling layout for NEXT-8

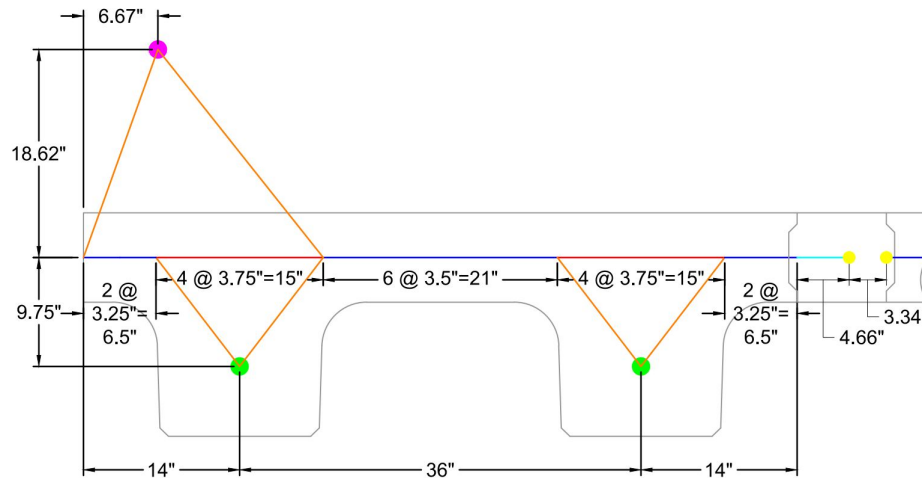


Figure 7.20: Shell modeling layout for NEXT-6

7.6 Bridge Live loads

To appropriately assess the behavior of the NEXT-D bridge it is important to apply loads which are typical to the bridge. As such, the live loads prescribed in the bridge design specifications were used. The design loads for decks are as specified in LRFD Article 3.6.1.3.3: when the deck is spanned mainly transversely, either the design truck of Article 3.6.1.2.2 (known as the HS20 truck) or the design tandem of 3.6.1.2.3 needs to be applied (AASHTO, 2012). The amplification of the wheel loads from centrifugal and braking forces can be ignored. The design truck (Figure 7.21) consists of an 8 kip front axle, a 32 kip rear axle on the tractor, and a 32 kip axle on the trailer. The spacing between axles on the tractor is 14 ft. and the spacing between the rear axle of the tractor and the trailer axle is a minimum of 14 ft. but not more than 30 ft. The axle loads are split evenly between the driver's side and passenger's side of the truck and the tires on an axle are spaced 6 ft.

apart. The spacing used should maximize the demand of the design. The design tandem (Figure 7.22) consists of two 25 kip axles with 6 ft. between each tire on an axle and 4 ft. between axles.

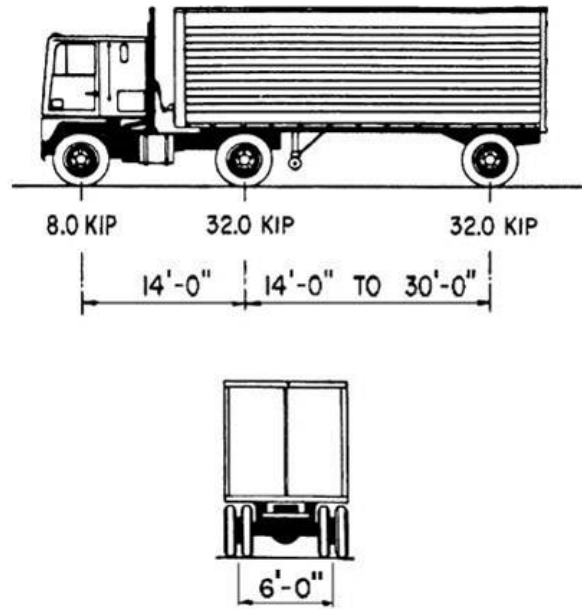


Figure 7.21: AASHTO design truck (AASHTO, 2012)

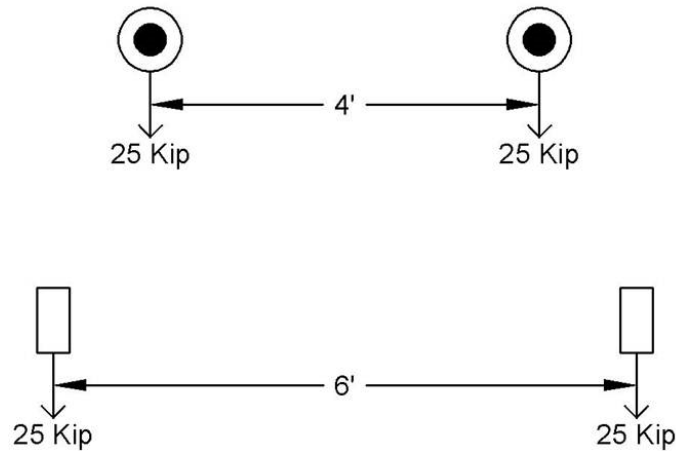


Figure 7.22: AASHTO design tandem (AASHTO, 2012)

According to LRFD Article 3.6.1.2.5, the contact area of wheel loads may be modeled as rectangular with a width of 20 in. and a length of 10 in. The force of the tire is to be uniformly distributed over the contact area. In the case studied, the wheel loads were applied as patch loads

with widths between 14 and 15 in. and a length of 12 in. The dimensions of the wheel load were driven by the dimensions of the shell and solid elements of the deck. The load modeled is actually pretty conservative in the sense that the patch load area does not include the spreading length of the deck depth.

7.7 Shell FEM vs Solid FEM

The design truck and design tandem loads were applied to the NEXT-6 and NEXT-8 for both shell models and solid models. The loads were moving transversely (Figure 7.23), with the shear key transverse demands monitored. Moment and shear influence lines were generated for the left and right sides of the shear key. This process was repeated over the supports of the bridge, at quarter-span of the bridge, and at mid-span of the bridge.

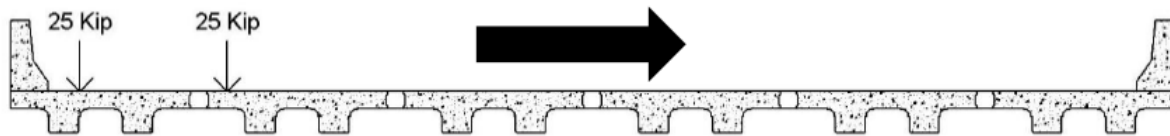


Figure 7.23: Design tandem moving transversely

Typical influence lines of NEXT-6 under the design tandem loading at mid-span are shown in Figure 7.24 and Figure 7.25. The keys are labeled in sequence from one side of the bridge to the other. The location of the load on the x-axis refers to the point midway between the left and right wheels. Each figure shows the influence lines for all seven shear keys.

The shear and moment influence lines for the solid model and shell model closely resemble each other with the exception of the outermost keys. Influence lines for the shear keys of an eight-ft. NEXT-D bridge under the design tandem loading at mid-span are shown in Figure 7.26 and Figure 7.27.

Similarly to the 6 ft. model, the greatest shear and negative moment demands clearly exist in the outermost keys. These differences can be attributed to the difference between the connection of the parapet to the bridge for the solid model and the shell model. By getting rid of the parapets, the influence lines for these models with the design tandem load applied at mid-span are shown in Figure 7.28 through Figure 7.31. The influence lines for the outermost keys for the solid and shell models align much more closely with each other than the influence lines for the bridge models with parapets. For the influence lines of the outermost keys, compared with the solid model, the difference in the critical demands between the two types of models are all within 10 percent, proving that the cause for the large demand variations in the solid and shell models stem from the difference between the connections of the parapet to the bridge deck.

In the solid model, the parapet and the deck are connected by sharing the same nodes at the interface. In the shell model, the parapet is connected to the bridge deck by rigid links. The way that the parapet is modeled in the shell model is more representative of the real-life parapet

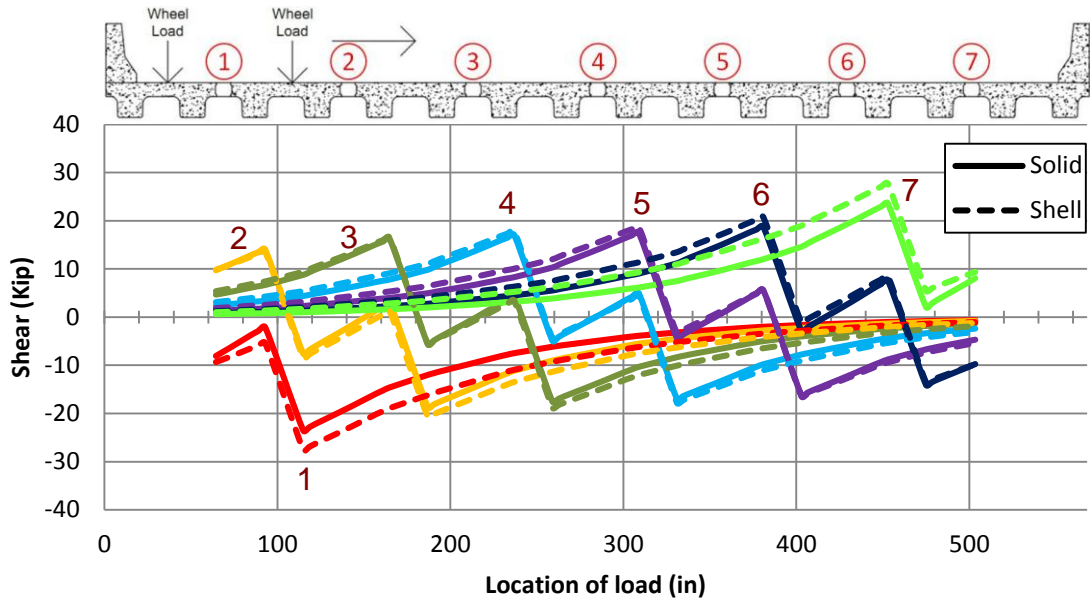


Figure 7.24: Shear influence line for the shear keys in the NEXT-6 bridge under a design tandem loading at mid-span

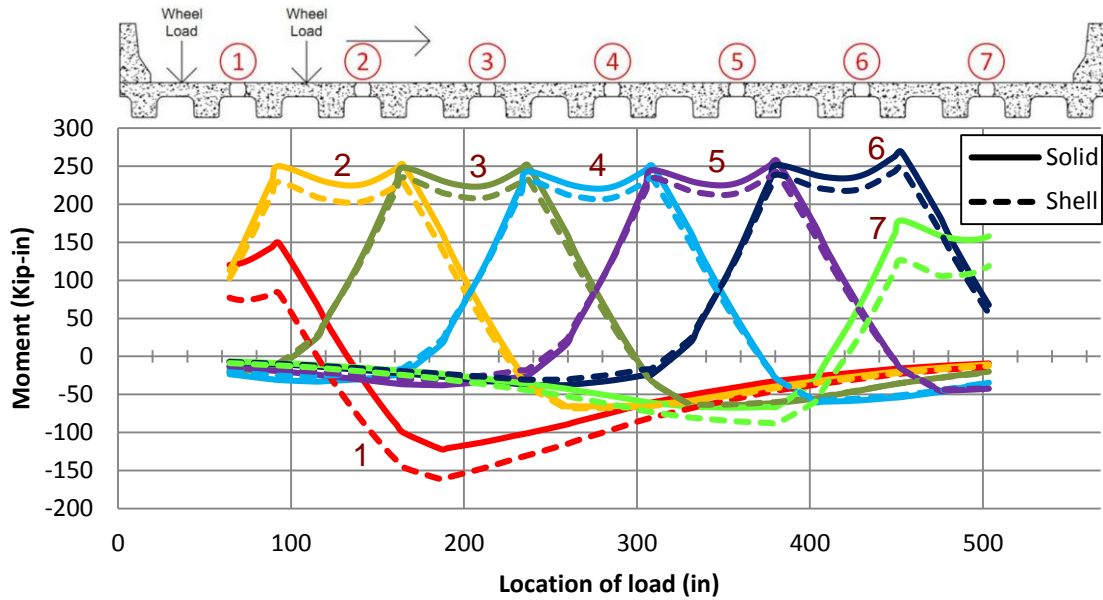


Figure 7.25: Moment influence line for the left side of the shear keys in the NEXT-6 bridge under a design tandem loading at mid-span

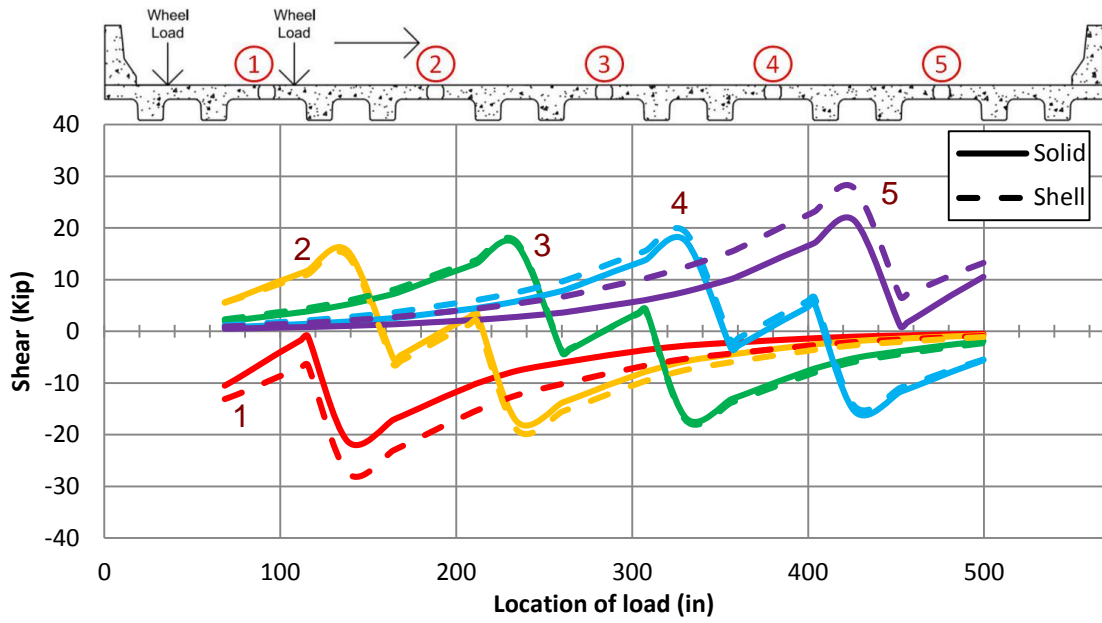


Figure 7.26: Shear influence line for the shear keys in the NEXT-8 bridge under a design tandem loading at mid-span

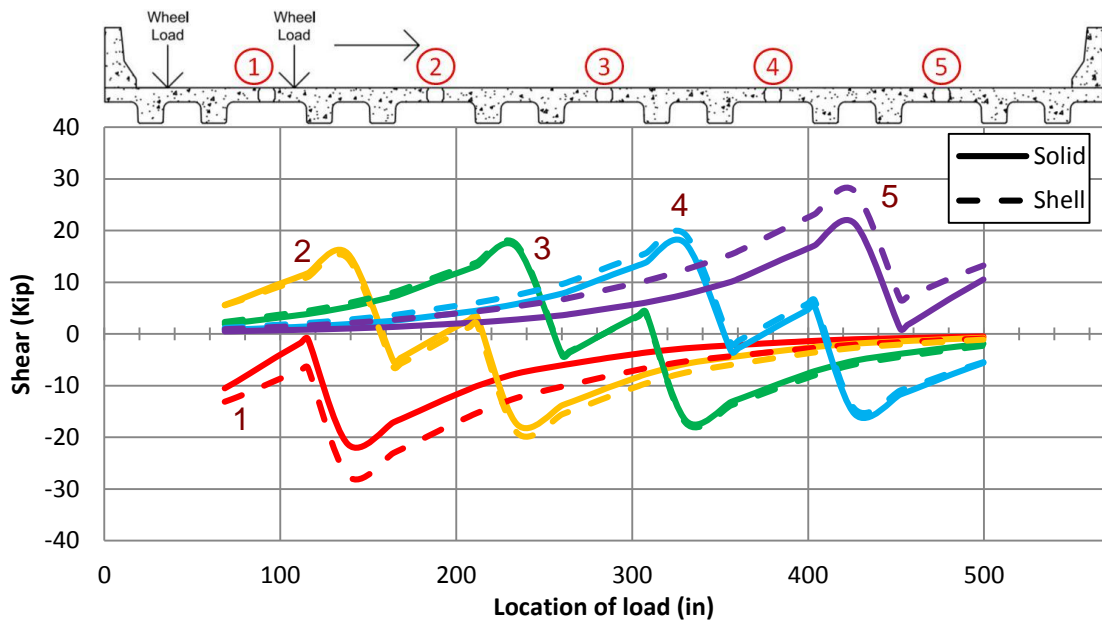


Figure 7.27: Moment influence line for the left side of the shear keys in the NEXT-8 bridge under a design tandem loading at mid-span

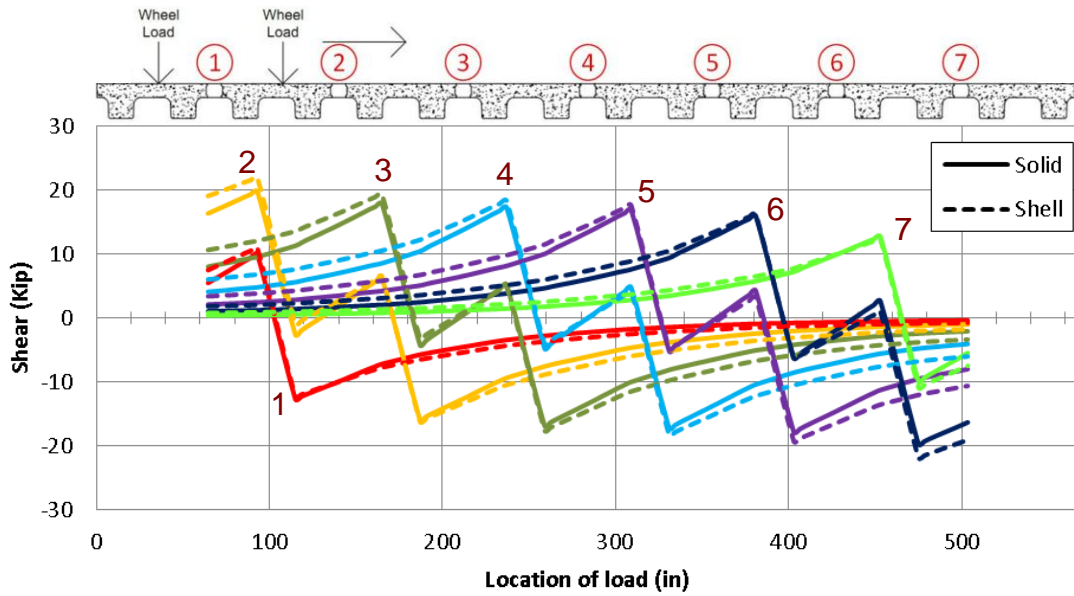


Figure 7.28: Shear influence line for the shear keys in the NEXT-6 bridge without parapets under a design tandem loading at mid-span

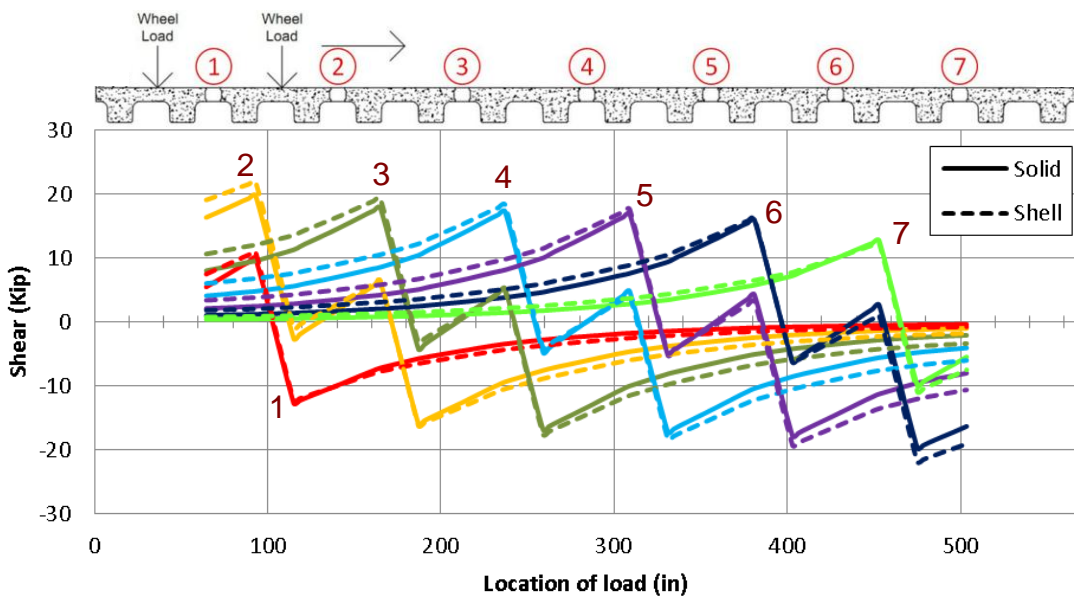


Figure 7.29: Moment influence line for the left side of the shear keys in the NEXT-6 bridge without parapets under a design tandem loading at mid-span

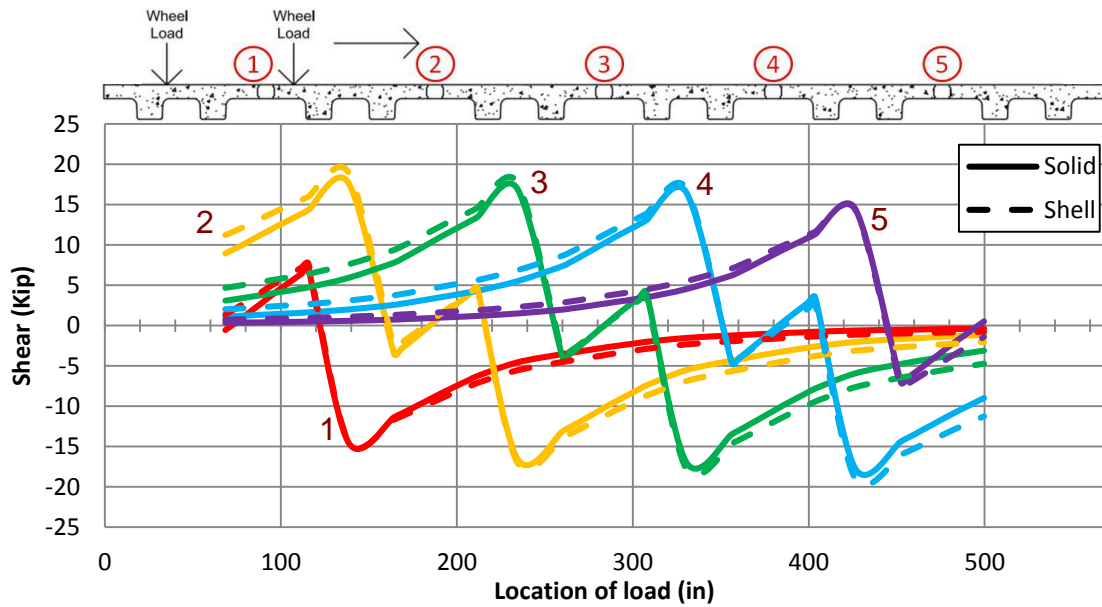


Figure 7.30: Shear influence line for the shear keys in the NEXT-8 bridge without parapets under a design tandem loading at mid-span

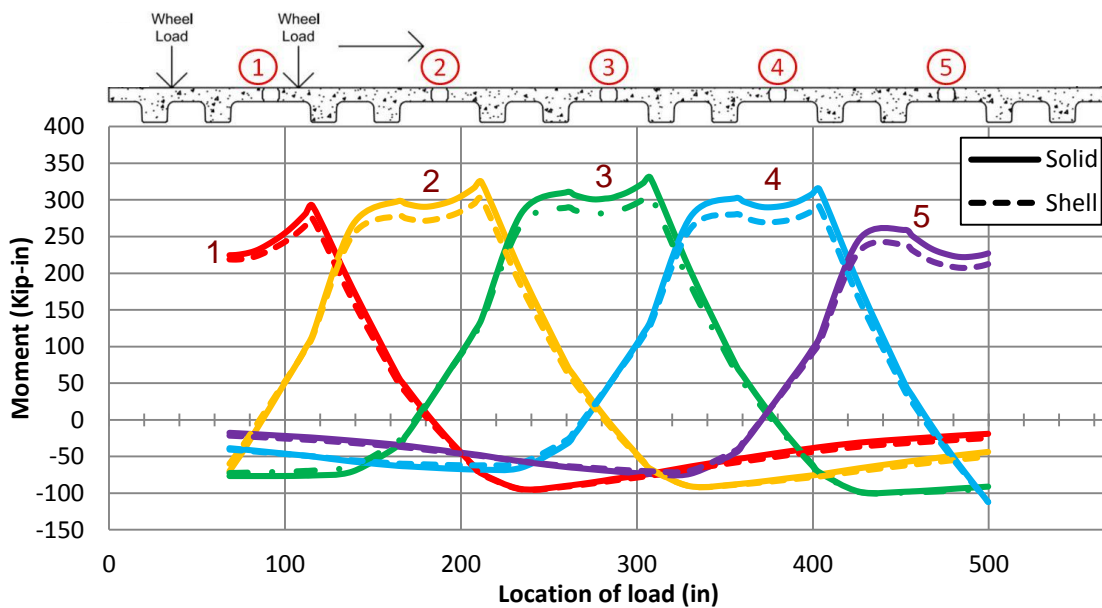


Figure 7.31: Moment influence line for the left side of the shear keys in the NEXT-8 bridge with no parapets bridge under a design tandem loading at mid-span

to deck connection because in reality, the parapet is not integral with the bridge deck across its entire width. As such, the shell model was deemed to be an adequate solution for determining the demands in a NEXT-D bridge. This selection also saves a lot of effort in the sense that data is much easier to be obtained from the shell model than the solid model. From this point on, all the results are given by the shell model.

7.8 Strip Width Determination for AASHTO Live Loads

Once the shell model was chosen as an adequate representation of the bridge, the design tandem loading was moved across the bridge models longitudinally (Figure 7.32) at each of the transverse critical locations for shear, positive moment, and negative moment in the key to locate the longitudinal critical loading position. The critical shear demands (shear, positive moment, and negative moment) all occur when the loading is at the mid-span of the bridge.

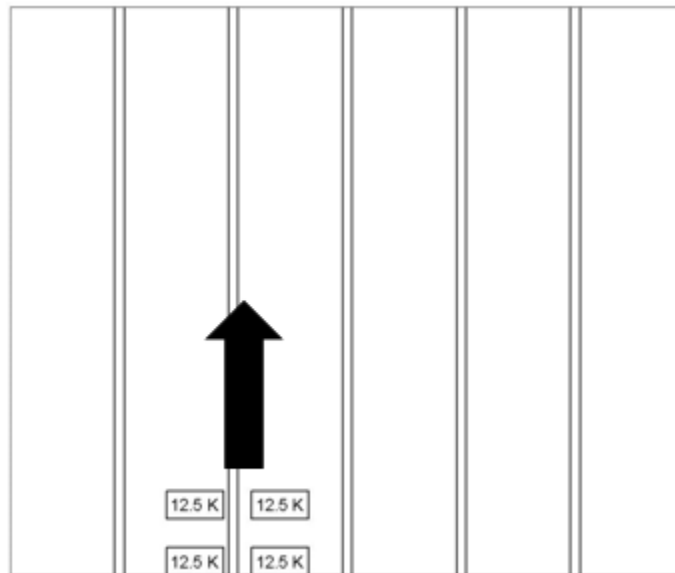


Figure 7.32: Design tandem longitudinal load placement

The longitudinal shear key demand distributions were investigated for the single 32 kip axle of the design truck, the two 32 kip axles of the design truck spaced 14 ft., and the design tandem. The demands are obtained from each shear key frame element, and plotted against the longitudinal location of the shear key element. As an illustration, the longitudinal shear key demand distributions for NEXT-8 are shown from Figure 7.33 through Figure 7.35.

Generally the high demand magnitudes concentrate within a certain distance under the critical loading position and spread out to the entire length of the bridge. Compared with the single 32 kip axle of the design truck, the demand distributions for the design tandem are more widely spread out, so are the demand distributions for the two 32 kip axles of the design truck. As such, the

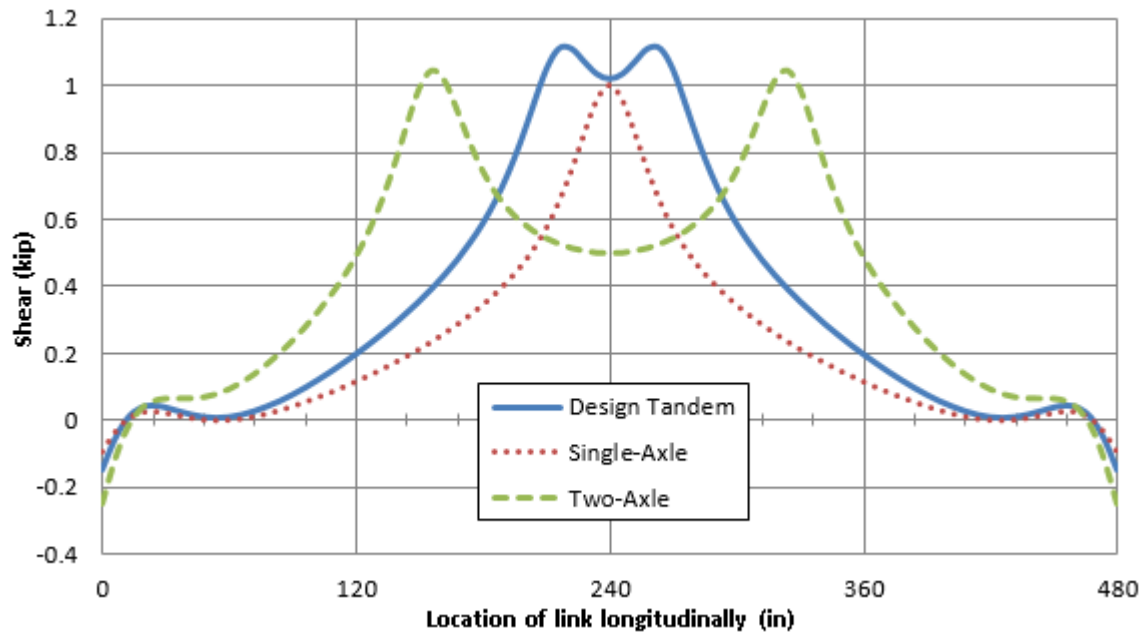


Figure 7.33: Shear in each shear key element of Key 5 along the length of an 8 ft. section NEXT-D bridge with load at the critical shear location

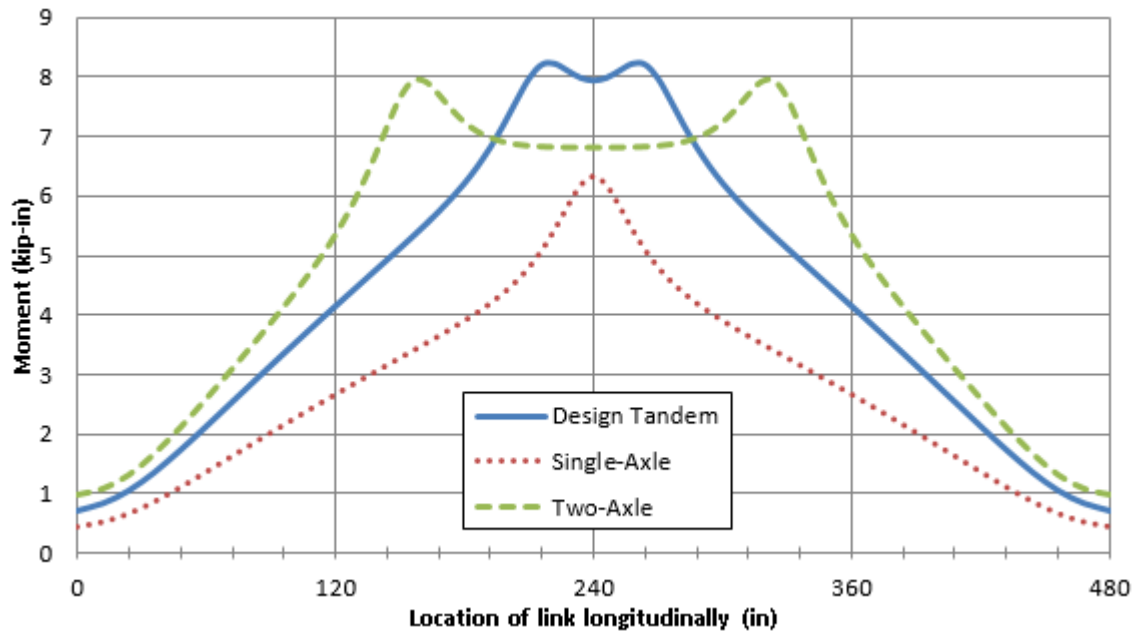


Figure 7.34: Moment in each shear key element of Key 4 along the length of an 8 ft. section NEXT-D bridge with load at the critical positive moment location

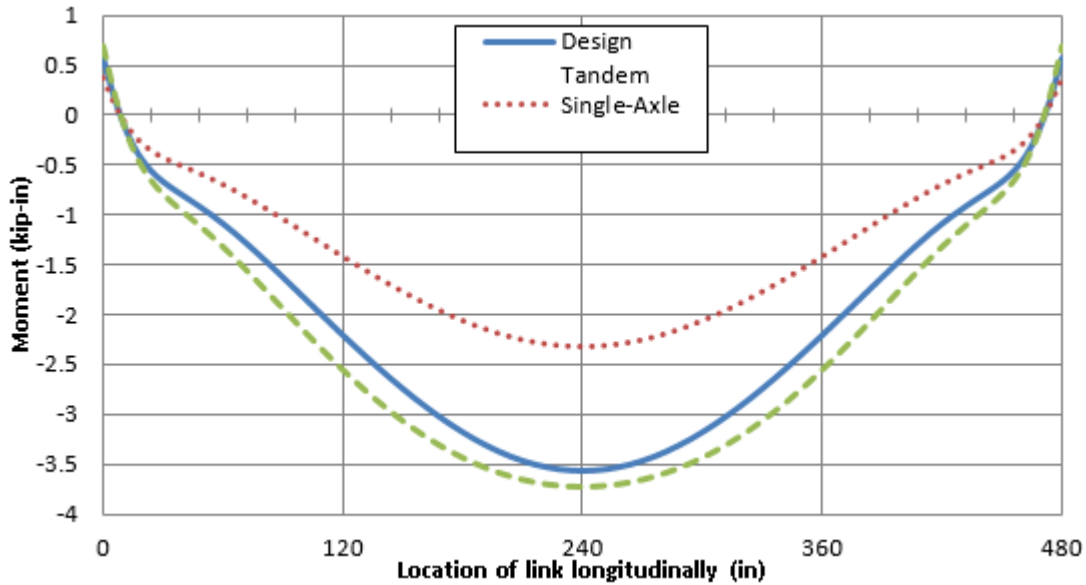


Figure 7.35: Moment in each shear key element of Key 5 along the length of an 8 ft. section NEXT-D bridge with load at the critical negative moment location

geometry of the live loads was used to recommend a strip width. This means that the strip width is independent of bridge width, span length, number of design lanes, etc. For the design tandem, the recommended strip width is 10 ft. For the single-axle load of the design truck, the recommended strip width is 14 ft. The recommended strip width for the two-axle load is 28 ft. These widths were determined based on the spacing of the axles and the closest possible spacing of an additional axle. If each strip width is designed to be able to withstand the critical demand in the entire span length of the bridge, then even if more than one truck is in a lane at a time, the bridge will be ensured to have enough capacity to function without failure. This strip width determination for all three loads is shown in Figure 7.36 through Figure 7.38.

7.9 Design Tandem vs Design Truck

The critical transverse shear key demands were normalized by the recommended strip widths for each load case so that the demands on a 1-ft strip are determined. These demands are shown in Table 7.5 and Table 7.6 for the NEXT-6 and NEXT-8 respectively.

Although the two 32 kip axles of the design truck result in the largest total demands, the critical normalized demands are from the design tandem for both the NEXT-6 and NEXT-8. It is also observed that the normalized demands for the NEXT-8 are more critical than those for the NEXT-6. This difference is particularly distinct for the positive moment demand due to the longer deck span of the NEXT-8.

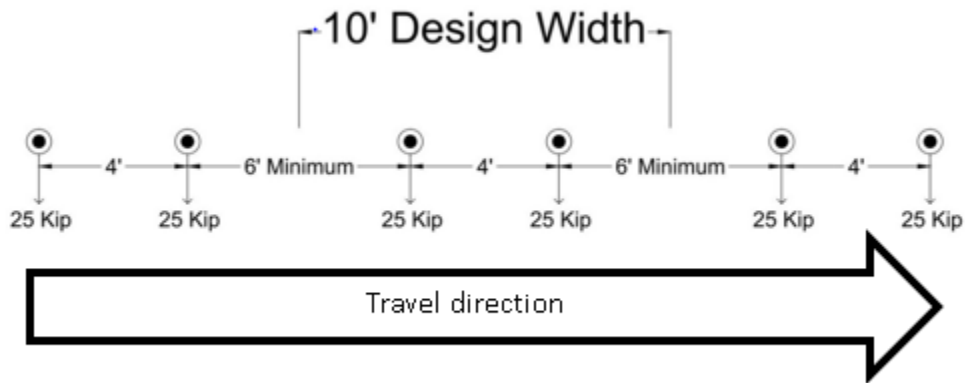


Figure 7.36: Design tandem strip width determination

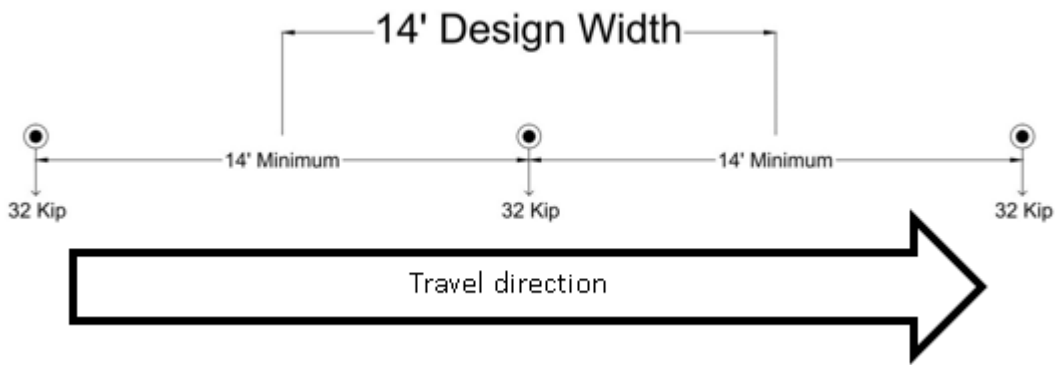


Figure 7.37: Single 32 kip axle strip width determination

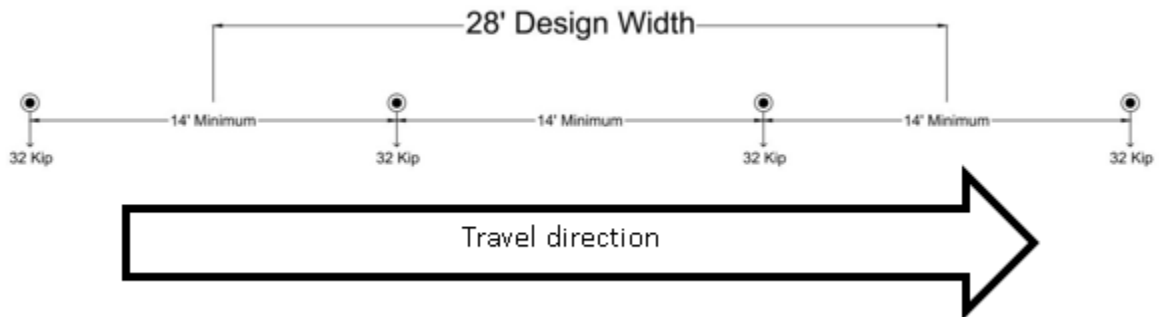


Figure 7.38: Two 32 kip axle strip width determination

Table 7.5: Demand per foot for the NEXT-6 bridge based on recommended strip widths

	Design Tandem	Single Axle	Two Axles	Units
Strip width:	10	14	28	ft
Max shear:	2.78	1.27	1.21	$\frac{kip}{ft}$
Max positive moment:	24.84	11.47	10.06	$\frac{(kip-in)}{ft}$
Max negative moment:	-16.41	-7.58	-6.55	$\frac{(kip-in)}{ft}$

Table 7.6: Demand per foot for the NEXT-8 bridge based on recommended strip widths

	Design Tandem	Single Axle	Two Axles	Units
Strip width:	10	14	28	ft
Max shear:	2.80	1.29	1.21	$\frac{kip}{ft}$
Max positive moment:	34.36	15.87	13.90	$\frac{(kip-in)}{ft}$
Max negative moment:	-16.78	-7.76	-6.67	$\frac{(kip-in)}{ft}$

7.10 Calibration of Shear Key Finite Element Model

In order to get the demand distribution for NEXT-D beam bridge, the shear key stiffness is essential. Here the stiffness matrix (Figure 7.39) is assumed to be symmetric with the following terms K11, K22, K33, K66, and K26 that are expected to be determined from the shear key finite element models (FEM) subjected to axial tension in X (local 1) direction, shear in Y (local 2) direction, shear in Z (local 3) direction, and bending in Z (local 6) direction respectively. The local axis was defined before but is repeated here for convenience (Figure 7.40). In the matrix, there is one term that is available from experimental data (K66). The idea is to calibrate this term against experimental data and use the calibrated model to get K26 and other terms from a detailed FEM model of the shear key. Some of the stiffness terms should be elastic-cracked stiffness, obtained after crack happens but before steel yields at the fatigue load level. However this may not apply to other stiffness terms, for which the load level may not be big enough to cause interface cracking to happen. In another word, the same load that causes interface crack in bending or axial tension may not cause cracking in shear.

7.10.1 Model Introduction

7.10.1.1 Geometry

The original shear key finite element models were built by Flores Duron (2009) in ANSYS 12 (ANSYS-Inc., 2009), which had a #5 headed reinforcement at 6 in. on center. As the configuration of the rebar was switched to #4 U-bar at 8 in. on center and dimensions of the shear key were changed, new models were built. The final shear key configuration adopted for the NEXT-D bridge

$$\begin{matrix}
 & \mathbf{1} & \mathbf{2} & \mathbf{3} & \mathbf{4} & \mathbf{5} & \mathbf{6} \\
 \mathbf{1} & K_{11} & 0 & 0 & 0 & 0 & 0 \\
 \mathbf{2} & & K_{22} & 0 & 0 & 0 & K_{26} \\
 \mathbf{3} & & & K_{33} & 0 & K_{35} & 0 \\
 \mathbf{4} & & & & K_{44} & 0 & 0 \\
 \mathbf{5} & & & & & K_{55} & 0 \\
 \mathbf{6} & & (\text{Sym.}) & & & & K_{66}
 \end{matrix}$$

Figure 7.39: Shear key stiffness matrix

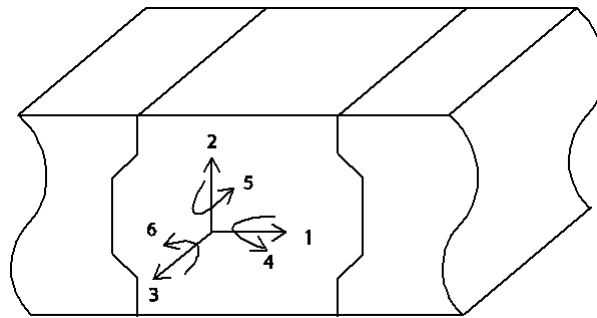


Figure 7.40: Shear key local axis

is illustrated in Figure 7.41. The new shear key model is 4 in. in the longitudinal direction, which is the center to center distance of the staggered U-bar within the shear key. The model is 8 in. tall representing the depth of the deck. A beam flange length of 12 in. was modeled on each side of the shear key. Refer to Figure 7.42 for the finite element model geometry.

7.10.1.2 Material models

In the FEM, the solid 65 element with cracking capability is used to model concrete and UHPC with PVA fiber, and the solid 185 element with plasticity, stress stiffening, and large strain capabilities is used to model the U-bar.

The stress-strain behavior proposed by Graybeal (2007) is used to model the UHPC. This behavior was originally proposed to be representative of UHPC reinforced with steel fiber. Although PVA fiber provides less strength than does steel fiber, its effectiveness in controlling crack formation and propagation is like the steel fiber. Considering that in the shear key FEM to be calibrated the load to be exerted only needs to be sufficient to obtain the elastic-cracked stiffness, the linear stress-strain behavior is deemed sufficient for UHPC with PVA.



Figure 7.41: Shear key configuration

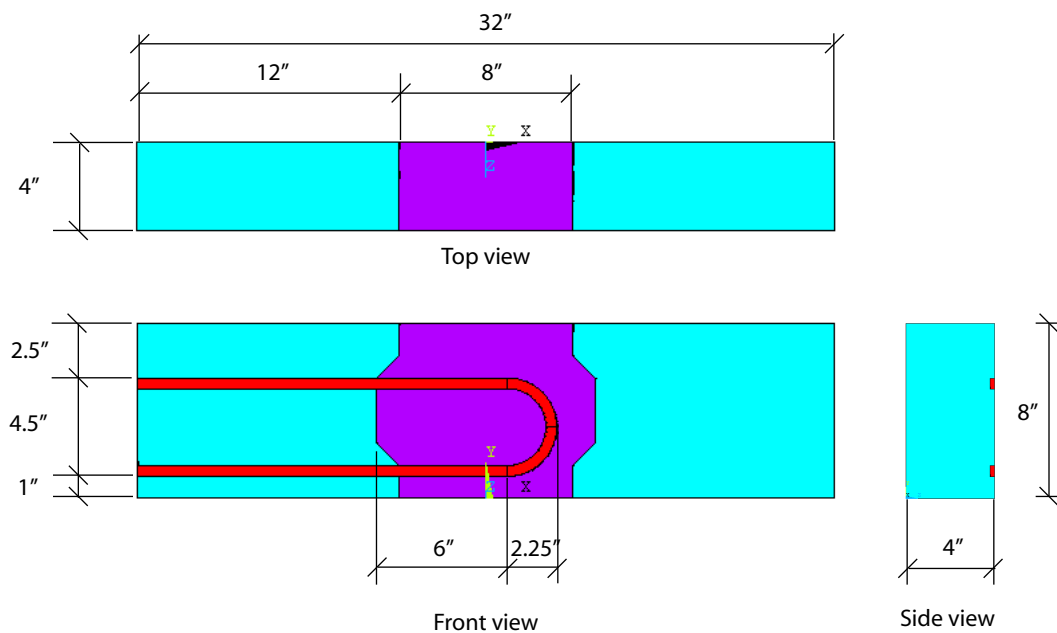


Figure 7.42: Shear key FEM geometry

The linear stress-strain behavior proposed by Graybeal (2007) is based on a series of test conducted on UHPC with steel fiber. the stress-strain relationship of the cylinders tested 8 weeks after casting shows a 5 percent of divergence from linear behavior up to about 70 percent of the compressive strength (18.1 ksi). And the cylinders tested 2 weeks after casting show the similar stress-strain behavior up to about 50 percent of the compressive strength (16 ksi).

In the current study, the compressive strength of UHPC with PVA fiber is 18 ksi at the age of 2 weeks and 22.3 ksi at the age of 8 weeks. According to the formula proposed by Graybeal (Eq 7.1), the secant Young's modulus of UHPC with PVA fiber with respect to strain at the peak stress is about 6200 ksi at the age of 2 weeks and 6900 ksi at the age of 8 weeks. Results show that before a divergence of 5 percent from linear behavior occurs, the Young's modulus is much higher than that predicted by the formula. The values calculated above are increased by 10 percent, which

Table 7.7: Material properties in the shear key FEM

Material	Young's modulus (ksi)	Density (pcf)	Poisson's ratio
Concrete	5600	150	0.2
UHPC with PVA	7200	155	0.19
Steel	29000 (pre-yield)	481	0.3
	2.9 (post-yield)		

gives a range from 6820 ksi to 7590 ksi. Taking the average value, the Young's modulus of the shear key material is set to be 7200 ksi. The Poisson's ratio is assigned 0.19 as that for UHPC with steel fiber (Graybeal, 2007).

$$E_c = 46200\sqrt{f'_c} \quad (7.1)$$

For concrete, the compressive strength at the age of slab test is 9600 psi. It should be noted that this comes from a design mix with a specified strength of 6500 psi. Since calibration of the model is desired, the actual strength and not the design strength is used. Considering the load level to be applied, a linear elastic model is used. The Young's modulus for concrete is set to be 5600 ksi according to the formula from ACI 8.5.1 (Eq 7.2) (ACI, 2011) which is nominally identical to the AASHTO equation for normal weight concrete as specified in section 5.4.2.4 (AASHTO, 2012). Both cracking and crushing of UHPC and concrete are disabled. The reasons are as follows. First, before reinforcement yields, crushing of concrete and UHPC is not supposed to happen. Second, although cracking is expected in the model, its existence causes convergence issues. Third, by disabling concrete and UHPC cracking, only the bond is permitted to crack. The lumped crack is assumed to have the equivalent effect on the shear key stiffness as that of the distributed cracks. For steel, a bilinear elastic-plastic model from Hsu (1993) is applied, in which the initial Young's modulus is 29000 ksi, and the Young's modulus after yielding is 2.9 ksi. Enhanced strain formulation for the solid 185 element is applied to prevent shear locking in all the FEMs by setting KEYOPT (2) = 2. A summary of the above material properties and material models are displayed in Table 7.7 and Figure 7.43.

$$E_c = 57000\sqrt{f'_c} \quad (7.2)$$

7.10.1.3 Contact elements

7.10.1.3.1 Key options Surface-to-surface contact pairs (conta 174 and target170) are used to model the contact between UHPC with steel, concrete with steel, and concrete with UHPC. The contacts in the study are all asymmetric, which means all contact elements are on one surface and all target elements on the other surface. Since a target surface can penetrate the contact surface, when assigning the target and contact surfaces, the target surface assigned to the more rigid material. Therefore in the contact with steel, steel is the target surface, and in the contact between concrete and UHPC, UHPC is the target surface. Pure penalty method is selected (KEYOPT (2) = 1) when modeling contact, which uses springs to model the contact behaviors in both normal and tangential

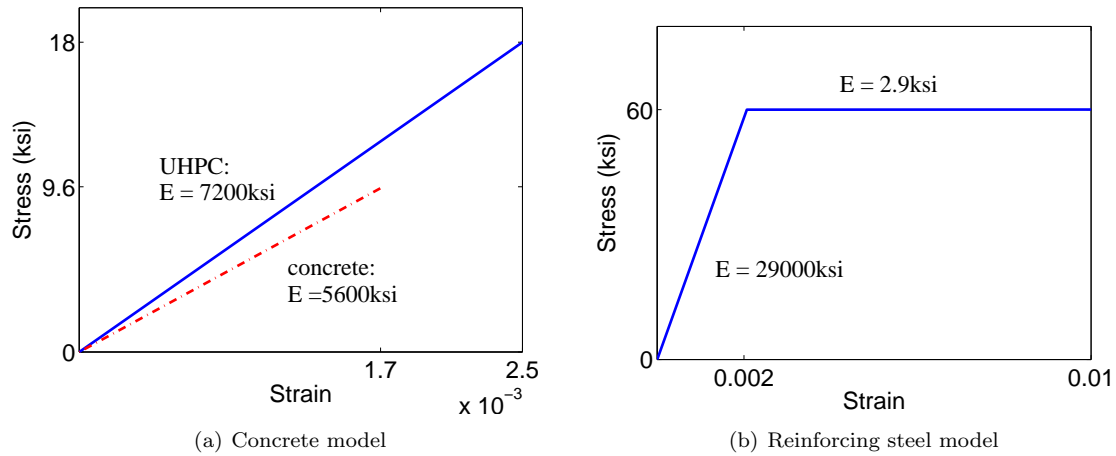


Figure 7.43: Material model

directions. At each iteration, except in the very first one, the normal contact stiffness (KN) is updated automatically depending on the current mean stress of the underlying elements and the allowable penetration (FTOLN). The tangential contact stiffness (KT) is updated automatically at each iteration based on the current contact pressure, friction coefficient (Mu), and allowable slippage (SLTO). This automatic update of stiffness based on the mean stress of each element is obtained by setting KEYOPT (10) = 5. Bonded (always) contact (KEYOPT (12) = 5) is chosen so that there is no sliding or separation between different materials. An initial ‘perfect’ contact status is created which has no initial penetration, gap, or initial force in between the contact elements by setting KEYOPT (5) = 3 and KEYOPT (9) = 1 under the condition of bonded (always) contact. Contact is detected within the pinball region of the Gaussian points. This pinball region is defined by setting the parameter of PINB, which is the radius centering on the Gaussian point. To help convergence, an aggressive refinement of stiffness is chosen by setting KEYOPT (6) = 2.

7.10.1.3.2 Real constants The contact element and target element are associated together by sharing the same real constant set as described next. Based on the problem studied and the element key options selected, six real constants are singled out for further study. They are the normal penalty stiffness factor FKN, penetration tolerance factor FTOLN, tangent penalty stiffness factor FTN, allowable elastic slip SLTO, pinball region PINB, and contact opening stiffness FKOP. The normal penalty stiffness factor FKN is used to modify the default normal contact stiffness, which is determined by material properties, element size, and the total number of degrees of freedom in the model. The usual factor range of FKN is from 0.01 to 1. Since ANSYS 12, this factor is never influenced by plasticity of any material model defined. Therefore in the case studied, even in the presence of the plasticity of steel material model, this factor will not be reduced. An ideal stiffness should be one that is neither too high to cause convergence issue, nor too low to cause too much penetration. In the case of bending, a smaller value would be more appropriate. In

the bending model, both FKN for the contact between concrete and grout, and the contact with steel will need to be calibrated. The factor FTOLN is used to specify the penetration range. As long as the penetration is within this range, compatibility is satisfied. In the model, this factor is set to the default value 0.1. The tangential penalty stiffness factor FKT is used to modify the tangential contact stiffness, the default value of which corresponds to the default value of FKT = 1. The tangential contact stiffness KT is proportional to the penalty stiffness factor FKT, contact pressure, and friction coefficient. In the bonded (always) contact, the value of friction coefficient is default to 1. The allowable elastic slip SLTO sets the maximum sliding distance upon each update of tangential contact stiffness at each iteration. Larger values of FTOLN and SLTO although can help convergence, but may compromise accuracy. In the bending model, both FKT and SLTO are set to default values. The contact opening stiffness FKOP is the stiffness factor applied when contact opens for the bonded-always contact. A positive value of FKOP is a scalar that when multiplied by the closed contact stiffness gives the contact opening stiffness. The value of PINB is determined by considering the target surface, contact surface behavior, and deformation setting. In the model studied, the contact is bonded (always), and large deformation is turned on (NLGEOM, ON), therefore the default value of PINB is 0.5. However, considering that there are several convex regions of the U-bar, a smaller value 0.1 is used for PINB.

7.10.1.4 Debonding model

Debonding happens either as separation in the normal direction or the sliding in the tangential direction or both. When the normal contact stress exceeds the maximum normal contact stress specified, separation occurs. Similarly, when the tangential contact stress exceeds the maximum tangential contact stress, sliding occurs. Debonding under bonded-always contact and pure penalty method is modeled using cohesive zone model (czm) (Alfano and Crisfield, 2001). Two bilinear material models can be used to define czm, one is by specifying tractions and separations and the other is tractions and critical fracture energies. In this study the first model is used. It should be noted that the area covered by the bilinear traction- separation curve gives the critical fracture energy. In this sense, these two bilinear material models are equivalent. There are three types of debonding behaviors. Mode I debonding (Figure 7.44) is separation-dominated, which means the slip constitutive behavior follows the separation constitutive behavior. Debonding completes when the normal contact stress reaches zero. In this mode, the maximum tensile stress (σ) and the separation gap at the completion of debonding (u) need to be specified. Mode II debonding is slip dominated. The parameters required for this mode include the maximum tangential stress and the slippage at the completion of debonding. Mode III debonding is a mixture of Mode I and Mode II. In the current study, the Mode I debonding model is chosen for the contact between concrete and grout and the Mode II debonding model is chosen for the contact with steel.

In the FEM, the interface between the UHPC and the concrete is assumed to be the location of the crack (debonding). In the real case, however, since the bond is stronger than concrete, cracking actually occurs in the concrete. Therefore, in the model, the maximum normal contact stress should come from the properties of concrete. In a previous study (Julander, 2009), the bond is weaker

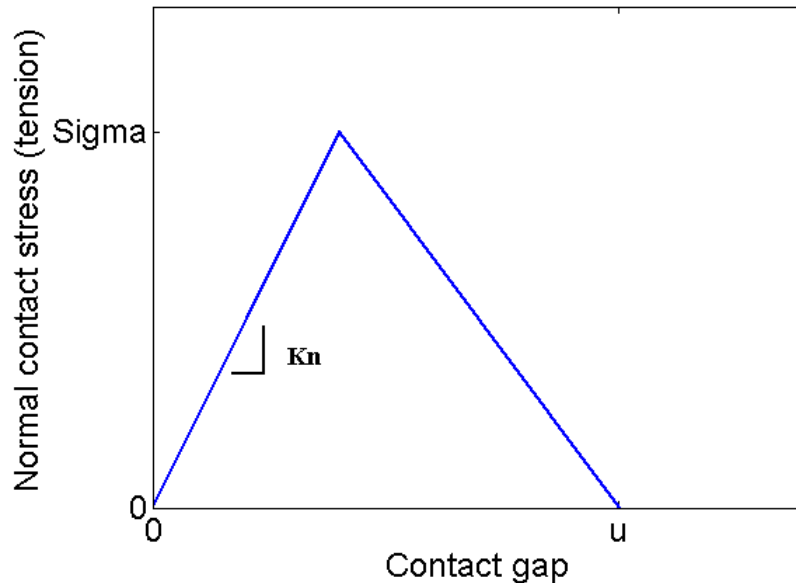


Figure 7.44: Mode I debonding model

than the concrete, and this value is set to be 23 percent of the tensile stress of concrete. In the current study, the direct tensile stress from concrete cylinder test at the comparable age is about 400 psi. Considering the material variability and inherent defects in the direct tension tests, a range from 200 psi to 600 psi is chosen. This value, together with the separation gap at the completion of debonding in the czm will be determined later during the calibration process.

For the contact between UHPC with steel reinforcement, Perry and Royce (2010) performed direct tensile pull-off tests on rebar with various diameters (0.511 in., 0.629 in. and 0.748 in.) which were either in epoxy coated or black steel bars. The UHPC used had steel fibers in it and the compressive strength at 28 days was 20 ksi. The failure behavior for all the tests was rebar failure. In the current study, #4 deformed bar is used, which is comparable to one type of rebar used in Perry's study. The influence of PVA fiber in UHPC on the pull-out behavior is neglected. As such sliding between rebar and UHPC is deemed to never happen, and the values of sliding stress and sliding distance at the completion of debonding are set to 60 ksi and 2 in.

For the contact between concrete and steel, Tastani and Pantazopoulou (2002) carried out direct tensile pull-off tests between rebar ($f_y = 60$ ksi, diameter = 0.55 in, clear cover = 1.7 in.) and normal strength concrete with a compressive strength of 4.5 ksi at test. The bond stress Vs rebar slip relationship (Figure 7.45) showed a maximum debonding stress of about 550 psi and the tangential slipping distance at the completion of debonding approaching to 1 in. According to Tastani's study, the eccentric pullout test results in much larger bond stress than that in the direct tensile pull-off test due to increasing friction caused by rebar curvature. Since a higher strength concrete and rebar with smaller diameter (0.5 in.) are used in the current study, a higher value of

maximum debonding stress 600 psi is applied, and a value of 1 in. is assigned to the tangential slip distance at the completion of debonding. For the bending model, these two values could be larger.

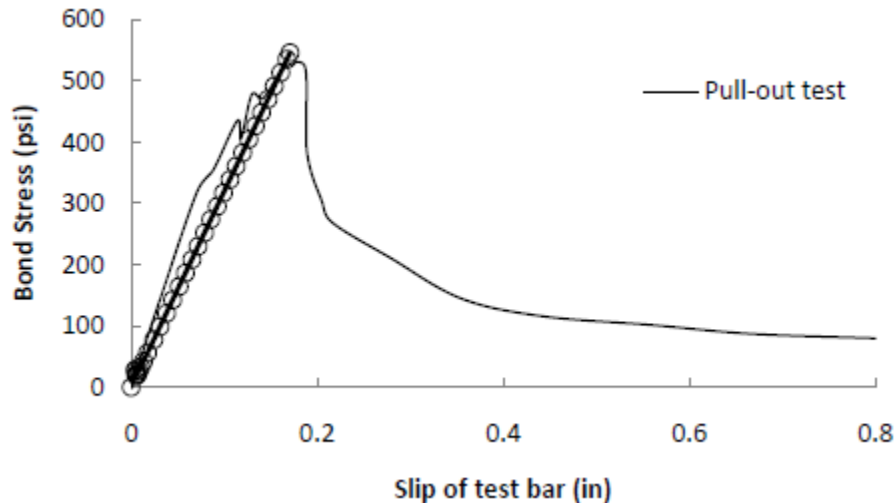


Figure 7.45: Rebar behavior under pull-off test (Tastani and Pantazopoulou, 2002)

For each debonding model, damping is used to help convergence. Its value should be smaller than the smallest time step so that the separation or sliding stress can be correctly identified. In the model, a value of 0.00001 is assigned to damping. A summary of the parameters used in the FEM are listed in Table 7.8.

7.10.1.5 Meshing

Meshing is an important process in finite element modeling in the sense that the results and computational time are sensitive to it. A finer mesh can improve the results but may also increase the computational time considerably. For the model considered, ANSYS recommends the use of brick elements for solid 65, which is simple to be implemented in the beam. For the shear key, however, due to the curvature of the U-bar, this requirement is not easy to be achieved. Nevertheless, efforts were made to divide the volume of the shear key into smaller volumes to facilitate the mesh using brick elements. The region of the U-bar curvature is specially addressed by using elements with smaller sizes. The divided volume is shown in Figure 7.46 and the final mesh is shown in Figure 7.47.

7.10.1.6 Boundary conditions and applied displacements

The shear key FEM is used to determine the translational stiffness of the shear key in the global x, y, and z directions and the bending stiffness around the global z direction. As such four finite element models were created with different bounding conditions aimed at determining the required stiffness terms for the stiffness matrix of the shear key.

Table 7.8: Parameter summary in the shear key FEM

Parameters	Value	Note
FKN	0.01-1	
FTOLN	0.1	default
FKT	1	default
Mu	1	default for bonded (always) contact
SLTO		default
PINB	0.1	
FKOP	0-1	
damping	0.00001	Smaller than the smallest time step
Normal contact stress Gap at the completion of debonding	200 psi-600 psi to be calibrated	contact between concrete and UHPC
Tangential contact stress Slip distance at the completion of debonding	60000 psi 2	contact between UHPC and steel
Tangential contact stress Slip distance at the completion of debonding	600 psi 1	contact between concrete and steel

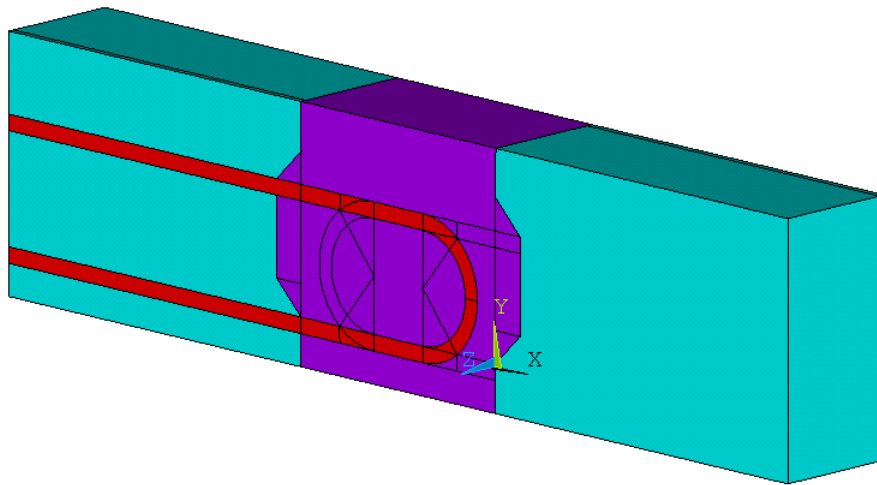


Figure 7.46: Volume division for mesh using brick elements

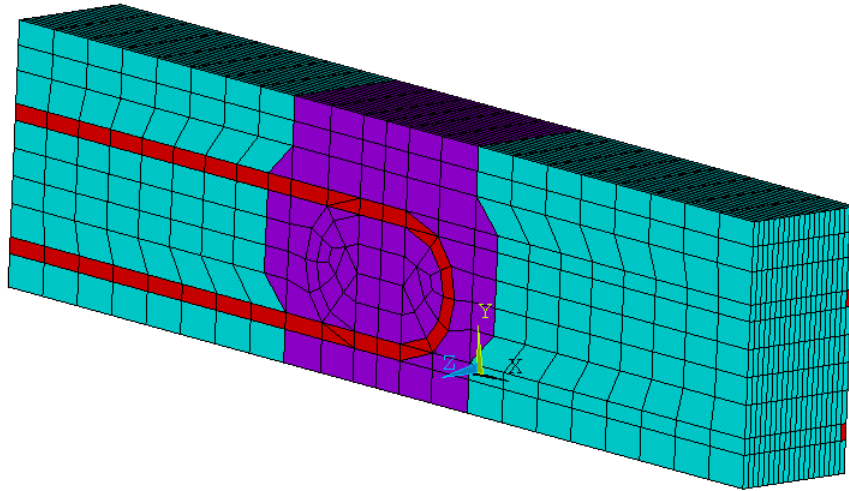


Figure 7.47: Shear key FEM after mesh

7.10.1.6.1 FEM-Rz This model is used to determine the shear key bending stiffness around the global z axis. For this analysis, the nodes located on the bottom corners of the exterior left face of the left beam flange and the exterior right face of the right beam flange are restricted in the Y direction. Additionally, translation along the X -axis (transversal direction) is restricted on the bottom nodes of the exterior left face of the left beam to create a simply supported condition. External displacement is applied to the line of nodes located 1.5 in. from each side of the shear key to create a pure bending situation. Finally, translation along the Z -axis (longitudinal direction of the bridge) was restricted on the front and back faces of the model so that there would be no longitudinal deformation. This reason behind this is that in the real bridge, a 4 in. wide section longitudinally should not cause longitudinal deformations due to the restraints given. Indeed this could be termed a plane strain problem. Refer to Figure 7.48 for the detailed boundary conditions and applied displacements.

7.10.1.6.2 FEM-X This model is to determine the translational stiffness in the transverse direction, which is in alignment with global X axis in the FEM. For this analysis, the nodes located on the exterior left face of the left beam flange were restricted in the X direction and external displacement in the X direction was applied to the nodes on the exterior right face of the right beam. Additionally, translation along the Y -axis (vertical direction) was restricted on the bottom nodes of the exterior face of the left beam to create a fixed support condition. Finally, translation along the Z -axis (longitudinal direction of the bridge) was restricted on the front and back faces of the model for the same reason as mentioned in 7.10.1.6.1. Refer to Figure 7.49 for the detailed boundary conditions and applied displacements.

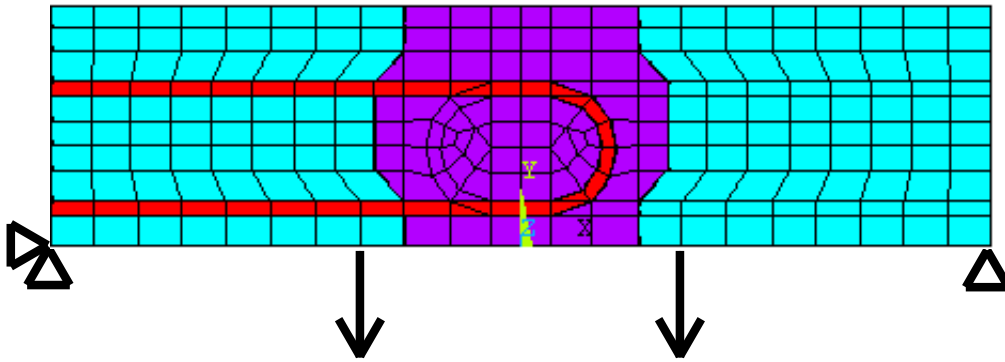


Figure 7.48: Boundary conditions and displacements for FEM-Rz

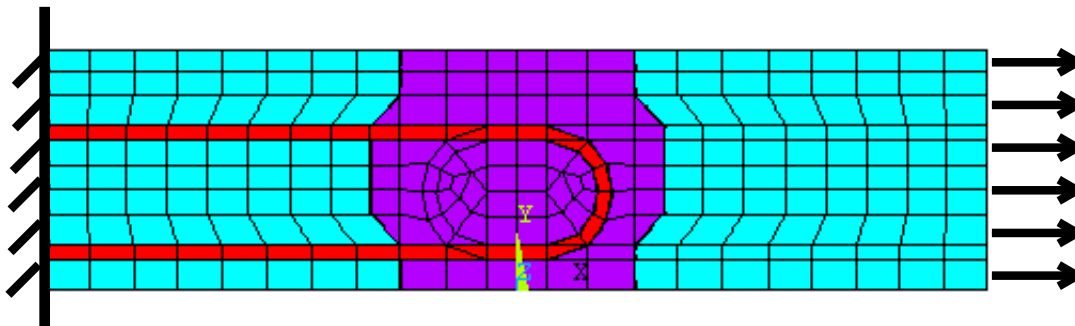


Figure 7.49: Boundary conditions and displacements for FEM-X

7.10.1.6.3 FEM-Y This model is to determine the translational stiffness in the vertical direction, which is in alignment with global Y axis in the FEM. For this analysis, the bottom nodes and top nodes of the left beam flange were restricted along the Y-axis and external displacement in the Y direction was applied to the bottom and top nodes of the right beam. Additionally, translation along the X-axis (transverse direction of the bridge) was restricted on the bottom nodes located on the exterior left face of the left beam to create a simply supported condition. Finally, translation along the Z-axis (longitudinal direction of the bridge) was restricted on the front and back faces of the model. Refer to Figure 7.50 for the detailed boundary conditions and applied displacements.

7.10.1.6.4 FEM-Z This model is to determine the translational stiffness in the longitudinal direction, which is in alignment with global Z axis in the FEM. For this analysis, the nodes located on the exterior front and back faces of the left beam flange were restricted in the Z direction and the

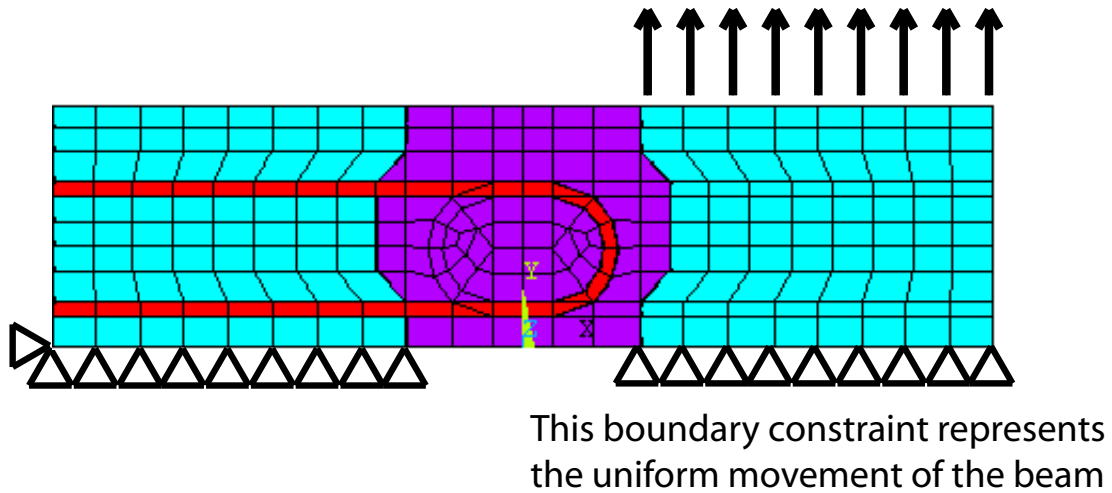


Figure 7.50: Boundary conditions and displacements for FEM-Y

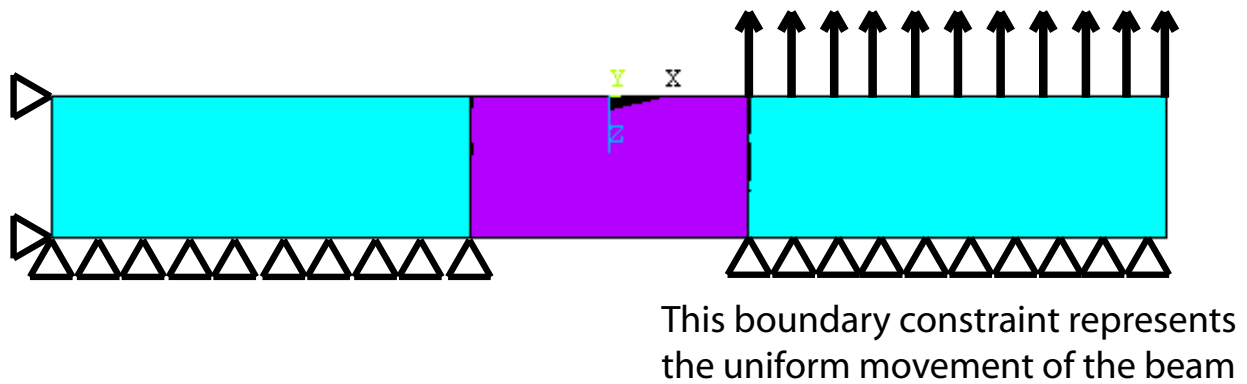


Figure 7.51: Boundary conditions and displacements for FEM-Z

external displacement in the z direction was applied to the nodes on the front and back faces of the right beam flange. Additionally, translation along the X-axis (transverse direction of the bridge) and the Y-axis (vertical direction) was restricted on the bottom corner nodes of the left and right beam. Finally, considering that in the real bridge the rotation of the shear key along Y axis would not occur, translation along the X-axis was restricted for all the nodes inside the shear key. Also nodes on the front and back faces of the shear key are coupled together to prevent the relative movement. Refer to Figure 7.51 for the detailed boundary conditions and applied displacements.

7.10.1.7 Response Monitoring

7.10.1.7.1 FEM-Rz To get the bending stiffness, both bending moment and the rotation in the shear key are needed. In the FEM, the shear key is in pure bending. Bending moment in the shear key is obtained by using the reaction force multiplied by the moment arm. As far as shear key

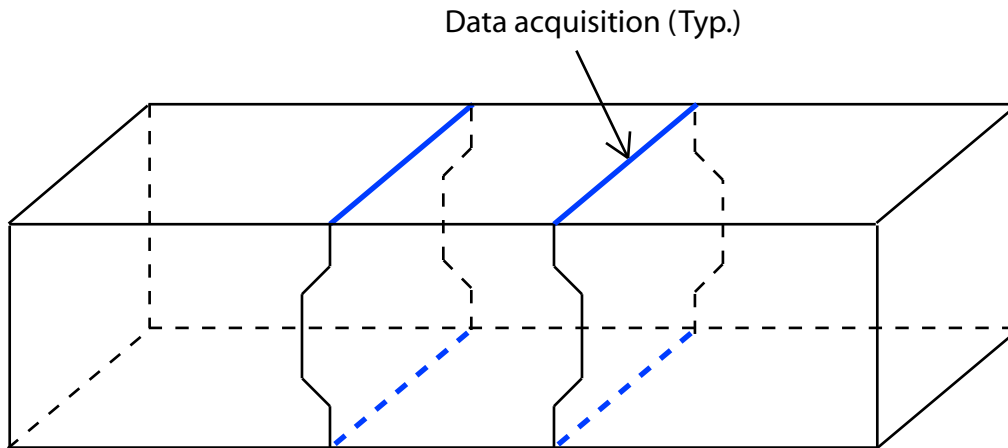


Figure 7.52: Data acquisition in FEM-Rz

rotation is concerned, in the experiment, top and bottom LVDTs were put across the shear key and cracks in the adjacent concrete to determine the shear key rotation. A similar method is used in the FEM where displacement response is acquired at the interface points of the bottom and on the top edges on the concrete slab rather than the shear key (Figure 7.52). After all, it is the stiffness of the shear key with adjacent cracked concrete that matters when determining demands rather than the shear key itself.

7.10.1.7.2 FEM-X/Y/Z For these three FEMs, the displacement responses are monitored at the shear key interface nodes on the beams for the determination of the average relative movement in the $X/Y/Z$ direction. The reaction forces are collected to calculate the force on the shear key in the $X/Y/Z$ direction. In this way the load-displacement curves of the shear key are obtained.

7.10.2 Feature Selection

The shear key FEM in bending is calibrated against the moment-rotation curve from the experiment labeled STA-04. A conversion is made of the curve to change from a 40 in. wide slab in the experiment to the 4 in. wide shear key in the model (Figure 7.53). Here in the curve, the elastic-cracked stiffness is only one value. In the real case however, within the fatigue load level, the elastic-cracked rotational stiffness changes its magnitude depending upon the level of cracking in the concrete adjacent to the shear key. In another words, the elastic-cracked stiffness is actually within a range, the upper bound of which is the pre-cracking stiffness and the lower bound is the stiffness when the first steel yields. This influence of this range of shear key stiffness on the measured load demands is considered later in a sensitivity study. During the calibration, both the pre-cracking behavior and post-cracking behavior are used as features. It is expected that through this process, all the sensitive parameters can be calibrated.

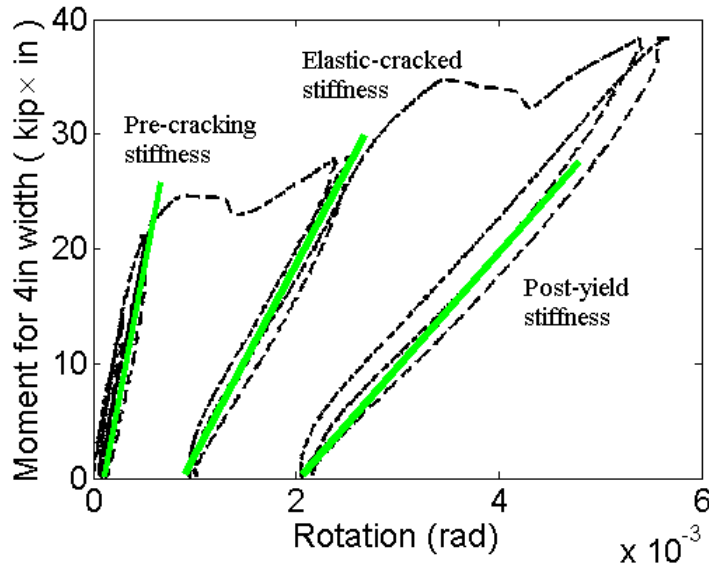


Figure 7.53: Converted moment-rotation

7.10.3 Parameter Calibration

The calibration underwent two phases. These were the calibrating of the pre-cracking behavior and of the post-cracking behavior of the moment-rotation curve.

7.10.3.1 Pre-cracking behavior

For the pre-cracking stiffness, an intensive sensitivity study shows that the pre-cracking stiffness is sensitive to only the following parameters: normal penalty stiffness factor between concrete and grout FKN_CG, normal penalty stiffness factor for the contact with steel FKN_CS, Young's modulus of concrete, and Young's modulus of UHPC. A full-factorial sensitivity study of the above mentioned parameters was carried out with FKN_CG ranging from 0.025 to 0.08, E_conc from 5000 ksi to 6600 ksi, E_UHPC from 5600 ksi to 8000 ksi, and FKN_CS from 0.001 to 1 (Figure 7.54). The correlation between these parameters and the pre-cracking stiffness (Table 7.9) shows that within the ranges specified, the pre-cracking stiffness is most sensitive to FKN_CG, followed by E_conc, while it is relatively insensitive to E_UHPC and FKN_CS. This implies that the pre-cracking stiffness is controlled by the weak material. With E_UHPC at a value of 7200 ksi, and E_conc at a value of 5600 ksi, FKN_CG is calibrated to be 0.048. It is also observed that with other parameters at their nominal values, a five percent divergence from the pre-cracking stiffness can either result from E_conc ranging from 5200 ksi to 6000 ksi, or E_UHPC ranging from 6000 ksi to 8400 ksi, implying that the material variability from batch to batch has insignificant impact on the pre-cracking stiffness.

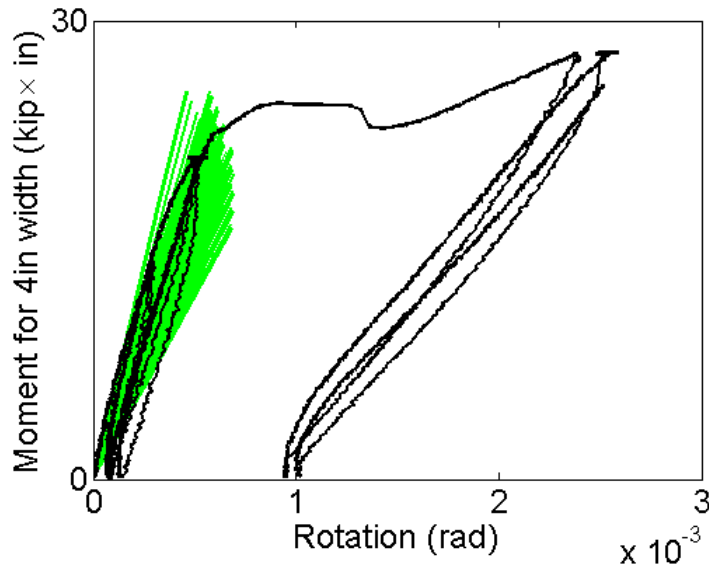


Figure 7.54: Calibration of pre-cracking behavior

Table 7.9: Correlation coefficients

	FKN_CG	E_conc	E_UHPC	FKN_CS	Pre-cracking stiffness
FKN_CG	1	-0.0813	-0.1578	0.1488	0.8839
E_conc	-0.0813	1	0.5440	-0.0332	0.3298
E_UHPC	-0.1578	0.5440	1	0.0410	0.2058
FKN_CS	0.1488	-0.0332	0.0410	1	0.2222
Pre-cracking stiffness	0.8839	0.3298	0.2058	0.2222	1

7.10.3.2 Post-cracking behavior

With all the other parameters at their nominal values or default values, the post-cracking behavior is found out to be quite sensitive to FKN_CS, fracture energy (sigma and gap at the completion of debonding), and relatively insensitive to the stiffness factor after cracking FKOP. A combination of FKN_CS = 0.001, sigma = 230 psi, gap = 0.0013 and FKOP = 0.5 gives a post-cracking behavior that agrees fairly well with the experimental data. Since the magnitude of elastic-cracked stiffness varies depending upon the seriousness of the interface cracks, a displacement study and full cycle study are carried out. Under a displacement of 0.017in, the model is unloaded and loaded to the same displacement. The calibrated moment-rotation curve is shown in Figure 7.55a. A small deviation exists between the post-cracking curves, which is mainly due to the displacement exerted. A larger displacement could bring these two curves closer, but at a significant cost of computational time. Since the post-cracking stiffness determined this way from the FEM is close

to that from the experiment, the calibration is deemed to be sufficient. As such the stiffness term K_{66} is obtained by fitting the curve to a straight line. Based on the bending model, the stiffness term of K_{26} (the force in y direction caused by a unit rotation) is also determined. It is also found out that a 5 percent divergence from the pre-cracking stiffness does not have much influence on the elastic-cracked stiffness (Figure 7.55b).

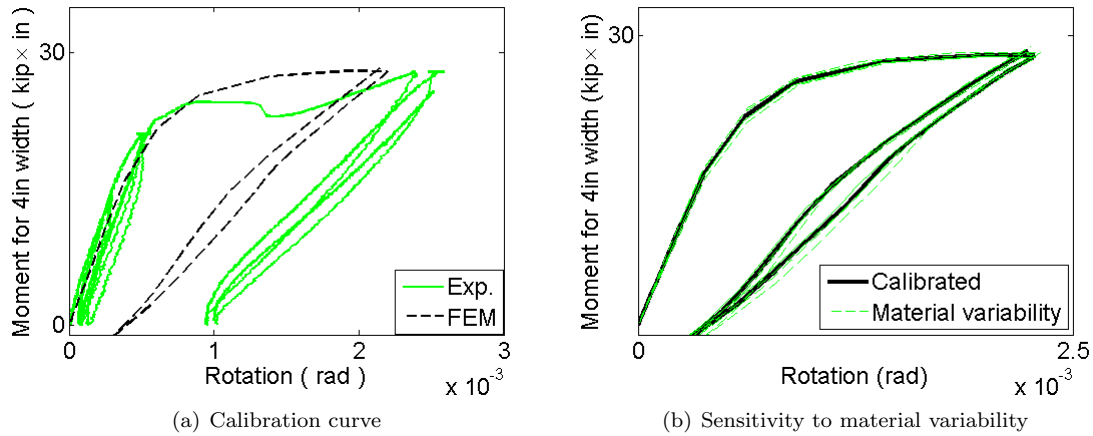


Figure 7.55: Calibrated moment-rotation curve

7.10.4 Stiffness Matrix Determination

This calibrated bending model is then used to get stiffness terms from other models including the model subjected to axial tension in the direction of X and the models subjected to shear in both Y and Z directions. For each model, several studies are conducted including a displacement study, support study, sensitivity to other parameters other than those calibrated above, and sometimes full-cycle study. As in the bending model, the stiffness in these other models is not sensitive to other parameters. For the model subjected to axial tension, cracking is deemed to occur under fatigue loads and the elastic-cracked stiffness is used. For the other two models subjected to shear, the pre-cracking stiffness is used. The load-displacement curve for each model is displayed in Figure 7.56, and the final stiffness matrix is given in Figure 7.57.

7.11 Closure

This chapter mainly talks about the method that is used for demand evaluation through the use of a bridge FEM and a shear key FEM. The shear key FEM provides the shear key stiffness matrix calibrated through experimental data, which is then converted and fed into the bridge FEM for further demand determination. This method requires an appropriate modeling of the bridge FEM, and of equal importance, a reasonable stiffness matrix obtained through the calibration of the shear key FEM.

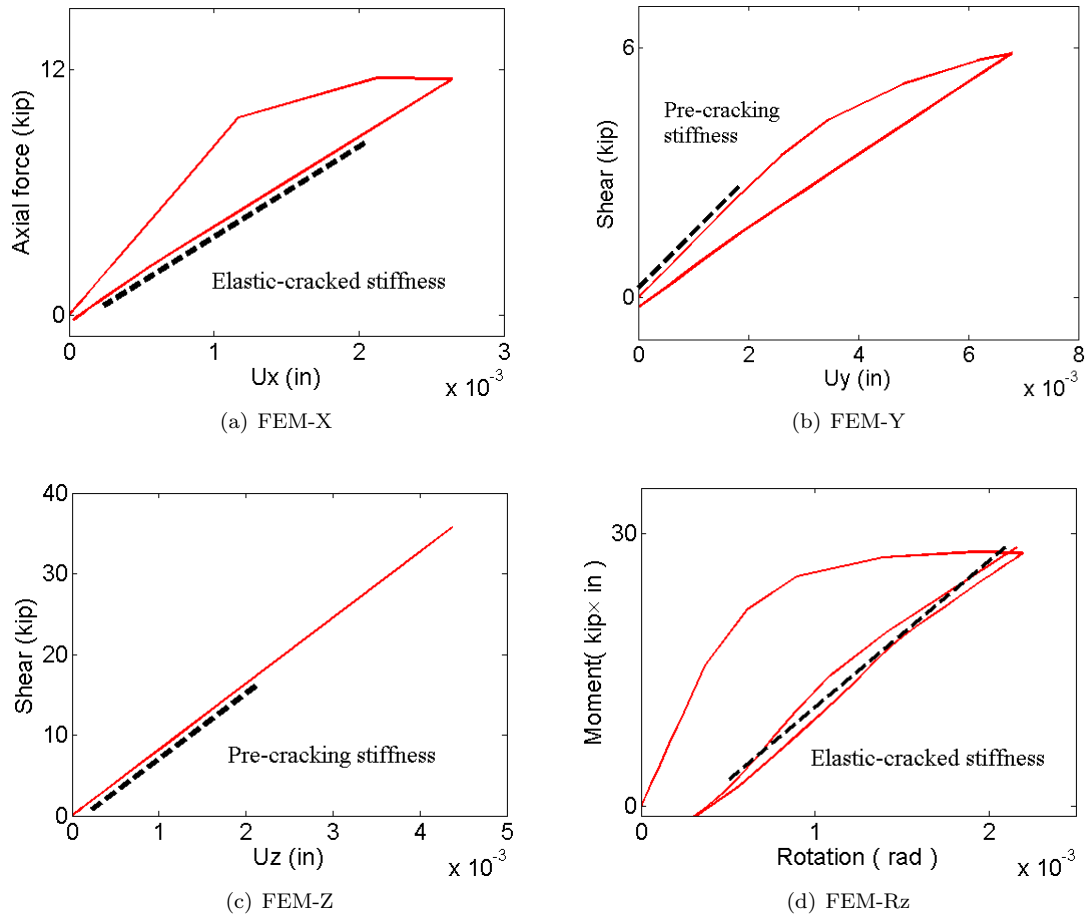


Figure 7.56: Load-displacement curve for stiffness determination

	1	2	3	4	5	6
1	4376	0	0	0	0	0
2		1340	0	0	0	1478
3			8171	0	--	0
4				--	0	0
5					--	0
6		(Sym.)				15960

Figure 7.57: Shear key stiffness based on the 4 in. FEM in units of kips and in.

The bridge FEM is validated by using both solid modeling and shell modeling, the results from which are close to each other except those for the exterior beams due to the different connection between parapets and the deck. Since the modeling of this connection in the shell model is much closer to the reality, the shell model is selected. AASHTO's strip method for deck design does not consider the varying deck spans which is pretty common for the NEXT-D bridges. For the NEXT-D bridge FEMs studied, the transverse shear key demand distributions in the longitudinal direction under corresponding critical loading positions are spreading across the whole span length; as such the strip width is determined based on the geometry of the AASHTO live loads. For the three live load cases studied (design tandem, single 32 kip axle of the design truck, and two 32 kip axles of the design truck spaced 14 ft apart), the recommended strip width is 10 ft for design tandem, 14 ft for the single-axle case, and 28 ft for the two-axle case. Using the strip width recommended above, even if more than one truck is in a lane at a time, the bridge will be ensured to have enough capacity to function without failure. The normalized shear key transverse live load demands show that the critical demands are from the design tandem for both NEXT-6 and NEXT-8. It is also observed that the normalized transverse demands for NEXT-8 are more critical than those for NEXT-6. This difference is particularly distinct for the positive moment demand due to the longer deck span of the NEXT-8.

The shear key FEM is based on the assumptions that the lumped crack at the interface has the same effect on stiffness as distributed cracks. In the model, the bond is stronger than the concrete so that the debonding properties are controlled by the concrete. The stiffness matrix is obtained depending on the parameters from the calibrated shear key FEM subjected to bending, which is calibrated against the elastic-cracked stiffness of shear. The shear key stiffness is more sensitive to the rigidity of the weak material (concrete) than the strong material (UHPC with PVA). The main function of the shear key material is to provide a bond that is stronger than concrete.

There are a lot of factors that can influence the stiffness matrix. The material properties could change and the concrete and the UHPC can undergo creep and shrinkage. The general formula for Young's modulus may not be suitable for a particular case. The debonding model or certain parameters suitable for the bending FEM may not be appropriate for the shear FEM. The lumped crack may exert different effects on the stiffness than the distributed cracks. Moreover, the elastic-cracked stiffness covers a range rather than a single value. Talking about all of these factors, however, does not discourage the use of FEM. Rather, the model is valuable in the sense that it provides a reference for the stiffness to be used, and it is robust in the sense that out of the so many parameters, only a few of them have significant influences on the stiffness. In addition, the stiffness is not influenced that much by material properties. Varying E_{conc} from 5200 ksi to 6000 ksi, or E_{UHPC} from 6000 ksi to 8400 ksi results in pre-cracking stiffness within five percent divergence and little change of elastic-cracked stiffness. After all, the objective of obtaining a shear key stiffness matrix is to determine the demands on the NEXT-D beam bridge. Therefore rather than figuring out all the uncertainties involved, a sensitivity study of the shear key stiffness's influence on the demand distribution is more direct and effective, which will be talked about in the next chapter.

Chapter 8

NEXT-D Bridge Design

A highway bridge is designed on a component basis. In this project, the following components of a typical NEXT-D bridge are designed: parapet, overhang, beam and deck.

8.1 Parapet and overhang design

The parapet designed is a New Jersey type of parapet. It is designed to the load level TL4 (LRFD Article 13.7.2) under the Extreme Event II limit state based on yield line analysis. When performing yield line analysis, the critical length of yield line failure pattern and the nominal resistance are determined using formulas in LRFD Article A13.3.1 with the following assumptions.

1. The parapet is of uniform thickness;
2. The overhang is strong enough to force the yield line pattern to remain within the parapet;
3. The parapet wall must be long enough so that the yield line pattern can happen;
4. The positive and negative wall resisting moments are equal.

A yield line analysis for parapets with variable thicknesses was conducted by Calloway Calloway (1993). The LRFD method is four percent conservative according to Calloway and at the same time more computationally convenient. During the design, it is found that the end zone impact causes more demands than those resulting from the impact within the wall segment. As such, the middle zone and end zone were designed separately. The current parapet design in SCDOT using #5@12in throughout the entire length of the parapet is designed to the end impact condition and thus produces a conservative design in the middle zone. The deck overhang must be designed to have a larger capacity than the parapet it supports. Therefore, the overdesign in the middle zone of the parapet also causes a more stringent design to be used for the design of the overhang. The benefit, however, is that it is more construction friendly and the same reinforcement design can be used throughout the overhang. Finally this conventional design, as per the SCDOT's request, is used.

The basic concept for the deck overhang design is that the overhang must be stronger than the parapet; so that the damage will remain in the parapet as much as possible which is more easily repaired than the overhang. The standard overhang width for NEXT-8 is 2.5 ft., and for NEXT-6 is 1.5 ft., which does not satisfy the minimum requirement (2 ft.-3 in.) specified in SCDOT Bridge Design Manual 12.2.5.5 to accommodate drainage (SCDOT, 2006). As such, the overhang width is set to be 2.5 ft. for both NEXT-6 and NEXT-8 and any width section in between. For the overhang design, the Extreme Event II limit state controls. The overhang is designed considering not only the negative moment resulting from the transverse collision load on the parapet, but also the axial tension caused by the collision load. The collision load effects on the overhang are calculated by assuming that the collision loads spread at a slope of 45 degree from the top of the parapet to the interface. Therefore when the impact happens within the wall, the spreading length of the collision load at the interface is two times the height of the parapet; and when the impact happens at the end of the wall, the spreading length is the height of the parapet. When calculating the axial tensile capacity of the overhang, the transverse rebar are assumed to all yield. Refer to Appendix F for the detailed parapet and overhang design. This is actually a typical detail used by SCDOT.

8.2 Beam analysis and design

8.2.1 Refined analysis using 3D finite element model

LRFD Article 4.6.2.2b specifies that for stemmed beams with shear keys, if the stem spacing is less than 4 ft. or more than 10 ft., a refined analysis needs to be performed to determine the live load flexural moment for interior beams (AASHTO, 2012). For both the NEXT-6 and NEXT-8, the stem spacing is 3 ft.; therefore a refined analysis is needed. The requirement however does not necessarily mean that the AASHTO live load distribution formulas do not apply to the NEXT-D Beam Bridge, rather it means that the formulas were developed without considering the above ranges. Three dimensional finite element models of 40 ft. span NEXT-6 and NEXT-8 bridges were built using SAP2000 by Funcik, (2011) as discussed in the previous chapter. It should be noted that those models are base models. There are a few updates about this model concerning geometry, material properties, and component stiffness as follows.

8.2.2 Geometry and material properties

The overhang length for both the NEXT-6 and NEXT-8 is updated to 2.5 ft. measured from the centerline of the exterior stem of the exterior beam to the edge of the overhang. As such, the width of the NEXT-8 Bridge remains 48 ft., while the width of the NEXT-6 Bridge is expanded to 50 ft. According to LRFD Article 4.6.3.1, the structurally continuous parapet, acting compositely with the deck, can be considered to be structurally active at service and fatigue limit states (AASHTO, 2012). Therefore the parapets are present in the model when determining the load distribution factors and demands to ascertain their influence. However, to be consistent with the requirements of the SCDOT Bridge Design Manual Section 14.1.1.2 the parapet was not included in the capacity calculation of the bridge. The stem depth to be designed for both the NEXT-6 and NEXT-8, after

a discussion with SCDOT, is determined to be 13 in. giving an overall section depth of 21 in. In the bridge FEM, this depth used remains 12 in. as determined by Deery (2010) to be the minimum feasible depth. To account for the effect of stem depth on demands, a sensitivity study is carried out later.

Young's modulus, used for the parapet, is 3600 ksi which corresponds to a design compressive strength of 4000 psi. For the precast beam, Young's modulus is 5600 ksi corresponding to a compressive strength of 9600 psi according to the experimental data. Notice that the design compressive strength for the precast at service is 6500 psi, which results in a smaller Young's modulus. However, this difference in Young's modulus should not be a concern for live load distribution factor determination. In addition to the 40 ft. span, NEXT-D bridges with span lengths of 30 ft. and 22 ft. are also modeled and designed. To be clear, the design strength used for the actual capacity design of the beams later in this chapter is 6500 psi. The 9600 psi actual strength of this 6500 psi design strength was to capture the actual behavior for demand determination sensitivity.

8.2.3 Component stiffness

Relative stiffness among components is important for demand determination. For the shear key stiffness, the matrix obtained from the shear key FEMs is used as a target. Before this matrix is used, a few modifications are made. First, the matrix is based on a 4 in. wide shear key FEM. It is converted to be used for the 6 in. spaced shear key frame elements by multiplying a factor of 1.5 assuming that all the stiffness terms are proportional to the shear key width. Second, there is a term missing in the matrix, which is the rotational stiffness K_{44} . Since this term is necessary, the torsional constant of the shear key frame element is assumed. Considering that it is much easier for the shear key to bend than to rotate, a value which is ten times that of the bending stiffness is assigned to the torsional stiffness. A sensitivity study using the design tandem load shows that the transverse demands are insensitive to the change of this term. For the NEXT-6, by amplifying or decreasing this term 100 times, the change of maximum positive moment is within 1.5 percent, and the change of critical negative moment is within 6 percent. For the NEXT-8, the percentages are within 1 percent for maximum positive moment, and 1.5 percent for critical negative moment. Based on the updated stiffness matrix, as given in Figure 8.1, the input parameters are determined for the shear key frame element. Refer to Appendix G for the detailed calculation shown in a spreadsheet. Since the calculated length of the frame element is smaller than 8 in., equal constraints are applied to both ends of the shear key frame element, which gives the desired stiffness terms in the matrix.

8.3 Live load distribution factor

8.3.1 Definition

The live load distribution factor (LDF) is defined as “the critical load actions (either moment or shear) under either a single design truck or multiple design trucks spaced transversely based on refined analysis, multiplied by multiple presence factors specified in AASHTO LRFD Table 3.6.1.1.2-1, the result of which is then divided by the corresponding load actions obtained from beam line

$$\begin{array}{c}
 \mathbf{1} \\
 \mathbf{2} \\
 \mathbf{3} \\
 \mathbf{4} \\
 \mathbf{5} \\
 \mathbf{6}
 \end{array}
 \left(
 \begin{array}{cccccc}
 \mathbf{1} & \mathbf{2} & \mathbf{3} & \mathbf{4} & \mathbf{5} & \mathbf{6} \\
 6564 & 0 & 0 & 0 & 0 & 0 \\
 & 2010 & 0 & 0 & 0 & 2217 \\
 & & 12256 & 0 & 13519 & 0 \\
 & & & 239400 & 0 & 0 \\
 & & & & 145980 & 0 \\
 & (\text{Sym.}) & & & & 23940
 \end{array}
 \right)$$

Figure 8.1: Stiffness matrix for shear key frame element in the bridge FEM in units of kips and inches

analysis under a single design truck”. The current live load distribution factor formulas in the LRFD Design Specifications are based on design trucks and already include multiple presence factors except for those calculated based on the lever rule method. For the NEXT-D beam bridges with varying span lengths, if the load distribution factors are close to that based on AASHTO LRFD formulas, the beam design would be much more efficient by using a commercial bridge design software rather than performing refined analyses.

8.3.2 Beam line analysis

The design truck as described in LRFD Article 3.6.1.2.2, with a distance of 14 ft. between the two 32 kip axles, is applied to both the beam line analysis and the bridge model for maximum load effects. When performing a beam line analysis, the critical demand is determined following the guidance below:

1. The maximum shear due to moving concentrated loads occurs at one support when one of the loads is at the support.
2. The maximum bending moment produced by moving concentrated loads occurs under one of the loads when that load is as far from one support as the center of gravity of all the moving loads on the beam is from the other support. The critical moment happens under the load that is closest to the center of gravity of all the moving loads on the beam.

Therefore, for shear, the rear 32 kip axle is positioned on the support. The critical load configuration for moment depends on the span length. For the 40 ft. span the three-axle truck dominates – see Figure 8.2; for the 30 ft. span the two–32 kip axle condition controls (Figure 8.3); and for the 22 ft. span, the single 32 kip axle condition controls when the axle is placed in the middle of the span. The critical demands based on beam line analysis are listed in Appendix H.

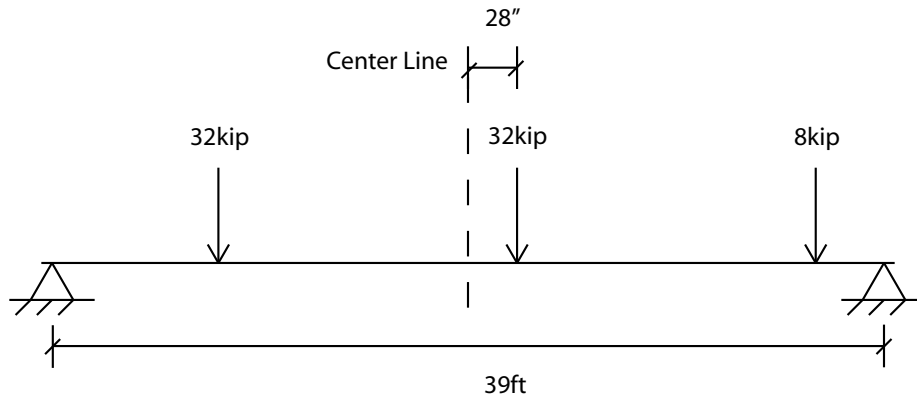


Figure 8.2: Critical load position for the 40 ft. span in beam line analysis

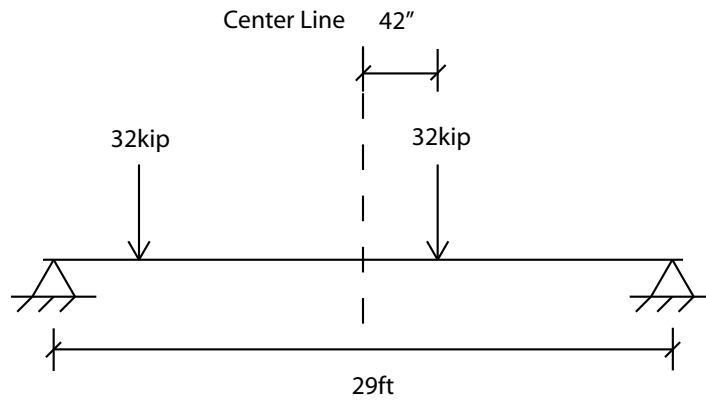


Figure 8.3: Critical load position for the 30 ft. span in beam line analysis

8.3.3 Critical Demands Based on 3D FEM

Since there are three design lanes (LRFD Art. 3.6.1.1.1) for the bridges under design, a maximum number of three design trucks are positioned side by side on the bridge FEM. Wheel loads are modeled as patch loads as described in Chapter 7, which is conservative in the sense that the spreading length (depth of the deck) is not considered, resulting in a more focused load. The center of any wheel load of any design truck is placed no closer than 2 ft. from the face of the parapet as specified in LRFD Article 3.6.1.3. The critical load position for critical shear and positive moment are as described in the beam line analysis, so are the corresponding critical cross sections. In the FEM, the section cut command is used to define a critical cross section in the beam, which includes the frame joints of the stem and the shell joints of the deck. For the exterior beam, the parapet is not included in the section cut. When defining the section cut, the centroid of the section should

Table 8.1: Load distribution factors for NEXT-8

Span length (ft)	Girder location	Number of lanes loaded	Positive moment		Shear	
			3D FEM	AASHTO	3D FEM	AASHTO
40	Exterior	1	0.368	0.813	0.755	0.813
		2	0.369	0.590	0.744	0.563
		3	0.299	0.590	0.571	0.563
	Interior	1	0.412	0.516	0.631	0.680
		2	0.591	0.678	0.720	0.814
		3	0.643	0.678	0.651	0.814
30	Exterior	1	0.316	0.813	0.751	0.813
		2	0.279	0.639	0.704	0.563
		3	0.207	0.639	0.522	0.563
	Interior	1	0.465	0.573	0.681	0.680
		2	0.670	0.734	0.764	0.814
		3	0.710	0.734	0.684	0.814
22	Exterior	1	0.437	0.813	0.740	0.813
		2	0.371	0.697	0.657	0.563
		3	0.267	0.697	0.475	0.563
	Interior	1	0.547	0.644	0.735	0.680
		2	0.714	0.801	0.807	0.814
		3	0.696	0.801	0.712	0.814

be specified in order to get the right longitudinal moment. The load is then moved transversely - element by element - in order to get the maximum demand at the critical locations for both the interior beam and exterior beam.

8.3.4 Live load distribution factor determination

The beam demands determined from the bridge FEM and the beam line analysis are listed in Appendix H. Multiple presence factors 1.2, 1, and 0.85 are applied to the one-truck, two-truck, and three-truck load cases separately. Finally the load distribution factors are determined. For the one-truck load case, the summation of the load factors does not give 1.0, which is due to the contribution of parapet and shear key, and the precision of the load position and section cut position in the FEM. These factors are then scaled up so that the summation is 1.0 to neglect the contribution of the parapet in the design as per the SCDOT Bridge Design manual 14.1.1.2 (SCDOT, 2006). Load distribution factors in the two-truck, and three-truck load cases are processed the same way. The final load distribution factors for the NEXT-8 and the NEXT-6 are listed in Table 8.1 and Table 8.2. The values highlighted are obtained based on the lever rule method, which assumes that the deck is simply supported on the interior girders and continuous over the exterior girder. In the calculation, a whole beam is assumed as a support.

Table 8.2: Load distribution factors for NEXT-6

Span length (ft)	Girder location	Number of lanes loaded	Positive moment		Shear	
			3D FEM	AASHTO	3D FEM	AASHTO
40	Exterior	1	0.250	0.683	0.652	0.683
		2	0.271	0.480	0.626	0.464
		3	0.255	0.480	0.545	0.464
	Interior	1	0.291	0.431	0.527	0.600
		2	0.437	0.552	0.694	0.671
		3	0.475	0.552	0.608	0.671
30	Exterior	1	0.203	0.683	0.633	0.683
		2	0.192	0.519	0.591	0.464
		3	0.167	0.519	0.504	0.464
	Interior	1	0.351	0.478	0.523	0.600
		2	0.472	0.596	0.735	0.671
		3	0.506	0.596	0.637	0.671
22	Exterior	1	0.345	0.683	0.619	0.683
		2	0.294	0.565	0.554	0.464
		3	0.239	0.565	0.465	0.464
	Interior	1	0.395	0.535	0.614	0.600
		2	0.534	0.649	0.779	0.671
		3	0.519	0.649	0.668	0.671

The axle load is applied 2 ft. from the face of the parapet. The reaction in the exterior beam is then multiplied by the multiple presence factor of 1.2. Comparing with the LDFs based on AASHTO's formula for cross section I (sufficiently connected to act as a unit - AASHTO Table 4.6.2.2.2), similar results are observed for the interior beams in all the cases. For the exterior beam, AASHTO's method gives similar shear LDFs to those from the FEM, but is notably conservative in predicting the moment LDFs. Except for a few cases, the AASHTO's method generally gives appropriate LDFs. Some of the FEM values do exceed the AASHTO values by as much as 35%, however this is not true for the critical load cases. Rather, for the critical values only a few cases may exceed between 2 and 16%. This only occurs in a very few cases is hence deemed to be an acceptable range. Particularly since the LDFs reported for the FEM are conservative since they neglect the contribution of the parapet. As such the AASHTO's approximate method is recommended for the NEXT-D beam design.

8.4 Beam design

The beam is designed using the bridge design software CONSPAN (Bentley Systems, 2012) which includes prestressing strand and vertical reinforcement design. For a specific design, CONSPAN checks the stress of prestressing strands and the precast beam at various stages and different limit states. It does this for the bending and shear strengths at strength limit states. In addition

it also provides a summary of deflection and camber, and information for longitudinal bonded reinforcement design in the deck and vertical reinforcement design in the beam anchorage zone. Take the NEXT-8 40 ft. span bridge for example, the following paragraphs will cover detailed design inputs including bridge modeling, material properties, and loads.

8.4.1 Geometry

The overall bridge width is 48 ft. The shear key is not modeled; rather its width is included in the Double-Tee beam (Figure 8.4). Therefore each beam is 8 ft. wide. The properties of the beam cross section used are those automatically calculated by CONSPAN. The left and right curb width is 19 in., resulting in a distance of 11 in. from the interior face of the parapet to the centerline of the exterior stem of the exterior beam. This information is used for calculating the live load distribution factor based on the lever rule and determining design lanes, which is three in this case. The release span length is set to the same as the total span length, which is 39 ft and 10.5 in., and the bearing to bearing distance is 39 ft. At this stage the beam cross section is type I without post-tension, but the beams are not considered sufficiently connected to act as a unit, which results in live load distribution factors that are not desired. In order to get the appropriate distribution factors, post-tension is added by checking the box ‘Post-Tensioned’ in the geometry tab. It should be noted that for NEXT-6 bridge, due to the geometry difference between the interior beam and the exterior beam, the modeling is not as straight-forward as the NEXT-8’s. The asymmetric geometry of the exterior beam cannot be directly modeled. This aspect is taken care of by utilizing the same geometry as that of the interior beam but the cross section properties are obtained from the real cross section to make sure that the beam self-weight and stress calculations are right (Figure 8.5). The effective flange width of the exterior beam is assigned 7 ft., which ensures the correct flexural resistance.

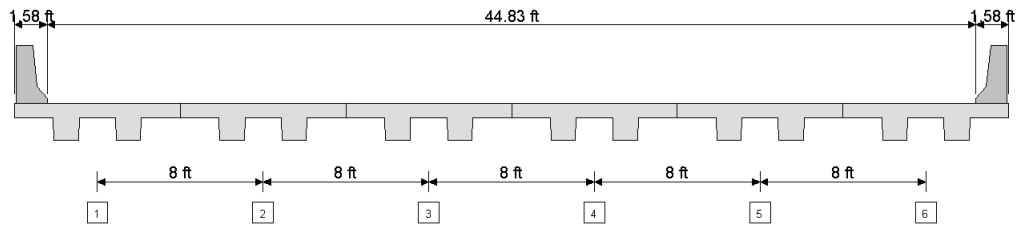


Figure 8.4: Model geometry of NEXT 8 in CONSPAN

8.4.2 Material properties

The compressive strength of the precast beam is 5200 psi at release, and 6500 psi at service. The unit weight of the precast is assigned a value of 150 pcf. It is assumed that the shear key has the same unit weight as that of the precast. For calculating the beam self-weight, considering the presence of reinforcement, this density is appropriate; while when calculating the Young’s modulus

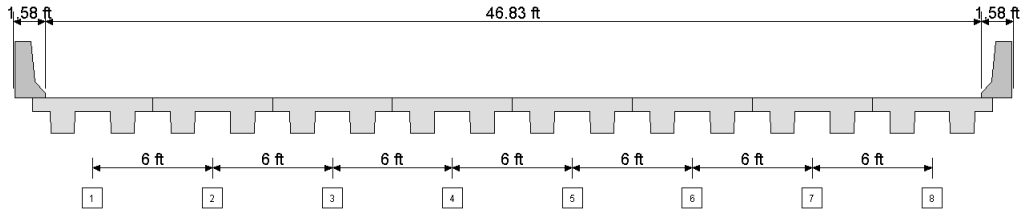


Figure 8.5: Model geometry of NEXT 6 in CONSPAN

using LRFD equation 5.4.2.4-1, this density may be a little bit larger. Since high strength concrete is used and the precast has high quality control, the Young's modulus is directly calculated based on the density of 150 pcf. A smaller Young's modulus can be directly input in the tab however. Bonded low relaxation strands with diameter of 0.5 in., tensile strength of 270 ksi, and a Young's modulus of 28500 ksi are used to produce a straight strand pattern. At the top of each stem (7.5 in. to the strand center from the top of the deck), two strands are provided to support the deck reinforcement. For the plain longitudinal reinforcement, the Young's modulus is 29000 ksi, and the yield stress is 60 ksi. For vertical reinforcement, #4 reinforcing steel is used in the NEXT-D beams. Transformed area of the prestressing strand is not applied according to SCDOT Bridge Design Manual Section 15.5.6.3. SCDOT (2006).

8.4.3 Loads

The dead load of the parapet is uniformly distributed to the exterior beam and the adjacent interior beam. In CONSPAN, this load is input as a line load on the precast over the design span length. The dead load of the bituminous wearing surface, which has an average depth of 4 in., covers an area in between the inner faces of the two parapets. In CONSPAN, this load is split uniformly to each beam as line load on the precast over the design span length. The beam self-weight is automatically calculated by the software. The vehicular live load applied is HL-93 as specified in LRFD Article 3.6.1.2. All of the factors are based on the AASHTO LRFD method. Although the bridge has an ADTT less than 5000, this advantage is not taken to reduce the impact factor, and the bridge is designed for an ADTT of 5000.

8.4.4 Comments concerning beam design

When calculating the prestress loss, the approximate method is used. When checking the tensile stress in concrete before prestress losses against the limits provided in LRFD Table 5.9.4.1.2-1, it was found out that bonded reinforcement needs to be provided above the top transverse reinforcement. The area of the bonded reinforcement is calculated based on LRFD Figure C5.9.4.1.2-1. In the anchorage zone, within a distance of $\frac{h}{4}$ from the end of the beam, where h is the total height of the beam, vertical reinforcement is provided as specified in LRFD Article 5.10.10.1. The area of this reinforcement is proportional to the total area of prestressing strands used. Therefore it is important to design the beam to be structurally efficient. Compared with other interior beams,

the first interior beam, due to the additional parapet load exerted, has to take more demand and therefore needs more strands in some cases. Since the difference is not significant, all the other interior beams are designed the same as the first one. The exterior beam, in some cases, due to the smaller live load distribution factors than those of the interior beam, attracts less demand and requires fewer strands. However, LRFD Article 2.5.2.7 requires that in general the exterior beam should not have less resistance than that of the interior beam. Taking this suggestion, the exterior beam is designed the same as the interior beam in these cases. The load factors calculated by lever rule in CONSPAN v12 were manually updated to the accurate values.

A hand-calculation example for the first interior beam design of NEXT-8 40 ft. span is provided in Appendix I. Refer to Appendix J for detailed drawings of all designed cases with Appendix K given all of the CONSPAN input and output for all cases.

8.5 Deck analysis and design

8.5.1 Refined analysis using 3D finite element model

LRFD Article 3.6.1.3.3 specifies that when the refined methods are used to analyze decks, if the slab spans primarily in the transverse direction, only the axles of the design truck of Article 3.6.1.2.2 or design tandem of Article 3.6.1.2.3 shall be applied to the deck slab. According to the previous chapter, the most critical normalized live load demand results from the design tandem. As such a single design tandem is applied to the bridge FEM, moving across the bridge model element by element both transversely and longitudinally. The tandem is positioned as specified in LRFD Article 3.6.1.3 such that the center of any wheel load is not closer than 2 ft. from the face of the parapet for the deck design. Article 3.6.1.3.4 of the AASHTO specifications also suggests checking the overhang design for a vertical load positioned 1 ft from the face of the parapet (AASHTO, 2012). However, this design case is not applicable to the proposed NEXT-D section because the overhang is only 30 in. wide. This would then place the vertical load directly over the beam stem and not on the overhang. The dead loads, as described above, include beam self weight, parapet self weight, and bituminous wearing surface self weight. Section cuts are created at critical cross sections: sections beside the stem, sections in the middle of two stems of a beam, and sections besides the shear key (Figure 8.6). The live load and dead load demands at the critical sections from the FEM are then normalized by the distribution widths of 10 ft. and the bridge total length respectively to get the demands for a 1 ft. wide strip. Typical normalized dead load demand distributions and the envelope of normalized live load demand distributions (NEXT-8 40 ft. span) are displayed in Figure 8.7. The normalized live load demands are then factored by the multiple presence factor 1.2 (LRFD Table 3.6.1.1.2-1) and the impact factor 1.33 (LRFD Table 3.6.2.1-1). These are combined with the normalized dead load demands using load factors as specified in LRFD Table 3.4.1-1 for strength I and service I limit states (Figure 8.8).

Notice that there are two different alternating spans for the deck, one includes the shear key (span w/ key) and the other does not (span w/o key). For the span without a shear key, the positive moment demand is higher than that in the span with a shear key. This is different when compared

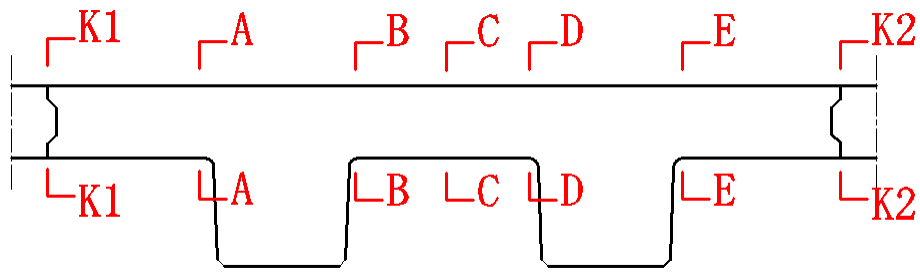


Figure 8.6: Section cuts in the bridge FEM

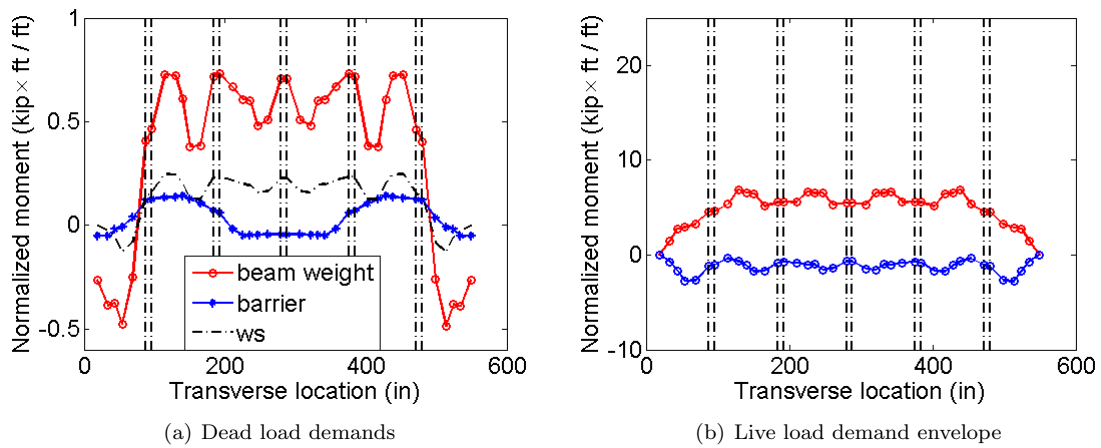


Figure 8.7: Transverse demand distribution for NEXT-8 in the bridge FEM

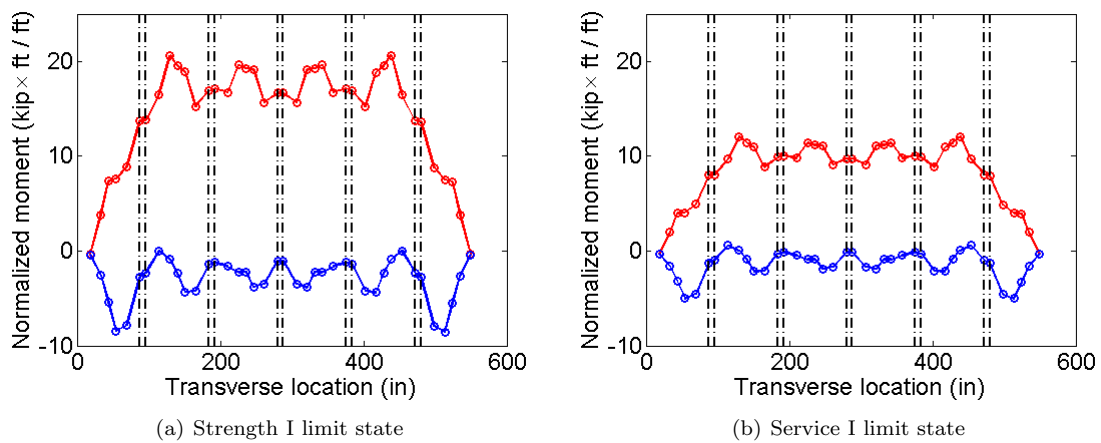


Figure 8.8: Design normalized demands for NEXT-8

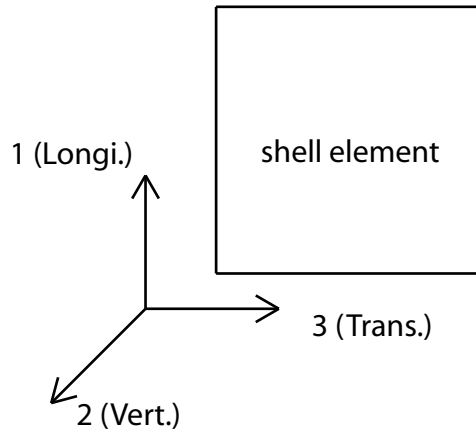


Figure 8.9: Local axis for a shell element in the bridge FEM

with the AASHTO strip method discussed later, where the larger spans result in a larger positive moment. This is because in the 3D FEM, the stiffness of the shear key is not as large as that within the stem of a beam and thus attracts less positive moment demand. However, in the AASHTO strip method, the stiffness of all the components are the same and the demand distribution is controlled by the support spacing.

When determining the transverse demands, the elastic-cracked stiffness is applied to the shear key. To be consistent, the post-cracked stiffness is applied to the deck by assigning a value of 0.35 to both bending m_{11} and bending m_{12} modifiers for the shell element, where m_{11} is the modifier for the transverse bending stiffness, and m_{12} is the modifier that represents the influence of transverse bending stiffness on torsional stiffness in local 2 direction (Figure 8.9). The transverse bending stiffness will be weakened by the existence of longitudinal cracks, which will also lead to the reduction of the torsional stiffness. Therefore a reduction factor of 0.35 is assigned for both modifiers.

The demands determined this way in the FEM can be used directly for the bridges studied. However, considering the future alteration of the bridge geometry, running the 3D FEM to determine deck demands is complex and time-consuming. A general formula for the deck demands will facilitate the design of NEXT-D bridges with different spans and different beam spacing. Since the AASHTO strip method is popularly used for deck demand determination, it is expected that a relationship between the 3D FEM demands and those from the AASHTO strip method can be established.

8.5.2 AASHTO method

8.5.2.1 Modeling

The AASHTO strip method assumes that the deck is continuous and the supports are all rigid. This method results in larger negative demands in the middle of the longitudinal span because it does not consider the deformation of the supports in real cases. In the 1D AASHTO FEM, the deck (including the shear key) is modeled using frame elements and the stems are modeled as rigid

supports (Figure 8.10). This can be performed in any basic analysis package. The real stem spacing and overhang length are used in the FEM. For the NEXT-8, the rigid supports representing the stems are spaced at alternating distances: 3 ft. and 5 ft. For the NEXT-6, the supports are spaced at 3 ft. In both the NEXT-6 and NEXT-8, the distance from the outer rigid support to the edge of the overhang is 2.5 ft. The deck is meshed into smaller frame elements with the same size, which in this case is 3 in. As far as the live load is concerned, LRFD 3.6.1.3.3 specifies that where the slab spans primarily in the transverse direction, only the axles of the design truck or design tandem shall be applied to the deck slab. It also states that the centrifugal and braking forces need not be considered in the deck design. Two axles of the design tandem result in larger critical demands than a single 32 kip axle of the design truck does. However, since the design tandem has a wider distribution width, the normalized demand on a 1 ft. cross section will be reduced. Therefore in the FEM, a single 32 kip axle load of the design truck is applied. The two 16 kip point loads spaced 6 ft. apart are applied as frame joint loads and positioned no closer than 2 ft. from the face of the parapet. In the case studied, the furthest loading position should be 43 in. (1 in. + 18 in. parapet width + 2 ft.) from the edge of the overhang. In the finite element model, this distance is 42 in., which is equivalent to the total length of 14 frame elements. Multiple trucks can be considered but with many permutations. It is therefore decided to use only one design truck with the result multiplied by the multiple presence factor of 1.2. Within the distance specified, the design truck point loads are moving together element by element, creating 141 load cases for the NEXT-8 and 149 load cases for the NEXT-6.

The dead loads on a 1 ft. strip are applied on the AASHTO FEM as line loads. The distribution of the dead loads are as that in the 3D FEM, i.e, each beam takes its own weight, which is uniformly distributed on the beam; parapet self-weight is uniformly distributed to the exterior beam and the first interior beam; and the self-weight of the wearing surface is uniformly distributed in-between the innerfaces of the two parapets.

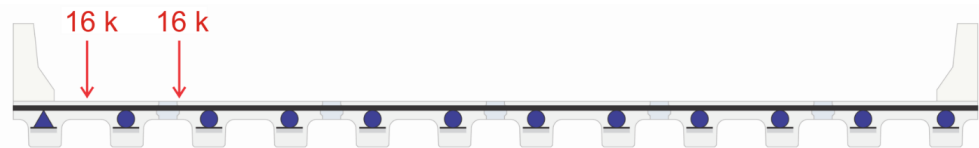


Figure 8.10: AASHTO model of NEXT-8 using SAP2000

8.5.2.2 Data acquisition

For the frame element, compared with the global x, y, z axis, local axis in the case studied are as follows:

- Local axis 1 is the longitudinal axis of the element directed from end I to end J (positive x) (see Figure 8.11);
- The local 2 axis is taken as the upward z;

- The local 3 axis lies in x-y plane, and is the downward y.

Therefore the frame joint moment in local 2 direction (m_2) is desired. The positive m_2 is defined from the frame element end i, which, in the case studied, results in a negative moment (tension on top of the bridge deck) Therefore when processing results, this sign is reversed so that the positive value of m_2 represents positive moment. This moment m_2 is monitored at each frame joint for each load case. The whole process – adding load patterns, applying frame joint loads, running analysis, and acquiring data— was completed by running a MATLAB code, which gives a final matrix containing m_2 at each frame element joint for each load case. However in actual use, influence lines may be used to identify critical loading locations. According to LRFD Article 4.6.2.1, when the strip method is used, the critical positive moment and negative moment within the deck should be used for the deck design. As such, the critical positive moment and negative moment caused by the live load are recorded for later use. For the NEXT-8, the total critical positive moment is 156.73 kip-in, and the critical negative moment is -95.11 kip-in. For the NEXT-6, the total critical positive moment is 123.09 kip-in, and the critical negative moment is -51.8 kip-in. The total live load demands are then normalized using the strip widths specified in LRFD Table 4.6.2.1.3-1 for the cast-in-place concrete deck without stay-in-place concrete formwork. For the NEXT-8, the strip width is 52.4 in. for positive moment demand, and 60 in. for negative moment demand using the average stem spacing of 4 ft. For the NEXT-6, the strip width is 45.8 in. for positive moment demand, and 57 in. for negative moment demand using the stem spacing of 3 ft. The normalized dead load demand distributions and envelope of normalized live load demand distributions are displayed in Figure 8.12. For the NEXT-8, the critical normalized positive moment demand is 2.99 kip-ft/ft, and the critical normalized negative moment demand is -1.59 kip-ft/ft. For the NEXT-6, the critical normalized positive moment demand is 2.69 kip-ft/ft, and the critical normalized negative moment demand is -0.91 kip-ft/ft.

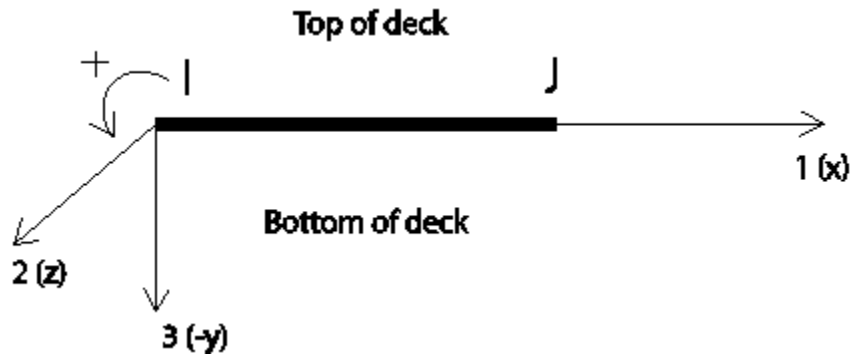


Figure 8.11: Output convention for frame element in SAP2000

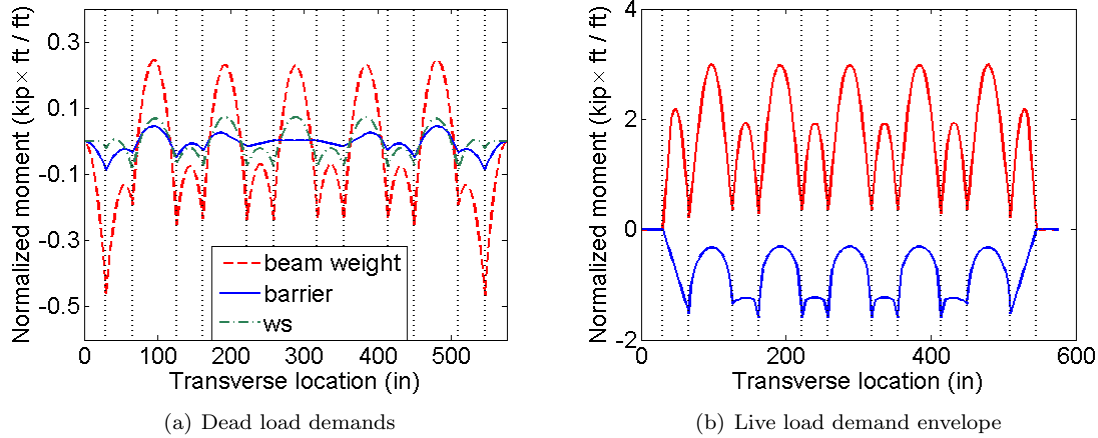


Figure 8.12: Transverse demand distribution for NEXT-8 in the AASHTO model

8.5.3 Formula development

8.5.3.1 Live load effect

AASHTO makes some general assumptions of effective strip width for positive moment and negative moment based on regular layouts. For the NEXT-D beam bridge, the usual case is that the stem spacing varies. For instance in the NEXT-8, the stem spacing alternates between 3 ft. and 5 ft. Also the AASHTO strip method does not consider the influence of span length. Simulation results however show that for both the NEXT-6 and NEXT-8, as the span length increases, the normalized live load moment demands also increase; and for the same span length, the normalized live load moment demands in NEXT-8 are always more critical than those in the NEXT-6. Based on this phenomenon, the normalized moment demands caused by the live load are considered highly correlated with design span length and stem spacing for the NEXT-D Beam Bridge. This is particularly the case for the positive moment demands.

In the 3D FEM, five span lengths are studied for the NEXT-8 (48 ft. wide) and the NEXT-6 (50 ft. wide): 22 ft., 26 ft., 30 ft., 35 ft., and 40 ft. with design span lengths of 21 ft., 25 ft., 29 ft., 34 ft., and 39 ft. respectively. The envelope distributions of the normalized live load transverse moment demand for all the five spans for both the NEXT-6 and NEXT-8 are displayed in Figure 8.13. The critical positive moment demands in the two deck spans are recorded. Meanwhile, the critical negative moment demands for both interior beam and exterior beam are also recorded. In order to establish a relationship of demands between the 3D FEM and the AASHTO strip-method, the critical positive moment demands in the 3D FEM are divided by the maximum positive moment from the AASHTO method, and the critical negative moment demands in the 3D FEM are divided by the minimum negative moment from the AASHTO method. As stated before, these critical demand ratios increase their magnitudes as the span length and average beam spacing increase (Figure 8.14). For simplicity, the ratios are modified so that they are linearly dependent upon the span lengths. It is observed that for the NEXT-6, the negative moment obtained from AASHTO is

much more conservative due to the rigid support assumption. In the formula, the demand ratio is assumed to be linearly dependent on the exponential form of the design span length multiplied by the exponential form of the average stem spacing as follows:

$$R = ax + b \quad (8.1)$$

$$x = l_{design}^m S_{design}^n \quad (8.2)$$

where, R is the demand ratio, l_{design} is the design span length (ft), which is the distance between supports; and S_{design} is the average stem spacing (ft). For the NEXT-6, the average stem spacing is 3 ft. For the NEXT-8 with an alternating stem spacing of 3 ft and 5 ft, the average stem spacing is 4 ft. Other parameters including a , b , m , and n are constant coefficients, of which m and n are determined first so that the demand ratios of the NEXT-6 and NEXT-8 are approximately on a linear line (Figure 8.15). After that, the equation of the line is obtained and a and b are determined. Following this procedure, the formulas for the live load demands are given below. The negative moment in the interior beam is directly taken as the AASHTO FEM value, which is proper for NEXT-8 and fairly conservative for NEXT-6 (Figure 8.14c) due to the rigid support assumption. For bridges of 22 ft. span and 30 ft. span, the critical negative moment demand in the interior beams of NEXT-6 from AASHTO FEM is so conservative that it even exceeds the critical demand in the exterior beam, which, according to the 3D simulation, is not correct. Therefore when applying the formula for negative moment demand in the interior beam, this value shall not exceed that in the exterior beam.

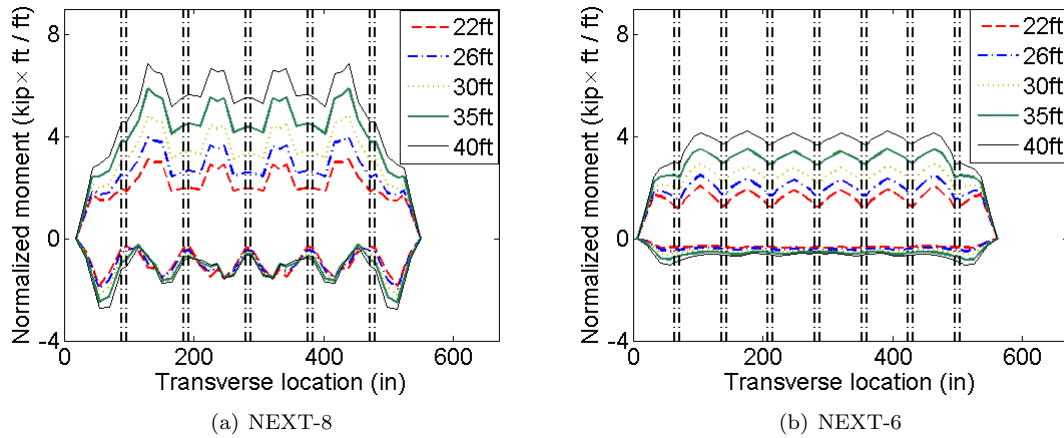


Figure 8.13: Live load transverse demand envelope in bridge FEM

Positive moment demand in the span without shear key:

$$M_{positive} = M_{p_AASHTO} [0.77 + 0.0027(l_{design}^{1.3} S_{design}^{1.4} - 244)] \quad (8.3)$$

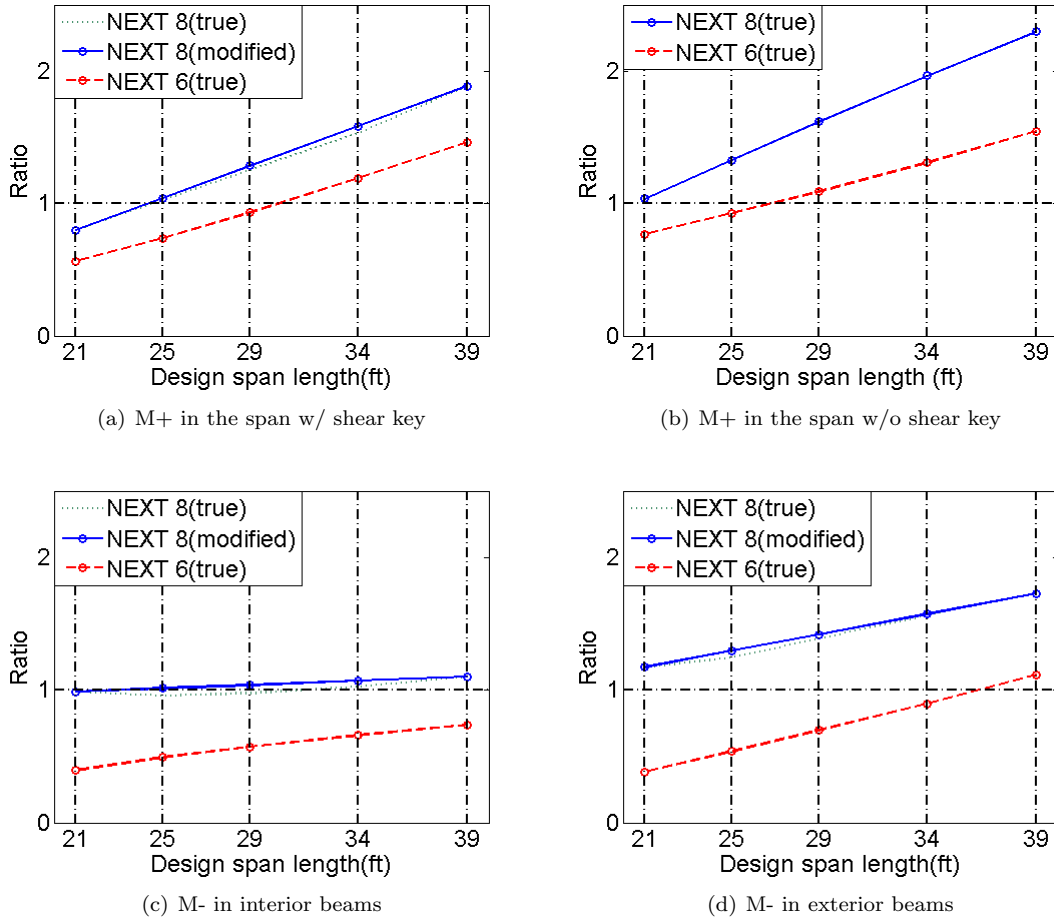


Figure 8.14: Critical demand ratios of bridge FEM result over AASHTO method result

Positive moment demand in the span with shear key:

$$M_{positive} = M_{p_AASHTO}[0.58 + 0.0196(l_{design}^1 S_{design}^{0.8} - 51)] \quad (8.4)$$

Negative moment demand in the exterior beam:

$$M_{negative} = M_{n_AASHTO}[0.4 + 6.28(l_{design}^{0.1} S_{design}^{0.2} - 1.69)] \quad (8.5)$$

Negative moment demand in the interior beam:

$$M_{negative} = M_{n_AASHTO} \quad (8.6)$$

where M_{p_AASHTO} and M_{n_AASHTO} represent the critical positive and negative moment demands separately in the 1-D analysis model caused by a single 32-kip axle of the design truck, and $M_{positive}$

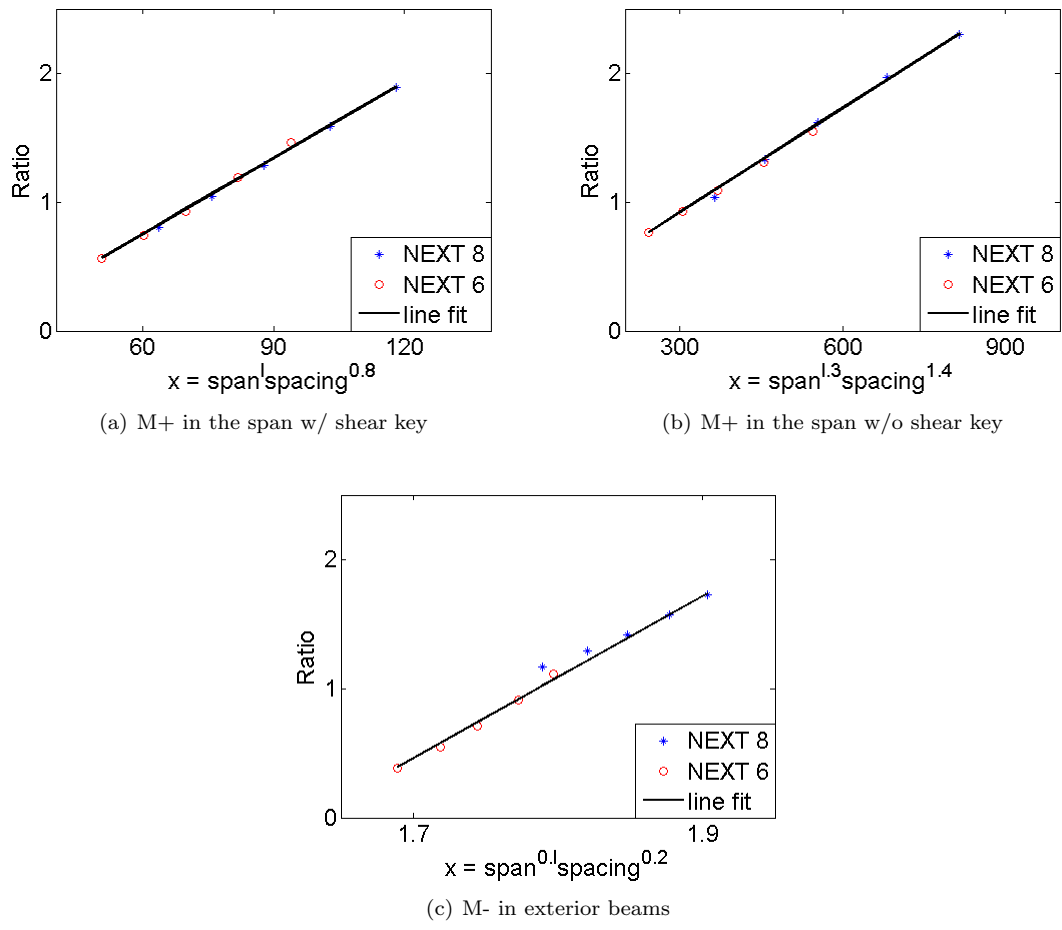


Figure 8.15: Deck demand formula development

and $M_{negative}$ represent the critical positive and negative moment demands separately caused by the live load to be used for design. **It should be stressed that when dealing with the negative moment demand in the interior beam, the value shall not exceed that in the exterior beam.**

The above formulas apply to both the NEXT-6 and the NEXT-8 and any width in between. The range of applicable spans, without further verification, is between 22 ft. to 40 ft. The formulas above are based on a constant stem depth of 12 in. and do not consider the change of the shear key stiffness. Increasing the stem depth or decreasing the shear key stiffness will decrease the transverse demands in the deck as talked about later. Thus, the developed formulas provide a conservative and acceptable demand estimate for stem depths of 12 in. or greater.

8.5.3.2 Dead load effect

Dead load effects - including the demands from beam self-weight, parapet self-weight, and wearing surface self-weight - are also determined based on the 1D FEM. The dead load demands at each frame element joint are then combined together for Strength I and Service I limit states using the factors as specified in LRFD Table 3.4.1-1 and Table 3.4.1-2. The moment distributions due to dead load effect for each limit state are given in Figure 8.16 and Figure 8.17. The factored critical positive and negative moment demands due to the dead loads for each limit state are listed in Table 8.3 for later final design demand determination.

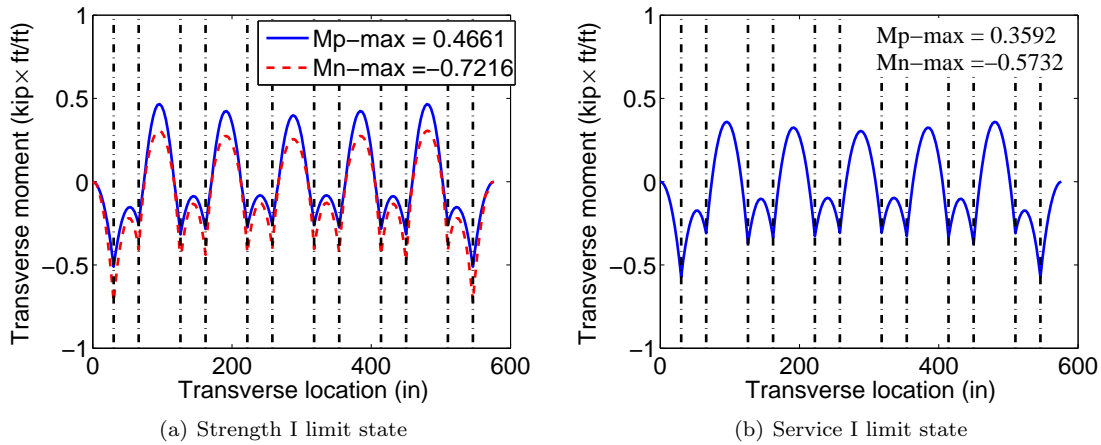


Figure 8.16: Factored dead load effect for NEXT-8

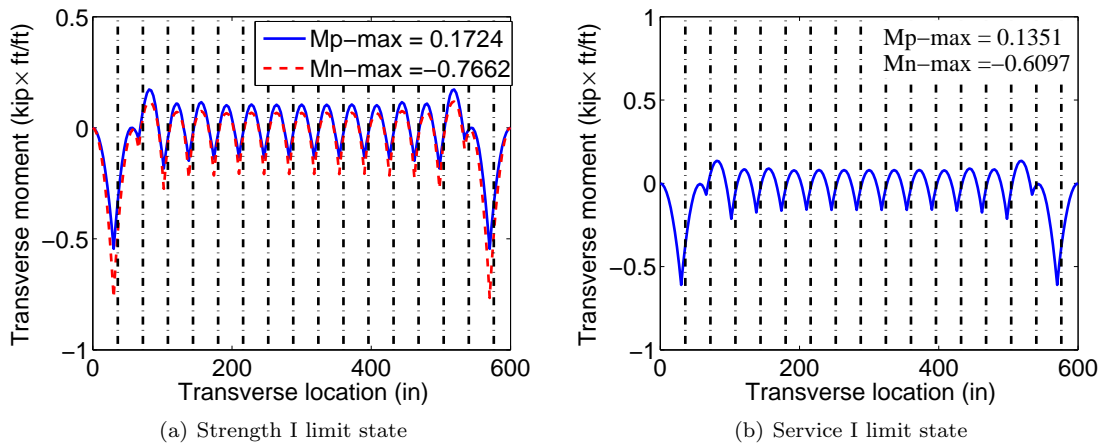


Figure 8.17: Factored dead load effect for NEXT-6

Table 8.3: Factored moment demand caused by dead load

Demand	NEXT-8		NEXT-6	
	Strength I	Service I	Strength I	Service I
M_{p_DL} (kip-ft/ft)	0.4661	0.3592	0.1724	0.1351
M_{n_DL} (kip-ft/ft)	-0.7216	-0.5732	-0.7662	-0.6097

8.5.3.3 Final design demand determination

The final design positive moment demand (M_{p_total}) is determined by summing up the factored live load effect and four times the factored dead load effect (Equation 8.7). The final design negative moment demand (M_{n_total}) is determined by summing up the factored live load effect and the factored dead load effect (Equation 8.8).

$$M_{p_total} = M_{positive} \times IM \times m \times LF + 4M_{p_DL} \quad (8.7)$$

$$M_{n_total} = M_{negative} \times IM \times m \times LF + M_{n_DL} \quad (8.8)$$

where,

$M_{positive}$ = unfactored positive moment demand from live load based on Equation 8.3 and Equation 8.4, (kip-ft/ft)

$M_{negative}$ = unfactored negative moment demand from live load based on Equation 8.5 and Equation 8.6, (kip-ft/ft)

M_{p_DL} = factored positive moment demand from dead load, (kip-ft/ft)

M_{n_DL} = factored negative moment demand from dead load, (kip-ft/ft)

IM = dynamic load allowance percent, $IM = 1.33$ (LRFD Table 3.6.2.1-1)

m = multiple presence factor, $m = 1.2$ (LRFD Table 3.6.1.1.2-1)]

LF = load combination factor, $LF = 1.75$ for Strength I limit state, and 1 for Service I limit state (LRFD Table 3.4.1-1)

The multiplier 4 for the design positive moment demand is to account for the large increase of positive moment demand due to dead loads as the span length increases (see Figure 8.18 and Figure 8.19). There is not much change of negative moment demand with span length change in each design limit state, therefore a multiplier of 1 is used.

The design demands obtained this way are compared with the 3D FEM results (in bracket) in Table 8.4 to Table 8.7. Most of the demands from the proposed formula are conservative. The unconservative values are highlighted. Taking the 3D FEM's results as the "correct" values, the maximum percentage error of the unconservative demands is less than six percent.

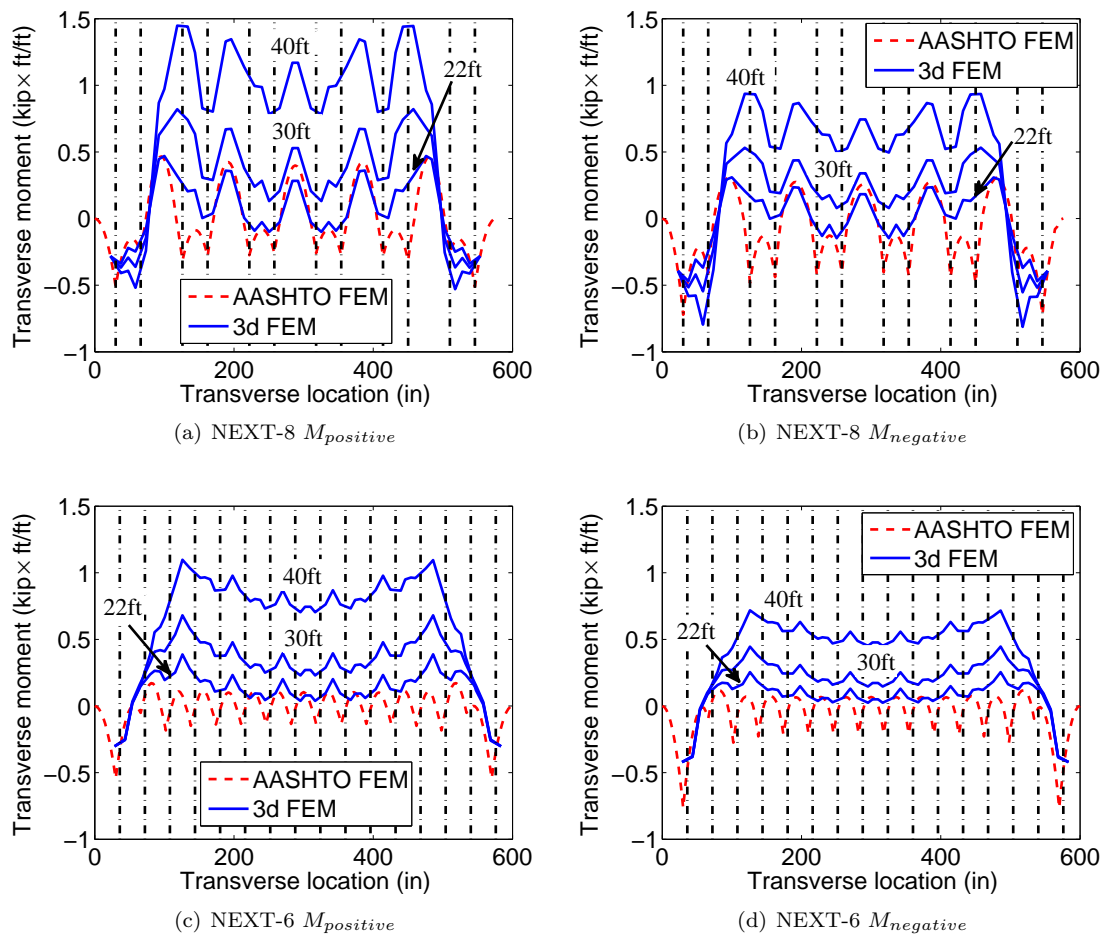


Figure 8.18: Comparison between dead load effect of 3D FEM and AASHTO 1D FEM in Strength I limit state

Table 8.4: NEXT-8 — Design demands provided by the formula vs demands from the bridge FEM (shown in parentheses) for the strength I limit state

	Critical section location	22 ft.	30 ft.	40 ft.
M+ (kip-ft/ft)	Span w/o key	11.02 (8.87)	15.30 (14.25)	21.18(20.65)
	Span w/ key	8.78(7.00)	12.75(11.31)	17.72(17.12)
M- (kip-ft/ft)	Exterior beam	-5.25(-5.56)	-6.88(-6.70)	-8.42(-8.45)
	Interior beam	-5.15(-4.52)	-5.15(-4.19)	-5.15(-4.34)

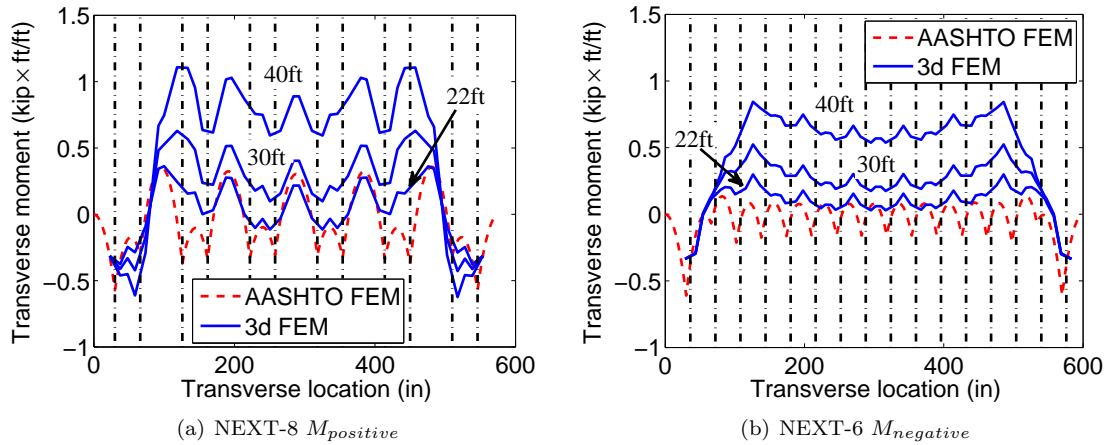


Figure 8.19: Comparison between dead load effect of 3D FEM and AASHTO 1D FEM in Service I limit state

Table 8.5: NEXT-8 — Design demands provided by the formula vs demands from the bridge FEM (shown in parentheses) for the service I limit state

Critical section location		22 ft.	30 ft.	40 ft.
M+ (kip-ft/ft)	Span w/o key	6.67(5.10)	9.12(8.29)	12.47(12.08)
	Span w/ key	5.39(4.06)	7.66(6.62)	10.50(10.04)
M- (kip-ft/ft)	Exterior beam	-3.16(-3.25)	-4.09(-3.94)	-4.97(-4.98)
	Interior beam	-3.10(-2.61)	-3.10(-2.34)	-3.10(-2.15)

Table 8.6: NEXT-6 — Design demands provided by the formula vs demands from the bridge FEM (shown in parentheses) for the strength I limit state

Critical section location		22 ft.	30 ft.	40 ft.
M+ (kip-ft/ft)	Span w/o key	6.46(6.15)	9.04(8.85)	12.57(12.70)
	Span w/ key	4.98(4.35)	7.81(7.37)	11.36(11.84)
M- (kip-ft/ft)	All beams	-1.77(-0.98)	-2.65(-1.55)	-3.49(-2.61)

Table 8.7: NEXT-6 — Design demands provided by the formula vs demands from the bridge FEM (shown in parentheses) for the service I limit state

Critical section location		22 ft.	30 ft.	40 ft.
M+ (kip-ft/ft)	Span w/o key	3.84(3.59)	5.31(5.19)	7.33(7.47)
	Span w/ key	2.99(2.51)	4.61(4.28)	6.64(6.94)
M- (kip-ft/ft)	All beams	-1.18(-0.54)	-1.69(-0.82)	-2.16(-1.43)

8.6 Sensitivity study

8.6.1 Sensitivity of demand distribution to shear key stiffness

There are many sources that can lead to a change of shear key stiffness. In the case studied, the bond is stronger than the concrete, and the interface crack actually happens in the adjacent concrete. Therefore the material variability of the concrete is one source. Second, the elastic-crack stiffness of the shear key actually covers a range of values depending upon the seriousness of the crack. Third, the change of rebar configuration can also change the shear key stiffness. Some of these sources can also change the stiffness of the precast beam. It is important to keep in mind that the transverse demand distribution is dependent upon the ratio of the stiffness among the relevant components rather than the change of stiffness of a single component. This sensitivity study of transverse demand distribution to shear key stiffness answers the question: How does the demand change from a condition when the shear key interface is intact to the condition where serious shear key interface cracks exist. In the 3D FEM, shear key stiffness is changed by either increasing or decreasing the modifier of moment of inertia of the shear key frame element. With the modifier of 1 as the reference value, other modifiers include 0.1, 5, 10, and 100. The design tandem load is applied, running element by element both transversely and longitudinally with no wheels closer than 2 ft. from the face of the parapet. The transverse live load demand distribution envelope corresponding to each modifier is displayed in Figure 8.20.

For the NEXT-8, the following trends are observed. It is seen that for the positive moment demand, as the stiffness modifier changes from 1 to 0.1, there is a big drop in the demand in both the shear key and the precast beam. The shear key acts similar to an internal hinge when the modifier is 0.1, meaning severe cracks happened. As the modifier changes from 5 to 100, there is only a very small change of the demand distribution and magnitudes, implying the shear key interface is close being fully intact. For the negative moment, the increase of shear key stiffness attracts more demands to the shear key itself, but subtracts demands in the precast beam. There is little change of demands as the modifier increases from 1 to 100. The trend seen in the negative moment is also seen for the shear. For the NEXT-6, the change of positive moment demand distribution is similar to that of the NEXT-8, with the only difference being for the negative moment demand. As the shear key stiffness increases, both the negative moment demands in the key and in the precast increase. There is not much change of negative moment demand as the modifier changes from 1 to 100. As in the NEXT-8, the change of shear is similar to the change of negative moment demand.

8.6.2 Sensitivity of demand distribution to stem depth

As the bridge span length increases, the stem depth may also need to be increased. The increase in stem depth will result in a larger stem stiffness, causing demand redistribution. To better understand the influence of stem stiffness on transverse demand distribution, for each span length, a sensitivity study is carried out using different stem depths: 12 in. (current), 16 in., and 20 in., which correspond to an overall section depth of 20 in., 24 in., and 28 in. (NEXT 20D, NEXT 24D, NEXT 28D) respectively. The live load demand distribution envelope is displayed in Figure 8.21. Similar

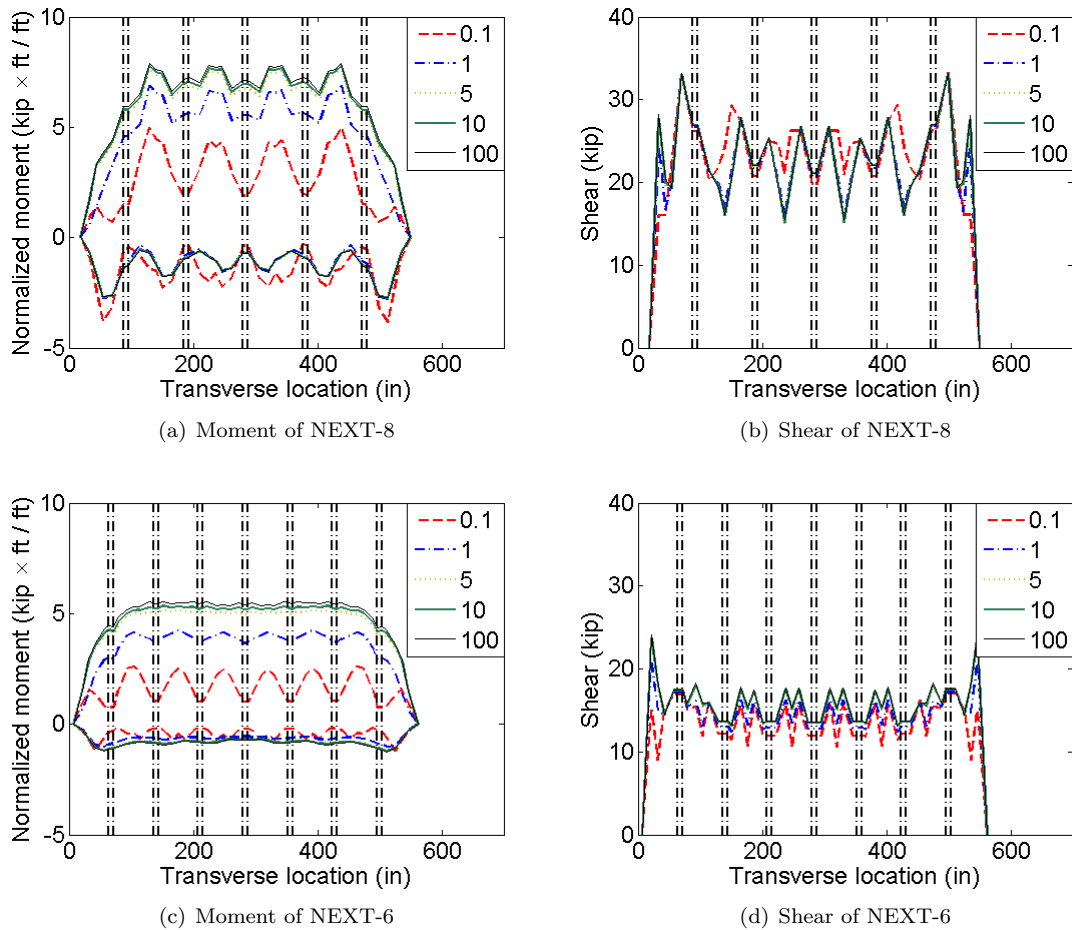


Figure 8.20: Sensitivity of transverse demand envelope to shear key stiffness

trends are found for all of the cases: as the stem depth increases, the positive moment demands both in the shear key and the precast beam decrease. There is very little change of negative moment demands and shear demands. The increase in stem stiffness attracts more demands to the stem itself, and therefore the demands in the deck decrease.

8.6.3 Sensitivity of demand distribution to Young’s modulus of concrete

The material properties of concrete used in the 3D FEM are obtained based on the cylinder test results during the specimen test day. The Young’s modulus of concrete is directly related to the component’s stiffness, and therefore the demand distribution. The current value of Young’s modulus used in the 3D FEM is 5600 ksi corresponding to a compressive strength of 9.6 ksi. Considering the material variability that is inevitably involved or the change of the concrete design strength in the future, Young’s modulus of 4415 ksi and 5100 ksi corresponding to compressive strengths of 6 ksi and 8 ksi are also investigated for each span length. Within this range of Young’s modulus (from

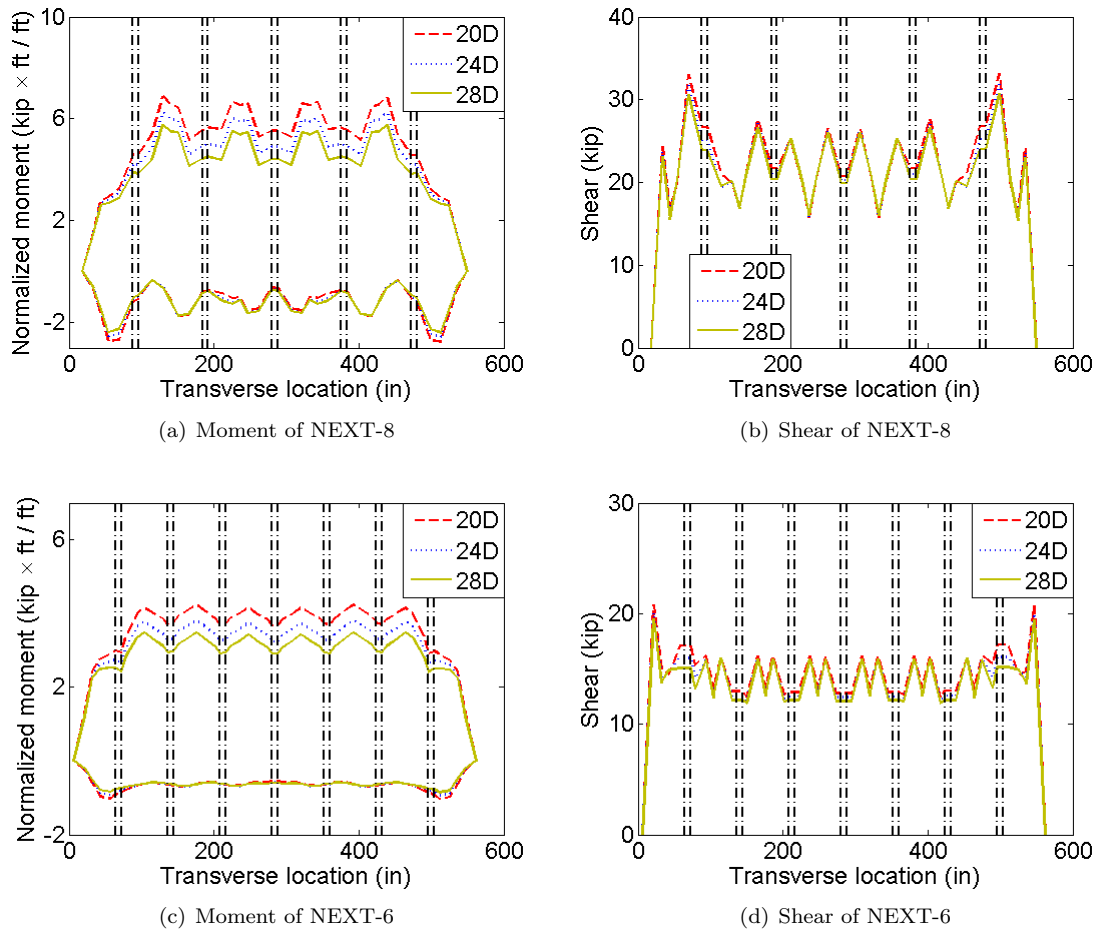


Figure 8.21: Sensitivity of transverse demand envelope to stem depth

4415 ksi to 5600 ksi) there is little change of live load demand distribution envelope for all the cases (Figure 8.22).

8.7 Deck design

The deck is designed based on the demands obtained from the formulas proposed. In general there are four steps to determine the design demands in Strength I and Service I limit states.

Step 1, Determine M_{p_AASHTO} and M_{n_AASHTO} : Establish the 1D AASHTO FEM using the true geometry of the overhang length and stem spacing. The deck is modeled as a continuous beam and stems are modeled as rigid supports. A single 32 kip axle of the design truck is modeled as two 16 kip point loads. The load is positioned no closer than 2 ft. from the face of the parapet as specified in LRFD Article. 3.6.1.3. Determine the critical positive and negative moment demands, which should be normalized based on the strip width specified in LRFD

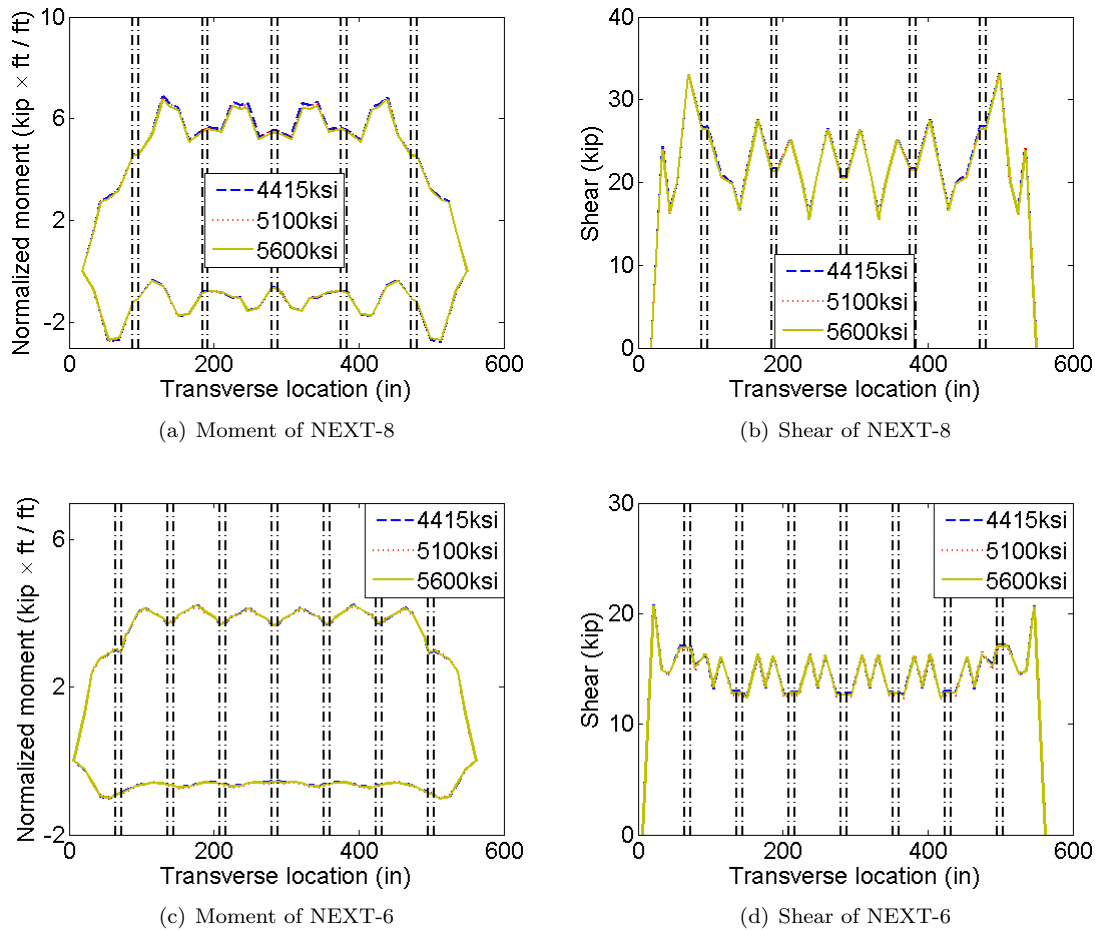


Figure 8.22: Sensitivity of transverse demand envelope to concrete Young's modulus

Table 4.6.2.1.3-1 for cast-in-place concrete deck without stay-in-place concrete formwork. In this way M_{p_AASHTO} and M_{n_AASHTO} are obtained. Influence lines may assist in this step.

Step 2, Determine $M_{positive}$ and $M_{negative}$: Use Equation 8.3 and Equation 8.4 to determine the unfactored positive moment demand due to live load for the deck span without shear key and the deck span with shear key respectively. Use Equation 8.5 and Equation 8.6 to determine the unfactored negative moment demand due to live load for the exterior beam and interior beam respectively. The negative moment demand in the interior beam shall not be more than that in the exterior beam.

Step 3, Determine M_{p_DL} and M_{n_DL} : Use the 1D beam FEM to determine the moment demands on a 1 ft. strip from dead loads (line loads). The dead loads include beam self-weight, parapet self-weight, and wearing surface self-weight. For beam self weight, each beam takes its own weight, which is uniformly distributed to the whole width of the beam. The parapet self-weight is uniformly distributed to the exterior beam and the first interior beam. The self-

weight of the wearing surface is distributed uniformly in-between the inner faces of the two parapets. The dead load effects are combined based on the factors provided in LRFD Table 3.4.1-1 and Table 3.4.1-2 for Strength I and Service I limit states. The critical positive and negative moment demands are then obtained (M_{p_DL} and M_{n_DL}) for each design limit state.

Step 4, Determine M_{p_total} and M_{n_total} : The final design positive moment demand M_{p_total} for each limit state is determined by multiplying $M_{positive}$ by IM (dynamic load allowance percent), m (multiple presence factor), and LF (load factor), the result of which is added to four times M_{p_DL} (see Equation 8.7). The final design negative moment demand M_{n_total} for each limit state is determined by multiplying $M_{negative}$ by IM, m, and LF, the result of which is added to M_{p_DL} (see Equation 8.8).

The deck is then designed for capacity in Strength I limit state and cracking control in Service I limit state. For the positive moment design in both limit states, the larger positive moment demand in the span without shear key is taken care of by considering the overlapping of the development length of the reinforcement. Demand-capacity charts in Figure 8.23 provide a direct comparison between current demands for strength I and service I limit states and capacities from various rebar configurations (Table 8.8). Take the NEXT-8 with a 22 ft. span for instance, the cracking control determines the final rebar configuration, which is #4@7in.; while for the 40 ft. span, the capacity determines the final rebar configuration, which is #4@5in. The final reinforcement designs for the NEXT-8 and the NEXT-6 with various spans are listed in Table 8.9 and Table 8.10. Other requirements that are checked include minimum transverse reinforcement requirement (LRFD Article 5.7.3.3), distribution reinforcement requirement (LRFD Article 9.7.3.2), temperature and shrinkage reinforcement requirement (LRFD Article 5.10.8), and bonded reinforcement requirement (LRFD Article 5.9.4.1). Refer to Appendix I and J for detailed deck design drawings and calculations.

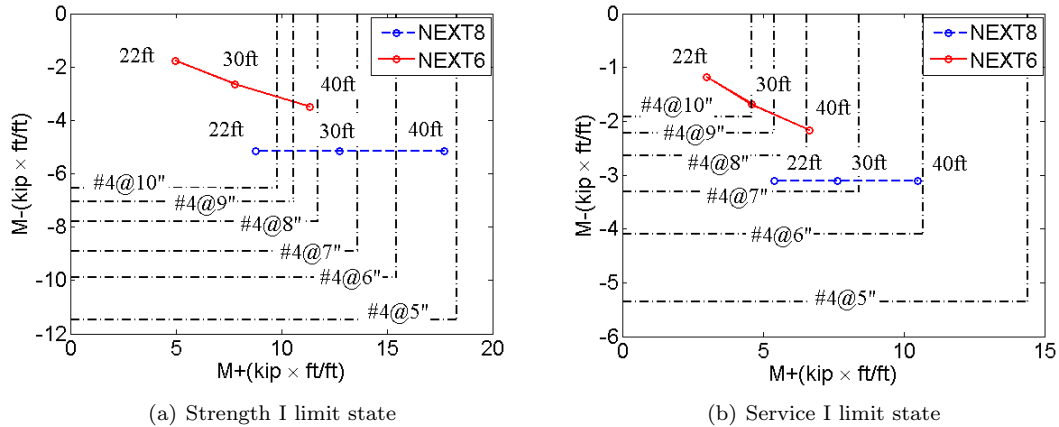


Figure 8.23: Demand vs capacity provided by various rebar configurations

Table 8.8: Reinforcing bar configuration capacities

Rebar configure	$A_s(in^2/ft)$	Strength I limit state		Service I limit state	
		M+ (kip-ft/ft)	M- (kip-ft/ft)	M+ (kip-ft/ft)	M- (kip-ft/ft)
#4@5"	0.47	18.29	-11.47	14.41	-5.36
#4@6"	0.39	15.43	-9.88	10.69	-4.10
#4@7"	0.34	13.59	-8.90	8.42	-3.32
#4@8"	0.29	11.71	-7.80	6.56	-2.64
#4@9"	0.26	10.56	-7.05	5.41	-2.22
#4@10"	0.24	9.79	-6.55	4.61	-1.92

Table 8.9: NEXT-8 — Final design capacity vs demand

Span length (ft)	Rebar config.	Strength I				Service I			
		M+ (kip-ft/ft)		M- (kip-ft/ft)		M+ (kip-ft/ft)		M- (kip-ft/ft)	
		Dem.	Cap.	Dem.	Cap.	Dem.	Cap.	Dem.	Cap.
22	#4@7"	8.78	13.59	-5.15	-8.90	5.39	8.42	-3.10	-3.32
30	#4@7"	12.75	13.59	-5.15	-8.90	7.66	8.42	-3.10	-3.32
40	#4@5"	17.72	18.29	-5.15	-11.47	10.50	14.41	-3.10	-5.36

8.8 Closure

This Chapter addresses the design of the parapet, deck overhang, deck and beam. The typical parapet design that has been used in the SCDOT is adopted for the NEXT-D Beam Bridge. The reinforcing steel configuration is designed to the end zone impact along the entire length of the parapet. This produces a very conservative design for the middle zone of the parapet. The effect of this over design is also felt within the deck overhang. The overhang must be stronger than the parapet to keep the damage within the parapet. As a result, the design of the deck overhang must be more robust than would be otherwise required. The advantage to this approach, however, is that the same rebar configuration (#5@12in) can be used throughout the parapet, which is a more construction friendly detail.

The overhang is designed considering not only the negative moment caused by the collision load, but also the axial tensile force due to the collision effect. The precast beam is designed using the live load distribution factors from AASHTO for cross section type I as specified in AASHTO LRFD Table 4.6.2.2.1-1, which is confirmed through finite element analysis. For the deck design, the live load effects are determined using Equation 8.3 to Equation 8.6, in which, the live load effect is a function of design span length and average stem spacing. Other parameters in the function are obtained based on line-fit. The proposed formulas are developed based on a constant stem depth of 12 in. and do not consider the change of shear key stiffness. Increasing the stem depth or decreasing shear key stiffness will decrease the transverse demands in the deck. The change of concrete Young's modulus from 4415 ksi to 5600 ksi exerts little influence on the live load demand distribution. The dead load effect is also obtained based on the 1D FEM. The final design demands in Strength I and

Table 8.10: NEXT-6 — Final design capacity vs demand

Span length (ft)	Rebar config.	Strength I				Service I			
		M+ (kip-ft/ft)		M- (kip-ft/ft)		M+ (kip-ft/ft)		M- (kip-ft/ft)	
		Dem.	Cap.	Dem.	Cap.	Dem.	Cap.	Dem.	Cap.
22	#4@10"	4.98	9.79	-1.77	-6.55	2.99	4.61	-1.18	-1.92
30	#4@10"	7.81	9.79	-2.65	-6.55	4.61	4.61	-1.69	-1.92
40	#4@7"	11.36	13.59	-3.49	-8.90	6.64	8.42	-2.16	-3.32

Service I limit states are obtained by combining live load effects and dead load effects together using Equation 8.7 and Equation 8.8.

The conclusions chapter of this report will provide a basic and succinct outline of the design guideline recommendations to be used for the modified NEXT-D beam to be used in South Carolina. The recommendations are restricted to the design space prescribed by the SCDOT which is 22 ft. 40 ft. spans and beam widths between 6 ft. and 8 ft. The details of these designs are found in Appendix J.

This page intentionally left blank

Chapter 9

Summary and Conclusions

9.1 Summary

Many state departments of transportation are in need of the development of a precast concrete solution for the construction of short span bridges that meet the objectives of accelerated bridge construction but do not have restrictions on the level of traffic service and are durable. This means that minimal maintenance to the superstructure and wearing surface would be needed. The South Carolina Department of Transportation funded a study to conduct a literature review and survey all other state departments of transportation to determine new design strategies for short span bridges. One of the surprising conclusions of the literature review/survey is that there is considerable research/design activity related to the construction of short span bridges, but little consensus among state departments of transportation. Based upon an initial report prepared by the authors of this reports and discussions during a briefing with both steering committee members and other stakeholders present, a decision was made to further investigate whether the NEXT-D bridge system is a plausible alternative to flat slab bridges which are on high volume roadways.

After additional research and discussions with the developers of the NEXT-D bridge system, the authors recommended to the South Carolina Department of Transportation that the scope and funding of the research project be expanded to allow for structural testing of the critical shear key detail of the NEXT-D bridge system and also do an extensive finite element study to better understand the load demand for this bridge type. The request was accepted and a plan for an experimental test program was developed and implemented. The demand evaluation required both crude and refined finite element analyses. It also relied on feedback from the experimental program to calibrate the computer models. From both the experimental activities and the computer modeling a bridge design was carried out and proposed for adoption within the State of South Carolina.

9.2 Conclusions

Some general conclusions of this research are:

- There is interdependency between the stiffness of the shear key and the demand that it attracts under loading. A stiff shear key needs to be stronger, so a viable solution could be a shear key with less stiffness – more is not necessarily better. This stiffness directly impacts the loads it attracts.
- The effectiveness of a precast concrete bridge system is highly dependent upon the design of the connections to transform the assemblage of discrete elements into a monolithic system.
- The design of a precast bridge to meet an accelerated construction schedule requires critical coordination among the department of transportation, the bridge engineer, the precast producer, material suppliers and the contractor.
- The UHPC with PVA fiber is a plausible material for use in the shear key between the NEXT-D beam sections. Indeed it is the recommended material to use as it achieves a balance between performance and inherent stiffness.

9.2.1 Design Guidelines for modified NEXT-D

The researchers recommended that the South Carolina Department of Transportation adopt a precast bridge design based on using NEXT-D beam elements with a modified cross section that is more amenable to the shorter spans of interest to the Department. While the report provides critical details for the design of a modified NEXT-D bridge and the recommendation for the shear key material, the following list provides the general design guidelines that should be followed by bridge engineers:

1. For the parapet design, use the current steel reinforcement configuration as currently recommended for precast concrete hollow core bridges. One change required is the length of the dowel bar anchored into the deck needs to be changed to a 90-degree standard hook.
2. For the overhang, the design needs to consider the axial tensile force caused by the collision loads.
3. For the deck design, use the strip method. Follow this four-step procedure to determine the design demands on a 1 ft. strip for Strength I and Service I limit states:

Step 1: **Determine M_{p_AASHTO} and M_{n_AASHTO} :** Establish the 1D FEM beam model using the true geometry of the overhang length and stem spacing. The deck (including the shear key) is modeled as a continuous beam and stems are modeled as rigid supports. A single 32 kip axle of the design truck is modeled as two 16 kip point loads. The load is positioned no closer than 2 ft. from the face of the parapet as specified in LRFD Article. 3.6.1.3.1. However, a little bit conservativeness is OK to accommodate the mesh in the AASHTO FEM. Determine the critical positive and negative moment demands, which should be normalized based on the strip width specified in LRFD Table 4.6.2.1.3-1 for cast-in-place concrete deck without stay-in-place concrete formwork. In this way M_{p_AASHTO} and

M_{n_AASHTO} are obtained. Note that influence lines most certainly could be used for this step.

- Step 2: **Determine $M_{positive}$ and $M_{negative}$:** Follow the formulas proposed for modifying the demand values M_{p_AASHTO} and M_{n_AASHTO} for the unfactored live load effects $M_{positive}$ and $M_{negative}$. These formulas are:

Positive moment demand in the span without shear key:

$$M_{positive} = M_{p_AASHTO}[0.77 + 0.0027(l_{design}^{1.3}S_{design}^{1.4} - 244)] \quad (9.1)$$

Positive moment demand in the span with shear key:

$$M_{positive} = M_{p_AASHTO}[0.58 + 0.0196(l_{design}^1S_{design}^{0.8} - 51)] \quad (9.2)$$

Negative moment demand in the exterior beam:

$$M_{negative} = M_{n_AASHTO}[0.4 + 6.28(l_{design}^{0.1}S_{design}^{0.2} - 1.69)] \quad (9.3)$$

Negative moment demand in the interior beam:

$$M_{negative} = M_{n_AASHTO} \quad (9.4)$$

where

l_{design} = the design span length (ft)

S_{design} = the average stem spacing (ft).

The negative moment demand in the interior beam shall not exceed that in the exterior beam.

- Step 3: **Determine M_{p_DL} and M_{n_DL} :** Use the 1D FEM to determine the moment demands on a 1 ft. strip from dead loads (line loads). The dead loads include beam self-weight, parapet self-weight, and wearing surface self-weight. For beam self-weight, each beam takes its own weight, which is uniformly distributed to the whole width of the beam. The parapet self-weight is uniformly distributed to the exterior beam and the first interior beam. The self-weight of the wearing surface is distributed uniformly in-between the inner faces of the two parapets. The dead load effects are combined based on the factors provided in LRFD Table 3.4.1-1 and Table 3.4.1-2 for Strength I and Service I limit states. The critical positive and negative moment demands are then obtained (M_{p_DL} and M_{n_DL}) for each design limit state.

- Step 4: **Determine M_{p_total} and M_{n_total} :** The final design positive moment demand M_{p_total} and negative moment demand M_{n_total} for each limit state is determined using the following formulas.

$$M_{p_total} = M_{positive} \times IM \times m \times LF + 4M_{p_DL} \quad (9.5)$$

$$M_{n_total} = M_{negative} \times IM \times m \times LF + M_{n_DL} \quad (9.6)$$

where,

IM = dynamic load allowance percent, $IM = 1.33$ (LRFD Table 3.6.2.1-1)

m = multiple presence factor, $m = 1.2$ (LRFD Table 3.6.1.1.2-1)

LF = load combination factor, $LF = 1.75$ for StrengthI limit state, and 1 for Service I limit state (LRFD Table 3.4.1-1)

The multiplier 4 for the positive moment demand due to dead load is to account for the big influence of span length change on critical positive moment demand. This influence, however, does not impact negative moment demand as much. Therefore a multiplier of 1 is used for the negative moment demand due to dead load.

4. For the beam design, use the live load distribution factors provided by AASHTO for cross section I as specified in AASHTO LRFD Table 4.6.2.2.1-1. The dead loads due to beam self-weight, parapet self-weight, and wearing surface self-weight are distributed as mentioned in Step 3.

9.2.2 Further Research

It should be noted that the recommendations provided in this report are based on limited experimental testing by both the authors of this report and investigators at other universities, industry research and development labs at state and federal transportation research labs. The results of this collected research, field experience with existing cast-in-place and precast bridges and sound engineering judgment allow the authors to believe with a reasonable degree of confidence that the construction of a bridge using the provided recommendations will lead to durable bridges that are cost effective and can be constructed using an accelerated schedule.

Given below are a few recommendations for further research that would address some of the limitations of this study, provide actual data on the performance of an SCDOT NEXT-D bridge and expand the selection of shear key materials:

- Test continuity details to produce continuous spans for multi-span bridges.
- Develop generic mix designs for shear key material. This recommendation comes from recognizing that all property characteristics of current UHPCs may not be required for use as a shear key material.
- Test using straight bars extending into the shear key rather than a U-bar.
- Construct a bridge on a low volume roadway and monitor the construction of the bridge and the structural performance under both typical traffic and controlled loading.

References

- AASHTO (2007). *AASHTO LRFD Bridge Design Specification*. American Association of State Highway and Transportation Officials, Washington, DC, 4th edition.
- AASHTO (2012). *AASHTO LRFD Bridge Design Specification*. American Association of State Highway and Transportation Officials, Washington, DC, 5th edition.
- ACI (1974). “Considerations for design of concrete structures subjected to fatigue loading.” *ACI Journal Proceedings*, 71(3).
- ACI (2009). *ACI 550.1R-09: Guide to Emulating Cast-in-Place Detailing for Seismic Design of Precast Concrete Structures*. American Concrete Institute, Farmington Hills, MI (February 2009).
- ACI (2011). *ACI 318-11: Building Code Requirements for Structural Concrete and Commentary*. American Concrete Institute, Farmington Hills, MI.
- Alfano, G. and Crisfield, M. A. (2001). “Finite element interface models for the delamination analysis of laminated composites: mechanical and computational issues.” *International Journal for Numerical Methods in Engineering*, 50(7), 1701–36.
- ANSYS-Inc. (2009). “Ansys academic research, version 12.0.
- ASTM (2004). “Standard test method for tensile strength of concrete surfaces and the bond strength or tensile strength of concrete repair and overlay materials by direct tension (pull-off method).” *Report No. C1583/C1583M-04*, ASTM International, <www.astm.org>.
- ASTM (2007a). “Standard practice for making and curing concrete test specimens in the laboratory.” *Report No. C192/C192M-07*, ASTM International, <www.astm.org>.
- ASTM (2007b). “Standard test method for flow of hydraulic cement mortar.” *Report No. C1437-07*, ASTM International, <www.astm.org>.
- ASTM (2010). “Standard test method for compressive strength of cylindrical concrete specimens.” *Report No. C39/C39M-10*, ASTM International, <www.astm.org>.
- ASTM (2011). “Standard test method for splitting tensile strength of cylindrical concrete specimens.” *Report No. C496/C496M-11*, ASTM International, <www.astm.org>.
- Badie, S. S. and Tadros, M. K. (2008). “Full-depth precast concrete bridge deck panel systems.” *Report No. NCHRP 584*, Transportation Research Board.
- Badwan, I. Z. and Liang, R. Y. (2007). “Performance evaluation of precast posttensioned concrete multibeam deck.” *Journal of Performance of Constructed Facilities*, 21(5), 368–374.
- Barker, R. and Puckett, J. (2007). *Design of Highway Bridges: An LRFD Approach*. John Wiley & Sons, Inc., Hoboken, NJ, 2nd edition.

- Baur, K., Culmo, M., Dillman, B., Lorah, D., and Medlock, R. (2010). "The NEXT Beam: A robust double-tee prestressed beam." *2010 FHWA Bridge Conference* (April).
- Bentley Systems, I. (2012). "LEAP CONSPAN V8i - version 12.
- Bergeron, K. A. (2008). "Leap, not creep: delivery and deployment of vanguard technologies promise to lead the way to faster, safer, better highway construction." *Public Roads* (01/01).
- Big-R-Bridge (2010). "Vehicular bridges for accelerated construction — Big R Bridge, date accessed: May 20, 2010, <<http://www.bigrmfg.com/products/modular/>>.
- Calloway, B. R. (1993). "Yield line analysis of an AASHTO New Jersey parapet wall." Ph.D. thesis, Virginia Polytechnic Institute and State University, Blacksburg, VA.
- Cangiano, S., Meda, A., and Plizzari, G. A. (2009). "Rapid hardening concrete for the construction of a small span bridge." *Construction & Building Materials*, 23(3), 1329–37.
- Cho, A. (2007). "Utah embraces accelerated construction method.." *ENR* (11/05).
- Collins, M. P. and Mitchell, D. (2001). *Prestressed Concrete Structures*. Prentice Hall international series in civil engineering and engineering mechanics. Prentice Hall.
- CSI (2011a). *CSI Analysis Reference Manual*. Computers and Structures, Inc., Berkeley, CA.
- CSI (2011b). "Csi wiki knowledge base, date accessed: 7/10/11., <<https://wiki.csiberkeley.com/display/kb/Home>>.
- CSI (2011c). "SAP2000 Advanced, version 15.
- Culmo, M. P. (2009). "Connection details for prefabricated bridge elements and systems." *Report no.*, Federal Highway Administration.
- Culmo, M. P. and Seraderian, R. (2010). "Personal communication, september 1, 2010.
- Deery, D. P. (2010). "Investigation of northeast extreme tee (NEXT) D beam bridges as an alternative to precast hollow core bridges: An exploration of appropriate slab design forces." M.S. thesis, Clemson University, Clemson, SC.
- El-Remaily, A., Tadros, M. K., Yamane, T., and Krause, G. (1996). "Transverse design of adjacent precast prestressed concrete box girder bridges." *PCI Journal*, 41(4), 96–113.
- ERICO (2010). "Lenton Interlok, date accessed: 5/5/10, <<http://www.erico.com/products/InterLock.asp>>.
- FHWA (2011). "General guidelines for refined analysis of deck slabs, date accessed: 11/17/11., <<http://www.fhwa.dot.gov/bridge/lrfd/pscusappb.htm>>.
- Flores-Duron, A. (2011). "Behavior of the NEXT-D beam shear key: A finite element approach." M.S. thesis, Clemson University, Clemson, SC.
- Fu, C. C. and Jeong, S. (2009). "Behavior and analysis of an instrumented slab bridge." *Report no.*, University of Maryland.
- Gordon, J. E. (1991). *The New Science of Strong Materials or Why You Don't Fall through the Floor*. Princeton University Press, Princeton, NJ.
- Grace, N. F. and Jensen, E. (2008). "Use of unbonded cfcc for transverse post-tensioning of side-by-side box-beam bridges." *Report No. Research Report RC-1509*, Michigan Department of Transportation.

- Graybeal, B. A. (2006). "Material property characterization of ultra-high performance concrete." *Report No. FHWA-HRT-06-103*, Federal Highway Administration.
- Graybeal, B. A. (2007). "Compressive behavior of ultra-high-performance fiber-reinforced concrete." *ACI Materials Journal*, 104(2), 146–152.
- Graybeal, B. A. (2010a). "Behavior of field-cast ultra-high performance concrete bridge deck connections under cyclic and static structural loading." *Report No. FHWA-HRT-11-023*, Federal Highway Administration.
- Graybeal, B. A. (2010b). "Behavior of ultra-high performance concrete connections between precast bridge deck elements." *2010 Concrete Bridge Conference: Achieving Safe, Smart & Sustainable Bridges*.
- Graybeal, B. A. and Hartmann, J. L. (2003). "Ultra-high performance concrete material properties." *Transportation Research Board Conference*, 2.
- Hartle, R. A. (2009). "I-70 overpass beam failure - Lakeview Drive bridge." *Ohio Bridge Conference*.
- Hlavacs, G. M., Long, T., Miller, R. A., and Baseheart, T. M. (1996). "Nondestructive determination of response of shear keys to environmental and structural cyclic loading." *Transportation Research Record*, 1574, 18–24.
- Hsu, T. T. C. (1993). *Unified Theory for Reinforced Concrete*. CRC Press, Inc., Boca Raton, FL.
- Huckelbridge Jr., A. A., El-Esnawi, H., and Moses, F. (1995). "Shear key performance in multibeam box girder bridges." *Journal of Performance of Constructed Facilities*, 9(4), 271–285.
- Jansson, P. O. (2008). "Evaluation of grout-filled mechanical splices for precast concrete construction." *Report No. R-1512*, Michigan Department of Transportation (May 2008).
- Jones, L. H. (2010). "Inspection methods & techniques to determine non visible corrosion of prestressing strands in concrete bridge components." M.S. thesis, Lehigh University, Bethlehem, PA.
- Julander, J. L. (2009). "Finite element modeling of full depth precast concrete transverse bridge deck connections." M.S. thesis, Utah State University, Logan, UT.
- Kim, J.-H. J., Jin, W. N., Ho, J. K., Jae, H. K., Sung, B. K., and Keun, J. B. (2008). "Overview and applications of precast, prestressed concrete adjacent box-beam bridges in South Korea." *PCI Journal*, 53(4), 83–107.
- Konda, T. F., Klaiber, F. W., Wipf, T. J., and Schoellen, T. P. (2007). "Precast modified beam-in-slab bridge system an alternative replacement for low-volume roads." *Transportation Research Record*, 1(1989), 335–346.
- Lall, J., Alampalli, S., and DiCocco, E. F. (1998). "Performance of full-depth shear keys in adjacent prestressed box beam bridges." *PCI Journal*, 43(2), 72–79.
- Miller, R. A., Hlavacs, G. M., Long, T., and Greuel, A. (1999). "Full-scale testing of shear keys for adjacent box girder bridges." *PCI Journal*, 44(6), 80–90.
- MoDOT (2010). "Bridge standard drawings for the Missouri Department of Transportation, date accessed: 5/5/2010, <http://www.modot.mo.gov/business/consultant_resources/bridgestandards.htm>. id: 1.
- Nims, D. K. and Devabahktuni, V. (2011). "Magnetic sensor for nondestructive evaluation of deteriorated prestressing strand." *Report No. UTUTC-IU-12*, University of Toledo University Transportation Center.

- NYSDOT (2010a). “Bridge detail sheets, date accessed: 10/25/2010, <<https://www.dot.ny.gov/main/business-center/engineering/cadd-info/drawings>>.
- NYSDOT (2010b). *NYSDOT Design Manual - Chapter 3 - Deck Systems*. New York State Department of Transportation, New York.
- ODOT (2010). “Standard bridge drawings for the Ohio Department of Transportation, date accessed: 5/5/2010., <<http://www.dot.state.oh.us/Divisions/HighwayOps/Structures/standard/Bridges/Pages/StandardBridgeDrawings.aspx>>.
- Oesterle, R. G. and Elremaily, A. F. (2009). “Design and construction guidelines for long-span decked precast, prestressed concrete girder bridges.” *Report No. NCHRP 12-69*, National Cooperative Highway Research Program.
- PCINE (2010). “PCI Northeast: Northeast extreme tee (NEXT) beam, date accessed: 6/1/2010., <http://pcine.org/index.cfm/resources/bridge/Northeast_Extreme_Tee_Beam>.
- PennDOT (2006). “Adaption to presentation to AASHTO T-18 Committee to inform other states of the SR 1014 over I-70 beam collapse, date accessed: 6/1/10., <<http://design.transportation.org/Documents/Scott,Non-compositeAdjacentBoxBeamBridges,Region1.ppt>>.
- Perry, V. and Royce, M. (2010). “Innovative field-cast UHPC joints for precast bridge decks (full-depth precast deck panels), Oneonta, NY-Design, prototype testing and construction.” *2010 Concrete Bridge Conference: Achieving Safe, Smart & Sustainable Bridges*.
- Ralls, M. L., Tang, B., Bhid, S., Calvert, E., Capers, H., Dorgan, D., Matsumoto, E., Napier, C., Nickas, W., and Russell, H. (2005). “Prefabricated bridge elements and systems in Japan and Europe.” *Report No. FHWA-PL-05-003*, Federal Highway Administration.
- Roscoe-Bridge (2010). “County vehicular bridges - Roscoe Bridge - vehicle, trail, and pedestrian bridges, date accessed: 5/5/2010., <<http://www.roscoebridge.com/?a=12&b=county-vehicular-bridges>>.
- Russell, H. G. (2009). “Adjacent precast concrete box beam bridges: Connection details.” *Report No. NCHRP 393*, Transportation Research Board.
- Saadeghvaziri, M. A., Yin, L., and Spillers, W. R. (2006). “Development of high performance continuity connection using CFRP composites.” *2006 ASCE Structures Congress*, Washington, DC, Federal Highway Administration.
- Sawyer, H. A. (1964). “Design of concrete frames for two failure states.” *Proc., Int. Symposium on the Flexural Mechanics of Reinforced Concrete, ASCE-ACI*, 405–431.
- SCDOT (2006). *Bridge Design Manual*. South Carolina Department of Transportation, Columbia, SC.
- SCDOT (2010). “Bridge standard drawings - South Carolina Department of Transportation, date accessed: 5/11/2010., <http://www.scdot.org/doing/sd_Book.aspx>.
- Skogman, B. C., Tadros, M. K., and Grasmick, R. (1988). “Ductility of reinforced and prestressed concrete flexural members.” *PCI Journal*, 33(6), 94–107.
- Tastani, S. P. and Pantazopoulou, S. J. (2002). “Experimental evaluation of the direct tension-pullout bond test.” *Bond in Concrete from Research to Standards*.

TXDOT (2009). *Texas Department of Transportation Bridge Design Manual - LRFD*. Texas Department of Transportation, Austin, TX.

TxDOT (2010). “Bridge standards (English), date accessed: 5/5/2010., <<http://www.txdot.gov/insdot/orgchart/cmd/cserve/standard/bridge-e.htm>>.

WSDOT (2010). “Bridge standard drawings - Washington State Department of Transportation, date accessed: 5/11/2010., <<http://www.wsdot.wa.gov/eesc/bridge/drawings/>>.

This page intentionally left blank

Appendices

This page intentionally left blank

Appendix A

Department of Transportation Web Survey

Survey of Adjacent Beam Bridge Design and Construction Practices

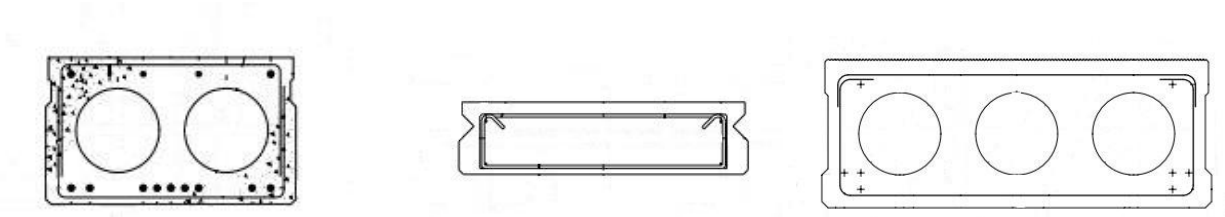
We are researching improved methods of accelerated bridge construction for short span bridges for the South Carolina Department of Transportation. Our goal in utilizing this survey is to gather construction and performance information about precast adjacent beam bridges. We aim to minimize cracking along the longitudinal joints of the bridge and create continuity details over interior bents. The survey will inquire about the design and erection of your adjacent beam members and the experienced performance of these bridges. By gathering this information from other DOTs, we hope to produce a standard with improved shear key and continuity performance that may be used on higher ADT roads.

In return for helping us gather information on these systems, we will send you a summary report of our findings from the survey.

What State are you representing? _____

Low Profile Adjacent Beam (LPAB) Bridges: Voided Slab/Hollow Core/Deck Beams/Solid Slab (sections and pictures shown below)

LPAB Sections:



Hollow Core:



**** If you do not use low profile adjacent beam (LPAB) bridges, please skip to part B.**

General:

How long have you been using LPAB bridges?

- Past 2 years
- Past 5 years
- Past 10 years
- Past 20 years
- Past 50 years

About how many LPAB bridges have you built in the past 10 years?

- 5 or less
- 6 to 10
- 11 to 20
- 21 to 50
- More than 50

What is the maximum span of your LPAB bridges?

- 20 feet or less
- 21 to 25 feet
- 26 to 30 feet
- 31 to 40 feet
- More than 40 feet

Are the LPAB bridge details available on your website the most current plans?

- Yes
- No

Website: _____

Do you limit the use of LPAB bridges to a particular ADT?

- Yes
 - What is the maximum ADT for use?
 - Less than or equal to 1500
 - Less than or equal to 3000
 - Less than or equal to 5000
 - Less than or equal to 10,000
 - More than 10,000
- No

Do you permit using LPAB bridges on the National Highway System?

- Yes No

Have you had any recent major changes to the standards for this bridge type?

- Yes No

What were the major design/construction changes?

Has there been noticeable improvement in performance after the changes were implemented?

- Yes No Too early to tell

Construction:

What is the average time needed to erect one span of a LPAB bridge?

- Less than 1 week
 1 to 2 weeks
 2 to 3 weeks
 3 to 4 weeks
 More than 4 weeks

What workforce constructs these bridges?

- In house
 Contractor
 Both

Post-Tensioning:

When do you apply the post-tensioning force to the bridge?

- After grouting the shear keys
 Before grouting the shear keys
 Contractor's Preference

What post-tensioning material do you use?

- Strands Rods Contractor's Preference

Do you have a target contact stress for post-tensioning?

- Yes: _____ kips/ft² No

Grouting/Shear Key:

What depth are the shear keys?

- Partial Depth Full Depth

Where are the shear keys located?

- Near the top face of the member
 At the center of gravity of the member

What type of grout is used in the longitudinal shear keys?

- Non-shrink Epoxy Cast-in-place concrete
 Other: _____

Do you require a concrete overlay on the LPAB bridge members?

- Yes
- Is the overlay reinforced?
 Yes No
- No
- Is an asphalt overlay required?
 Yes No
 - Do you provide waterproofing?
 Yes No

Have you tried placing mild reinforcing steel transversely through the shear key?

- Yes No

Do you use any other method of shear transfer (other than mild reinforcing or shear key)?

- Yes: _____
 No

About what percentage of these bridges experience longitudinal reflective cracking along the shear keys?

- 0 to 20%
 21 to 40%
 41 to 60%
 61 to 80%
 81 to 100%

Do these cracks occur more in bridges with an ADT over 3000?

- Yes No

On the scale below, identify how concerned you are about these cracks distressing the bridge.

(Not concerned) 1 2 3 4 5 6 7 8 9 10 (Very concerned)

Longitudinal Continuity:

Do you ever make your multi-span LPAB bridges longitudinally continuous?

- Yes No

- Do you account for positive restraint moments when designing continuity diaphragms?

- Yes No

- If yes, what is the average girder age when continuity is established?

- 7 days or less
- 8 to 24 days
- 25 to 90 days
- Greater than 90 days
- Not Considered

Alternative:

Do you have an alternative system for this bridge type that is considered rapid construction?

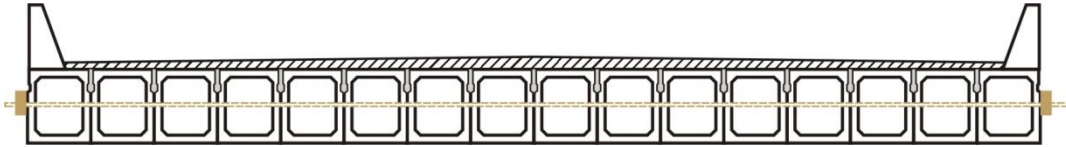
- Yes: _____
 No

Are there any other alternative systems that you are interested in?

- Yes: _____
 No

High Profile Adjacent Beam (HPAB) Bridges: Box Beams

HPAB Section:



*** If you do not use high profile adjacent beam (HPAB) bridges, please skip to part C.*

General:

How long have you been using HPAB bridges?

- Past 2 years
- Past 5 years
- Past 10 years
- Past 20 years
- Past 50 years

About how many HPAB bridges have you built in the past 10 years?

- 5 or less
- 6 to 10
- 11 to 20
- 21 to 50
- More than 50

What is the maximum span of your HPAB bridges?

- 20 feet or less
- 21 to 25 feet
- 26 to 30 feet
- 31 to 40 feet
- More than 40 feet

Are the HPAB bridge details available on your website the most current plans?

- Yes No

Website: _____

Do you limit the use of HPAB bridges to a particular ADT?

- Yes

What is the maximum ADT for use?

- Less than or equal to 1500
 Less than or equal to 3000
 Less than or equal to 5000
 Less than or equal to 10,000
 More than 10,000

- No

Do you permit using HPAB bridges on the National Highway System?

- Yes No

Have you had any recent major changes to the standards for this bridge type?

- Yes No

What were the major design/construction changes?

Has there been noticeable improvement in performance after the changes were implemented?

- Yes No Too early to tell

Construction:

What is the average time needed to erect one span of a HPAB bridge?

- Less than 1 week
 1 to 2 weeks
 2 to 3 weeks
 3 to 4 weeks
 More than 4 weeks

What workforce constructs these bridges?

- In house
- Contractor
- Both

Post-Tensioning:

When do you apply the post-tensioning force to the bridge?

- After grouting the shear keys
- Before grouting the shear keys
- Contractor's Preference

What post-tensioning material do you use?

- Strands
- Rods
- Contractor's Preference

Do you have a target contact stress for post-tensioning?

- Yes: _____ kips/ft²
- No

Grouting/Shear Key:

What depth are the shear keys?

- Partial Depth
- Full Depth

Where are the shear keys located?

- Near the top face of the member
- At the center of gravity of the member

What type of grout is used in the longitudinal shear keys?

- Non-shrink
- Epoxy
- Cast-in-place concrete
- Other: _____

Do you require a concrete overlay on the HPAB bridge members?

- Yes

Is the overlay reinforced?

- Yes
- No
- No

Is an asphalt overlay required?

- Yes No

Do you provide waterproofing?

- Yes No

Have you tried placing mild reinforcing steel transversely through the shear key?

- Yes No

Do you use any other method of shear transfer (other than mild reinforcing or shear key)?

Yes: _____

- No

About what percentage of these bridges experience longitudinal reflective cracking along the shear keys?

- 0 to 20%
 21 to 40%
 41 to 60%
 61 to 80%
 81 to 100%

Do these cracks occur more in bridges with an ADT over 3000?

- Yes No

On the scale below, identify how concerned you are about these cracks distressing the bridge.

(Not concerned) 1 2 3 4 5 6 7 8 9 10 (Very concerned)

Longitudinal Continuity:

Do you ever make your multi-span HPAB bridges longitudinally continuous?

- Yes No

Do you account for positive restraint moments when designing continuity diaphragms?

- Yes No

If yes, what is the average girder age when continuity is established?

- 7 days or less
 8 to 24 days
 25 to 90 days

- Greater than 90 days
- Not Considered

Alternative:

Do you have an alternative system for this bridge type that is considered rapid construction?

- Yes: _____
- No

Are there any other alternative systems that you are interested in?

- Yes: _____
- No

C. Alternatives

*** If you skipped parts A & B (you do not use low or high profile adjacent beam bridges) please complete this section. Otherwise, please skip to Part D.*

Do you have an alternative system for these bridge types that is considered rapid construction?

- Yes: _____
- No

Are there any other alternative systems that you are interested in?

- Yes: _____
- No

D. Follow Up

- Information:

Name: _____

State: _____

Position: _____

Phone: _____

E-mail: _____

- Is it OK to call you for a follow-up conversation?

- Yes
- No

- Would you like to have the results of this survey sent to you?

- Yes
- No

This page intentionally left blank

Appendix B

Phone Interview Transcripts

B.1 Phone Interview with Thomas Domagalski

Engineer of Bridge Design of the Illinois Department of Transportation
By Sara Roberts, Clemson University
Date: Wednesday March 24th, 2010
Time: 4:15 PM EST

Follow up questions for survey of adjacent box beam bridges.

S: You said you changed the keyway design recently. What kind of changes did you make to it?

T: We made it bigger. Wider and deeper.

S: Why did you make this change?

T: Well the shear key, they pour grout in there. We didn't think it was wide enough so they could vibrate it. So we made it wide enough so they could use a pencil vibrator to make sure it's mixed up really well and well distributed throughout the whole shear key.

S: What was the purpose for thickening the bottom slab of the member?

T: We wanted to get more clearance on the strands underneath. We were at one inch and we thickened it a half inch so we could have a half inch more cover for the prestressing strands.

S: Why don't you have a target post tensioning force?

T: We didn't think we needed one. I guess we looked at various other states and a lot of other states didn't have a force there so. And also, when you put these beams together, if you're on a skew, your transverse ties can only tie two beams together because we put them at right angles. That would be a lot of extra field work if we did a post tensioning force at location on every beam we installed. So we decided against it.

S: On the survey you said you had a 1 - 2 week erection time per span. Does that include curing of the concrete overlay you require?

T: No. The overlay would need to cure for about 4 to 7 days.

S: How thick do you usually make your concrete overlay?

T: We usually put a 5" overlay on ours. It's reinforced with a rebar mat: #5 at 12" centers in both directions. So that prevents some reflective cracking coming up if the shear key does start moving

differently.

S: Do you have any alternative system you would like to try or that you heard may be better?

T: Well there's a lot of ideas out there. Nebraska wants to actually pour a real wide shear key and try to post tension the tops of the slabs. It just gets into a thing of ease of construction. We don't think we're going to get a lot more cracks coming up though there, there's a possibility but it's something that we can live with. We have epoxy coated bars in the overlay, so we're not really worried there's going to be a lot of deterioration.

S: Does your DOT have an interest in rapid construction since you have a shorter season to build?

T: We're not looking at accelerated construction in the sense of the national effort of building bridges off the road way and then rolling them in. That's what we consider rapid construction and we're not interested in that. Our precast box beam bridges that we put up, that's pretty fast. We're pretty well satisfied with the time of construction for those.

B.2 Phone Interview with Julius Volgyi

Assistant State Structure & Bridge Engineer of the Virginia Department of Transportation
By Sara Roberts, Clemson University
Date: Wednesday March 24th, 2010
Time: 10:00 PM EST

Follow up questions for survey of adjacent box beam bridges.

S: Why do you construct so few low profile box beams?

V: There's basically very few places we use them right now. The second thing is the joint material has not been the greatest. Most of these we don't have a concrete slab on top, we have an asphalt surface. When we do get cracks we get intrusion of the salt water, and we don't keep the vent holes open so that garbage collects in there so it's been a maintenance nuisance and headache all the way around. So we typically do not recommend their use but every once in a while they may have a use for it.

S: So the voided slabs perform better in this area?

V: Yeah, I think so. But the limit on those is about a 45 foot span so if you need a longer span you need to look at some of the alternatives.

S: You said the box beam details you have online aren't the most current. Do you have the most current details available anywhere we could look at?

V: Not the box beams, but for the other stuff we have PDFs? Standards for the joints and that kind of stuff. Those are on our website if you look under VDOT and the structural bridge division for manuals you'll see the volume 5 series. If you go to volume parts 4 and 5 you should find them in there.

S: You said you don't usually use a concrete overlay on your beams. Do you ever use a concrete overlay or do you just always use the asphalt?

V: I think there's only 2 or 3 projects that I know of where someone actually put a slab on top, a 4.5 or 5 inch slab.

S: Do you know how much that extends the construction time for the bridge?

V: The slab has to stand up to 28 days before it gets its strength and before you can release it to traffic, so I would say at least a good month.

S: How did you select your post tensioning contact stress?

V: That I don't know. It was kind of a handed down number and I'm not sure where they borrowed that detail from. Right off hand I don't know.

S: Has the reflective cracking been a setback or hindrance when choosing this type of bridge?

V: Definitely.

S: You said you have a full depth shear key on the hollow core beams. Has that been a help at all in comparison to having just a partial depth shear key?

V: That I don't know. That joint detail has only been out for about 10 years or so, so time will tell if the joint is any better or not.

S: Why do you not make the bridges continuous?

V: That's just our preference.

S: Have you ever had a need to make them continuous?

V: No because these are typically on small secondary projects on single span type structures and there's probably no need to make them continuous.

S: Do you have any alternatives you think would be better so you wouldn't have to worry about the longitudinal cracking? Any other short span systems?

V: Not off hand no.

S: So you don't have any you think you would like to try?

V: Nope.

B.3 Phone Interview with Suresh Patel

Senior Structural Engineer of the Missouri Department of Transportation

By Sara Roberts, Clemson University

Date: Thursday March 25th, 2010

Time: 3:45 PM EST

Follow up questions for survey of adjacent box beam bridges.

S: Why does your DOT build such a low number of low profile box beams?

P: The problem is the maintenance. In the history, you may not have problem in South Carolina, but in Missouri that is the main problem because of the salted waters that run through. Constant cracks happen even if you have a deck or asphalt surface on the top. As time pass, it will crack and water leaks through and then it will rust. Sometimes we use it if there is a time requirement and it is economical, usually with a 6" concrete top surface. These days we are thinking of using more though, bridge research is doing research now.

S: Does the 1 -2 week construction time for one span include the curing of the concrete overlay?

P: No that is not considered in that, that requires more time to reach the concrete compressive strength. That time is just for getting the box beams put into place and grouted.

S: Why don't you have a standard target post tensioning force?

P: We do not post tension, we generally use rods and tighten them enough to close the gap at the bottom.

S: What is the usual thickness for your concrete overlay?

P: 5.5", some cases we may have asphalt surface if it is low ADT.

S: Do you think there's a specific reason such a small percentage of your bridges show longitudinal cracking? Do you think you have a better system?

P: No, like I said we do not have that big of a history. Like some states have been using for a long time, but we do not have that many bridges built in the last several years and we have not experienced that problem yet. That doesn't mean we won't. Like as time passes, maybe they have longer time than us. And it depends on what day. Sometimes it's the spans, sometimes it's the ADT, or the temperature, it's so many things involved in that. I do not know if other states have the same top surface, so it's hard to compare.

S: Can you give me an overview of the system you use to create the continuity?

P: That one we generally have a pour, like our prestressed beam girder. We bend the strands from both beams and we put the rebar in the transverse direction and then we pour the concrete. Just like a diaphragm for a prestressed beam girder.

S: Have you ever used any other sort of continuity details or looked into newer methods?

P: No I have heard of any changes. We have not had any problems. Most of our bridges are prestressed I girder and it's working for those and it is working for this beam also. Sometimes it may be complicated to insert those tie bars because of the skew or the grade difference, so we may have to have a little bit wider gap. When you have a greater than twenty-five degree skew it may be hard to install.

S: Pouring this continuity diaphragm, about how long does it extend the time of construction for the bridge?

P: That I do not know. Maybe a week or two, generally it does not hold the whole bridge construction that long.

S: So it doesn't significantly extend the time?

P: Not much. By the time you do other things. It's not that's the only thing you have to do at that time. It's difficult to separate the time just for that activity.

S: What method do you use to estimate the positive moment restraints when designing the diaphragm?

P: Depends on the strand requirements and you use that for your hand calculations. Determining how many strands need to be bended based on the moment connection.

S: The research group I'm working with is a little confused on what the positive moment restraints are and how they affect the design. Can you help us at all with that?

P: That I may have to think about. But, like I said it should be just like our prestressed I girder. Maybe you may need 30 total strands, but not all of those strands need to be bended, that is the calculation, to determine how many need to be bended and the rest need to be trimmed or cut to create that moment connection.

S: You said in the survey that the average girder age you use is 25 to 90 days before you establish continuity. Does having to wait for that prolong the construction time also?

P: That I am not sure.

S: Have you experienced any cracking around the diaphragms?

P: No. I'm not aware of any cracking at the diaphragm location. But the box beams usually require more shear reinforcement at the end. You do not need, but for the bonding, we put about 3 or 4 inch spacing at the end. Those kind of cracks we have had before without that shear reinforcement.

S: Do you have any alternative systems you would like to try rather than using these box beams?

P: If there is something economically good then we will do. If you find something and send me the report then we may try that. But I doubt, I have not seen anything where the reliability remains consistent. This system is good, but if there is something better economically or feasible to do quickly, we will use it. But I'm not aware of any.

B.4 Phone Interview with Tim Keller

State Bridge Engineer of the Ohio Department of Transportation

By Sara Roberts, Clemson University

Date: Tuesday March 30th, 2010

Time: 2:15 PM EST

Follow up questions for survey of adjacent box beam bridges.

S: What's the reason that your DOT constructs so few low profile box beams?

T: I want to make sure I know the definition of low profile box beams? Non-voided boxes?

S: They can be voided, but generally less than two feet in thickness and the high profile box beams were thicker sections.

T: OK. Generally it's a span length issue, for those span lengths we would tend to use a different structure. Bottom line is economy, those don't do well in this state. Economically they can't compete.

S: What do you use instead?

T: You're generally talking about a 20-30 foot span length, we will use a three sided culvert or a slab bridge. Most of the time a three sided culvert.

S: The slab bridge is just cast-in-place concrete?

T: Yes.

S: You said in the low profile box beams, you have used waterproofing under asphalt before. Has that been effective in keeping water out or have you had problems with it?

T: Problems. It has not been effective.

S: For all of your box beams, you said you don't use them on the NHS and not on high ADT roads, what is your reasoning for doing that?

T: Because we have not gotten good performance out of them.

S: And is that mainly due to shear key problems or is something else that is a problem?

T: The problem is, and it's all kinda interrelated, the shear keys don't hold up and they leak. The membranes aren't holding up or aren't installed properly, or all of the above, and joints are leaking and deteriorating the boxes at the joints. So the issue were having because they're not performing well when we put them on an NHS system that traditionally high ADTs and high ADTTs, when we go in to work on those, we create real maintenance and MOT nightmares. So it hurts when I do that. So because of the performance of this structure type and putting them on high ADT and ADTT routes, it just doesn't make any sense.

S: The post tensioning force you said on the survey was a contact stress of 75 to 100 psi, how did you decide on that number?

T: Ok I forget what the question was, was the question what we're currently doing or what we want to do?

S: I think it was what your currently doing.

T: Ok what we're currently doing is putting tie rods between them and just tightening them up. There's no requirement. To call it post tensioning transversely right now would be not correct. There's very little load on those tie rods. Now what we're proposing to do, and we've done about half a dozen of these, and these are not on the low profile they're on our deeper box, is to transversely post tension the box together. And the reason we're doing that is to get the performance out of the structure type. So we've done a handful of them and we have another handful of them in place, and the question is how much post tensioning should you put in to achieve the performance. The only area that has any specification that even remotely resembles what we're doing is the segmental box, and to get 200 psi across the gross cross sectional area of a prestressed box beam is possible but it's not really economical. To put that much post tensioning in, you need a lot of ducts and a lot of pt. So the question is what should that be. Well we try to get about 100 psi across the gross cross sectional area, that gets closer to what we traditionally used as far as number of diaphragms. It's still more than we have used, but it's getting somewhere down to what I think is a reasonable amount. Even then we still struggle with some of the deeper boxes to get 100. We've usually gotten somewhere about 90 psi on those. It really comes down to... yes you can get 200 but I don't think you need 200. The work we've done so far shows you really don't need 200, and 100 is probably a better target.

S: The 1 week erection time you said on the survey, does that include the curing of the concrete overlay when you use one?

T: No. For an asphalt one you can get them put in in a week, but once you go to the concrete no.

S: About how much time does that add on?

T: About 2 weeks depending on the structure type and what kind of railing you have. If you're using a metal railing, it adds about two weeks because you can install the railing in the second week of cure time. Generally we can get strength in those two weeks to put traffic on it, but generally we still have to put a concrete barrier if we're using one and you still have to stripe it.

S: Now you guys use some continuity diaphragms with your box beams?

T: At piers?

S: Yes. What method do you use to calculate the positive moment restraints?

T: We have a standard detail for all our boxes so we don't design it. We had some research done for us to determine how much continuity steel we should be using. So we use the same detail on all our designs. And I have no idea how they got to that I'd have to go back to the research and dig it up.

S: Did they research within the DOT or did they have an institution do it?

T: University of Cincinnati did the work for us: Dr. Rick Miller.

S: The continuity diaphragm, does that severely extend the time of construction?

T: It depends. If it's an asphalt wearing surface, which I'm not a big fan of at all, then yes it does extend it. If it's a concrete overlay, not that much, some but not as much as you'd think. Most of them have been asking to pour that with the deck. We generally don't like doing that, we generally require that to be poured separate, but occasionally depending on the situation we might pour it with the deck.

S: Have you experienced any cracking on the continuity diaphragm?

T: Oh yes.

S: Just like transverse cracks across the bridge?

T: We've seen a lot of different types of cracking there. Now what we have done, we've kind of changed our process in our load rating analysis. When we do an analysis to run our permit vehicles across, we do that analysis based on simple span. We do not use continuity for live load. So if it cracks and is behaving as simple span it works, so we're probably a little unique there.

S: Are there any other different continuity details you have heard of or would like to try?

T: I don't know, I don't know what's out there. The more reinforcing you put in there, the wider your pier caps have to be so you're trying balancing two things out: need for more room between the beams to get more reinforcing steel in and the width of your pier caps. The continuity diaphragms have not been a real problem for us. The biggest issue I'm having is shear keys and the leaking joints, and we just have a nightmare in front of us we have to deal with now. Those bridges were really a 25 year then you throw the beams away put new beams in, we'll we just can't afford that. We have an inventory of almost 5,000 of these bridges in the state and we just can't afford to build bridges for 25 years and then throw them away. So something's got to change.

S: Are there any new or innovative systems you have heard of or would like to try? Or would think might work?

T: Well I really thing the transverse post tensioning will work and will give us a viable structure type. That's where we're at. There was some discussion of moving the shear keys down and revising the shear key detail. The research we had Dr. Miller do with shear keys, it's a temperature problem with those shear keys, they're cracked before the load's every put on them. I just don't believe that the shear keys are gonna hold up unless we put a compressive load across them.

Dr. Miller has done a lot of work for us and he's extremely knowledgeable about the whole issue. You're more than welcome to give him a call and use my name and say I told you I could call him.

S: Since you're in a cold climate, do you have any interest in rapid construction since you have a shorter construction period during the year?

T: The answer is sure, but it's got nothing to do with the winters around here. It really has to do with the amount of volume we have on our roadways. When we close a high ADT road way, we create all kind of backlog. So our challenge isn't because of weather, it's because of the volume of vehicles we have on some of our routes. It puts a real challenge in place.

The bigger challenge is... It's not about how fast you do it, though sometimes it is. If you're doing a five mile stretch of four lane divided highway, and the bridge is on critical path for two months, I need that bridge done in two months, I don't need it done in two weeks. So the challenge is identifying how long that structure is on critical path. Now if it's a standalone bridge where the bridge is on critical path the whole time, then it's how fast can you get it done. So if you need the bridge done in a week, you can do that, it costs you more, so it needs to be a location where it makes sense. The challenge isn't the technology to get it done, because there's plenty of technology out there, the challenge is: 'what's my target?.'

B.5 Phone Interview with Terry Frake and Steve Beck

Engineer of Structural Design of the Michigan Department of Transportation

By Sara Roberts, Clemson University

Date: Tuesday April 6th, 2010

Time: 4:00 PM EST

Follow up questions for survey of adjacent box beam bridges.

B: We have a long long history with box beams and in the early days they were pretty bad so our maintenance force to this day are pretty much against them. But we used them without post tensioning, without a concrete overlay, with bituminous and cardboard forms and they were very bad. It's very hard for them to separate old news from new news. If you talked to one of our maintenance guys right now, they would contend that even our new system isn't so good. So, even with ourselves we do have some argument. We find that they can get us out of a lot of problems with underclearance and we have a new system that's not so bad, although we ourselves are looking at changing our post tensioning scheme to be better.

S: About how many have you built in the last 10 years?

B: Lots and lots. Typically in Michigan our first choice is prestressed I beams, our next choice would be the box beams. We've built plenty of these, both side-by-side and spread.

F: Sometimes we're forced into box beam design if we have underclearance issues because we can get by using a shallower superstructure using boxes than with I beams.

S: The details for these you have on your website, are these the most current?

B: Yes

S: Do you limit them on high ADT roads or on the NHS?

B: No, we'll use them anywhere.

S: About how long does it take to erect your box beams?

B: I'd have to check with our construction guys, there's nothing really special about them.

S: Do you always use a concrete overlay on top?

B: Yes. Lower governments occasionally use asphalt by itself, but we never use anything but concrete.

S: What is your average thickness for that overlay?

B: 6 inch overlay.

S: Do you have a target contact stress between the boxes for transverse post tensioning?

B: Actually we didn't and we just did a research project on it and now we do but I don't have the numbers on me. We're having a flux on this. It more or less was by empirical means in the past. But we just did a giant research project on increasing the force tremendously by numbers of location and by total force in the post tensioning. We have not adopted that at this point, but I can give you better numbers when we do.

S: Do you grout the shear keys before or after post tensioning?

B: We grout them before.

S: Have you used any other method of shear transfer other than shear keys or using an overlay?

B: No. But this research project that I'm alluding to, they criticized that our shear keys were very shallow, so we're going to more of a full depth shear key. But we've not used any other method.

S: So you're thinking about increasing the shear key depth?

B: Yes. What's really kept us from adopting this is right now the post tensioning can be done by Joe's post tensioning and garage door openers, and we've been scared by some people that we're asking them to really get into the business. Now, that's not going to prevent us, but we've had a little bit of cold feet. I don't know how true this is but sometimes contractors worry you about things that they just need to be tugged into doing.

S: About how many of your box beams experience longitudinal reflective cracking through the deck at the joints?

B: I'm not really sure. That's what first caused this. First we saw them on skews and our maintenance people tell us we are seeing some longitudinal cracking from our post tensioning. 25%.

S: So you feel like it's not a real big problem?

B: Well unfortunately you're talking to a designer and we're akin to being able to put anything on paper. It's gotten us out of certain situations and our modern designs are so much better that I'm going to tell you it's worth the trouble that it causes, but I wouldn't say that's a universal undoubted opinion.

S: Have you ever made your bridges continuous between spans?

B: Yes, we do that continuous for live load. The boxes themselves are designed simple spans and then we'll do the deck itself for live load.

S: Do you know of any good alternatives to box beams that would work well and get rid of the cracking problem?

B: We have looked at, we haven't done much with them, there are some alternate I beam shapes that kinda mimic the box beams, at least section modulus wise. I know other states use tubs and whatnot. We're kinda anti-steel here because the paint system tends to cost more, but certainly a steel section can get you anything you want.

S: I read a research paper from your DOT about using grout filled mechanical splices on your bridges. Do you use those commonly?

B: Grout filled mechanical splices? I would not say commonly.

S: I think it was about connecting continuity rebar.

B: Oh, I see. We have not used those. If we were to go to true continuity we would use some type of continuous cable through it and we'd splice it.

F: I'll tell you that we are in the process of going through our most recent call for research projects, and we have had some younger design engineers who've come into the department the last five years or so that have extensive design. They've looked at the design of in their college days and they question why MDOT doesn't use more of them. So, we've got some ideas right now for research projects we've been trying to get going to see if our old ingrained biases are still valid or maybe we need to work harder and change some minds. Because, we don't want to limit their usefulness in certain situations. We're looking at it but it's a slow process.

B.6 Phone Interview with John Holt

Texas Department of Transportation
By Daniel Deery, Clemson University
Date: Monday March 29th, 2010

Follow up questions for survey of adjacent box beam bridges.

D: Do you ever use a concrete or asphalt overlay on your adjacent box beam bridges?

H: Yes we use both on the adjacent box beams.

D: Does the erection time you listed in the survey account for curing of the concrete overlay?

H: What time did I list for the erection time?

D: Less than a week.

H: That would not include curing of the concrete deck.

D: Is there a particular reason you do not have a target post-tensioning force?

H: That is something that has evolved over the years through trial and error. We now have more than we've ever had which is 1 tendon every 5 or 10 feet or so at 31 kips initial tension. It seems to be working okay.

D: How do you account for shear transfer for the LPAB bridges? Do you use a shear key or a reinforced concrete topping or something else?

H: We have a pretty robust concrete shear key. The sides of our beams are not vertical like a PCI box, years ago when they were developed they had a side face like an AASHTO I beam, and we get pretty good lock up and it seems to be adequate with the post-tensioning we use. We only use post-tensioning when we are topping the boxes with an asphalt concrete pavement. When we have the concrete deck on it that is 5" thick we do not use post-tensioning and probably 99% of the time we are not using the asphalt and post-tensioning system, it is just a concrete deck the vast majority of the time. Those seem to be holding up pretty good.

D: Has the longitudinal relative cracking been a setback or hindrance with these types of bridges? We had a question about how many bridges experience this type of cracking issue...

H: Not since we have gone to a 5" deck, it has not been a problem.

D: So that has not been a concern or hindrance with using these bridges?

H: No, not now.

D: Is there a particular reason you do not make these bridges continuous? Would it prolong the construction?

H: Years ago, I can't say we did continuous with box beams at all, we may have... but we found with I-beams we weren't saving anything. It complicated the analysis a little bit, and the strand savings was inconsequential in the big picture compared to the simplicity of just using simple spans. Not to say we didn't have problems with going continuous for live load anyway with end anchorage and stuff like that.

D: What are the advantages of using the Decked Slab Beam system you have on your website?

H: For the same depth they usually span farther, they use fewer beam lines to haul out to a jobsite, they install quicker since there is really no field placed concrete to complete the superstructure, it's just grout and some welding. They are used so far primarily on low-volume roads where we wanted to replace a bridge very quickly. We have built some in a week or less. They are fairly new; they've only been out for about 4 years or so.

D: Do you find these Deck Slab Beam bridges limit the cracking at all?

H: We haven't seen any cracking with the deck slab beams, but of course they have not been out that long yet.

D: Are there any other alternatives you may be interested in looking into or any others you use that we haven't already mentioned?

H: We haven't really used state-wide spread box beams, but we are starting to look at it right now with a conventional 8" concrete deck and spacing the beams out about 8 or 10 feet or so. We're finding we can span just as far as we can with the adjacent beam set up and this is a lower cost because beams are expensive and when you are setting them side by side the cost adds up real quick.

D: Is that also fairly rapid construction?

H: No, that is not very rapid, it would just be for cost-savings.

B.7 Phone Interview with Paul Chung

California Department of Transportation
By Daniel Deery, Clemson University
Date: Tuesday March 30th, 2010

Follow up questions for survey of adjacent box beam bridges.

D: Is there a reason you do not construct too many LPAB bridges?

C: That is because in California the majority of our bridges are cast-in-place box girders, not so much precast, so we do not have too many of these adjacent box beams.

D: Do you have any other alternatives that you would consider rapid construction?

C: Rapid Construction typically would be precast, and most are precast I-girders or what we have in California are bulb T girders.

D: Are these details available anywhere?

C: I think some of the standard plans are online but I need to check whether it is Internet or intranet and I will get back to you on that and I can send you the files.

D: Do you take into account the curing of the concrete overlay when you list the erection time as 3-4 weeks for one span?

C: For adjacent box beams we normally have a concrete deck so we do take that into account.

D: Is there any particular reason you do not have a target post-tensioning force?

C: Typically we do say what the post-tensioning force required is on our plans and the contractors figure out the strand configuration to meet that force.

D: Have you found that longitudinal relative cracking has been a setback or hindrance when you use these adjacent beam sections?

C: No because we haven't seen too much of that problem.

D: So are you generally pleased with these sections?

C: Yeah, on the projects we have done, we haven't heard any complaints from our maintenance people so it's been pretty good.

D: You mentioned you were interested in spliced precast girder systems as an alternative. Would this be considered a rapid construction method and what are the advantages of this system?

C: It would be part of a rapid construction method and the advantage is you can handle longer spans. We post-tension these spliced girders and we can optimize the structure depth. When these precast girders are not spliced they are only simply supported for dead load so the design is less efficient. So the splice makes it more efficient and allows for a longer span.

D: Would this take 3-4 weeks to erect a span as well?

C: It would probably take a week or so longer because you would have to splice it and put it together. Some of our construction is on site and some is off-site and requires some special picking or hauling equipment. But probably a week longer.

D: Do you make these bridges continuous?

C: Yes.

D: How do you provide the longitudinal continuity?

C: We typically put the splice at the bent cap and the bent cap is cast-in-place so we use the cast-in-place portion and we use the post-tensioning through that section to make them continuous.

D: When you make these bridges continuous does it prolong the construction time at all?

C: From our experience it is not significant.

D: Do you know the method you use to account for positive moment restraints at the continuity diaphragm?

C: If our engineers did it by hand they would use a conjugate beam theory to do it. We also have sophisticated tools where we actually look at the finite element and we also account for the creep and shrinkage effects to get the positive moment and the redistribution of those moments. Most of the time now we do use these tools to account for the changing distribution of the positive moments.

D: You mentioned that you have a pretty high girder age when these are made continuous, would that prolong the construction?

C: I think typically the girders are aged off-site.

B.8 Phone Interview with Benjamin Tang

Oregon Department of Transportation

By Daniel Deery, Clemson University

Date: Tuesday March 30th, 2010

Follow up questions for survey of adjacent box beam bridges.

D: On LPAB and HPAB bridges, do you ever use a concrete overlay or do you only use an asphalt overlay?

T: I do not know about specifically Oregon, but I believe that they do. For deck beams they do use generally an overlay but not asphalt overlay.

D: For one span of these bridges, you answered on the survey it only takes less than one week to erect; does this consider the curing of the concrete overlay?

T: That's correct, you could do it today in less time.

D: If you use a concrete overlay, will the erection time be increased?

T: You say erect a box beam, so you would have to allow some time for placing the overlay, it depends on how thick the overlay is. Some could be just a couple of days or a couple of hours or some just require a 7-day cure. I'm speaking in general terms though because my experience is more than just ODOT.

D: Do you know what sort of post-tensioning material Oregon uses?

T: If you are post-tensioning a box beam, the prestressed will be strands, the post-tensioning most likely will be just bars.

D: For the survey, we asked for a target post-tensioning force, do you know what that is for Oregon?

T: I do not have that number; it could be in our standards.

D: It seems Oregon has built these bridges for awhile (50 years) and they've built 21-50 in the last ten years. Do you know if these bridges have had any longitudinal cracking issues and if this has been a hindrance for these bridges?

T: Not on the longitudinal cracking, I don't believe there is any at all. I'm not aware of any in Oregon. But there might be some reflective cracking in the earlier designs.

D: Does it seem they are pleased with the details they have?

T: Yeah, I think we use them, I think we use them here.

D: Do you of any rapid construction alternatives that are being used?

T: The box beam, if you design them in a way you can quickly put them together, we have some of those box beams that we can erect over a weekend. Those would be more on our local bridges, or at least on low-volume bridges.

D: Do you know if they are ever made longitudinally continuous?

T: Yeah they are, usually a single-span. We're not talking about multiple spans here? Most of them are single-span bridges.

D: I was referring to multiple span continuous bridges.

T: That I couldn't answer. They usually just put in a diaphragm with the prestressed beams but design it like a simple-span even though they may have some negative steel on top if they have a deck on top. Then that way you have to put a deck on top, to put the negative steel moment up there.

D: Thank you for your time.

T: If you have any other questions, call us back because I think Craig Shike will be the person to ask. I think what I gave you is good enough for the general questions about low-profile beams.

B.9 Phone Interview with Jugesh Kapur

Washington Department of Transportation

By Daniel Deery, Clemson University

Date: Friday April 2th, 2010

Follow up questions for survey of adjacent box beam bridges.

D: Why do you not construct HPAB bridges?

K: Because we have other structure types that are just as or even more efficient that have been part of our inventory for a long time.

D: Have you ever experimented with using these types of bridges?

K: No.

D: Why did you begin using 5" concrete topping on your bridges is that to help with shear transfer?

K: No that is just to control the reflective cracking that occurs on these types of elements. You get longitudinal cracks across the bridge where the joint is so the topping is able to bind everything together and avoid those kinds of cracks.

D: Have you noticed a good deal of longitudinal relative cracking in these bridges?

K: Yes there have been issues, not with the box type, but if we used a voided slab or a T-beam without any topping or overlay there is definitely some cracking that goes on.

D: Is this a cause for alarm or hindrance when choosing this bridge type even though only 0-20% experience the cracking?

K: Yes, especially when the ADT is high.

D: You mentioned it takes less than 1 week to erect one span of these bridges, does this account for the curing of the concrete overlay?

K: Yes that can be done, although we may not put traffic on it but the construction can be done within one week.

D: How do you provide longitudinal continuity for these bridges?

K: Generally we extend rebars and strands at the intermediate piers and then we provide longitudinal reinforcement in the topping over the pier at the negative moment location.

D: So you just use a cast-in-place concrete diaphragm?

K: Yes.

D: Have you ever used a different continuity detail?

K: The one I just mentioned is the most common.

D: Does this continuity diaphragm prolong the construction time?

K: Yes it does add some time to it. Everything is precast, but this has to be cast and then we must wait for it to be cured before traffic can be put on the bridge.

D: What method do you use to estimate the positive moment restraints for the continuity diagram?

K: This is earthquake country here, so we take the plastic hinging moment in the column and split that evenly between the adjacent spans. So the strands for example that are extended from the superstructure are designed to take half of the plastic moment of the column on either side.

D: You mentioned the girder age is 25-90 days, does this also prolong construction or is this age accounted for off-site?

K: That is accounted for off-site, at the pre-casting yard, but it depends on the manufacturer. If you wait too long you get into camber issues that can impact what you expected on the bridge.

D: What are the advantages of using the decked bulb-T system that you mentioned earlier compared to other traditional LPAB bridges? Does this system limit the longitudinal reflective cracking at all?

K: It is just faster construction but we still use topping on those as well.

D: Are the details for this system available on your website as well?

K: The details of the girders are but the topping is simply 5" thick with one mat of reinforcement longitudinally and one mat of reinforcement transversely.

D: Are there any other alternatives that you use? In the survey you mentioned precast concrete deck form panels...

K: No, I think we have been using mainly a lot of precast girder types and now we are trying to adapt to precast slabs but we are taking a cautious approach for the slabs. We are using these precast form panels only in the positive moment areas so that they stay in compression and there is no cracking or if the bridge is totally post-tensioned so everything is kept in compression. Those are the two situations where we are going with precast slabs also. But 7 out of 10 bridges we build are precast prestressed concrete, so everything is geared to rapid construction.

D: I noticed your shear key detail in these adjacent beam bridges, with the rod going through the shear key. What are the advantages of this detail?

K: It is mainly to control cracking in the longitudinal direction. We've been refining this detail to make it more constructable so no special grouting has to be used, you can use your normal concrete in that key which has been made a little wider. There is just a little strip at the bottom to hold the concrete.

D: In addition to all of these things we've mentioned, have you been looking for any other alternatives or are you happy with the options you are using?

K: We are pretty happy because with our inventory of prestressed elements we can span up to 200 feet by using post-tensioning and splicing them together and we've done some amazing structures with splicing and post-tensioning. We have an inventory to take care of short spans as well as long spans where they are competitive with steel.

B.10 Phone Interview with George Christian

New York Department of Transportation

By Daniel Deery, Clemson University

Date: Tuesday April 6th, 2010

Follow up questions for survey of adjacent box beam bridges.

D: I see you have the slab unit bridges and the box beam bridges that you use as adjacent beam bridges. About how long have you been using these bridges and do you still use them often?

C: We have built quite a few of them over the years; I'm sure many hundreds of them. We're not building quite as many as we used to because we've had some issues partly with deck cracking and partly because some of the older ones are starting to corrode, the bottoms are eroding. They are pretty hard to maintain once they start corroding. We've been short spans up to 90-100 feet mostly over streams because they have a low profile and a smooth bottom so for hydraulics they are good.

D: Do you limit these bridges based on ADT?

C: No we use them on all highway systems and even interstates.

D: Is a 5" concrete overlay required on all bridges?

C: Actually a 6" overlay is required. We do have our standards on the website.

D: Is that to help with shear transfer or to help control cracking at the joints?

C: It's a combination of shear transfer and durability. Maintaining a reasonable amount of cover over whatever rebar we have in there. It's a monolithic deck we don't put an overlay over that.

D: Is this normally a composite deck?

C: Generally they are composite yes, we usually make them composite.

D: Is your shear key partial or full depth?

C: We've been using full depth shear keys maybe for the last 20 or so years. The earlier ones probably built in the 70s were partial depth.

D: Do you know why the switch was made?

C: To reduce the amount of longitudinal cracking in the decks. I couldn't tell you when we switched but I'm sure it's been 20 years.

D: Is longitudinal reflective cracking something you've noticed on a lot of these bridges or is this not an issue?

C: We see some of it. We've reduced it quite a bit due to the longitudinal shear keys and also because we've increased the amount of transverse post-tensioning, we put a lot more in than we used to. I wouldn't say we eliminated it but we reduced it quite a bit.

D: Do you have a target contact stress for the post-tensioning?

C: I don't know it by stress but depending on what the span length is and depending on whether its at the quarter points, midpoints or ends it affects how many tendons we use. We use standard patterns.

D: Do you apply this force before or after grouting the shear key?

C: After.

D: Have you had any recent changes to any of these details?

C: We used to use mesh in the deck but now we specify rebar. It makes for better shear transfer I guess. Also the shear key, we changed that.

D: Do you ever make these bridges longitudinally continuous?

C: We make them continuous for live load but we don't really make them fully continuous for dead and live load. We will make a continuity pour and put heavy reinforcement in the deck and put restraint reinforcement in there. That's pretty common. We do that as a matter of practice usually on multi-span bridges.

D: Does continuity prolong construction?

C: That really hasn't been an issue. It doesn't really take that much longer really you still pour the deck the same and you don't have to install the joint system.

D: Do you know how you account for the positive restraint moments?

C: I'm not exactly sure I'm kind of an older guy and when I used to do it in design there was an old PCA method we used to use. I'm sure we are following whatever is in LRFD now. If you want more information I can have somebody in our design group talk to you.

D: Do you know what the average girder age is when continuity is established?

C: That is a factor but I'm not sure if we specify a certain age... I think you have to account for it in the design. One of the things we do is make them continuous for live load but we still design the positive moment regions as simple spans, which goes back to an old NCHRP report and it covers all bases in case the girders are too early of an age or there is too much creep or shrinkage. So we don't count on the continuity to reduce the live load positive moment but we will design for the negative moment.

D: Do you have any other alternative bridge types in addition to the adjacent beam bridges that you would consider rapid construction?

C: If we are trying to keep it to rapid construction, well we have done a couple of things. We just did one bridge that was a deck bulb-T, it was an experimental bridge and we used the ultra HPC with closures... we just did that this past year and it seemed to work out pretty good. We have done a number of bridges using the "inverse system" you know with the upside down steel composite beams that come in panels and you put them side-by-side. We've done a number of bridges that way. We just led a contract where we are going to do this "next T" thing which is something the New England PCA came up with which is almost like a "double T" kind of system. It is sort of like adjacent except you just put them next to each other and you pour a deck over them while its still forming. We're going to do a job in NYC using those. Those are the ones that probably compare to what we would use an adjacent box or adjacent slab beam bridge for similar span lengths and rapid construction.

C: Yeah I don't think the cracking problem is fully gone (laughs). We've tried to do things but the cracking thing is not as bad as where we've seen some of the old ones deteriorate due to strand corrosion but we've gone to HPC mixes that have corrosion inhibitors in there for our beams themselves so we are trying to improve durability that way.

D: And you said that these adjacent beam bridges are not used as much now as they used to be?

C: I wouldn't say we've eliminated using them, we still do them. But we may think about other methods if we can. Some of our regional maintenance people have kind of soured on them a little bit. We've got some that are almost 40 years old so you know you will start to see some issues with them.

D: Why is it that the maintenance people are not happy with them?

C: Well when they start to corrode... There is no easy way to fix them.

B.11 Phone Interview with Paul Liles

Georgia Department of Transportation

By Daniel Deery, Clemson University

Date: Tuesday April 6th, 2010

Follow up questions for survey of adjacent box beam bridges.

D: Do you use LPAB bridges? Voided Slab, Hollow Core... etc for a low profile...

L: Yeah those hollow boxes... we use them very sparingly, we use them if we have a very difficult clearance problem.

D: About how long have you been using them?

L: About as long as I can remember but we probably do not do more than a few a year.

D: What is the maximum span that you use?

L: About 40 feet.

D: Are these plans available on your website?

L: No they aren't available, we'd have to send them to you. We have them, just some old bridges we've done.

D: Do you limit these to a particular ADT?

L: No we never worried about the ADT, but there are other bridges that are cheaper and seem to be easier so we only use these with a real clearance problem.

D: How long does it take to erect one span of these?

L: Pretty quick, I don't know... we put them in, it's all precast so once you've done your substructure they go in pretty fast and we put an asphalt riding surface on them. We don't like doing that but we do it.

D: Have you noticed a good amount of longitudinal reflective cracking on these bridges along the longitudinal joints?

L: No we haven't. It might very well be there and might be hidden by the asphalt. That's the big thing in research is how it cracks the shear key up but we haven't noticed it. It may be that our routes do not have much traffic on them. But we didn't plan it that way.

D: What is your shear key detail? Partial Depth/Full Depth... Location?

L: It is partial depth between the beams and is located in the upper half or maybe more towards the middle but it's a shear key that's just an indentation of both beams and it looks like what I've seen in other states... no invention on our part.

D: Have you ever tried placing mild reinforcing steel through the shear key?

L: No the only thing is we do have that rod that goes through and connects all the beams together, there is usually one of those in the middle of the span. It probably goes through the shear key. It's a steel rod and it is threaded and tensioned a little bit but it's not like a pre-stressing strand or anything it does put some force in it and they call it post-tensioning and it is tensioned just a little bit.

D: Have you ever made these bridges longitudinally continuous for multi-spans?

L: No we have never made them continuous we always had simple spans.

D: What are the alternatives you would use for rapid construction for short spans?

L: Usually what we've told them on the rapid construction end of it is we just sort of bite the bullet and give them a real short time frame and they get out there and really aggressively build a bridge. We haven't had one where we really wanted to get it done in 2 or 3 weeks or something. If you give them a year they take a year if you give them 6 months they take 6 months. If you told them they had to do it in a few weeks they would probably count on doing it in a few months and just put the penalty in their bid. That's my guess. The other alternative is they may propose some sort of rapid construction thing like precast the bridge and roll it into place or use boxes and bring them in precast or something but we just haven't really had to do that. We generally just give them a tight time frame and say build it.

D: So most of these bridges are contractor erected?

L: We prepare the plans and they are all bid out and the contractors build them. We do very little in-house construction. A little bit of maintenance and that's about it.

D: What about more high-profile adjacent beam bridges?

L: We've done some with higher profile where they have gone in and used the boxes like a beam and we call them spread boxes. They spread them apart so its like every other one in there is a beam so they are not really connected so they aren't adjacent boxes but they are still boxes they are just behaving like a beam. We've done a few of those. Consultants did them we did not design them in-house. I guess they work okay it just behaves like a beam then. But they aren't adjacent its every other one.

D: So you don't use many of these adjacent beams either way?

L: No I'd say 1 or 2 a year is about all we do. It has to be a really dictated situation with clearance where we can't raise the grade and absolutely have to go with a minimum depth structure. I think you can get down to a 27" box, they are pretty thin. I think that's what it was. That's your whole depth and then the overlay on top so that's about as small as we can get.

D: You said you normally use asphalt for the overlay?

L: Well we have, the older ones we did them that way. Now our maintenance people are real down on putting asphalt on bridges but it's been out there a long time. We haven't put a concrete overlay on any of them but we might one day.

L: I think our detail is pretty much the normal bread-and-butter... I don't think there is anything unusual about it. We just don't have that many of them. We've minimized our cracking by minimizing the use of them. There was a survey done by Henry Russell or someone that did it, sort of a nationwide survey... not sure if you all have access to that. It wasn't more than a year ago. Let me know if you cannot find it.

D: I'll look into that. Thanks for your time.

B.12 Notes on Phone Interview with Ed Wasserman

Tennessee Department of Transportation
By Sara Roberts, Clemson University
Date: Friday, June 18th, 2010

- Started building adjacent box beams in the late 50s to late 60s during the infancy of prestress in Tennessee.
- Generally tensioned together with high strength rods at the 1/3 points.
- Believes that there was a nominal value for post tensioning, but they were probably never tightened down with a torque wrench to check it.
- First bridges only used an asphalt overlay.
- After 10-12 years, it was noticed that the boxes were not deflecting uniformly and longitudinal cracks were appearing along the joints through the asphalt.
- Began having issues with leakage through the joints
- In the early 70s, they start requiring a 4" concrete overlay with one mat of reinforcing.
- On high volume highways, they included continuity bars in the concrete overlay over bents and also let the overlay be cast down the side of the exterior beams to "clamp" the box beams together.
- In the 90s, they began sorting out the older bridges that were still usable. They scraped the asphalt off them and blasted the top of the boxes. Then put a 4" concrete overlay with one mat of reinforcing down on all of them.
- The low volume roads with the new concrete overlay performed very well, but those on high volume roads began to show longitudinal cracks through the concrete.
- 25-30 years ago, they determined that spread box beams were the more economical option rather than using adjacent box beams because they:
 - have less members and cost less
 - the service life is 3x to 4x as long as the adjacent boxes
 - However, they are slower due to formwork and need an extra 4" of concrete slab on them, but they feel the performance and cost outweigh the cons.
- However, when clearance is not an issue, box beams are not used. They usually go to using AASHTO I girders or double tees for longer spans.

B.13 Notes on Phone Interview with Rita Seraderian

PCI is working on a manual for side-by-side box beams

Contact: Rita Seraderian
Title: Executive Director of PCI North East
Email: seraderian@PCINE.org
Phone: 888-700-5670
Location: Belmont, Massachusetts
By Sara Roberts, Clemson University
Date: Monday, June 21st, 2010

- Is not working on a side-by-side box beam manual
- Believes Massachusetts DOT has a matrix for determining post tensioning forces
- Her department is working on the NEXT beam (Northeast Extreme Tee beam)
 - pcine.org \Rightarrow Bridge Resources \Rightarrow NEXT beam standards
 - NEXT F is the stay-in-place formwork for an eight inch slab
 - NEXT D has the deck incorporated and requires eight inch wide shear keys between members
 - The first fabricated bridge is getting ready to be installed in New York
 - Pennsylvania has just adopted this section to replace their box beam bridges.

Appendix C

Contractor and Fabricator Interview Transcripts

C.1 Email Interview with Troy M. Jenkins, PE (New York Fabricator)

Chief Engineer, Northeast Precast Products
By Daniel Deery, Clemson University
Date: Tuesday May 18th, 2010
Time: 1:00 PM EST

D: Do you prefer/not-prefer these adjacent beam details over alternative bridge types? Why?

J: For our fabrication, there really is no difference between a spread box beam or an adjacent. Shear keys and tie rods are not difficult items to deal with. For design, we typically only see adjacent box beams when the vertical clearance cannot be met with a spread beam.

D: What are the difficult details to work with? If you had the option, is there any part of the details you would change? Why?

J: Some states do not permit a joint between the beams. This causes issues in the field because beams are not always perfectly straight and spaces end up between the beams anyway.

D: Is there any part of the shear key detail, in particular, that you would change? Why or why not? Does the shear key for these bridge types vary from other bridge types you work with, and if so which do you prefer and why? Are your shear keys smooth? Are you willing to sandblast the shear key or use another method to roughen it? Some research has shown this can increase the effectiveness of the shear key. Is it a problem to work with more transverse rods in these bridges? Is it difficult to align the ducts for the rods for these bridges?

J: Every state has its own rules for shear keys. Some sandblast some don't. Some have the tie rod in the key some don't, some use a full depth key at the tie rod. Some have full depth key full length of beam. Some use strand instead of tie rods.

D: Do you have a preference on the type and location of shear key? For instance, preferences on: the tie rods in key or not, full or partial depth, and location of partial depth?

J: We really don't have a preference.

D: Is your stockpile capacity limited to any degree? When providing continuity for these bridges, girder age plays a large role, and this age is usually accounted for off-site in order to not significantly delay the construction. Is this a concern when dealing with these bridge types?

J: I don't understand the question...

D: I'm referring to AASHTO design examples that state 90-day girder age must be reached in order to ignore creep and shrinkage restraint moment effects. Does this impact you at all?

J: We don't have a problem with the 90-day rule because we can submit for payment after we hit 28-day strength. Project schedule needs to permit this time. Some states like PA design the deck steel assuming the beams are 28 days old.

D: Are there any particular details associated with these adjacent types that are more expensive than alternative bridge types?

J: To sand blast keys, we need to double pick each beam for the staging area of sandblasting. Anytime we are required to use closed loop stirrups our costs go up.

D: Overall, are you satisfied with the details for these adjacent beam bridges?

J: Yes. We work in about 9 states and all details are different. We can deal with all of them. The only issue we see is because we use tub forms, if the shear key gets too thick (3/4") for too low in the beam, we cannot get the beams out of the forms.

D: Are you informed of the performance of these bridges?

J: Yes. I sit on a few committees such as PCEF and PCI Bridge.

D: Is there anything else you think would be helpful for us to know?

J: We should all know that the box beams of 15 years ago are not the same as those made today. We no longer use cardboard hollow beams. The center void is now formed with Styrofoam. The concretes we use today are durable and stronger. PCI certified plants are required to closely follow Quality Procedure Manuals that didn't exist 15 years ago and are subject to random audits both in-house and independent. We have also learned that joints in bridges need to be shifted off the bridges to keep the chlorides from destroying the ends of the girders.

C.2 Phone Interview with Mark D. Losee (New York Fabricator)

Pre-Stress Manager, Jefferson Concrete

By Daniel Deery, Clemson University

Date: Thursday May 20th, 2010

Time: 10:00 AM EST

D: You did a job on 4/21 with box beams, correct?

L: Yes it had 4' and 3' boxes, 2'-6" by 85' long, it had a skew; it was tensioned in 5 locations with 3 tendons in each location.

D: Do you prefer/not-prefer these adjacent beam details over alternative bridge types? Why?

L: They work pretty well, I started in 1980 and they originally a small keyway, then they switched to full-depth shear key, more labor for full keyway for fabrication... no big deal though.

D: What are the difficult details to worth with? If you had the option, is there any part of the details you would change? Why?

L: There are a few details I don't really like anymore. One is they've started doing is: usually you have U bars in bottoms of beams, now they are running U bars but they'll come half-way across the beam and put rebar in middle so it's a pain to tie all these in, U-bars and bulkheads quite a bit harder to do it, and I don't really know what purpose is, I'm not an engineer. It used to be first 6 inches they'd put bars in but now it has changed and it's hard to tie it all together. Not a huge deal.

D: Is there any part of the shear key detail, in particular, that you would change? Why or why not? Does the shear key for these bridge types vary from other bridge types you work with, and if so which do you prefer and why?

L: Shear key is fine.

D: Are your shear keys smooth? Are you willing to sandblast the shear key or use another method to roughen it?

L: We power wash the shear keys, we water blast them, about to 12,000 psi or 13,000 psi, and if its less than a week they can get it with 7,000 psi but if its about 10 days then they use at least 9,000 psi. We also treat it with a silane sealer protects it from getting chlorides infiltrated.

D: Is it a problem to work with more transverse rods in these bridges? Is it difficult to align the ducts for the rods for these bridges?

L: Originally skewed ones were tough, problem made better because they used to be 2" plates, now 3" plates are used so as long as the layout is good you don't run into any problems. Only thing I will tell you with the state ones they have this new very, very bad design with tendons. On one particular project, where they were replacing 23 beams, first they put all of the traffic on the inside lanes and replaced outside ones with six on each side, so they got those tensioned up, and then in stage 2 they dropped the beams in. They are curving the tendons and starting in the middle (not simply running it from side to side) and coming out at the top. The problem is: when you go to tension it, 1st one is tight, 2nd one gets caught wrapped around it, and you wonder, will it pinch it? I'm worried about losing compression or ripping top of it off. If there's one design I don't like it's this. It's also a bad safety issue too before the composite deck is poured. I've seen these cut loose before and it will do major damage. Also, the duct is facing the top of the road, so moisture will go down into the duct and cause problems. Also, some contractors like to start running tendons when they are setting them but I usually tell contractor not to, I say he can set them all down before they do it.

D: Is your stockpile capacity limited to any degree? When providing continuity for these bridges, girder age plays a large role, and this age is usually accounted for off-site in order to not significantly delay the construction. Is this a concern when dealing with these bridge types?

L: The state is holding you to 60 days from time of the last pour until the deck pour. Funny thing is I am doing a job now for Delta and they are holding me to 60 days for a single-span... I wanted to tell them it's not necessary and they are not interpreting the rule correctly but oh well. Problem with this is, the contractor normally has to wait 60 days because I can get them out really quick, maybe in about a week. One thing is, in my opinion, the beams on trailers riding to the jobsite are having their camber messed with anyways so who cares for single spans. For multi-spans though I guess it makes sense.

D: Do you ever have to account for this girder age or does the contractor always have to? If it is a rapid job is it possible for you to account for the age?

L: It's up to contractor, if he wants to get it quick and set it and wait before he pours the deck then that's fine, but most will wait a least a month for me to hold onto it until they get it to take some time out of project.

D: So overall, are you satisfied with the details for these adjacent beam bridges?

L: The state likes them for low-profile bridges. The state is having problems with the older adjacent box beams (his comments suggested corrosion issues). I've heard from someone else one time the cardboard forms used on the bridge (it was an older one) had collapsed and clogged up the drain holes at the bottom of the box so water was stored in there... well one was poked through with some rebar and they told me that water drained for 2 days. Some other cases they've checked and they are full of water as well. We've switched our forms to foam now so the newer ones should be better than those.

D: Are you familiar with the Pennsylvania collapse a few years back? It was attributed mostly to corroded strands, mostly due to water in the box due to open joints on the fascia beam.

L: We've used foam since the mid-90's until now, used to be all cardboard. Also 3/8" strands are worse too and those were probably used in the Pennsylvania collapse. We use a thicker strand now, which helps as well. New York has taken steps to increase the longevity of their adjacent box beams. New York has looked into double bulb T but they are so heavy, about 120,000 pounds, so many don't like them because of that. They look like parking garages from below... very wide and large... the new design isn't smooth under so stuff can get caught which was one of the advantages of adjacent beams, the low profile and smooth bottoms.

D: When I spoke with the DOT they made it seem like New York was using less and less adjacent box beams, have you noticed this as well?

L: Yes, they have. The beams built in 1970's and early 1980's they are starting to see issues so now the state is looking at the New England bulb-T, and newer ideas are more and more what I think New York is going to do. The water issue is because maintenance is not done... yeah I know they are supposed to be "maintenance free" but you have to do SOMETHING! It's not a problem with the beam but with maintenance. But you cannot compare the stuff in early 70's and 80's to now it's so different: different strand sizes, different sealers, forms, concrete strength, etc. I think the new design won't fly either though so I'm not too worried about them going away. Most counties love adjacent box beams: they are friendly to put in and you don't have to worry about deck or much open space. You can set the bridge and have it grouted on Monday, and they've had it opened within 2 or 3 days after it was set... it wasn't composite, wasn't a deck pour, but still very fast. They can have adjacent box beams open to traffic within 2 weeks and with a deck pour usually a month.

D: Thanks for your time and information.

L: By the way, check out "Concrete Products May of 2010" in that there is an article with the new beam the state is leaning towards but it's very heavy so probably not great with contractors.

C.3 Phone Interview with JR Parimuha (North Carolina Fabricator)

Florence Concrete Products
By Daniel Deery, Clemson University
Date: Thursday May 27th, 2010
Time: 4:00 PM EST

D: The NCDOT has used you on a cored slab bridge without an overlay, correct?

P: Yes, they just ground the top down.

D: Do you prefer the adjacent box beam and cored slab bridges?

P: Yes we love the adjacent box beams; it's what we produce the most.

D: Any particular reason why?

P: I think it's easier for contractors, you do not have decking and such (I guess compared with girders) but you also don't have formwork or any of that either. You can make sure everything fits good before it gets to the job site. Obviously when the contractor lays it down all he has to do is pour a rail or use a precast rail and pour an overlay or not even that now with the ones you mentioned.

D: Are they using hot-mix or concrete for the overlay?

P: South Carolina pretty much uses asphalt, but North Carolina uses both, probably 75% asphalt and the rest concrete. We do both overlays.

D: What are your thoughts on the details without an overlay? I know many have not been done yet...

P: I think it's a good system, one thing we need to look at is the grout used to patch the hold-down locations. It's a threaded rod that holds the void in place until the concrete gets hard, then you back out that rod and you fill the hole where the threaded rod was with grout. That can chip out when you do not use an overlay and you come back and grind the top. I think it's a great idea though, I know South Carolina uses some solid ones without voids so that would avoid this problem.

D: Are these bridges post-tensioned transversely or are tie rods being used?

P: In SC they used to use strands for construction and tie rods for maintenance, but now all of SC uses tie rods, which is still post-tensioning but rods instead of strands. North Carolina always uses the strands, they use a 6/10 cable jacked at 44,000 lbs and for their bigger boxes they use a double 6/10 and two separate ducts next to each other, which gives them a little more post-tensioning. South Carolina could try this; I think that's a good way to get more post-tensioning, using a double duct. It's not a big deal for producers to put those in.

D: Are there any details with these bridges that you do not prefer or would like to see changed?

P: I think we're used to the details, it is something we've done forever. You have to look at how long the bridges have been there and how long they've been using the system. This is an effective and efficient way to do smaller bridges, especially secondary bridges. The thing I don't like is they limit these to certain volume roads; y'all should be able to find a way that we can use them on more roads. Without topping, that would be great. We do some heights (in North Carolina) that South Carolina does not use, we do 18" ones and we have narrow ones we use for shorter spans as well. I think what y'all are researching is something in shear transfer and all that... some people say there is some cracking going on and there is, you can see it, but it's nothing that's causing any problems I don't think. Maybe visually, aesthetically... but I think we could do some things differently if y'all felt like we needed to. There is room for improvement. This is not something we'd love to do but it's something we could do. The details are pretty basic, they are supposed to be easy to do and cost efficient, which they are. If you look at South Carolina maintenance bridges they do not even recess for the post-tensioning they use a galvanized 1.25" rod and there is not even a grout pocket. All we do is put a PVC pipe in there where that is and make sure we're at the right locations and we fit them up in the yard and make sure we can see through the hole and we send them out. They do not even use dowels in those systems, they probably should, but they were just made to be easy. But I think it's a good system.

D: Have you heard of any durability issues dealing with corrosive salts and water getting into the voids in these beams and causing an issue in North or South Carolina?

P: I haven't at all. I know that did happen up North, with how water got in there and ate the beam from the inside out, but we haven't seen that around here and there are a lot of old bridges around here. That was a long box beam too, maybe had some more issues, most of ours are a lot smaller. I think that span was in the 100-foot range... but I haven't heard of any. I know I've heard

people saying inspecting can be a problem but I don't think that's a reason to jump the gun and stop using something. You could put void drains in there. We've never had a problem with it, not that I know of, I've never heard of any around here. That's one that comes up and gives adjacent box bridges a bad name. I don't think that should be a reason to get rid of them, if you are worried about moisture in there well then let's figure out a way to get it out of there, you know? Some of those states up North are still using them, and they are still standing. The void drains are going to be more expensive to put in, but we will if they think we need them. Not sure if that's something we need to jump the gun on or not. I don't think if you look at these you would see a problem with that though. I think these things are pretty beefy and hold a lot more than they are designed for. They are a lot stronger and more durable than people think... which they need to be, you definitely do not want to be designing for "exact" in the bridge industry.

D: Have you ever dealt with making these bridges continuous for multi-span?

P: No, I never have. That is an option though we could have some bars sticking out of the ends and take some special headers and things. We have done it in North Carolina before but it was a federal job. We did some box beams that had continuous steel sticking out of the ends but it was a single span it was more or less to make it continuous with the approaches, it was not multi-span.

D: Thanks for your time; we're interviewing the fabricators and contractors to get a good idea of their perspectives before we turn in some options to the DOT.

P: I know a few contractors, are you looking for references?

D: Sure.

P: One that would be a good one to talk to is Randall Gettis with Sanford Contracting, they do a lot in North Carolina and are big across the country. They could give you a very fair opinion on things. Another is United Contractors, which is a big one in South Carolina. Jim Fitsmorris is a designer for Triplett King, works for United, he would be a great source, and he designs all types. He is a good one to write down because we just did a box beam in South Carolina, and I think it was the first one, it was actually grouted before it was post-tensioned, but Jim Fitsmorris was the one that worked with the state on designing that. Jim's phone number is 803-980-6025 and Randall's is 919-775-7882. If you all have any more questions feel free to give me a call.

C.4 Phone Interview with Gary Fisher (Texas Fabricator)

Flexicore

By Daniel Deery, Clemson University

Date: Thursday May 20th, 2010

Time: 4:00 PM EST

D: We've been doing some research with SCDOT with adjacent box beam bridges and we've talked to the TXDOT about their adjacent beam options and they gave us your information as a fabricator they use frequently. You do the deck slab beam and adjacent box beam bridges, correct?

F: Yes.

D: Do you prefer one or the other?

F: I guess there are fewer deck slabs, when you do those. It's kind of like a single-T as opposed to a double-T. The box beams and deck slabs are both adjacent to each other and the contractors like that because they can put them down and then immediately work on the deck. I don't know if there is that much difference in making one or the other. We don't really prefer one to the other. As for advantages, fewer deck slab beams than box beams, but the deck slabs are heavier and cost more, so they require bigger cranes for contractors and are more freight. However, there are fewer picks for deck slabs. For a single span structure you can probably do them both in half of a day. Four

deck slabs versus five or six box beams probably isn't much time difference.

D: What are the difficult details from your perspective?

F: Details as in shear connectors?

D: Any detail associated with these sections... is any more difficult than other sections you work on?

F: Let's see... of course you don't have the shear connectors on the adjacent box beams, and you do have them on the deck slabs. On occasion that is more difficult to make sure they stay flush with the top slab, we ran into that a little at the beginning but we've pretty much taken care of it now... it was more of a learning curve I guess you could say. I know we didn't have any problems but some of our competitors had some problems with the deck slabs when they first came out with the ends bulging out. So TXDOT made a modification where you could make the wing part about 0.5" longer than the bottom part of the deck slab. We never really had any problems with that but I guess one of the other competitors had that problem. Issues with box beams... you know just details like making sure the void doesn't float up on you, of course you have that in deck slabs too.

D: Do you use Styrofoam forms for that?

F: Yes we use a solid piece of Styrofoam for that. We hold them in place and that's an issue you just have to check, we very rarely have had problems with that but that's just an issue you have to be aware of because that could come back to haunt you. I guess putting the plates in the deck slabs is a little bit difficult... more or less like double-Ts it's just a little time consuming. You have all that reinforcing there in the top, all that longitudinal steel and transverse steel all crossing and you have plates in there and bars sticking back in there so its just a lot in a small area. Just a few minor details but just things we've actually worked out on doing the products. The deck slabs are similar to a double-T in that aspect.

D: Have you noticed any concerns with using the welds in the shear keys from a fatigue perspective?

F: You mean the welds not being completely done or breaking or something?

D: Have you used these for about 4 years or something like that?

F: Probably close to about 4 years, I think the first structure was probably in 2006 or 2007, something like that. I haven't heard of any issues, the only issue I heard of was after the deck slab wings had been welded together and before the keyway had been grouted a truck drove over it and it cracked I didn't see this a TXDOT engineer told me what he saw. He then realized pouring the grout in the keyway made a pretty big difference in that connection, I think everybody thought that welding the plates was holding it all together, but the grout serves a pretty big function.

D: I mean over time welds are more prone to having a stress riser and a fatigue issue so I was just curious if anyone had noticed that? I know they haven't been used for very long so it might be too early to tell. We didn't know if fatigue was a concern or not with the shear transfer going through that detail.

F: I haven't really heard of any long-term issues with that but we probably haven't done the deck slabs long enough for there to be an issue. You might see an issue in some of the older double-Ts, which are actually a similar connection, but we didn't start using that connection in those until about 10 years ago. It was a different type of weld plate and the plates weren't spaced as closely together as they are now, maybe that was why they spaced the plates closer together or put more of them in the sides because they had noticed some sort of fatigue with them. The only other issue is I know in some of the commercial, non-state products we make, we put a very small plate in the sides at quarter or mid-points on the beam, not very many of them, not like TXDOT where they are every ten feet... and we had some contractors on these when they put the screed across they noticed after they poured the deck there were cracks along the outside beam because that outside beam was taking all the load because of the screed so they were getting the reflective cracks. TXDOT uses that real big keyway, so I haven't heard anything similar happening to them. The commercial projects use something like an AASHTO keyway that is near the top and about " wide on each side of the

beam and maybe only 7" deep. So that's when we've put those little weld plates on the sides and that seems to get rid of that cracking from the screed running across it. Once the concrete hardens those plates really don't do anything anyways. I know that's not what you're asking anyways... I don't think I've ever heard of any fatigue issues... we probably haven't been doing the deck slabs long enough to hear of those issues.

D: Do you have any issues with the robust shear key for the adjacent box beam bridges? It seems to be performing well.

F: It adds extra dead load to your structure, being a large keyway. Although, theoretically, it makes the beam a little bit lighter, a similar weight to a similar AASHTO height beam but when you add the dead load of the keyway grout it makes the structure a heavier one than an AASHTO height beam. There is no real difficulty in manufacturing. There might be some issues with reinforcing if reinforcing is not bent correctly there may be an issue. I'm talking at the bottom of the beam, we used to do all one bar, but now there is a combination of three bars, one bar on each side that encases your strands and then a U-shaped bar that does not encapsulate all the strands it just goes up into the thin area where the keyway comes in. We used to have problems with the rebar manufacturers with the single bar where they wouldn't have the right bend or the bars either did not have enough cover or they would be too small and there would be some deflection in your strand. But since they've gone to the different reinforcing where you've got three bars instead of one it seems to alleviate that problem. Now there are loose bars and you can pull them in as tight as you want and it cannot deflect the strands because its not a single bar and you can still ensure you get the right amount of cover without making it too tight. Dealing with the keyway itself though we really don't have any problem with it, not with pouring it or setting it up.

D: Do you ever do any projects making these bridges longitudinally continuous? I know Texas has some details where they use a composite deck to make the bridges continuous for live load, are you familiar with that?

F: I've noticed they've put expansion joints in there but they normally do it every other span. I have also noticed structures being completely continuous over multiple spans, I don't know if that is a good or a bad issue. I know our concrete is different than what they are putting on the topping so there may be some expansion differences in our concrete and the deck.

D: I ask that question because there is an AASHTO design example for continuous bridges where you must account for the girder age in order to determine whether or not you can neglect creep and shrinkage which causes positive restraint moments over the bents that are made continuous for live load. If the girder age is at least 90 days old once the deck is poured you can ignore the effects, so I didn't know whether you had to account for a certain age for your beams in your yard before they go to the site or anything like that.

F: We've had beams here for over a year due to some design issues. They just now started taking beams that they were supposed to take last year at this time. But I can't think of any issues that you are referring to. On occasion we'll have beams here for 60+ days but that may be it was a phase project and there may be multiple width beams like a small number of 4 footers and we just produced them all at the same time. There is no reason to string it out if we can do all the same ones at once so those may end up sitting here for a long period of time.

D: If they did require you to keep them would it be an issue?

F: That is an issue to hang on to stuff longer than required and having it take up space. I know if you talk to some of the other prestressers that do girder projects they may have lots of them on site for a long period of time but typically for box beams they are for shorter spans so you don't have to keep beams like that for very long unless on the job site there is some sort of a delay or a design issue. We are always looking to maximize our storage so we don't run into an issue of being short on storage.

D: Overall, you seem to be pretty satisfied with both of these bridge types adjacent box beams and deck slab beams, you don't see many causes for concern with these?

F: No. I think the contractors like the adjacent box beams as I said before because you can put those down right up against each other and then you have a work area to work on. You don't have to wait around to either weld in metal deck or put deck panels on top like you would for a girder project so there's some more time that you'd have an issue with. So the contractors can get their jobs done sooner and then maybe they can do an extra job or two and make some more money. That's my view on box beams I think box beams are a lot better than girders but that is probably because we don't make girders.

C.5 Email Interview with Chuck Prussack, PE (Washington Fabricator)

Vice President/General Manager, Central Pre-Mix Prestress Company

By Daniel Deery, Clemson University

Date: Thursday April 29th, 2010

Time: 9:00 PM EST

Daniel Deery's questions posed in the email:

- Do you prefer/not-prefer these adjacent beam details over alternative bridge types? Why?
- What are the difficult details to worth with? If you had the option, is there any part of the details you would change? Why?
- Is there any part of the shear key detail, in particular, that you would change? Why or why not? Does the shear key for these bridge types vary from other bridge types you work with, and if so which do you prefer and why?
- Are your shear keys smooth? Are you willing to sandblast the shear key or use another method to roughen it? Some research has shown this can increase the effectiveness of the shear key.
- Is it a problem to work with more transverse rods in these bridges? Is it difficult to align the ducts for the rods for these bridges?
- Is your stockpile capacity limited to any degree? When providing continuity for these bridges, girder age plays a large role, and this age is usually accounted for off-site in order to not significantly delay the construction. Is this a concern when dealing with these bridge types?
- Are there any particular details associated with these adjacent types that are more expensive than alternative bridge types?
- Overall, are you satisfied with the details for these adjacent beam bridges?
- Are you informed of the performance of these bridges?
- Is there anything else you think would be helpful for us to know?

Chuck Prussack's Email Response:

"We build what you are calling "adjacent beam" bridges, and have for 50 years, with generally excellent service life for the thousands of bridges we have built. Most of this type of bridge we have done are not for the DOT, which is basically a prestressed girder with cast-in-place deck design agency, but for cities, counties, USFS, etc.

Many of the adjacent member bridges we have done do not have any type of overlay, they have weld ties at usually about 5' on-center and use a full-length grouted keyway. The remainder of the adjacent member bridges we have done either use a cast-in-place deck or asphalt overlay. Both of these types of bridges are performing well, and do not have reflective cracking to my knowledge.

In Washington we use weld ties at 5' on-center typically, even on slab bridges, as opposed to transverse high-strength rods.

We typically sandblast the keyways at the plant. The keyway configuration is based on an earlier NCHRP study by Mattock and Stanton.

We have been involved with the drawings and concept for this type bridge for 50 years, so generally are happy with all the details since we participated in their generation.

I'm not a big fan of transverse rods because they end up too far apart and contribute to differential movement, which causes reflective cracking. Whatever is used, weld ties or rods, in my opinion they should be about 5' on-center max to provide a tensile tie across the keyway with the grout providing the shear capacity.

Girder age is not an issue.

I think adjacent member bridges are an excellent way to build a bridge because: the entire section is plant cast which gives better control and concrete than field, they lend themselves to staged construction, they can be built more quickly, they are safer over roadways since there is an immediate work platform", and they can give an owner good results even if the contractor is less sophisticated.

There have been two current NCHRP projects that examine more robust joints if your state needs to go that direction, Cathy French and Ralph Oesterle are their respective PI's."

C.6 Email Interview with Bill Heston (North Carolina Contractor)

Balfour Beatty

By Daniel Deery, Clemson University

Date: Friday May 28th, 2010

Time: 4:00 PM EST

D: Do you prefer/not-prefer these cored slab details over alternative bridge types? Is there an alternative bridge you prefer to build? Why?

H: Cored slab bridges are well suited where span lengths can be short and top-down construction method is preferred/required. Details for this bridge type work well for the application and result in a relatively inexpensive solution. However, BBII prefers to build larger bridges in areas that typically call for longer span lengths with steel plate girders or prestressed/precast concrete girders, particularly when traversing water and/or wetlands. This type of bridge allows us to utilize our larger (175T 230T) cranes and heavy-duty temporary work trestle that the smaller bridge builders typically don't have.

D: How long does it take to erect one span of these bridges? How does this compare to alternatives?

H: Of course, the time to complete one span of any bridge type is dependent on its width. Considering a normal 2-lane cored slab bridge with shoulders, built using the top-down method, a full cycle for a standard 50' span takes about six weeks. The same width precast concrete girder bridge, built from a temporary work trestle alongside the new bridge, will take roughly the same amount of time to construct a single span that is typically about twice as long. This can be accomplished since work is done from the side, enabling multiple activities to proceed simultaneously (e.g. deck placement in one span, girder erection in the next, cap construction in the next, pile driving or drilled shafts in the next).

D: Could you step through a construction sequence for this bridge type?

H: Here is a very general work sequence:

1. Excavate first end bent
2. Drive end bent pile
3. Form & place end bent concrete & cure
4. Backfill end bent
5. Place rip-rap slope protection at end bent
6. Drive pile at first intermediate bent
7. Construct intermediate cap & cure concrete
8. Set first span bearings and cored slabs & install temp handrail
9. Install transverse PT strands/anchors and stress
10. Grout cored slab keys, PT strand anchor blockouts
11. Repeat until structure complete
12. Place concrete barrier
13. Place concrete wearing surface
14. Place approach slabs
15. Install expansion joints

D: What are the difficult details to work with? If you had the option, is there any part of the details you would change? Why?

H: The hardest details to work with are the shear keys and concrete wearing surface (when specified). See shear key discussion that follows. As for wearing surface, AC paving would be much preferred.

D: Is there any part of the shear key detail, in particular, that you would change? Why or why not? Does the shear key for these bridge types vary from other bridge types you work with, and if so which do you prefer and why?

H: Key width is too narrow, causing significant quantities of grout to be wasted and too much time to ensure they are properly filled. The keys could be twice as wide, use about the same amount of grout, and make filling faster and quality more consistent. Other bridge types we work with typically don't have grouted keys.

D: When do you grout the shear keys? Would grouting the shear key after post-tensioning be more difficult? This has been found to improve the performance, ensuring compression in the grout.

H: In our experience shear keys are required to be grouted after post-tensioning grouting before is not an option.

D: Is it difficult to achieve the target post-tensioning force (is there a target you try to hit)?

H: There is a specified force and strand elongation. We don't find it difficult to achieve.

D: Is it a problem to work with more transverse rods in these bridges, or is that not a concern? Is it difficult to align the ducts for the rods for these bridges?

H: In our experience, one or two (depending on bridge width & span length) single 0.6" high strength post-tensioning strands are required. Non-corrosive (PVC) pipes are embedded at the correct location in each cored slab by the fabricator. Alignment is not an issue.

D: In your opinion, do you feel that concrete topping on these bridges is valuable to make these bridges continuous? Do you find it valuable for anything else?

H: We can't make an engineering judgment about the need for or type of wearing surface. However, we have seen cored slab bridges with no wearing surface, asphalt wearing surfaces, and concrete wearing surfaces. Of these, concrete is the most expensive and least preferred.

D: Are there any particular details associated with these cored slab types that are more expensive than alternative bridge types?

H: Again, on a cubic yard basis, a concrete wearing surface on a cored slab bridge is much more expensive than a CIP deck on a prestressed girder bridge.

D: Overall, are you satisfied with the details for these cored slab bridges?

H: Yes, overall we are fine with the details as they are.

D: Are you informed of the performance of these bridges?

H: We are typically out of the loop when it comes to performance of any bridge type once construction is completed.

C.7 Phone Interview with Sandy Tesch (Texas Contractor)

ConStar Construction
By Daniel Deery, Clemson University
Date: Wednesday May 19th, 2010
Time: 4:00 PM EST

T: You had talked to L.L. & F. about the bridge beams?

D: Correct did you do deck slab beams for them or the adjacent box beams?

T: It would be the deck slab beams.

D: We're doing some research at Clemson University here in South Carolina with the SCDOT dealing with adjacent beam bridges and their alternatives and we've talked to TXDOT about these bridge details and they listed L.L. & F. as one of their contractors for deck slab beams and L.L. & F. sent us on to you.

T: Yeah, we did one, actually two; we were only the second or third one in Texas at that time to actually be constructed. Are the ones you are looking at the ones with voids inside them to make them lighter?

D: Yes.

T: Yes, they have a flange and inside the member itself is a void, it's not solid concrete in the bottom or something. It makes them instead of 100,000+ pounds ours were 80,000 pounds or so or less.

D: Do you prefer this type of bridge compared to its alternatives?

T: Actually we do mainly smaller ones for the smaller bridges. I think it's pretty advantageous because of the time frame. You set it in there and you grout in between them and you are pretty much done. The only problem we had was ours was on a skew and I don't think they had the bearing pads exactly designed right... they were showing two bearing pads on one side and one on the other... they should've had two on each end of each one. Also, since ours was on a skew I don't

know why but it made the member twist a little and they ended up actually putting hot-mix on top to level it out. I think now they might be pouring concrete on top. As far as the one that wasn't a skew bridge I heard they didn't have any problems.

D: How long does it take to erect one span of these bridges?

T: For a deck-slab member, just installing it, you can do it easily in one day, not counting the grout; it would probably take you another day to do all the grout.

D: And there is normally a concrete or hot-mix overlay?

T: There probably wouldn't have been in our case except for the irregularity in the top, after they twisted a little. It wasn't a real straight structure on top, level I mean. The irregularity probably could've been avoided if they let us use different sized bearing pads to kind of adjust they didn't actually know what they wanted to do at the time they were pretty new at this but since then they may have worked it out.

D: Could you step me through a construction sequence for this bridge type?

T: In the beginning your bridge is the same, ours was a single span, but you have to go through all the steps to pour the abutments on both ends, then a lot of the care in this becomes you have to have a pretty large crane. The expense in these is the actual crane. To give you an idea for ours it was one day and it was mainly mobilization but it was \$15,000, for one day. But we actually set all the beams probably in two to three hours, but it takes that large of a crane maybe a half-day almost to come in and set up and then you do the work and then a half-day to tear down and leave. The actual placement of the deck slabs is minimal compared to the move-in and move-out. Then after that we had to have a certified welder because of the V-shaped section between the beams, and they have plates welded every 6 or 7 feet, I can't remember, and then you have to put a rod in there and weld it on both sides. Then after that, which that probably took 1 to 2 days to weld all the rods, then it's just a matter of grout placement. You pretty much have to do that in 1 day, so it takes roughly 1 week. It's fast, if you don't have any problems with twisting or anything, you can complete that bridge in a week pretty easy.

D: What's the most difficult detail to work with for this type of bridge in your opinion?

T: Probably the open space of the area you are working in, because of the size of the crane you have to make sure that large of a crane can spin around and move around in that area. We actually stayed on one side I guess you could try it if you had two spans you could try from both sides but we only had one span and we did it from one side of course. That was the hardest part, making sure the crane could fit on one side. Because it was minimum we had to have a 350 ton hydraulic but they ended up sending us a 500 since the 350 wasn't available but the 500 set it pretty smooth and easily, it worked out pretty good actually.

D: Is there any part of the shear key (V-detail) that you would like to change?

T: No, it was pretty simple. You just take, whatever it is, 11-inch rods, and drop them down in there. It's more of a problem as far as TXDOT is concerned you have to have a certified bridge welder which is not always available. I actually got the welder I use all the time to get certified and do it but it took more time to do all the certification than to do the welding on the bridge.

D: We've found some cases where these bridges have been made continuous for multi-spans, have you worked on any of these?

T: No sir.

D: Overall you said you are pretty satisfied with this type of bridge compared to the alternatives?

T: Yes and it looks like in Texas here TXDOT uses them mainly on single span and maybe double but they do use them some on multi-span.

D: Do you have anything else you think may be helpful for us to know?

T: To me, I'm not trying to knock them but I think the manufacturer of the beams know more about them than TXDOT, they actually designed them I think TXDOT just took their design and turned it into a standard. And they are pretty knowledgeable, in Houston, TX is one of the manufacturers, they are actually the most economical they seem to be the cheapest on every bridge I've ever dealt with.

D: What's their name again?

T: Flexicore. I think they are the originators on those bridges but I'm not positive.

Appendix D

Mini-Workshop Questionnaires

D.1 Contractor Questionnaire

Questions are set in the context of a 48' wide x 40' single span bridge

What is the maximum section weight which is reasonable to set without taking extraordinary measures?

Inverted-Tee

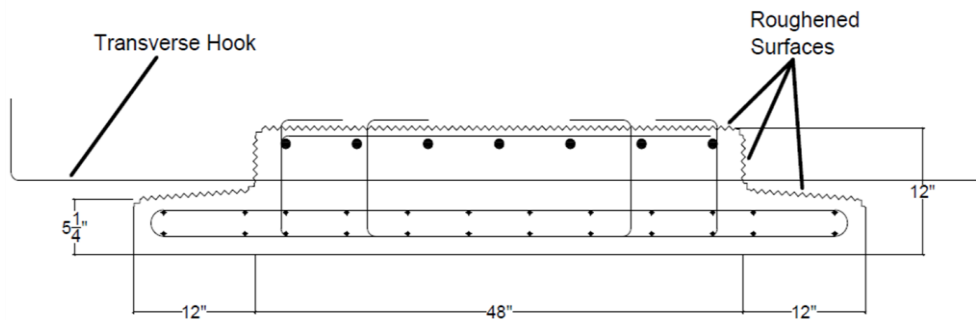
1. What is the relative time, compared to hollow-core bridge to construct one span (i.e. set beams, place reinforcement and any concrete/grout) – Please circle one.

More than 50% less	Between 25% and 50% less	Between 5% and 25% less	Between 5% less and 5% more
Between 5% and 25% more	Between 25% and 50% more	More than 50% more	

2. What is the relative erection cost, compared to hollow-core bridge to construct one span? (i.e. set beams, place reinforcement and any concrete/grout, crane capacity) – Please circle one.

More than 50% less	Between 25% and 50% less	Between 5% and 25% less	Between 5% less and 5% more
Between 5% and 25% more	Between 25% and 50% more	More than 50% more	

3. What details of the proposed section are construction friendly?
4. What details of the proposed section are construction unfriendly? Why?
5. What modifications (keeping with the spirit of detail) would you propose to ease construction difficulties and cost? (You may make mark-ups on the next page)
6. Would light-weight concrete make a big difference in construction time and/or cost?



NEXT-D

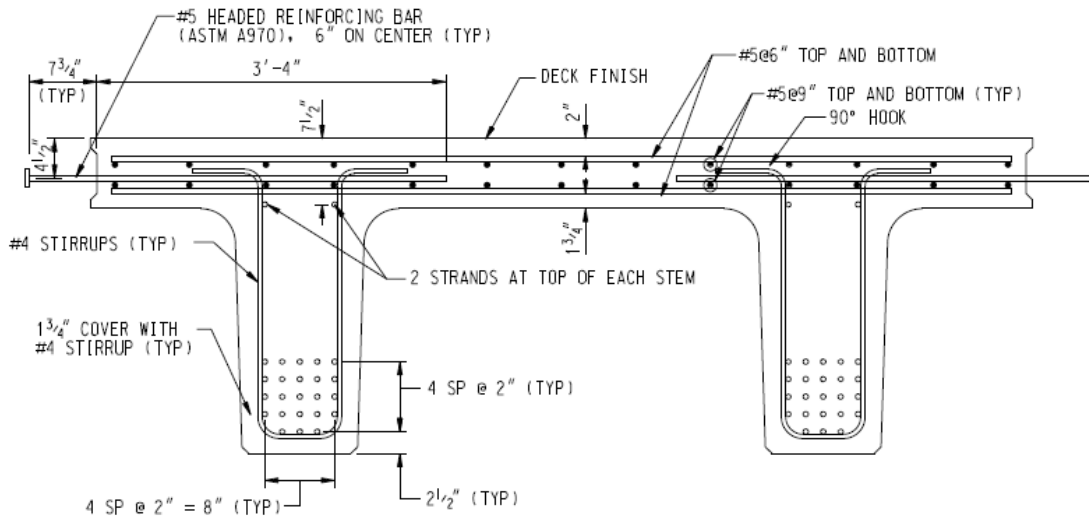
1. What is the relative time, compared to hollow-core bridge to construct one span (i.e. set beams, place reinforcement and any concrete/grout) – Please circle one.

More than 50% less	Between 25% and 50% less	Between 5% and 25% less	Between 5% less and 5% more
Between 5% and 25% more	Between 25% and 50% more	More than 50% more	

2. What is the relative erection cost, compared to hollow-core bridge to construct one span? (i.e. set beams, place reinforcement and any concrete/grout, crane capacity) – Please circle one.

More than 50% less	Between 25% and 50% less	Between 5% and 25% less	Between 5% less and 5% more
Between 5% and 25% more	Between 25% and 50% more	More than 50% more	

3. What details of the proposed section are construction friendly?
4. What details of the proposed section are construction unfriendly? Why?
5. What modifications (keeping with the spirit of detail) would you propose to ease construction difficulties and cost? (You may make mark-ups on the next page)
6. Would light-weight concrete make a big difference in construction time and/or cost?



Clemson Adaptation

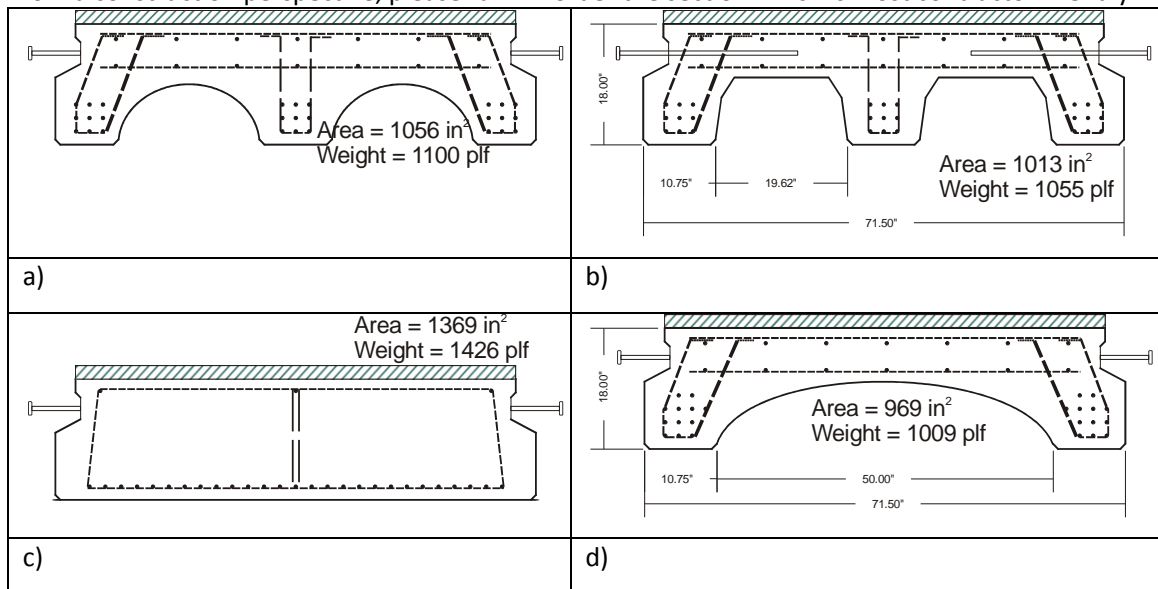
1. What is the relative time, compared to hollow-core bridge to construct one span (i.e. set beams, place reinforcement and any concrete/grout) – Please circle one.

More than 50% less	Between 25% and 50% less	Between 5% and 25% less	Between 5% less and 5% more
Between 5% and 25% more	Between 25% and 50% more	More than 50% more	

2. What is the relative erection cost, compared to hollow-core bridge to construct one span? (i.e. set beams, place reinforcement and any concrete/grout, crane capacity) – Please circle one.

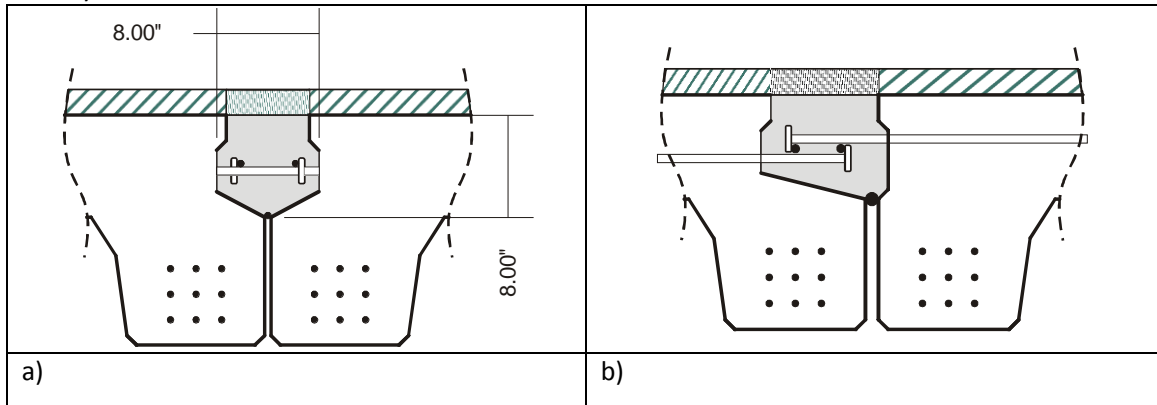
More than 50% less	Between 25% and 50% less	Between 5% and 25% less	Between 5% less and 5% more
Between 5% and 25% more	Between 25% and 50% more	More than 50% more	

3. What details of the proposed section are construction friendly?
4. What details of the proposed section are construction unfriendly? Why?
5. What modifications (keeping with the spirit of detail) would you propose to ease construction difficulties and cost? (You may make mark-ups on the next page)
6. Would light-weight concrete make a big difference in construction time and/or cost?
7. From a construction perspective, please rank in order the section which is most contractor friendly.

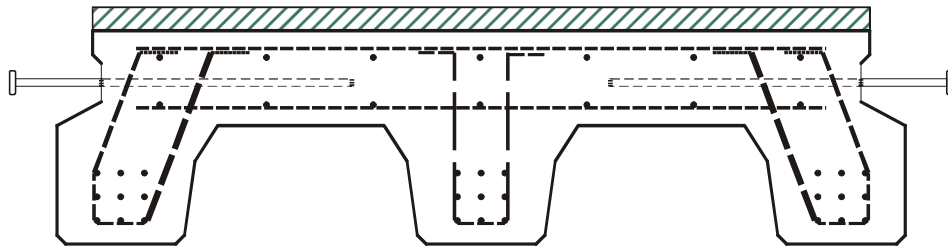


Justification (if any):

8. From a construction perspective, please identify the shear key detail which is most contractor friendly.



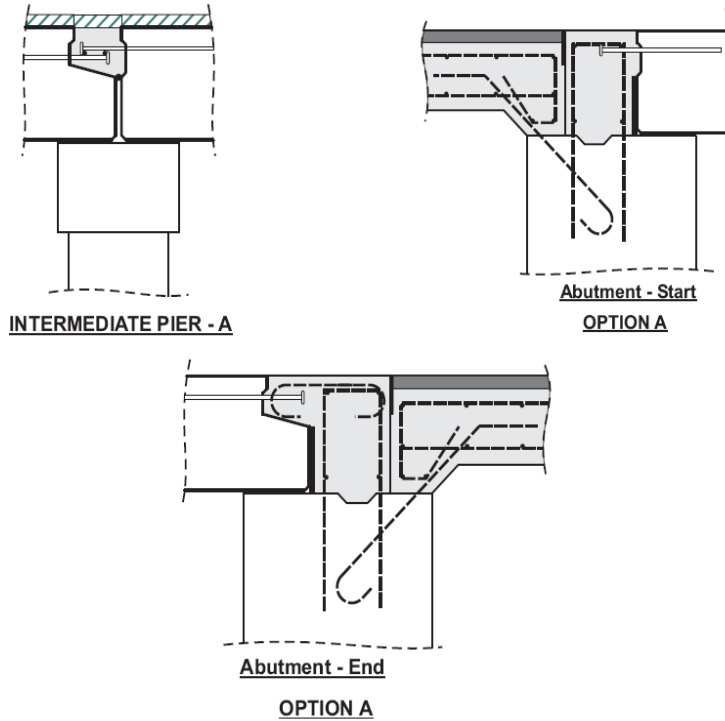
Justification (if any):



Continuity – Headed Option

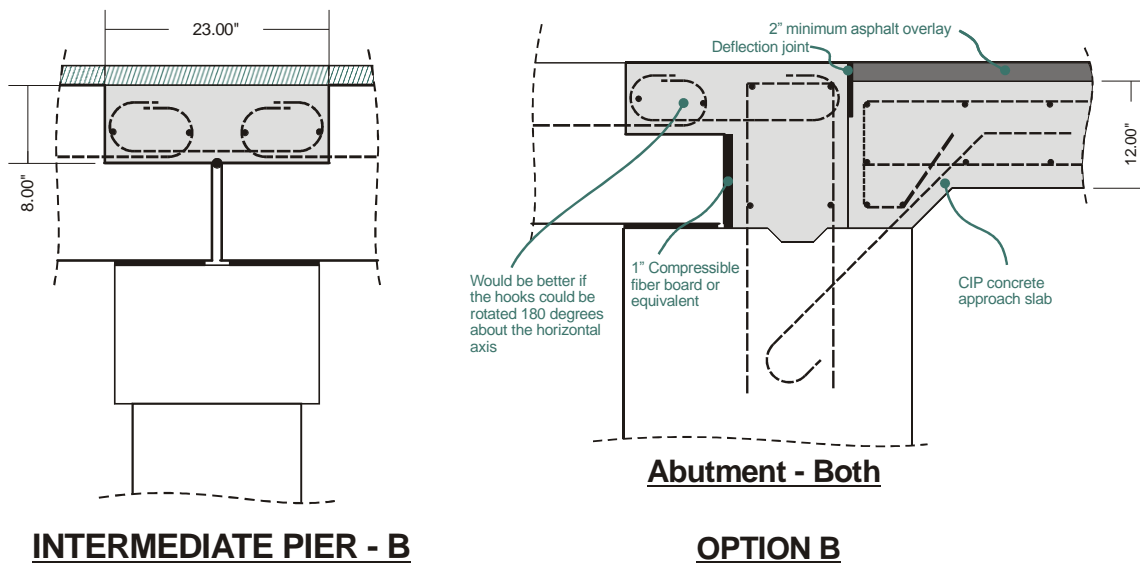
This option requires the spans to be set starting from one end of the bridge and working to the other end. This is to avoid conflict with protruding studs.

1. What aspects of the proposed details are construction friendly?
2. What aspects of the proposed details are construction unfriendly? Why?
3. What modifications (keeping with the spirit of detail) would you propose to ease construction difficulties and cost? (You may make mark-ups on the next page)
4. Is the fact that the profile at each end of a section is not identical overly problematic?



Continuity – Hook Option

1. What aspects of the proposed details are construction friendly?
2. What aspects of the proposed details are construction unfriendly? Why?
3. What modifications (keeping with the spirit of detail) would you propose to ease construction difficulties and cost? (You may make mark-ups on the figures above)



D.2 Fabricator Questionnaire

Inverted-Tee

1. Fabrication difficulty compared with cored-slab

Easier		Neutral		More Difficult
1	2	3	4	5
2. What details of the proposed section are fabrication friendly?
3. What details of the proposed section are fabrication unfriendly? Why?
4. What modifications (keeping with the spirit of detail) would you propose to ease fabrication and transport difficulties and cost? (You may make mark-ups on the next page)
5. What impact would light-weight concrete have on fabrication cost?

NEXT-D

1. Fabrication difficulty compared with cored-slab

Easier		Neutral		More Difficult
1	2	3	4	5
2. What details of the proposed section are fabrication friendly?
3. What details of the proposed section are fabrication unfriendly? Why?
4. What modifications (keeping with the spirit of detail) would you propose to ease fabrication and transport difficulties and cost? (You may make mark-ups on the next page)
5. What impact would light-weight concrete have on fabrication cost?

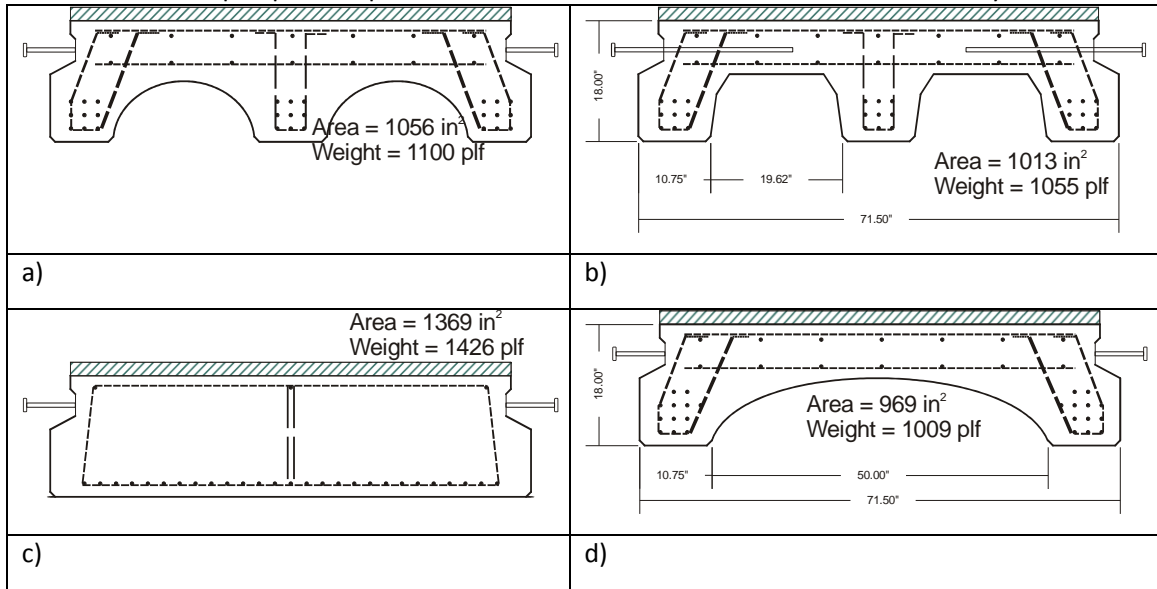
Clemson Adaptation

1. Fabrication difficulty compared with cored-slab

Easier		Neutral		More Difficult
1	2	3	4	5
2. What details of the proposed section are fabrication friendly?
3. What details of the proposed section are fabrication unfriendly? Why?
4. What modifications (keeping with the spirit of detail) would you propose to ease fabrication and transport difficulties and cost? (You may make mark-ups on the next page)

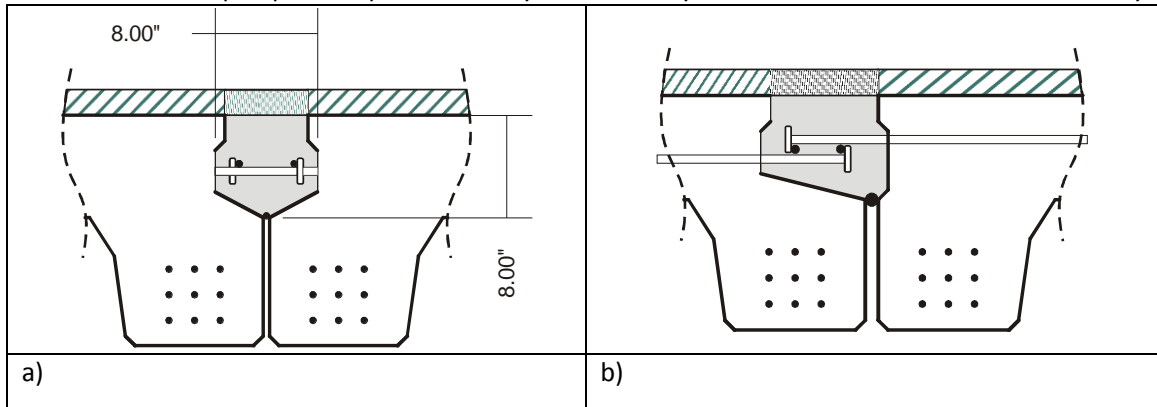
5. What impact would light-weight concrete have on fabrication cost?

6. From a fabrication perspective, please rank in order the section most fabricator friendly.



Justification (if any):

7. From a fabrication perspective, please identify the shear key detail which is most contractor friendly.



Justification (if any):

Continuity – Headed Option

1. What aspects of the proposed details are fabrication friendly?
2. What aspects of the proposed details are fabrication unfriendly? Why?
3. What modifications (keeping with the spirit of detail) would you propose to ease fabrication and transport difficulties and cost?
4. Is the fact that the profile at each end of a section is not identical overly problematic?

Continuity – Hook Option

1. What aspects of the proposed details are fabrication friendly?
2. What aspects of the proposed details are fabrication unfriendly? Why?
3. What modifications (keeping with the spirit of detail) would you propose to ease fabrication and transport difficulties and cost?

This page intentionally left blank

Appendix E

Letter from PCINE

September 13, 2010

Bryant G. Nielson, SE (Utah)
Assistant Professor
Department of Civil Engineering
Clemson University
Clemson, SC 29634-0911

Subject: Recommended Research for NEXT D Beams

Dear Professor Nielson:

It was a pleasure speaking with you the other day regarding the development of the NEXT D Beams in the northeast. As we discussed, the beam was developed by a committee of DOT bridge engineers from the six New England states and New York State.

The basis of the development of the section was that the beam could be used as an adjacent deck section with a simple closure pour connection between the units. The detail chosen for the closure pour joint is based on research being done at the University of Tennessee Knoxville. In that research, the team determined that a headed reinforcing bar could be developed in approximately 6 inches when cast in 7000 psi grout. This research identified the resistance of the section, but not the potential load side of the design equation.

Our committee took that research and applied it to the NEXT D Beam. Our design is based on treating each stem as a stringer beam and the top flange as a concrete deck. The AASHTO LRFD strip method was then applied to determine the moments acting on the joint. The bars were then placed just below mid-depth of the top flange so that the section could resist the AASHTO positive moments while also being able to resist minor potential negative moments.

This approach may be appropriate; however we are not sure that it is an accurate depiction of the actual forces in the connection. It would be helpful to study the forces acting on this connection for various beam configurations. The maximum beam spacing should generate the highest moments and the minimum beam spacing should generate the highest shear values. For this reason, a parametric study of the different beam configurations would be useful. The intent of this study would be to identify if the AASHTO LRFD Strip method is a reasonable method for designing the connection between the units, or if another method is more appropriate..

If you have any question or require additional information, please do not hesitate to contact me at 860-290-4100 or Rita Seraderian at 888-700-5670.

Sincerely,



Michael P. Culmo, P.E.
Vice President of Transportation and Structures

mpc
cc: Rita Seraderian, PCI Northeast

Appendix F

Parapet and Deck Design for NEXT-D Beam

Parapet and Overhang Design Outline:

- 1) Design criteria
 - 1.1) Deck properties:
 - 1.2) Deck overhang properties:
- 2) Continuous parapet design---Impacts are within the wall segment
 - 2.1) Basic parameters:
 - 2.2) Flexural resistance of wall about vertical axis--- M_w (kip*ft)
 - 2.3) Flexural resistance of wall about an axis parallel to the longitudinal axis of the bridge--- M_c (kip*ft/ft)
 - 2.4) Determine critical length of yield line failure pattern --- L_c
 - 2.5) Determine nominal resistance to transverse load --- R_w
 - 2.6) Shear transfer between concrete parapet and deck
 - 2.7) Top reinforcement of the overhang:
- 3) Continuous parapet design---Impacts at the end of the wall
 - 3.1) Determine critical length of yield line failure pattern --- L_c
 - 3.2) Determine nominal resistance to transverse load --- R_w
 - 3.3) Shear transfer between concrete parapet and deck
 - 3.4) Top reinforcement of the overhang:
- 4) Development length of bars in the overhang
 - 4.1 #5 bars
 - 4.2 #4 bars
- 5) Summary
 - 5.1) Parapet reinforcement capacity VS demand
 - 5.2) Overhang reinforcement capacity VS demand

1. Design criteria

1.1 Deck properties:

Cross section:	NEXT-8	
Deck top cover:	Cover _t := 2.5in	AASHTO LRFD Table 5.12.3-1
Deck bottom cover:	Cover _b := 1.0in	AASHTO LRFD Table 5.12.3-1
Reinforced concrete density:	W _c := 150pcf	
Concrete 28-day compressive strength:	f _c := 6.5ksi	AASHTO LRFD 5.4.2.1
Reinforcement strength:	f _y := 60ksi	AASHTO LRFD 5.4.3 & 6.10.3.7
Bituminous wearing surface:	W _{fws} := 140pcf	AASHTO LRFD Table 3.5.1-1

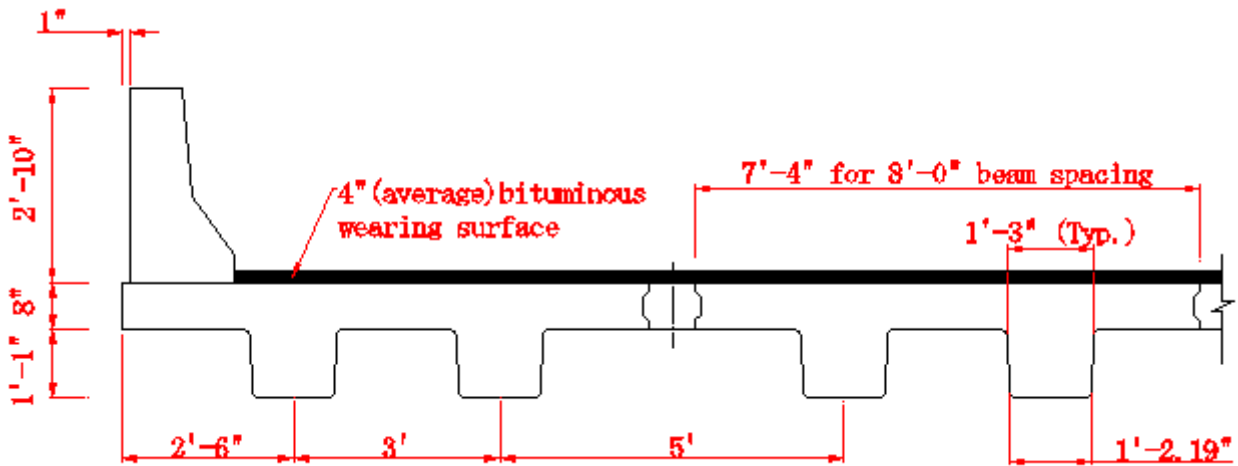


Figure F.1: NEXT-8 transversal cross section

Note: the minimum asphalt thickness is 2" at the gutterline.

1.2 Deck overhang properties:

1.2.1 Overhang width

SCDOT 12.2.5.5: The minimum overhang width is 2ft 3in. This is to accommodate the drainage. The maximum overhang width requirement is applied typically for a CIP slab casting on top of existing beams, thus not applied for NEXT-D design.

The standard overhang width is 2ft 6in for NEXT-8, and 1ft 6in for NEXT-6, which does not satisfy the minimum requirement. In the design, an overhang width of 2ft 6in will be applied for both NEXT-8 and NEXT-6. Therefore the parapet and overhang design for NEXT-8 and NEXT-6 will be the same.

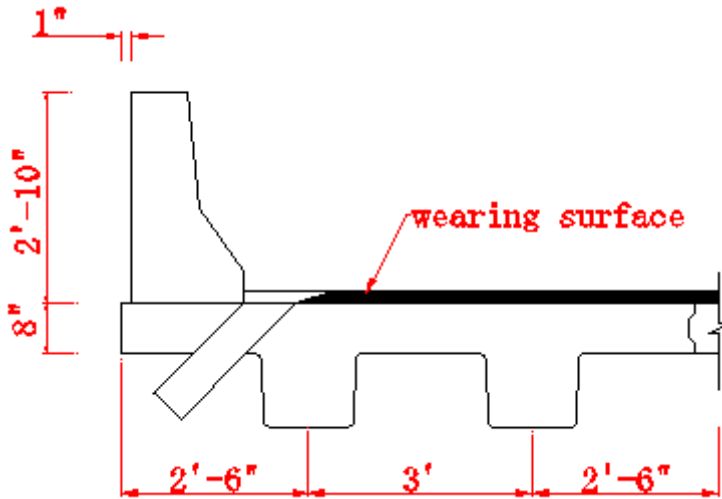


Figure F.2: Standard NEXT-8

1.2.2 Overhang thickness

AASHTO LRFD 13.7.3.1.2: For concrete deck overhangs supporting concrete parapets, the minimum overhang thickness should be 8 in, which is used in the design.

1.2.3 In summary, overhang parameters chosen in the design are:

Overhang width: $Wid_o := 2.5ft$

Overhang Thickness: $h_o := 8in$

Load: TL-4(test level 4)

AASHTO LRFD 13.7.2: TL-4 is for high speed highways, freeways, expressways, and Interstate highways with a mixture of trucks and heavy vehicles

Use #5 bars for the longitudinal bars, and #5@12in for the vertical bars

2.1 Basic parameters:

Properties of #5 bar: $d_5 := 0.625\text{in}$ $A_5 := 0.31\text{in}^2$

Properties of section 1: $H_1 := 19\text{in}$ $L_1 := 9\text{in}$

Properties of section 2: $H_2 := 10\text{in}$ $L_2 := 11\text{in}$

Properties of section 3: $H_3 := 5\text{in}$ $L_3 := 18\text{in}$

Note that when determining vertical rebar capacity, the average thickness of the section is used as shown in section 2.3.

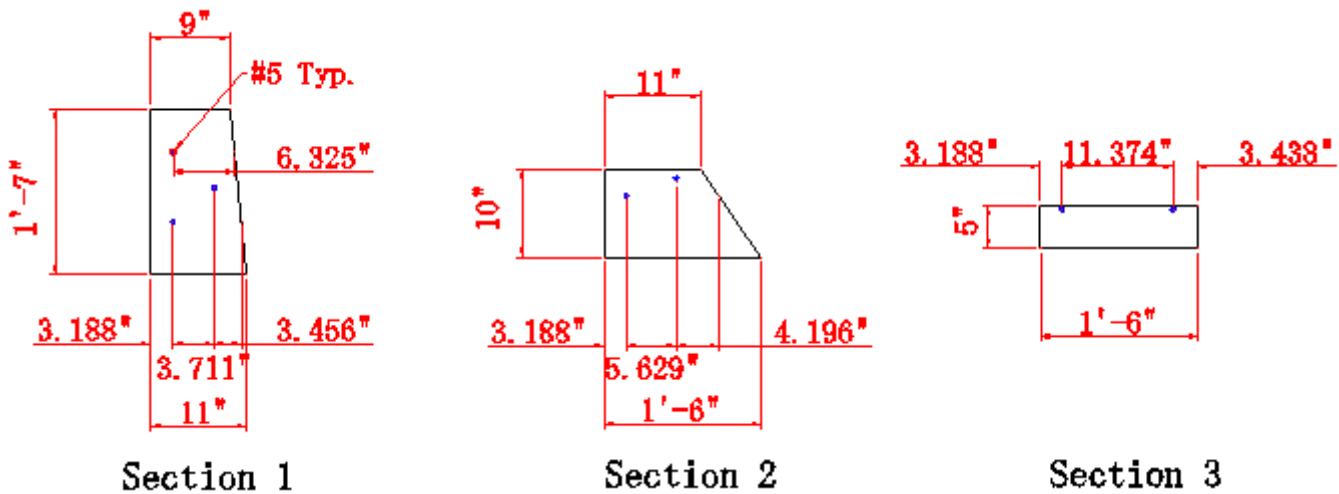


Figure F.5: Section dimensions

Height of the parapet: $H_p := 34\text{in}$

Area of the parapet: $A_p := \frac{L_1 + L_2}{2} \cdot H_1 + \frac{L_2 + L_3}{2} \cdot H_2 + L_3 \cdot H_3 = 425 \cdot \text{in}^2$

density of the parapet: $\rho_p := 150\text{pcf}$

Weight of the parapet: $P_p := A_p \cdot \rho_p = 0.443 \cdot \frac{\text{kip}}{\text{ft}}$

Design strength of the parapet: $f'_{cp} := 4\text{ksi}$

TL - 4 (Test level 4) AASHTO LRFD Table A13.2-1

Transverse load: $F_t := 54\text{kip}$ $L_t := 3.5\text{ft}$
 Longitudinal load: $F_L := 18\text{kip}$ $L_L := 3.5\text{ft}$
 Vertical load (down): $F_v := 18\text{kip}$ $L_v := 18\text{ft}$

2.2 Flexural resistance of wall about vertical axis--- M_w (kip*ft)

Positive moment represent compression at the slop face

Yield line analysis will be carried out without considering the contribution of compression rebar unless necessary. The result therefore will be conservative

When calculating R_w , Calloway (1993) found that the use of average M_w and M_c can give R_w that is 4% less than that calculated by the more correct method, which is more conservative and simpler to compute.

2.2.1 section 1

Positive moment:

$$d_{1_pos} := \frac{3.711\text{in} + 3.456\text{in} + 6.325\text{in}}{2} = 6.746\text{in}$$

$$a_{1_pos} := \frac{0.61\text{in}^2 \cdot f_y}{0.85 \cdot f_{cp} \cdot H_1} = 0.567\text{in}$$

where, $H_1 = 19\text{in}$ $f_{cp} = 4\text{ksi}$ $f_y = 60\text{ksi}$

$$\phi M_{w1_pos} := 1 \cdot 0.61\text{in}^2 \cdot f_y \cdot \left(d_{1_pos} - \frac{a_{1_pos}}{2} \right) = 19.711\text{kip}\cdot\text{ft}$$

Negative moment:

$$d_{1_neg} := 3.188\text{in} + 3.711\text{in} = 6.899\text{in}$$

$$a_{1_neg} := \frac{A_5 \cdot f_y}{0.85 \cdot f_{cp} \cdot H_1} = 0.288\text{in} \quad \text{where, } A_5 = 0.31\text{in}^2$$

$$\phi M_{w1_neg} := 1 A_5 \cdot f_y \cdot \left(d_{1_neg} - \frac{a_{1_neg}}{2} \right) = 10.47\text{kip}\cdot\text{ft}$$

Average moment:

$$\phi M_{w1_aver} := \frac{1}{2} \cdot (\phi M_{w1_pos} + \phi M_{w1_neg}) = 15.091\text{kip}\cdot\text{ft}$$

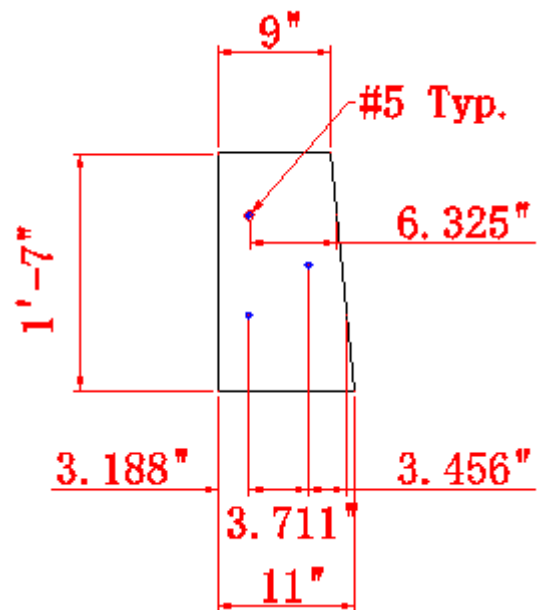


Figure F.6: Section 1

2.2.2 section 2

Positive moment:

$$d_{2_pos} := 5.629\text{in} + 4.196\text{in} = 9.825\text{in}$$

$$a_{2_pos} := \frac{A_5 \cdot f_y}{0.85 \cdot f_{cp} \cdot H_2} = 0.547\text{in} \quad \text{where,} \quad H_2 = 10\text{in}$$

$$\phi M_{w2_pos} := 1A_5 \cdot f_y \cdot \left(d_{2_pos} - \frac{a_{2_pos}}{2} \right) = 14.805 \cdot \text{kip} \cdot \text{ft}$$

Negative moment:

$$d_{2_neg} := 3.188\text{in} + 5.629\text{in} = 8.817\text{in}$$

$$a_{2_neg} := a_{2_pos}$$

$$\phi M_{w2_neg} := 1A_5 \cdot f_y \cdot \left(d_{2_neg} - \frac{a_{2_neg}}{2} \right) = 13.242 \cdot \text{kip} \cdot \text{ft}$$

Average moment:

$$\phi M_{w2_aver} := \frac{1}{2} \cdot (\phi M_{w2_pos} + \phi M_{w2_neg}) = 14.024 \cdot \text{kip} \cdot \text{ft}$$

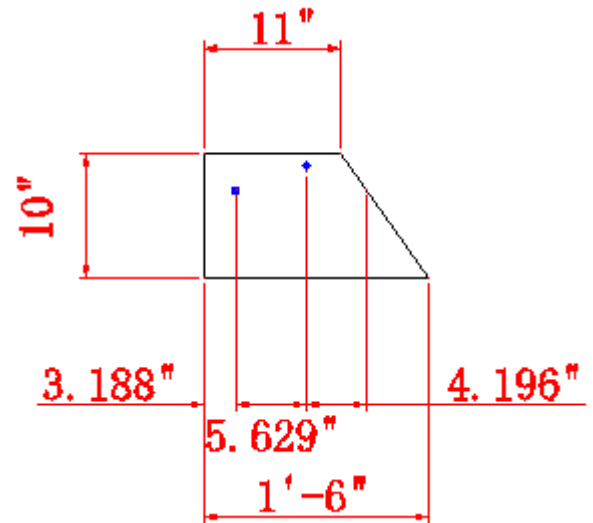


Figure F.7: Section 2

2.2.3 section 3

Positive moment:

$$d_{3_pos} := 11.374\text{in} + 3.438\text{in} = 14.812\text{in}$$

$$a_{3_pos} := \frac{A_5 \cdot f_y}{0.85 \cdot f_{cp} \cdot H_3} = 1.094\text{in} \quad \text{where,} \quad H_3 = 5\text{in}$$

$$\phi M_{w3_pos} := 1A_5 \cdot f_y \cdot \left(d_{3_pos} - \frac{a_{3_pos}}{2} \right) = 22.111 \cdot \text{kip} \cdot \text{ft}$$

Negative moment:

$$d_{3_neg} := 11.374\text{in} + 3.188\text{in} = 14.562\text{in}$$

$$a_{3_neg} := a_{3_pos}$$

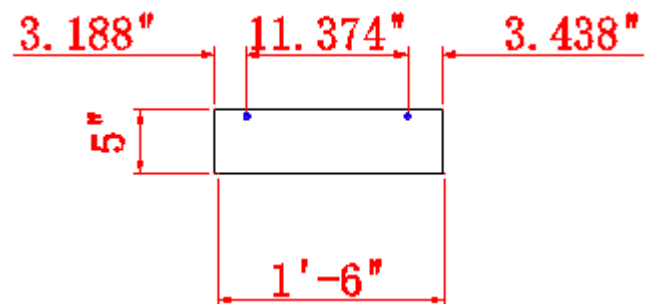


Figure F.8: Section 3

$$\phi M_{w3_neg} := 1A_s \cdot f_y \cdot \left(d_{3_neg} - \frac{a_{3_neg}}{2} \right) = 21.723 \cdot \text{kip} \cdot \text{ft}$$

Average moment:

$$\phi M_{w3_aver} := \frac{1}{2} \cdot (\phi M_{w3_pos} + \phi M_{w3_neg}) = 21.917 \cdot \text{kip} \cdot \text{ft}$$

2.2.4 Determine M_w

$$M_w := \phi M_{w1_aver} + \phi M_{w2_aver} + \phi M_{w3_aver} = 51.031 \cdot \text{kip} \cdot \text{ft}$$

2.3 Flexural resistance of wall about an axis parallel to the longitudinal axis of the bridge— M_c (kip*ft/ft)

Only negative moment capacity is needed

When calculating moment, d is the average value—10in for section 1, 14.5in for section 2, and 18in for section 3.

Note: in Figure F.9, the dimension 2.828" and 3.433" represent the distance from rebar center to the concrete edge in the horizontal direction. Since the rebar follows the slope of the concrete edge for each section, this distance does not vary with the height for each section. Refer to the triangle for the calculation of the dimension 3.433:

$$a := 2.5\text{in} + \frac{d_5}{2} = 2.813 \cdot \text{in} \quad \text{where, } 2.5\text{in is the clear cover}$$

$$\text{By using similar triangle of section 2, } \cos\theta := \frac{10}{\sqrt{10^2 + 7^2}} = 0.819$$

$$\text{Therefore, } b := \frac{a}{\cos\theta} = 3.433 \cdot \text{in}$$

2.3.1 section 1

$$A_s := 0.31\text{in}^2$$

$$d_{c1} := 10\text{in} - 2.828\text{in} = 7.172 \cdot \text{in}$$

$$a_{c1} := \frac{A_s \cdot f_y}{0.85 \cdot f_{cp} \cdot 12\text{in}} = 0.456 \cdot \text{in} \quad \text{where, } f_{cp} = 4 \cdot \text{ksi}$$

$$\phi M_{c1} := \frac{1 \cdot A_s \cdot f_y \cdot \left(d_{c1} - \frac{a_{c1}}{2} \right)}{1\text{ft}} = 10.763 \cdot \frac{\text{kip} \cdot \text{ft}}{\text{ft}}$$

2.3.2 section 2

$$d_{c2} := 14.5\text{in} - 3.433\text{in} = 11.067 \cdot \text{in}$$

$$a_{c2} := a_{c1}$$

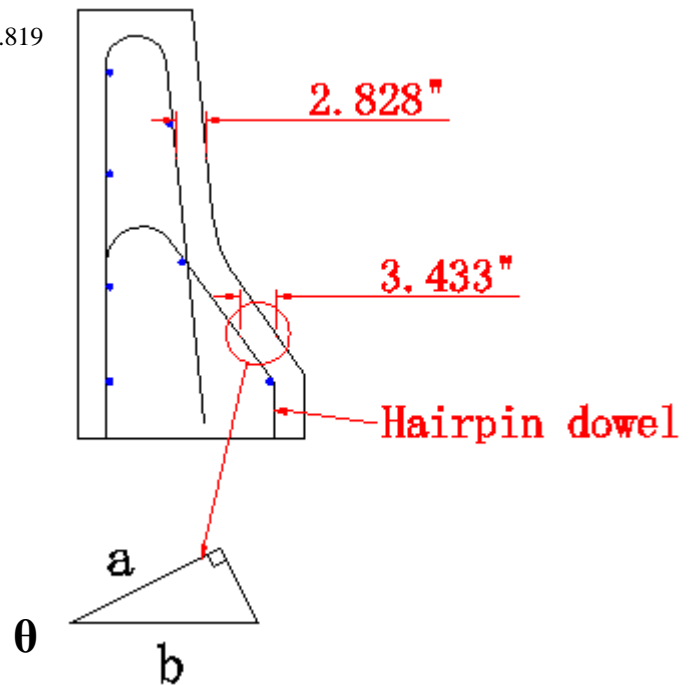


Figure F.9: Vertical rebar configuration

$$\phi M_{c2} := \frac{1 \cdot A_s \cdot f_y \cdot \left(d_{c2} - \frac{a_{c2}}{2} \right)}{1 \text{ ft}} = 16.801 \cdot \frac{\text{kip} \cdot \text{ft}}{\text{ft}}$$

Note: only the hairpin dowel is anchored, therefore only the hairpin dowel is considered in calculating ϕM_{c2} and ϕM_{c3}

2.3.3 section 3

$$d_{c3} := L_3 - 2.5 \text{ in} - \frac{d_5}{2} = 15.188 \text{ in} \quad \text{where,} \quad L_3 = 18 \text{ in} \quad d_5 = 0.625 \text{ in}$$

$$a_{c3} := a_{c1}$$

$$\phi M_{c3} := \frac{1 \cdot A_s \cdot f_y \cdot \left(d_{c3} - \frac{a_{c3}}{2} \right)}{1 \text{ ft}} = 23.187 \cdot \frac{\text{kip} \cdot \text{ft}}{\text{ft}} \quad \text{where,} \quad A_s = 0.31 \cdot \text{in}^2$$

2.3.4 Determine M_c

$$M_c := \frac{\phi M_{c1} \cdot H_1 + \phi M_{c2} \cdot H_2 + \phi M_{c3} \cdot H_3}{H_1 + H_2 + H_3} = 14.366 \cdot \frac{\text{kip} \cdot \text{ft}}{\text{ft}}$$

$$\text{where,} \quad H_1 = 19 \text{ in} \quad H_2 = 10 \text{ in} \quad H_3 = 5 \text{ in}$$

2.4 Determine critical length of yield line failure pattern --- L_c

Since we do not have top beam in this parapet design, therefore the flexural capacity along the vertical axis is zero, i.e. $M_b := 0 \text{ kip} \cdot \text{ft}$

$$L_c := \frac{L_t}{2} + \sqrt{\left(\frac{L_t}{2} \right)^2 + \frac{8 \cdot H_p \cdot (M_b + M_w)}{M_c}} = 10.892 \cdot \text{ft} \quad \text{AASHTO LRFD A13.3.1-2}$$

$$\text{where,} \quad L_t = 3.5 \text{ ft} \quad H_p = 34 \text{ in} \quad M_b = 0 \quad M_w = 51.031 \cdot \text{kip} \cdot \text{ft} \quad M_c = 14.366 \cdot \frac{\text{kip} \cdot \text{ft}}{\text{ft}}$$

2.5 Determine nominal resistance to transverse load --- R_w

$$R_w := \frac{2}{2 \cdot L_c - L_t} \cdot \left(8 \cdot M_b + 8 M_w + \frac{M_c \cdot L_c^2}{H_p} \right) = 110.455 \cdot \text{kip} \quad F_t = 54 \cdot \text{kip} \quad \text{OK} \quad \text{AASHTO LRFD A13.3.1-1}$$

The above calculations of L_c and R_w are derived from a uniform thickness barrier wall by Hirsh(1978). An yield line analysis for parapets with changing thicknesses was conducted by Calloway(1993). Hirsh's method using an average of M_w and M_c gives a R_w that is 4% less (conservative) than the more correct value and at the same time saves a lot of effort. Therefore the average values of M_w and M_c are used.

2.6 Shear transfer between concrete parapet and deck

2.6.1 External shear force---T (kip/ft)

The shear force due to vehicle collision transferred to the interface can be calculated as:

$$L_c + 2 \cdot H_p = 16.559 \cdot \text{ft} \quad \text{where,} \quad H_p = 34 \cdot \text{in}$$

$$T := \frac{R_w}{L_c + 2 \cdot H_p} = 6.67 \cdot \frac{\text{kip}}{\text{ft}} \quad \text{AASHTO LRFD A13.4.2}$$

This calculation assumes that the load spreads out at a 1:1 slope from the top of the parapet to the interface

2.6.2 Interface shear reinforcement

2.6.2.1 Parameters selection:

AASHTO LRFD 5.8.4.3: 'For concrete placed against a clean concrete surface, free of laitance, but not intentionally roughened:

cohesion factor:	$c := 0.075 \text{ksi}$
friction factor:	$\mu := 0.6$
fraction of concrete strength available to resist interface shear:	$K_1 := 0.2$
limiting interface shear resistance	$K_2 := 0.8 \text{ksi}$

2.6.2.2 Nominal interface shear resistance V_n : AASHTO LRFD 5.8.4.1

Area of concrete considered to be engaged in interface shear transfer:

$$A_{cv} := \frac{18 \text{in} \cdot 12 \text{in}}{1 \text{ft}} = 216 \cdot \frac{\text{in}^2}{\text{ft}}$$

Area of interface shear reinforcement crossing the shear plane within the area :

$$A_{vf} := \frac{A_5}{1 \text{ft}} = 0.31 \cdot \frac{\text{in}^2}{\text{ft}}$$

According to AASHTO LRFD C5.8.4.1, all reinforcement considered that make a contribution to interface shear resistance must be fully developed, therefore only the 90 degree hook of hairpin dowel is considered

$$\text{Permanent compressive force:} \quad P_c := P_p = 0.443 \cdot \frac{\text{kip}}{\text{ft}}$$

nominal shear resistance is considered to be composed of cohesion and shear friction:

$$V_n := c \cdot A_{cv} + \mu \cdot (A_{vf} \cdot f_y + P_c) = 27.626 \cdot \frac{\text{kip}}{\text{ft}} \quad \text{AASHTO LRFD C5.8.4.1}$$

$$< K_1 \cdot f'_{cp} \cdot A_{cv} = 172.8 \cdot \frac{\text{kip}}{\text{ft}}$$

$$< K_2 \cdot A_{cv} = 172.8 \cdot \frac{\text{kip}}{\text{ft}}$$

$$\phi V_n := 1 \cdot V_n = 27.626 \cdot \frac{\text{kip}}{\text{ft}} > T = 6.67 \cdot \frac{\text{kip}}{\text{ft}} \quad \text{OK} \quad \phi \text{ -- AASHTO LRFD C5.8.4.1}$$

2.6.2.3) Minimum area of interface shear reinforcement :

$$A_{\min} := \frac{0.05 \cdot A_{cv}}{\frac{f_y}{\text{ksi}}} = 0.18 \cdot \frac{\text{in}^2}{\text{ft}} < A_{vf} = 0.31 \cdot \frac{\text{in}^2}{\text{ft}} \quad \text{OK} \quad \text{AASHTO LRFD 5.8.4.4-1}$$

2.6.2.4) Development length of the hairpin dowel :

$$\text{Basic development length: } l_{hb} := \frac{38 \cdot d_5}{\sqrt{\frac{f_c}{\text{ksi}}}} = 9.316 \cdot \text{in} \quad \text{AASHTO LRFD 5.11.2.4.1-1}$$

$$\text{where, } f'_c = 6.5 \cdot \text{ksi} \quad d_5 = 0.625 \cdot \text{in}$$

Modification factors:

Sufficient cover: 0.7 AASHTO LRFD 5.11.2.4.2

The development length now is:

$$l_{dh} := l_{hb} \cdot 0.7 = 6.521 \cdot \text{in}$$

$$> 8 \cdot d_5 = 5 \cdot \text{in}$$

$$> 6 \cdot \text{in}$$

Therefore the development length should be :

$$l_{dh} = 6.521 \cdot \text{in}$$

The available development length is:

$$8 \cdot \text{in} - 1 \cdot \text{in} = 7 \cdot \text{in}$$

$$> l_{dh} = 6.521 \cdot \text{in} \quad \text{OK}$$

The extension for the standard 90° hook at the free end of the bar is: $12 \cdot d_5 + 4 \cdot d_5 = 10 \cdot \text{in}$

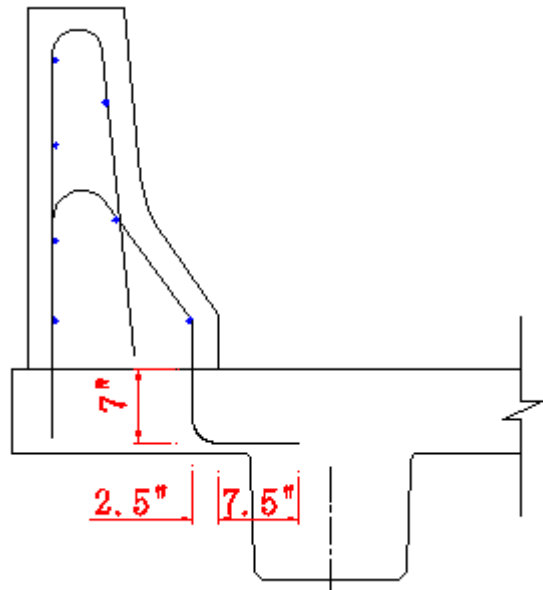


Figure F.10: Development length for hairpin dowel

2.7 Top reinforcement of the overhang:

For the exterior face of the exterior support (cross section 1-1), The moment demand comes from two parts: vehicle collision load and dead load in the overhang region.

2.7.1 Calculate M_U :

2.7.1.1 The collision moment at the base:

$$M_{CT} := -\frac{R_w \cdot H_p}{L_c + 2 \cdot H_p} = -18.9 \frac{\text{kip} \cdot \text{ft}}{\text{ft}} \quad \text{where,} \quad H_p = 34 \cdot \text{in} \quad R_w = 110.455 \cdot \text{kip} \quad L_c = 130.706 \cdot \text{in}$$

2.7.1.2 The dead load induced moment at the base:

2.7.1.2.1 Calculate center of gravity (CG.) of the parapet

Assume the parapet material is homogeneous

$$A'_1 := L_1 \cdot H_1 = 171 \cdot \text{in}^2 \quad CG_1 := 4.5 \text{in} \quad \text{where,} \quad L_1 = 9 \cdot \text{in} \quad H_1 = 19 \cdot \text{in}$$

$$A'_2 := L_2 \cdot H_2 = 110 \cdot \text{in}^2 \quad CG_2 := 5.5 \text{in} \quad \text{where,} \quad L_2 = 11 \cdot \text{in} \quad H_2 = 10 \cdot \text{in}$$

$$A'_3 := L_3 \cdot H_3 = 90 \cdot \text{in}^2 \quad CG_3 := 9 \text{in} \quad \text{where,} \quad L_3 = 18 \cdot \text{in} \quad H_3 = 5 \cdot \text{in}$$

$$A'_4 := \frac{1}{2} \cdot [(L_2 - L_1)H_1] = 19 \cdot \text{in}^2 \quad CG_4 := 9 \text{in} + \frac{2}{3} \text{in} = 9.667 \cdot \text{in}$$

$$A'_5 := \frac{1}{2} \cdot [(L_3 - L_2)H_2] = 35 \cdot \text{in}^2 \quad CG_5 := 11 \text{in} + \frac{7}{3} \text{in} = 13.333 \cdot \text{in}$$

$$x := \frac{A'_1 \cdot CG_1 + A'_2 \cdot CG_2 + A'_3 \cdot CG_3 + A'_4 \cdot CG_4 + A'_5 \cdot CG_5}{A'_1 + A'_2 + A'_3 + A'_4 + A'_5} = 6.67 \cdot \text{in}$$

$$y := 34 - \frac{A'_1 \cdot \frac{19}{2} + A'_2 \cdot 24 + A'_3 \cdot 31.5 + A'_4 \cdot \frac{38}{3} + A'_5 \cdot \left(\frac{20}{3} + 19\right)}{A'_1 + A'_2 + A'_3 + A'_4 + A'_5} = 14.615 \text{ in} \quad \text{=<from the bottom of the parapet}$$

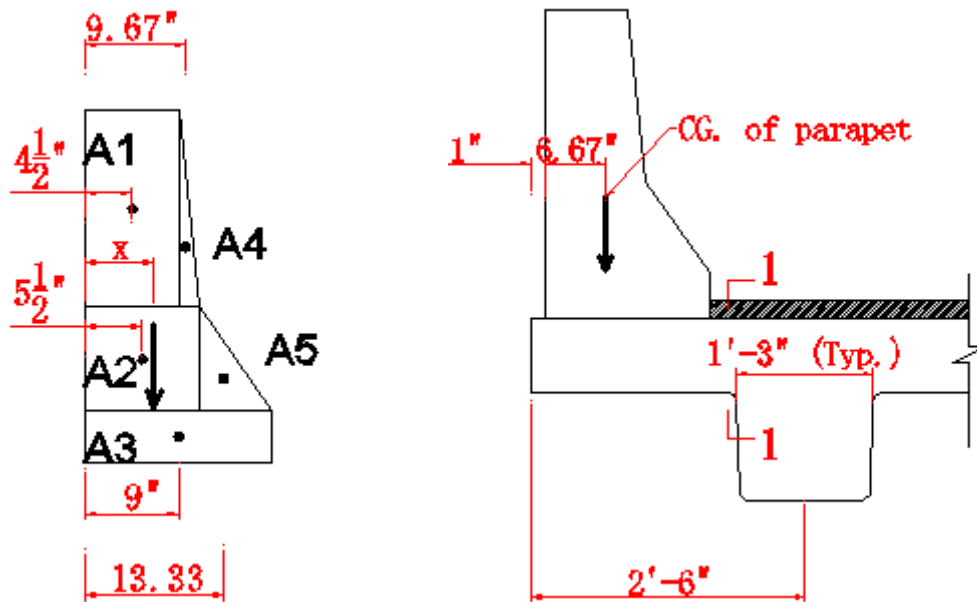


Figure F.11: Calculation of center of gravity

2.7.1.2.2 Basic parameters:

Overhang dead load: $\omega_o := W_c \cdot h_o = 100 \cdot \text{psf}$ where, $W_c = 150 \cdot \text{pcf}$ $h_o = 8 \cdot \text{in}$

Parapet dead load: $P_p = 0.443 \cdot \frac{\text{kip}}{\text{ft}}$

4in future wearing surface dead load: $\omega_{fws} := W_{fws} \cdot 4 \text{in} = 46.667 \cdot \text{psf}$ where, $W_{fws} = 140 \cdot \text{pcf}$

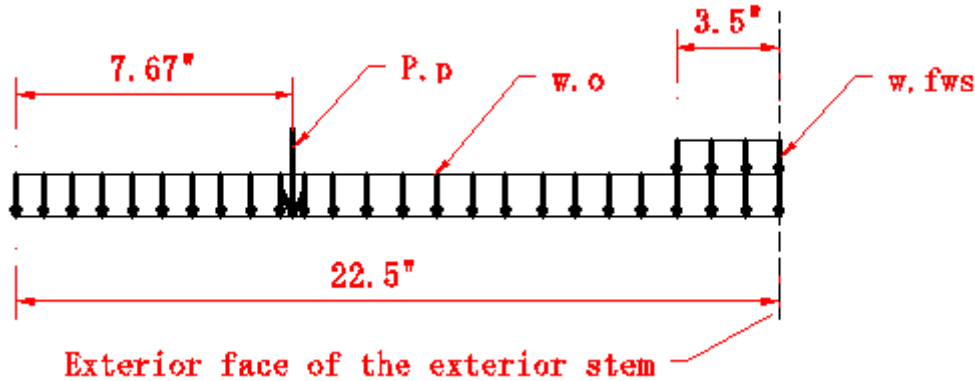


Figure F.12: Dead load configuration for cross section 1-1

2.7.1.2.3 Dead load moments at cross section 1-1:

$$M_o := -\frac{\omega_o \cdot (22.5 \text{in})^2}{2} = -0.176 \cdot \frac{\text{kip} \cdot \text{ft}}{\text{ft}}$$

$$M_p := -P_p \cdot (22.5 \text{in} - 7.67 \text{in}) = -0.547 \cdot \frac{\text{kip} \cdot \text{ft}}{\text{ft}}$$

$$M_{fws} := -\frac{\omega_{fws} \cdot (3.5 \text{in})^2}{2} = -1.985 \times 10^{-3} \cdot \frac{\text{kip} \cdot \text{ft}}{\text{ft}}$$

2.7.1.3 Design factors for extreme event II:

Resistance factor: $\phi := 1$ AASHTO LRFD 1.3.2.1

Load factors: AASHTO LRFD Table 3.4.1-1 & Table 3.4.1-2

DC: $\gamma_{p_DC} := 1.25$ <---maximum

DW: $\gamma_{p_DW} := 1.5$ <---maximum

CT: $\gamma_{p_CT} := 1$

Load modifiers: AASHTO LRFD Table 3.4.1-1

Ductility factor: $\eta_D := 1$ AASHTO LRFD 1.3.3

Redundancy factor: $\eta_R := 1$ AASHTO LRFD 1.3.4

Importance factor: $\eta_I := 1$ AASHTO LRFD 1.3.5

$$\eta := \eta_D \cdot \eta_R \cdot \eta_I = 1$$

2.7.1.4) Determine M_u :

$$M_u := \eta \left[\gamma_{p_DC} (M_o + M_p) + \gamma_{p_DW} M_{fws} + \gamma_{p_CT} M_{CT} \right] = -19.806 \cdot \frac{\text{kip}\cdot\text{ft}}{\text{ft}}$$

2.7.2 Calculate P_u :

$$P_u := T = 6.67 \cdot \frac{\text{kip}}{\text{ft}} \quad \text{AASHTO LRFD A13.4.2}$$

It should be noted that when calculating the demands at cross 1-1, the live load demands calculated are actually the demands at the section where gutterline is located. In order to calculate the live load demands at cross section 1-1, the demand at the gutterline cross section need to be spread at an angle. In the case studied, since the distance between the gutterline cross section and cross section 1-1 is short, spreading angle is not used. Therefore the combined demands (live load+dead load) are conservative for cross section 1-1. And if the demand requirement at cross section 1-1 can be satisfied, the one at the gutterline cross section can also be satisfied provided that sufficient rebar development length is provided.

2.7.3 Check rebar capacity --- For the U-bar configuration of #4@10" in the beam

2.7.3.1 Calculate ϕM_n :

Try **#5@4"** for top bar in the deck overhang.

$$d_5 = 0.625 \cdot \text{in}$$

The area of top bar is:

$$A_{st} := 0.92 \frac{\text{in}^2}{\text{ft}}$$

$$d := h_o - \text{Cover}_t - \frac{d_5}{2} = 5.188 \cdot \text{in}$$

$$\text{where, } h_o = 8 \cdot \text{in} \quad \text{Cover}_t = 2.5 \cdot \text{in}$$

$$a := \frac{A_{st} \cdot f_y}{0.85 \cdot f_c} = 0.833 \cdot \text{in} \quad \text{where, } f_c = 6.5 \cdot \text{ksi}$$

$$\phi M_n := \phi \cdot A_{st} \cdot f_y \cdot \left(d - \frac{a}{2} \right) = 21.948 \cdot \frac{\text{kip}\cdot\text{ft}}{\text{ft}}$$

$$\text{where, } \phi = 1$$

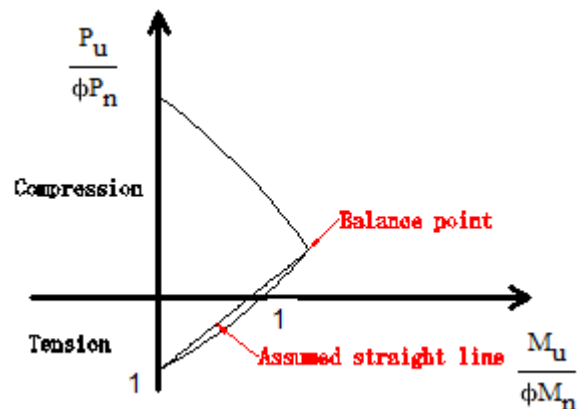


Figure F.13: Interaction curve

2.7.3.2 Calculate ϕP_n :

Assume that only the rebar resists the tensile force and all of them are yielded.

$$A_s := A_{st} + 0.24 \frac{\text{in}^2}{\text{ft}} = 1.16 \cdot \frac{\text{in}^2}{\text{ft}}$$

$$\phi P_n := \phi \cdot A_s \cdot f_y = 69.6 \cdot \frac{\text{kip}}{\text{ft}}$$

2.7.3.3 Check M_u :

Assume the interaction curve between moment and axial tension is a straight line (Figure F.13)

$$\phi M_n \cdot \left(1 - \frac{P_u}{\phi P_n} \right) = 19.844 \cdot \frac{\text{kip} \cdot \text{ft}}{\text{ft}} > -M_u = 19.806 \cdot \frac{\text{kip} \cdot \text{ft}}{\text{ft}} \quad \underline{\text{OK}}$$

3. Continuous parapet design----Impacts at the end of the wall

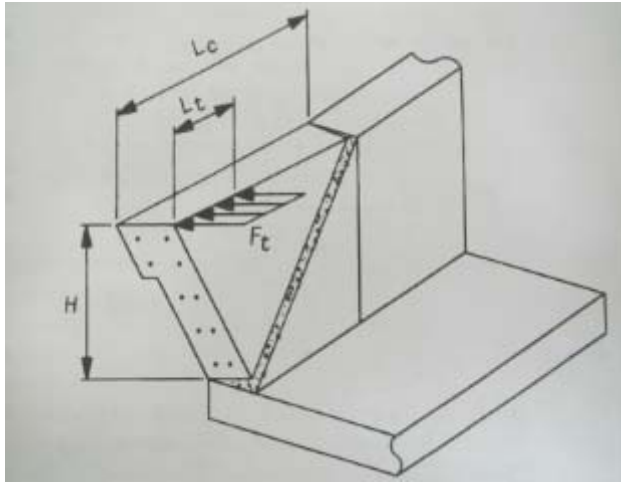


Figure F.14: Yield line pattern for impacts at the end of the wall segment adapted from LRFD CA 13.3.1

3.1 Determine critical length of yield line failure pattern ---- L_c

$$L_c := \frac{L_t}{2} + \sqrt{\left(\frac{L_t}{2} \right)^2 + \frac{H_p \cdot (M_b + M_w)}{M_c}} = 5.373 \cdot \text{ft} \quad \text{AASHTO LRFD A13.3.1-4}$$

where, $L_t = 42 \cdot \text{in}$ $H_p = 34 \cdot \text{in}$ $M_b = 0$ $M_w = 51.031 \cdot \text{kip} \cdot \text{ft}$ $M_c = 14.366 \cdot \text{kip} \cdot \frac{\text{ft}}{\text{ft}}$

3.2 Determine nominal resistance to transverse load ---- R_w

$$R_w := \frac{2}{2 \cdot L_c - L_t} \cdot \left(M_b + M_w + \frac{M_c \cdot L_c^2}{H_p} \right) = 54.487 \cdot \text{kip} > F_t = 54 \cdot \text{kip}$$

OK AASHTO LRFD A13.3.1-3

3.3 Shear transfer between concrete parapet and deck

The following procedure is just as what has been done in 2.6

The shear force due to vehicle collision transferred to the interface can be calculated as:

$$T := \frac{R_w}{L_c + H_p} = 6.64 \cdot \frac{\text{kip}}{\text{ft}} < 6.67 \frac{\text{kip}}{\text{ft}} \leq T \text{ for the middle zone}$$

Since it is the end of the parapet, the spreading length for T should be $L_c + H_p$

Nominal interface shear resistance, and minimum area of interface shear reinforcement will definitely be satisfied.

Development length of the hairpin dowel in the end zone will be the same as that in the middle zone:

3.4 Top reinforcement of the overhang:

3.4.1 Calculate M_u :

3.4.1.1 The collision moment at the base:

$$M_{CT} := -\frac{R_w \cdot H_p}{L_c + H_p} = -18.812 \cdot \frac{\text{kip} \cdot \text{ft}}{\text{ft}}$$

3.4.1.2 The dead load induced moment at the base at cross section 1-1 **as determined before:**

$$M_o = -0.176 \cdot \frac{\text{kip} \cdot \text{ft}}{\text{ft}} \quad M_p = -0.547 \cdot \frac{\text{kip} \cdot \text{ft}}{\text{ft}}$$

$$M_{fws} = -1.985 \times 10^{-3} \cdot \frac{\text{kip} \cdot \text{ft}}{\text{ft}}$$

3.4.1.3 Determine M_u :

$$M_u := \eta \cdot [\gamma_{p_DC} \cdot (M_o + M_p) + \gamma_{p_DW} \cdot M_{fws} + \gamma_{p_CT} \cdot M_{CT}] = -19.719 \cdot \frac{\text{kip} \cdot \text{ft}}{\text{ft}}$$

3.4.2 Calculate P_u :

$$P_u := T = 6.64 \cdot \frac{\text{kip}}{\text{ft}} \quad \text{AASHTO LRFD A13.4.2}$$

3.4.3 Check the original overhang reinforcement capacity **as determined before:**

$$\phi M_n = 21.948 \cdot \frac{\text{kip} \cdot \text{ft}}{\text{ft}} \quad \phi P_n = 69.6 \cdot \frac{\text{kip}}{\text{ft}}$$

$$\phi M_n \cdot \left(1 - \frac{P_u}{\phi P_n}\right) = 19.854 \cdot \frac{\text{kip} \cdot \text{ft}}{\text{ft}} > -M_u = 19.719 \cdot \frac{\text{kip} \cdot \text{ft}}{\text{ft}} \quad \text{OK}$$

4. Development length or bars in the overhang

4.1 #5 bars $d_5 = 0.625 \cdot \text{in}$ $A_5 = 0.31 \cdot \text{in}^2$

Available embedment length is calculated from the interior face of the parapet, i.e, the cross section at the gutterline. In this way, the cross section at the gutterline does not need to be checked for capacity :

According to SCDOT 17.3.7.3, the clear cover for transverse rebar in the overhang from the edge of the slab should be 3in. Therefore,

$$l_{\text{available}} := 18\text{in} + 1\text{in} - 3\text{in} = 16\text{in}$$

Straight development:

$$l_{\text{hb}} := \max\left(\frac{1.25 \cdot A_5 \cdot f_y \cdot \text{in}}{\sqrt{\frac{f_c}{\text{ksi}} \cdot \text{kip}}}, 0.4 \cdot \frac{d_5 \cdot f_y}{\text{ksi}}\right) = 15\text{in} \quad \text{where, } f_c = 6.5\text{ksi} \quad \text{AASHTO LRFD 5.11.2.1.1}$$

$$f_{\text{modS}} := 1 \quad \text{where, } f_{\text{modS}} \text{ is the modification factor for development length} \quad \text{AASHTO LRFD 5.11.2.1.2 and 5.11.2.1.3}$$

$$l_{\text{dh}} := \max(f_{\text{modS}} \cdot l_{\text{hb}}, 12\text{in}) = 15\text{in} < l_{\text{available}} = 16\text{in} \quad \text{OK}$$

4.2 #4 bars $A_4 := 0.2\text{in}^2$ $d_4 := 0.5\text{in}$

Straight development:

$$l_{\text{hb}} := \max\left(\frac{1.25 \cdot A_4 \cdot f_y \cdot \text{in}}{\sqrt{\frac{f_c}{\text{ksi}} \cdot \text{kip}}}, 0.4 \cdot \frac{d_4 \cdot f_y}{\text{ksi}}\right) = 12\text{in}$$

$$f_{\text{modS}} := 1 \quad \text{AASHTO LRFD 5.11.2.1.2 and 5.11.2.1.3}$$

$$l_{\text{dh}} := \max(f_{\text{modS}} \cdot l_{\text{hb}}, 12\text{in}) = 12\text{in}$$

5. Summary

5.1 Parapet reinforcement capacity VS demand

Vertical: #5@12in Longitudinal: #5

Middle zone:

$$R_w := \frac{2}{2 \cdot L_c - L_t} \cdot \left(8 \cdot M_b + 8M_w + \frac{M_c \cdot L_c^2}{H_p} \right) = 110.455 \cdot \text{kip} > F_t = 54 \cdot \text{kip} \quad \text{OK}$$

End zone:

$$R_w := \frac{2}{2 \cdot L_c - L_t} \cdot \left(M_b + M_w + \frac{M_c \cdot L_c^2}{H_p} \right) = 54.487 \cdot \text{kip} > F_t = 54 \cdot \text{kip} \quad \text{OK}$$

5.2 Overhang reinforcement capacity VS demand

Top bar: #5@4in

Bottom bar: #4@10in

Note: #4@10in is the worst situation considered

Impact within the wall segment

$$\phi M_n \cdot \left(1 - \frac{P_u}{\phi P_n} \right) = 19.844 \cdot \frac{\text{kip} \cdot \text{ft}}{\text{ft}} > -M_u = 19.806 \cdot \frac{\text{kip} \cdot \text{ft}}{\text{ft}} \quad \underline{\text{OK}}$$

Impact at the end of the wall segment

$$\phi M_n \cdot \left(1 - \frac{P_u}{\phi P_n} \right) = 19.854 \cdot \frac{\text{kip} \cdot \text{ft}}{\text{ft}} > -M_u = 19.719 \cdot \frac{\text{kip} \cdot \text{ft}}{\text{ft}} \quad \underline{\text{OK}}$$

This page intentionally left blank

NEXT-6---Deck Design Outline:

1. Deck properties:
2. 3d finite element method---Loads and load effects:
 - 2.1 Dead load:
 - 2.2 Live load
 - 2.3 Moment distribution
 - 2.4 Distribution strip width:
 - 2.5 Load combination
 - 2.6 Design demands for a 1ft strip:
3. Demands based on 1d AASHTO FEM:
4. 40ft bridge design--- #4 @ 7in
 - 4.1 Development length
 - 4.2. Limits of reinforcement
 - 4.2.1 Maximum reinforcement
 - 4.2.2 Minimum reinforcement
 - 4.3. Distribution reinforcement
 - 4.4. Shrinkage and temperature reinforcement
 - 4.5. Control of cracking
 - 4.5.1 Check of the positive moment reinforcement
 - 4.5.2 Check of the negative moment reinforcement
5. 30ft bridge design using #4@10in
 - 5.1 Development length
 - 5.2. Minimum reinforcement
 - 5.2.1 Positive moment
 - 5.2.2 Negative moment
 - 5.3. Distribution reinforcement
 - 5.4. Shrinkage and temperature reinforcement
 - 5.5. Control of cracking
 - 5.5.1 Check of the positive moment reinforcement
 - 5.5.2 Check of the negative moment reinforcement
6. 22 ft bridge design using #4@10in
 - 6.1 Development length
 - 6.2. Distribution reinforcement
 - 6.3. Shrinkage and temperature reinforcement

7. Design summary

7.1 Reinforcement configuration

7.2 Criteria check

7.2.1 Demand VS Capacity

7.2.2 Minimum reinforcement check

7.2.3 Cracking control check

1. Deck properties:

Cross section:	NEXT-6
Effective width of a an interior beam (including shear key):	$b_{6int} := 6\text{ft}$
Area of an interior beam:	$A_{6int} := 955.4\text{in}^2$
Effective width of a an exterior beam (including shear key):	$b_{6ext} := 7\text{ft}$
Area of an exterior beam:	$A_{6ext} := 1051.4\text{in}^2$
Structural deck depth of the deck:	$h := 8\text{in}$
Moment of inertia considered:	$I := \frac{1}{12} \cdot 1\text{ft} \cdot h^3 = 512 \cdot \text{in}^4$
Section modulus:	$S_r := \frac{I}{h} \cdot 2 = 128 \cdot \text{in}^3$
Deck top cover:	$\text{Cover}_t := 2.5\text{in}$ AASHTO LRFD Table 5.12.3-1
Deck bottom cover:	$\text{Cover}_b := 1.0\text{in}$ AASHTO LRFD Table 5.12.3-1
Reinforced concrete density:	$w_c := 150\text{pcf}$
Concrete compressive strength (final):	$f'_c := 6.5\text{ksi}$
Rebar Young's modulus:	$E_s := 29000\text{ksi}$
Reinforcement strength:	$f_y := 60\text{ksi}$
Bituminous wearing surface:	$w_{fws} := 140\text{pcf}$ AASHTO LRFD Table 3.5.1-1

2. 3d finite element method----Loads and load effects:

2.1 Dead load:

DC :

parapet self weight : $w_p := 443\text{plf}$

Parapet self weight is uniformly distributed to the outer two beams. Therefore for each beam mentioned above,

$$w_b := \frac{w_p}{b_{6int} + b_{6ext}} = 0.034 \cdot \frac{\text{kip}}{\text{ft}^2} \quad \text{where,} \quad b_{6int} = 6 \cdot \text{ft} \quad b_{6ext} = 7 \cdot \text{ft}$$

Beam self weight:

Exterior beam:

$$w_{g_ext} := \frac{w_c \cdot A_{6ext}}{b_{6ext}} = 0.156 \cdot \frac{\text{kip}}{\text{ft}^2} \quad \text{where,} \quad A_{6ext} = 1.051 \times 10^3 \cdot \text{in}^2 \quad w_c = 150 \cdot \text{pcf}$$

Interior beam:

$$w_{g_int} := \frac{w_c \cdot A_{6int}}{b_{6int}} = 0.166 \cdot \frac{\text{kip}}{\text{ft}^2} \quad \text{where,} \quad A_{6int} = 955.4 \cdot \text{in}^2$$

DW :

Future wearing surface (4in on average):

$$DW := (4\text{in} \cdot w_{fws}) = 0.047 \cdot \frac{\text{kip}}{\text{ft}^2} \quad \text{where,} \quad w_{fws} = 140 \cdot \text{pcf}$$

The load from future wearing surface is distributed from face to face of the two parapets.

In the finite element model, the above area loads are distributed to the shell element of the slab. For the frame element of the shear key, according to the calculation in NEXT-8, the load exerted on the shear key has little influence on the demands, therefore load is not applied on the shear key for NEXT-6.

2.2 Live load

LRFD Art 3.6.1.3.3 specifies that when the refined methods are used to analyze decks, if the slab spans primarily in the transverse direction, only the axles of the design truck of Article 3.6.1.2.2 or design tandem of Article 3.6.1.2.3 shall be applied to the deck slab.

In order to obtain the most critical demand, a single design tandem specified in LRFD Art 3.6.1.2.3 is applied to the finite element model, moving across the bridge model transversely and longitudinally. The position of the tandem follows that specified in LRFD Art. 3.6.1.3: the design tandem shall be positioned transversely such that the center of any wheel load is not closer than: For the design of components other than deck overhang---2 ft from the edge of the design lane. In this case, the axle load is positioned no closer than 2ft from the face of the parapet.

2.3 Moment distribution

The total unfactored transverse moment demands on the deck for the 40ft span bridge resulting from the dead loads and live loads are displayed as follows, in which the black lines represent the location of the shear key:

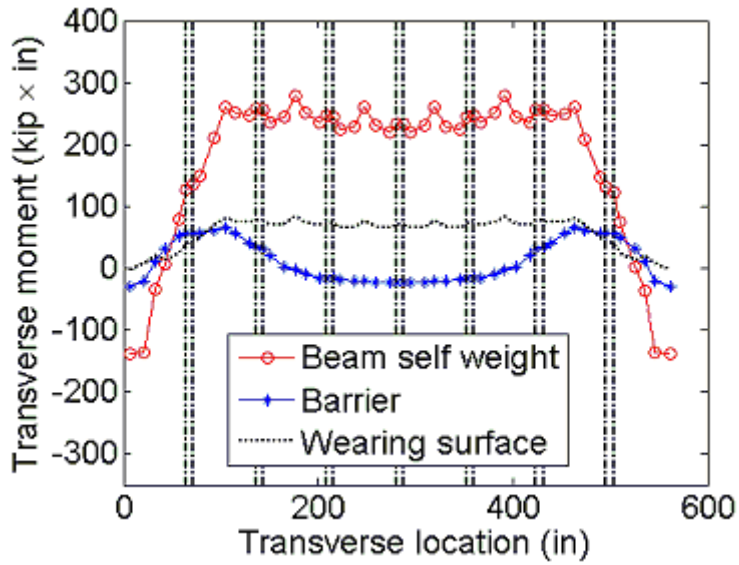


Figure F.15: Moment effects of dead loads

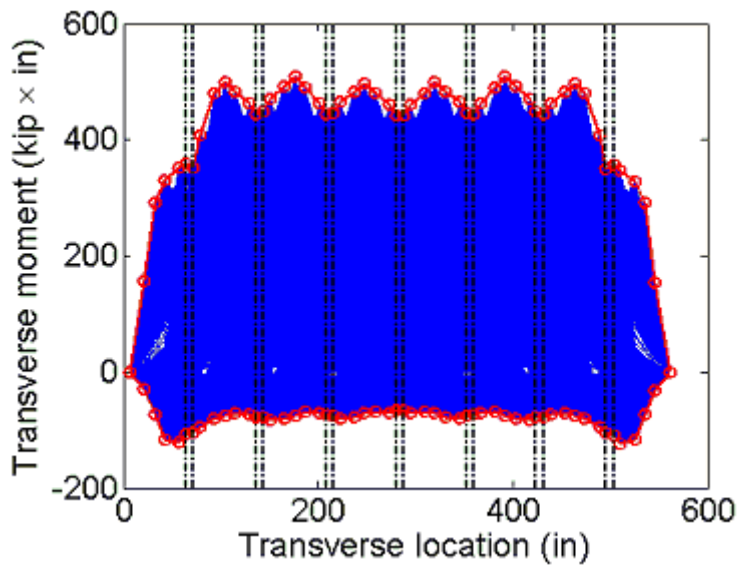


Figure F.16: Moment effects of design tandem

2.4 Distribution strip width:

The distribution width for the design tandem is 10ft

2.5 Load combination

LRFD Table 3.4.1-1

strength I limit state:

$$\text{Maximum } Q = 1.25(\text{DC}) + 1.50(\text{DW}) + 1.75(\text{LL} + \text{IM})$$

$$\text{Minimum } Q = 0.90(\text{DC}) + 0.65(\text{DW}) + 1.75(\text{LL} + \text{IM})$$

service I limit state:

$$Q = 1(\text{DC}) + 1(\text{DW}) + 1(\text{LL} + \text{IM})$$

where

LL = live load effect including multiple presence factor 1.2

IM = dynamic load allowance percentage IM := 1.33 LRFD Table 3.6.2.1-1

2.6 Design demands for a 1ft strip:

The dead load effect is divided by the total span length to get the normalized demand on a 1ft strip. And the live load effect is divided by the strip width 10ft to get the normalized demand on the 1ft strip. The resulting normalized transverse moment demands combined together for Strength I and Service I limit states for the 40ft span are displayed below. Positive moment means the bottom deck fiber is in tension

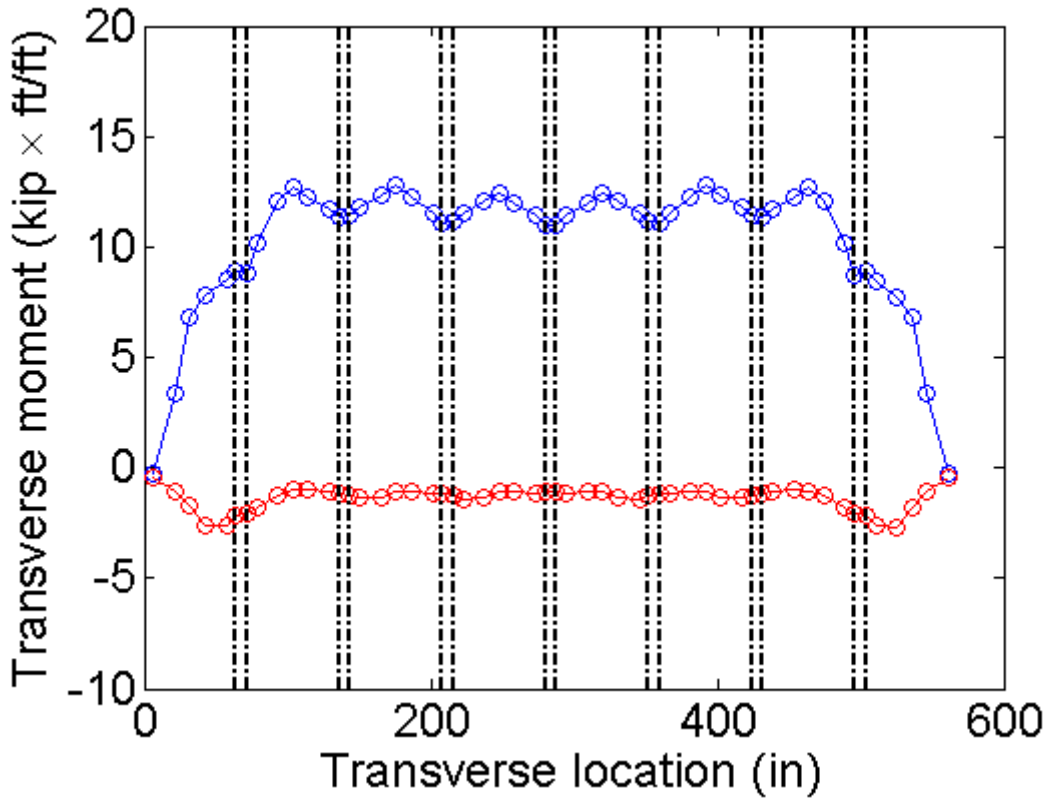


Figure F.17: Demand distribution in Strength I limit state

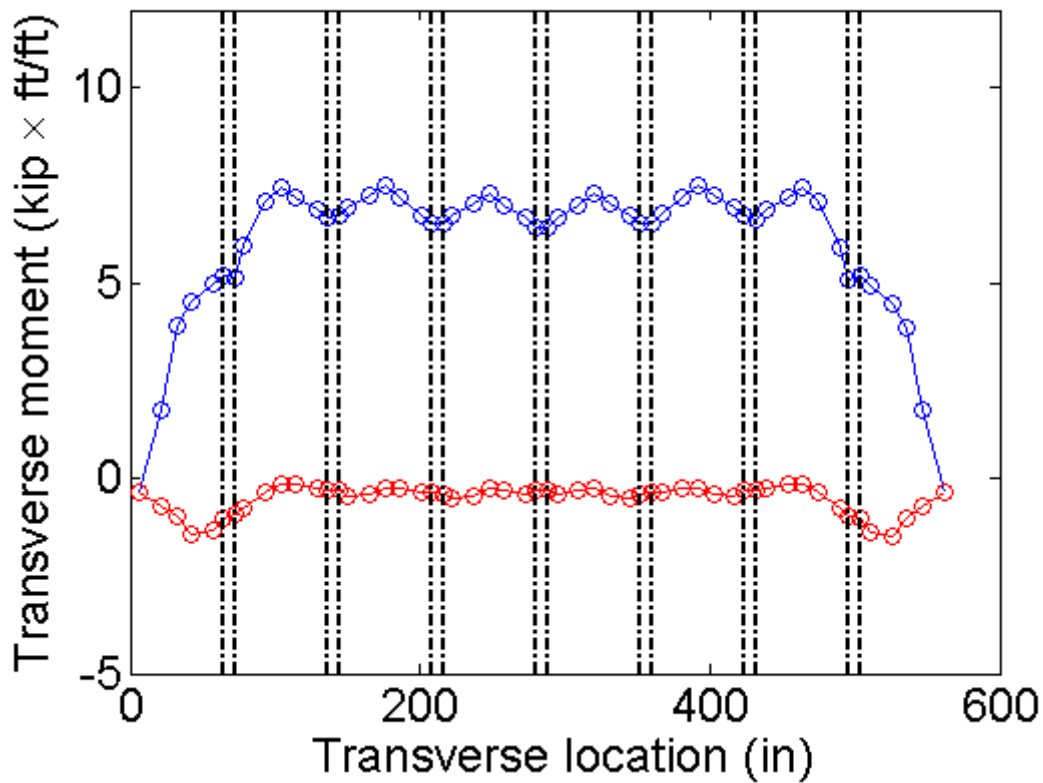


Figure F.18: Demand distribution in Service I limit state

A summary of the demands on a 1ft strip for the 22ft, 30ft, and 40ft spans are listed as follows:

		Strength I limit state		
	Location	22 ft	30 ft	40 ft
M+ (kip*ft/ft)	Span w/o key	6.15	8.85	12.70
M+ (kip*ft/ft)	Span w/ key	4.35	7.37	11.84
M- (kip*ft/ft)	Exterior beam	-0.89	-1.55	-2.61
M- (kip*ft/ft)	Interior beam	-0.98	-1.29	-1.41

Table 2

Service I limit state

	Location	22 ft	30 ft	40 ft
M+ (kip*ft/ft)	Span w/o key	3.59	5.19	7.47
M+ (kip*ft/ft)	Span w/ key	2.51	4.28	6.94
M- (kip*ft/ft)	Exterior beam	-0.45	-0.82	-1.43
M- (kip*ft/ft)	Interior beam	-0.54	-0.64	-0.51

Notice that in the deck span that has no shear key, the reinforcement is doubled by the development length, which will be considered in checking the moment capacity and cracking control.

3. Demands based on 1d AASHTO FEM:

The final design demands are calculated based on the results from 1d AASHTO FEM using a finite element software SAP2000. In the FEM, the deck (including shear key) is modeled as a continuous beam using frame elements and the stems are modeled as rigid supports. Refer to the deck design guideline in Chapter 9.2.1 for details.

From the 1d AASHTO FEM, the maximum positive moment and critical negative moment (unfactored) resulting from a single 32kip axle of the design truck as specified in LRFD Article 3.6.1.2.2 are:

$$M_{p_total} := 123.09 \text{kip}\cdot\text{in} \quad M_{n_total} := -51.80 \text{kip}\cdot\text{in}$$

The strip widths for positive and negative moment for cast-in-place deck without stay-in-place concrete formwork are: LRFD Table 4.6.2.1.3-1

$$M_{p_width} = 26 + 6.6 \cdot s_{design} \quad M_{n_width} = 48 + 3 \cdot s_{design}$$

where,

$$s_{design} = \text{average stem spacing (ft)} \quad s_{design} := 3$$

Therefore,

$$M_{p_width} := (26 + 6.6 \cdot s_{design}) \text{in} = 45.8 \cdot \text{in}$$

$$M_{n_width} := (48 + 3 \cdot s_{design}) \text{in} = 57 \cdot \text{in}$$

The normalized demands for a 1ft load strip are:

$$M_{n_AASHTO} := \frac{M_{n_total}}{M_{n_width}} = -0.909 \cdot \frac{\text{kip}\cdot\text{ft}}{\text{ft}}$$

$$M_{p_AASHTO} := \frac{M_{p_total}}{M_{p_width}} = 2.688 \cdot \frac{\text{kip}\cdot\text{ft}}{\text{ft}}$$

Based on the formula proposed, the design demands from the live load are:

Positive design moment:

$$\text{For span w/o key: } M_{\text{positive}} = M_{p_AASHTO} \cdot \left[0.77 + 0.0027 \cdot \left(l_{\text{design}}^{1.3} \cdot s_{\text{design}}^{1.4} - 244 \right) \right]$$

$$\text{For span w/ key: } M_{\text{positive}} = M_{p_AASHTO} \cdot \left[0.58 + 0.0196 \cdot \left(l_{\text{design}}^1 \cdot s_{\text{design}}^{0.8} - 51 \right) \right]$$

Negative design moment:

$$\text{For exterior beams: } M_{\text{negative}} = M_{n_AASHTO} \cdot \left[0.4 + 6.28 \cdot \left(l_{\text{design}}^{0.1} \cdot s_{\text{design}}^{0.2} - 1.69 \right) \right]$$

$$\text{For interior beams: } M_{\text{negative}} = M_{n_AASHTO}$$

The negative moment demand in the interior beam shall not exceed that in the exterior beam.

where,

l_{design} = design span length, (ft) $l_{\text{design}} = 39\text{ft}$ for the 40ft span bridge

M_{positive} = unfactored positive moment demand from live load (kip*ft/ft)

M_{negative} = unfactored negative moment demand from live load (kip*ft/ft)

Based on the formula, the normalized live load demands (kip*ft/ft) are:

Table 3	Location	22 ft	30 ft	40 ft
M_{positive} (kip*ft/ft)	Span w/o key	2.07	2.99	4.25
M_{positive} (kip*ft/ft)	Span w/ key	1.54	2.55	3.82
M_{negative} (kip*ft/ft)	Exterior beam	-0.36	-0.67	-0.97
M_{negative} (kip*ft/ft)	Interior beam	-0.91	-0.91	-0.91

Since the first two negative moment demands in the interior beam exceed those in the exterior beam, these two values will be equal to those in the exterior beam. There is not much difference between the negative moment values for the 40ft span, therefore, it is decided to use the negative moment demands in the exterior beam for all the beam design for NEXT-6.

Therefore the table above is updated to be:

Table 4	Location	22 ft	30 ft	40 ft
M_{positive} (kip*ft/ft)	Span w/o key	2.07	2.99	4.25
M_{positive} (kip*ft/ft)	Span w/ key	1.54	2.55	3.82
M_{negative} (kip*ft/ft)	All beams	-0.36	-0.67	-0.97

The dead load effect is obtained based on the 1d AASHTO FEM. The moment demands from beam self weight, barrier self weight, and wearing surface are combined for the Strength I limit state and Service limit state. For each limit state, both the maximum and minimum combined moment demands are obtained and listed in the following table.

Table 5	Strength I	Service I
$M_{\text{p_DL}}$	0.1724	0.1351
$M_{\text{n_DL}}$ (kip*ft/ft)	-0.7662	-0.6097

The total load effect is calculated as:

$$M_{\text{p_total}} = M_{\text{positive}} \cdot \text{IM} \cdot m \cdot \text{LF} + M_{\text{p_DL}} \cdot 4$$

$$M_{\text{n_total}} = M_{\text{negative}} \cdot \text{IM} \cdot m \cdot \text{LF} + M_{\text{n_DL}}$$

where,

$M_{\text{p_total}}$ = final design positive moment demand for either Strength I or Service I limit state (kip*ft/ft)

$M_{\text{n_total}}$ = final design negative moment demand for either Strength I or Service I limit state (kip*ft/ft)

M_{positive} = unfactored positive moment demand from live load (kip*ft/ft)

M_{negative} = unfactored negative moment demand from live load (kip*ft/ft)

$M_{\text{p_DL}}$ = factored positive moment demand from dead load (kip*ft/ft)

$M_{\text{n_DL}}$ = factored negative moment demand from dead load (kip*ft/ft)

IM = dynamic load allowance percent, IM = 1.33 LRFD Table 3.6.2.1-1

m = multiple presence factor, MP = 1.2 LRFD Table 3.6.1.1.2-1

LF = live load factor, LL = 1.75 for Strength I limit state, and 1 for Service I limit state
LRFD Table 3.4.1-1

The final design demands for Strength I and Service I limit states are listed in Table 6 and 7. The values given in bracket are the demands based on 3d FEM results. The percentage errors for the unconservative demands are also given by taking the 3d FEM results as the 'correct' values. The unconservative values are all within five percentage of the FEM results.

Table 6

		Strength I limit state			
		Location	22 ft	30 ft	40 ft
M_{p_total} (kip*ft/ft)	Span w/o key		6.46 (6.15)	9.04 (8.85)	12.57 (12.70) -1.0%
M_{p_total} (kip*ft/ft)	Span w/ key		4.98 (4.35)	7.81 (7.37)	11.36 (11.84) -4.1%
M_{n_total} (kip*ft/ft)	All beams		-1.77 (-0.98)	-2.65 (-1.55)	-3.49 (-2.61)

Table 7

		Service I limit state			
		Location	22 ft	30 ft	40 ft
M_{p_total} (kip*ft/ft)	Span w/o key		3.84 (3.59)	5.31 (5.19)	7.33 (7.47) -2.0%
M_{p_total} (kip*ft/ft)	Span w/ key		2.99 (2.51)	4.61 (4.28)	6.64 (6.94) -4.3%
M_{n_total} (kip*ft/ft)	All beams		-1.18 (-0.54)	-1.69 (-0.82)	-2.16 (-1.43)

Comparing the demands with capacities provided by various rebar configurations:

Table 8	Location	Demand			Capacity provided			
		22 ft	30 ft	40 ft	#4@7in	#4@8in	#4@9in	#4@10in
M_{p_total} (kip*ft/ft)	Span w/o key	6.46	9.04	12.57	N/A	N/A	N/A	N/A
M_{p_total} (kip*ft/ft)	Span w/ key	4.98	7.81	11.36	13.59	11.71	10.56	9.79
M_{n_total} (kip*ft/ft)	All beams	-1.77	-2.65	-3.49	-8.90	-7.80	-7.05	-6.55

For the deck span without shear key---which is the deck in-between the two stems of a beam--- due to the development length of the rebar, the actual capacity is larger than that in the span with shear key. This also applies to the table in section 4, 5, 6, and 7.2.

4. 40ft bridge design--- #4 @ 7in

A summary of the normalized demands in Strength I limit state for the 40ft span, according to Table 6, is as follows:

Table 9	Location	Demand	Capacity provided by #4@7in Ubar
M_{p_total} (kip*ft/ft)	Span w/o key	12.57	N/A
M_{p_total} (kip*ft/ft)	Span w/ key	11.36	13.59
M_{n_total} (kip*ft/ft)	All beams	-3.49	-8.90

4.1 Development length

Rebar area: $A_4 := 0.2\text{in}^2$ Rebar diameter: $d_4 := 0.5\text{in}$

Straight development: LRFD Art. 5.11.2.1

$$l_{hb} := \max\left(\frac{1.25 \cdot A_4 \cdot f_y \cdot \text{in}}{\sqrt{\frac{f'_c}{\text{ksi}} \cdot \text{kip}}}, 0.4 \cdot \frac{d_4 \cdot f_y}{\text{ksi}}\right) = 12 \cdot \text{in} \quad \text{where, } f'_c = 6.5 \cdot \text{ksi} \quad f_y = 60 \cdot \text{ksi}$$

$$f_{\text{modS}} := 1$$

$$l_{dh} := \max(f_{\text{modS}} \cdot l_{hb}, 12\text{in}) = 12 \cdot \text{in}$$

According to LRFD Art. 5.11.1.2.1, except at supports of simple spans and at the free ends of cantilevers, reinforcement shall be extended beyond the point at which it is no longer required to resist flexure for a distance calculated above.

Interior beam:

For the both positive and negative reinforcement, this point is taken at the centerline of the beam

4.2. Limits of reinforcement

4.2.1 Maximum reinforcement

The check of maximum reinforcement limits was removed from the LRFD Specifications in 2005. LRFD Art. 5.7.3.3.1

4.2.2 Minimum reinforcement

At any section of a noncompression-controlled flexural component, the amount of prestressed and nonprestressed tensile reinforcement shall be adequate to develop a factored flexural resistance, M_r , at least equal to the lesser of:

1. 1.33 times the factored moment required by the applicable strength load combination specified in Table 3.4.1-1 (Strength I); and

$$2. M_{cr} = \gamma_3 \cdot (\gamma_1 \cdot f_r) \cdot S_r \quad \text{LRFD Eq. 5.7.3.3.2-1}$$

The above equation is a simplified form of LRFD Equation 5.7.3.3.2-1 because no composite section exists, therefore the composite and noncomposite section modulus are the same. Also since there is no transverse post-tensioning, the cracking moment capacity won't be increased.

where,

f_r = modulus of rupture of concrete LRFD Art 5.4.2.6

$$f_r := 0.37 \sqrt{\frac{f_c}{\text{ksi}}} \text{ ksi} = 0.943 \cdot \text{ksi}$$

S_r = section modulus for the extreme fiber of the section where tensile stress is caused by externally applied loads (in³) $S_r = 128 \cdot \text{in}^3$

γ_1 = flexural cracking variability factor

$\gamma_1 := 1.2$ for precast segmental structures

γ_3 = ratio of specified minimum yield strength to ultimate tensile strength of the reinforcement

$\gamma_3 := 0.75$ for A 706, Grade 60 reinforcement

$$M_{cr} := \gamma_3 \cdot (\gamma_1 \cdot f_r) \cdot S_r = 9.056 \cdot \text{kip} \cdot \text{ft}$$

The above M_{cr} applies to any cross section in the deck

4.2.2.1 Positive moment

The factored normalized positive moment demand in Strength I limit state in the deck span with shear key, according to Table 9, is:

$$M_u := 11.36 \text{ kip} \cdot \text{ft}$$

$$\text{Thus, } 1.33 \cdot M_u = 15.109 \cdot \text{kip} \cdot \text{ft} > M_{cr} = 9.056 \cdot \text{kip} \cdot \text{ft}$$

Therefore M_{cr} requirement controls.

The factored capacity provided by #4@7in is:

$$M_r := 13.59 \text{ kip} \cdot \text{ft} > M_{cr} = 9.056 \cdot \text{kip} \cdot \text{ft} \quad \text{OK}$$

This criteria can be met at every deck section.

4.2.2.2 Negative moment

The factored normalized negative moment demand in Strength I limit state for all the beams, according to Table 9, is:

$$M_u := -3.49 \text{ kip} \cdot \text{ft}$$

$$\text{Thus, } |1.33 \cdot M_u| = 4.642 \cdot \text{kip} \cdot \text{ft} < M_{cr} = 9.056 \cdot \text{kip} \cdot \text{ft}$$

Therefore $|1.33 \cdot M_u|$ requirement controls.

The least negative moment capacity comes from the rebar configuration of #4 @7in

$$|M_r| = 8.9 \text{ kip}\cdot\text{ft} > |1.33 \cdot M_u| = 4.642 \cdot \text{kip}\cdot\text{ft} \quad \text{OK}$$

Therefore this criteria can be met at every deck section.

4.3. Distribution reinforcement

The required area of secondary reinforcement at the bottom of the deck is a percentage of the primary positive moment reinforcement. For primary reinforcement perpendicular to traffic, LRFD Art. 9.7.3.2 specifies that the percentage should be:

$$\text{Percentage} = \frac{220}{\sqrt{S}} \leq 67\%$$

where

S = the effective span length (ft) LRFD Art. 9.7.2.3

$$S := 3 \text{ ft} - 15 \text{ in} = 21 \cdot \text{in}$$

$$\text{Percentage} := \frac{220}{\sqrt{\frac{S}{\text{ft}}}} = 166.304\% \quad \text{use} \quad 67\%$$

For both the Interior beam and exterior beam

Positive moment reinforcement in the transverse direction (#4@7in): $A_s := 0.34 \frac{\text{in}^2}{\text{ft}}$

$$A_s \cdot 67\% = 0.228 \cdot \frac{\text{in}^2}{\text{ft}}$$

For longitudinal bottom bar, Use #4@10in, which gives $0.24 \frac{\text{in}^2}{\text{ft}}$

4.4. Shrinkage and temperature reinforcement

The minimum reinforcement area per foot, on each face and in each direction, shall satisfy:

$$A_{s_TS} \geq \frac{1.3 \cdot b \cdot h}{2 \cdot (b + h) \cdot f_y} \quad \text{LRFD Eq. 5.10.8-1}$$

where

A_{s_TS} = area of reinforcement in each direction and each face (in^2/ft)

b = least width of component section (in) b := 1ft

h = least thickness of component section (in) h = 8·in

f_y = specified yield strength of reinforcing bars $f_y = 60 \text{ ksi} \leq 75 \text{ ksi}$

Therefore

$$A_{s_TS} \geq 1 \cdot \frac{1.3 \cdot 12 \cdot 8}{2 \cdot (12 + 8) \cdot 60} \cdot \frac{\text{in}^2}{\text{ft}} = 0.052 \cdot \frac{\text{in}^2}{\text{ft}}$$

Use $A_{s_TS} := 0.11 \frac{\text{in}^2}{\text{ft}}$ LRFD Eq. 5.10.8-2

This requirement can be satisfied in each direction and each face. Since the deck depth is more than 6in, the shrinkage and temperature rebars need to be provided equally on both layers. The maximum spacing of the rebar shall not exceed either 3 times the deck depth or 18in. The top longitudinal bars are provided by the bonded reinforcement, which is #4 @7in for the exterior beam, and #4@10in for the interior beam as calculated below.

From CONSPAN, at release, the tension stress in the top fiber of the **exterior beam** at the transfer cross section is:

$$f_t := -0.476 \text{ksi}$$

The compressive stress in the bottom fiber of the beam at the same cross section is:

$$f_b := 2.78 \text{ksi}$$

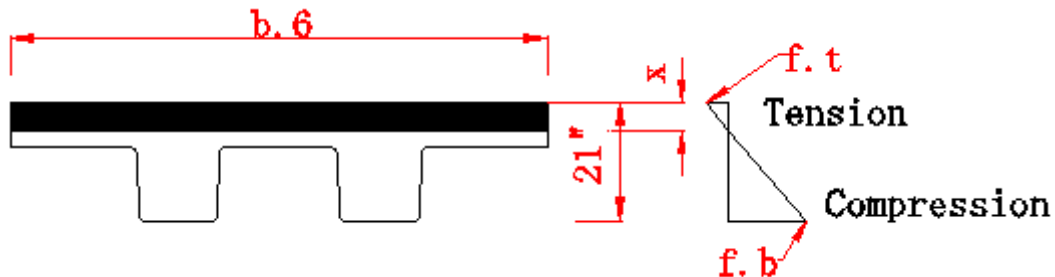


Figure F.19: Stress distribution adapted from LRFD C5.9.4.1.2

The depth of the tensile zone x is: LRFD C5.9.4.1.2

$$\frac{-f_t}{x} = \frac{f_b}{21\text{in} - x}$$

$$x := -\frac{21 \cdot f_t \cdot \text{in}}{f_b - f_t} = 3.07 \cdot \text{in} < 8\text{in}$$

The tensile force T in the concrete is: $T := \frac{f_t}{2} \cdot b_{6\text{ext}} \cdot x$

where, $b_{6\text{ext}}$ is the width of the beam at top $b_{6\text{ext}} = 84 \cdot \text{in}$

Therefore $T := \frac{-f_t}{2} \cdot b_{6\text{ext}} \cdot x = 61.376 \cdot \text{kip}$

The required area of bonded reinforcement is: $A_{\text{req}} = \frac{T}{f_s}$

where $f_s := 0.5 \cdot f_y = 30 \cdot \text{ksi}$ LRFD C5.9.4.1.2

$$\text{Therefore } A_{\text{req}} := \frac{T}{f_s \cdot b_{\text{ext}}} = 0.292 \cdot \frac{\text{in}^2}{\text{ft}}$$

Use #4 @ 7in within the tensile zone $A_s := 0.34 \frac{\text{in}^2}{\text{ft}} > A_{\text{req}}$ **OK**

From CONSPAN, at release, the tension stress in the top fiber of the **interior beam** at the transfer cross section is:

$$f_t := -0.398 \text{ksi}$$

The compressive stress in the bottom fiber of the beam at the same cross section is:

$$f_b := 2.392 \text{ksi}$$

The depth of the tensile zone x is: LRFD C5.9.4.1.2

$$\frac{-f_t}{x} = \frac{f_b}{21 \text{in} - x}$$
$$x := -\frac{21 \cdot f_t \cdot \text{in}}{f_b - f_t} = 2.996 \cdot \text{in} < 8 \text{in}$$

The tensile force T in the concrete is: $T := \frac{f_t}{2} \cdot b_{\text{int}} \cdot x$

where, b_{int} is the width of the beam at top $b_{\text{int}} = 72 \cdot \text{in}$

$$\text{Therefore } T := \frac{-f_t}{2} \cdot b_{\text{int}} \cdot x = 42.922 \cdot \text{kip}$$

The required area of bonded reinforcement is: $A_{\text{req}} = \frac{T}{f_s}$

where $f_s := 0.5 \cdot f_y = 30 \cdot \text{ksi}$ LRFD C5.9.4.1.2

$$\text{Therefore } A_{\text{req}} := \frac{T}{f_s \cdot b_{\text{int}}} = 0.238 \cdot \frac{\text{in}^2}{\text{ft}}$$

Use #4 @ 10in within the tensile zone $A_s := 0.24 \frac{\text{in}^2}{\text{ft}} > A_{\text{req}}$ **OK**

4.5. Control of cracking LRFD Art. A.5.7.3.4

In the longitudinal direction, due to the existence of prestress strands, cracking is assumed to not happen. Therefore only in the transverse direction, cracking is considered.

The spacing of mild steel reinforcement in the layer closest to the tension face shall satisfy the following:

$$s \leq \frac{700 \cdot \gamma_e}{\beta_s \cdot f_{ss}} - 2 \cdot d_c$$

in which, $\beta_s = 1 + \frac{d_c}{0.7 \cdot (h - d_c)}$

where

γ_e = exposure factor
 = 1.00 for Class 1 exposure condition
 = 0.75 for Class 2 exposure condition

$\gamma_e := 0.75$ SCDOT Bridge Design Manual 15.1.7

d_c = thickness of concrete cover measured from extreme tension fiber to center of the flexural reinforcement located closest thereto (in)

f_{ss} = tensile stress in steel reinforcement at the service limit state (ksi)

h = overall thickness or depth of the component (in) $h = 8 \cdot \text{in}$

LRFD Art. 3.4.1 specifies that Service I limit state should be investigated for crack control in reinforced concrete structures. According to the previous calculation in Table 7, the final design demands for the 40ft span in the Service I limit state are summarized below:

Table 10	Location	Demand
M_{p_total} (kip*ft/ft)	Span w/o key	7.33
M_{p_total} (kip*ft/ft)	Span w/ key	6.64
M_{n_total} (kip*ft/ft)	All beams	-2.06

The section is transformed elastic, cracked cross section. LRFD Art. 5.7.1

modulus of elasticity, ksi = $33000 \cdot K_1 \cdot w_c^{1.5} \cdot \sqrt{f'_c}$ LRFD Eq 5.4.2.4-1

where

correction factor for source of aggregate: $K_1 := 1$

unit weight of concrete: $w_c = 150 \cdot \text{pcf}$

This unit weight is higher than what is given in LRFD Table 3.5.1-1. It is to be used for deck design unless more precise information is provided.

f'_c = specified compressive strength of concrete, ksi $f'_c = 6.5 \cdot \text{ksi}$

Therefore, the modulus of elasticity:

$$E_c := 33000 \cdot K_1 \cdot \left(\frac{w_c}{1000 \text{pcf}} \right)^{1.5} \cdot \sqrt{\frac{f'_c}{\text{ksi}}} \text{ksi} = 4.888 \times 10^3 \cdot \text{ksi}$$

Modulus ratio:

$$n_c := \frac{E_s}{E_c} = 5.933$$

where, $E_s = 2.9 \times 10^4 \cdot \text{ksi}$

4.5.1 Check of the positive moment reinforcement

Check the maximum positive moment against rebar configuration of #4@7in

According to Table 10, $M_{\text{pos}} := 6.64 \frac{\text{kip} \cdot \text{ft}}{\text{ft}}$

4.5.1.1 Cracked moment of inertia

For a 1ft cross section, $b := 1\text{ft}$

The distance from the top fiber of the deck to the bottom layer of reinforcement:

$$d := h - \text{Cover}_b - 0.5 \cdot d_4 = 6.75 \cdot \text{in}$$

The distance from the bottom fiber of the deck to the top layer of reinforcement:

$$d' := h - \text{Cover}_t - 0.5 \cdot d_4 = 5.25 \cdot \text{in}$$

$$\text{Bottom layer of rebar: } A_s := 0.34 \frac{\text{in}^2}{\text{ft}}$$

$$\text{Top layer of rebar: } A'_s := 0.34 \frac{\text{in}^2}{\text{ft}}$$

The location of neutral axis x measured from the top fiber of the beam is determined as below.

Sum of statical moments about the neutral axis gives:

$$\frac{1}{2} \cdot x^2 = n_c \cdot A_s \cdot (d - x) + n_c \cdot A'_s \cdot (h - d' - x)$$

$$x := \sqrt{n_c \cdot \left(A_s^2 \cdot n_c + A'_s{}^2 \cdot n_c + 2 \cdot A_s \cdot d - 2 \cdot A'_s \cdot d' + 2 \cdot A'_s \cdot h + 2 \cdot A_s \cdot A'_s \cdot n_c \right)} - A_s \cdot n_c - A'_s \cdot n_c = 1.482 \cdot \text{in}$$

The cracked moment of inertia therefore is:

$$I_{\text{cr}} := \frac{b \cdot x^3}{3} + n_c \cdot A_s \cdot b \cdot (d - x)^2 + n_c \cdot A'_s \cdot b \cdot (h - d' - x)^2 = 72.247 \cdot \text{in}^4$$

4.5.1.2 Tensile stress in the bottom steel

$$f_{\text{ss}} := n_c \cdot \frac{M_{\text{pos}} \cdot b}{I_{\text{cr}}} \cdot (d - x) = 34.47 \cdot \text{ksi}$$

where, $n_c = 5.933$

4.5.1.3 Rebar spacing

The thickness of concrete cover measured from extreme tension fiber to center of the flexural reinforcement located closest thereto (in) is:

$$d_c := h - d = 1.25 \cdot \text{in} \quad \text{where, } h = 8 \cdot \text{in}$$

Therefore:

$$\beta_s := 1 + \frac{d_c}{0.7 \cdot (h - d_c)} = 1.265$$

$$\text{where, } h = 8 \cdot \text{in}$$

So that the maximum rebar spacing is:

$$s_{\max} := \frac{700 \cdot \gamma_e}{\beta_s \cdot \frac{f_{ss}}{\text{ksi}}} \text{in} - 2 \cdot d_c = 9.544 \cdot \text{in} > 7 \text{in} \quad \text{OK} \quad \text{where, } \gamma_e = 0.75$$

4.5.2 Check of the negative moment reinforcement

Check the maximum negative moment demand against the #4@7in

$$\text{According to Table 10, } M_{\text{neg}} := 2.06 \frac{\text{kip} \cdot \text{ft}}{\text{ft}}$$

4.5.2.1 Cracked moment of inertia

For a 1ft cross section, $b := 1 \text{ft}$

$$\text{Bottom layer of rebar: } A_s := 0.34 \frac{\text{in}^2}{\text{ft}}$$

$$\text{Top layer of rebar: } A'_s := 0.34 \frac{\text{in}^2}{\text{ft}}$$

The location of neutral axis x measured from the bottom fiber of the beam is determined as below.

Sum of statical moments about the neutral axis gives:

$$\frac{1}{2} \cdot x^2 = n_c \cdot A_s \cdot (h - d - x) + n_c \cdot A'_s \cdot (d' - x) \quad \text{where, } n_c = 5.933 \quad d = 6.75 \cdot \text{in} \quad d' = 5.25 \cdot \text{in}$$

$$x := \sqrt{n_c \cdot \left(A_s^2 \cdot n_c + A'_s{}^2 \cdot n_c - 2 \cdot A_s \cdot d + 2 \cdot A'_s \cdot d' + 2 \cdot A_s \cdot h + 2 \cdot A_s \cdot A'_s \cdot n_c \right)} - A_s \cdot n_c - A'_s \cdot n_c = 1.18 \cdot \text{in}$$

The cracked moment of inertia therefore is:

$$I_{cr} := \frac{b \cdot x^3}{3} + n_c \cdot A_s \cdot b \cdot (h - d - x)^2 + n_c \cdot A'_s \cdot b \cdot (d' - x)^2 = 39.998 \cdot \text{in}^4$$

4.5.2.2 Tensile stress in the top steel

$$f_{ss} := n_c \cdot \frac{M_{\text{neg}} \cdot b}{I_{cr}} \cdot (d' - x) = 14.925 \cdot \text{ksi}$$

4.5.2.3 Rebar spacing

The thickness of concrete cover measured from extreme tension fiber to center of the flexural reinforcement located closest thereto (in) is:

$$d_c := h - d' = 2.75 \cdot \text{in} \quad \text{where,} \quad h = 8 \cdot \text{in} \quad d' = 5.25 \cdot \text{in}$$

$$\text{Therefore: } \beta_s := 1 + \frac{d_c}{0.7 \cdot (h - d_c)} = 1.748$$

So that the maximum rebar spacing is:

$$s_{\max} := \frac{700 \cdot \gamma_e}{\beta_s \cdot \frac{f_{ss}}{\text{ksi}}} \text{in} - 2 \cdot d_c = 14.62 \cdot \text{in} > 7 \text{in} \quad \underline{\text{OK}}$$

5. 30 ft bridge design using #4@10in

A summary of the demands in Strength I limit state on a 1ft strip for the 30ft span, according to Table 6, is as follows:

Table 11

	Location	Demand	Capacity provided by #4@10in Ubar
M_{p_total} (kip*ft/ft)	Span w/o key	9.04	N/A
M_{p_total} (kip*ft/ft)	Span w/ key	7.81	9.79
M_{n_total} (kip*ft/ft)	All beams	-2.65	-6.55

5.1 Development length

The development length for #4 bar is just as determined before: $l_{dh} = 12 \cdot \text{in}$

Interior beam:

For both the positive and negative moment reinforcement, this point where the development length begins is taken at the centerline of the beam.

5.2. Minimum reinforcement

LRFD Art. 5.7.3.3.1

At any section of a noncompression-controlled flexural component, the amount of prestressed and nonprestressed tensile reinforcement shall be adequate to develop a factored flexural resistance, M_r , at least equal to the lesser of:

- 1.33 times the factored moment required by the applicable strength load combination specified in Table 3.4.1-1 (Strength I); and
- $M_{cr} = 9.056 \cdot \text{kip} \cdot \text{ft}$

The above M_{cr} applies to any cross section in the deck

5.2.1 Positive moment

The factored positive moment required by strength I load combination in between beams, according to Table 11, is:

$$M_u := 7.81 \text{ kip}\cdot\text{ft}$$

$$\text{Thus, } 1.33 \cdot M_u = 10.387 \cdot \text{kip}\cdot\text{ft} > M_{cr} = 9.056 \cdot \text{kip}\cdot\text{ft}$$

Therefore M_{cr} requirement controls.

The factored capacity provided by #4@10in is:

$$M_r := 9.79 \text{ kip}\cdot\text{ft} > M_{cr} = 9.056 \cdot \text{kip}\cdot\text{ft} \quad \mathbf{OK}$$

5.2.2 Negative moment

The critical factored negative moment required by strength I load combination, according to Table 11, is:

$$M_u := -2.65 \text{ kip}\cdot\text{ft}$$

$$\text{Thus, } |1.33 \cdot M_u| = 3.524 \cdot \text{kip}\cdot\text{ft} < M_{cr} = 9.056 \cdot \text{kip}\cdot\text{ft}$$

Therefore $|1.33 \cdot M_u|$ requirement controls.

The least negative moment capacity comes from the rebar configuration of #4 @10in

$$|M_r| = 6.55 \text{ kip}\cdot\text{ft} > |1.33 \cdot M_u| = 3.524 \cdot \text{kip}\cdot\text{ft} \quad \mathbf{OK}$$

Therefore this criteria can be met at every deck section.

5.3. Distribution reinforcement

As determined before, the minimum percentage of bottom longitudinal reinforcement should be:

$$\text{Percentage} := 67\%$$

For both the Interior beam and exterior beam

$$\text{Positive moment reinforcement in the transverse direction (\#4@10in): } A_s := 0.24 \frac{\text{in}^2}{\text{ft}}$$

$$A_s \cdot 67\% = 0.161 \frac{\text{in}^2}{\text{ft}}$$

$$\text{For longitudinal bottom bar, Use \#4@12in, which gives } 0.2 \frac{\text{in}^2}{\text{ft}}$$

5.4. Shrinkage and temperature reinforcement

As determined before, the minimum reinforcement area per foot, on each face and in each direction, shall be:

$$A_{s_TS} := 0.11 \frac{\text{in}^2}{\text{ft}}$$

This criteria can be met on each face and in each direction. But this reinforcement need to be provided equally on both layers. The maximum spacing of the rebar shall not exceed either 3 times the deck depth or 18in. The top longitudinal bars are provided by the bonded reinforcement, which is #4 @16in for both the interior and exterior beams.

From CONSPAN, at release, the tension stress in the top fiber of the **exterior beam** at the transfer cross section is: $f_t := -0.26\text{ksi}$

The compressive stress in the bottom fiber of the beam at the same cross section is:

$$f_b := 1.678\text{ksi}$$

Refer to Figure F.19, the depth of the tensile zone x is: LRFD C5.9.4.1.2

$$\frac{-f_t}{x} = \frac{f_b}{21\text{in} - x}$$

$$x := -\frac{21 \cdot f_t \cdot \text{in}}{f_b - f_t} = 2.817 \cdot \text{in} < 8\text{in}$$

The tensile force T in the concrete is: $T := \frac{f_t}{2} \cdot b_{6\text{ext}} \cdot x$

where, $b_{6\text{ext}}$ is the width of the beam at top $b_{6\text{ext}} = 84 \cdot \text{in}$

Therefore $T := \frac{-f_t}{2} \cdot b_{6\text{ext}} \cdot x = 30.765 \cdot \text{kip}$

The required area of bonded reinforcement is: $A_{\text{req}} := \frac{T}{f_s}$

where $f_s := 0.5 \cdot f_y = 30 \cdot \text{ksi}$ LRFD C5.9.4.1.2

Therefore $A_{\text{req}} := \frac{T}{f_s \cdot b_{6\text{ext}}} = 0.147 \cdot \frac{\text{in}^2}{\text{ft}}$

Use #4 @16in within the tensile zone $A_s := 0.15 \cdot \frac{\text{in}^2}{\text{ft}} > A_{\text{req}}$ **OK**

From CONSPAN, at release, the tension stress in the top fiber of the **interior beam** at the transfer cross section is: $f_t := -0.26\text{ksi}$

The compressive stress in the bottom fiber of the beam at the same cross section is:

$$f_b := 1.706\text{ksi}$$

The depth of the tensile zone x is: LRFD C5.9.4.1.2

$$\frac{-f_t}{x} = \frac{f_b}{21\text{in} - x}$$

$$x := -\frac{21 \cdot f_t \cdot \text{in}}{f_b - f_t} = 2.777 \cdot \text{in} < 8\text{in}$$

The tensile force T in the concrete is: $T := \frac{f_t}{2} \cdot b_{6\text{int}} \cdot x$

where, $b_{6\text{int}}$ is the width of the beam at top $b_{6\text{int}} = 72 \cdot \text{in}$

Therefore $T := \frac{-f_t}{2} \cdot b_{\text{Gint}} \cdot x = 25.995 \cdot \text{kip}$

The required area of bonded reinforcement is: $A_{\text{req}} := \frac{T}{f_s}$

where $f_s := 0.5 \cdot f_y = 30 \cdot \text{ksi}$ LRFD C5.9.4.1.2

Therefore $A_{\text{req}} := \frac{T}{f_s \cdot b_{\text{Gint}}} = 0.144 \cdot \frac{\text{in}^2}{\text{ft}}$

Use #4 @16in within the tensile zone $A_s := 0.15 \frac{\text{in}^2}{\text{ft}} > A_{\text{req}}$ **OK**
LRFD Art. A.5.7.3.4

5.5. Control of cracking

A summary of the demands on a 1ft strip in Service I limit state for the 30ft span, according to Table 7, is as follows:

Table 12	Location	Demand
M_{p_total} (kip*ft/ft)	Span w/o key	5.31
M_{p_total} (kip*ft/ft)	Span w/ key	4.61
M_{n_total} (kip*ft/ft)	All beams	-2.06

The section is transformed elastic, cracked cross section. LRFD Art. 5.7.1

5.5.1 Check of the positive moment reinforcement

Check the positive moment against rebar configuration of #4@10in

According to Table 12, $M_{\text{pos}} := 4.61 \frac{\text{kip} \cdot \text{ft}}{\text{ft}}$

5.5.1.1 Cracked moment of inertia

For a 1ft cross section, $b := 1\text{ft}$

The distance from the top fiber of the deck to the bottom layer of reinforcement:

$$d := h - \text{Cover}_b - 0.5 \cdot d_4 = 6.75 \cdot \text{in}$$

The distance from the bottom fiber of the deck to the top layer of reinforcement:

$$d' := h - \text{Cover}_t - 0.5 \cdot d_4 = 5.25 \cdot \text{in}$$

Bottom layer of rebar: $A_s := 0.24 \frac{\text{in}^2}{\text{ft}}$

Top layer of rebar: $A'_s := 0.24 \frac{\text{in}^2}{\text{ft}}$

The location of neutral axis x measured from the top fiber of the beam is determined as below.

Sum of statical moments about the neutral axis gives:

$$\frac{1}{2} \cdot x^2 = n_c \cdot A_s \cdot (d - x) + n_c \cdot A'_s \cdot (h - d' - x) \quad \text{where, } n_c = 5.933$$

$$x := \sqrt{n_c \cdot \left(A_s^2 \cdot n_c + A'_s{}^2 \cdot n_c + 2 \cdot A_s \cdot d - 2 \cdot A'_s \cdot d' + 2 \cdot A'_s \cdot h + 2 \cdot A_s \cdot A'_s \cdot n_c \right)} - A_s \cdot n_c - A'_s \cdot n_c = 1.283 \cdot \text{in}$$

$$< h - d' = 2.75 \cdot \text{in}$$

The cracked moment of inertia therefore is:

$$I_{cr} := \frac{b \cdot x^3}{3} + n_c \cdot A_s \cdot b \cdot (d - x)^2 + n_c \cdot A'_s \cdot b \cdot (h - d' - x)^2 = 54.072 \cdot \text{in}^4$$

$$\text{where, } n_c = 5.933 \quad h = 8 \cdot \text{in}$$

5.5.1.2 Tensile stress in the bottom steel

$$f_{ss} := n_c \cdot \frac{M_{\text{pos}} \cdot b}{I_{cr}} \cdot (d - x) = 33.186 \cdot \text{ksi}$$

5.5.1.3 Rebar spacing

The thickness of concrete cover measured from extreme tension fiber to center of the flexural reinforcement located closest thereto (in) is:

$$d_c := h - d = 1.25 \cdot \text{in} \quad \text{where, } h = 8 \cdot \text{in}$$

$$\text{Therefore: } \beta_s := 1 + \frac{d_c}{0.7 \cdot (h - d_c)} = 1.265$$

So that the maximum rebar spacing is:

$$s_{\text{max}} := \frac{700 \cdot \gamma_e}{\beta_s \cdot \frac{f_{ss}}{\text{ksi}}} \text{in} - 2 \cdot d_c = 10.01 \cdot \text{in} > 10 \text{in} \quad \underline{\text{OK}} \quad \text{where, } \gamma_e = 0.75$$

5.5.2 Check of the negative moment reinforcement

Check the maximum negative moment demand against the #4@10in rebar configuration

$$\text{According to Table 12, } M_{\text{neg}} := 1.69 \frac{\text{kip} \cdot \text{ft}}{\text{ft}}$$

5.5.2.1 Cracked moment of inertia

For a 1ft cross section, $b := 1 \text{ft}$

$$\text{Bottom layer of rebar: } A_s = 0.24 \cdot \frac{\text{in}^2}{\text{ft}}$$

$$\text{Top layer of rebar: } A'_s = 0.24 \cdot \frac{\text{in}^2}{\text{ft}}$$

The location of neutral axis x measured from the bottom fiber of the beam is determined as below.

Sum of statical moments about the neutral axis gives:

$$\frac{1}{2} \cdot x^2 = n_c \cdot A_s \cdot (h - d - x) + n_c \cdot A'_s \cdot (d' - x) \quad \text{where, } n_c = 5.933 \quad d = 6.75 \cdot \text{in} \quad d' = 5.25 \cdot \text{in}$$

$$x := \sqrt{n_c \cdot \left(A_s^2 \cdot n_c + A'_s{}^2 \cdot n_c - 2 \cdot A_s \cdot d + 2 \cdot A'_s \cdot d' + 2 \cdot A_s \cdot h + 2 \cdot A_s \cdot A'_s \cdot n_c \right)} - A_s \cdot n_c - A'_s \cdot n_c = 1.027 \cdot \text{in}$$

The cracked moment of inertia therefore is:

$$I_{cr} := \frac{b \cdot x^3}{3} + n_c \cdot A_s \cdot b \cdot (h - d - x)^2 + n_c \cdot A'_s \cdot b \cdot (d' - x)^2 = 29.798 \cdot \text{in}^4$$

5.5.2.2 Tensile stress in the top steel

$$f_{ss} := n_c \cdot \frac{M_{neg} \cdot b}{I_{cr}} \cdot (d' - x) = 17.052 \cdot \text{ksi}$$

5.5.2.3 Rebar spacing

The thickness of concrete cover measured from extreme tension fiber to center of the flexural reinforcement located closest thereto (in) is:

$$d_c := h - d' = 2.75 \cdot \text{in}$$

$$\text{where, } h = 8 \cdot \text{in} \quad d' = 5.25 \cdot \text{in}$$

Therefore:

$$\beta_s := 1 + \frac{d_c}{0.7 \cdot (h - d_c)} = 1.748$$

So that the maximum rebar spacing is:

$$s_{max} := \frac{700 \cdot \gamma_e}{\beta_s \cdot \frac{f_{ss}}{\text{ksi}}} \cdot \text{in} - 2 \cdot d_c = 12.111 \cdot \text{in} > 10 \text{in} \quad \text{OK}$$

6. 22 ft bridge design using #4@10in

A summary of the demands for Strength I limit state on a 1ft strip for the 22ft span, according to Table 6, is as follows:

Table 13	Location	Demand	Capacity provided by #4@10in Ubar
M_{p_total} (kip*ft/ft)	Span w/o key	6.46	N/A
M_{p_total} (kip*ft/ft)	Span w/ key	4.98	9.79
M_{n_total} (kip*ft/ft)	All beams	-1.77	-6.55

Compared with the 30ft bridge design, with the same reinforcement configuration and smaller demands (Table 6 and 7), the requirements of minimum reinforcement and cracking control reinforcement are definitely satisfied.

6.1 Development length

The development length for #4 bar is as determined before: $l_{dh} = 12 \cdot \text{in}$

For both the positive and negative moment reinforcement, this point where the development length begins is taken at the centerline of the beam.

6.2 Distribution reinforcement

For longitudinal bottom bar, Use #4@12in (refer the 30ft bridge design)

6.3. Shrinkage and temperature reinforcement

As determined before, the minimum reinforcement area per foot, on each face and in each direction, shall be:

$$A_{s_TS} := 0.11 \frac{\text{in}^2}{\text{ft}}$$

This criteria can be met on each face and in each direction. The maximum spacing of the rebar shall not exceed either 3 times the deck depth or 18in. For the top longitudinal bar, use #4@18in. There is no bonding reinforcement needed as shown below:

From CONSPAN, at release, the maximum tension stress in the top fiber of the beam at the transfer cross section is 0.148ksi, which is smaller than the limiting tensile stress of concrete 0.2ksi

7. Design summary

7.1 Reinforcement configuration

	Main bar (transverse)	Development length (in)	Cut-off point (Interior beam)	Distribution bottom rebar (longitudinal)	Top rebar (longitudinal)
40ft	#4@7in	12in	centerline of the beam	#4@10in	#4@7in (exterior beam) #4@10in (interior beam)
30ft	#4@10in	12in	centerline of the beam	#4@12in	#4@16in Use #4@12
22ft	#4@10in	12in	centerline of the beam	#4@12in	#4@18in Use #4@12

Note: bonded reinforcement needs to be provided within the tension zone of concrete at the transfer cross section at the time of release.

7.2 Criteria check

7.2.1 Demand VS Capacity

	<u>40 ft span</u>		Capacity provided by #4@7in Ubar
	Location	Demand	
M_{p_total} (kip*ft/ft)	Span w/o key	12.57	N/A
M_{p_total} (kip*ft/ft)	Span w/ key	11.36	13.59
M_{n_total} (kip*ft/ft)	All beams	-3.49	-8.90

	<u>30 ft span</u>		Capacity provided by #4@10in Ubar
	Location	Demand	
M_{p_total} (kip*ft/ft)	Span w/o key	9.04	N/A
M_{p_total} (kip*ft/ft)	Span w/ key	7.81	9.79
M_{n_total} (kip*ft/ft)	All beams	-2.65	-6.55

	<u>22 ft span</u>		Capacity provided by #4@10in Ubar
	Location	Demand	
M_{p_total} (kip*ft/ft)	Span w/o key	6.46	N/A
M_{p_total} (kip*ft/ft)	Span w/ key	4.98	9.79
M_{n_total} (kip*ft/ft)	All beams	-1.77	-6.55

Note: the positive moment capacity in the deck span without shear key, due to the development length of the reinforcing steel, is larger than that in the deck span with shear key.

7.2.2 Minimum reinforcement check

40 ft span

M+ rebar	#4@7in	$M_r := 13.59 \text{ kip}\cdot\text{ft}$	>	$M_{cr} = 9.056 \text{ kip}\cdot\text{ft}$	OK
M- rebar	#4@7in	$ M_r = 8.9 \text{ kip}\cdot\text{ft}$	>	$ 1.33 \cdot M_u = 4.642 \text{ kip}\cdot\text{ft}$	OK

30 ft span

M+ rebar	#4@10in	$M_r := 9.79 \text{ kip}\cdot\text{ft}$	>	$M_{cr} = 9.056 \text{ kip}\cdot\text{ft}$	OK
M- rebar	#4@10in	$ M_r = 6.55 \text{ kip}\cdot\text{ft}$	>	$ 1.33 \cdot M_u = 3.524 \text{ kip}\cdot\text{ft}$	OK

22 ft span

With the same rebar configuration with 30ft span and less demands, this requirement needs not to be checked.

The minimum reinforcement requirement can be satisfied at any cross section.

7.2.3 Cracking control check

40 ft span

M +	Maximum moment Transversally	#4@7in	$s_{\max} := \frac{700 \cdot \gamma_e}{\beta_s \cdot \frac{f_{ss}}{\text{ksi}}} \text{in} - 2 \cdot d_c = 9.544 \cdot \text{in} > 7 \text{in}$	OK
-----	---------------------------------	--------	--	-----------

M -	Minimum moment Transversally	#4@7in	$s_{\max} := \frac{700 \cdot \gamma_e}{\beta_s \cdot \frac{f_{ss}}{\text{ksi}}} \text{in} - 2 \cdot d_c = 14.62 \cdot \text{in} > 7 \text{in}$	OK
-----	---------------------------------	--------	--	-----------

30 ft span

M +	Maximum moment Transversally	#4@10in	$s_{\max} := \frac{700 \cdot \gamma_e}{\beta_s \cdot \frac{f_{ss}}{\text{ksi}}} \text{in} - 2 \cdot d_c = 10.01 \cdot \text{in} > 10 \text{in}$	OK
-----	---------------------------------	---------	---	-----------

M -	Minimum moment Transversally	#4@10in	$s_{\max} := \frac{700 \cdot \gamma_e}{\beta_s \cdot \frac{f_{ss}}{\text{ksi}}} \text{in} - 2 \cdot d_c = 12.111 \cdot \text{in} > 10 \text{in}$	OK
-----	---------------------------------	---------	--	-----------

22 ft span

With the same rebar configuration with 30ft span and less demands, this requirement needs not to be checked.

NEXT-8---Deck Design Outline:

1. Deck properties
2. 3d finite element method--- Loads and load effects
 - 2.1 Dead load:
 - 2.2 Live load
 - 2.3 Moment distribution
 - 2.4 Distribution strip width
 - 2.5 Load combination
 - 2.6 Design demands for a 1ft strip
3. Demands based on 1d AASHTO FEM
4. Moment capacity
 - 4.1 The moment capacity of the current U-bar configuration: #4@8in c2c
 - 4.1.1 Negative moment capacity
 - 4.1.2 Positive moment capacity
 - 4.2 Capacities provided by various rebar configurations:
5. 40 ft bridge design--- #4@5
 - 5.1 Development length
 - 5.2. Limits of reinforcement
 - 5.2.1 Maximum reinforcement
 - 5.2.2 Minimum reinforcement
 - 5.3 Distribution reinforcement
 - 5.4 Shrinkage and temperature reinforcement
 - 5.5 Control of cracking
 - 5.5.1 Check of the positive moment reinforcement
 - 5.5.2 Check of the negative moment reinforcement
6. 30ft bridge design --- #4 @ 7in
 - 6.1 Development length
 - 6.2 Minimum reinforcement
 - 6.2.1 Positive moment
 - 6.2.2 Negative moment
 - 6.3 Distribution reinforcement
 - 6.4. Shrinkage and temperature reinforcement
 - 6.5 Control of cracking

- 6.5.1 Check of the positive moment reinforcement
 - 6.5.2 Check of the negative moment reinforcement
- 7. 22ft bridge design using #4@7in
 - 7.1 Development length
 - 7.2 Distribution reinforcement
 - 7.3 Shrinkage and temperature reinforcement
- 8. Design summary
 - 8.1 Reinforcement configuration
 - 8.2 Criteria check
 - 8.2.1 Demand VS Capacity
 - 8.2.2 Minimum reinforcement check
 - 8.2.3 Cracking control check

1. Deck properties:

Cross section:	NEXT-8
Area of a single beam cross section:	$A_g := 1147.4 \text{ in}^2$
Effective width of a single cross section (including shear key):	$b_g := 8 \text{ ft}$
Structural deck depth:	$h := 8 \text{ in}$
Moment of inertia considered:	$I := \frac{1}{12} \cdot 1 \text{ ft} \cdot h^3 = 512 \cdot \text{in}^4$
Section modulus:	$S_r := \frac{I}{h} \cdot 2 = 128 \cdot \text{in}^3$
Deck top cover:	$\text{Cover}_t := 2.5 \text{ in}$ AASHTO LRFD Table 5.12.3-1
Deck bottom cover:	$\text{Cover}_b := 1.0 \text{ in}$ AASHTO LRFD Table 5.12.3-1
Reinforced concrete density:	$w_c := 150 \text{ pcf}$
Concrete compressive strength (final)	$f'_c := 6.5 \text{ ksi}$
Rebar Young's modulus:	$E_s := 29000 \text{ ksi}$
Reinforcement strength:	$f_y := 60 \text{ ksi}$
Bituminous wearing surface:	$w_{fws} := 140 \text{ pcf}$ AASHTO LRFD Table 3.5.1-1

2. 3d finite element method--- Loads and load effects:

2.1 Dead load:

DC :

parapet self weight : $w_p := 443 \text{ plf}$

Parapet self weight is uniformly distributed to the outer two beams. Therefore for each beam mentioned above,

$$w_b := \frac{w_p}{b_g \cdot 2} = 0.028 \cdot \frac{\text{kip}}{\text{ft}^2} \quad \text{where, } b_g = 8 \cdot \text{ft}$$

Beam self weight:

$$w_g := \frac{w_c \cdot A_g}{b_g} = 0.149 \cdot \frac{\text{kip}}{\text{ft}^2} \quad \text{where, } A_g = 1.147 \times 10^3 \cdot \text{in}^2 \quad w_c = 150 \cdot \text{pcf}$$

DW :

Wearing surface (4in on average):

$$DW := (4\text{in} \cdot w_{fws}) = 0.047 \cdot \frac{\text{kip}}{\text{ft}^2} \quad \text{where,} \quad w_{fws} = 140 \cdot \text{pcf}$$

The load from wearing surface is distributed from face to face of the two parapets.

In the finite element model, the above area loads are distributed to the shell element of the slab. For the frame element of the shear key, the area load is converted to uniformly distributed line load to each element. An example is provided for the 40ft-span NEXT8 bridge.

Bridge span length: $l := 40\text{ft}$

Number of frame elements for each shear key: $n := 81$

parapet self weight is distributed to the outer two shear keys :

$$w_{bk} := \frac{w_b \cdot l}{n} = 0.014 \cdot \frac{\text{kip}}{\text{ft}} \quad \text{where,} \quad w_b = 0.028 \cdot \frac{\text{kip}}{\text{ft}^2}$$

Beam self weight:

$$w_{gk} := \frac{w_g \cdot l}{n} = 0.074 \cdot \frac{\text{kip}}{\text{ft}} \quad \text{where,} \quad w_g = 0.149 \cdot \frac{\text{kip}}{\text{ft}^2}$$

Wearing surface load:

$$w_{dwk} := \frac{DW \cdot l}{n} = 0.023 \cdot \frac{\text{kip}}{\text{ft}} \quad \text{where,} \quad DW = 0.047 \cdot \frac{\text{kip}}{\text{ft}^2}$$

Simulation results show insignificant influence of the loads from the shear key on demands.

2.2 Live load

LRFD Art 3.6.1.3.3 specifies that when the refined methods are used to analyze decks, if the slab spans primarily in the transverse direction, only the axles of the design truck of Article 3.6.1.2.2 or design tandem of Article 3.6.1.2.3 shall be applied to the deck slab.

In order to obtain the most critical demand, a single design tandem specified in LRFD Art 3.6.1.2.3 is applied to the finite element model, moving across the bridge model transversely and longitudinally. The position of the tandem follows that specified in LRFD Art. 3.6.1.3: the design tandem shall be positioned transversely such that the center of any wheel load is not closer than: For the design of components other than deck overhang---2 ft from the edge of the design lane. In this case, the axle load is positioned no closer than 2ft from the face of the parapet.

2.3 Moment distribution

The total unfactored transverse moment demand on the deck for the 40ft span bridge resulting from the dead loads and live loads are displayed as follows, in which the black lines represent the location of the shear key:

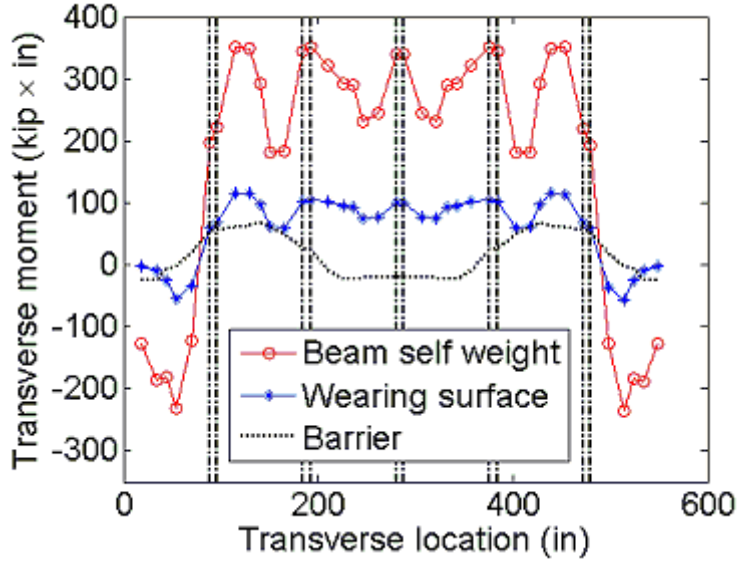


Figure F.20: Moment effects of dead loads

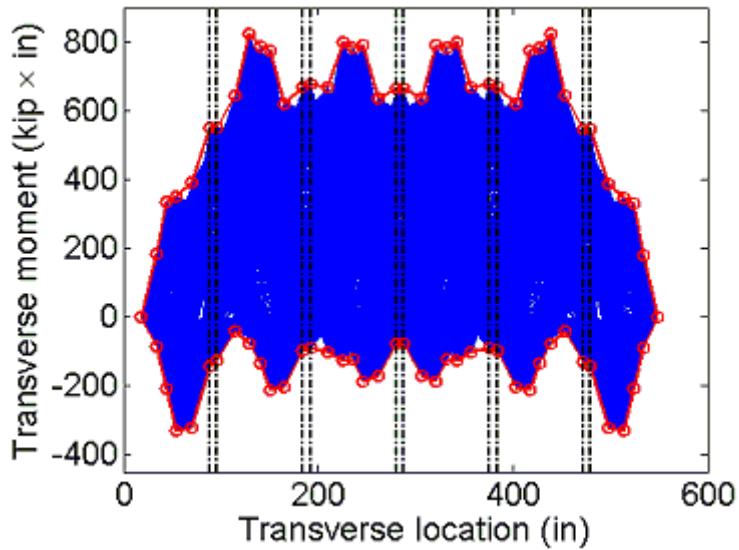


Figure F.21: Moment effects of design tandem

2.4 Distribution strip width:

The distribution width for the design tandem is 10ft

2.5 Load combination

LRFD Table 3.4.1-1

strength I limit state:

$$\text{Maximum } Q = 1.25(\text{DC}) + 1.50(\text{DW}) + 1.75(\text{LL} + \text{IM})$$

$$\text{Minimum } Q = 0.90(\text{DC}) + 0.65(\text{DW}) + 1.75(\text{LL} + \text{IM})$$

service I limit state:

$$Q = 1(\text{DC}) + 1(\text{DW}) + 1(\text{LL} + \text{IM})$$

where

LL = live load effect including multiple presence factor 1.2

IM = dynamic load allowance $\text{IM} := 1.33$ LRFD Table 3.6.2.1-1

2.6 Design demands for a 1ft strip:

The total dead load effect is divided by the total span length to get the normalized demand on a 1ft strip. And the live load effect is divided by the strip width 10ft to get the normalized demand on the 1ft strip. The resulting normalized transverse moment demands combined for Strength I and Service I limit states for the 40ft span are displayed below. Positive moment means the bottom deck fiber is in tension

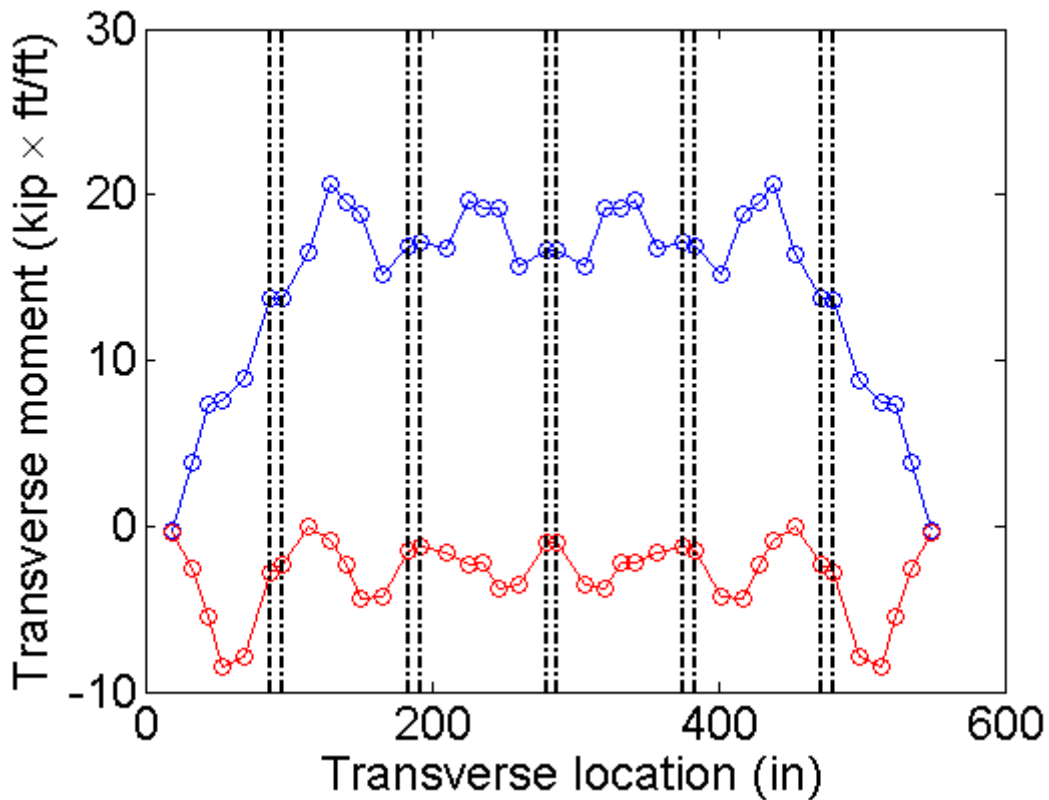


Figure F.22: Demand distribution in Strength I limit state

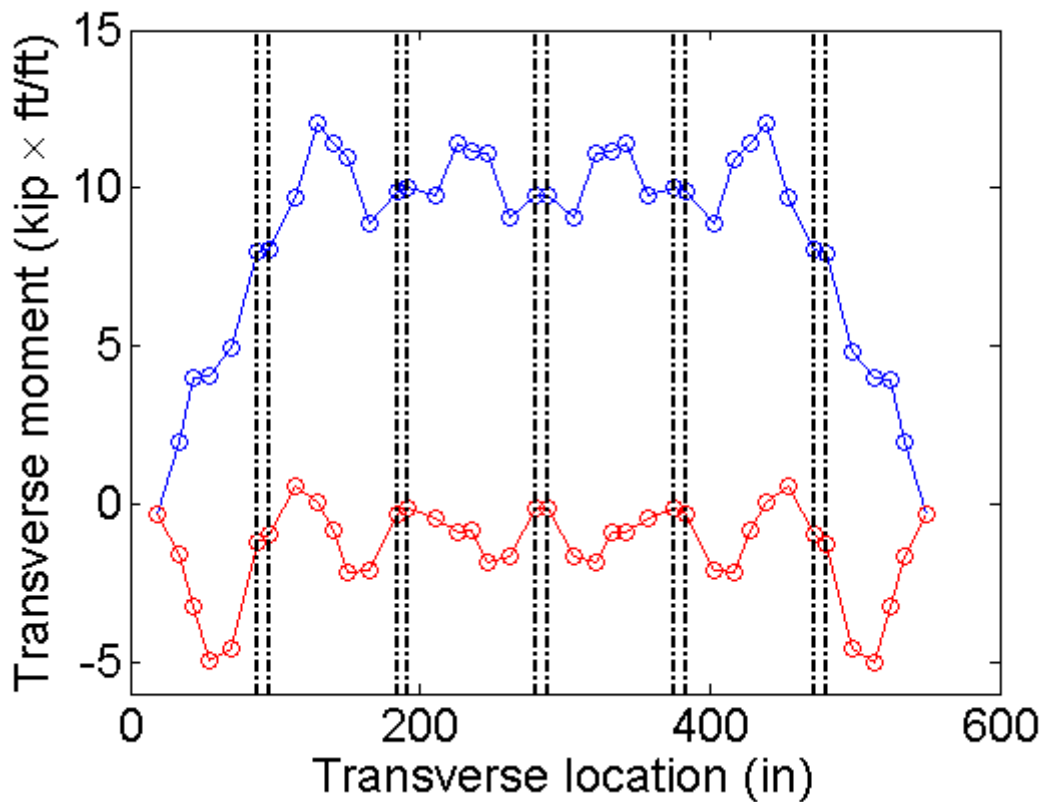


Figure F.23: Demand distribution in Service I limit state

A summary of the demands on a 1ft strip for the 22ft, 30ft, and 40ft spans are listed in Table 1 and Table 2:

Table 1

Strength I limit state

	Location	22 ft	30 ft	40 ft
M+ (kip*ft/ft)	3 ft span	8.87	14.25	20.65
M+ (kip*ft/ft)	5 ft span	7.00	11.31	17.12
M- (kip*ft/ft)	Exterior beam	-5.56	-6.70	-8.45
M- (kip*ft/ft)	Interior beam	-4.52	-4.19	-4.34

Table 2 Service I limit state

	Location	22 ft	30 ft	40 ft
M+ (kip*ft/ft)	3 ft span	5.10	8.29	12.08
M+ (kip*ft/ft)	5 ft span	4.06	6.62	10.04
M- (kip*ft/ft)	Exterior beam	-3.25	-3.94	-4.98
M- (kip*ft/ft)	Interior beam	-2.61	-2.34	-2.15

Notice that within the 3ft span, the reinforcement is doubled by the development length, which will be considered in checking the moment capacity and cracking control requirement.

3. Demands based on 1d AASHTO FEM:

The final design demands are calculated based on the results from 1d AASHTO FEM using a finite element software SAP2000. In the FEM, the deck (including shear key) is modeled as a continuous beam using frame elements and the stems are modeled as rigid supports. Refer to the deck design guideline in Chapter 9.2.1 for details.

From the 1d AASHTO FEM, the maximum positive moment and critical negative moment (unfactored) resulting from a single 32kip axle of design truck as specified in LRFD Article 3.6.1.2.2 are:

$$M_{p_total} := 156.73 \text{ kip}\cdot\text{in} \quad M_{n_total} := -95.11 \text{ kip}\cdot\text{in}$$

The strip widths for positive and negative moment for cast-in-place deck without stay-in-place concrete formwork are: LRFD Table 4.6.2.1.3-1

$$M_{p_width} = 26 + 6.6 \cdot s_{design} \quad M_{n_width} = 48 + 3 \cdot s_{design}$$

where,

$$s_{design} = \text{average stem spacing (ft)} \quad s_{design} := 4$$

Therefore,

$$M_{p_width} := (26 + 6.6 \cdot s_{design}) \text{ in} = 52.4 \cdot \text{in}$$

$$M_{n_width} := (48 + 3 \cdot s_{design}) \text{ in} = 60 \cdot \text{in}$$

The normalized demands for a 1ft load strip are:

$$M_{p_AASHTO} := \frac{M_{p_total}}{M_{p_width}} = 2.991 \cdot \frac{\text{kip}\cdot\text{ft}}{\text{ft}}$$

$$M_{n_AASHTO} := \frac{M_{n_total}}{M_{n_width}} = -1.585 \cdot \frac{\text{kip}\cdot\text{ft}}{\text{ft}}$$

Based on the formula proposed, the normalized design demands are:

Positive design moment:

$$\text{For the 3ft span: } M_{\text{positive}} = M_{p_AASHTO} \cdot \left[0.77 + 0.0027 \cdot \left(l_{\text{design}}^{1.3} \cdot s_{\text{design}}^{1.4} - 244 \right) \right]$$

$$\text{For the 5ft span: } M_{\text{positive}} = M_{p_AASHTO} \cdot \left[0.58 + 0.0196 \cdot \left(l_{\text{design}}^1 \cdot s_{\text{design}}^{0.8} - 51 \right) \right]$$

Negative design moment:

$$\text{For the exterior beam: } M_{\text{negative}} = M_{n_AASHTO} \cdot \left[0.4 + 6.28 \cdot \left(l_{\text{design}}^{0.1} \cdot s_{\text{design}}^{0.2} - 1.69 \right) \right]$$

$$\text{For the interior beam: } M_{\text{negative}} = M_{n_AASHTO}$$

The negative moment demand in the interior beam shall not exceed that in the exterior beam.

where,

l_{design} = design span length, (ft) $l_{\text{design}} = 39\text{ft}$ for the 40ft span bridge

M_{positive} = unfactored positive moment demand from live load (kip*ft/ft)

M_{negative} = unfactored negative moment demand from live load (kip*ft/ft)

Based on the formula, the normalized live load demands (kip*ft/ft) are:

Table 3	Location	22 ft	30 ft	40 ft
M_{positive} (kip*ft/ft)	3 ft span	3.28	4.81	6.92
M_{positive} (kip*ft/ft)	5 ft span	2.48	3.90	5.68
M_{negative} (kip*ft/ft)	Exterior beam	-1.62	-2.20	-2.76
M_{negative} (kip*ft/ft)	Interior beam	-1.59	-1.59	-1.59

The dead load effect is obtained based on the 1d AASHTO FEM. The moment demands from beam self weight, barrier self weight, and wearing surface are combined for the Strength I limit state and Service I limit state. For each limit state, both the maximum and minimum combined moment demands are obtained and listed in Table 4.

	Strength I	Service I
M_{p_DL}	0.4661	0.3592
M_{n_DL} (kip*ft/ft)	-0.7216	-0.5732

The total load effect is calculated as:

$$M_{p_total} = M_{positive} \cdot IM \cdot m \cdot LF + M_{p_DL} \cdot 4$$

$$M_{n_total} = M_{negative} \cdot IM \cdot m \cdot LF + M_{n_DL}$$

where,

M_{p_total} = final design positive moment demand for either Strength I or Service I limit state (kip*ft/ft)

M_{n_total} = final design negative moment demand for either Strength I or Service I limit state (kip*ft/ft)

$M_{positive}$ = unfactored positive moment demand from live load (kip*ft/ft)

$M_{negative}$ = unfactored negative moment demand from live load (kip*ft/ft)

M_{p_DL} = factored positive moment demand from dead load (kip*ft/ft)

M_{n_DL} = factored negative moment demand from dead load (kip*ft/ft)

IM = dynamic load allowance percent, IM = 1.33 LRFD Table 3.6.2.1-1

m = multiple presence factor, MP = 1.2 LRFD Table 3.6.1.1.2-1

LF = live load factor, LL = 1.75 for Strength I limit state, and 1 for Service I limit state
LRFD Table 3.4.1-1

The final design demands for Strength I and Service I limit states are listed in Table 5 and 6. The values given in bracket are the demands based on 3d FEM results. The percentage errors for the unconservative demands are also given by taking the 3d FEM results as the 'correct' values. The unconservative values are all within six percentage of the FEM results.

	Location	Strength I limit state			
		22 ft	30 ft	40 ft	
M_{p_total} (kip*ft/ft)	3 ft span	11.02 (8.87)	15.30 (14.25)	21.18 (20.65)	
M_{p_total} (kip*ft/ft)	5 ft span	8.78 (7.00)	12.75 (11.31)	17.72 (17.12)	
M_{n_total} (kip*ft/ft)	Exterior beam	-5.25 (-5.56)	-6.88 (-6.70)	-8.42 (-8.45)	-0.3%
M_{n_total} (kip*ft/ft)	Interior beam	-5.15 (-4.52)	-5.15 (-4.19)	-5.15 (-4.34)	

Table 6

	Location	Service I limit state					
		22 ft		30 ft		40 ft	
M_{p_total} (kip*ft/ft)	3 ft span	6.67	(5.10)	9.12	(8.29)	12.47	(12.08)
M_{p_total} (kip*ft/ft)	5 ft span	5.39	(4.06)	7.66	(6.62)	10.50	(10.04)
M_{n_total} (kip*ft/ft)	Exterior beam	-3.16	(-3.25) -2.9%	-4.09	(-3.94)	-4.97	(-4.98) -0.2%
M_{n_total} (kip*ft/ft)	Interior beam	-3.10	(-2.61)	-3.10	(-2.34)	-3.10	(-2.15)

4. Moment capacity

4.1 The moment capacity of the U-bar configuration used in experiments: #4@8in c2c

Rebar diameter: $d_4 := 0.5\text{in}$

Area of top layer of rebar: $A'_s := 0.29 \frac{\text{in}^2}{\text{ft}}$

Area of bottom layer of rebar: $A_s := A'_s$

Distance from the bottom beam fiber to the centroid of the top bar:

$$d' := h - \text{Cover}_t - 0.5 \cdot d_4 = 5.25 \cdot \text{in} \quad \text{where, } \text{Cover}_t = 2.5 \cdot \text{in} \quad h = 8 \cdot \text{in}$$

Distance from the top beam fiber to the centroid of the bottom bar:

$$d := h - \text{Cover}_b - 0.5 \cdot d_4 = 6.75 \cdot \text{in} \quad \text{where, } \text{Cover}_b = 1 \cdot \text{in}$$

$$\beta_1 := 0.85 - \left(\frac{f'_c - 4000\text{psi}}{1000\text{psi}} \right) \cdot 0.05 = 0.725 \quad \text{where, } f'_c = 6.5 \cdot \text{ksi} \quad \text{LRFD Article 5.7.2.2}$$

4.1.1 Negative moment capacity

For negative moment capacity, assume both sides of bars are in tension and yield

$$A_s \cdot f_y + A'_s \cdot f_y = 0.85 \cdot f'_c \cdot \beta_1 c_o$$

$$c_o := \frac{1.1764705882352941176 \cdot (A_s \cdot f_y + A'_s \cdot f_y)}{f'_c \cdot \beta_1} = 0.724 \cdot \text{in}$$

< $h - d = 1.25 \cdot \text{in}$ Therefore both layers of bars are in tension

Strain in the bottom layer of rebar:

$$\varepsilon := -\frac{c_o - (h - d)}{c_o} \cdot 0.003 = 2.18 \times 10^{-3} > \frac{f_y}{E_s} = 2.069 \times 10^{-3}$$

Strain in the top layer of rebar:

$$\varepsilon := -\frac{c_o - d'}{c_o} \cdot 0.003 = 0.019 > 0.005$$

Therefore cross section is tension-controlled LRFD Article 5.7.2.1

Therefore both layers of rebars yield. Assumption is valid

$$a_o := \beta_1 \cdot c_o = 0.525 \cdot \text{in} \quad \text{where,} \quad \beta_1 = 0.725$$

Negative moment capacity:

$$\phi M_n = -\phi \cdot \left[A_s \cdot f_y \cdot \left(h - d - \frac{a_o}{2} \right) + A'_s \cdot f_y \cdot \left(d' - \frac{a_o}{2} \right) \right]$$

where

ϕ = resistance factor LRFD Art. 5.5.4.2.1

$\phi := 0.9$ tension controlled reinforced concrete sections

$$\phi M_n := -\phi \cdot \left[A_s \cdot f_y \cdot \left(h - d - \frac{a_o}{2} \right) + A'_s \cdot f_y \cdot \left(d' - \frac{a_o}{2} \right) \right] = -7.798 \cdot \frac{\text{kip} \cdot \text{ft}}{\text{ft}}$$

4.1.2 Positive moment capacity

Assume both sides of bars are in tension and yield

$$A_s \cdot f_y + A'_s \cdot f_y = 0.85 \cdot f_c \cdot \beta_1 c_o$$

$$c_o := \frac{1.1764705882352941176 \cdot (A_s \cdot f_y + A'_s \cdot f_y)}{f_c \cdot \beta_1} = 0.724 \cdot \text{in}$$

< $h - d' = 2.75 \cdot \text{in}$ Therefore both layers of bars are in tension

Strain in the top layer of rebar:

$$\epsilon := -\frac{c_o - (h - d')}{c_o} \cdot 0.003 = 8.395 \times 10^{-3} > \frac{f_y}{E_s} = 2.069 \times 10^{-3}$$

where, $d' = 5.25 \cdot \text{in}$

Strain in the bottom layer of rebar:

$$\epsilon := -\frac{c_o - d}{c_o} \cdot 0.003 = 0.025 > 0.005 \quad \text{where, } d = 6.75 \cdot \text{in}$$

Cross section is tension-controlled

Therefore both layers of rebars yield. Assumption is valid

$$a_o := \beta_1 \cdot c_o = 0.525 \cdot \text{in}$$

Positive moment capacity:

$$\phi M_n := \phi \cdot \left[A'_s \cdot f_y \cdot \left(h - d' - \frac{a_o}{2} \right) + A_s \cdot f_y \cdot \left(d - \frac{a_o}{2} \right) \right] = 11.713 \cdot \frac{\text{kip} \cdot \text{ft}}{\text{ft}}$$

4.2 Capacities provided by various rebar configurations:

Like the calculation procedures above, several different rebar configurations are considered. The capacities are provided below:

Table 7

	#4@9in	#4@8in	#4@7in	#4@6in	#4@5in
M+ (kip*ft/ft)	10.56	11.71	13.59	15.43	18.29
M- (kip*ft/ft)	-7.05	-7.80	-8.90	-9.87	-11.47

5. 40 ft bridge design--- #4@5

The normalized moment demands in strength I limit state, according to Table 5, is:

Table 8

	Location	Demand	Capacity provided by #4@5in Ubar
M_{p_total} (kip*ft/ft)	3 ft span	21.18	N/A
M_{p_total} (kip*ft/ft)	5 ft span	17.72	18.29
M_{n_total} (kip*ft/ft)	Exterior beam	-8.42	-11.47
M_{n_total} (kip*ft/ft)	Interior beam	-5.15	-11.47

For the 3ft-span deck ---which is the deck in-between the two stems of a beam--- due to the development length of the rebar, the actual capacity is larger than that in the 5ft-span deck.

5.1 Development length

Rebar area: $A_4 := 0.2\text{in}^2$ Rebar diameter: $d_4 := 0.5\text{in}$

Straight development: LRFD Art. 5.11.2.1

$$l_{hb} := \max\left(\frac{1.25 \cdot A_4 \cdot f_y \cdot \text{in}}{\sqrt{\frac{f_c}{\text{ksi}} \cdot \text{kip}}}, 0.4 \cdot \frac{d_4 \cdot f_y}{\text{ksi}}\right) = 12 \cdot \text{in} \quad \text{where, } f_c = 6.5 \cdot \text{ksi} \quad f_y = 60 \cdot \text{ksi}$$

$$f_{\text{modS}} := 1$$

$$l_{dh} := \max(f_{\text{modS}} \cdot l_{hb}, 12\text{in}) = 12 \cdot \text{in}$$

According to LRFD Art. 5.11.1.2.1, except at supports of simple spans and at the free ends of cantilevers, reinforcement shall be extended beyond the point at which it is no longer required to resist flexure for a distance calculated above.

Interior beam:

For the positive reinforcement, since additional moment capacity is needed within the 3ft deck but not within the stem, this point is taken at the inner face of each stem.

For the negative reinforcement, the point where the development length begins is taken at the centerline of the beam. The development length is at least 12in as determined above. In the design, the two legs of the U-bar will be made of the same length.

5.2. Limits of reinforcement

5.2.1 Maximum reinforcement

The check of maximum reinforcement limits was removed from the LRFD Specifications in 2005. LRFD Art. 5.7.3.3.1

5.2.2 Minimum reinforcement

At any section of a noncompression-controlled flexural component, the amount of prestressed and nonprestressed tensile reinforcement shall be adequate to develop a factored flexural resistance, M_r , at least equal to the lesser of:

1. 1.33 times the factored moment required by the applicable strength load combination specified in Table 3.4.1-1 (Strength I); and

2. $M_{cr} = \gamma_3 \cdot (\gamma_1 \cdot f_r) \cdot S_r$ LRFD Eq. 5.7.3.3.2-1

The above equation is a simplified form of LRFD Equation 5.7.3.3.2-1 because no composite section exists, therefore the composite and noncomposite section modulus are the same. Also since there is no transverse post-tensioning, the cracking moment capacity won't be increased.

where,

f_r = modulus of rupture of concrete LRFD Art 5.4.2.6

$$f_r := 0.37 \sqrt{\frac{f_c}{\text{ksi}}} \text{ ksi} = 0.943 \cdot \text{ksi}$$

S_r = section modulus for the extreme fiber of the section where tensile stress is caused by externally applied loads (in³) $S_r = 128 \cdot \text{in}^3$

γ_1 = flexural cracking variability factor

$\gamma_1 := 1.2$ for precast segmental structures

γ_3 = ratio of specified minimum yield strength to ultimate tensile strength of the reinforcement

$\gamma_3 := 0.75$ for A 706, Grade 60 reinforcement

Therefore, $M_{cr} := \gamma_3 \cdot (\gamma_1 \cdot f_r) \cdot S_r = 9.056 \cdot \text{kip} \cdot \text{ft}$

The above M_{cr} applies to any cross section in the deck

5.2.2.1 Positive moment

The factored positive moment required by strength I load combination within the 5ft deck for a 1ft strip, according to Table 8, is:

$$M_u := 17.72 \text{ kip} \cdot \text{ft}$$

Thus, $1.33 \cdot M_u = 23.568 \cdot \text{kip} \cdot \text{ft} > M_{cr} = 9.056 \cdot \text{kip} \cdot \text{ft}$

Therefore M_{cr} requirement controls.

The factored capacity provided by #4@5in is:

$$M_r := 18.29 \text{ kip} \cdot \text{ft} > M_{cr} = 9.056 \cdot \text{kip} \cdot \text{ft} \quad \mathbf{OK}$$

This criteria can be met at every deck section.

5.2.2.2 Negative moment

5.2.2.2.1 Interior beam

The factored negative moment required by strength I load combination for the interior beam, according to Table 8, is:

$$M_u := -5.15 \text{ kip}\cdot\text{ft}$$

$$\text{Thus, } |1.33 \cdot M_u| = 6.849 \cdot \text{kip}\cdot\text{ft} < M_{cr} = 9.056 \cdot \text{kip}\cdot\text{ft}$$

Therefore $|1.33 \cdot M_u|$ requirement controls.

The factored negative moment resistance provided by #4@5in is :

$$|M_r| = 11.47 \text{ kip}\cdot\text{ft} > |1.33 \cdot M_u| = 6.849 \cdot \text{kip}\cdot\text{ft} \quad \underline{\text{OK}}$$

5.2.2.2.2 Exterior beam

The factored negative moment required by strength I load combination for the exterior beam, according to Table 8, is:

$$M_u := -8.42 \text{ kip}\cdot\text{ft}$$

$$\text{Thus, } |1.33 \cdot M_u| = 11.199 \cdot \text{kip}\cdot\text{ft} > M_{cr} = 9.056 \cdot \text{kip}\cdot\text{ft}$$

Therefore M_{cr} requirement controls.

The least negative moment capacity comes from the rebar configuration of #4 @5in

$$|M_r| = 11.47 \text{ kip}\cdot\text{ft} > M_{cr} = 9.056 \cdot \text{kip}\cdot\text{ft} \quad \underline{\text{OK}}$$

Therefore this criteria can be met at every deck section.

5.3 Distribution reinforcement

The required area of secondary reinforcement at the bottom of the deck is a percentage of the primary positive moment reinforcement. For primary reinforcement perpendicular to traffic, LRFD Art. 9.7.3.2 specifies that the percentage should be:

$$\text{Percentage} = \frac{220}{\sqrt{S}} \leq 67\%$$

where

S = the effective span length (ft) LRFD Art. 9.7.2.3

S := 5ft - 15in = 45·in Compared with the 3ft span, the 5ft span gives less percentage

$$\text{Percentage} := \frac{220}{\sqrt{\frac{S}{\text{ft}}}} = 113.60\% \quad \text{use} \quad 67\%$$

For both the Interior beam and exterior beam:

Positive moment reinforcement in the transverse direction (#4@5in): $A_s := 0.47 \frac{\text{in}^2}{\text{ft}}$

$$A_s \cdot 67\% = 0.315 \cdot \frac{\text{in}^2}{\text{ft}}$$

For longitudinal bottom bar, Use #4@7in, which gives $0.34 \frac{\text{in}^2}{\text{ft}}$

5.4. Shrinkage and temperature reinforcement

The minimum reinforcement area per foot, on each face and in each direction, shall satisfy:

$$A_{s_TS} \geq \frac{1.3 \cdot b \cdot h}{2 \cdot (b + h) \cdot f_y} \quad \text{LRFD Eq. 5.10.8-1}$$

where

A_{s_TS} = area of reinforcement in each direction and each face (in^2/ft)

b = least width of component section (in) $b := 1\text{ft}$

h = least thickness of component section (in) $h = 8\text{-in}$

f_y = specified yield strength of reinforcing bars $f_y = 60\text{ksi} \leq 75\text{ksi}$

Therefore

$$A_{s_TS} \geq \frac{1.3 \cdot 12 \cdot 8}{2 \cdot (12 + 8) \cdot 60} \cdot \frac{\text{in}^2}{\text{ft}} = 0.052 \cdot \frac{\text{in}^2}{\text{ft}}$$

$$\text{Use } A_{s_TS} := 0.11 \frac{\text{in}^2}{\text{ft}} \quad \text{LRFD Eq. 5.10.8-2}$$

This requirement can be satisfied in each direction and each face.

Since the deck depth is more than 6in, the shrinkage and temperature rebars need to be provided equally on both layers. The maximum spacing of the rebar should not exceed either 3 times the deck depth or 18in. The top longitudinal bars are provided by the bonded reinforcement, which is #4@7in for both interior and exterior beams as calculated below:

From CONSPAN, at release, the tension stress in the top fiber of the **interior beam** at the transfer cross section is:

$$f_t := -0.472\text{ksi}$$

The compressive stress in the bottom fiber of the beam at the same cross section is:

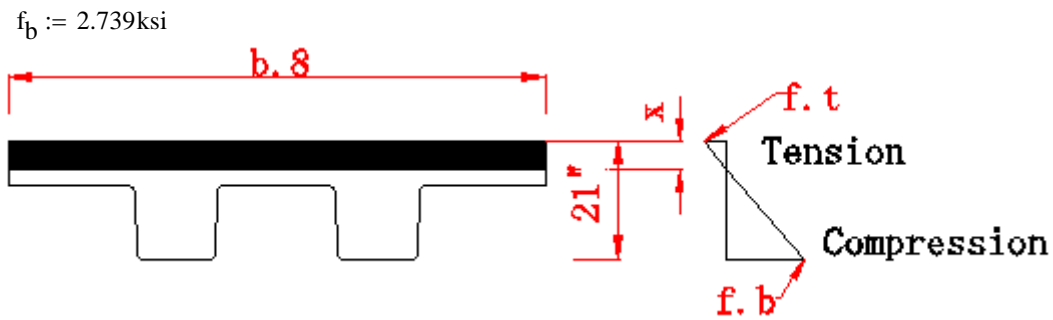


Figure F.24: Stress distribution adapted from LRFD C5.9.4.1.2

The depth of the tensile zone x is: LRFD C5.9.4.1.2

$$\frac{-f_t}{x} = \frac{f_b}{21\text{in} - x}$$

$$x := -\frac{21 \cdot f_t \cdot \text{in}}{f_b - f_t} = 3.087 \cdot \text{in} < 8\text{in}$$

The tensile force T in the concrete is: $T := \frac{f_t}{2} \cdot b_8 \cdot x$

where, b_8 is the width of the beam at top $b_8 = 96\text{in}$

Therefore $T := \frac{-f_t}{2} \cdot b_8 \cdot x = 69.937 \cdot \text{kip}$

The required area of bonded reinforcement is: $A_{\text{req}} = \frac{T}{f_s}$

where $f_s := 0.5 \cdot f_y = 30 \cdot \text{ksi}$ LRFD C5.9.4.1.2

Therefore $A_{\text{req}} := \frac{T}{f_s \cdot b_8} = 0.291 \cdot \frac{\text{in}^2}{\text{ft}}$

Use #4 @ 7in within the tensile zone $A_s := 0.34 \frac{\text{in}^2}{\text{ft}} > A_{\text{req}}$ **OK**

From CONSPAN, at release, the tension stress in the top fiber of the **exterior beam** at the transfer cross section is:

$$f_t := -0.53\text{ksi}$$

The compressive stress in the bottom fiber of the beam at the same cross section is:

$$f_b := 3.117\text{ksi}$$

The depth of the tensile zone x is: LRFD C5.9.4.1.2

$$\frac{-f_t}{x} = \frac{f_b}{21\text{in} - x}$$

$$x := \frac{21 \cdot f_t \cdot \text{in}}{f_b - f_t} = 3.052 \cdot \text{in} < 8\text{in}$$

The tensile force T in the concrete is: $T := \frac{f_t}{2} \cdot b_g \cdot x$

where, b_g is the width of the beam at top $b_g = 96 \cdot \text{in}$

Therefore $T := \frac{-f_t}{2} \cdot b_g \cdot x = 77.638 \cdot \text{kip}$

The required area of bonded reinforcement is: $A_{\text{req}} = \frac{T}{f_s}$

where $f_s := 0.5 \cdot f_y = 30 \cdot \text{ksi}$ LRFD C5.9.4.1.2

Therefore $A_{\text{req}} := \frac{T}{f_s \cdot b_g} = 0.323 \cdot \frac{\text{in}^2}{\text{ft}}$

Use #4 @ 7in within the tensile zone $A_s := 0.34 \frac{\text{in}^2}{\text{ft}} > A_{\text{req}}$ **OK**

5.5 Control of cracking LRFD Art. A.5.7.3.4

In the longitudinal direction, due to the existence of prestress strands, cracking is assumed to not happen. Therefore only in the transverse direction, cracking is considered.

The spacing of mild steel reinforcement in the layer closest to the tension face shall satisfy the following:

$$s \leq \frac{700 \cdot \gamma_e}{\beta_s \cdot f_{ss}} - 2 \cdot d_c \text{ in which, } \beta_s = 1 + \frac{d_c}{0.7 \cdot (h - d_c)}$$

where

γ_e = exposure factor
 = 1.00 for Class 1 exposure condition
 = 0.75 for Class 2 exposure condition

$\gamma_e := 0.75$ for deck SCDOT Bridge Design Manual 15.1.7

d_c = thickness of concrete cover measured from extreme tension fiber to center of the flexural reinforcement located closest thereto (in)

f_{ss} = tensile stress in steel reinforcement at the service limit state (ksi)

h = overall thickness or depth of the component (in) $h = 8 \cdot \text{in}$

The load effects determined for the Service I limit state for the NEXT-8 40ft span, according to Table 6, is displayed below.

Table 9	location	Demand
M_{p_total} (kip*ft/ft)	3 ft span	12.47
M_{p_total} (kip*ft/ft)	5 ft span	10.50
M_{n_total} (kip*ft/ft)	Exterior beam	-4.97
M_{n_total} (kip*ft/ft)	Interior beam	-3.10

The section is transformed elastic, cracked cross section. LRFD Art. 5.7.1

$$\text{modulus of elasticity, ksi} = 33000 \cdot K_1 \cdot w_c^{1.5} \cdot \sqrt{f'_c} \quad \text{LRFD Eq 5.4.2.4-1}$$

where

$$K_1 = \text{correction factor for source of aggregate:} \quad K_1 := 1$$

$$w_c = \text{unit weight of concrete(kcf):} \quad w_c = 150 \cdot \text{pcf}$$

This unit weight is higher than what is given in LRFD Table 3.5.1-1. It is to be used for deck design unless more precise information is provided.

$$f'_c = \text{specified compressive strength of concrete, ksi} \quad f'_c = 6.5 \cdot \text{ksi}$$

Therefore, the modulus of elasticity:

$$E_c := 33000 \cdot K_1 \cdot \left(\frac{w_c}{1000 \text{pcf}} \right)^{1.5} \cdot \sqrt{\frac{f'_c}{\text{ksi}}} \text{ ksi} = 4.888 \times 10^3 \cdot \text{ksi}$$

$$\text{Modulus ratio:} \quad n_c := \frac{E_s}{E_c} = 5.933 \quad \text{where,} \quad E_s = 2.9 \times 10^4 \cdot \text{ksi}$$

5.5.1 Check of the positive moment reinforcement

$$\text{For the 5ft deck with \#4@5in, according to Table 9,} \quad M_{pos} := 10.5 \frac{\text{kip} \cdot \text{ft}}{\text{ft}}$$

5.5.1.1 Cracked moment of inertia

Assume both layers of bars are in tension.

$$\text{For a 1ft cross section,} \quad b := 1 \text{ft}$$

$$\text{Bottom layer of rebar:} \quad A_s := 0.47 \frac{\text{in}^2}{\text{ft}}$$

Top layer of rebar: $A'_s := 0.47 \frac{\text{in}^2}{\text{ft}}$

Distance from center of bottom rebar to the top fiber of the beam is:

$$d := h - \text{Cover}_b - \frac{d_4}{2} = 6.75 \cdot \text{in}$$

Distance from center of top rebar to the bottom fiber of the beam is:

$$d' := h - \text{Cover}_t - \frac{d_4}{2} = 5.25 \cdot \text{in}$$

The location of neutral axis x measured from the top fiber of the beam is determined as below.

Sum of statical moments about the neutral axis gives:

$$\frac{1}{2} \cdot x^2 = n_c \cdot A_s \cdot (d - x) + n_c \cdot A'_s \cdot (h - d' - x)$$

$$x := \sqrt{n_c \cdot \left(A_s^2 \cdot n_c + A'_s{}^2 \cdot n_c + 2 \cdot A_s \cdot d - 2 \cdot A'_s \cdot d' + 2 \cdot A'_s \cdot h + 2 \cdot A_s \cdot A'_s \cdot n_c \right)} - A_s \cdot n_c - A'_s \cdot n_c = 1.687 \cdot \text{in}$$

The cracked moment of inertia is:

$$I_{cr} := \frac{b \cdot x^3}{3} + n_c \cdot A_s \cdot b \cdot (d - x)^2 + n_c \cdot A'_s \cdot b \cdot (h - d' - x)^2 = 93.839 \cdot \text{in}^4$$

5.5.1.2 Tensile stress in the bottom steel

$$f_{ss} := n_c \cdot \frac{M_{\text{pos}} \cdot b}{I_{cr}} \cdot (d - x) = 40.333 \cdot \text{ksi}$$

5.5.1.3 Rebar spacing

The thickness of concrete cover measured from extreme tension fiber to center of the flexural reinforcement located closest thereto (in) is:

$$d_c := h - d = 1.25 \cdot \text{in} \quad \text{where,} \quad h = 8 \cdot \text{in}$$

Therefore:

$$\beta_s := 1 + \frac{d_c}{0.7 \cdot (h - d_c)} = 1.265$$

So that the maximum rebar spacing is:

$$s_{\text{max}} := \frac{700 \cdot \gamma_e}{\beta_s \cdot \frac{f_{ss}}{\text{ksi}}} \text{in} - 2 \cdot d_c = 7.793 \cdot \text{in} > 5 \text{in} \quad \text{OK} \quad \text{where,} \quad \gamma_e = 0.75$$

5.5.2 Check of the negative moment reinforcement

Check the most critical negative moment against #4@5in

According to Table 9, $M_{neg} := 4.97 \frac{\text{kip}\cdot\text{ft}}{\text{ft}}$

5.5.2.1 Cracked moment of inertia

Assume both layers of bars are in tension.

For a 1ft cross section, $b := 1\text{ft}$

Bottom layer of rebar: $A_s := 0.47 \frac{\text{in}^2}{\text{ft}}$

Top layer of rebar: $A'_s := 0.47 \frac{\text{in}^2}{\text{ft}}$

The location of neutral axis x measured from the bottom fiber of the beam is determined as below.

Sum of statical moments about the neutral axis gives:

$$\frac{1}{2} \cdot x^2 = n_c \cdot A_s \cdot (h - d - x) + n_c \cdot A'_s \cdot (d' - x) \quad \text{where, } n_c = 5.933 \quad d = 6.75 \cdot \text{in} \quad d' = 5.25 \cdot \text{in}$$

$$x := \sqrt{n_c \cdot \left(A_s^2 \cdot n_c + A'_s{}^2 \cdot n_c - 2 \cdot A_s \cdot d + 2 \cdot A'_s \cdot d' + 2 \cdot A_s \cdot h + 2 \cdot A_s \cdot A'_s \cdot n_c \right) - A_s \cdot n_c - A'_s \cdot n_c} = 1.334 \cdot \text{in}$$

The cracked moment of inertia is:

$$I_{cr} := \frac{b \cdot x^3}{3} + n_c \cdot A_s \cdot b \cdot (h - d - x)^2 + n_c \cdot A'_s \cdot b \cdot (d' - x)^2 = 52.279 \cdot \text{in}^4$$

5.5.2.2 Tensile stress in the top steel

$$f_{ss} := n_c \cdot \frac{M_{neg} \cdot b}{I_{cr}} \cdot (d' - x) = 26.503 \cdot \text{ksi}$$

5.5.2.3 Rebar spacing

The thickness of concrete cover measured from extreme tension fiber to center of the flexural reinforcement located closest thereto (in) is:

$$d_c := h - d' = 2.75 \cdot \text{in}$$

Therefore:

$$\beta_s := 1 + \frac{d_c}{0.7 \cdot (h - d_c)} = 1.748$$

So that the maximum rebar spacing is:

$$s_{\max} := \frac{700 \cdot \gamma_e}{\beta_s \cdot \frac{f_{ss}}{\text{ksi}}} \text{in} - 2 \cdot d_c = 5.83 \cdot \text{in} > 5 \text{in} \quad \text{OK}$$

Therefore this requirement can be satisfied at any cross section

6. 30ft bridge design--- #4 @ 7in

The normalized moment demands in strength I limit state, according to Table 5, is:

Table 10	Location	Demand	Capacity provided by #4@7in Ubar
M_{p_total} (kip*ft/ft)	3 ft span	15.30	N/A
M_{p_total} (kip*ft/ft)	5 ft span	12.75	13.59
M_{n_total} (kip*ft/ft)	Exterior beam	-6.88	-8.90
M_{n_total} (kip*ft/ft)	Interior beam	-5.15	-8.90

6.1 Development length

The development length for #4 bar is as determined before: $l_{dh} = 12 \cdot \text{in}$

Interior beam:

For positive moment reinforcement, additional moment capacity is needed within the 3ft deck. Therefore the beginning point of the development length is taken at the inner face of each stem.

For negative moment reinforcement, The point where the development length begins is taken at the centerline of the 3ft span between the two stems. The development length is 12in as determined above. In the design, the two legs of the U-bar will be made of the same length.

6.2. Minimum reinforcement

LRFD Art. 5.7.3.3.1

At any section of a noncompression-controlled flexural component, the amount of prestressed and nonprestressed tensile reinforcement shall be adequate to develop a factored flexural resistance, M_p , at least equal to the lesser of:

- 1.33 times the factored moment required by the applicable strength load combination specified in Table 3.4.1-1 (Strength I); and
- $M_{cr} = 9.056 \cdot \text{kip} \cdot \text{ft}$

6.2.1 Positive moment

The factored positive moment required by strength I load combination within the 5ft deck for a 1ft strip, according to Table 10, is:

$$M_u := 12.75 \text{ kip}\cdot\text{ft}$$

$$\text{Thus, } 1.33 \cdot M_u = 16.957 \cdot \text{kip}\cdot\text{ft} > M_{cr} = 9.056 \cdot \text{kip}\cdot\text{ft}$$

Therefore M_{cr} requirement controls.

The factored capacity provided by #4@7in is:

$$M_r := 13.59 \text{ kip}\cdot\text{ft} > M_{cr} = 9.056 \cdot \text{kip}\cdot\text{ft} \quad \mathbf{OK}$$

This criteria can be met at every deck section.

6.2.2 Negative moment

6.2.2.1 Interior beam

The factored negative moment required by strength I load combination for the interior beam, according to Table 10, is:

$$M_u := -5.15 \text{ kip}\cdot\text{ft}$$

$$\text{Thus, } |1.33 \cdot M_u| = 6.849 \cdot \text{kip}\cdot\text{ft} < M_{cr} = 9.056 \cdot \text{kip}\cdot\text{ft}$$

Therefore $|1.33 \cdot M_u|$ requirement controls.

The factored negative moment resistance provided by #4@7in is :

$$|M_r| = 8.90 \text{ kip}\cdot\text{ft} > |1.33 \cdot M_u| = 6.849 \cdot \text{kip}\cdot\text{ft} \quad \mathbf{OK}$$

6.2.2.2 Exterior beam

The factored negative moment required by strength I load combination for the exterior beam is:

$$M_u := -6.88 \text{ kip}\cdot\text{ft}$$

$$\text{Thus, } |1.33 \cdot M_u| = 9.15 \cdot \text{kip}\cdot\text{ft} > M_{cr} = 9.056 \cdot \text{kip}\cdot\text{ft}$$

Therefore M_{cr} requirement controls.

The factored negative moment capacity provided by #4@7in is :

$$|M_r| = 8.90 \text{ kip}\cdot\text{ft} < M_{cr} = 9.056 \cdot \text{kip}\cdot\text{ft}$$

Therefore additional bars in the overhang need to extend beyond the point of critical demand for a distance of its development length.

6.3 Distribution reinforcement

As determined before, the minimum percentage of bottom longitudinal reinforcement should be:

$$\text{Percentage} := 67\%$$

For both the Interior beam and exterior beam

$$\text{Positive moment reinforcement in the transverse direction (\#4@7in): } A_s := 0.34 \frac{\text{in}^2}{\text{ft}}$$

$$A_s \cdot 67\% = 0.228 \cdot \frac{\text{in}^2}{\text{ft}}$$

$$\text{For longitudinal bottom bar, Use \#4@10in, which gives } 0.24 \frac{\text{in}^2}{\text{ft}}$$

6.4. Shrinkage and temperature reinforcement

As determined before, the minimum reinforcement area per foot, on each face and in each direction, shall be:

$$A_{s_TS} := 0.11 \frac{\text{in}^2}{\text{ft}}$$

This criteria can be met on each face and in each direction. The top longitudinal bars are provided by the bonded reinforcement, which is #4 @10in for the exterior beam, and #4@12in for the interior beam. The calculation is provided here.

From CONSPAN, at release, the tension stress in the top fiber of the **exterior beam** at the transfer cross section is:

$$f_t := -0.368 \text{ksi}$$

The compressive stress in the bottom fiber of the beam at the same cross section is:

$$f_b := 2.125 \text{ksi}$$

Refer to Figure F.24, the depth of the tensile zone x is: LRFD C5.9.4.1.2

$$\frac{-f_t}{x} = \frac{f_b}{21 \text{in} - x}$$

$$x := -\frac{21 \cdot f_t \cdot \text{in}}{f_b - f_t} = 3.1 \cdot \text{in} < 8 \text{in}$$

$$\text{The tensile force T in the concrete is: } T := \frac{f_t}{2} \cdot b_g \cdot x$$

$$\text{where, } b_g \text{ is the width of the beam at top } b_g = 96 \cdot \text{in}$$

$$\text{Therefore } T := \frac{-f_t}{2} \cdot b_g \cdot x = 54.756 \cdot \text{kip}$$

$$\text{The required area of bonded reinforcement is: } A_{\text{req}} = \frac{T}{f_s}$$

where $f_s := 0.5 \cdot f_y = 30 \cdot \text{ksi}$ LRFD C5.9.4.1.2

$$\text{Therefore } A_{\text{req}} := \frac{T}{f_s \cdot b_g} = 0.228 \cdot \frac{\text{in}^2}{\text{ft}}$$

Use #4 @ 10in within the tensile zone $A_s := 0.24 \frac{\text{in}^2}{\text{ft}} > A_{\text{req}}$ **OK**

From CONSPAN, at release, the tension stress in the top fiber of the **interior beam** at the transfer cross section is:

$$f_t := -0.314 \text{ksi}$$

The compressive stress in the bottom fiber of the beam at the same cross section is:

$$f_b := 1.889 \text{ksi}$$

The depth of the tensile zone x is: LRFD C5.9.4.1.2

$$\frac{-f_t}{x} = \frac{f_b}{21 \text{in} - x}$$

$$x := -\frac{21 \cdot f_t \cdot \text{in}}{f_b - f_t} = 2.993 \cdot \text{in} < 8 \text{in}$$

The tensile force T in the concrete is: $T := \frac{f_t}{2} \cdot b_g \cdot x$

where, b_g is the width of the beam at top $b_g = 96 \cdot \text{in}$

$$\text{Therefore } T := \frac{-f_t}{2} \cdot b_g \cdot x = 45.113 \cdot \text{kip}$$

The required area of bonded reinforcement is: $A_{\text{req}} = \frac{T}{f_s}$

where $f_s := 0.5 \cdot f_y = 30 \cdot \text{ksi}$ LRFD C5.9.4.1.2

$$\text{Therefore } A_{\text{req}} := \frac{T}{f_s \cdot b_g} = 0.188 \cdot \frac{\text{in}^2}{\text{ft}}$$

Use #4 @ 12in within the tensile zone $A_s := 0.2 \frac{\text{in}^2}{\text{ft}} > A_{\text{req}}$ **OK**

6.5. Control of cracking LRFD Art. A.5.7.3.4

In the longitudinal direction, due to the existence of prestress strands, cracking is assumed to not happen. Therefore only in the transverse direction, cracking is considered.

A summary of the demands on a 1ft strip for the 30ft span in Service I limit state, according to Table 6, is as follows:

Table 11 location Demand

	location	Demand
M_{p_total} (kip*ft/ft)	3 ft span	9.12
M_{p_total} (kip*ft/ft)	5 ft span	7.66
M_{n_total} (kip*ft/ft)	Exterior beam	-4.09
M_{n_total} (kip*ft/ft)	Interior beam	-3.10

The section is transformed elastic, cracked cross section. LRFD Art. 5.7.1

6.5.1 Check of the positive moment reinforcement

For the 5ft deck with #4@7in, according to Table 11, $M_{pos} := 7.66 \frac{\text{kip}\cdot\text{ft}}{\text{ft}}$

6.5.1.1 Cracked moment of inertia

For a 1ft cross section, $b := 1\text{ft}$

Bottom layer of rebar: $A_s := 0.34 \frac{\text{in}^2}{\text{ft}}$

Top layer of rebar: $A'_s := 0.34 \frac{\text{in}^2}{\text{ft}}$

The location of neutral axis x measured from the top fiber of the beam is determined as below.

Sum of statical moments about the neutral axis gives:

$$\frac{1}{2} \cdot x^2 = n_c \cdot A_s \cdot (d - x) + n_c \cdot A'_s \cdot (h - d' - x) \quad \text{where, } n_c = 5.933 \quad d = 6.75 \cdot \text{in} \quad d' = 5.25 \cdot \text{in}$$

$$x := \sqrt{n_c \cdot \left(A_s^2 \cdot n_c + A'_s{}^2 \cdot n_c + 2 \cdot A_s \cdot d - 2 \cdot A'_s \cdot d' + 2 \cdot A'_s \cdot h + 2 \cdot A_s \cdot A'_s \cdot n_c \right) - A_s \cdot n_c - A'_s \cdot n_c} = 1.482 \cdot \text{in}$$

The cracked moment of inertia therefore is:

$$I_{cr} := \frac{b \cdot x^3}{3} + n_c \cdot A_s \cdot b \cdot (d - x)^2 + n_c \cdot A'_s \cdot b \cdot (h - d' - x)^2 = 72.247 \cdot \text{in}^4$$

6.5.1.2 Tensile stress in the bottom steel

$$f_{ss} := n_c \cdot \frac{M_{pos} \cdot b}{I_{cr}} \cdot (d - x) = 39.765 \cdot \text{ksi}$$

6.5.1.3 Rebar spacing

The thickness of concrete cover measured from extreme tension fiber to center of the flexural reinforcement located closest thereto (in) is:

$$d_c := h - d = 1.25 \cdot \text{in} \quad \text{where, } h = 8 \cdot \text{in}$$

Therefore: $\beta_s := 1 + \frac{d_c}{0.7 \cdot (h - d_c)} = 1.265$

So that the maximum rebar spacing is:

$$s_{\max} := \frac{700 \cdot \gamma_e}{\beta_s \cdot \frac{f_{ss}}{\text{ksi}}} \text{in} - 2 \cdot d_c = 7.941 \cdot \text{in} > 7 \text{in} \quad \text{where, } \gamma_e = 0.75 \quad \underline{\text{OK}}$$

6.5.2 Check of the negative moment reinforcement

For the interior beams with #4@7in, according to Table 11, $M_{\text{neg}} := 3.10 \frac{\text{kip} \cdot \text{ft}}{\text{ft}}$

6.5.2.1 Cracked moment of inertia

For a 1ft cross section, $b := 1 \text{ft}$

Bottom layer of rebar: $A_s := 0.34 \frac{\text{in}^2}{\text{ft}}$

Top layer of rebar: $A'_s := 0.34 \frac{\text{in}^2}{\text{ft}}$

The location of neutral axis x measured from the bottom fiber of the beam is determined as below.

Sum of statical moments about the neutral axis gives:

$$\frac{1}{2} \cdot x^2 = n_c \cdot A_s \cdot (h - d - x) + n_c \cdot A'_s \cdot (d' - x) \quad \text{where, } n_c = 5.933 \quad d = 6.75 \cdot \text{in} \quad d' = 5.25 \cdot \text{in}$$

$$x := \sqrt{n_c \cdot \left(A_s^2 \cdot n_c + A'_s^2 \cdot n_c - 2 \cdot A_s \cdot d + 2 \cdot A'_s \cdot d' + 2 \cdot A_s \cdot h + 2 \cdot A_s \cdot A'_s \cdot n_c \right) - A_s \cdot n_c - A'_s \cdot n_c} = 1.18 \cdot \text{in}$$

The cracked moment of inertia therefore is:

$$I_{\text{cr}} := \frac{b \cdot x^3}{3} + n_c \cdot A_s \cdot b \cdot (h - d - x)^2 + n_c \cdot A'_s \cdot b \cdot (d' - x)^2 = 39.998 \cdot \text{in}^4$$

6.5.2.2 Tensile stress in the top steel

$$f_{ss} := n_c \cdot \frac{M_{\text{neg}} \cdot b}{I_{\text{cr}}} \cdot (d' - x) = 22.46 \cdot \text{ksi}$$

6.5.2.3 Rebar spacing

The thickness of concrete cover measured from extreme tension fiber to center of the flexural reinforcement located closest thereto (in) is:

$$d_c := h - d' = 2.75 \cdot \text{in} \quad \text{where, } h = 8 \cdot \text{in}$$

$$\text{Therefore: } \beta_s := 1 + \frac{d_c}{0.7 \cdot (h - d_c)} = 1.748$$

So that the maximum rebar spacing is:

$$s_{\max} := \frac{700 \cdot \gamma_e}{\beta_s \cdot \frac{f_{ss}}{\text{ksi}}} \text{in} - 2 \cdot d_c = 7.87 \cdot \text{in} > 7 \text{in} \quad \underline{\text{OK}}$$

7. 22ft bridge design using #4@7in

Compared with the 30ft bridge design, with the same reinforcement configuration and smaller demands (Table 5 and 6), the requirements of minimum reinforcement and cracking control reinforcement are definitely satisfied.

7.1 Development length

The development length for #4 bar is as determined before: $l_{dh} = 12 \cdot \text{in}$

For both the positive and negative moment reinforcement, this point where the development length begins is taken at the centerline of the beam.

7.2 Distribution reinforcement

For longitudinal bottom bar, Use #4@10in (refer the 30ft bridge design)

7.3. Shrinkage and temperature reinforcement

As determined before, the minimum reinforcement area per foot, on each face and in each direction, shall be:

$$A_{s_TS} := 0.11 \frac{\text{in}^2}{\text{ft}}$$

This criteria can be met on each face and in each direction. But this reinforcement need to be provided equally on both layers. The maximum spacing of the rebar shall not exceed either 3 times the deck depth or 18in. For the top longitudinal bar, use #4@18in. There is no bonding reinforcement needed as shown below:

From CONSPAN, at release, the tension stress in the top fiber of the beam at the transfer cross section is:

$$f_t := -0.152 \text{ksi}$$

which is smaller than the limiting tensile stress of concrete 0.2ksi

8. Design summary

8.1 Reinforcement configuration

	Main bar (transverse)	Development length (in)	Cut-off point (Interior beam)	Distribution bottom rebar (longitudinal)	Top rebar (longitudinal)
40ft	#4@5in	12in	inner face of each stem	#4@7in	#4 @7in
30ft	#4@7in	12in	inner face of each stem	#4@10in	#4 @10in (exterior beam) #4 @12in (interior beam) Use #4@10in
22ft	#4@7in	12in	centerline between two stems	#4@10in	#4 @18in Use #4@10in

Note: bonded reinforcement needs to be provided within the tension zone of concrete at the transfer cross section at the time of release.

8.2 Criteria check

8.2.1 Demand VS Capacity

		<u>40 ft span</u>	Capacity provided by #4@5in Ubar
	Location	Demand	
M+ (kip*ft/ft)	3 ft deck	21.18	N/A
M+ (kip*ft/ft)	5 ft deck	17.72	18.29
M- (kip*ft/ft)	exterior beam	-8.42	-11.47
M- (kip*ft/ft)	interior beam	-5.15	-11.47

		<u>30 ft span</u>	Capacity provided by #4@7in Ubar
	Location	Demand	
M+ (kip*ft/ft)	3 ft deck	15.30	N/A
M+ (kip*ft/ft)	5 ft deck	12.75	13.59
M- (kip*ft/ft)	exterior beam	-6.88	-8.90
M- (kip*ft/ft)	interior beam	-5.15	-8.90

	Location	22 ft span Demand	Capacity provided by #4@7in Ubar
M+ (kip*ft/ft)	3 ft deck	11.02	N/A
M+ (kip*ft/ft)	5 ft deck	8.78	13.59
M- (kip*ft/ft)	exterior beam	-5.25	-8.90
M- (kip*ft/ft)	interior beam	-5.15	-8.90

Note: the positive moment capacity in the 3ft deck span, due to the development length of the reinforcing steel, is larger than that in the 5ft deck span.

8.2.2 Minimum reinforcement check

40 ft span

M+ rebar	Any cross section	#4@5in	$M_r := 18.29 \text{ kip}\cdot\text{ft}$	$>$	$M_{cr} = 9.056 \cdot \text{kip}\cdot\text{ft}$	OK
M- rebar	Interior beam	#4@5in	$ M_r = 11.47 \text{ kip}\cdot\text{ft}$	$>$	$ 1.33 \cdot M_{u1} = 6.849 \cdot \text{kip}\cdot\text{ft}$	OK
	Exterior beam	#4@5in	$ M_r = 11.47 \text{ kip}\cdot\text{ft}$	$>$	$M_{cr} = 9.056 \cdot \text{kip}\cdot\text{ft}$	OK

30 ft span

M+ rebar	Any cross section	#4@7in	$M_r := 13.59 \text{ kip}\cdot\text{ft}$	$>$	$M_{cr} = 9.056 \cdot \text{kip}\cdot\text{ft}$	OK
M- rebar	Interior beam	#4@7in	$ M_r = 8.90 \text{ kip}\cdot\text{ft}$	$>$	$ 1.33 \cdot M_{u1} = 6.849 \cdot \text{kip}\cdot\text{ft}$	OK
	Exterior beam	#4@7in	$ M_r = 8.90 \text{ kip}\cdot\text{ft}$	$<$	$M_{cr} = 9.056 \cdot \text{kip}\cdot\text{ft}$	

Overhang reinforcement needs to extend beyond the critical negative moment demand point for a length of its development length

22 ft span

With the same rebar configuration with 30ft span and less demands, this requirement is satisfied at any cross section

8.2.3 Cracking control check

40 ft span

M +	5ft deck	#4@5in	$s_{\max} := \frac{700 \cdot \gamma_e}{\beta_s \cdot \frac{f_{ss}}{\text{ksi}}} \text{in} - 2 \cdot d_c = 7.793 \cdot \text{in} > 5 \text{in}$	OK
-----	----------	--------	--	-----------

M - Exterior beams		#4@5in	$s_{\max} := \frac{700 \cdot \gamma_e}{\beta_s \cdot \frac{f_{ss}}{\text{ksi}}} \text{in} - 2 \cdot d_c = 5.83 \cdot \text{in} > 5 \text{in}$	OK
--------------------	--	--------	---	-----------

Note: Positive moment demand in the 5ft span deck is the most critical, and negative moment demand in the exterior beam is most critical.

30 ft span

M +	5ft deck	#4@7in	$s_{\max} := \frac{700 \cdot \gamma_e}{\beta_s \cdot \frac{f_{ss}}{\text{ksi}}} \text{in} - 2 \cdot d_c = 7.941 \cdot \text{in} > 7 \text{in}$	OK
-----	----------	--------	--	-----------

M - Interior beams		#4@7in	$s_{\max} := \frac{700 \cdot \gamma_e}{\beta_s \cdot \frac{f_{ss}}{\text{ksi}}} \text{in} - 2 \cdot d_c = 7.87 \cdot \text{in} > 7 \text{in}$	OK
--------------------	--	--------	---	-----------

For exterior beams, due to the extension of the overhang reinforcement (see the minimum reinforcement check), this criteria can be satisfied.

22 ft span

With the same rebar configuration with 30ft span and less demands, this requirement can be satisfied at any cross section.

Appendix G

Shear Key Modeling

Inputs			Targeted Stiffness Matrix (δ) for a single shear key element in SAP2000						
Property	Value	Units	***Units are kips, inches, and radians						
$f'_c =$	9600	psi							
$\nu =$	0.2	-							
Calculated Values			U1	U2	U3	R1	R2	R3	
Property	Value	Units	6564	0	0	0	0	0	
			0	2010	0	0	0	2217	
			0	0	12256.5	0	0	0	
$E =$	5584.8	ksi $E = 57\sqrt{f'_c}$	0	0	0	239400	0	0	
			0	0	0	0	0	0	
$G =$	2327.0	ksi $G = \frac{E}{2(1+\nu)}$	0	2217	0	0	0	23940	
			Stiffness Matrix (δ) Based on Inputs						
			***Units are kips, inches, and radians						
$L =$	2.206	in $L = 2 \cdot \left(\frac{\delta_{U2_R3}}{\delta_{U2_U2}} \right)$	U1	U2	U3	R1	R2	R3	
			6564	0	0	0	0	0	
			0	2010	0	0	0	2217	
			0	0	12256.5	0	13519	0	
$J =$	226.947	in ⁴ $J = \frac{\delta_{R1_R1} \cdot L}{G}$	0	0	0	239400	0	0	
			0	0	0	0	145980	0	
$A =$	2.593	in ² $A = \frac{\delta_{U1_U1} \cdot L}{E}$	0	2217	0	0	0	23940	
$\beta_s =$	25.370	- $\beta_s = \frac{12 \cdot \delta_{R3_R3}}{L^2 \cdot \delta_{U2_U2}} - 4$	U1	U2	U3	R1	R2	R3	
			$=A \cdot E / L$	0	0	0	0	0	
			0	$=12 \cdot X_3$	0	0	0	$=6 \cdot L \cdot X_3$	
$I_3 =$	8.490	in ⁴ $I_3 = \frac{L^3 \cdot \delta_{U2_U2} \cdot (1 + \beta_s)}{12 \cdot E}$	U3	0	$=12 \cdot X_2$	0	$=6 \cdot L \cdot X_2$	0	
			0	0	0	$=J \cdot G / L$	0	0	
$f_{s,2} =$	1.309	- $f_{s,2} = \frac{\beta_s \cdot G \cdot A \cdot L^2}{12 \cdot E \cdot I_3}$	R1	0	0	$=6 \cdot L \cdot X_2$	0	0	
			0	0	0	0	$=L^2 \cdot (4 + \beta_s) \cdot X_2$	0	
$A_{v,2} =$	1.981	in ² $A_{v,2} = \frac{A}{f_{s,2}}$	R2	0	$=6 \cdot L \cdot X_3$	0	0	$=L^2 \cdot (4 + \beta_s) \cdot X_3$	
			R3	0	0	0	0	0	
			$X_3 =$	167.50	$X_3 = EI_y / (L^3 \cdot (1 + \beta_s))$				
			$X_2 =$	1021.38	$X_2 = EI_y / (L^3 \cdot (1 + \beta_s))$				
$I_2 =$	51.771	in ⁴ $I_2 = \frac{L^3 \cdot \delta_{U3_U3} \cdot (1 + \beta_s)}{12 \cdot E}$							
$f_{s,3} =$	0.215	- $f_{s,3} = \frac{\beta_s \cdot G \cdot A \cdot L^2}{12 \cdot E \cdot I_2}$							
$A_{v,3} =$	12.077	in ² $A_{v,3} = \frac{A}{f_{s,3}}$							

This page intentionally left blank

Appendix H

Load Distribution Calculations

NEXT-8 Positive Moment Distribution Factor---40ft span					
Load case	Stem	Beam line analysis	Design truck---Three axles		
		Moment (kip*ft)	Max moment	Distribution factor	Scaled LDF
One design truck exterior girder	1	432.05	58.09	0.1344	0.3069
	2	432.05	65.09	0.1506	0.3439
	3	432.05	35.15	0.0813	0.1857
	4	432.05	19.22	0.0445	0.1016
	5	432.05	8.87	0.0205	0.0469
	6	432.05	2.87	0.0066	0.0152
	sum	432.05	189.28	0.4381	1.0000
Two design trucks exterior girder	1	432.05	11.38	0.0264	0.0483
	2	432.05	33.91	0.0785	0.1438
	3	432.05	69.85	0.1617	0.2961
	4	432.05	125.49	0.2905	0.5320
	5	432.05	144.21	0.3338	0.6113
	6	432.05	86.95	0.2012	0.3686
	sum	864.10	471.80	1.0920	2.0000
Three design trucks exterior girder	1	432.05	35.78	0.0828	0.1339
	2	432.05	100.90	0.2335	0.3777
	3	432.05	183.86	0.4256	0.6883
	4	432.05	207.16	0.4795	0.7755
	5	432.05	179.77	0.4161	0.6730
	6	432.05	93.90	0.2173	0.3515
	sum	1296.15	801.38	1.8548	3.0000
One design truck interior girder	1	432.05	22.44	0.0519	0.0747
	2	432.05	61.48	0.1423	0.2047
	3	432.05	103.01	0.2384	0.3430
	4	432.05	68.41	0.1583	0.2278
	5	432.05	33.36	0.0772	0.1111
	6	432.05	11.59	0.0268	0.0386
	sum	432.05	300.28	0.6950	1.0000
Two design trucks interior girder	1	432.05	45.78	0.1060	0.1572
	2	432.05	122.74	0.2841	0.4214
	3	432.05	172.04	0.3982	0.5907
	4	432.05	143.11	0.3312	0.4913
	5	432.05	72.77	0.1684	0.2498
	6	432.05	26.08	0.0604	0.0895
	sum	864.10	582.52	1.3483	2.0000
Three design trucks interior girder	1	432.05	58.70	0.1359	0.2096
	2	432.05	151.95	0.3517	0.5426
	3	432.05	212.02	0.4907	0.7570
	4	432.05	211.49	0.4895	0.7551
	5	432.05	149.12	0.3451	0.5325
	6	432.05	56.92	0.1317	0.2032
	sum	1296.15	840.20	1.9447	3.0000

NEXT-8 Positive Moment Distribution Factor---30ft span					
	Stem	Beam line analysis	Design truck---Two axle		
		Moment (kip*ft)	Max moment	Distribution factor	Scaled LDF
One design truck exterior girder	1	267.03	0.50	0.0019	0.0044
	2	267.03	3.17	0.0119	0.0283
	3	267.03	8.69	0.0325	0.0778
	4	267.03	20.69	0.0775	0.1851
	5	267.03	49.33	0.1847	0.4413
	6	267.03	29.40	0.1101	0.2630
	sum	267.03	111.77	0.4186	1.0000
Two design trucks exterior girder	1	267.03	2.27	0.0085	0.0161
	2	267.03	13.98	0.0524	0.0991
	3	267.03	36.66	0.1373	0.2598
	4	267.03	85.36	0.3197	0.6048
	5	267.03	104.60	0.3917	0.7411
	6	267.03	39.40	0.1475	0.2792
	sum	534.07	282.27	1.0570	2.0000
Three design trucks exterior girder	1	267.03	9.70	0.0363	0.0588
	2	267.03	59.89	0.2243	0.3633
	3	267.03	118.89	0.4452	0.7211
	4	267.03	143.56	0.5376	0.8708
	5	267.03	122.44	0.4585	0.7427
	6	267.03	40.09	0.1501	0.2432
	sum	801.10	494.57	1.8521	3.0000
One design truck interior girder	1	267.03	5.61	0.0210	0.0292
	2	267.03	32.55	0.1219	0.1694
	3	267.03	74.38	0.2785	0.3871
	4	267.03	55.67	0.2085	0.2897
	5	267.03	20.45	0.0766	0.1064
	6	267.03	3.48	0.0130	0.0181
	sum	168.00	192.13	0.7195	1.0000
Two design trucks interior girder	1	267.03	15.80	0.0592	0.0866
	2	267.03	86.20	0.3228	0.4728
	3	267.03	122.11	0.4573	0.6698
	4	267.03	95.25	0.3567	0.5225
	5	267.03	38.67	0.1448	0.2121
	6	267.03	6.59	0.0247	0.0362
	sum	534.07	364.62	1.3654	2.0000
Three design trucks interior girder	1	267.03	27.93	0.1046	0.1605
	2	267.03	109.13	0.4087	0.6273
	3	267.03	145.41	0.5446	0.8359
	4	267.03	137.72	0.5157	0.7916
	5	267.03	86.67	0.3246	0.4982
	6	267.03	15.04	0.0563	0.0864
	sum	801.10	521.90	1.9544	3.0000

NEXT-8 Positive Moment Distribution Factor---22ft span					
	Stem	Beam line analysis	Design truck---One axle		
		Moment (kip*ft)	Max moment	Distribution factor	Scaled LDF
One design truck exterior girder	1	168.00	34.80	0.2072	0.3640
	2	168.00	43.70	0.2601	0.4571
	3	168.00	12.70	0.0756	0.1329
	4	168.00	3.45	0.0206	0.0361
	5	168.00	0.82	0.0049	0.0086
	6	168.00	0.12	0.0007	0.0013
	sum	168.00	95.60	0.5691	1.0000
Two design trucks exterior girder	1	168.00	0.90	0.0054	0.0076
	2	168.00	5.79	0.0345	0.0485
	3	168.00	22.33	0.1329	0.1870
	4	168.00	70.58	0.4201	0.5909
	5	168.00	94.93	0.5651	0.7947
	6	168.00	44.37	0.2641	0.3714
	sum	336.00	238.91	1.4221	2.0000
Three design trucks exterior girder	1	168.00	6.71	0.0400	0.0492
	2	168.00	40.68	0.2422	0.2982
	3	168.00	98.77	0.5879	0.7239
	4	168.00	115.34	0.6865	0.8453
	5	168.00	105.02	0.6251	0.7697
	6	168.00	42.81	0.2548	0.3137
	sum	504.00	409.33	2.4365	3.0000
One design truck interior girder	1	168.00	5.53	0.0329	0.0361
	2	168.00	33.13	0.1972	0.2162
	3	168.00	69.81	0.4155	0.4556
	4	168.00	34.42	0.2049	0.2246
	5	168.00	8.91	0.0531	0.0582
	6	168.00	1.43	0.0085	0.0093
	sum	168.00	153.22	0.9120	1.0000
Two design trucks interior girder	1	168.00	14.34	0.0853	0.0962
	2	168.00	71.82	0.4275	0.4817
	3	168.00	106.40	0.6333	0.7136
	4	168.00	77.14	0.4592	0.5174
	5	168.00	24.42	0.1454	0.1638
	6	168.00	4.09	0.0244	0.0274
	sum	336.00	298.21	1.7751	2.0000
Three design trucks interior girder	1	168.00	18.08	0.1076	0.1249
	2	168.00	82.24	0.4895	0.5680
	3	168.00	118.55	0.7056	0.8188
	4	168.00	118.29	0.7041	0.8170
	5	168.00	80.12	0.4769	0.5534
	6	168.00	17.07	0.1016	0.1179
	sum	504.00	434.35	2.5854	3.0000

NEXT-8 Shear Distribution Factor---40ft span					
Load case	Stem	Beam line analysis		Design truck--Three axles	
		Reaction (kips)	Max reactions	Distribution factor	Scaled LDF
One design truck Exterior	1	54.77	0.31	0.0057	0.0058
	2	54.77	0.07	0.0013	0.0014
	3	54.77	0.59	0.0108	0.0110
	4	54.77	2.31	0.0422	0.0429
	5	54.77	16.66	0.3042	0.3094
	6	54.77	33.90	0.6189	0.6295
	sum	54.77	53.85	0.9831	1.0000
Two design trucks Exterior	1	54.77	1.38	0.0252	0.0256
	2	54.77	0.67	0.0122	0.0124
	3	54.77	3.25	0.0594	0.0604
	4	54.77	26.04	0.4754	0.4835
	5	54.77	36.32	0.6631	0.6744
	6	54.77	40.04	0.7311	0.7437
	sum	109.54	107.69	1.9663	2.0000
Three design trucks Exterior	1	54.77	6.05	0.1105	0.1124
	2	54.77	9.53	0.1739	0.1769
	3	54.77	32.86	0.6000	0.6102
	4	54.77	38.99	0.7118	0.7240
	5	54.77	37.92	0.6923	0.7042
	6	54.77	36.20	0.6609	0.6722
	sum	164.31	161.54	2.9494	3.0000
One design truck Interior	1	54.77	4.29	0.0783	0.0796
	2	54.77	8.68	0.1584	0.1611
	3	54.77	28.33	0.5173	0.5262
	4	54.77	9.40	0.1716	0.1745
	5	54.77	1.53	0.0279	0.0284
	6	54.77	1.62	0.0296	0.0301
	sum	54.77	53.85	0.9832	1.0000
Two design trucks Interior	1	54.77	8.17	0.1492	0.1517
	2	54.77	24.10	0.4401	0.4477
	3	54.77	38.75	0.7076	0.7197
	4	54.77	29.42	0.5371	0.5463
	5	54.77	3.17	0.0579	0.0589
	6	54.77	4.07	0.0744	0.0757
	sum	109.54	107.69	1.9663	2.0000
Three design trucks Interior	1	54.77	11.50	0.2100	0.2136
	2	54.77	28.68	0.5236	0.5325
	3	54.77	41.27	0.7535	0.7664
	4	54.77	41.25	0.7532	0.7661
	5	54.77	28.04	0.5119	0.5207
	6	54.77	10.80	0.1973	0.2007
	sum	164.31	161.54	2.9495	3.0000

NEXT-8 Shear Distribution Factor---30ft span					
	Stem	Beam line analysis	Design truck--Three axles		
		Reaction (kips)	Max reactions	Distribution factor	Scaled LDF
One design truck exterior girder	1	48.83	0.08	0.0016	0.0017
	2	48.83	0.05	0.0009	0.0010
	3	48.83	0.34	0.0070	0.0072
	4	48.83	1.73	0.0354	0.0363
	5	48.83	15.62	0.3198	0.3282
	6	48.83	29.77	0.6098	0.6257
	sum		48.83	47.59	0.9746
Two design trucks exterior girder	1	48.83	0.46	0.0094	0.0096
	2	48.83	0.42	0.0087	0.0089
	3	48.83	2.20	0.0450	0.0462
	4	48.83	24.23	0.4963	0.5093
	5	48.83	34.35	0.7036	0.7219
	6	48.83	33.50	0.6862	0.7041
	sum		97.66	95.17	1.9491
Three design trucks exterior girder	1	48.83	3.13	0.0640	0.0657
	2	48.83	8.45	0.1730	0.1775
	3	48.83	30.31	0.6208	0.6370
	4	48.83	35.97	0.7366	0.7558
	5	48.83	35.67	0.7305	0.7496
	6	48.83	29.23	0.5987	0.6143
	sum		146.48	142.76	2.9237
One design truck interior girder	1	48.83	2.55	0.0522	0.0535
	2	48.83	7.83	0.1604	0.1646
	3	48.83	27.00	0.5529	0.5674
	4	48.83	8.35	0.1710	0.1755
	5	48.83	1.19	0.0244	0.0250
	6	48.83	0.67	0.0137	0.0140
	sum		48.83	47.59	0.9746
Two design trucks interior girder	1	48.83	4.72	0.0966	0.0992
	2	48.83	22.55	0.4618	0.4738
	3	48.83	36.35	0.7445	0.7640
	4	48.83	27.36	0.5602	0.5749
	5	48.83	2.35	0.0481	0.0493
	6	48.83	1.85	0.0379	0.0389
	sum		97.66	95.17	1.9491
Three design trucks interior girder	1	48.83	6.09	0.1247	0.1280
	2	48.83	26.40	0.5408	0.5549
	3	48.83	38.29	0.7841	0.8046
	4	48.83	38.27	0.7838	0.8042
	5	48.83	26.92	0.5514	0.5658
	6	48.83	6.79	0.1390	0.1426
	sum		146.48	142.76	2.9237

NEXT-8 Shear Distribution Factor---22ft span					
	Stem	Beam line analysis	Design truck--Two 32 axles		
		Reaction (kips)	Max reactions	Distribution factor	Scaled LDF
One design truck exterior girder	1	42.67	0.01	0.0001	0.0002
	2	42.67	0.01	0.0003	0.0003
	3	42.67	0.14	0.0034	0.0035
	4	42.67	1.14	0.0267	0.0277
	5	42.67	14.47	0.3392	0.3518
	6	42.67	25.37	0.5946	0.6166
	sum		42.67	41.14	0.9643
Two design trucks exterior girder	1	42.67	0.06	0.0015	0.0015
	2	42.67	0.15	0.0035	0.0037
	3	42.67	1.04	0.0244	0.0253
	4	42.67	22.00	0.5156	0.5347
	5	42.67	31.99	0.7498	0.7776
	6	42.67	27.04	0.6337	0.6572
	sum		85.33	82.29	1.9286
Three design trucks exterior girder	1	42.67	1.27	0.0298	0.0309
	2	42.67	7.08	0.1659	0.1721
	3	42.67	27.09	0.6349	0.6584
	4	42.67	32.10	0.7522	0.7801
	5	42.67	32.92	0.7715	0.8001
	6	42.67	22.97	0.5384	0.5584
	sum		128.00	123.43	2.8928
One design truck interior girder	1	42.67	1.18	0.0277	0.0287
	2	42.67	6.81	0.1597	0.1656
	3	42.67	25.18	0.5903	0.6121
	4	42.67	7.01	0.1642	0.1703
	5	42.67	0.80	0.0187	0.0193
	6	42.67	0.16	0.0038	0.0039
	sum		42.67	41.14	0.9643
Two design trucks interior girder	1	42.67	1.85	0.0434	0.0450
	2	42.67	20.75	0.4863	0.5043
	3	42.67	33.19	0.7780	0.8068
	4	42.67	24.69	0.5787	0.6001
	5	42.67	1.31	0.0307	0.0319
	6	42.67	0.49	0.0114	0.0118
	sum		85.33	82.29	1.9286
Three design trucks interior girder	1	42.67	2.48	0.0582	0.0603
	2	42.67	24.26	0.5687	0.5897
	3	42.67	34.47	0.8079	0.8378
	4	42.67	34.43	0.8070	0.8369
	5	42.67	24.75	0.5801	0.6016
	6	42.67	3.03	0.0710	0.0737
	sum		128.001	123.4286	2.8928

NEXT-6 Positive Moment Distribution Factor---40ft span						
Load case	Stem	Beam line analysis	Design truck---Three axles			
		Moment (kip*ft)	Max moment	Distribution factor	Scaled LDF	
One design truck exterior girder	1	432.05	2.85	0.0066	0.0123	
	2	432.05	6.41	0.0148	0.0275	
	3	432.05	11.92	0.0276	0.0512	
	4	432.05	19.90	0.0461	0.0855	
	5	432.05	31.09	0.0720	0.1336	
	6	432.05	47.62	0.1102	0.2046	
	7	432.05	64.43	0.1491	0.2768	
	8	432.05	48.54	0.1124	0.2085	
	sum	432.05	232.76	0.5387	1.0000	
Two design trucks exterior girder	1	432.05	69.23	0.1602	0.2711	
	2	432.05	104.46	0.2418	0.4090	
	3	432.05	115.08	0.2664	0.4506	
	4	432.05	95.76	0.2216	0.3750	
	5	432.05	60.07	0.1390	0.2352	
	6	432.05	36.93	0.0855	0.1446	
	7	432.05	20.17	0.0467	0.0790	
	8	432.05	9.09	0.0210	0.0356	
	sum	864.10	510.79	1.1822	2.0000	
Three design trucks exterior girder	1	432.05	79.61	0.1843	0.3005	
	2	432.05	124.08	0.2872	0.4683	
	3	432.05	147.29	0.3409	0.5559	
	4	432.05	156.05	0.3612	0.5890	
	5	432.05	131.00	0.3032	0.4944	
	6	432.05	86.49	0.2002	0.3264	
	7	432.05	47.90	0.1109	0.1808	
	8	432.05	22.45	0.0520	0.0847	
	sum	1296.15	794.88	1.8398	3.0000	
One design truck interior girder	1	432.05	11.35	0.0263	0.0343	
	2	432.05	24.22	0.0561	0.0732	
	3	432.05	42.67	0.0988	0.1290	
	4	432.05	72.83	0.1686	0.2202	
	5	432.05	80.16	0.1855	0.2424	
	6	432.05	54.39	0.1259	0.1644	
	7	432.05	30.52	0.0706	0.0923	
	8	432.05	14.61	0.0338	0.0442	
	sum	432.05	330.74	0.7655	1.0000	
Two design trucks interior girder	1	432.05	32.75	0.0758	0.1085	
	2	432.05	68.34	0.1582	0.2265	
	3	432.05	111.39	0.2578	0.3692	
	4	432.05	131.96	0.3054	0.4373	
	5	432.05	116.10	0.2687	0.3848	
	6	432.05	78.69	0.1821	0.2608	
	7	432.05	43.64	0.1010	0.1446	
	8	432.05	20.59	0.0477	0.0682	
	sum	864.10	603.46	1.3967	2.0000	
Three design trucks interior girder	1	432.05	37.17	0.0860	0.1295	
	2	432.05	78.35	0.1813	0.2729	
	3	432.05	128.40	0.2972	0.4472	
	4	432.05	160.54	0.3716	0.5591	
	5	432.05	159.94	0.3702	0.5570	
	6	432.05	144.02	0.3333	0.5016	
	7	432.05	103.39	0.2393	0.3601	
	8	432.05	49.56	0.1147	0.1726	
	sum	1296.15	861.3783	1.9937	3.0000	

NEXT-6 Positive Moment Distribution Factor---30ft span					
	Stem	Beam line analysis	Design truck---Two axles		Scaled LDF
		Moment (kip*ft)	Max moment	Distribution factor	
One design truck exterior girder	1	267.03	22.53	0.0844	0.1694
	2	267.03	47.48	0.1778	0.3568
	3	267.03	32.05	0.1200	0.2409
	4	267.03	16.08	0.0602	0.1209
	5	267.03	8.42	0.0315	0.0633
	6	267.03	4.20	0.0157	0.0316
	7	267.03	1.91	0.0071	0.0143
	8	267.03	0.39	0.0015	0.0029
	sum	267.03	133.06	0.4983	1.0000
Two design trucks exterior girder	1	267.03	29.52	0.1105	0.1921
	2	267.03	76.11	0.2850	0.4952
	3	267.03	82.83	0.3102	0.5389
	4	267.03	62.26	0.2331	0.4051
	5	267.03	31.62	0.1184	0.2057
	6	267.03	16.05	0.0601	0.1044
	7	267.03	7.44	0.0279	0.0484
	8	267.03	1.56	0.0058	0.0101
	sum	534.07	307.39	1.1511	2.0000
Three design trucks exterior girder	1	267.03	31.40	0.1176	0.1966
	2	267.03	84.18	0.3152	0.5272
	3	267.03	98.70	0.3696	0.6181
	4	267.03	101.71	0.3809	0.6369
	5	267.03	84.43	0.3162	0.5288
	6	267.03	50.77	0.1901	0.3180
	7	267.03	22.85	0.0856	0.1431
	8	267.03	5.01	0.0188	0.0314
	sum	801.10	479.04	1.7939	3.0000
One design truck interior girder	1	267.03	4.98	0.0187	0.0249
	2	267.03	22.10	0.0828	0.1105
	3	267.03	48.38	0.1812	0.2419
	4	267.03	58.42	0.2188	0.2921
	5	267.03	37.47	0.1403	0.1874
	6	267.03	18.20	0.0682	0.0910
	7	267.03	8.59	0.0322	0.0430
	8	267.03	1.84	0.0069	0.0092
	sum	267.03	199.99	0.7489	1.0000
Two design trucks interior girder	1	267.03	7.10	0.0266	0.0368
	2	267.03	31.84	0.1192	0.1652
	3	267.03	67.06	0.2511	0.3481
	4	267.03	90.98	0.3407	0.4722
	5	267.03	88.88	0.3328	0.4613
	6	267.03	63.71	0.2386	0.3307
	7	267.03	29.29	0.1097	0.1520
	8	267.03	6.50	0.0243	0.0337
	sum	534.07	385.34	1.4430	2.0000
Three design trucks interior girder	1	267.03	13.72	0.0514	0.0769
	2	267.03	61.43	0.2301	0.3444
	3	267.03	94.00	0.3520	0.5269
	4	267.03	106.30	0.3981	0.5959
	5	267.03	104.56	0.3915	0.5861
	6	267.03	88.06	0.3298	0.4936
	7	267.03	55.14	0.2065	0.3091
	8	267.03	11.99	0.0449	0.0672
	sum	801.10	535.19	2.0042	3.0000

NEXT-6 Positive Moment Distribution Factor---22ft span					
	Stem	Beam line analysis	Design truck---One axle		Scaled LDF
		Moment (kip*ft)	Max moment	Distribution factor	
One design truck exterior girder	1	168.00	29.21	0.1739	0.2874
	2	168.00	40.70	0.2423	0.4005
	3	168.00	19.42	0.1156	0.1910
	4	168.00	7.73	0.0460	0.0760
	5	168.00	2.99	0.0178	0.0294
	6	168.00	1.11	0.0066	0.0109
	7	168.00	0.39	0.0023	0.0038
	8	168.00	0.10	0.0006	0.0009
	sum	168.00	101.64	0.6050	1.0000
Two design trucks exterior girder	1	168.00	36.38	0.2165	0.2942
	2	168.00	67.62	0.4025	0.5468
	3	168.00	68.98	0.4106	0.5578
	4	168.00	47.36	0.2819	0.3830
	5	168.00	17.34	0.1032	0.1402
	6	168.00	6.66	0.0397	0.0539
	7	168.00	2.37	0.0141	0.0192
	8	168.00	0.59	0.0035	0.0048
	sum	336.00	247.31	1.4721	2.0000
Three design trucks exterior girder	1	168.00	37.83	0.2252	0.2813
	2	168.00	73.28	0.4362	0.5450
	3	168.00	84.30	0.5018	0.6270
	4	168.00	88.79	0.5285	0.6603
	5	168.00	68.29	0.4065	0.5079
	6	168.00	34.98	0.2082	0.2601
	7	168.00	12.65	0.0753	0.0941
	8	168.00	3.25	0.0194	0.0242
	sum	504.00	403.37	2.4010	3.0000
One design truck interior girder	1	168.00	2.79	0.0166	0.0179
	2	168.00	10.72	0.0638	0.0687
	3	168.00	29.66	0.1766	0.1901
	4	168.00	51.40	0.3059	0.3294
	5	168.00	40.27	0.2397	0.2581
	6	168.00	14.50	0.0863	0.0929
	7	168.00	5.33	0.0317	0.0342
	8	168.00	1.36	0.0081	0.0087
	sum	168.00	156.02	0.9287	1.0000
Two design trucks interior girder	1	168.00	8.26	0.0491	0.0541
	2	168.00	31.94	0.1901	0.2094
	3	168.00	64.84	0.3860	0.4251
	4	168.00	81.52	0.4852	0.5344
	5	168.00	66.76	0.3974	0.4376
	6	168.00	35.62	0.2120	0.2335
	7	168.00	12.85	0.0765	0.0842
	8	168.00	3.31	0.0197	0.0217
	sum	336.00	305.10	1.8161	2.0000
Three design trucks interior girder	1	168.00	8.92	0.0531	0.0605
	2	168.00	34.69	0.2065	0.2353
	3	168.00	69.34	0.4127	0.4704
	4	168.00	90.05	0.5360	0.6109
	5	168.00	87.21	0.5191	0.5917
	6	168.00	80.95	0.4818	0.5492
	7	168.00	55.40	0.3297	0.3758
	8	168.00	15.65	0.0932	0.1062
	sum	504.00	442.19	2.6321	3.0000

NEXT-6 Shear Distribution Factor---40ft span						
Load case	Stem	Beam line analysis		Design truck---Three axles		Scaled LDF
		Shear (kip)	Max shear	Distribution factor		
One design truck exterior girder	1	54.77	0.22	0.0040	0.0042	
	2	54.77	0.11	0.0020	0.0021	
	3	54.77	0.05	0.0009	0.0010	
	4	54.77	0.23	0.0041	0.0043	
	5	54.77	0.64	0.0118	0.0123	
	6	54.77	1.08	0.0197	0.0206	
	7	54.77	21.50	0.3926	0.4117	
	8	54.77	28.39	0.5184	0.5437	
	sum	54.77	52.23	0.9536	1.0000	
Two design trucks exterior girder	1	54.77	0.89	0.0163	0.0171	
	2	54.77	0.29	0.0053	0.0056	
	3	54.77	0.69	0.0127	0.0133	
	4	54.77	2.88	0.0526	0.0552	
	5	54.77	18.17	0.3318	0.3481	
	6	54.77	21.38	0.3903	0.4095	
	7	54.77	27.44	0.5010	0.5257	
	8	54.77	32.66	0.5963	0.6256	
	sum	109.54	104.41	1.9063	2.0000	
Three design trucks exterior girder	1	54.77	33.29	0.6079	0.6411	
	2	54.77	27.13	0.4954	0.5224	
	3	54.77	23.70	0.4327	0.4563	
	4	54.77	36.80	0.6719	0.7086	
	5	54.77	24.83	0.4534	0.4782	
	6	54.77	6.63	0.1211	0.1277	
	7	54.77	0.42	0.0076	0.0080	
	8	54.77	3.00	0.0547	0.0577	
	sum	164.31	155.80	2.8447	3.0000	
One design truck interior girder	1	54.77	2.88	0.0525	0.0529	
	2	54.77	0.75	0.0138	0.0139	
	3	54.77	21.80	0.3980	0.4011	
	4	54.77	23.86	0.4357	0.4391	
	5	54.77	2.84	0.0518	0.0522	
	6	54.77	1.05	0.0192	0.0193	
	7	54.77	0.17	0.0032	0.0032	
	8	54.77	0.99	0.0181	0.0182	
	sum	54.77	54.34	0.9922	1.0000	
Two design trucks interior girder	1	54.77	2.69	0.0491	0.0514	
	2	54.77	0.55	0.0100	0.0105	
	3	54.77	6.49	0.1184	0.1240	
	4	54.77	24.23	0.4423	0.4633	
	5	54.77	36.30	0.6628	0.6942	
	6	54.77	22.77	0.4158	0.4355	
	7	54.77	5.61	0.1024	0.1072	
	8	54.77	5.95	0.1087	0.1138	
	sum	109.54	104.59	1.9096	2.0000	
Three design trucks interior girder	1	54.77	7.72	0.1409	0.1488	
	2	54.77	21.51	0.3928	0.4147	
	3	54.77	28.78	0.5254	0.5548	
	4	54.77	25.63	0.4679	0.4941	
	5	54.77	37.12	0.6777	0.7156	
	6	54.77	23.01	0.4202	0.4437	
	7	54.77	5.43	0.0991	0.1046	
	8	54.77	6.42	0.1172	0.1237	
	sum	164.31	155.61	2.8412	3.0000	

NEXT-6 Shear Distribution Factor---30ft span					
	Stem	Beam line analysis	Design truck---Three axles		Scaled LDF
		Shear (kip)	Max shear	Distribution factor	
One design truck exterior girder	1	48.83	24.13	0.4941	0.5275
	2	48.83	20.19	0.4135	0.4414
	3	48.83	0.76	0.0155	0.0165
	4	48.83	0.43	0.0087	0.0093
	5	48.83	0.12	0.0024	0.0026
	6	48.83	0.02	0.0005	0.0005
	7	48.83	0.04	0.0007	0.0008
	8	48.83	0.06	0.0013	0.0014
	sum	48.83	45.74	0.9367	1.0000
Two design trucks exterior girder	1	48.83	26.68	0.5464	0.5910
	2	48.83	25.43	0.5207	0.5632
	3	48.83	19.30	0.3953	0.4275
	4	48.83	16.12	0.3301	0.3571
	5	48.83	2.01	0.0412	0.0445
	6	48.83	0.39	0.0080	0.0086
	7	48.83	0.09	0.0019	0.0021
	8	48.83	0.27	0.0055	0.0060
	sum	97.66	90.29	1.8492	2.0000
Three design trucks exterior girder	1	48.83	27.21	0.5572	0.5928
	2	48.83	25.52	0.5227	0.5561
	3	48.83	21.09	0.4319	0.4595
	4	48.83	34.10	0.6984	0.7430
	5	48.83	22.64	0.4636	0.4932
	6	48.83	5.38	0.1101	0.1172
	7	48.83	0.53	0.0108	0.0115
	8	48.83	1.22	0.0251	0.0267
	sum	146.48	137.69	2.8199	3.0000
One design truck interior girder	1	48.83	0.57	0.0118	0.0117
	2	48.83	0.08	0.0017	0.0017
	3	48.83	1.65	0.0337	0.0334
	4	48.83	20.11	0.4119	0.4085
	5	48.83	21.48	0.4398	0.4361
	6	48.83	3.95	0.0808	0.0801
	7	48.83	0.48	0.0097	0.0097
	8	48.83	0.93	0.0190	0.0188
	sum	48.83	49.24	1.0085	1.0000
Two design trucks interior girder	1	48.83	1.14	0.0233	0.0246
	2	48.83	0.56	0.0115	0.0122
	3	48.83	5.27	0.1080	0.1141
	4	48.83	22.18	0.4543	0.4800
	5	48.83	33.97	0.6957	0.7351
	6	48.83	20.89	0.4278	0.4520
	7	48.83	5.14	0.1053	0.1112
	8	48.83	3.27	0.0670	0.0708
	sum	97.66	92.43	1.8929	2.0000
Three design trucks interior girder	1	48.83	3.77	0.0772	0.0823
	2	48.83	20.74	0.4248	0.4525
	3	48.83	26.42	0.5410	0.5763
	4	48.83	22.75	0.4659	0.4962
	5	48.83	34.36	0.7038	0.7497
	6	48.83	20.99	0.4299	0.4579
	7	48.83	5.08	0.1040	0.1107
	8	48.83	3.41	0.0698	0.0744
	sum	146.48	137.52	2.8164	3.0000

NEXT-6 Shear Distribution Factor---22ft span					
	Stem	Beam line analysis	Design truck---Two axles		Scaled LDF
		Shear (kip)	Max shear	Distribution factor	
One design truck exterior girder	1	42.67	20.50	0.4804	0.5161
	2	42.67	19.00	0.4453	0.4784
	3	42.67	0.11	0.0025	0.0027
	4	42.67	0.08	0.0019	0.0021
	5	42.67	0.01	0.0003	0.0003
	6	42.67	0.00	0.0000	0.0000
	7	42.67	0.01	0.0002	0.0002
	8	42.67	0.01	0.0001	0.0001
	sum	42.67	39.71	0.9308	1.0000
Two design trucks exterior girder	1	42.67	21.61	0.5064	0.5545
	2	42.67	23.49	0.5505	0.6028
	3	42.67	16.86	0.3953	0.4328
	4	42.67	14.46	0.3388	0.3710
	5	42.67	1.29	0.0302	0.0331
	6	42.67	0.18	0.0041	0.0045
	7	42.67	0.01	0.0003	0.0003
	8	42.67	0.03	0.0008	0.0009
	sum	85.33	77.93	1.8264	2.0000
Three design trucks exterior girder	1	42.67	21.72	0.5090	0.5472
	2	42.67	23.58	0.5526	0.5942
	3	42.67	17.98	0.4213	0.4530
	4	42.67	30.95	0.7253	0.7799
	5	42.67	20.09	0.4708	0.5062
	6	42.67	3.98	0.0933	0.1003
	7	42.67	0.46	0.0107	0.0116
	8	42.67	0.30	0.0070	0.0075
	sum	128.00	119.05	2.7901	3.0000
One design truck interior girder	1	42.67	0.11	0.0026	0.0027
	2	42.67	0.03	0.0008	0.0008
	3	42.67	0.02	0.0004	0.0004
	4	42.67	20.86	0.4889	0.5116
	5	42.67	19.57	0.4586	0.4799
	6	42.67	0.01	0.0001	0.0001
	7	42.67	0.03	0.0006	0.0006
	8	42.67	0.15	0.0036	0.0037
	sum	42.67	40.77	0.9556	1.0000
Two design trucks interior girder	1	42.67	0.29	0.0067	0.0072
	2	42.67	0.46	0.0107	0.0115
	3	42.67	3.91	0.0917	0.0979
	4	42.67	19.75	0.4628	0.4942
	5	42.67	31.11	0.7292	0.7787
	6	42.67	18.56	0.4349	0.4644
	7	42.67	4.44	0.1042	0.1112
	8	42.67	1.40	0.0327	0.0350
	sum	85.33	79.91	1.8730	2.0000
Three design trucks interior girder	1	42.67	0.75	0.0176	0.0190
	2	42.67	19.65	0.4605	0.4957
	3	42.67	23.58	0.5526	0.5949
	4	42.67	19.37	0.4540	0.4888
	5	42.67	31.15	0.7301	0.7860
	6	42.67	18.56	0.4350	0.4683
	7	42.67	4.43	0.1038	0.1117
	8	42.67	1.41	0.0331	0.0356
	sum	128.00	118.90	2.7867	3.0000

This page intentionally left blank

Appendix I

Sample Bridge Calculations for NEXT-8 40 ft.

NEXT-8 Beam2 Design Check Outline:

1. Overview
2. Basic properties
3. Gross cross-section properties for a beam section including shear key:
4. Shear forces and bending moments:
 - 4.1 Shear forces and bending moments due to dead loads:
 - 4.1.1 Dead loads
 - 4.1.2 Unfactored shear forces and bending moments:
 - 4.2 Shear forces and bending moments due to live loads:
 - 4.2.1 Live loads
 - 4.2.2 Live load distribution factors for a typical interior beam
 - 4.2.3 Dynamic allowance
 - 4.2.4 Unfactored shear forces and bending moments
 - 4.2.5 Load combinations
5. Prestress loss
 - 5.1 Strand pattern:
 - 5.2 Gross cross section properties at the middle span:
 - 5.3 Prestress losses
 - 5.3.1 Elastic shortening
 - 5.3.2 Time-dependent losses using approximate method
 - 5.3.3 Total losses at transfer
 - 5.3.4 Total losses at service loads
6. Stress at limit states:
 - 6.1 Concrete stresses at transfer:
 - 6.1.1 Stress limits for concrete
 - 6.1.2 Stresses at transfer length section of bonded strands
 - 6.2 Concrete stresses at service loads after losses
 - 6.2.1 Stress limits for concrete
 - 6.2.2 Stresses at midspan or transfer length cross section
 - 6.3 Fatigue stress limit

- 7. Strength limit state
 - 7.1 Strain in strands
 - 7.2 Stress in strands
 - 7.3 Total force in each row of strands
 - 7.4 Moment contributed by each row of strand
 - 7.5 Moment capacity
- 8. Limits of reinforcement
 - 8.1 Maximum reinforcement
 - 8.2 Minimum reinforcement
- 9. Anchorage zone reinforcement
 - 10.1 Anchorage zone reinforcement
 - 10.2 Confinement reinforcement

1. Overview

In addition to the design of NEXT-D bridges using CONSPAN, a hand-calculation is provided here for the first interior pretensioned prestressed concrete beam of NEXT-8 beam bridge. In the calculation, the design span length is 39ft from center to center of bearings, and the total span length is 40ft. The overall width of the bridge is 48ft, and the roadway width between the interior faces of parapets is 44.83ft. An average 4-in bituminous overlay will be used for wearing surface. This example includes the load effect calculation from prestress load, dead loads, and HL-93 live loads, stress check of concrete and prestress tendon at different stages and different limit states, moment capacity check, reinforcement requirement check, and pretensioned anchorage zone check. Four design limit states are investigated, including Service I, Service III, Fatigue, and Strength I limit states. The format follows the example design of NEXTD 36 D provided by PCI bridge design manual. This hand calculation is provided as a comparison with the corresponding results provided by CONSPAN, the bridge model in which has a total span length of 39ft 10.5in.

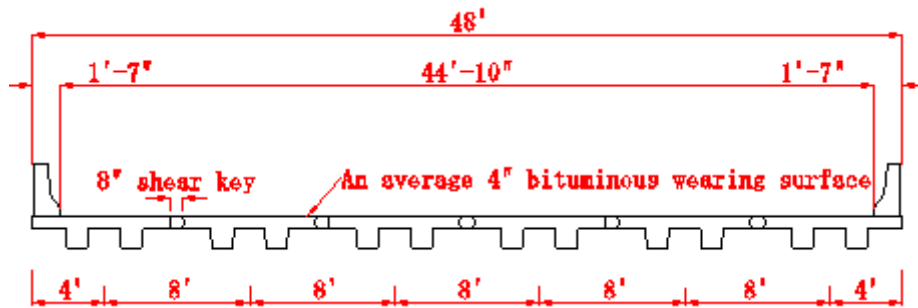


Figure I.1: NEXT-8 Bridge Cross Section

2. Basic properties:

Overall beam length = 40ft

Design span = 39ft

Required concrete compressive strength at transfer: $f'_{ct} := 5.2\text{ksi}$

Specified concrete compressive strength for use in design: $f'_c := 6.5\text{ksi}$

Precast beam unit weight: $w_c := 0.15 \frac{\text{kip}}{\text{ft}^3}$

Note: the shear key weight is included in the precast beam weight, and its density is assumed to be the same as the precast beam.

Modulus of elasticity, ksi = $33000 \cdot K_1 \cdot w_c^{1.5} \cdot \sqrt{f'_c}$ LRFD Eq 5.4.2.4-1

where

Correction factor for source of aggregate: $K_1 := 1$

Unit weight of concrete: $w_c = 150 \cdot \text{pcf}$

For Young's modulus calculation, this unit weight is higher than what is given in LRFD Table 3.5.1-1. It is to be used for design check unless more precise information is provided.

f'_c = specified compressive strength of concrete, ksi

Therefore, the modulus of elasticity for:

$$\text{precast beam at transfer: } E_{ct} := 33000 \cdot K_1 \cdot \left(\frac{w_c}{1000\text{pcf}} \right)^{1.5} \cdot \sqrt{\frac{f'_{ct}}{\text{ksi}}} \text{ ksi} = 4.372 \times 10^3 \cdot \text{ksi}$$

$$\text{precast beam at service loads: } E_c := 33000 \cdot K_1 \cdot \left(\frac{w_c}{1000\text{pcf}} \right)^{1.5} \cdot \sqrt{\frac{f'_c}{\text{ksi}}} \text{ ksi} = 4.888 \times 10^3 \cdot \text{ksi}$$

Future bituminous wearing surface (average 4in) : $w_{fws} := 140\text{pcf}$ LRFD Table 3.5.1-1

New Jersey-type barrier on each side: $w_p := 443\text{plf}$

Prestressing strands: 0.5-in.-dia., seven-wire, low-relaxation

Area of one strand = 0.153in²

Specified tensile strength: $f_{pu} := 270\text{ksi}$

Yield strength: $f_{py} := 0.9 \cdot f_{pu} = 243 \cdot \text{ksi}$ LRFD Table 5.4.4.1-1

Stress limits for prestressing strands (pretensioning): LRFD Table 5.9.3-1

before transfer: $f_{pt} \leq 0.75f_{pu} = 202.5 \cdot \text{ksi}$

at service limit state (after all losses), $f_{pe} \leq 0.8f_{py} = 194.4 \cdot \text{ksi}$

Modulus of elasticity, $E_p := 28500\text{ksi}$ LRFD Art. 5.4.4.2

Reinforcing bars:

Yield strength, $f_y := 60\text{ksi}$

Modulus of elasticity, $E_s := 29000\text{ksi}$

3. Gross cross-section properties for a beam section including shear key:

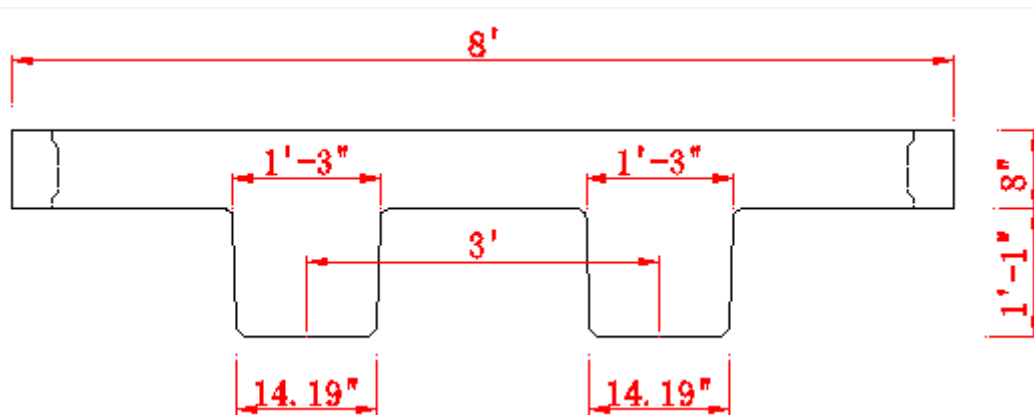


Figure I.2 Cross Section of Beam 2

Area of cross section of precast beam: $A_g := 1147.4 \text{ in}^2$

Overall depth of precast beam: $h := 21 \text{ in}$

Moment of inertia about the centroid of the noncomposite precast beam: $I_g := 37120 \text{ in}^4$

Distance from centroid to the extreme bottom fiber of the beam: $y_b := 13.54 \text{ in}$

Distance from centroid to the extreme top fiber of the beam: $y_t := h - y_b = 7.46 \text{ in}$

Section modulus for extreme bottom fiber of the beam: $S_b := \frac{I_g}{y_b} = 2.742 \times 10^3 \cdot \text{in}^3$

Section modulus for extreme top fiber of the beam: $S_t := \frac{I_g}{y_t} = 4.976 \times 10^3 \cdot \text{in}^3$

4. Shear forces and bending moments:

4.1 Shear forces and bending moments due to dead loads:

4.1.1 Dead loads

DC = dead load of structural components and nonstructural attachments

LRFD Art. 3.3.2

Beam self weight (including shear key weight): $w_g := w_c \cdot A_g = 1.195 \cdot \frac{\text{kip}}{\text{ft}}$

LRFD Article 4.6.2.2.1 states that permanent loads of and on the deck (barrier and wearing surface loads) may be distributed uniformly among all the beams if the following conditions are met:

a. Width of deck is constant **OK**

b. Number of beams (N_b) not less than four $N_b := 6$

c. Beams are parallel and approximately of the same stiffness **OK**

d. The roadway part of the overhang, $d_e \leq 3\text{ft}$.

$$d_e := 2.5\text{ft} - 1\text{in} - 18\text{in} = 0.917\text{ft} \quad \text{OK}$$

e. Curvature is less than specified in LRFD Specifications, (curvature = 0⁰) **OK**

f. Cross section of the bridge is consistent with one of the cross sections given in LRFD Table 4.6.2.2.1-1. The bridge is "sufficiently connected to act as unit" and the bridge type is (i). **OK**

Since these criteria are satisfied, the wearing surface loads are distributed equally among the six beams.

DW = dead load of wearing surface per each beam:

LRFD Art. 3.3.2

$$DW := \frac{(4\text{in} \cdot w_{\text{fws}}) \cdot 44.83\text{ft}}{6} = 0.349 \cdot \frac{\text{kip}}{\text{ft}} \quad \text{where,} \quad w_{\text{fws}} = 140 \cdot \text{pcf}$$

For the barriers, their weights are decided to be distributed to only the exterior beam and the adjacent interior beam.

$$\text{Barrier weight per each beam : } w_b := \frac{w_p}{2} = 0.221 \cdot \frac{\text{kip}}{\text{ft}}$$

4.1.2 Unfactored shear forces and bending moments:

Values of shear forces and bending moments for a typical interior beam under the self weight of beam (including shear key weight), barriers, and wearing surface are calculated using finite element software SAP2000, which agree with CONSPAN results. For these calculations, the span length (L) is the design span, 39ft. However, for calculations of stresses and deformations at the time prestress is transferred, the overall length of the precast member, 40ft, is used.

4.2 Shear forces and bending moments due to live loads:

4.2.1 Live loads

Design live load is HL-93, which consists of a combination of: LRFD 3.6.1.2.1

1. Design truck or design tandem with dynamic allowance

LRFD 3.6.1.2.2 and 3.6.1.2.3

2. Design lane load of 0.64klf without dynamic allowance LRFD 3.6.1.2.4

4.2.2 Live load distribution factors for a typical interior beam

The live load bending moments and shear forces are determined by using the simplified distribution factor formulas (LRFD Art. 4.6.2.2), provided that the following conditions are met:

LRFD Art.4.6.2.2.1

a. Width of deck is constant **OK**

- b. Number of beams (N_b) not less than four $N_b := 6$ **OK**
- c. Beams are parallel and approximately of the same stiffness **OK**
- d. The roadway part of the overhang, $d_e \leq 3\text{ft}$.

$$d_e := 2.5\text{ft} - 1\text{in} - 18\text{in} = 0.917\text{ft} < 3\text{ft} \quad \text{OK}$$

- e. Curvature is less than specified in LRFD Specifications, (curvature = 0⁰) **OK**
- f. For a precast concrete double-tee section with shear keys without transverse post-tensioning, the bridge type is (i) LRFD Table 4.6.2.2.1-1

Number of design lanes = the integer part of the ratio ($w/12$), where w is the clear roadway width, in ft, between the curbs LRFD Art. 3.6.1.1.1

$$w := 44.83\text{ft} \quad \frac{w}{12\text{ft}} = 3.736$$

Number of design lanes: $N_L := 3$

4.2.2.1 Distribution factor for bending moments for cross section type I

- a. For all limit states except fatigue limit state:

Regardless of number of loaded lanes:

$$\text{DFM} = 0.075 + (S/9.5)^{0.6}(S/L)^{0.2}(K_g/12/L/t_s^3)^{0.1} \quad \text{LRFD Table 4.6.2.2.2b-1}$$

Provided that:

$$3.5 \leq S \leq 16 \quad S := 8\text{ft} \quad \text{OK}$$

$$4.5 \leq t_s \leq 12 \quad t_s := 8\text{in} \quad \text{OK}$$

$$20 \leq L \leq 240 \quad L := 39\text{ft} \quad \text{OK}$$

$$N_b \geq 4 \quad N_b = 6 \quad \text{OK}$$

$$10000 \leq K_g \leq 7000000 \quad \text{OK (see below)}$$

where

DFM = distribution factor for moment for interior beam

S = beam spacing, ft

t_s = structural depth of concrete deck, in

L = beam span, ft

K_g = longitudinal stiffness parameter, $\text{in}^4 = n(I_{bs} + A_{bs}e_g^2)$

where

n = modular ratio between beam and deck slab concrete

$$n := \frac{E_c}{E_c} = 1$$

I_{bs} = moment of inertia of the beam in⁴

A_{bs} = cross-sectional area of the beam, in²

e_g = distance between the centers of gravity of the basic beam and deck, in

LRFD Article 4.6.2.2 is unclear on how to calculate K_g for bridges without a composite deck. In this design, both the stems and the flange are considered together as a beam.

Therefore, $K_g := I_g + A_g \cdot y_t^2 = 1.01 \times 10^5 \cdot \text{in}^4$

$$\text{DFM} := 0.075 + \left(\frac{S}{9.5\text{ft}}\right)^{0.6} \cdot \left(\frac{S}{L}\right)^{0.2} \cdot \left(\frac{\frac{K_g}{\text{in}^4}}{12 \frac{L}{\text{ft}} \cdot \frac{t_s^3}{\text{in}^3}}\right)^{0.1} = 0.678 \text{ lanes /beam}$$

Conspan DFM = 0.677 **OK**

For one design lane loaded:

$$\text{DFM} := 0.06 + \left(\frac{S}{14\text{ft}}\right)^{0.4} \cdot \left(\frac{S}{L}\right)^{0.3} \cdot \left(\frac{\frac{K_g}{\text{in}^4}}{12 \frac{L}{\text{ft}} \cdot \frac{t_s^3}{\text{in}^3}}\right)^{0.1} = 0.516 \text{ lanes /beam}$$

Conspan DFM = 0.514 **OK**

Thus, the case of two or more lanes loaded controls and $\text{DFM} := 0.677 \text{ lanes/beam}$

b. For fatigue limit state:

The distribution factor for fatigue load should be calculated based on a single design truck without the multiple presence factor 1.2 specified in LRFD Article 3.6.1.1.2. Therefore the factor for fatigue limit state is:

$$\text{DFM} := \frac{0.514}{1.2} = 0.428 \text{ lanes /beam}$$

4.2.2.2 Distribution factor for shear force

For two or more lanes loaded:

$$\text{DFV} = 0.2 + (S/12) - (S/35)^2$$

Provided that:

$$3.5 \leq S \leq 16 \quad S := 8\text{ft} \quad \text{OK}$$

$$4.5 \leq t_s \leq 12 \quad t_s := 8\text{in} \quad \text{OK}$$

$$20 \leq L \leq 240 \quad L := 39\text{ft} \quad \text{OK}$$

$$N_b \geq 4 \quad N_b = 6 \quad \text{OK}$$

where

DFV = distribution factor for shear for interior beam

S = beam spacing, ft

Therefore, the distribution factor for shear force is:

$$\text{DFV} := 0.2 + \frac{S}{12\text{ft}} - \left(\frac{S}{35\text{ft}} \right)^2 = 0.814 \quad \text{lanes /beam}$$

$$\text{Conspan DFM} = 0.825 \quad \text{OK}$$

For one design lane loaded:

$$\text{DFV} := 0.36 + \frac{S}{25\text{ft}} = 0.68 \quad \text{lanes /beam}$$

$$\text{Conspan DFM} = 0.681 \quad \text{OK}$$

Thus, the case of two or more lanes loaded controls and DFV = 0.825 lanes/beam

4.2.3 Dynamic allowance

LRFD Tabel 3.6.2.1-1

IM := 15% for fatigue and fracture limit states

IM := 33% for all other limit states

where IM = dynamic load allowance, applied to design truck and design tandem

4.2.4 Unfactored shear forces and bending moments

4.2.4.1 Due to truck load; V_{LT} and M_{LT}

a. For all limit states except for fatigue limit state:

Shear force and bending moment envelopes on a per-lane basis are calculated using SAP2000. The results agree with CONSPAN results and are not given here. Truck load shear forces and bending moments per beam are:

$$\begin{aligned} V_{LT} &= (\text{shear force per lane})(\text{DFV})(1+\text{IM}) \\ &= (\text{shear force per lane})(0.825)(1+0.33) \\ &= (\text{shear force per lane})(1.097)\text{kips} \end{aligned}$$

$$\begin{aligned}
M_{LT} &= (\text{bending moment per lane})(DFV)(1+IM) \\
&= (\text{bending moment per lane})(0.677)(1+0.33) \\
&= (\text{bending moment per lane})(0.9)\text{kips}
\end{aligned}$$

b. For fatigue limit state:

Article 3.6.1.4.1 in the LRFD Specifications states that fatigue load is a single design truck which has the same axle weight used in all other limit states but with a constant spacing of 30ft between the 32-kip axles. bending moment envelope on a per-lane basis is calculated using SAP2000.

Therefore, bending moment of fatigue truck load is:

$$\begin{aligned}
M_f &= (\text{bending moment per lane})(DFM)(1+IM) \\
&= (\text{bending moment per lane})(0.428)(1+0.15) \\
&= (\text{bending moment per lane})(0.492)\text{ft-kips}
\end{aligned}$$

4.2.4.2 Due to Design lane load; V_{LL} and M_{LL}

To obtain the maximum shear force at a section located at a distance (x) from the left support under a uniformly distributed load of 0.64kips/ft, load the member to the right of the section under consideration. Therefore, the maximum shear force per lane is:

$$V_x = \frac{0.32(L - x)^2}{L} \quad \text{for } x \leq 0.5L$$

where V_x is in Kips/lane and L and x are in ft.

The maximum bending moment at any section is also calculated using SAP2000. Lane load shear force and bending moment per typical interior beam are as follows:

$$\begin{aligned}
V_{LL} &= (\text{lane load shear force})(DFV) \\
&= (\text{lane load shear force})(0.825) \text{ kips}
\end{aligned}$$

For all limit states except for fatigue limit state:

$$\begin{aligned}
M_{LL} &= (\text{lane load bending moment})(DFM) \\
&= (\text{lane load bending moment})(0.677) \text{ ft-kips}
\end{aligned}$$

Note that dynamic allowance is not applied to the design lane loading.

4.2.5 Load combinations

LRFD Art. 3.4

Total factored load is taken as:

$$Q = \sum \eta_i \gamma_i Q_i \quad \text{LRFD Art. 3.4.1-1}$$

where

η_i = a load modifier relating to ductility, redundancy, and operational importance.

LRFD Art. 1.3.2.1

γ_i = load factors

LRFD Table 3.4.1-1

Q_i = force effects from specified loads

Investigating different limit states given in LRFD Article 3.4.1, the following limit states are applicable:

Service I: check compressive stresses in prestressed concrete components:

$$Q = 1.00 (DC + DW) + 1.00(LL+IM)$$

Service III: check tensile stresses in prestressed concrete components:

$$Q = 1.00 (DC + DW) + 0.80(LL+IM) \quad \text{LRFD Table 3.4.1-1}$$

Strength I: check ultimate strength: LRFD Tables 3.4.1-1 and 3.4.1-2

$$\text{Maximum } Q = 1.25(DC)+1.50(DW)+1.75(LL+IM)$$

$$\text{Minimum } Q = 0.90(DC)+0.65(DW)+1.75(LL+IM)$$

This load combination is the general load combination for strength limit state design. Since only critical positive moment needs to be investigated, only the first combination will be applied.

Fatigue I: check stress range in strands:

$$Q = 1.50(LL+IM) \quad \text{LRFD Table 3.4.1-1}$$

This load combination is a special load combination to check the tensile stress range in the strands due to live load and dynamic allowance.

5. Prestress loss

5.1 Strand pattern:

Strand type: 1/2-270K-LL, low relaxation strands

Quantity : 26

Pattern : straight

End pattern:

4 @ 13.5in

2 @ 6.5in

10 @ 4.5in

10 @ 2.5in

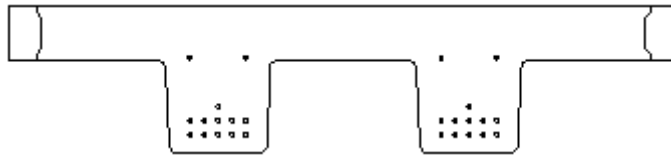


Figure I.3: End Strand Pattern

Parameters:

Strand diameter: 0.5in

Strand area: 0.153in^2

Tensile strength: $f_{pu} := 270\text{ksi}$

5.2 Gross cross section properties at the middle span:

The distance between center of gravity of strands and the bottom concrete fiber of the beam is:

$$y_{bs} := \frac{10 \cdot (2.5\text{in} + 4.5\text{in}) + 2 \cdot 6.5\text{in} + 4 \cdot 13.5\text{in}}{26} = 5.269 \cdot \text{in}$$

Gross cross section at transfer:

$$A_{ti} = \text{area of gross cross section at transfer: } A_{ti} := A_g = 1.147 \times 10^3 \cdot \text{in}^2$$

$$I_{ti} = \text{moment of inertia of the gross cross section at transfer: } I_{ti} := I_g = 3.712 \times 10^4 \cdot \text{in}^4$$

$$y_{bti} = \text{distance from the centroid of the gross cross section to the extreme bottom fiber of the beam at transfer: } y_{bti} := y_b = 13.54 \cdot \text{in}$$

e_{ti} = eccentricity of strands with respect to gross cross section at transfer:

$$e_{ti} := y_{bti} - y_{bs} = 8.271 \cdot \text{in}$$

S_{bti} = section modulus for the extreme bottom fiber of the gross cross section at transfer

$$s_{bti} := \frac{I_{ti}}{y_{bti}} = 2.742 \times 10^3 \cdot \text{in}^3$$

S_{tti} = section modulus for the extreme top fiber of the gross cross section at transfer

$$s_{tti} := \frac{I_{ti}}{h - y_{bti}} = 4.976 \times 10^3 \cdot \text{in}^3$$

Gross cross section at final time:

$$A_{tf} = \text{area of gross cross section at final time: } A_{tf} := A_g = 1.147 \times 10^3 \cdot \text{in}^2$$

$$I_{tf} = \text{moment of inertia of the gross cross section at final time: } I_{tf} := I_g = 3.712 \times 10^4 \cdot \text{in}^4$$

$$y_{btf} = \text{distance from the centroid of the gross cross section to the extreme bottom fiber of the beam at final time: } y_{btf} := y_b = 13.54 \cdot \text{in}$$

e_{tf} = eccentricity of strands with respect to the gross cross section at final time:

$$e_{tf} := y_{btf} - y_{bs} = 8.271 \cdot \text{in}$$

S_{btf} = section modulus for the extreme bottom fiber of the gross cross section at final time

$$s_{btf} := \frac{I_{tf}}{y_{btf}} = 2.742 \times 10^3 \cdot \text{in}^3$$

S_{ttf} = section modulus for the extreme top fiber of the gross cross section at final time

$$s_{\text{ttf}} := \frac{I_{\text{tf}}}{h - y_{\text{btf}}} = 4.976 \times 10^3 \cdot \text{in}^3$$

5.3 Prestress losses

Total prestress loss:

$$\Delta f_{\text{pT}} = \Delta f_{\text{pES}} + \Delta f_{\text{pLT}}$$

where

Δf_{pT} = total loss in prestressing steel stress

Δf_{pES} = sum of all losses or gains due to elastic shortening or extension at the time of application of prestress and /or external loads

Δf_{pLT} = long-term losses due to shrinkage and creep of concrete, and relaxation of steel after transfer. In this design, the approximate estimates of time-dependent losses are used.

5.3.1 Elastic shortening

$$\Delta f_{\text{pES}} = \frac{E_{\text{p}}}{E_{\text{ct}}} f_{\text{cgp}} \quad \text{LRFD Eq. 5.9.5.2.3a-1}$$

where

E_{p} = modulus of elasticity of prestressing strands $E_{\text{p}} = 2.85 \times 10^4 \cdot \text{ksi}$

E_{ct} = modulus of elasticity of beam concrete at transfer $E_{\text{ct}} = 4.372 \times 10^3 \cdot \text{ksi}$

f_{cgp} = sum of concrete stresses at the center of gravity of prestressing strands due to prestressing force at transfer and the self weight of the member at sections of maximum moment.

When gross section properties are used to calculate concrete stress, the effects of losses and gains due to elastic deformations Δf_{pES} should be included in calculating f_{cgp}

$$f_{\text{cgp}} = \frac{P_{\text{pi}} - \Delta f_{\text{pES}} \cdot (26 \cdot 0.153 \text{in}^2)}{A_{\text{ti}}} + \frac{\left[P_{\text{pi}} - \Delta f_{\text{pES}} \cdot (26 \cdot 0.153 \text{in}^2) \right] \cdot e_{\text{ti}}^2}{I_{\text{ti}}} - \frac{M_{\text{g}} \cdot e_{\text{ti}}}{I_{\text{ti}}}$$

where

P_{pi} = total prestressing force before transfer:

$$P_{\text{pi}} := 26 \cdot 0.153 \text{in}^2 \cdot 0.75 \cdot f_{\text{pu}} = 805.545 \cdot \text{kip}$$

e_{ti} = eccentricity of strands at midspan at transfer

$$e_{\text{ti}} = 8.271 \cdot \text{in}$$

M_g should be calculated based on the overall beam length of 40 ft. Here, the M_g using the design span length of 39 is applied, which will give a larger stress in concrete.

$$M_g := 227.24 \text{ kip}\cdot\text{ft}$$

Therefore,

$$f_{cgp} = \frac{P_{pi} - \frac{E_p}{E_{ct}} f_{cgp} \cdot (26 \cdot 0.153 \text{ in}^2)}{A_{ti}} + \frac{\left[P_{pi} - \frac{E_p}{E_{ct}} f_{cgp} \cdot (26 \cdot 0.153 \text{ in}^2) \right] \cdot e_{ti}^2}{I_{ti}} - \frac{M_g \cdot e_{ti}}{I_{ti}}$$

$$f_{cgp} := \frac{500.0 \cdot A_{ti} \cdot E_{ct} \cdot P_{pi} \cdot e_{ti}^2 - 500.0 \cdot A_{ti} \cdot E_{ct} \cdot M_g \cdot e_{ti} + 500.0 \cdot E_{ct} \cdot I_{ti} \cdot P_{pi}}{1989.0 \cdot A_{ti} \cdot E_p \cdot e_{ti}^2 \cdot \text{in}^2 + 1989.0 \cdot E_p \cdot I_{ti} \cdot \text{in}^2 + 500.0 \cdot A_{ti} \cdot E_{ct} \cdot I_{ti}} = 1.475 \times 10^3 \text{ psi}$$

$$\text{CONSPAN : } f_{cgp} = 1.474 \text{ ksi}$$

$$\Delta f_{pES} := \frac{E_p}{E_{ct}} f_{cgp} = 9.617 \cdot \text{ksi} \quad \text{CONSPAN : } f_{pES} = 9.61 \text{ ksi}$$

5.3.2 Time-dependent losses using approximate method

The long-term prestress loss, Δf_{pLT} , due to creep of concrete, shrinkage of concrete, and relaxation of steel shall be estimated using the following formula:

$$\Delta f_{pLT} = 10.0 \cdot \frac{f_{pi} \cdot A_{ps}}{A_g} \cdot \gamma_h \cdot \gamma_{st} + 12.0 \cdot \gamma_h \cdot \gamma_{st} + \Delta f_{pR} \quad \text{LRFD Eq. 5.9.5.3-1}$$

with the first term corresponds to creep losses, the second term to shrinkage losses, and the third to relaxation losses.

where

f_{pi} = prestressing steel stress immediately prior to transfer (ksi)

$$f_{pi} := 0.75 \cdot f_{pu} = 202.5 \cdot \text{ksi}$$

$$A_{ps} = \text{area of prestressing steel (in}^2) \quad A_{ps} := 26 \cdot 0.153 \text{ in}^2 = 3.978 \cdot \text{in}^2$$

γ_h = correction factor for relative humidity of the ambient air

$$\gamma_h = 1.7 - 0.01 \cdot H$$

in which,

H = the average annual ambient relative humidity (%) $H := 75$

$$\text{Therefore } \gamma_h := 1.7 - 0.01 \cdot H = 0.95$$

γ_{st} = correction factor for specified concrete strength at time of prestress transfer to the concrete member

$$\gamma_{st} := \frac{5}{\left(1 + \frac{f'_{ct}}{\text{ksi}}\right)} = 0.806$$

Δf_{pR} = an estimate of relaxation loss taken as 2.4ksi for low relaxation strand. $\Delta f_{pR} := 2.4\text{ksi}$

Therefore

$$\Delta f_{pLT} := 10.0 \cdot \frac{f_{pi} \cdot A_{ps}}{A_g} \cdot \gamma_h \cdot \gamma_{st} + 12.0\text{ksi} \cdot \gamma_h \cdot \gamma_{st} + \Delta f_{pR} = 16.972 \cdot \text{ksi}$$

CONSPAN : $f_{pLT} = 16.97\text{ksi}$

5.3.3 Total losses at transfer

AASHTO LRFD C5.9.5.2.3a and C5.9.5.3 indicate that the losses or gains due to elastic deformation must be included in determining the total prestress losses and the effective stress in prestressing strands.

$$\Delta f_{pi} := \Delta f_{pES} = 9.617 \cdot \text{ksi}$$

Effective stress in tendons immediately after transfer, $f_{pt} := f_{pi} - \Delta f_{pi} = 192.883 \cdot \text{ksi}$

Total prestressing force after transfer, $P_{pt} := f_{pt} \cdot A_{ps} = 767.29 \cdot \text{kip}$

$$\text{Initial loss, \%} = (\text{Total losses at transfer}) / (f_{pi}) = \frac{\Delta f_{pi}}{f_{pi}} \cdot 100 = 4.749$$

When determining the concrete stress using gross cross section properties, the strand force is that at transfer:

The total prestressing force at transfer, $P_{pt} = 767.29 \cdot \text{kip}$

5.3.4 Total losses at service loads

Total loss due to elastic shortening at transfer and long-term losses (Service III) is:

$$\Delta f_{pT} := \Delta f_{pES} + \Delta f_{pLT} = 26.589 \cdot \text{ksi}$$

The elastic gain due to superimposed dead load, and live load is:

$$\begin{aligned} & \left[(M_p + M_{ws}) + 0.8 \cdot (M_{LL} + M_{LT}) \right] \cdot \frac{e_{tf}}{I_{tf}} \cdot \frac{E_p}{E_c} \\ & = (716.7\text{kip}\cdot\text{ft} - 227.24\text{kip}\cdot\text{ft}) \left(\frac{e_{tf}}{I_{tf}} \cdot \frac{E_p}{E_c} \right) = 7.631 \cdot \text{ksi} \end{aligned}$$

The effective stress in strands after all losses and gains:

$$f_{pe} := f_{pi} - \Delta f_{pT} + 7.631 \text{ ksi} = 183.542 \cdot \text{ksi} \quad \text{CONSPAN: } f_{pe} = 183 \text{ ksi}$$

Check prestressing stress limit at service limit state: LRFD Table 5.9.3-1

$$0.8f_{py} = 194.4 \cdot \text{ksi} > f_{pe} = 183.542 \cdot \text{ksi} \quad \text{OK}$$

$$\text{Force per strand after all losses and gains} = f_{pe} \cdot 0.153 \text{ in}^2 = 28.082 \cdot \text{kip}$$

Therefore, the total prestressing force after all losses = $28.016 \text{ kip} \cdot 26 = 728.416 \cdot \text{kip}$

$$\text{Final loss percentage} = \frac{f_{pi} - f_{pe}}{f_{pi}} \cdot 100 = 9.362$$

CONSPAN considers an adjustment of prestress loss due to superimposed dead load, and live load. CONSPAN : =9.63%

Force per strand with elastic loss and total time-dependent losses =

$$(f_{pi} - \Delta f_{pT}) \cdot 0.153 \text{ in}^2 = 26.914 \cdot \text{kip}$$

Total prestressing force, $P_{pe} := 26.914 \text{ kip} \cdot 26 = 699.764 \cdot \text{kip}$

CONSPAN considers the effect due to superimposed dead load, and live load.

$$\text{CONSPAN : } P_{pe} := 183 \text{ ksi} \cdot 0.153 \text{ in}^2 \cdot 26 = 727.974 \cdot \text{kip}$$

6. Stress at limit states:

6.1 Concrete stresses at transfer:

Because the gross cross section is used, the total prestressing force at transfer,

$$P_{pt} = 767.29 \cdot \text{kip}$$

6.1.1 Stress limits for concrete LRFD Art. 5.9.4

Compression:

$$0.6f'_{ct} = 3.12 \cdot \text{ksi}$$

where f'_{ct} = concrete strength at transfer = 5.2ksi

Tension:

In areas other than the precompressed tensile zone and without bonded auxiliary reinforcement

$$-0.0948 \cdot \sqrt{\frac{f'_{ct}}{\text{ksi}}} \text{ ksi} = -0.216 \cdot \text{ksi} \leq -0.2 \text{ ksi}$$

Therefore, -0.2ksi (controls)

with bonded auxiliary reinforcement sufficient to resist the tensile force in the concrete computed assuming an uncracked section, where reinforcement is proportioned using a stress of $0.5f_y$, not to exceed 30ksi.

$$-0.24 \sqrt{\frac{f_{ct}}{\text{ksi}}} \text{ksi} = -0.547 \cdot \text{ksi}$$

6.1.2 Stresses at transfer length section of bonded strands

Stresses at this location are checked since this cross section is most critical as reflected from CONSPAN result summary.

Transfer length = 60 (strand diameter) = $60 \cdot 0.5\text{in} = 2.5 \cdot \text{ft}$

$$M_g := \frac{w_g \cdot 40\text{ft}}{2} \cdot 2.5\text{ft} - \frac{w_g \cdot (2.5\text{ft})^2}{2} = 56.025 \cdot \text{kip} \cdot \text{ft} \quad \text{where,} \quad w_g = 1.195 \cdot \text{klf}$$

Compute concrete stress in the top of beam:

$$f_t := \frac{P_{pt}}{A_{ti}} - \frac{P_{pt} \cdot e_{ti}}{s_{tti}} + \frac{M_g}{s_{tti}} = -0.472 \cdot \text{ksi} \quad \text{CONSPAN } f_t = -0.472\text{ksi}$$

Tensile stress limit for concrete with bonded reinforcement: -0.547ksi **OK**

Bonded auxiliary reinforcement must be provided in the top of the beam.

In order to determine the required bonded reinforcement area, the tensile zone needs to be determined first by using the stresses at extreme fibers.

Compute concrete stress in bottom of beam:

$$f_b := \frac{P_{pt}}{A_{ti}} + \frac{P_{pt} \cdot e_{ti}}{s_{bti}} - \frac{M_g}{s_{bti}} = 2.738 \cdot \text{ksi} \quad \text{CONSPAN } f_b = 2.739\text{ksi}$$

Compressive stress limit for concrete: 3.12ksi **OK**

The depth of the tensile zone x is: LRFD C5.9.4.1.2

$$\frac{-f_t}{x} = \frac{f_b}{h - x}$$

$$x := -\frac{f_t \cdot h}{f_b - f_t} = 3.085 \cdot \text{in} < 8\text{in}$$

The tensile force in the concrete T is: $T = \frac{f_t}{2} \cdot b \cdot x$

where b is the width of the beam at top $b := 96\text{in}$

Therefore $T := \frac{-f_t}{2} \cdot b \cdot x = 69.825 \cdot \text{kip}$

The required area of bonded reinforcement is: $A_{req} = \frac{T}{f_s}$

where $f_s := 0.5 \cdot f_y = 30 \cdot \text{ksi}$

Therefore $A_{req} := \frac{T}{f_s \cdot b} = 0.291 \cdot \frac{\text{in}^2}{\text{ft}}$

Use #4 @ 7in within the tensile zone $A_s := 0.34 \frac{\text{in}^2}{\text{ft}} > A_{req}$ **OK**

6.2 Concrete stresses at service loads after losses LRFD Art. 5.9.4.2

With elastic loss and total time-dependent losses, $P_{pe} = 727.974 \cdot \text{kip}$

6.2.1 Stress limits for concrete

Compression:

Due to the sum of effective prestress, permanent loads, and transient loads (i.e. all dead loads and live loads), for load combination Service I (final 1 in CONSPAN)

for precast beams: $0.6\phi_w f'_c$

where ϕ_w is a reduction factor, it shall be taken to be equal to 1.0 when the web and flange slenderness ratios, calculated according to Article 5.7.4.7.1 are not greater than 15. This condition is satisfied for the NEXT-8 beam. Therefore $\phi_w := 1$ $0.6\phi_w f'_c = 3.9 \cdot \text{ksi}$

Due to sum of effective prestress and permanent loads (i.e. beam self weight including shear key, weight of future wearing surface, and weight of barriers), for load combination Service I (final II in CONSPAN):

for precast beams: $0.45f'_c = 2.925 \cdot \text{ksi}$

Tension:

LRFD Table 5.9.4.2.2-1

For components with bonded prestressing tendons or reinforcement that are subjected to not worse than moderate corrosion conditions

for load combination Service III:

for precast beams $-0.19 \sqrt{\frac{f'_c}{\text{ksi}}} \text{ ksi} = -0.484 \cdot \text{ksi}$

6.2.2 Stresses at midspan or transfer length cross section

6.2.2.1 Concrete compressive stress at top fiber of the beam at middle span

To check top compressive stresses, middle span is the critical cross section. Two cases are considered:

1. Under permanent loads and prestress, load combination service I

$$f_{tg} := \frac{P_{pe}}{A_{tf}} - \frac{P_{pe} \cdot e_{tf}}{s_{tff}} + \frac{227.24 \text{kip} \cdot \text{ft} + 42.02 \text{kip} \cdot \text{ft} + 66.35 \text{kip} \cdot \text{ft}}{s_{tff}} = 0.234 \cdot \text{ksi}$$

Compressive stress limit: 2.925ksi **OK** CONSPAN $f_{tg} = 0.234 \text{ksi}$

2. Under prestress, permanent and transient loads, load combination Service I:

$$f_{tg} := \frac{P_{pe}}{A_{tf}} - \frac{P_{pe} \cdot e_{tf}}{s_{tff}} + \frac{812 \text{kip} \cdot \text{ft}}{s_{tff}} = 1.383 \cdot \text{ksi} \quad \text{CONSPAN } f_{tg} = 1.383 \text{ksi}$$

Compressive stress limit: 3.9ksi **OK**

6.2.2.2 Concrete compressive stress at bottom fiber of the beam at transfer cross section

Only the case under permanent loads and prestress need to be considered. And the transfer cross section is critical.

Load combination Service I

$$f_{tg} := \frac{P_{pe}}{A_{tf}} + \frac{P_{pe} \cdot e_{tf}}{s_{btf}} - \frac{42.43 \text{kip} \cdot \text{ft} + 7.846 \text{kip} \cdot \text{ft} + 12.388 \text{kip} \cdot \text{ft}}{s_{btf}} = 2.556 \cdot \text{ksi}$$

CONSPAN $f_{tg} = 2.536 \text{ksi}$

Compressive stress limit: 2.925ksi **OK**

6.2.2.3 Concrete tensile stress in bottom of beam at middle span, load combination Service III

$$f_b := \frac{P_{pe}}{A_{tf}} + \frac{P_{pe} \cdot e_{tf}}{s_{btf}} - \frac{716.7 \text{kip} \cdot \text{ft}}{s_{btf}} = -0.306 \cdot \text{ksi} \quad \text{CONSPAN } f_b = -0.306 \text{ksi}$$

Tensile stress limit: **OK**
-0.484 ksi

6.3 Fatigue stress limit

LRFD Article 5.5.3.1 states that in fully prestressed components other than segmentally constructed bridges, the compressive stress due to Fatigue I load combination and one half the sum of effective prestress and permanent loads shall not exceed $0.4f_c'$ after losses.

At middle span, the unfactored fatigue bending moment is 247kip*ft. Therefore, stress at the top fiber of the beam is:

$$\frac{247 \text{kip} \cdot \text{ft}}{s_{tff}} + \frac{1}{2} \left(\frac{P_{pe}}{A_{tf}} - \frac{P_{pe} \cdot e_{tf}}{s_{tff}} + \frac{227.24 \text{kip} \cdot \text{ft} + 42.02 \text{kip} \cdot \text{ft} + 66.35 \text{kip} \cdot \text{ft}}{s_{tff}} \right) = 0.713 \cdot \text{ksi}$$

CONSPAN 0.713ksi

< $0.4f_c' = 2.6 \cdot \text{ksi}$ **OK**

At the transfer length cross section, the unfactored fatigue bending moment is 51.2 kip·ft. Therefore, stress at the bottom fiber of the beam is:

$$-\frac{51.2 \text{kip}\cdot\text{ft}}{s_{\text{btf}}} + \frac{1}{2} \left(\frac{P_{\text{pe}}}{A_{\text{tf}}} + \frac{P_{\text{pe}} \cdot e_{\text{tf}}}{s_{\text{btf}}} - \frac{42.43 \text{kip}\cdot\text{ft} + 7.846 \text{kip}\cdot\text{ft} + 12.388 \text{kip}\cdot\text{ft}}{s_{\text{btf}}} \right) = 1.054 \cdot \text{ksi}$$

CONSPAN 1.037ksi

$$< 0.4f'_c = 2.6 \cdot \text{ksi} \quad \text{OK}$$

7. Strength limit state

Total ultimate bending moment for strength I is:

$$M_u = 1.25(\text{DC}) + 1.5(\text{DW}) + 1.75(\text{LL} + \text{IM})$$

From CONSPAN or SAP2000, this ultimate bending moment is

$$M_u := 1269.8 \text{kip}\cdot\text{ft}$$

Strain compatibility method is used without consideration of the contribution of any rebar, which is what CONSPAN does. The procedure here is the same as that used in CONSPAN. The whole procedure is iterative. A loop can be used to locate the neutral axis c. By trial and error, c is as below.

$$c := 2.76 \text{in}$$

β_1 = stress factor of compression block

$$= 0.85 \text{ for } f'_c \leq 4 \text{ksi}$$

$$= 0.85 - 0.05 (f'_c - 4) \geq 0.65 \text{ for } f'_c > 4 \text{ksi}$$

$$\beta_1 := 0.85 - 0.05 \left(\frac{f'_c}{\text{ksi}} - 4 \right) = 0.725$$

where, f'_c = specified compressive strength of concrete $f'_c = 6.5 \cdot \text{ksi}$

a = depth of the equivalent stress block, in.

$$a := \beta_1 \cdot c = 2.001 \cdot \text{in} \quad \text{CONSPAN: } a = 2 \text{in}$$

7.1 Strain in strands

7.1.1 After all the prestress losses, assume each strands has the same stress, when the beam is under the action of prestressing force alone. At this time, the strain in each strand is:

$$\epsilon_{\text{psln}} := \frac{f_{\text{pe}}}{E_p}$$

where

f_{pe} = stress in strands after elastic and long-term loss due to creep, shrinkage, and steel relaxation. $f_{\text{pe}} := f_{\text{pi}} - \Delta f_{\text{pT}} = 175.911 \cdot \text{ksi}$

$$\epsilon_{ps1n} := \frac{f_{pe}}{E_p} = 6.172 \times 10^{-3}$$

7.1.2 As the beam concrete is totally decompressed (strain is zero), the increment in strand strain is equal to the strain in surrounding concrete with P_e acting alone. The strain in strand now is:

$$\epsilon_{ps2n} := \frac{P_{pe}}{E_c \cdot A_{tf}} + \frac{P_{pe} \cdot e_{tf}^2}{E_c \cdot I_{tf}}$$

where

P_e = the total prestressing force in the beam after long-term loss

$$P_{pe} = 7.28 \times 10^5 \text{ lbf}$$

Therefore,

$$\epsilon_{ps2n} := \frac{P_{pe}}{E_c \cdot A_{tf}} + \frac{P_{pe} \cdot e_{tf}^2}{E_c \cdot I_{tf}} = 4.043 \times 10^{-4}$$

7.1.3 The third component of strains in each row of strand is:

$$\text{Row 1: } \epsilon_{ps31} := 0.003 \cdot \frac{(h - 2.5in - c)}{c} = 0.017$$

$$\text{Row 2: } \epsilon_{ps32} := 0.003 \cdot \frac{(h - 4.5in - c)}{c} = 0.015$$

$$\text{Row 3: } \epsilon_{ps33} := 0.003 \cdot \frac{(h - 6.5in - c)}{c} = 0.013$$

$$\text{Row 4: } \epsilon_{ps34} := 0.003 \cdot \frac{(h - 13.5in - c)}{c} = 5.152 \times 10^{-3}$$

7.1.4 The total strain in each row of strand is:

$$\text{Row 1: } \epsilon_{ps1} := \epsilon_{ps1n} + \epsilon_{ps2n} + \epsilon_{ps31} = 0.024 \quad > \quad 0.0086$$

$$\text{Row 2: } \epsilon_{ps2} := \epsilon_{ps1n} + \epsilon_{ps2n} + \epsilon_{ps32} = 0.022 \quad > \quad 0.0086$$

$$\text{Row 3: } \epsilon_{ps3} := \epsilon_{ps1n} + \epsilon_{ps2n} + \epsilon_{ps33} = 0.019 \quad > \quad 0.0086$$

$$\text{Row 4: } \epsilon_{ps4} := \epsilon_{ps1n} + \epsilon_{ps2n} + \epsilon_{ps34} = 0.012 \quad > \quad 0.0086$$

7.2 The stress in each row of strand is:

$$\text{Row 1: } f_{ps1} := f_{pu} - \frac{0.04}{\epsilon_{ps1} - 0.007} \text{ksi} = 267.603 \cdot \text{ksi}$$

$$\text{Row 2: } f_{ps2} := f_{pu} - \frac{0.04}{\epsilon_{ps2} - 0.007} \text{ksi} = 267.244 \cdot \text{ksi}$$

$$\text{Row 3: } f_{ps3} := f_{pu} - \frac{0.04}{\epsilon_{ps3} - 0.007} \text{ksi} = 266.758 \cdot \text{ksi}$$

$$\text{Row 4: } f_{ps4} := f_{pu} - \frac{0.04}{\epsilon_{ps4} - 0.007} \text{ksi} = 261.541 \cdot \text{ksi}$$

7.3 Total force in each row of strand is:

$$\text{Row 1: } F_{p1} := f_{ps1} \cdot 10 \cdot 0.153 \text{in}^2 = 409.432 \cdot \text{kip}$$

$$\text{Row 2: } F_{p2} := f_{ps2} \cdot 10 \cdot 0.153 \text{in}^2 = 408.883 \cdot \text{kip}$$

$$\text{Row 3: } F_{p3} := f_{ps3} \cdot 2 \cdot 0.153 \text{in}^2 = 81.628 \cdot \text{kip}$$

$$\text{Row 4: } F_{p4} := f_{ps4} \cdot 4 \cdot 0.153 \text{in}^2 = 160.063 \cdot \text{kip}$$

Check force balance

$$F_p := F_{p1} + F_{p2} + F_{p3} + F_{p4} = 1.06 \times 10^3 \cdot \text{kip}$$

$$F_c := 0.85 \cdot f'_c \cdot a \cdot b$$

where

$$f'_c = \text{specified compressive strength of concrete} \quad f'_c = 6.5 \cdot \text{ksi}$$

$$b = \text{width of compression flange} \quad b := 96 \text{in}$$

Therefore

$$F_c := 0.85 \cdot f'_c \cdot a \cdot b = 1.061 \times 10^3 \cdot \text{kip} \text{ close to } F_p \quad \mathbf{OK}$$

7.4 Moment contributed by each row of strand is:

$$\text{Row 1: } M_{p1} := F_{p1} \cdot \left(h - 2.5 \text{in} - \frac{a}{2} \right) = 597.071 \cdot \text{kip} \cdot \text{ft}$$

$$\text{Row 2: } M_{p2} := F_{p2} \cdot \left(h - 4.5 \text{in} - \frac{a}{2} \right) = 528.123 \cdot \text{kip} \cdot \text{ft}$$

$$\text{Row 3: } M_{p3} := F_{p3} \cdot \left(h - 6.5 \text{in} - \frac{a}{2} \right) = 91.828 \cdot \text{kip} \cdot \text{ft}$$

Row 4: $M_{p4} := F_{p4} \cdot \left(h - 13.5 \text{ in} - \frac{a}{2} \right) = 86.694 \cdot \text{kip} \cdot \text{ft}$

7.5 Moment capacity

$$M_n := M_{p1} + M_{p2} + M_{p3} + M_{p4} = 1.304 \times 10^3 \cdot \text{kip} \cdot \text{ft}$$

CONSPAN: $M_n = 1304.2 \text{ kip} \cdot \text{ft}$

Factored flexural resistance:

$$M_r = \phi \cdot M_n \quad \text{LRFD Eq. 5.7.3.2.1-1}$$

where

ϕ = resistance factor LRFD Art. 5.5.4.2.1

$\phi := 1$ tension controlled prestressed concrete sections

$$M_r := \phi \cdot M_n = 1.304 \times 10^3 \cdot \text{kip} \cdot \text{ft} > M_u = 1.27 \times 10^3 \cdot \text{kip} \cdot \text{ft} \quad \text{OK}$$

8. Limits of reinforcement

8.1 Maximum reinforcement

The check of maximum reinforcement limits was removed from the LRFD Specifications in 2005. LRFD Art. 5.7.3.3.1

8.2 Minimum reinforcement

At any section of a noncompression-controlled flexural component, the amount of prestressed and nonprestressed tensile reinforcement shall be adequate to develop a factored flexural resistance, M_r , at least equal to the lesser of:

1. 1.33 times the factored moment required by the applicable strength load combination specified in Table 3.4.1-1 (Strength I); and

$$2. M_{cr} = \gamma_3 \cdot (\gamma_1 \cdot f_r + \gamma_2 \cdot f_{cpe}) \cdot s_{btf} \quad \text{LRFD Eq. 5.7.3.3.2-1}$$

The above equation is a simplified form of LRFD Equation 5.7.3.3.2-1 because no composite section exists, therefore the composite and noncomposite section modulus are the same.

where,

f_r = modulus of rupture of concrete LRFD Art 5.4.2.6

$$f_r := 0.37 \sqrt{\frac{f_c}{\text{ksi}}} \text{ ksi} = 0.943 \cdot \text{ksi}$$

f_{cpe} = compressive stress in concrete due to effective prestress forces only (after allowance for all prestress losses) at extreme fiber of section where tensile stress is caused by externally applied loads (ksi) (bottom fiber)

$$f_{cpe} := \frac{P_{pe}}{A_{tf}} + \frac{P_{pe} \cdot e_{tf}}{s_{btf}} = 2.831 \cdot \text{ksi}$$

s_{btf} = section modulus for the extreme fiber of the section where tensile stress is caused by externally applied loads (in³) $s_{btf} = 2.742 \times 10^3 \cdot \text{in}^3$

γ_1 = flexural cracking variability factor

$\gamma_1 := 1.2$ for precast segmental structures

γ_2 = prestress variability factor

$\gamma_2 := 1.1$ for bonded tendons

γ_3 = ratio of specified minimum yield strength to ultimate tensile strength of the reinforcement

$\gamma_3 := 1$ for prestressed concrete structures

$$M_{cr} := \gamma_3 \cdot (\gamma_1 \cdot f_r + \gamma_2 \cdot f_{cpe}) \cdot s_{btf} = 969.969 \cdot \text{kip} \cdot \text{ft}$$

The above M_{cr} applies to any cross section in between the two transfer length cross sections. At other cross sections, M_{cr} is smaller due to the smaller effective prestress P_{pe} .

The factored moment required by strength I load combination at the middle span is:

$$M_u = 1.27 \times 10^3 \cdot \text{kip} \cdot \text{ft}$$

$$\text{Thus, } 1.33 \cdot M_u = 1.689 \times 10^3 \cdot \text{kip} \cdot \text{ft} > M_{cr} = 969.969 \cdot \text{kip} \cdot \text{ft}$$

Therefore M_{cr} requirement controls.

$$M_r = 1.304 \times 10^3 \cdot \text{kip} \cdot \text{ft} > M_{cr} = 969.969 \cdot \text{kip} \cdot \text{ft} \quad \underline{\text{OK}}$$

Note : the LRFD specifications requires that this criterion be met at every section. At cross sections within the development length of prestress strands, the moment capacity is reduced. But those cross sections are not checked here.

9. Anchorage zone reinforcement

LRFD Art. 5.10.10

Design of the anchorage zone reinforcement is computed using the force in the strands just prior to transfer.

$$P_{pi} = 805.545 \cdot \text{kip}$$

The splitting resistance of pretensioned anchorage zones provided by reinforcement in the ends of pretensioned beams shall be taken as:

$$P_r := f_s \cdot A_s \geq 0.04 \cdot P_{pi} = 32.222 \cdot \text{kip}$$

where

A_s = total area of vertical reinforcement located within a distance of $h/4$ from the end of the beam, in^2

f_s = stress in steel, but not taken greater than 20ksi

$$A_s := \frac{0.04 \cdot P_{pi}}{20 \text{ksi}} = 1.611 \cdot \text{in}^2$$

At least 1.611 in^2 of vertical transverse reinforcement should be provided within a distance of ($h/4 = 21 \text{ in}/4 = 5.25 \text{ in}$) from the end of the beam.

Use 3 No.4 four-leg bars at 1.5in spacing starting at 2.25in from the end of the beam

$$\text{The provided } A_s := 3 \cdot 4 \cdot 0.2 \text{ in}^2 = 2.4 \text{ in}^2 > 1.611 \text{ in}^2 \quad \mathbf{OK}$$

Appendix J

Bridge Drawings

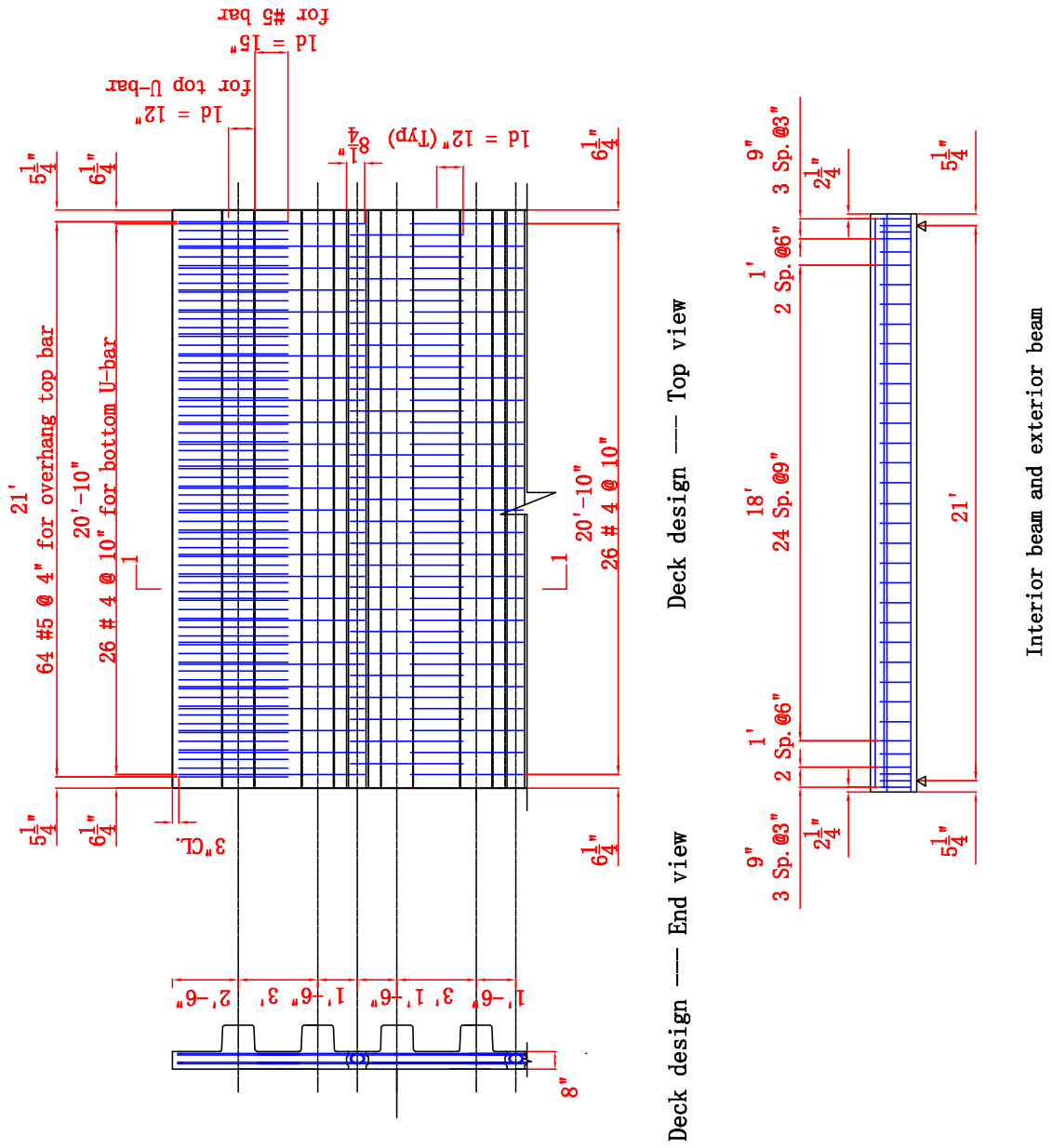


Figure J.1: NEXT-6 22 ft. deck and beam detail

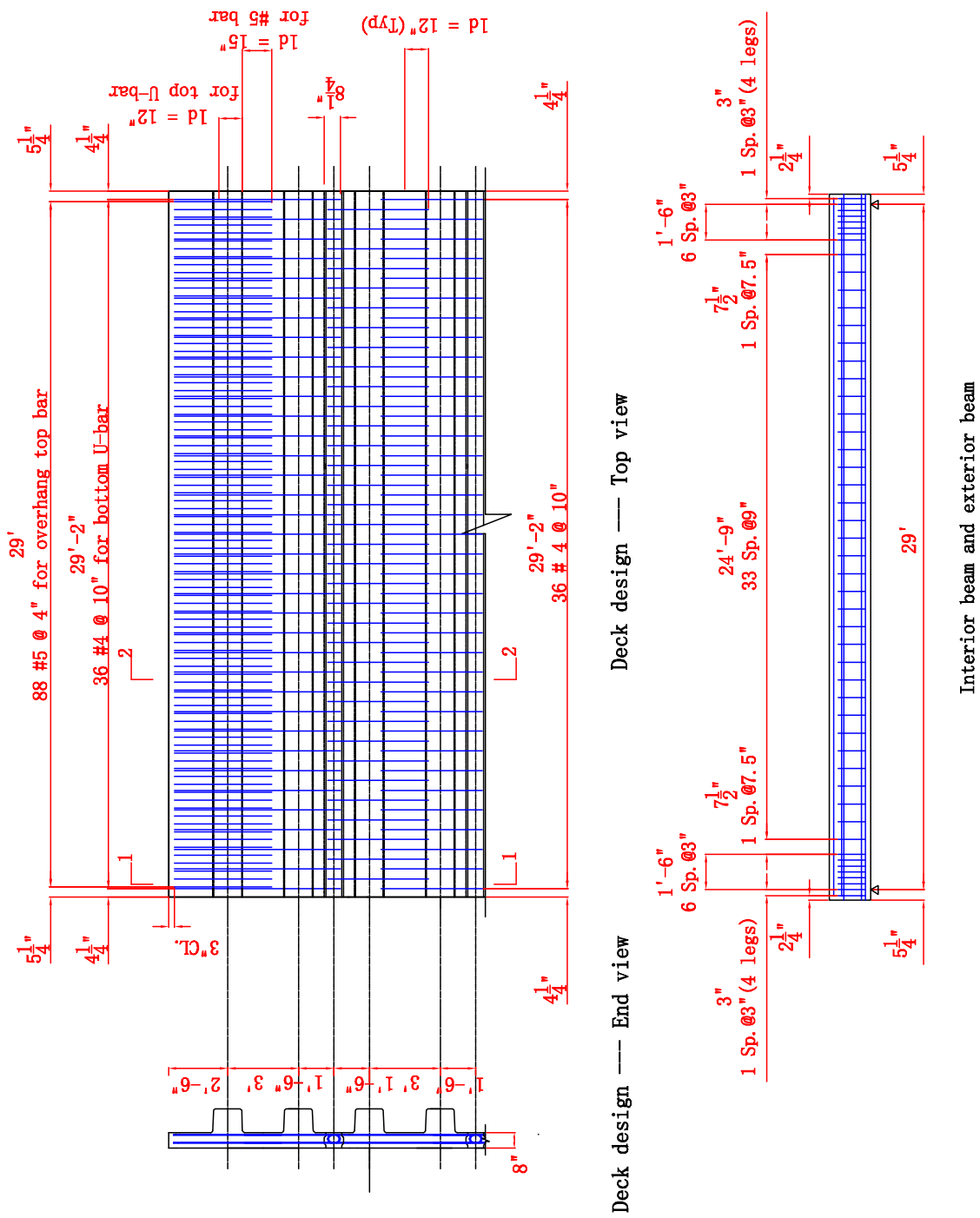


Figure J.2: NEXT-6 30 ft. deck and beam detail

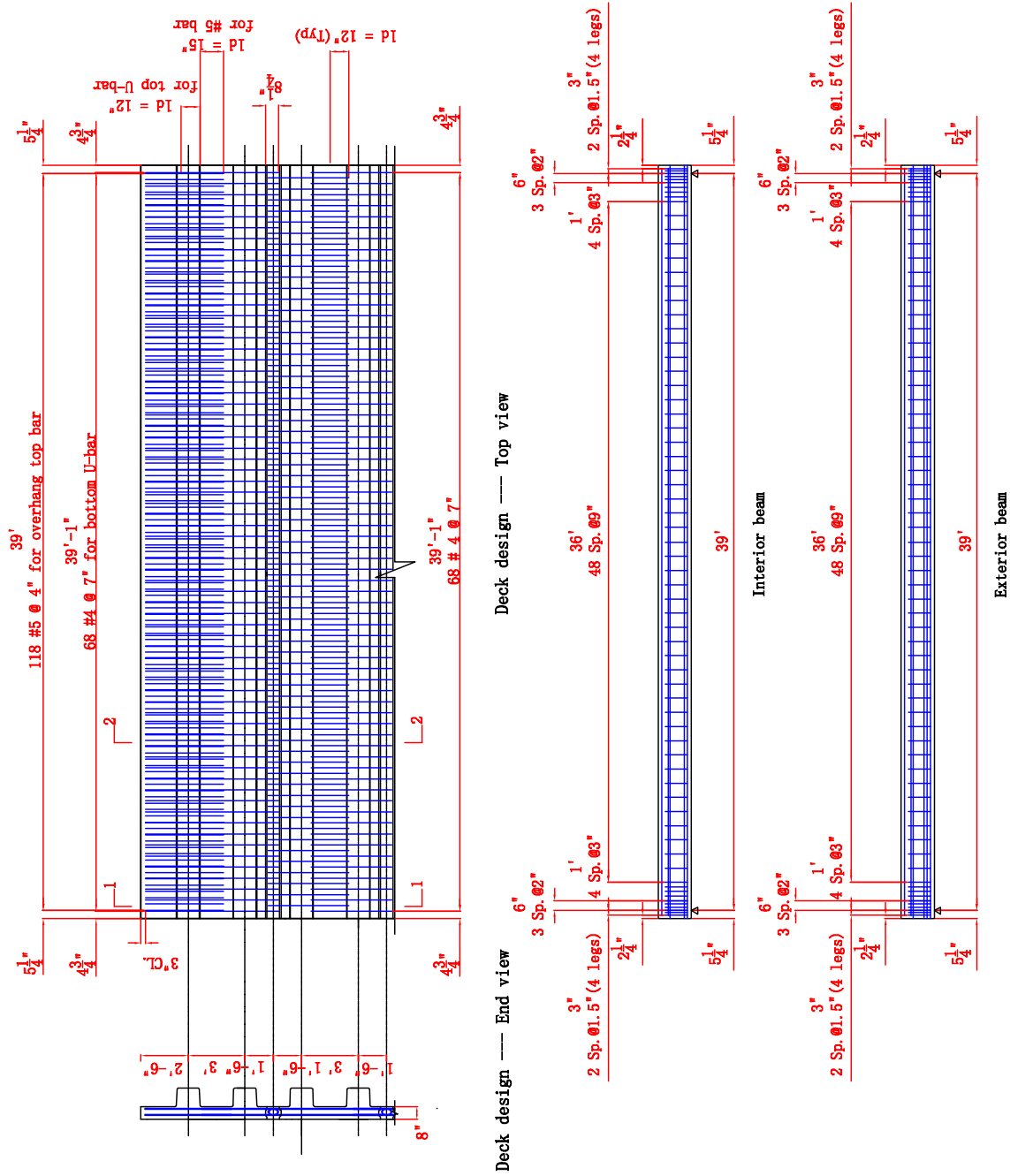


Figure J.3: NEXT-6 40 ft. deck and beam detail

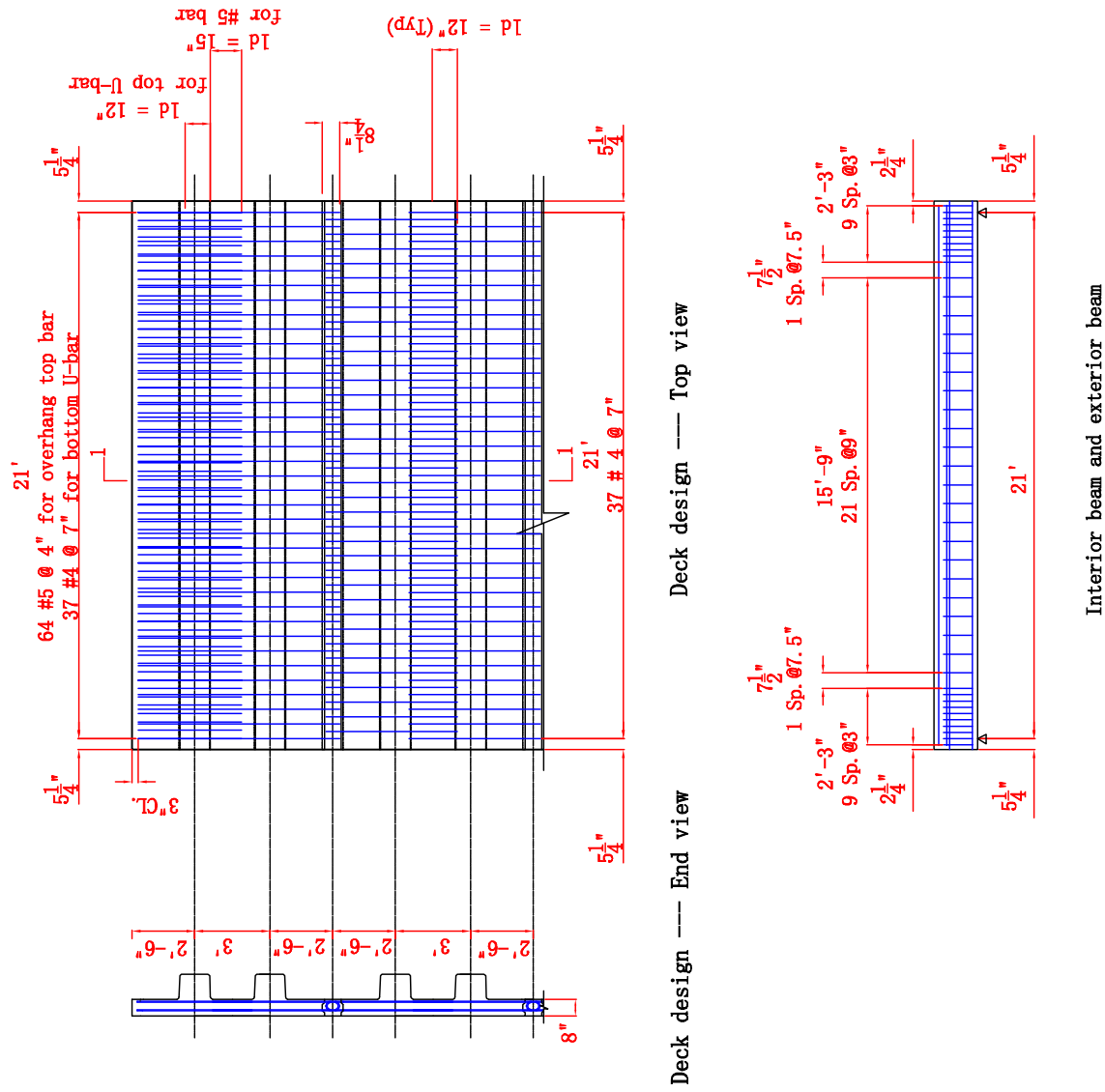


Figure J.4: NEXT-8 20 ft. deck and beam detail

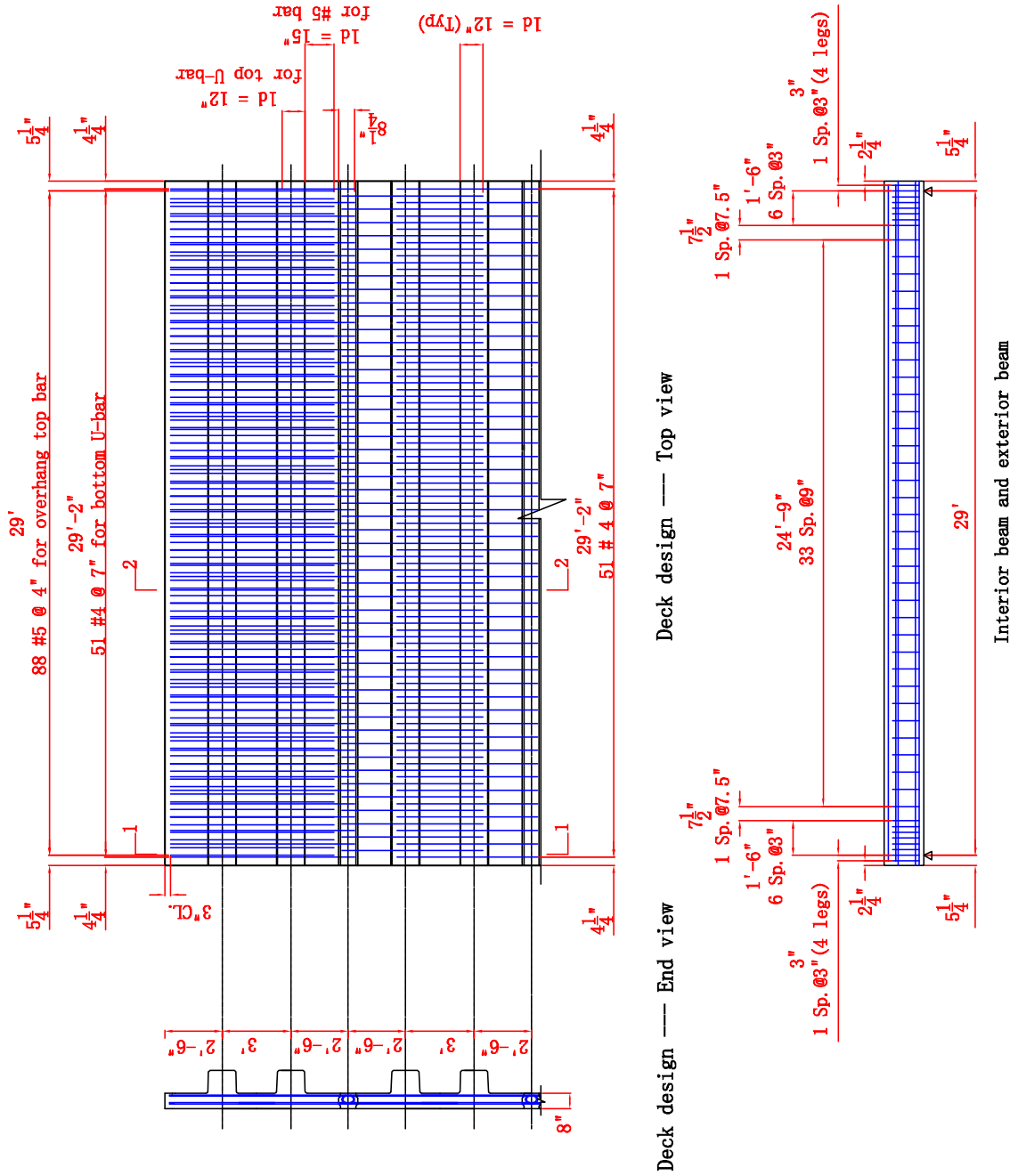


Figure J.5: NEXT-8 30 ft. deck and beam detail

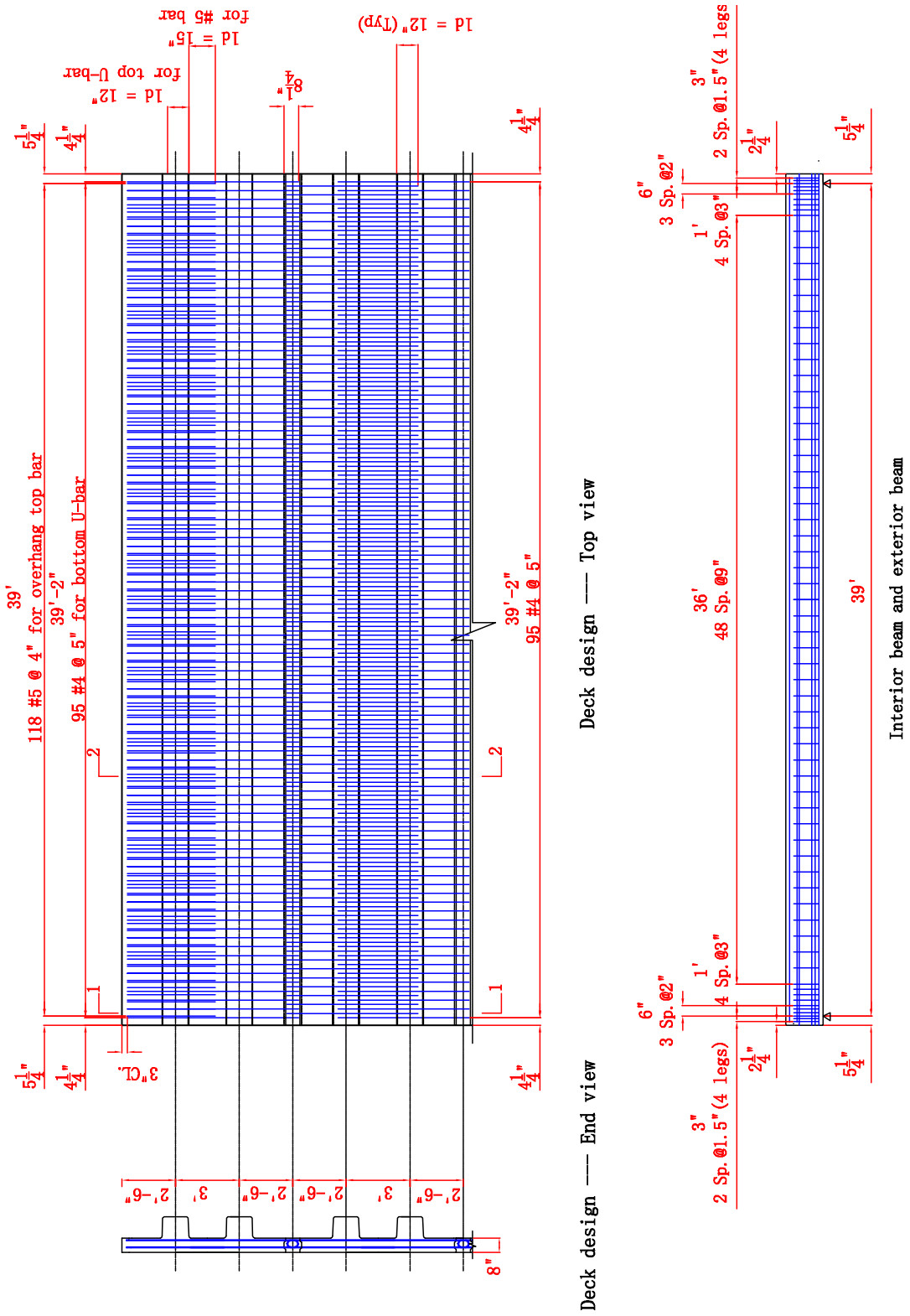
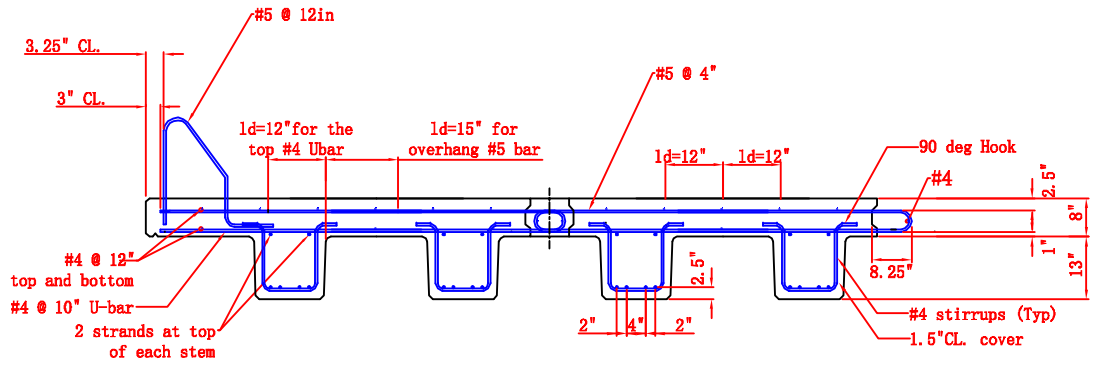
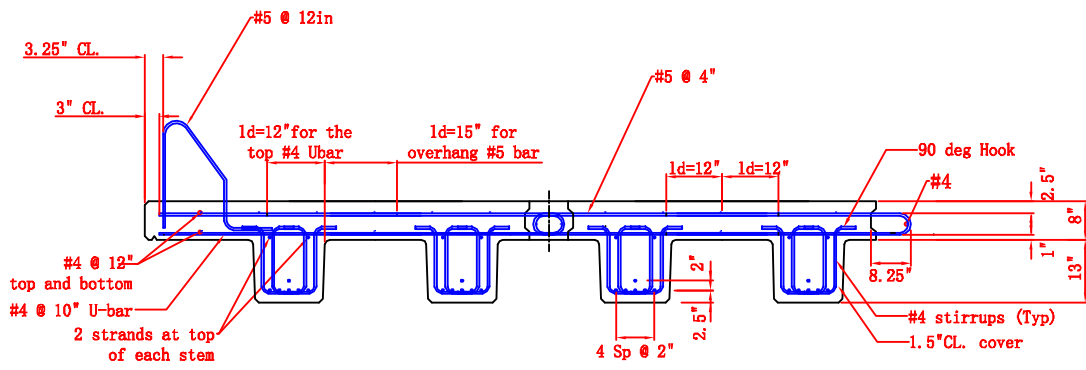


Figure J.6: NEXT-8 40 ft. deck and beam detail

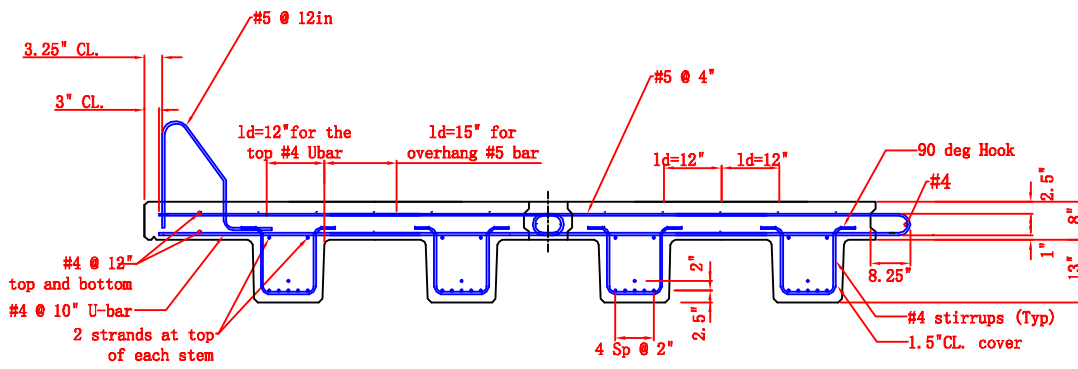


Cross section 1-1

Figure J.7: NEXT-6 22 ft. deck and beam cross-section detail

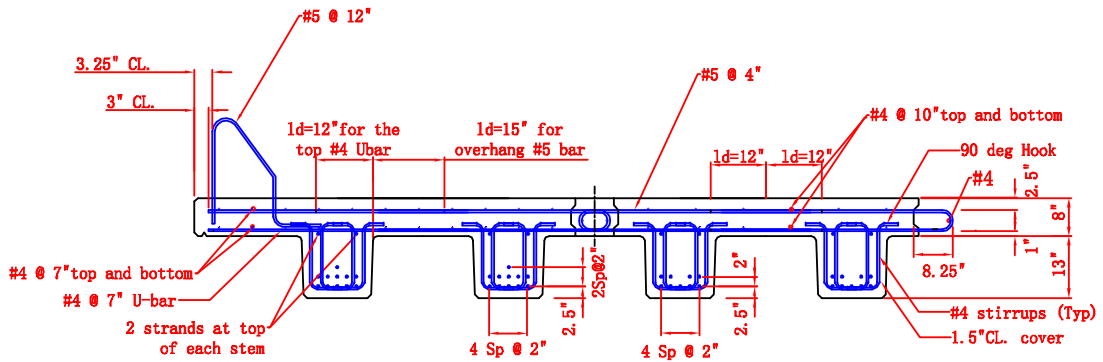


Cross Section 1-1 Anchorage zone

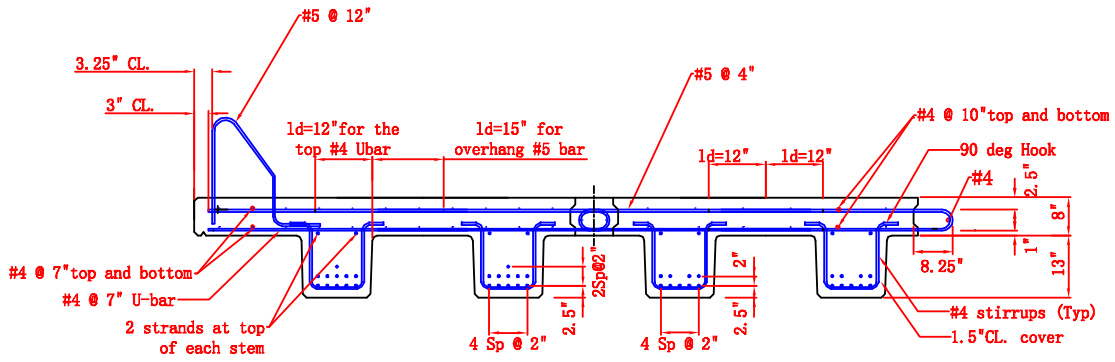


Cross Section 2-2 Other zone

Figure J.8: NEXT-6 30 ft. deck and beam cross-section detail

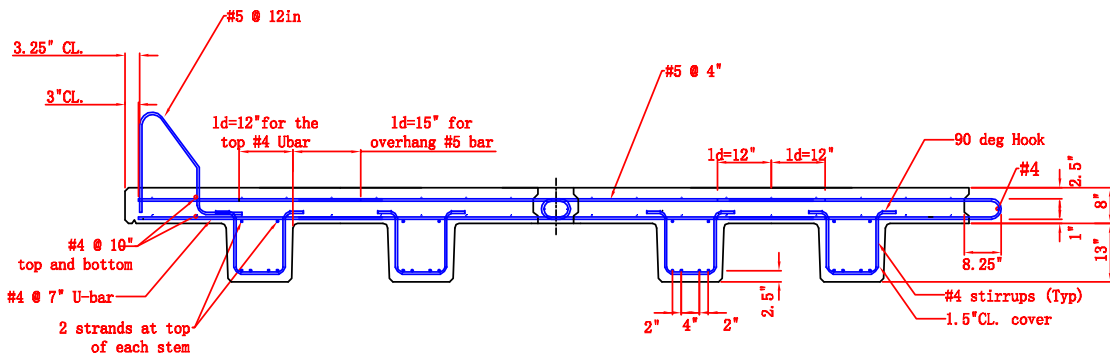


Cross Section 1-1 Anchorage zone



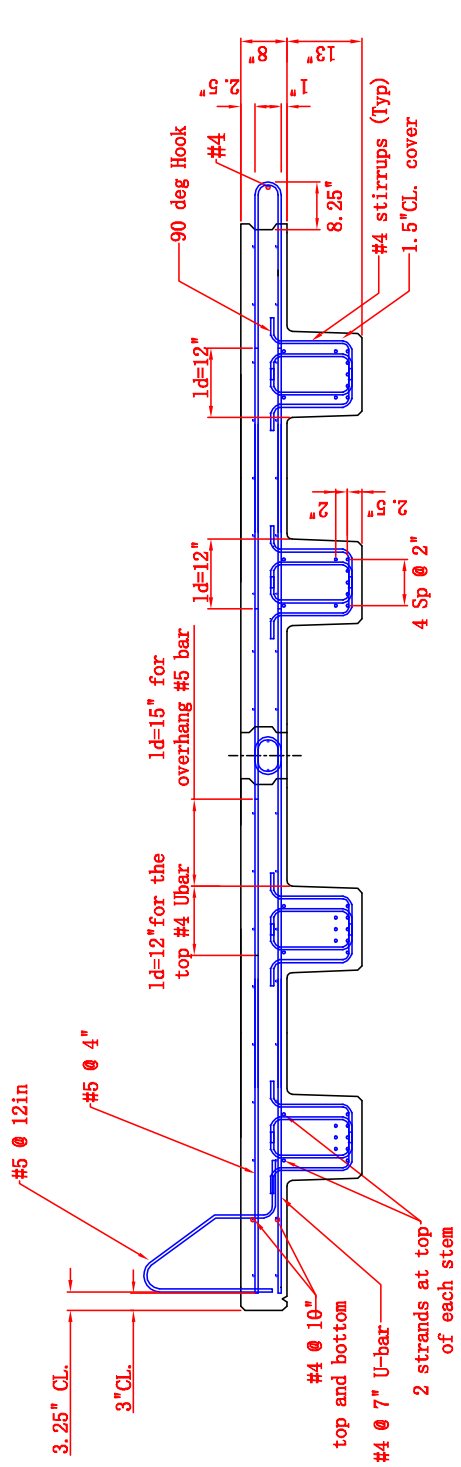
Cross Section 2-2 Other zone

Figure J.9: NEXT-6 40 ft. deck and beam cross-section detail

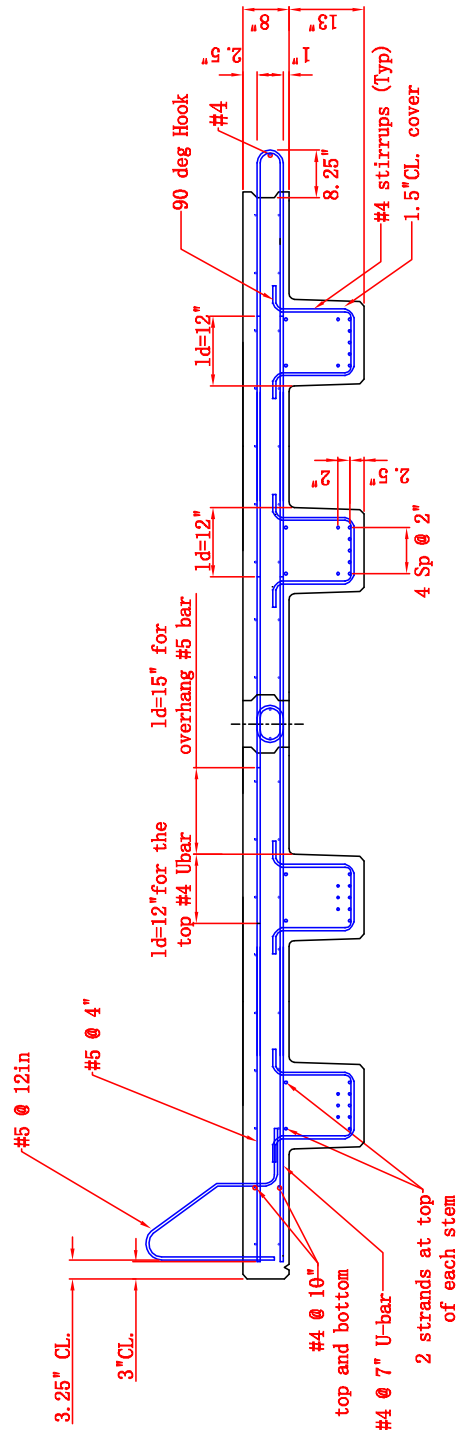


Cross section 1-1

Figure J.10: NEXT-8 22 ft. deck and beam cross-section detail



Cross Section 1-1 Anchorage zone



Cross Section 2-2 Other zone

Figure J.11: NEXT-8 30 ft. deck and beam cross-section detail

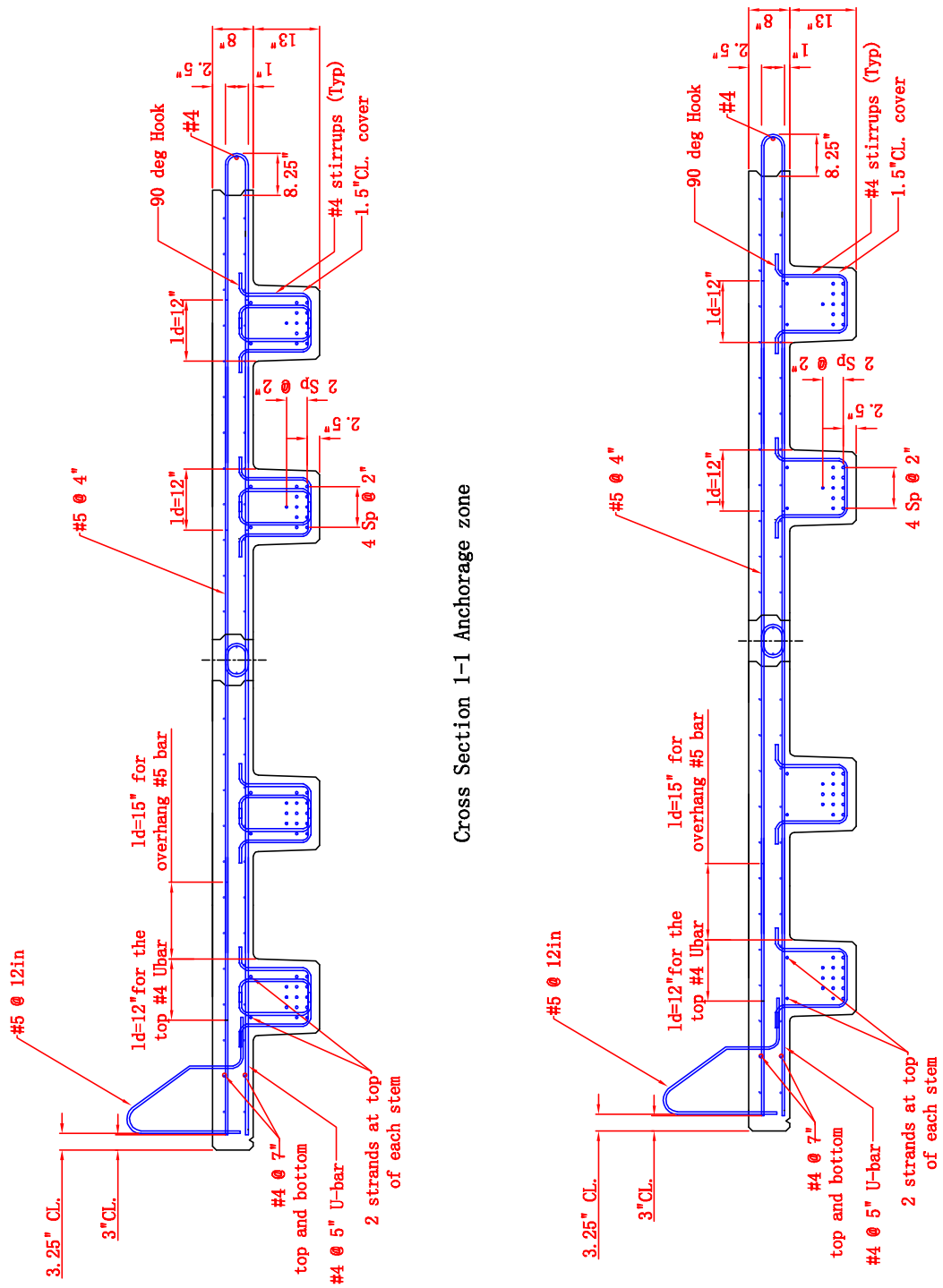


Figure J.12: NEXT-8 40 ft. deck and beam cross-section detail

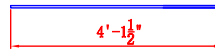
Notes:

1. · denotes straight strands, only straight strands are used
2. Strand type is 1/2-270k-LL low relaxation strands
3. Except for the T&S bar, the rebar dimensions shown to the left apply to all the other spans of NEXT-6
For the length and splice of T&S bar, follow the usual practice.
4. The distribution of T&S bar should not follow that given in CONSPAN, because the beam geometry in CONSPAN does not consider shear key, or the asymmetrical geometry of the exterior beam.
5. The prestressing strand patterns shown are the final patterns
6. The top two prestressing strands are at a fully prestressed.
7. The vertical bars are all #4

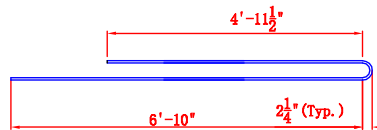
Bars:

Exterior beam:

Top overhang bar: #5

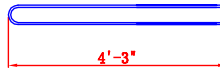


U bar: #4



Interior beam:

U bar: #4



Others:

Vertical bar #4

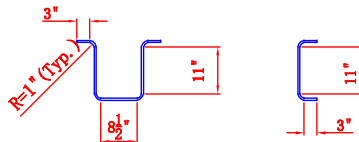


Figure J.13: NEXT-6 notes and bar details

Notes:

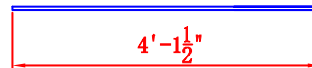
1. · denotes straight strands, only straight strands are used
2. Strand type is 1/2-270k-LL low relaxation strands
3. For the length and splice of T&S bar, follow the usual practice.
4. The distribution of T&S bar should not follow that given in CONSPAN, because the beam geometry in CONSPAN does not consider shear key, or the asymmetrical geometry of the exterior beam.
5. The prestressing strand patterns shown are the final patterns
6. The top two prestressing strands are at a fully prestressed.
7. The vertical bars are all #4

Figure J.14: NEXT-8 notes

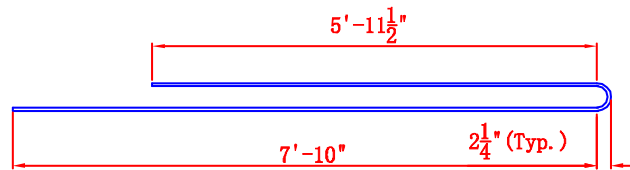
Bars:

Exterior beam:

Top overhang bar: #5

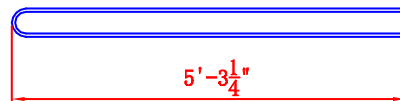


U bar: #4



Interior beam:

U bar: #4



Others:

Vertical bar #4

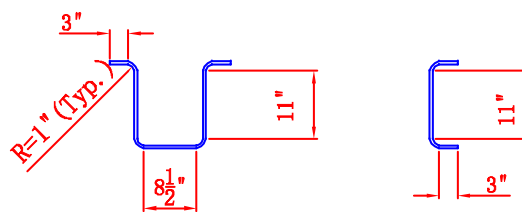
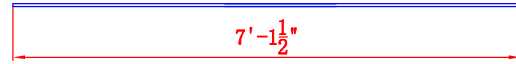


Figure J.15: NEXT-8 22 ft. bar details

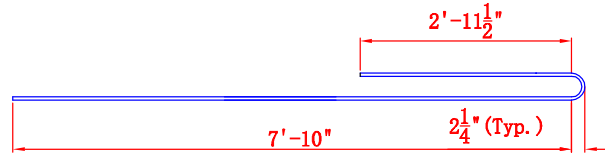
Bars:

Exterior beam:

Top overhang bar: #5

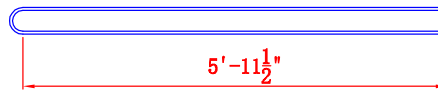


U bar: #4



Interior beam:

U bar: #4



Others:

Vertical bar #4

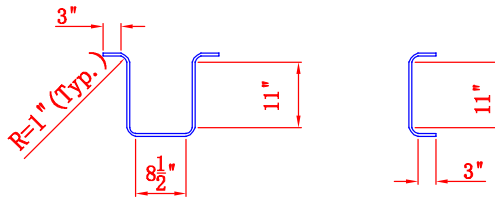
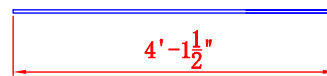


Figure J.16: NEXT-8 30 ft. bar details

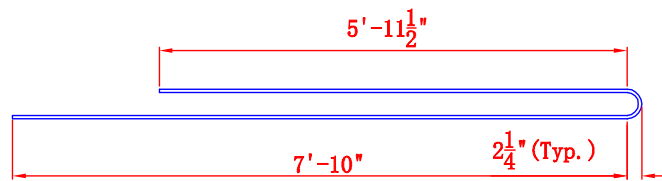
Bars:

Exterior beam:

Top overhang bar: #5

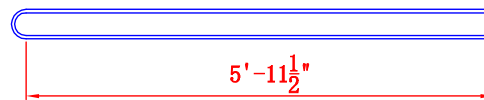


U bar: #4



Interior beam:

U bar: #4



Others:

Vertical bar #4

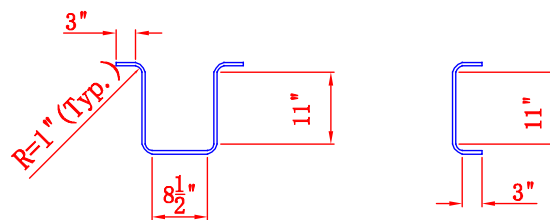


Figure J.17: NEXT-8 40 ft. bar details

This page intentionally left blank

Appendix K

CONSPAN Input and Output

K.1 NEXT-6 40 ft. - Input



		Sheet #	1		
		Job #			
Program:	LEAP® CONSPAN® V8i (SELECTseries 5)	Academic Use Only	Designed	HS	
Version:	12.01.00.57	Copyright © Bentley Systems, Inc. 1984 - 2012	Date	Oct/17/2013	
		www.bentley.com	Phone: 1-800-778-4277	Checked	
File Name:	NEXT D6-39ft105nonTransform.csl			Date	

PROJECT DATA

Project:	NEXT6-40ft
Designer:	HS
Date:	Oct/17/2013
Checked By:	
Date Checked:	
User job number:	
State:	SC, State Job #:
State	None
Specification:	
Design Code:	AASHTO LRFD - [6th Edition, 2012]
Units:	US
Span Type:	Simple Span
Flared Girder:	No
File Name:	C:\SCDOT\HUAN\SCDOT\CONSPAN BRIDGE\FinalDesign\ModifiedDesign\NEXT D6-39ft105nonTransform.csl



Sheet #	2
Job #	
Program:	LEAP® CONSPAN® V8i (SELECTseries 5)
Version:	12.01.00.57
Copyright © Bentley Systems, Inc. 1984 - 2012	www.bentley.com
Phone: 1-800-778-4277	
File Name:	NEXT D6-39ft105nonTransform.csl

GEOMETRY DATA

BRIDGE LAYOUT

Overall Width (ft)	50.000
Left curb (ft)	1.583
Right curb (ft)	1.583
Curb-to-curb width (ft)	46.833
Number of spans	1
Number of lanes	3
Lane width (ft)	12.000
Eff Deck thick (in)	0.000
Sacrificial thick (in)	0.000
Haunch thickness (in)	0.000
Haunch width (in)	0.000
Bridge c/s,MI(Ixx) (in4)	271025.88

SPAN DATA

Precast length,	ft =	39.875
Bearing-to-bearing,	ft =	39.000
Release span,	ft =	39.875

BEAM DATA

No	ID	Loc-prev ft	Area in2	MI(Ixx) in4	Height in	Yb in	B-topg in	B-trib ft
1	Next D6-21-exterior	4.000	1051.5	35359.5	21.00	13.23	72.00	7.000
2	Next D6-21-interior	6.000	955.4	33347.0	21.00	12.85	72.00	6.000
3	Next D6-21-interior	6.000	955.4	33347.0	21.00	12.85	72.00	6.000
4	Next D6-21-interior	6.000	955.4	33347.0	21.00	12.85	72.00	6.000
5	Next D6-21-interior	6.000	955.4	33347.0	21.00	12.85	72.00	6.000
6	Next D6-21-interior	6.000	955.4	33347.0	21.00	12.85	72.00	6.000
7	Next D6-21-interior	6.000	955.4	33347.0	21.00	12.85	72.00	6.000
8	Next D6-21-exterior	6.000	1051.5	35359.5	21.00	13.23	72.00	7.000

MATERIAL DATA - Project Level

As defined in Material Tab. For beam level properties look at Beam Specific output.

CONCRETE PROPERTIES

	Precast Release	Precast Final	C.I.P
f'c (ksi)	5.200	6.500	6.500
Wc (pcf)	150.000	150.000	150.000
Ec (ksi)	4371.720	4887.730	4887.730
K1	1.000	1.000	1.000
Thermal coeff.(1/°F)	0.00000600		

STRAND AND REBAR PROPERTIES



				Sheet #	3
				Job #	
Program:	LEAP® CONSPAN® V8i (SELECTseries 5)	Academic Use Only		Designed	HS
Version:	12.01.00.57	Copyright © Bentley Systems, Inc. 1984 - 2012		Date	Oct/17/2013
		www.bentley.com	Phone: 1-800-778-4277	Checked	
File Name:	NEXT D6-39ft105nonTransform.csl			Date	

PRESTRESSED STEEL:

1/2-270K-LL, Low relaxation strands
Straight Pattern
Strand Diameter = 0.500 in
Tensile Strength(fpu) = 270.0 ksi
Use transformed strand and rebar: No

REINFORCING STEEL:

Tension/Shear steel: fy = 60.0 ksi Es = 29000 ksi fs = 24.0 ksi



Sheet #	4
Job #	
Program:	LEAP® CONSPAN® V8i (SELECTseries 5)
Version:	12.01.00.57
Copyright © Bentley Systems, Inc. 1984 - 2012	Date
www.bentley.com	Checked
Phone: 1-800-778-4277	Date

Academic Use Only	Designed	HS
File Name: NEXT D6-39ft105nonTransform.csl	Date	

LOADS DATA

Loads generated using Permanent Load Wizard: NO
DEAD LOADS ON PRECAST
 UNITS: (Point: kips, Location: ft, Line: klf, Trapez: klf)

Span	Beam	DC/DW	Type	Mag.1	Loc.1	Mag.2	Loc.2	Description
1	1	DC	Line	0.221	0.000	0.221	39.000	Barrier Parapet
1	1	DW	Line	0.273	0.000	0.273	39.000	4 in bituminous wearing
1	2	DC	Line	0.221	0.000	0.221	39.000	Barrier Parapet
1	2	DW	Line	0.273	0.000	0.273	39.000	4 in bituminous wearing
1	3	DW	Line	0.273	0.000	0.273	39.000	4 in bituminous wearing
1	4	DW	Line	0.273	0.000	0.273	39.000	4 in bituminous wearing
1	5	DW	Line	0.273	0.000	0.273	39.000	4 in bituminous wearing
1	6	DW	Line	0.273	0.000	0.273	39.000	4 in bituminous wearing
1	7	DC	Line	0.221	0.000	0.221	39.000	Barrier Parapet
1	7	DW	Line	0.273	0.000	0.273	39.000	4 in bituminous wearing
1	8	DC	Line	0.221	0.000	0.221	39.000	Barrier Parapet
1	8	DW	Line	0.273	0.000	0.273	39.000	4 in bituminous wearing

DIAPHRAGM LOADS - NONE

DEAD LOADS ON COMPOSITE - NONE

TEMPERATURE LOADS - NONE

LIVE LOADS

Live load deflection: included.

ID	Type
Design Lane	Design Lane
Design Tandem	Design Tandem
Design Truck	Design Truck

Pedestrian Load - NONE



Sheet #	5
Job #	
Program:	LEAP® CONSPAN® V8i (SELECTseries 5)
Version:	12.01.00.57
File Name:	NEXT D6-39ft105nonTransform.csl

Academic Use Only	Designed	HS
Copyright © Bentley Systems, Inc. 1984 - 2012	Date	Oct/17/2013
www.bentley.com Phone: 1-800-778-4277	Checked	
	Date	

LIVE LOADS USED

LIVE LOAD LIBRARY: Default.cs3

1 ID: Design Lane

Description:	Design Lane as in AASHTO-LRFD
Type:	Design Lane

Lane Load:	Intensity = 0.64 klf, Width = 10.00 ft
------------	--

2 ID: Design Tandem

Description:	Design Tandem as in AASHTO-LRFD
Type:	Design Tandem

First Axle Magnitude = 25.00 k, Wheel Spacing = 6.00 ft, Truck Width = 10.00 ft

#	Magnitude, k	Max Spacing, ft	Min Spacing, ft	Increment, ft
1	25.00	4.00	4.00	0.00

3 ID: Design Truck

Description:	Design Truck as in AASHTO-LRFD
Type:	Design Truck

First Axle Magnitude = 8.00 k, Wheel Spacing = 6.00 ft, Truck Width = 10.00 ft
--

#	Magnitude, k	Max Spacing, ft	Min Spacing, ft	Increment, ft
1	32.00	14.00	14.00	0.00
2	32.00	30.00	14.00	2.00


4 ID: Fatigue Truck

Description:	Fatigue Truck as in AASHTO-LRFD
Type:	Fatigue Truck

First Axle Magnitude = 8.00 k, Wheel Spacing = 6.00 ft, Truck Width = 10.00 ft
--

#	Magnitude, k	Max Spacing, ft	Min Spacing, ft	Increment, ft
1	32.00	14.00	14.00	0.00
2	32.00	30.00	30.00	0.00

RATING LOADS - NONE

		Sheet #	6
		Job #	
Program:	LEAP® CONSPAN® V8i (SELECTseries 5)	Academic Use Only	Designed HS
Version:	12.01.00.57	Copyright © Bentley Systems, Inc. 1984 - 2012	Date Oct/17/2013
		www.bentley.com Phone: 1-800-778-4277	Checked
File Name:	NEXT D6-39ft105nonTransform.csl		Date

ANALYSIS DATA

ANALYSIS PARAMETERS DATA

Truck impact:	1.330
Lane impact:	1.000
Strength II impact:	1.330
Fatigue impact:	1.150

DISTRIBUTION FACTORS (Art. 4.6.2.2):

Is Span Post-tensioned:	YES
ADTT (Average Daily Truck Traffic) :	5000
Percent of the specified force effect :	1.00

NOTE: Beam specific dead and live load DFs are printed in beam level reports.

LOAD FACTORS: (Table 3.4.1-1 & 3.4.1-2)

	Live	DC(max)	DC(min)	DW(max)	DW(min)
Service I:	1.00	1.00	-	1.00	-
Service III:	0.80	1.00	-	1.00	-
Strength I:	1.75	1.25	0.90	1.50	0.65
Fatigue I:	1.50	-	-	-	-

Ductility Factor:	1.00
Redundancy Factor:	1.00
Importance Factor:	1.00



Sheet #	7
Job #	
Program:	LEAP® CONSPAN® V8i (SELECTseries 5)
Version:	12.01.00.57
File Name:	NEXT D6-39ft105nonTransform.csl

Academic Use Only	Designed	HS
Copyright © Bentley Systems, Inc. 1984 - 2012	Date	Oct/17/2013
www.bentley.com	Checked	
Phone: 1-800-778-4277	Date	

PROJECT DESIGN PARAMETERS

MULTIPLIERS:

Trans len mult:	Bonded	1.00
	Debonded	1.00
Dev len mult:	Bonded	1.00
	Debonded	2.00

Camber & Deflection Multiplier (PCI ref.)

	Erection	Final
Prestress:	1.80	2.45
Self. Wt:	1.85	2.70
Deck + Haunch:		2.30
Diaphragm:		3.00
DL-Prec.:		3.00
DL-Comp.:		3.00

MOMENT AND SHEAR PROVISIONS:

Ultimate Moment Capacity, Mr-prvd computed:	Strain Compatibility method.
Ultimate Concrete Strain:	0.0030
Horizontal Shear, Beam and Slab effects in Vu:	EXCLUDED

STRESS LIMITS (Art. 5.9.4):

STRESS LIMITS AT RELEASE BEFORE LOSSES:

	PRECAST	
Strength	5.20	ksi
Elasticity	4371.7	ksi
Max comp	3.12	ksi
Max tens	-0.20	ksi
Max tens, w/reinf	-0.55	ksi

STRESS LIMITS AT FINAL AFTER LOSSES:

	PRECAST		DECK	
Strength	6.50	ksi	6.50	ksi
Elasticity	4887.73	ksi	4887.73	ksi

STRESS LIMITS AT FINAL 1 (P/S + DL + LL):

	PRECAST		DECK	
Max comp	3.90	ksi	3.90	ksi

STRESS LIMITS AT FINAL 2 (P/S + DL):

	PRECAST		DECK	
Max comp	2.93	ksi	2.93	ksi



Sheet #	8
Job #	
Program:	LEAP® CONSPAN® V8i (SELECTseries 5)
Version:	12.01.00.57
File Name:	NEXT D6-39ft105nonTransform.csl

Academic Use Only
 Copyright © Bentley Systems, Inc. 1984 - 2012
www.bentley.com Phone: 1-800-778-4277

FATIGUE I STRESS LIMITS AT FINAL 3 (50% P/S + 50% DL + F_LL) (Art. 5.5.3.1):

	PRECAST		DECK	
Max comp	2.60	ksi	-	ksi

SERVICE III (Tension):

	PRECAST		DECK	
Max tens	-0.48	ksi	-0.48	ksi

RESISTANCE FACTORS (Art. 5.5.4.2):

Flexure Reinforced	
Compression controlled sections	0.75
Tension controlled sections	0.90
Flexure Prestressed	
Compression controlled sections	0.75
Tension controlled sections	1.00
Shear	0.90

PRESTRESS LOSSES:

Time Dependent Losses, Approximate Method (Art.5.9.5.3)
Days to release = 0.75
Rel. Humid.(RH) = 75.0 %



		Sheet #	9
		Job #	
Program:	LEAP® CONSPAN® V8i (SELECTseries 5)	Academic Use Only	Designed
Version:	12.01.00.57	Copyright © Bentley Systems, Inc. 1984 - 2012	Date
		www.bentley.com	Phone: 1-800-778-4277
File Name:	NEXT D6-39ft105nonTransform.csl	Checked	Date

RATING PARAMETERS

Rating Factors	References	Values
Condition Factor	Table 6A.4.2.3-1	1.00
System Factor for Flexural Effect	Table 6A.4.2.4-1	1.00
System Factor for Shear Effect	Art. 6A.4.2.4	1.00
ADTT	Section C3.6.1.1.2	5000
Dynamic Load Factor for Design Level	Art. 6A.4.3.3	0.33
Dynamic Load Factor for Legal and Permit Level	Table C6A.4.4.3-1	0.33

For Flexural Effect: Condition Factor * System Factor = 1.00 >= 0.85 (Art. 6A.4.2.1) OK

For Shear Effect: Condition Factor * System Factor = 1.00 >= 0.85 (Art. 6A.4.2.1 and 6A.4.2.4) OK

Dead Load Factors (Table 6A.4.2.2-1)

Limit State	DC	DW
Strength I	1.25	1.50
Strength II	1.25	1.50
Service I	1.00	1.00
Service III	1.00	1.00

Allowable Stresses (ksi)

Rating Level	Concrete Compression	Concrete Tension	Steel
Design Inventory	0.60 x f'c = 3.90	0.19 x sqrt(f'c) = 0.48	0.90 x f'y = 218.70
Design Operating	0.60 x f'c = 3.90	0.19 x sqrt(f'c) = 0.48	0.90 x f'y = 218.70
Legal	0.60 x f'c = 3.90	0.19 x sqrt(f'c) = 0.48	-
Permit	0.60 x f'c = 3.90	0.19 x sqrt(f'c) = 0.48	0.90 x f'y = 218.70

Consider shear reinf. across plane (FDOT alternative): No



Sheet #	10
Job #	
Program:	LEAP® CONSPAN® V8i (SELECTseries 5)
Version:	12.01.00.57
File Name:	NEXT D6-39ft105nonTransform.csl
Academic Use Only	
Copyright © Bentley Systems, Inc. 1984 - 2012	
www.bentley.com	Phone: 1-800-778-4277
Designed	HS
Date	Oct/17/2013
Checked	
Date	

BEAM REINFORCEMENT

BEAM SPECIFIC MATERIAL PROPERTIES:

Span#, Beam#	Tendon-ID	Girder-f'ci ksi	Girder-f'c ksi	Deck-f'c ksi
Span:1, Beam:1	1/2-270K-LL	5.20	6.50	6.50
Span:1, Beam:2	1/2-270K-LL	5.20	6.50	6.50
Span:1, Beam:3	1/2-270K-LL	5.20	6.50	6.50
Span:1, Beam:4	1/2-270K-LL	5.20	6.50	6.50
Span:1, Beam:5	1/2-270K-LL	5.20	6.50	6.50
Span:1, Beam:6	1/2-270K-LL	5.20	6.50	6.50
Span:1, Beam:7	1/2-270K-LL	5.20	6.50	6.50
Span:1, Beam:8	1/2-270K-LL	5.20	6.50	6.50

Span:1, Beam:1

PRESTRESSED STEEL:

26 strands, 1/2-270K-LL, Low relaxation strands
Straight Pattern

END PATTERN (Ycg = 5.27 in):

10 @ 2.500 in	10 @ 4.500 in	2 @ 6.500 in	4 @ 13.500 in
---------------	---------------	--------------	---------------

REINFORCING STEEL:

Tension	steel:	
fy	60.0	ksi
Es	29000	ksi
fs	24.0	ksi

Stirrups:

# legs	Size	fy (ksi)	Area (in2)	Spacing (in)	Start (ft)	End (ft)	Extends into Deck
4	US#4[M13]	60.0	0.80	1.50	0.1900	0.4400	No
2	US#4[M13]	60.0	0.40	2.00	0.4400	0.9400	No
2	US#4[M13]	60.0	0.40	3.00	0.9400	1.9400	No
2	US#4[M13]	60.0	0.40	9.00	1.9400	37.9400	No
2	US#4[M13]	60.0	0.40	3.00	37.9400	38.9400	No
2	US#4[M13]	60.0	0.40	2.00	38.9400	39.4400	No
4	US#4[M13]	60.0	0.80	1.50	39.4400	39.6900	No

Top Steel:



Sheet #	11
Job #	
Program:	LEAP® CONSPAN® V8i (SELECTseries 5)
Version:	12.01.00.57
Copyright © Bentley Systems, Inc. 1984 - 2012	www.bentley.com
Phone: 1-800-778-4277	
File Name:	NEXT D6-39ft105nonTransform.csl

Academic Use Only	Designed	HS
Date	Oct/17/2013	
Checked		
Date		

#bars	Size	Dist. from Top (in)	Area (in2)	Start (ft)	End (ft)	Side Cover (in)
11	US#4[M13]	2.25	2.200	0.1667	39.7083	1.00
11	US#4[M13]	6.25	2.200	0.1667	39.7083	1.00

Bottom Steel:

#bars	Size	Dist. from Top (in)	Area (in2)	Start (ft)	End (ft)	Side Cover (in)
-------	------	---------------------	------------	------------	----------	-----------------

Span:1, Beam:2

PRESTRESSED STEEL:

22 strands, 1/2-270K-LL, Low relaxation strands
Straight Pattern

END PATTERN (Ycg = 5.23 in):

10 @ 2.500 in	8 @ 4.500 in	4 @ 13.500 in
---------------	--------------	---------------

REINFORCING STEEL:

Tension	steel:	
fy	60.0	ksi
Es	29000	ksi
fs	24.0	ksi

Stirrups:

# legs	Size	fy (ksi)	Area (in2)	Spacing (in)	Start (ft)	End (ft)	Extends into Deck
4	US#4[M13]	60.0	0.80	1.50	0.1900	0.4400	No
2	US#4[M13]	60.0	0.40	2.00	0.4400	0.9400	No
2	US#4[M13]	60.0	0.40	3.00	0.9400	1.9400	No
2	US#4[M13]	60.0	0.40	9.00	1.9400	37.9400	No
2	US#4[M13]	60.0	0.40	3.00	37.9400	38.9400	No
2	US#4[M13]	60.0	0.40	2.00	38.9400	39.4400	No
4	US#4[M13]	60.0	0.80	1.50	39.4400	39.6900	No

Top Steel:

#bars	Size	Dist. from Top (in)	Area (in2)	Start (ft)	End (ft)	Side Cover (in)
6	US#4[M13]	2.25	1.200	0.1667	39.7083	7.00
6	US#4[M13]	6.25	1.200	0.1667	39.7083	444 7.00



Sheet #	12
Job #	
Program:	LEAP® CONSPAN® V8i (SELECTseries 5)
Version:	12.01.00.57
File Name:	NEXT D6-39ft105nonTransform.csl

Academic Use Only	Designed	HS
Copyright © Bentley Systems, Inc. 1984 - 2012	Date	Oct/17/2013
www.bentley.com Phone: 1-800-778-4277	Checked	
	Date	

Bottom Steel:

#bars	Size	Dist. from Top (in)	Area (in ²)	Start (ft)	End (ft)	Side Cover (in)
-------	------	---------------------	-------------------------	------------	----------	-----------------

Span:1, Beam:3

PRESTRESSED STEEL:

22 strands, 1/2-270K-LL, Low relaxation strands
Straight Pattern

END PATTERN (Ycg = 5.23 in):

10 @ 2.500 in	8 @ 4.500 in	4 @ 13.500 in
---------------	--------------	---------------

REINFORCING STEEL:

Tension	steel:	
fy	60.0	ksi
Es	29000	ksi
fs	24.0	ksi

Stirrups:

# legs	Size	fy (ksi)	Area (in ²)	Spacing (in)	Start (ft)	End (ft)	Extends into Deck
4	US#4[M13]	60.0	0.80	1.50	0.1900	0.4400	No
2	US#4[M13]	60.0	0.40	2.00	0.4400	0.9400	No
2	US#4[M13]	60.0	0.40	3.00	0.9400	1.9400	No
2	US#4[M13]	60.0	0.40	9.00	1.9400	37.9400	No
2	US#4[M13]	60.0	0.40	3.00	37.9400	38.9400	No
2	US#4[M13]	60.0	0.40	2.00	38.9400	39.4400	No
4	US#4[M13]	60.0	0.80	1.50	39.4400	39.6900	No

Top Steel:

#bars	Size	Dist. from Top (in)	Area (in ²)	Start (ft)	End (ft)	Side Cover (in)
6	US#4[M13]	2.25	1.200	0.1667	39.7083	7.00
6	US#4[M13]	6.25	1.200	0.1667	39.7083	7.00

Bottom Steel:

#bars	Size	Dist. from Top (in)	Area (in ²)	Start (ft)	End (ft)	Side Cover (in)
-------	------	---------------------	-------------------------	------------	----------	-----------------

445



		Sheet #	13
		Job #	
Program:	LEAP® CONSPAN® V8i (SELECTseries 5)	Academic Use Only	Designed HS
Version:	12.01.00.57	Copyright © Bentley Systems, Inc. 1984 - 2012	Date Oct/17/2013
		www.bentley.com	Phone: 1-800-778-4277
File Name:	NEXT D6-39ft105nonTransform.csl		Checked
			Date

Span:1, Beam:4

PRESTRESSED STEEL:

22 strands, 1/2-270K-LL, Low relaxation strands
Straight Pattern

END PATTERN (Ycg = 5.23 in):

10 @ 2.500 in	8 @ 4.500 in	4 @ 13.500 in
---------------	--------------	---------------

REINFORCING STEEL:

Tension	steel:	
fy	60.0	ksi
Es	29000	ksi
fs	24.0	ksi

Stirrups:

# legs	Size	fy (ksi)	Area (in2)	Spacing (in)	Start (ft)	End (ft)	Extends into Deck
4	US#4[M13]	60.0	0.80	1.50	0.1900	0.4400	No
2	US#4[M13]	60.0	0.40	2.00	0.4400	0.9400	No
2	US#4[M13]	60.0	0.40	3.00	0.9400	1.9400	No
2	US#4[M13]	60.0	0.40	9.00	1.9400	37.9400	No
2	US#4[M13]	60.0	0.40	3.00	37.9400	38.9400	No
2	US#4[M13]	60.0	0.40	2.00	38.9400	39.4400	No
4	US#4[M13]	60.0	0.80	1.50	39.4400	39.6900	No

Top Steel:

#bars	Size	Dist. from Top (in)	Area (in2)	Start (ft)	End (ft)	Side Cover (in)
6	US#4[M13]	2.25	1.200	0.1667	39.7083	7.00
6	US#4[M13]	6.25	1.200	0.1667	39.7083	7.00

Bottom Steel:

#bars	Size	Dist. from Top (in)	Area (in2)	Start (ft)	End (ft)	Side Cover (in)
-------	------	---------------------	------------	------------	----------	-----------------

Span:1, Beam:5



Sheet #	14
Job #	
Program:	LEAP® CONSPAN® V8i (SELECTseries 5)
Version:	12.01.00.57
File Name:	NEXT D6-39ft105nonTransform.csl

Academic Use Only	Designed	HS
Copyright © Bentley Systems, Inc. 1984 - 2012	Date	Oct/17/2013
www.bentley.com	Checked	
Phone: 1-800-778-4277	Date	

PRESTRESSED STEEL:

22 strands, 1/2-270K-LL, Low relaxation strands
Straight Pattern

END PATTERN (Ycg = 5.23 in):

10 @ 2.500 in | 8 @ 4.500 in | 4 @ 13.500 in |

REINFORCING STEEL:

Tension steel:		
fy	60.0	ksi
Es	29000	ksi
fs	24.0	ksi

Stirrups:

# legs	Size	fy (ksi)	Area (in2)	Spacing (in)	Start (ft)	End (ft)	Extends into Deck
4	US#4[M13]	60.0	0.80	1.50	0.1900	0.4400	No
2	US#4[M13]	60.0	0.40	2.00	0.4400	0.9400	No
2	US#4[M13]	60.0	0.40	3.00	0.9400	1.9400	No
2	US#4[M13]	60.0	0.40	9.00	1.9400	37.9400	No
2	US#4[M13]	60.0	0.40	3.00	37.9400	38.9400	No
2	US#4[M13]	60.0	0.40	2.00	38.9400	39.4400	No
4	US#4[M13]	60.0	0.80	1.50	39.4400	39.6900	No

Top Steel:

#bars	Size	Dist. from Top (in)	Area (in2)	Start (ft)	End (ft)	Side Cover (in)
6	US#4[M13]	2.25	1.200	0.1667	39.7083	7.00
6	US#4[M13]	6.25	1.200	0.1667	39.7083	7.00

Bottom Steel:

#bars	Size	Dist. from Top (in)	Area (in2)	Start (ft)	End (ft)	Side Cover (in)

Span:1, Beam:6

PRESTRESSED STEEL:

22 strands, 1/2-270K-LL, Low relaxation strands
Straight Pattern



Sheet #	15
Job #	
Program:	LEAP® CONSPAN® V8i (SELECTseries 5)
Version:	12.01.00.57
File Name:	NEXT D6-39ft105nonTransform.csl

Academic Use Only	Designed	HS
Copyright © Bentley Systems, Inc. 1984 - 2012	Date	Oct/17/2013
www.bentley.com	Checked	
Phone: 1-800-778-4277	Date	

END PATTERN (Ycg = 5.23 in):

10 @ 2.500 in	8 @ 4.500 in	4 @ 13.500 in
---------------	--------------	---------------

REINFORCING STEEL:

Tension steel:		
fy	60.0	ksi
Es	29000	ksi
fs	24.0	ksi

Stirrups:

# legs	Size	fy (ksi)	Area (in2)	Spacing (in)	Start (ft)	End (ft)	Extends into Deck
4	US#4[M13]	60.0	0.80	1.50	0.1900	0.4400	No
2	US#4[M13]	60.0	0.40	2.00	0.4400	0.9400	No
2	US#4[M13]	60.0	0.40	3.00	0.9400	1.9400	No
2	US#4[M13]	60.0	0.40	9.00	1.9400	37.9400	No
2	US#4[M13]	60.0	0.40	3.00	37.9400	38.9400	No
2	US#4[M13]	60.0	0.40	2.00	38.9400	39.4400	No
4	US#4[M13]	60.0	0.80	1.50	39.4400	39.6900	No

Top Steel:

#bars	Size	Dist. from Top (in)	Area (in2)	Start (ft)	End (ft)	Side Cover (in)
6	US#4[M13]	2.25	1.200	0.1667	39.7083	7.00
6	US#4[M13]	6.25	1.200	0.1667	39.7083	7.00

Bottom Steel:

#bars	Size	Dist. from Top (in)	Area (in2)	Start (ft)	End (ft)	Side Cover (in)
-------	------	---------------------	------------	------------	----------	-----------------

Span:1, Beam:7

PRESTRESSED STEEL:

22 strands, 1/2-270K-LL, Low relaxation strands
Straight Pattern

END PATTERN (Ycg = 5.23 in):



		Sheet #	16
		Job #	
Program:	LEAP® CONSPAN® V8i (SELECTseries 5)	Academic Use Only	Designed HS
Version:	12.01.00.57	Copyright © Bentley Systems, Inc. 1984 - 2012	Date Oct/17/2013
		www.bentley.com	Phone: 1-800-778-4277
File Name:	NEXT D6-39ft105nonTransform.csl		Date

10 @ 2.500 in | 8 @ 4.500 in | 4 @ 13.500 in |

REINFORCING STEEL:

Tension steel:		
fy	60.0	ksi
Es	29000	ksi
fs	24.0	ksi

Stirrups:

# legs	Size	fy (ksi)	Area (in2)	Spacing (in)	Start (ft)	End (ft)	Extends into Deck
4	US#4[M13]	60.0	0.80	1.50	0.1900	0.4400	No
2	US#4[M13]	60.0	0.40	2.00	0.4400	0.9400	No
2	US#4[M13]	60.0	0.40	3.00	0.9400	1.9400	No
2	US#4[M13]	60.0	0.40	9.00	1.9400	37.9400	No
2	US#4[M13]	60.0	0.40	3.00	37.9400	38.9400	No
2	US#4[M13]	60.0	0.40	2.00	38.9400	39.4400	No
4	US#4[M13]	60.0	0.80	1.50	39.4400	39.6900	No

Top Steel:

#bars	Size	Dist. from Top (in)	Area (in2)	Start (ft)	End (ft)	Side Cover (in)
6	US#4[M13]	2.25	1.200	0.1667	39.7083	7.00
6	US#4[M13]	6.25	1.200	0.1667	39.7083	7.00

Bottom Steel:

#bars	Size	Dist. from Top (in)	Area (in2)	Start (ft)	End (ft)	Side Cover (in)

Span:1, Beam:8

PRESTRESSED STEEL:

26 strands, 1/2-270K-LL, Low relaxation strands
Straight Pattern

END PATTERN (Ycg = 5.27 in):

10 @ 2.500 in | 10 @ 4.500 in | 2 @ 6.500 in | 4 @ 13.500 in

REINFORCING STEEL:



		Sheet #	17
		Job #	
Program:	LEAP® CONSPAN® V8i (SELECTseries 5)	Academic Use Only	Designed HS
Version:	12.01.00.57	Copyright © Bentley Systems, Inc. 1984 - 2012	Date Oct/17/2013
		www.bentley.com	Phone: 1-800-778-4277
File Name:	NEXT D6-39ft105nonTransform.csl		Checked
			Date

Tension steel:		
fy	60.0	ksi
Es	29000	ksi
fs	24.0	ksi

Stirrups:

# legs	Size	fy (ksi)	Area (in2)	Spacing (in)	Start (ft)	End (ft)	Extends into Deck
4	US#4[M13]	60.0	0.80	1.50	0.1900	0.4400	No
2	US#4[M13]	60.0	0.40	2.00	0.4400	0.9400	No
2	US#4[M13]	60.0	0.40	3.00	0.9400	1.9400	No
2	US#4[M13]	60.0	0.40	9.00	1.9400	37.9400	No
2	US#4[M13]	60.0	0.40	3.00	37.9400	38.9400	No
2	US#4[M13]	60.0	0.40	2.00	38.9400	39.4400	No
4	US#4[M13]	60.0	0.80	1.50	39.4400	39.6900	No

Top Steel:

#bars	Size	Dist. from Top (in)	Area (in2)	Start (ft)	End (ft)	Side Cover (in)
11	US#4[M13]	2.25	2.200	0.1667	39.7083	1.00
11	US#4[M13]	6.25	2.200	0.1667	39.7083	1.00

Bottom Steel:

#bars	Size	Dist. from Top (in)	Area (in2)	Start (ft)	End (ft)	Side Cover (in)
-------	------	---------------------	------------	------------	----------	-----------------

K.2 NEXT-6 40 ft. - Exterior Beam Output



Sheet #	1
Job #	
Program:	LEAP® CONSPAN® V8i (SELECTseries 5)
Version:	12.01.00.57
Copyright © Bentley Systems, Inc. 1984 - 2012	
www.bentley.com	Phone: 1-800-778-4277
File Name:	NEXT D6-39ft105nonTransform.csl
Designed	HS
Date	Oct/17/2013
Checked	
Date	

PROPERTIES

Span:1, Beam:1

PRECAST DATA:

Section Id	Next D6-21-exterior		
Type	Double Tee		
Flng width	Top	72.000	in
thick	Top	8.000	in
Stems	No	2	
	Top	15.000	in
	Bot	14.190	in
Shear width		29.190	in

Minimum Thickness Criteria, Article 5.14.1.2.2 checked: OK.

GENERAL BRIDGE DATA:

Bridge Width	50.00	ft
Curb-to-curb	46.83	ft
Beam Spac. Lt./Rt	4.00/ 6.00	ft
Lane width	12.00	ft
Number of lanes	3	
Interior/Exterior	Exterior	
Start Skew Angle	0.00	degrees
End Skew Angle	0.00	degrees

TOPPING DATA:

Deck	Thickness	0.000	in	
Haunch:	Thickness	0.000	in	
	Width	0.000	in	
Effective	width	84.000	in	(Art. 4.6.2.6.1)

GENERAL LOAD DATA:

DEAD LOADS ON PRECAST

UNITS: (Point: kips, Location: ft, Line: klf, Trapez: klf)

DC/DW	Type	Mag.1	Loc.1	Mag.2	Loc.2	Description
DC	Line	0.221	0.000	0.221	39.000	Barrier Parapet
DW	Line	0.273	0.000	0.273	39.000	4 in bituminous wearing

Dead loads on composite: See Project info for composite loads

GENERAL SPAN DATA:



		Sheet #	2
		Job #	
Program:	LEAP® CONSPAN® V8i (SELECTseries 5)	Academic Use Only	Designed HS
Version:	12.01.00.57	Copyright © Bentley Systems, Inc. 1984 - 2012	Date Oct/17/2013
		www.bentley.com	Phone: 1-800-778-4277
File Name:	NEXT D6-39ft105nonTransform.csl		Date

Overall length	39.875	ft
Release length	39.875	ft
Design length	39.000	ft

KERN POINTS:

Upper	15.77	in
Lower	8.90	in

DISTRIBUTION FACTORS (Art. 4.6.2.2):

Type i, post-tensioned

Live Moment	(2+ lanes loaded)	0.480	(Manual input)
Live Moment	(1 lane loaded)	0.683	(Manual input)
Live Shear	(2+ lanes loaded)	0.484	(Manual input)
Live Shear	(1 lane loaded)	0.683	(Manual input)

Pedestrian	0.125	(Manual input)
Comp. DC	0.125	(Calculated)
Comp. DW	0.125	(Calculated)

Dead Loads distributed equally to all beams

RESISTANCE FACTORS (Art. 5.5.4.2):

Flexure Reinforced	
Compression controlled sections	0.75
Tension controlled sections	0.90
Flexure Prestressed	
Compression controlled sections	0.75
Tension controlled sections	1.00
Shear	0.90

SECTION PROPERTIES:

	PRECAST		COMPOSITE		
Area	1051.5	in ²	1051.5	in ²	#
Total Height	21.00	in	21.00	in	
Mom. of Inertia (I _{xx})	35360	in ⁴	35360	in ⁴	#
Ht. of c.g.	13.23	in	13.23	in	#
Density	150.00	pcf	150.00	pcf	
Self-weight	1095.3	plf	1095.3	plf	
Mom. of Inertia (I _{yy})	533557.1	in ⁴			
Poisson's Ratio	0.2				
Thermal Coeff.	0.000006000	1/°F			



Sheet #	3
Job #	
Program:	LEAP® CONSPAN® V8i (SELECTseries 5)
Version:	12.01.00.57
File Name:	NEXT D6-39ft105nonTransform.csl
Academic Use Only	
Copyright © Bentley Systems, Inc. 1984 - 2012	
www.bentley.com	Phone: 1-800-778-4277
Designed	HS
Date	Oct/17/2013
Checked	
Date	

(#) Of Total Section using Ect/Ec = 1.0000
 Use transformed strand and rebar: No

Span:1, Beam:1

STRESS LIMITS (Art. 5.9.4):

STRESS LIMITS AT RELEASE BEFORE LOSSES:

	PRECAST	
Strength	5.20	ksi
Elasticity	4371.7	ksi
Max comp	3.12	ksi
Max tens	-0.20	ksi
Max tens, w/reinf	-0.55	ksi

STRESS LIMITS AT FINAL AFTER LOSSES:

	PRECAST		DECK	
Strength	6.50	ksi	6.50	ksi
Elasticity	4887.73	ksi	4887.73	ksi

STRESS LIMITS AT FINAL 1 (P/S + DL + LL):

	PRECAST		DECK	
Max comp	3.90	ksi	3.90	ksi

STRESS LIMITS AT FINAL 2 (P/S + DL):

	PRECAST		DECK	
Max comp	2.93	ksi	2.93	ksi

FATIGUE I STRESS LIMITS AT FINAL 3 (50% P/S + 50% DL + F_LL) (Art. 5.5.3.1):

	PRECAST		DECK	
Max comp	2.60	ksi	-	ksi

SERVICE III (Tension):

	PRECAST		DECK	
Max tens	-0.48	ksi	-0.48	ksi

Span:1, Beam:1

PRESTRESSED STEEL:

26 strands, 1/2-270K-LL, Low relaxation strands

Straight Pattern



		Sheet #	4
		Job #	
Program:	LEAP® CONSPAN® V8i (SELECTseries 5)	Academic Use Only	Designed HS
Version:	12.01.00.57	Copyright © Bentley Systems, Inc. 1984 - 2012	Date Oct/17/2013
		www.bentley.com	Phone: 1-800-778-4277
File Name:	NEXT D6-39ft105nonTransform.csl	Checked	Date

END PATTERN (Ycg = 5.27 in):

10 @ 2.500 in	10 @ 4.500 in	2 @ 6.500 in	4 @ 13.500 in
---------------	---------------	--------------	---------------

Strand Diameter	0.500	in
Strand Area	0.153	in ²
Total Strand Area	3.978	in ²
Trans. Len, bonded	2.500	ft
Trans. Len, debonded	2.500	ft
Dev. Len, bonded	5.521	ft
Dev. Len, debonded	11.041	ft
Holddown Force	0.000	kips
Tensile Strength(fpu)	270.0	ksi
Initial Prestress = 0.75fpu	202.5	ksi
Initial Pull	805.5	kips
Beam Shrtng (PL/AE)	0.080	in

Span:1, Beam:1

ESTIMATED QUANTITIES

Prestressing (linear ft)	Strands (LB/1000ft)	(LB)	Beam Vol(C.Y.)	Concrete Wt(LB)	Stirrups (LB)	Longitudinal Bars (LB)
1036.750	520	539.110	10.784	43674.430	166.757	592.097

Span:1, Beam:1

REINFORCING STEEL:

Tension	steel:	
fy	60.0	ksi
Es	29000	ksi
fs	24.0	ksi

Stirrups:

# legs	Size	fy (ksi)	Area (in ²)	Spacing (in)	Start (ft)	End (ft)	Extends into Deck
4	US#4[M13]	60.0	0.80	1.50	0.1900	0.4400	No
2	US#4[M13]	60.0	0.40	2.00	0.4400	0.9400	No
2	US#4[M13]	60.0	0.40	3.00	0.9400	1.9400	No
2	US#4[M13]	60.0	0.40	9.00	1.9400	37.9400	No
2	US#4[M13]	60.0	0.40	3.00	37.9400	38.9400	No
2	US#4[M13]	60.0	0.40	2.00	38.9400	39.4400	No
4	US#4[M13]	60.0	0.80	1.50	39.4400	39.6900	No

Top Steel:

#bars	Size	Dist. from Top (in)	Area (in ²)	Start (ft)	End (ft)	Side Cover (in)
11	US#4[M13]	2.25	2.200	0.1667	39.7083	455 1.00
11	US#4[M13]	6.25	2.200	0.1667	39.7083	1.00



		Sheet #	5	
		Job #		
Program:	LEAP® CONSPAN® V8i (SELECTseries 5)	Academic Use Only	Designed	HS
Version:	12.01.00.57	Copyright © Bentley Systems, Inc. 1984 - 2012	Date	Oct/17/2013
		www.bentley.com	Phone: 1-800-778-4277	Checked
File Name:	NEXT D6-39ft105nonTransform.csl		Date	

Bottom Steel:

#bars	Size	Dist. from Top (in)	Area (in2)	Start (ft)	End (ft)	Side Cover (in)
-------	------	---------------------	------------	------------	----------	-----------------

LOSSES

Note: Values are calculated at Midspan

Str. area	3.9780	in2
Ycg	5.27	in
P_init	805.5	kips
Ecc	7.96	in
Days to release	0.75	
Rel. Humid.(RH)	75.0	%
Es	28500.0	ksi
Eci	4372	ksi

AASHTO LOSSES

Elastic Shortening 10.03 ksi (Eq 5.9.5.2.3a-1), (fcgp= 1.538 ksi)

Elastic Gains		Gains		Adjustment	
due to Precast Loads		-1.48	ksi	0.09	ksi
due to Composite Loads		-0.00	ksi	0.00	ksi
due to Live Loads		-6.06	ksi	0.45	ksi

Time Dependent Losses (Approximate Method (Art.5.9.5.3))

	Initial	Final	
Steel relaxation	0.00 ksi	2.40 ksi	(Eq 5.9.5.3-1)
Concrete shrinkage	0.00 ksi	9.19 ksi	(Eq 5.9.5.3-1)
Concrete creep	0.00 ksi	5.87 ksi	(Eq 5.9.5.3-1)
Sub-total	10.03 ksi	10.47 ksi	(5.17 %)
Total Prestress Losses		20.49 ksi	(10.12 %)

Prestressing Stress Limit Check (Table 5.9.3.1)

initial fpi = 202.5 ksi < 0.75 fpu, OK
 initial fpe = 182.0 ksi < 0.80 fpy, OK



Sheet #	6
Job #	
Program:	LEAP® CONSPAN® V8i (SELECTseries 5)
Version:	12.01.00.57
Copyright © Bentley Systems, Inc. 1984 - 2012	www.bentley.com
Phone: 1-800-778-4277	
File Name:	NEXT D6-39ft105nonTransform.csl

Academic Use Only	Designed	HS
Copyright © Bentley Systems, Inc. 1984 - 2012	Date	Oct/17/2013
www.bentley.com	Checked	
Phone: 1-800-778-4277	Date	

SHEAR/MOMENT ENVELOPE (&REACTIONS)

SHEAR AND MOMENT ENVELOPE : Span : 1, Beam : 1, SERVICE I
 Shears: kips, Moments: kft

		Bearing	Trans	H/2	0.10L	0.20L	0.30L	0.40L	Midspan
Location,	ft	0.00	2.06	0.88	3.55	7.54	11.53	15.51	19.50
Self wt. :	M	0.0	41.7	18.3	68.9	129.9	173.4	199.5	208.2
(Max)	V	21.4	19.1	20.4	17.5	13.1	8.7	4.4	0.0
DL-Prec. :	M	-0.0	8.4	3.7	13.9	26.2	35.0	40.3	42.0
DC(Max)	V	4.3	3.9	4.1	3.5	2.6	1.8	0.9	0.0
DL-Prec. :	M	-0.0	10.4	4.6	17.2	32.4	43.2	49.7	51.9
DW(Max)	V	5.3	4.8	5.1	4.4	3.3	2.2	1.1	0.0
Deck + :	M	0.0	0.0	0.0	0.0	0.0	0.0	0.0	0.0
Haunch (Max)	V	0.0	0.0	0.0	0.0	0.0	0.0	0.0	0.0
Diaphragm :	M	0.0	0.0	0.0	0.0	0.0	0.0	0.0	0.0
(Max)	V	0.0	0.0	0.0	0.0	0.0	0.0	0.0	0.0
DL-Comp :	M	0.0	0.0	0.0	0.0	0.0	0.0	0.0	0.0
DC(Max)	V	0.0	0.0	0.0	0.0	0.0	0.0	0.0	0.0
DL-Comp :	M	0.0	0.0	0.0	0.0	0.0	0.0	0.0	0.0
DW(Max)	V	0.0	0.0	0.0	0.0	0.0	0.0	0.0	0.0
LL + I :	M+	-0.0	110.8	48.9	180.9	328.2	418.0	467.8	480.5
	V	58.3	53.6	56.3	50.2	41.9	33.7	4.1	20.4
LL + I :	M-	-0.0	-0.0	-0.0	0.0	0.0	0.0	0.0	0.0
	V	0.0	0.0	0.0	0.0	0.0	0.0	0.0	0.0
LL + I :	Vmx	58.3	53.6	56.3	50.2	42.1	34.4	28.0	22.5
	M	-0.0	111.9	49.8	180.9	317.5	396.9	434.2	439.0
Total :	M+	0.0	171.3	75.4	280.9	516.7	669.6	757.3	782.7
	V	89.3	81.3	85.9	75.5	60.9	46.4	10.4	20.4
Total :	M-	0.0	0.0	0.0	0.0	0.0	0.0	0.0	0.0
	V	0.0	0.0	0.0	0.0	0.0	0.0	0.0	0.0
Total :	Vmx	89.3	81.3	85.9	75.5	61.1	47.1	34.3	22.5
	M	0.0	172.4	76.3	280.9	506.0	648.5	723.7	741.1

		0.60L	0.70L	0.80L	0.90L	H/2	Trans	Bearing
Location,	ft	23.49	27.47	31.46	35.45	38.13	36.94	39.00
Self wt. :	M	199.5	173.4	129.9	68.9	18.3	41.7	0.0
(Max)	V	4.4	8.7	13.1	17.5	20.4	19.1	21.4
DL-Prec. :	M	40.3	35.0	26.2	13.9	3.7	8.4	0.0
DC(Max)	V	0.9	1.8	2.6	3.5	4.1	3.9	4.3
DL-Prec. :	M	49.7	43.2	32.4	17.2	4.6	10.4	-0.0
DW(Max)	V	1.1	2.2	3.3	4.4	5.1	4.8	5.3
Deck + :	M	0.0	0.0	0.0	0.0	0.0	0.0	0.0
Haunch (Max)	V	0.0	0.0	0.0	0.0	0.0	0.0	0.0
Diaphragm :	M	0.0	0.0	0.0	0.0	0.0	0.0	0.0
(Max)	V	0.0	0.0	0.0	0.0	0.0	0.0	0.0
DL-Comp :	M	0.0	0.0	0.0	0.0	0.0	0.0	0.0
DC(Max)	V	0.0	0.0	0.0	0.0	0.0	0.0	0.0
DL-Comp :	M	0.0	0.0	0.0	0.0	0.0	0.0	0.0
DW(Max)	V	0.0	0.0	0.0	0.0	0.0	0.0	0.0



Sheet #	7
Job #	
Program:	LEAP® CONSPAN® V8i (SELECTseries 5)
Version:	12.01.00.57
File Name:	NEXT D6-39ft105nonTransform.csl

Academic Use Only	Designed	HS
Copyright © Bentley Systems, Inc. 1984 - 2012	Date	Oct/17/2013
www.bentley.com	Checked	
Phone: 1-800-778-4277	Date	

		0.60L	0.70L	0.80L	0.90L	H/2	Trans	Bearing
LL + I :	M+	467.8	418.0	328.2	180.9	48.9	110.8	0.0
	V	4.1	33.7	41.9	50.2	56.3	53.6	58.3
LL + I :	M-	0.0	0.0	0.0	0.0	0.0	0.0	0.0
	V	0.0	0.0	0.0	0.0	0.0	0.0	0.0
LL + I :	Vmx	28.0	34.4	42.1	50.2	56.3	53.6	58.3
	M	434.2	396.9	317.5	180.9	49.8	111.9	0.0
Total :	M+	757.3	669.6	516.7	280.9	75.4	171.3	0.0
	V	10.4	46.4	60.9	75.5	85.9	81.3	89.3
Total :	M-	0.0	0.0	0.0	0.0	0.0	0.0	0.0
	V	0.0	0.0	0.0	0.0	0.0	0.0	0.0
Total :	Vmx	34.3	47.1	61.1	75.5	85.9	81.3	89.3
	M	723.7	648.5	506.0	280.9	76.3	172.4	0.0

REACTIONS (kips), SERVICE I

Load Type	Left Support	Right Support
Self Wt.	21.4	21.4
Deck+Haunch	0.0	0.0
Diaphragm	0.0	0.0
DL-Prec.(DC)	4.3	4.3
DL-Prec.(DW)	5.3	5.3
DL-Comp.(DC)	0.0	0.0
DL-Comp.(DW)	0.0	0.0
Live	67.2	67.2
Pedestrian	0.0	0.0

Upward reactions are positive.

Live Load reactions are per lane with no distribution factor and no impact.

Reactions are not multiplied by Load Modifiers (ductility, redundancy and operational importance).

Non-composite load types are per beam.

Composite and Pedestrian load types are per total bridge width.

SHEAR AND MOMENT ENVELOPE : Span : 1, Beam : 1, SERVICE III

Shears: kips, Moments: kft

		Bearing	Trans	H/2	0.10L	0.20L	0.30L	0.40L	Midspan
Location,	ft	0.00	2.06	0.88	3.55	7.54	11.53	15.51	19.50
Self wt. :	M	0.0	41.7	18.3	68.9	129.9	173.4	199.5	208.2
(Max)	V	21.4	19.1	20.4	17.5	13.1	8.7	4.4	0.0
DL-Prec. :	M	-0.0	8.4	3.7	13.9	26.2	35.0	40.3	42.0
DC(Max)	V	4.3	3.9	4.1	3.5	2.6	1.8	0.9	0.0
DL-Prec. :	M	-0.0	10.4	4.6	17.2	32.4	43.2	49.7	51.9
DW(Max)	V	5.3	4.8	5.1	4.4	3.3	2.2	1.1	0.0
Deck + :	M	0.0	0.0	0.0	0.0	0.0	0.0	0.0	0.0
Haunch (Max)	V	0.0	0.0	0.0	0.0	0.0	0.0	0.0	0.0



Sheet #	8
Job #	
Program:	LEAP® CONSPAN® V8i (SELECTseries 5)
Version:	12.01.00.57
Copyright © Bentley Systems, Inc. 1984 - 2012	www.bentley.com
Phone: 1-800-778-4277	
File Name:	NEXT D6-39ft105nonTransform.csl

		Bearing	Trans	H/2	0.10L	0.20L	0.30L	0.40L	Midspan
Diaphragm :	M	0.0	0.0	0.0	0.0	0.0	0.0	0.0	0.0
(Max)	V	0.0	0.0	0.0	0.0	0.0	0.0	0.0	0.0
DL-Comp :	M	0.0	0.0	0.0	0.0	0.0	0.0	0.0	0.0
DC(Max)	V	0.0	0.0	0.0	0.0	0.0	0.0	0.0	0.0
DL-Comp :	M	0.0	0.0	0.0	0.0	0.0	0.0	0.0	0.0
DW(Max)	V	0.0	0.0	0.0	0.0	0.0	0.0	0.0	0.0
LL + I :	M+	-0.0	88.6	39.2	144.7	262.6	334.4	374.2	384.4
	V	46.6	42.9	45.0	40.1	33.5	27.0	3.3	16.3
LL + I :	M-	-0.0	-0.0	-0.0	0.0	0.0	0.0	0.0	0.0
	V	0.0	0.0	0.0	0.0	0.0	0.0	0.0	0.0
LL + I :	Vmx	46.6	42.9	45.0	40.1	33.7	27.6	22.4	18.0
	M	-0.0	89.5	39.8	144.7	254.0	317.5	347.4	351.2
Total :	M+	0.0	149.2	65.7	244.7	451.0	586.0	663.7	686.6
	V	77.6	70.6	74.6	65.5	52.5	39.7	9.6	16.3
Total :	M-	0.0	0.0	0.0	0.0	0.0	0.0	0.0	0.0
	V	0.0	0.0	0.0	0.0	0.0	0.0	0.0	0.0
Total :	Vmx	77.6	70.6	74.6	65.5	52.7	40.2	28.7	18.0
	M	0.0	150.1	66.3	244.7	442.5	569.1	636.9	653.3

		0.60L	0.70L	0.80L	0.90L	H/2	Trans	Bearing
Location,	ft	23.49	27.47	31.46	35.45	38.13	36.94	39.00
Self wt. :	M	199.5	173.4	129.9	68.9	18.3	41.7	0.0
(Max)	V	4.4	8.7	13.1	17.5	20.4	19.1	21.4
DL-Prec. :	M	40.3	35.0	26.2	13.9	3.7	8.4	0.0
DC(Max)	V	0.9	1.8	2.6	3.5	4.1	3.9	4.3
DL-Prec. :	M	49.7	43.2	32.4	17.2	4.6	10.4	-0.0
DW(Max)	V	1.1	2.2	3.3	4.4	5.1	4.8	5.3
Deck + :	M	0.0	0.0	0.0	0.0	0.0	0.0	0.0
Haunch (Max)	V	0.0	0.0	0.0	0.0	0.0	0.0	0.0
Diaphragm :	M	0.0	0.0	0.0	0.0	0.0	0.0	0.0
(Max)	V	0.0	0.0	0.0	0.0	0.0	0.0	0.0
DL-Comp :	M	0.0	0.0	0.0	0.0	0.0	0.0	0.0
DC(Max)	V	0.0	0.0	0.0	0.0	0.0	0.0	0.0
DL-Comp :	M	0.0	0.0	0.0	0.0	0.0	0.0	0.0
DW(Max)	V	0.0	0.0	0.0	0.0	0.0	0.0	0.0
LL + I :	M+	374.2	334.4	262.6	144.7	39.2	88.6	0.0
	V	3.3	27.0	33.5	40.1	45.0	42.9	46.6
LL + I :	M-	0.0	0.0	0.0	0.0	0.0	0.0	0.0
	V	0.0	0.0	0.0	0.0	0.0	0.0	0.0
LL + I :	Vmx	22.4	27.6	33.7	40.1	45.0	42.9	46.6
	M	347.4	317.5	254.0	144.7	39.8	89.5	0.0
Total :	M+	663.7	586.0	451.0	244.7	65.7	149.2	0.0
	V	9.6	39.7	52.5	65.5	74.6	70.6	77.6
Total :	M-	0.0	0.0	0.0	0.0	0.0	0.0	0.0
	V	0.0	0.0	0.0	0.0	0.0	0.0	0.0
Total :	Vmx	28.7	40.2	52.7	65.5	74.6	70.6	77.6
	M	636.9	569.1	442.5	244.7	66.3	150.1	0.0



Sheet #	9
Job #	
Program:	LEAP® CONSPAN® V8i (SELECTseries 5)
Version:	12.01.00.57
Copyright © Bentley Systems, Inc. 1984 - 2012	Date
www.bentley.com	Phone: 1-800-778-4277
File Name:	NEXT D6-39ft105nonTransform.csl
Designed	HS
Checked	
Date	

SHEAR AND MOMENT ENVELOPE : Span : 1, Beam : 1, STRENGTH I
 Shears: kips, Moments: kft

		Bearing	Trans	H/2	0.10L	0.20L	0.30L	0.40L	Midspan
Location,	ft	0.00	2.06	0.88	3.55	7.54	11.53	15.51	19.50
Self wt. :	M	0.0	52.2	22.8	86.1	162.3	216.8	249.4	260.3
(Max)	V	26.7	23.9	25.5	21.8	16.4	10.9	5.5	0.0
Self wt. :	M	0.0	37.5	16.4	62.0	116.9	156.1	179.6	187.4
(Min)	V	19.2	17.2	18.4	15.7	11.8	7.9	3.9	0.0
DL-Prec. :	M	-0.0	10.5	4.6	17.4	32.8	43.7	50.3	52.5
DC(Max)	V	5.4	4.8	5.1	4.4	3.3	2.2	1.1	0.0
DL-Prec. :	M	-0.0	7.6	3.3	12.5	23.6	31.5	36.2	37.8
DC(Min)	V	3.9	3.5	3.7	3.2	2.4	1.6	0.8	0.0
DL-Prec. :	M	-0.0	15.6	6.8	25.8	48.6	64.8	74.6	77.9
DW(Max)	V	8.0	7.1	7.6	6.5	4.9	3.3	1.6	0.0
DL-Prec. :	M	-0.0	6.8	3.0	11.2	21.0	28.1	32.3	33.7
DW(Min)	V	3.5	3.1	3.3	2.8	2.1	1.4	0.7	0.0
Deck + :	M	0.0	0.0	0.0	0.0	0.0	0.0	0.0	0.0
Haunch (Max)	V	0.0	0.0	0.0	0.0	0.0	0.0	0.0	0.0
Deck + :	M	0.0	0.0	0.0	0.0	0.0	0.0	0.0	0.0
Haunch (Min)	V	0.0	0.0	0.0	0.0	0.0	0.0	0.0	0.0
Diaphragm :	M	0.0	0.0	0.0	0.0	0.0	0.0	0.0	0.0
(Max)	V	0.0	0.0	0.0	0.0	0.0	0.0	0.0	0.0
Diaphragm :	M	0.0	0.0	0.0	0.0	0.0	0.0	0.0	0.0
(Min)	V	0.0	0.0	0.0	0.0	0.0	0.0	0.0	0.0
DL-Comp :	M	0.0	0.0	0.0	0.0	0.0	0.0	0.0	0.0
DC(Max)	V	0.0	0.0	0.0	0.0	0.0	0.0	0.0	0.0
DL-Comp :	M	0.0	0.0	0.0	0.0	0.0	0.0	0.0	0.0
DC(Min)	V	0.0	0.0	0.0	0.0	0.0	0.0	0.0	0.0
DL-Comp :	M	0.0	0.0	0.0	0.0	0.0	0.0	0.0	0.0
DW(Max)	V	0.0	0.0	0.0	0.0	0.0	0.0	0.0	0.0
DL-Comp :	M	0.0	0.0	0.0	0.0	0.0	0.0	0.0	0.0
DW(Min)	V	0.0	0.0	0.0	0.0	0.0	0.0	0.0	0.0
LL + I :	M+	-0.0	193.9	85.6	316.6	574.4	731.4	818.6	840.9
	V	102.0	93.8	98.5	87.8	73.3	59.1	7.1	35.7
LL + I :	M-	-0.0	-0.0	-0.0	0.0	0.0	0.0	0.0	0.0
	V	0.0	0.0	0.0	0.0	0.0	0.0	0.0	0.0
LL + I :	Vmx	102.0	93.8	98.5	87.8	73.7	60.3	49.0	39.4
	M	-0.0	195.8	87.1	316.6	555.7	694.6	759.9	768.2
Total :	M+	0.0	272.2	119.9	445.9	818.1	1056.8	1192.9	1231.6
	V	142.1	129.6	136.8	120.6	97.9	75.4	15.3	35.7
Total :	M-	0.0	0.0	0.0	0.0	0.0	0.0	0.0	0.0
	V	0.0	0.0	0.0	0.0	0.0	0.0	0.0	0.0
Total :	Vmx	142.1	129.6	136.8	120.6	98.3	76.7	57.2	39.4
	M	0.0	265.3	117.5	431.3	771.8	983.2	1091.9	1114.8

		0.60L	0.70L	0.80L	0.90L	H/2	Trans	Bearing
Location,	ft	23.49	27.47	31.46	35.45	38.13	36.94	39.00
Self wt. :	M	249.4	216.8	162.3	86.1	22.8	5.5	0.0



Sheet #	10
Job #	
Program:	LEAP® CONSPAN® V8i (SELECTseries 5)
Version:	12.01.00.57
Copyright © Bentley Systems, Inc. 1984 - 2012	www.bentley.com
Phone: 1-800-778-4277	
File Name:	NEXT D6-39ft105nonTransform.csl

Academic Use Only	Designed	HS
Date	Oct/17/2013	
Checked		
Date		

		0.60L	0.70L	0.80L	0.90L	H/2	Trans	Bearing
(Max)	V	5.5	10.9	16.4	21.8	25.5	23.9	26.7
Self wt. :	M	179.6	156.1	116.9	62.0	16.4	37.5	0.0
(Min)	V	3.9	7.9	11.8	15.7	18.4	17.2	19.2
DL-Prec. :	M	50.3	43.7	32.8	17.4	4.6	10.5	0.0
DC(Max)	V	1.1	2.2	3.3	4.4	5.1	4.8	5.4
DL-Prec. :	M	36.2	31.5	23.6	12.5	3.3	7.6	0.0
DC(Min)	V	0.8	1.6	2.4	3.2	3.7	3.5	3.9
DL-Prec. :	M	74.6	64.8	48.6	25.8	6.8	15.6	-0.0
DW(Max)	V	1.6	3.3	4.9	6.5	7.6	7.1	8.0
DL-Prec. :	M	32.3	28.1	21.0	11.2	3.0	6.8	-0.0
DW(Min)	V	0.7	1.4	2.1	2.8	3.3	3.1	3.5
Deck + :	M	0.0	0.0	0.0	0.0	0.0	0.0	0.0
Haunch (Max)	V	0.0	0.0	0.0	0.0	0.0	0.0	0.0
Deck + :	M	0.0	0.0	0.0	0.0	0.0	0.0	0.0
Haunch (Min)	V	0.0	0.0	0.0	0.0	0.0	0.0	0.0
Diaphragm :	M	0.0	0.0	0.0	0.0	0.0	0.0	0.0
(Max)	V	0.0	0.0	0.0	0.0	0.0	0.0	0.0
Diaphragm :	M	0.0	0.0	0.0	0.0	0.0	0.0	0.0
(Min)	V	0.0	0.0	0.0	0.0	0.0	0.0	0.0
DL-Comp :	M	0.0	0.0	0.0	0.0	0.0	0.0	0.0
DC(Max)	V	0.0	0.0	0.0	0.0	0.0	0.0	0.0
DL-Comp :	M	0.0	0.0	0.0	0.0	0.0	0.0	0.0
DC(Min)	V	0.0	0.0	0.0	0.0	0.0	0.0	0.0
DL-Comp :	M	0.0	0.0	0.0	0.0	0.0	0.0	0.0
DW(Max)	V	0.0	0.0	0.0	0.0	0.0	0.0	0.0
DL-Comp :	M	0.0	0.0	0.0	0.0	0.0	0.0	0.0
DW(Min)	V	0.0	0.0	0.0	0.0	0.0	0.0	0.0
LL + I :	M+	818.6	731.4	574.4	316.6	85.6	193.9	0.0
	V	7.1	59.1	73.3	87.8	98.5	93.8	102.0
LL + I :	M-	0.0	0.0	0.0	0.0	0.0	0.0	0.0
	V	0.0	0.0	0.0	0.0	0.0	0.0	0.0
LL + I :	Vmx	49.0	60.3	73.7	87.8	98.5	93.8	102.0
	M	759.9	694.6	555.7	316.6	87.1	195.8	0.0
Total :	M+	1192.9	1056.8	818.1	445.9	119.9	272.2	0.0
	V	15.3	75.4	97.9	120.6	136.8	129.6	142.1
Total :	M-	0.0	0.0	0.0	0.0	0.0	0.0	0.0
	V	0.0	0.0	0.0	0.0	0.0	0.0	0.0
Total :	Vmx	57.2	76.7	98.3	120.6	136.8	129.6	142.1
	M	1091.9	983.2	771.8	431.3	117.5	265.3	0.0

REACTIONS (kips), STRENGTH I

Load Type	Left Support	Right Support
Self Wt.	26.7	26.7
Deck+Haunch	0.0	0.0
Diaphragm	0.0	0.0
DL-Prec.(DC)	5.4	5.4
DL-Prec.(DW)	8.0	8.0



Sheet #	11
Job #	
Program:	LEAP® CONSPAN® V8i (SELECTseries 5)
Version:	12.01.00.57
Copyright © Bentley Systems, Inc. 1984 - 2012	www.bentley.com
Phone: 1-800-778-4277	
File Name:	NEXT D6-39ft105nonTransform.csl

Academic Use Only	Designed	HS
Date	Oct/17/2013	
Checked		
Date		

Load Type	Left Support	Right Support
DL-Comp.(DC)	0.0	0.0
DL-Comp.(DW)	0.0	0.0
Live	117.7	117.7
Pedestrian	0.0	0.0

Upward reactions are positive.
 Live Load reactions are per lane with no distribution factor and no impact.
 Reactions are not multiplied by Load Modifiers (ductility, redundancy and operational importance).
 Non-composite load types are per beam.
 Composite and Pedestrian load types are per total bridge width.

SHEAR AND MOMENT ENVELOPE : Span : 1, Beam : 1, FATIGUE I
 Shears: kips, Moments: kft

		Bearing	Trans	H/2	0.10L	0.20L	0.30L	0.40L	Midspan
Location,	ft	0.00	2.06	0.88	3.55	7.54	11.53	15.51	19.50
Self wt. :	M	0.0	41.7	18.3	68.9	129.9	173.4	199.5	208.2
(Max)	V	21.4	19.1	20.4	17.5	13.1	8.7	4.4	0.0
Self wt. :	M	0.0	0.0	0.0	0.0	0.0	0.0	0.0	0.0
(Min)	V	0.0	0.0	0.0	0.0	0.0	0.0	0.0	0.0
DL-Prec. :	M	-0.0	8.4	3.7	13.9	26.2	35.0	40.3	42.0
DC(Max)	V	4.3	3.9	4.1	3.5	2.6	1.8	0.9	0.0
DL-Prec. :	M	-0.0	0.0	0.0	0.0	0.0	0.0	0.0	0.0
DC(Min)	V	0.0	0.0	0.0	0.0	0.0	0.0	0.0	0.0
DL-Prec. :	M	-0.0	10.4	4.6	17.2	32.4	43.2	49.7	51.9
DW(Max)	V	5.3	4.8	5.1	4.4	3.3	2.2	1.1	0.0
DL-Prec. :	M	-0.0	0.0	0.0	0.0	0.0	0.0	0.0	0.0
DW(Min)	V	0.0	0.0	0.0	0.0	0.0	0.0	0.0	0.0
Deck + :	M	0.0	0.0	0.0	0.0	0.0	0.0	0.0	0.0
Haunch (Max)	V	0.0	0.0	0.0	0.0	0.0	0.0	0.0	0.0
Deck + :	M	0.0	0.0	0.0	0.0	0.0	0.0	0.0	0.0
Haunch (Min)	V	0.0	0.0	0.0	0.0	0.0	0.0	0.0	0.0
Diaphragm :	M	0.0	0.0	0.0	0.0	0.0	0.0	0.0	0.0
(Max)	V	0.0	0.0	0.0	0.0	0.0	0.0	0.0	0.0
Diaphragm :	M	0.0	0.0	0.0	0.0	0.0	0.0	0.0	0.0
(Min)	V	0.0	0.0	0.0	0.0	0.0	0.0	0.0	0.0
DL-Comp :	M	0.0	0.0	0.0	0.0	0.0	0.0	0.0	0.0
DC(Max)	V	0.0	0.0	0.0	0.0	0.0	0.0	0.0	0.0
DL-Comp :	M	0.0	0.0	0.0	0.0	0.0	0.0	0.0	0.0
DC(Min)	V	0.0	0.0	0.0	0.0	0.0	0.0	0.0	0.0
DL-Comp :	M	0.0	0.0	0.0	0.0	0.0	0.0	0.0	0.0
DW(Max)	V	0.0	0.0	0.0	0.0	0.0	0.0	0.0	0.0
DL-Comp :	M	0.0	0.0	0.0	0.0	0.0	0.0	0.0	0.0
DW(Min)	V	0.0	0.0	0.0	0.0	0.0	0.0	0.0	0.0
LL + I :	M+	0.0	84.1	36.9	138.6	258.7	341.2	386.1	393.5
	V	46.4	42.1	44.6	39.0	34.3	29.6	24.9	20.2
LL + I :	M-	0.0	0.0	0.0	0.0	0.0	0.0	0.0	0.0



Sheet #	12
Job #	
Program:	LEAP® CONSPAN® V8i (SELECTseries 5)
Version:	12.01.00.57
Copyright © Bentley Systems, Inc. 1984 - 2012	www.bentley.com
Phone: 1-800-778-4277	
File Name:	NEXT D6-39ft105nonTransform.csl

		Bearing	Trans	H/2	0.10L	0.20L	0.30L	0.40L	Midspan
LL + I :	V	0.0	0.0	0.0	0.0	0.0	0.0	0.0	0.0
	Vmx	46.4	42.1	44.6	39.0	34.3	29.6	24.9	20.2
	M	0.0	84.1	36.9	138.6	258.7	341.2	386.1	393.5
Total :	M+	0.0	144.7	63.4	238.6	447.1	592.8	675.7	695.7
	V	77.4	69.8	74.2	64.4	53.3	42.3	31.2	20.2
Total :	M-	0.0	0.0	0.0	0.0	0.0	0.0	0.0	0.0
	V	0.0	0.0	0.0	0.0	0.0	0.0	0.0	0.0
Total :	Vmx	77.4	69.8	74.2	64.4	53.3	42.3	31.2	20.2
	M	0.0	144.7	63.4	238.6	447.1	592.8	675.7	695.7

		0.60L	0.70L	0.80L	0.90L	H/2	Trans	Bearing
Location,	ft	23.49	27.47	31.46	35.45	38.13	36.94	39.00
Self wt. :	M	199.5	173.4	129.9	68.9	18.3	41.7	0.0
(Max)	V	4.4	8.7	13.1	17.5	20.4	19.1	21.4
Self wt. :	M	0.0	0.0	0.0	0.0	0.0	0.0	0.0
(Min)	V	0.0	0.0	0.0	0.0	0.0	0.0	0.0
DL-Prec. :	M	40.3	35.0	26.2	13.9	3.7	8.4	0.0
DC(Max)	V	0.9	1.8	2.6	3.5	4.1	3.9	4.3
DL-Prec. :	M	0.0	0.0	0.0	0.0	0.0	0.0	0.0
DC(Min)	V	0.0	0.0	0.0	0.0	0.0	0.0	0.0
DL-Prec. :	M	49.7	43.2	32.4	17.2	4.6	10.4	-0.0
DW(Max)	V	1.1	2.2	3.3	4.4	5.1	4.8	5.3
DL-Prec. :	M	0.0	0.0	0.0	0.0	0.0	0.0	-0.0
DW(Min)	V	0.0	0.0	0.0	0.0	0.0	0.0	0.0
Deck + :	M	0.0	0.0	0.0	0.0	0.0	0.0	0.0
Haunch (Max)	V	0.0	0.0	0.0	0.0	0.0	0.0	0.0
Deck + :	M	0.0	0.0	0.0	0.0	0.0	0.0	0.0
Haunch (Min)	V	0.0	0.0	0.0	0.0	0.0	0.0	0.0
Diaphragm :	M	0.0	0.0	0.0	0.0	0.0	0.0	0.0
(Max)	V	0.0	0.0	0.0	0.0	0.0	0.0	0.0
Diaphragm :	M	0.0	0.0	0.0	0.0	0.0	0.0	0.0
(Min)	V	0.0	0.0	0.0	0.0	0.0	0.0	0.0
DL-Comp :	M	0.0	0.0	0.0	0.0	0.0	0.0	0.0
DC(Max)	V	0.0	0.0	0.0	0.0	0.0	0.0	0.0
DL-Comp :	M	0.0	0.0	0.0	0.0	0.0	0.0	0.0
DC(Min)	V	0.0	0.0	0.0	0.0	0.0	0.0	0.0
DL-Comp :	M	0.0	0.0	0.0	0.0	0.0	0.0	0.0
DW(Max)	V	0.0	0.0	0.0	0.0	0.0	0.0	0.0
DL-Comp :	M	0.0	0.0	0.0	0.0	0.0	0.0	0.0
DW(Min)	V	0.0	0.0	0.0	0.0	0.0	0.0	0.0
LL + I :	M+	386.1	341.2	258.7	138.6	36.9	84.1	0.0
	V	24.9	29.6	34.3	39.0	44.6	42.1	46.4
LL + I :	M-	0.0	0.0	0.0	0.0	0.0	0.0	0.0
	V	0.0	0.0	0.0	0.0	0.0	0.0	0.0
LL + I :	Vmx	24.9	29.6	34.3	39.0	44.6	42.1	46.4
	M	386.1	341.2	258.7	138.6	36.9	84.1	0.0
Total :	M+	675.7	592.8	447.1	238.6	63.4	144.7	0.0
	V	31.2	42.3	53.3	64.4	74.2	69.8	77.4
Total :	M-	0.0	0.0	0.0	0.0	0.0	0.0	0.0
	V	0.0	0.0	0.0	0.0	0.0	0.0	0.0
Total :	Vmx	31.2	42.3	53.3	64.4	74.2	69.8	77.4



		Sheet #	13		
		Job #			
Program:	LEAP® CONSPAN® V8i (SELECTseries 5)	Academic Use Only	Designed	HS	
Version:	12.01.00.57	Copyright © Bentley Systems, Inc. 1984 - 2012	Date	Oct/17/2013	
		www.bentley.com	Phone: 1-800-778-4277	Checked	
File Name:	NEXT D6-39ft105nonTransform.csl			Date	

	M	0.60L	0.70L	0.80L	0.90L	H/2	Trans	Bearing
		675.7	592.8	447.1	238.6	63.4	144.7	0.0



Sheet #	14
Job #	
Program:	LEAP® CONSPAN® V8i (SELECTseries 5)
Version:	12.01.00.57
Copyright © Bentley Systems, Inc. 1984 - 2012	www.bentley.com
Phone: 1-800-778-4277	
File Name:	NEXT D6-39ft105nonTransform.csl

Academic Use Only	Designed	HS
Date	Oct/17/2013	
Checked		
Date		

POSITIVE ENVELOPE STRESSES

Span : 1, Beam : 1, SERVICE I

RELEASE STRESSES, (ksi) (LOSS = 4.95 %)

Location, ft	Trans	0.10L /0.90L	0.20L /0.80L	0.30L /0.70L	0.40L /0.60L	Midspan
2.50	3.99	7.98	11.96	15.95	19.94	
Beam-Self						
Precast-top	0.135	0.207	0.367	0.482	0.551	0.574
Bottom	-0.230	-0.352	-0.626	-0.821	-0.938	-0.978
Prestress						
Precast-top	-0.611	-0.611	-0.611	-0.611	-0.611	-0.611
Bottom	3.010	3.010	3.010	3.010	3.010	3.010
Total						
Precast-top	-0.476	-0.405	-0.244	-0.129	-0.060	-0.037
Bottom	2.780	2.658	2.384	2.189	2.071	2.032

SERVICE I

POSITIVE ENVELOPE STRESSES, (ksi) (LOSS = 10.12 %)

Location, ft	Bearing	Trans	H/2	0.10L /0.90L	0.20L /0.80L	0.30L /0.70L	0.40L /0.60L	Midspan
0.00	2.06	0.88	3.55	7.54	11.53	15.51	19.50	
Prestress								
Precast-top	-0.101	-0.578	-0.303	-0.578	-0.578	-0.578	-0.578	-0.578
Bottom	0.498	2.846	1.494	2.846	2.846	2.846	2.846	2.846
Self wt.								
Precast-top	0.000	0.110	0.048	0.182	0.342	0.457	0.526	0.549
Bottom	-0.000	-0.187	-0.082	-0.309	-0.583	-0.779	-0.896	-0.935
DL-Prec (DC)								
Precast-top	-0.000	0.022	0.010	0.037	0.069	0.092	0.106	0.111
Bottom	0.000	-0.038	-0.017	-0.062	-0.118	-0.157	-0.181	-0.189
DL-Prec (DW)								
Precast-top	-0.000	0.027	0.012	0.045	0.085	0.114	0.131	0.137
Bottom	0.000	-0.047	-0.020	-0.077	-0.145	-0.194	-0.223	-0.233



Sheet #	15
Job #	
Program:	LEAP® CONSPAN® V8i (SELECTseries 5)
Version:	12.01.00.57
Copyright © Bentley Systems, Inc. 1984 - 2012	www.bentley.com
Phone: 1-800-778-4277	
File Name:	NEXT D6-39ft105nonTransform.csl
Designed	HS
Date	Oct/17/2013
Checked	
Date	

	Bearing	Trans	H/2	0.10L /0.90L	0.20L /0.80L	0.30L /0.70L	0.40L /0.60L	Midspan
Diaphragm								
Precast-top	-0.000	-0.000	-0.000	-0.000	-0.000	-0.000	-0.000	-0.000
Bottom	-0.000	-0.000	-0.000	-0.000	-0.000	-0.000	-0.000	-0.000
Deck + Haunch								
Precast-top	-0.000	-0.000	-0.000	-0.000	-0.000	-0.000	-0.000	-0.000
Bottom	-0.000	-0.000	-0.000	-0.000	-0.000	-0.000	-0.000	-0.000
DL-Comp (DC)								
Precast-top	-0.000	-0.000	-0.000	-0.000	-0.000	-0.000	-0.000	-0.000
Bottom	-0.000	-0.000	-0.000	-0.000	-0.000	-0.000	-0.000	-0.000
DL-Comp (DW)								
Precast-top	-0.000	-0.000	-0.000	-0.000	-0.000	-0.000	-0.000	-0.000
Bottom	-0.000	-0.000	-0.000	-0.000	-0.000	-0.000	-0.000	-0.000
LL+I(+)								
Precast-top	-0.000	0.292	0.129	0.477	0.865	1.102	1.233	1.267
Bottom	0.000	-0.498	-0.220	-0.812	-1.474	-1.877	-2.101	-2.158
Final 1 (P/S + DL + LL)								
Precast-top	-0.101	-0.126	-0.105	0.163	0.784	1.187	1.418	1.485
Bottom	0.498	2.077	1.155	1.585	0.526	-0.161	-0.555	-0.669
Final 2 (P/S + DL)								
Precast-top	-0.101	-0.418	-0.234	-0.314	-0.081	0.085	0.185	0.219
Bottom	0.498	2.574	1.375	2.397	2.000	1.716	1.546	1.489

Span : 1, Beam : 1, SERVICE III

RELEASE STRESSES, (ksi) (LOSS = 4.95 %)

Location, ft	Trans	0.10L /0.90L	0.20L /0.80L	0.30L /0.70L	0.40L /0.60L	Midspan
2.50	3.99	7.98	11.96	15.95	19.94	
Beam-Self						
Precast-top	0.135	0.207	0.367	0.482	0.551	0.574
Bottom	-0.230	-0.352	-0.626	-0.821	-0.938	-0.978
Prestress						
Precast-top	-0.611	-0.611	-0.611	-0.611	-0.611	-0.611
Bottom	3.010	3.010	3.010	3.010	3.010	3.010



Sheet #	16
Job #	
Program:	LEAP® CONSPAN® V8i (SELECTseries 5)
Version:	12.01.00.57
Copyright © Bentley Systems, Inc. 1984 - 2012	www.bentley.com
Phone: 1-800-778-4277	
File Name:	NEXT D6-39ft105nonTransform.csl

Academic Use Only	Designed	HS
Date	Oct/17/2013	
Checked		
Date		

	Trans	0.10L /0.90L	0.20L /0.80L	0.30L /0.70L	0.40L /0.60L	Midspan
Total						
Precast-top	-0.476	-0.405	-0.244	-0.129	-0.060	-0.037
Bottom	2.780	2.658	2.384	2.189	2.071	2.032
As_top, in2	1.756	1.347	0.571	0.000	0.000	0.000
Ast_prvd, in2	4.400	4.400	4.400	4.400	4.400	4.400

SERVICE III

POSITIVE ENVELOPE STRESSES, (ksi) (LOSS = 10.12 %)

	Bearing	Trans	H/2	0.10L /0.90L	0.20L /0.80L	0.30L /0.70L	0.40L /0.60L	Midspan
Location, ft	0.00	2.06	0.88	3.55	7.54	11.53	15.51	19.50
Prestress								
Precast-top	-0.101	-0.578	-0.303	-0.578	-0.578	-0.578	-0.578	-0.578
Bottom	0.498	2.846	1.494	2.846	2.846	2.846	2.846	2.846
Self wt.								
Precast-top	0.000	0.110	0.048	0.182	0.342	0.457	0.526	0.549
Bottom	-0.000	-0.187	-0.082	-0.309	-0.583	-0.779	-0.896	-0.935
DL-Prec (DC)								
Precast-top	-0.000	0.022	0.010	0.037	0.069	0.092	0.106	0.111
Bottom	0.000	-0.038	-0.017	-0.062	-0.118	-0.157	-0.181	-0.189
DL-Prec (DW)								
Precast-top	-0.000	0.027	0.012	0.045	0.085	0.114	0.131	0.137
Bottom	0.000	-0.047	-0.020	-0.077	-0.145	-0.194	-0.223	-0.233
Diaphragm								
Precast-top	-0.000	-0.000	-0.000	-0.000	-0.000	-0.000	-0.000	-0.000
Bottom	-0.000	-0.000	-0.000	-0.000	-0.000	-0.000	-0.000	-0.000
Deck + Haunch								
Precast-top	-0.000	-0.000	-0.000	-0.000	-0.000	-0.000	-0.000	-0.000
Bottom	-0.000	-0.000	-0.000	-0.000	-0.000	-0.000	-0.000	-0.000
DL-Comp (DC)								
Precast-top	-0.000	-0.000	-0.000	-0.000	-0.000	-0.000	-0.000	-0.000
Bottom	-0.000	-0.000	-0.000	-0.000	-0.000	-0.000	-0.000	-0.000
DL-Comp (DW)								
Precast-top	-0.000	-0.000	-0.000	-0.000	-0.000	-0.000	-0.000	-0.000



Sheet #	17
Job #	
Program:	LEAP® CONSPAN® V8i (SELECTseries 5)
Version:	12.01.00.57
Copyright © Bentley Systems, Inc. 1984 - 2012	www.bentley.com
Phone: 1-800-778-4277	
File Name:	NEXT D6-39ft105nonTransform.csl

Academic Use Only	Designed	HS
Date	Oct/17/2013	Checked
Date		

	Bearing	Trans	H/2	0.10L /0.90L	0.20L /0.80L	0.30L /0.70L	0.40L /0.60L	Midspan
Bottom	-0.000	-0.000	-0.000	-0.000	-0.000	-0.000	-0.000	-0.000
LL+I(+)								
Precast-top	-0.000	0.234	0.103	0.382	0.692	0.881	0.986	1.013
Bottom	0.000	-0.398	-0.176	-0.650	-1.179	-1.502	-1.680	-1.726
Final 1 (P/S + DL + LL)								
Precast-top	-0.101	-0.185	-0.130	0.067	0.611	0.967	1.172	1.232
Bottom	0.498	2.176	1.199	1.747	0.821	0.215	-0.134	-0.237

Span : 1, Beam : 1, FATIGUE I
 POSITIVE ENVELOPE STRESSES, (ksi)

Location, ft	Bearing	Trans	H/2	0.10L /0.90L	0.20L /0.80L	0.30L /0.70L	0.40L /0.60L	Midspan
	0.00	2.06	0.88	3.55	7.54	11.53	15.51	19.50
F_LL+I(+)								
Precast-top	-0.000	0.222	0.097	0.365	0.682	0.899	1.018	1.037
Bottom	-0.000	-0.378	-0.166	-0.622	-1.162	-1.532	-1.734	-1.767
Final 3 (50% P/S + 50% DL + F_LL)								
Precast-top	-0.051	0.013	-0.019	0.208	0.641	0.942	1.111	1.147
Bottom	0.249	0.909	0.522	0.576	-0.162	-0.674	-0.961	-1.023



Sheet #	18
Job #	
Program:	LEAP® CONSPAN® V8i (SELECTseries 5)
Version:	12.01.00.57
File Name:	NEXT D6-39ft105nonTransform.csl
Academic Use Only	Designed HS
Copyright © Bentley Systems, Inc. 1984 - 2012	Date Oct/17/2013
www.bentley.com	Checked
Phone: 1-800-778-4277	Date

VERTICAL/HORIZONTAL SHEAR

VERTICAL SHEAR (Art. 5.8) - Span : 1, Beam : 1, STRENGTH I
 Using General Beta Theta Equation procedure - Art.5.8.3.4.2

Location(ft)	Vu (kips)	bv (in)	de (in)	Aps (in ²)	Vp (kips)	eps_x	Theta	Vs-reqd (kips)	Av/s (in ² /ft)	Av-prvd (in ² /ft)	Al_reqd (in ²)
	Mcor (kft)	a (in)	dv (in)	fpo (ksi)	vu/fc	Vc-com (kips)	Beta	Max.spc. (in)	min.Av/s (in ² /ft)	pVn/Vu	Aps* (in ²)
Bearing :		0.44									
142.1	29.19	17.23	0.273	0.0	6.00e-3	50.0	122.8	1.716	6.400	0.00	
0.0	0.34	17.06	33.1	0.049	35.0	0.87	13.65	0.470	3.124	0.423	
Transfer :		2.50									
129.6	29.19	17.23	3.366	0.0	-0.12e-3	28.6	0.0	0.470	0.533	0.00	
265.3	1.92	16.27	189.0	0.047	201.3	5.26	13.02	0.470	1.951	2.418	
Critical :		1.81									
133.7	29.19	17.23	3.366	0.0	-0.14e-3	28.5	0.0	0.470	1.600	0.00	
176.4	1.39	16.53	189.0	0.047	208.3	5.36	13.22	0.470	3.040	1.755	
0.1L :		3.99									
120.6	29.19	17.23	3.366	0.0	-0.07e-3	28.7	0.0	0.470	0.533	0.00	
431.3	2.28	16.09	189.0	0.044	192.1	5.08	12.87	0.470	2.018	2.885	
0.2L :		7.97									
98.3	29.19	17.23	3.366	0.0	0.46e-3	30.6	0.0	0.470	0.533	0.00	
771.8	2.65	15.90	189.0	0.036	133.2	3.56	12.72	0.470	1.876	3.366	
0.3L :		11.96									
76.7	29.19	17.23	3.366	0.0	1.90e-3	35.7	11.1	0.470	0.533	0.00	
983.2	2.65	15.90	189.0	0.028	74.0	1.98	12.72	0.470	1.564	3.366	
0.4L :		15.95									
57.2	29.19	17.23	3.366	0.0	2.55e-3	37.9	1.9	0.470	0.533	0.00	
1091.9	2.65	15.90	189.0	0.021	61.6	1.65	12.72	0.470	1.826	3.366	
0.5L :		19.94									
39.4	29.19	17.23	3.366	0.0	2.55e-3	37.9	0.0	0.470	0.533	0.00	
1114.8	2.65	15.90	189.0	0.015	61.7	1.65	12.72	0.470	2.654	3.366	
0.6L :		23.93									
57.2	29.19	17.23	3.366	0.0	2.55e-3	37.9	1.9	0.470	0.533	0.00	
1091.9	2.65	15.90	189.0	0.021	61.6	1.65	12.72	0.470	1.826	3.366	
0.7L :		27.91									
76.7	29.19	17.23	3.366	0.0	1.90e-3	35.7	⁴⁶⁹ 11.1	0.470	0.533	0.00	



Sheet #	19
Job #	
Program:	LEAP® CONSPAN® V8i (SELECTseries 5)
Version:	12.01.00.57
Copyright © Bentley Systems, Inc. 1984 - 2012	www.bentley.com
Phone: 1-800-778-4277	
File Name:	NEXT D6-39ft105nonTransform.csl

Location(ft)	Vu (kips)	bv (in)	de (in)	Aps (in2)	Vp (kips)	eps_x	Theta	Vs-reqd (kips)	Av/s (in2/ft)	Av-prvd (in2/ft)	Al_reqd (in2)
Mcor (kft)	a (in)	dv (in)	fpo (ksi)	vu/fc	Vc-com (kips)	Beta	Max.spc. (in)	min.Av/s (in2/ft)	pVn/Vu	Aps* (in2)	
	983.2	2.65	15.90	189.0	0.028	74.0	1.98	12.72	0.470	1.564	3.366
0.8L :		31.90									
	98.3	29.19	17.23	3.366	0.0	0.46e-3	30.6	0.0	0.470	0.533	0.00
	771.8	2.65	15.90	189.0	0.036	133.2	3.56	12.72	0.470	1.876	3.366
0.9L :		35.89									
	120.6	29.19	17.23	3.366	0.0	-0.07e-3	28.7	0.0	0.470	0.533	0.00
	431.3	2.28	16.09	189.0	0.044	192.1	5.08	12.87	0.470	2.018	2.885
Critical :		38.06									
	133.7	29.19	17.23	3.366	0.0	-0.14e-3	28.5	0.0	0.470	1.600	0.00
	176.4	1.39	16.53	189.0	0.047	208.3	5.36	13.22	0.470	3.040	1.755
Transfer :		37.38									
	129.6	29.19	17.23	3.366	0.0	-0.12e-3	28.6	0.0	0.470	0.533	0.00
	265.3	1.92	16.27	189.0	0.047	201.3	5.26	13.02	0.470	1.951	2.418
Bearing :		39.44									
	142.1	29.19	17.23	0.273	0.0	6.00e-3	50.0	122.8	1.716	2.400	0.00
	0.0	0.34	17.06	33.1	0.049	35.0	0.87	13.65	0.470	1.310	0.423

ANCHORAGE ZONE REINFORCEMENT (Art. 5.10.10)
Span : 1, Beam : 1

Fpi (kips)	fs (ksi)	h/4 (in)	Abrst_rqrd (in2)
805.54	20.00	5.25	1.61



Sheet #	20
Job #	
Program:	LEAP® CONSPAN® V8i (SELECTseries 5)
Version:	12.01.00.57
Copyright © Bentley Systems, Inc. 1984 - 2012	Date
www.bentley.com	Checked
Phone: 1-800-778-4277	Date

Academic Use Only	Designed	HS
Copyright © Bentley Systems, Inc. 1984 - 2012	Date	Oct/17/2013
www.bentley.com	Checked	
Phone: 1-800-778-4277	Date	

File Name: NEXT D6-39ft105nonTransform.csl

CAMBER/DEFLECTION

CAMBER AND DEFLECTIONS: SERVICE I
(Span : 1, Beam : 1; Units: in)

	Release	Mult	Erection	Mult	Final
At 0.1 x L =	3.55 ft				
Prestress	0.400	1.80	0.721	2.45	0.981
Self Wt.	-0.127	1.85	-0.234	2.70	-0.342
Deck + Haunch			0.000	2.30	0.000
DL-Prec. (DC)			-0.019	3.00	-0.057
Diaphragm			0.000	3.00	0.000
DL-Prec. (DW)			-0.024	3.00	-0.071
DL-Comp. (DC)			0.000	3.00	0.000
DL-Comp. (DW)			0.000	3.00	0.000
Live Load					-0.172
Total	0.274		0.444		0.339

	Release	Mult	Erection	Mult	Final
At 0.2 x L =	7.54 ft				
Prestress	0.717	1.80	1.290	2.45	1.756
Self Wt.	-0.239	1.85	-0.443	2.70	-0.646
Deck + Haunch			0.000	2.30	0.000
DL-Prec. (DC)			-0.038	3.00	-0.115
Diaphragm			0.000	3.00	0.000
DL-Prec. (DW)			-0.047	3.00	-0.142
DL-Comp. (DC)			0.000	3.00	0.000
DL-Comp. (DW)			0.000	3.00	0.000
Live Load					-0.347
Total	0.477		0.761		0.505

	Release	Mult	Erection	Mult	Final
At 0.3 x L =	11.52 ft				
Prestress	0.942	1.80	1.696	2.45	2.309
Self Wt.	-0.328	1.85	-0.606	2.70	-0.885
Deck + Haunch			0.000	2.30	0.000
DL-Prec. (DC)			-0.054	3.00	-0.161
Diaphragm			0.000	3.00	0.000
DL-Prec. (DW)			-0.066	3.00	-0.199
DL-Comp. (DC)			0.000	3.00	0.000
DL-Comp. (DW)			0.000	3.00	0.000
Live Load					-0.482
Total	0.615		0.970		0.583

	Release	Mult	Erection	Mult	Final
At 0.4 x L =	15.51 ft				
Prestress	1.078	1.80	1.940	2.45	2.641



Sheet #	21
Job #	
Program:	LEAP® CONSPAN® V8i (SELECTseries 5)
Version:	12.01.00.57
Copyright © Bentley Systems, Inc. 1984 - 2012	www.bentley.com
Phone: 1-800-778-4277	
File Name:	NEXT D6-39ft105nonTransform.csl

Academic Use Only	Designed	HS
Date	Oct/17/2013	
Checked		
Date		

	Release	Mult	Erection	Mult	Final
Self Wt.	-0.384	1.85	-0.710	2.70	-1.036
Deck + Haunch			0.000	2.30	0.000
DL-Prec. (DC)			-0.063	3.00	-0.190
Diaphragm			0.000	3.00	0.000
DL-Prec. (DW)			-0.078	3.00	-0.234
DL-Comp. (DC)			0.000	3.00	0.000
DL-Comp. (DW)			0.000	3.00	0.000
Live Load					-0.567
Total	0.694		1.089		0.613

	Release	Mult	Erection	Mult	Final
At 0.5 x L = 19.50 ft					
Prestress	1.123	1.80	2.021	2.45	2.751
Self Wt.	-0.403	1.85	-0.746	2.70	-1.088
Deck + Haunch			0.000	2.30	0.000
DL-Prec. (DC)			-0.067	3.00	-0.200
Diaphragm			0.000	3.00	0.000
DL-Prec. (DW)			-0.082	3.00	-0.247
DL-Comp. (DC)			0.000	3.00	0.000
DL-Comp. (DW)			0.000	3.00	0.000
Live Load					-0.595
Total	0.720		1.127		0.622

	Release	Mult	Erection	Mult	Final
At 0.6 x L = 23.49 ft					
Prestress	1.078	1.80	1.940	2.45	2.641
Self Wt.	-0.384	1.85	-0.710	2.70	-1.036
Deck + Haunch			0.000	2.30	0.000
DL-Prec. (DC)			-0.063	3.00	-0.190
Diaphragm			0.000	3.00	0.000
DL-Prec. (DW)			-0.078	3.00	-0.234
DL-Comp. (DC)			0.000	3.00	0.000
DL-Comp. (DW)			0.000	3.00	0.000
Live Load					-0.567
Total	0.694		1.089		0.613

	Release	Mult	Erection	Mult	Final
At 0.7 x L = 27.48 ft					
Prestress	0.942	1.80	1.696	2.45	2.309
Self Wt.	-0.328	1.85	-0.606	2.70	-0.885
Deck + Haunch			0.000	2.30	0.000
DL-Prec. (DC)			-0.054	3.00	-0.161
Diaphragm			0.000	3.00	0.000
DL-Prec. (DW)			-0.066	3.00	-0.199
DL-Comp. (DC)			0.000	3.00	0.000
DL-Comp. (DW)			0.000	3.00	0.000
Live Load					-0.482



Sheet #	22
Job #	
Program:	LEAP® CONSPAN® V8i (SELECTseries 5)
Version:	12.01.00.57
Copyright © Bentley Systems, Inc. 1984 - 2012	www.bentley.com
Phone: 1-800-778-4277	
File Name:	NEXT D6-39ft105nonTransform.csl

Academic Use Only	Designed	HS
Date	Oct/17/2013	
Checked		
Date		

	Release	Mult	Erection	Mult	Final
Total	0.615		0.970		0.583

	Release	Mult	Erection	Mult	Final
At 0.8 x L = 31.46 ft					
Prestress	0.717	1.80	1.290	2.45	1.756
Self Wt.	-0.239	1.85	-0.443	2.70	-0.646
Deck + Haunch			0.000	2.30	0.000
DL-Prec. (DC)			-0.038	3.00	-0.115
Diaphragm			0.000	3.00	0.000
DL-Prec. (DW)			-0.047	3.00	-0.142
DL-Comp. (DC)			0.000	3.00	0.000
DL-Comp. (DW)			0.000	3.00	0.000
Live Load					-0.347
Total	0.477		0.761		0.505

	Release	Mult	Erection	Mult	Final
At 0.9 x L = 35.45 ft					
Prestress	0.400	1.80	0.721	2.45	0.981
Self Wt.	-0.127	1.85	-0.234	2.70	-0.342
Deck + Haunch			0.000	2.30	0.000
DL-Prec. (DC)			-0.019	3.00	-0.057
Diaphragm			0.000	3.00	0.000
DL-Prec. (DW)			-0.024	3.00	-0.071
DL-Comp. (DC)			0.000	3.00	0.000
DL-Comp. (DW)			0.000	3.00	0.000
Live Load					-0.172
Total	0.274		0.444		0.339



Sheet #	23
Job #	
Program:	LEAP® CONSPAN® V8i (SELECTseries 5)
Version:	12.01.00.57
File Name:	NEXT D6-39ft105nonTransform.csl
Academic Use Only	
Copyright © Bentley Systems, Inc. 1984 - 2012	
www.bentley.com	Phone: 1-800-778-4277
Designed	HS
Date	Oct/17/2013
Checked	
Date	

ULTIMATE MOMENT

ULTIMATE - Span : 1, Beam : 1, STRENGTH I
 (Mr-prvd computed by Strain Compatibility method. Ult. Conc. Strain = 0.00300)

Location (ft)	dp in	Aps in ²	fps ksi	c in	a in	Mr-prvd k.ft	c/dt	Phi	Mcr k.ft	min Mr k.ft	Crkg Ratio	Mu-p/r Ratio
Transfer	2.06											
272.2	15.8	2.858	266.7	2.6	1.9	940.1	0.142T	1.00	-	-	-	-
H/2	0.88											
119.9	15.7	1.501	268.5	1.4	1.0	511.5	0.075T	1.00	-	-	-	-
0.1L	3.55											
445.9	15.8	3.410	265.8	3.1	2.3	1104.8	0.169T	1.00	-	-	-	-
0.2L	7.54											
818.1	15.8	3.978	264.7	3.6	2.6	1268.8	0.196T	1.00	915.2	915.2	1.39	-
0.3L	11.53											
1056.8	15.8	3.978	264.7	3.6	2.6	1268.8	0.196T	1.00	915.2	915.2	1.39	-
0.4L	15.51											
1192.9	15.8	3.978	264.7	3.6	2.6	1268.8	0.196T	1.00	915.2	915.2	1.39	-
0.5L	19.50											
1231.6	15.8	3.978	264.7	3.6	2.6	1268.8	0.196T	1.00	915.2	915.2	1.39	-
0.6L	23.49											
1192.9	15.8	3.978	264.7	3.6	2.6	1268.8	0.196T	1.00	915.2	915.2	1.39	-
0.7L	27.48											
1056.8	15.8	3.978	264.7	3.6	2.6	1268.8	0.196T	1.00	915.2	915.2	1.39	-
0.8L	31.46											
818.1	15.8	3.978	264.7	3.6	2.6	1268.8	0.196T	1.00	915.2	915.2	1.39	-
0.9L	35.45											
445.9	15.8	3.410	265.8	3.1	2.3	1104.8	0.169T	1.00	-	-	-	-
H/2	38.13											
119.9	15.7	1.501	268.5	1.4	1.0	511.5	0.075T	1.00	-	-	-	-
Transfer	36.94											
272.2	15.8	2.858	266.7	2.6	1.9	940.1	0.142T	1.00	-	-	-	-

Legend: C = Compression-Controlled (c/dt > 0.600)
 I = In-Transition (0.60 >= c/dt > 0.375)
 T = Tension-Controlled (c/dt <= 0.375)
 Note : fr used for calculating Mcr is computed using AASHTO method (Art.5.4.2.6.)
 Consider Bottom Tension Steel Contribution : NO



Sheet #	24
Job #	
Program:	LEAP® CONSPAN® V8i (SELECTseries 5)
Version:	12.01.00.57
Copyright © Bentley Systems, Inc. 1984 - 2012	www.bentley.com
Phone: 1-800-778-4277	
File Name:	NEXT D6-39ft105nonTransform.csl

Academic Use Only	Designed	HS
Date	Oct/17/2013	Checked
Date		

DETENSIONING

Span : 1, Beam : 1; Groups 1-13; Units: ksi

Grp	Str	Ys,in	2.50ft
1	E	2.50	Ft 0.052
	M	2.50	Fb 0.062
2	E	13.50	Ft 0.112
	M	13.50	Fb 0.113
3	E	13.50	Ft 0.171
	M	13.50	Fb 0.163
4	E	6.50	Ft 0.140
	M	6.50	Fb 0.367
5	E	4.50	Ft 0.083
	M	4.50	Fb 0.616
6	E	4.50	Ft 0.026
	M	4.50	Fb 0.864
7	E	4.50	Ft -0.031
	M	4.50	Fb 1.113
8	E	4.50	Ft -0.088
	M	4.50	Fb 1.361
9	E	4.50	Ft -0.145
	M	4.50	Fb 1.610
10	E	2.50	Ft -0.228
	M	2.50	Fb 1.902
11	E	2.50	Ft -0.310
	M	2.50	Fb 2.195
12	E	2.50	Ft -0.393
	M	2.50	Fb 2.487
13	E	2.50	Ft -0.476
	M	2.50	Fb 2.780



		Sheet #	25
		Job #	
Program:	LEAP® CONSPAN® V8i (SELECTseries 5)	Academic Use Only	Designed HS
Version:	12.01.00.57	Copyright © Bentley Systems, Inc. 1984 - 2012	Date Oct/17/2013
		www.bentley.com	Phone: 1-800-778-4277
File Name:	NEXT D6-39ft105nonTransform.csl		Checked
			Date

DESIGN SUMMARY

Span: 1, Beam: 1, Exterior beam

Beam type:	Double Tee,	Next D6-21-exterior
Precast Length,	ft	39.88
Release Length,	ft	39.88
Strand Pattern:	Straight	
Strand:	1/2-270K-LL	
Strand Es,	ksi:	28500.0
No. of strands:	26	
	Draped:	0
	Straight:	26
Concrete Strength:		
	f'ci:	5.2 ksi
	f'c:	6.5 ksi
	f'ct:	6.5 ksi
Initial losses:	4.95 %	
Final losses:	10.12 %	

Specification	Allowable	Computed	Location	Status
Release Stresses (ksi) (Art. 5.9.4.1)				
Precast Bot (compression)	3.120	2.780	Trans	OK
Precast Top w/ no reinf. (tension)	-0.200	-0.476	Trans	
Precast Top w/ reinf. (tension)	-0.547			
Strength I (Art. 3.4.1, 5.7.3.1.1)	Provided	Required	Location	Status
Ult. Moment (k.ft)	1268.82	1231.60	Midspan	OK
Debonding Limits (Art. 5.11.4.3)	Allowable	Computed		Status
Max. Debond per Row	40.00 %	0.00 %		OK
Max. Debond Total	25.00 %	0.00 %		OK

Positive Moment Envelope Stresses (ksi) (Art. 3.4.1 and 5.9.4.2)



Sheet #	26
Job #	
Program:	LEAP® CONSPAN® V8i (SELECTseries 5)
Version:	12.01.00.57
Copyright © Bentley Systems, Inc. 1984 - 2012	www.bentley.com
Phone: 1-800-778-4277	
File Name:	NEXT D6-39ft105nonTransform.csl

Specification	Allow	Final 1 Comp	Loc.	Allow	Final 2 Comp	Loc.	Allow	Final 3 Comp	Loc.
Service I Limit State - Compressive	Stresses	Only							
Precast Top	3.900	1.485	Midspan	2.925	0.219	Midspan			
Precast Bot	3.900	2.077	Transfer	2.925	2.574	Transfer			
Service III Limit State - Tensile	Stresses	Only							
Precast Top	-0.484	-0.185	Transfer						
Precast Bot	-0.484	-0.237	Midspan						
Fatigue I Limit State - Compressive	Stresses	Only							
Precast Top							2.600	1.147	Midspan
Precast Bot							2.600	0.909	Transfer

CAMBER / DEFLECTION: (PCI Design Handbook - 4th Ed.- Table 4.6.2)
 0.5 x L = 19.50 ft

	Release	Mult	Erection	Mult	Final
Prestress	1.123	1.80	2.021	2.45	2.751
Self Wt.	-0.403	1.85	-0.746	2.70	-1.088
Deck + Haunch			0.000	2.30	0.000
DL-Prec. (DC)			-0.067	3.00	-0.200
Diaphragm			0.000	3.00	0.000
DL-Prec. (DW)			-0.082	3.00	-0.247
DL-Comp. (DC)			0.000	3.00	0.000
DL-Comp. (DW)			0.000	3.00	0.000
Live Load					-0.595
Total	0.720		1.127		0.622

Positive values indicate upward deflection.

K.3 NEXT-6 40 ft. - Interior Beam Output



Sheet #	1
Job #	
Program:	LEAP® CONSPAN® V8i (SELECTseries 5)
Version:	12.01.00.57
File Name:	NEXT D6-39ft105nonTransform.csl

Academic Use Only	Designed	HS
Copyright © Bentley Systems, Inc. 1984 - 2012	Date	Oct/17/2013
www.bentley.com	Checked	
Phone: 1-800-778-4277	Date	

PROPERTIES

Span:1, Beam:2

PRECAST DATA:

Section Id	Next D6-21-interior		
Type	Double Tee		
Fling width	Top	72.000	in
thick	Top	8.000	in
Stems	No	2	
	Top	15.000	in
	Bot	14.190	in
Shear width		29.190	in

Minimum Thickness Criteria, Article 5.14.1.2.2 checked: OK.

GENERAL BRIDGE DATA:

Bridge Width	50.00	ft
Curb-to-curb	46.83	ft
Beam Spac. Lt./Rt	6.00/ 6.00	ft
Lane width	12.00	ft
Number of lanes	3	
Interior/Exterior	Interior	
Start Skew Angle	0.00	degrees
End Skew Angle	0.00	degrees

TOPPING DATA:

Deck	Thickness	0.000	in	
Haunch:	Thickness	0.000	in	
	Width	0.000	in	
Effective	width	72.000	in	(Art. 4.6.2.6.1)

GENERAL LOAD DATA:

DEAD LOADS ON PRECAST

UNITS: (Point: kips, Location: ft, Line: klf, Trapez: klf)

DC/DW	Type	Mag.1	Loc.1	Mag.2	Loc.2	Description
DC	Line	0.221	0.000	0.221	39.000	Barrier Parapet
DW	Line	0.273	0.000	0.273	39.000	4 in bituminous wearing

Dead loads on composite: See Project info for composite loads

GENERAL SPAN DATA:



		Sheet #	2
		Job #	
Program:	LEAP® CONSPAN® V8i (SELECTseries 5)	Academic Use Only	Designed HS
Version:	12.01.00.57	Copyright © Bentley Systems, Inc. 1984 - 2012	Date Oct/17/2013
		www.bentley.com	Phone: 1-800-778-4277
File Name:	NEXT D6-39ft105nonTransform.csl		Checked
			Date

Overall length	39.875	ft
Release length	39.875	ft
Design length	39.000	ft

KERN POINTS:

Upper	15.57	in
Lower	8.57	in

DISTRIBUTION FACTORS (Art. 4.6.2.2):

Type i, post-tensioned

Live Moment	(2+ lanes loaded)	0.551	(Calculated)
Live Moment	(1 lane loaded)	0.430	(Calculated)
Live Shear	(2+ lanes loaded)	0.679	(Calculated)
Live Shear	(1 lane loaded)	0.601	(Calculated)

Pedestrian	0.125	(Calculated)
Comp. DC	0.125	(Calculated)
Comp. DW	0.125	(Calculated)

Dead Loads and Pedestrian Load distributed equally to all beams (Art. 4.6.2.2.1)

RESISTANCE FACTORS (Art. 5.5.4.2):

Flexure Reinforced	
Compression controlled sections	0.75
Tension controlled sections	0.90
Flexure Prestressed	
Compression controlled sections	0.75
Tension controlled sections	1.00
Shear	0.90

SECTION PROPERTIES:

	PRECAST		COMPOSITE		
Area	955.4	in ²	955.4	in ²	#
Total Height	21.00	in	21.00	in	
Mom. of Inertia (I _{xx})	33347	in ⁴	33347	in ⁴	#
Ht. of c.g.	12.85	in	12.85	in	#
Density	150.00	pcf	150.00	pcf	
Self-weight	995.2	plf	995.2	plf	
Mom. of Inertia (I _{yy})	378522.0	in ⁴			
Poisson's Ratio	0.2				
Thermal Coeff.	0.000006000	1/°F			



Sheet #	3
Job #	
Program:	LEAP® CONSPAN® V8i (SELECTseries 5)
Version:	12.01.00.57
File Name:	NEXT D6-39ft105nonTransform.csl
Academic Use Only	
Copyright © Bentley Systems, Inc. 1984 - 2012	
www.bentley.com	Phone: 1-800-778-4277
Designed	HS
Date	Oct/17/2013
Checked	
Date	

(#) Of Total Section using Ect/Ec = 1.0000
 Use transformed strand and rebar: No

Span:1, Beam:2

STRESS LIMITS (Art. 5.9.4):

STRESS LIMITS AT RELEASE BEFORE LOSSES:

	PRECAST	
Strength	5.20	ksi
Elasticity	4371.7	ksi
Max comp	3.12	ksi
Max tens	-0.20	ksi
Max tens, w/reinf	-0.55	ksi

STRESS LIMITS AT FINAL AFTER LOSSES:

	PRECAST		DECK	
Strength	6.50	ksi	6.50	ksi
Elasticity	4887.73	ksi	4887.73	ksi

STRESS LIMITS AT FINAL 1 (P/S + DL + LL):

	PRECAST		DECK	
Max comp	3.90	ksi	3.90	ksi

STRESS LIMITS AT FINAL 2 (P/S + DL):

	PRECAST		DECK	
Max comp	2.93	ksi	2.93	ksi

FATIGUE I STRESS LIMITS AT FINAL 3 (50% P/S + 50% DL + F_LL) (Art. 5.5.3.1):

	PRECAST		DECK	
Max comp	2.60	ksi	-	ksi

SERVICE III (Tension):

	PRECAST		DECK	
Max tens	-0.48	ksi	-0.48	ksi

Span:1, Beam:2

PRESTRESSED STEEL:

22 strands, 1/2-270K-LL, Low relaxation strands

Straight Pattern



		Sheet #	4
		Job #	
Program:	LEAP® CONSPAN® V8i (SELECTseries 5)	Academic Use Only	Designed HS
Version:	12.01.00.57	Copyright © Bentley Systems, Inc. 1984 - 2012	Date Oct/17/2013
		www.bentley.com	Phone: 1-800-778-4277
File Name:	NEXT D6-39ft105nonTransform.csl	Checked	Date

END PATTERN (Ycg = 5.23 in):

10 @ 2.500 in	8 @ 4.500 in	4 @ 13.500 in
---------------	--------------	---------------

Strand Diameter	0.500	in
Strand Area	0.153	in ²
Total Strand Area	3.366	in ²
Trans. Len, bonded	2.500	ft
Trans. Len, debonded	2.500	ft
Dev. Len, bonded	5.566	ft
Dev. Len, debonded	11.132	ft
Holddown Force	0.000	kips
Tensile Strength(fpu)	270.0	ksi
Initial Prestress = 0.75fpu	202.5	ksi
Initial Pull	681.6	kips
Beam Shrtng (PL/AE)	0.075	in

Span:1, Beam:2

ESTIMATED QUANTITIES

Prestressing (linear ft)	Strands (LB/1000ft)	(LB)	Beam Vol(C.Y.)	Concrete Wt(LB)	Stirrups (LB)	Longitudinal Bars (LB)
877.250	520	456.170	9.799	39684.020	166.757	322.962

Span:1, Beam:2

REINFORCING STEEL:

Tension	steel:	
fy	60.0	ksi
Es	29000	ksi
fs	24.0	ksi

Stirrups:

# legs	Size	fy (ksi)	Area (in ²)	Spacing (in)	Start (ft)	End (ft)	Extends into Deck
4	US#4[M13]	60.0	0.80	1.50	0.1900	0.4400	No
2	US#4[M13]	60.0	0.40	2.00	0.4400	0.9400	No
2	US#4[M13]	60.0	0.40	3.00	0.9400	1.9400	No
2	US#4[M13]	60.0	0.40	9.00	1.9400	37.9400	No
2	US#4[M13]	60.0	0.40	3.00	37.9400	38.9400	No
2	US#4[M13]	60.0	0.40	2.00	38.9400	39.4400	No
4	US#4[M13]	60.0	0.80	1.50	39.4400	39.6900	No

Top Steel:

#bars	Size	Dist. from Top (in)	Area (in ²)	Start (ft)	End (ft)	Side Cover (in)
6	US#4[M13]	2.25	1.200	0.1667	39.7083	482 7.00
6	US#4[M13]	6.25	1.200	0.1667	39.7083	7.00



		Sheet #	5	
		Job #		
Program:	LEAP® CONSPAN® V8i (SELECTseries 5)	Academic Use Only	Designed	HS
Version:	12.01.00.57	Copyright © Bentley Systems, Inc. 1984 - 2012	Date	Oct/17/2013
		www.bentley.com	Phone: 1-800-778-4277	Checked
File Name:	NEXT D6-39ft105nonTransform.csl		Date	

Bottom Steel:

#bars	Size	Dist. from Top (in)	Area (in ²)	Start (ft)	End (ft)	Side Cover (in)
-------	------	---------------------	-------------------------	------------	----------	-----------------

LOSSES

Note: Values are calculated at Midspan

Str. area	3.3660	in ²
Ycg	5.23	in
P_init	681.6	kips
Ecc	7.62	in
Days to release	0.75	
Rel. Humid.(RH)	75.0	%
Es	28500.0	ksi
Eci	4372	ksi

AASHTO LOSSES

Elastic Shortening 8.10 ksi (Eq 5.9.5.2.3a-1), (fcgp= 1.242 ksi)

Elastic Gains		Gains		Adjustment	
due to Precast Loads		-1.49	ksi	0.08	ksi
due to Composite Loads		-0.00	ksi	0.00	ksi
due to Live Loads		-4.96	ksi	0.32	ksi

Time Dependent Losses (Approximate Method (Art.5.9.5.3))

		Initial		Final	
Steel relaxation	0.00	ksi		2.40	ksi (Eq 5.9.5.3-1)
Concrete shrinkage	0.00	ksi		9.19	ksi (Eq 5.9.5.3-1)
Concrete creep	0.00	ksi		4.97	ksi (Eq 5.9.5.3-1)
Sub-total	8.10	ksi	(4.00 %)	10.50	ksi (5.19 %)
Total Prestress Losses				18.60	ksi (9.19 %)

Prestressing Stress Limit Check (Table 5.9.3.1)

initial fpi = 202.5 ksi < 0.75 fpu, OK
 initial fpe = 183.9 ksi < 0.80 fpy, OK



Sheet #	6
Job #	
Program:	LEAP® CONSPAN® V8i (SELECTseries 5)
Version:	12.01.00.57
Copyright © Bentley Systems, Inc. 1984 - 2012	Date
www.bentley.com	Phone: 1-800-778-4277
File Name:	NEXT D6-39ft105nonTransform.csl

SHEAR/MOMENT ENVELOPE (&REACTIONS)

SHEAR AND MOMENT ENVELOPE : Span : 1, Beam : 2, SERVICE I
 Shears: kips, Moments: kft

		Bearing	Trans	H/2	0.10L	0.20L	0.30L	0.40L	Midspan
Location,	ft	0.00	2.06	0.88	3.55	7.54	11.53	15.51	19.50
Self wt. :	M	0.0	37.9	16.6	62.6	118.0	157.6	181.3	189.2
(Max)	V	19.4	17.4	18.5	15.9	11.9	7.9	4.0	0.0
DL-Prec. :	M	0.0	8.4	3.7	13.9	26.2	35.0	40.3	42.0
DC(Max)	V	4.3	3.9	4.1	3.5	2.6	1.8	0.9	0.0
DL-Prec. :	M	0.0	10.4	4.6	17.2	32.4	43.2	49.7	51.9
DW(Max)	V	5.3	4.8	5.1	4.4	3.3	2.2	1.1	0.0
Deck + :	M	0.0	0.0	0.0	0.0	0.0	0.0	0.0	0.0
Haunch (Max)	V	0.0	0.0	0.0	0.0	0.0	0.0	0.0	0.0
Diaphragm :	M	0.0	0.0	0.0	0.0	0.0	0.0	0.0	0.0
(Max)	V	0.0	0.0	0.0	0.0	0.0	0.0	0.0	0.0
DL-Comp :	M	0.0	0.0	0.0	0.0	0.0	0.0	0.0	0.0
DC(Max)	V	0.0	0.0	0.0	0.0	0.0	0.0	0.0	0.0
DL-Comp :	M	0.0	0.0	0.0	0.0	0.0	0.0	0.0	0.0
DW(Max)	V	0.0	0.0	0.0	0.0	0.0	0.0	0.0	0.0
LL + I :	M+	-0.0	89.4	39.5	146.0	265.0	337.4	377.6	387.9
	V	57.9	53.2	55.9	49.9	41.6	33.5	4.0	20.3
LL + I :	M-	-0.0	-0.0	-0.0	0.0	0.0	0.0	0.0	0.0
	V	0.0	0.0	0.0	0.0	0.0	0.0	0.0	0.0
LL + I :	Vmx	57.9	53.2	55.9	49.9	41.9	34.2	27.8	22.4
	M	-0.0	90.3	40.2	146.0	256.3	320.4	350.5	354.4
Total :	M+	0.0	146.2	64.3	239.7	441.5	573.2	648.9	671.0
	V	87.0	79.2	83.7	73.6	59.5	45.4	10.0	20.3
Total :	M-	0.0	0.0	0.0	0.0	0.0	0.0	0.0	0.0
	V	0.0	0.0	0.0	0.0	0.0	0.0	0.0	0.0
Total :	Vmx	87.0	79.2	83.7	73.6	59.7	46.1	33.8	22.4
	M	0.0	147.1	65.0	239.7	432.9	556.2	621.8	637.5

		0.60L	0.70L	0.80L	0.90L	H/2	Trans	Bearing
Location,	ft	23.49	27.47	31.46	35.45	38.13	36.94	39.00
Self wt. :	M	181.3	157.6	118.0	62.6	16.6	37.9	0.0
(Max)	V	4.0	7.9	11.9	15.9	18.5	17.4	19.4
DL-Prec. :	M	40.3	35.0	26.2	13.9	3.7	8.4	-0.0
DC(Max)	V	0.9	1.8	2.6	3.5	4.1	3.9	4.3
DL-Prec. :	M	49.7	43.2	32.4	17.2	4.6	10.4	-0.0
DW(Max)	V	1.1	2.2	3.3	4.4	5.1	4.8	5.3
Deck + :	M	0.0	0.0	0.0	0.0	0.0	0.0	0.0
Haunch (Max)	V	0.0	0.0	0.0	0.0	0.0	0.0	0.0
Diaphragm :	M	0.0	0.0	0.0	0.0	0.0	0.0	0.0
(Max)	V	0.0	0.0	0.0	0.0	0.0	0.0	0.0
DL-Comp :	M	0.0	0.0	0.0	0.0	0.0	0.0	0.0
DC(Max)	V	0.0	0.0	0.0	0.0	0.0	0.0	0.0
DL-Comp :	M	0.0	0.0	0.0	0.0	0.0	0.0	0.0
DW(Max)	V	0.0	0.0	0.0	0.0	0.0	0.0	0.0



Sheet #	7
Job #	
Program:	LEAP® CONSPAN® V8i (SELECTseries 5)
Version:	12.01.00.57
Copyright © Bentley Systems, Inc. 1984 - 2012	www.bentley.com
Phone: 1-800-778-4277	
File Name:	NEXT D6-39ft105nonTransform.csl

Academic Use Only	Designed	HS
Date	Oct/17/2013	
Checked		
Date		

		0.60L	0.70L	0.80L	0.90L	H/2	Trans	Bearing
LL + I :	M+	377.6	337.4	265.0	146.0	39.5	89.4	0.0
	V	4.0	33.5	41.6	49.9	55.9	53.2	57.9
LL + I :	M-	0.0	0.0	0.0	0.0	0.0	0.0	0.0
	V	0.0	0.0	0.0	0.0	0.0	0.0	0.0
LL + I :	Vmx	27.8	34.2	41.9	49.9	55.9	53.2	57.9
	M	350.5	320.4	256.3	146.0	40.2	90.3	0.0
Total :	M+	648.9	573.2	441.5	239.7	64.3	146.2	0.0
	V	10.0	45.4	59.5	73.6	83.7	79.2	87.0
Total :	M-	0.0	0.0	0.0	0.0	0.0	0.0	0.0
	V	0.0	0.0	0.0	0.0	0.0	0.0	0.0
Total :	Vmx	33.8	46.1	59.7	73.6	83.7	79.2	87.0
	M	621.8	556.2	432.9	239.7	65.0	147.1	0.0

REACTIONS (kips), SERVICE I

Load Type	Left Support	Right Support
Self Wt.	19.4	19.4
Deck+Haunch	0.0	0.0
Diaphragm	0.0	0.0
DL-Prec.(DC)	4.3	4.3
DL-Prec.(DW)	5.3	5.3
DL-Comp.(DC)	0.0	0.0
DL-Comp.(DW)	0.0	0.0
Live	67.2	67.2
Pedestrian	0.0	0.0

Upward reactions are positive.

Live Load reactions are per lane with no distribution factor and no impact.

Reactions are not multiplied by Load Modifiers (ductility, redundancy and operational importance).

Non-composite load types are per beam.

Composite and Pedestrian load types are per total bridge width.

SHEAR AND MOMENT ENVELOPE : Span : 1, Beam : 2, SERVICE III

Shears: kips, Moments: kft

Location,	ft	Bearing	Trans	H/2	0.10L	0.20L	0.30L	0.40L	Midspan
Self wt. :	M	0.0	37.9	16.6	62.6	118.0	157.6	181.3	189.2
(Max)	V	19.4	17.4	18.5	15.9	11.9	7.9	4.0	0.0
DL-Prec. :	M	0.0	8.4	3.7	13.9	26.2	35.0	40.3	42.0
DC(Max)	V	4.3	3.9	4.1	3.5	2.6	1.8	0.9	0.0
DL-Prec. :	M	0.0	10.4	4.6	17.2	32.4	43.2	49.7	51.9
DW(Max)	V	5.3	4.8	5.1	4.4	3.3	2.2	1.1	0.0
Deck + :	M	0.0	0.0	0.0	0.0	0.0	0.0	0.0	0.0
Haunch (Max)	V	0.0	0.0	0.0	0.0	0.0	0.0	0.0	0.0



Sheet #	8
Job #	
Program:	LEAP® CONSPAN® V8i (SELECTseries 5)
Version:	12.01.00.57
Copyright © Bentley Systems, Inc. 1984 - 2012	www.bentley.com
Phone: 1-800-778-4277	
File Name:	NEXT D6-39ft105nonTransform.csl

		Bearing	Trans	H/2	0.10L	0.20L	0.30L	0.40L	Midspan
Diaphragm :	M	0.0	0.0	0.0	0.0	0.0	0.0	0.0	0.0
(Max)	V	0.0	0.0	0.0	0.0	0.0	0.0	0.0	0.0
DL-Comp :	M	0.0	0.0	0.0	0.0	0.0	0.0	0.0	0.0
DC(Max)	V	0.0	0.0	0.0	0.0	0.0	0.0	0.0	0.0
DL-Comp :	M	0.0	0.0	0.0	0.0	0.0	0.0	0.0	0.0
DW(Max)	V	0.0	0.0	0.0	0.0	0.0	0.0	0.0	0.0
LL + I :	M+	-0.0	71.6	31.6	116.8	212.0	269.9	302.1	310.3
	V	46.3	42.6	44.7	39.9	33.3	26.8	3.2	16.2
LL + I :	M-	-0.0	-0.0	-0.0	0.0	0.0	0.0	0.0	0.0
	V	0.0	0.0	0.0	0.0	0.0	0.0	0.0	0.0
LL + I :	Vmx	46.3	42.6	44.7	39.9	33.5	27.4	22.3	17.9
	M	-0.0	72.3	32.1	116.8	205.1	256.3	280.4	283.5
Total :	M+	0.0	128.3	56.4	210.5	388.6	505.7	573.4	593.5
	V	75.4	68.6	72.5	63.7	51.1	38.7	9.2	16.2
Total :	M-	0.0	0.0	0.0	0.0	0.0	0.0	0.0	0.0
	V	0.0	0.0	0.0	0.0	0.0	0.0	0.0	0.0
Total :	Vmx	75.4	68.6	72.5	63.7	51.3	39.3	28.2	17.9
	M	0.0	129.0	57.0	210.5	381.6	492.1	551.7	566.6

		0.60L	0.70L	0.80L	0.90L	H/2	Trans	Bearing
Location,	ft	23.49	27.47	31.46	35.45	38.13	36.94	39.00
Self wt. :	M	181.3	157.6	118.0	62.6	16.6	37.9	0.0
(Max)	V	4.0	7.9	11.9	15.9	18.5	17.4	19.4
DL-Prec. :	M	40.3	35.0	26.2	13.9	3.7	8.4	-0.0
DC(Max)	V	0.9	1.8	2.6	3.5	4.1	3.9	4.3
DL-Prec. :	M	49.7	43.2	32.4	17.2	4.6	10.4	-0.0
DW(Max)	V	1.1	2.2	3.3	4.4	5.1	4.8	5.3
Deck + :	M	0.0	0.0	0.0	0.0	0.0	0.0	0.0
Haunch (Max)	V	0.0	0.0	0.0	0.0	0.0	0.0	0.0
Diaphragm :	M	0.0	0.0	0.0	0.0	0.0	0.0	0.0
(Max)	V	0.0	0.0	0.0	0.0	0.0	0.0	0.0
DL-Comp :	M	0.0	0.0	0.0	0.0	0.0	0.0	0.0
DC(Max)	V	0.0	0.0	0.0	0.0	0.0	0.0	0.0
DL-Comp :	M	0.0	0.0	0.0	0.0	0.0	0.0	0.0
DW(Max)	V	0.0	0.0	0.0	0.0	0.0	0.0	0.0
LL + I :	M+	302.1	269.9	212.0	116.8	31.6	71.6	0.0
	V	3.2	26.8	33.3	39.9	44.7	42.6	46.3
LL + I :	M-	0.0	0.0	0.0	0.0	0.0	0.0	0.0
	V	0.0	0.0	0.0	0.0	0.0	0.0	0.0
LL + I :	Vmx	22.3	27.4	33.5	39.9	44.7	42.6	46.3
	M	280.4	256.3	205.1	116.8	32.1	72.3	0.0
Total :	M+	573.4	505.7	388.6	210.5	56.4	128.3	0.0
	V	9.2	38.7	51.1	63.7	72.5	68.6	75.4
Total :	M-	0.0	0.0	0.0	0.0	0.0	0.0	0.0
	V	0.0	0.0	0.0	0.0	0.0	0.0	0.0
Total :	Vmx	28.2	39.3	51.3	63.7	72.5	68.6	75.4
	M	551.7	492.1	381.6	210.5	57.0	129.0	0.0



Sheet #	9
Job #	
Program:	LEAP® CONSPAN® V8i (SELECTseries 5)
Version:	12.01.00.57
Copyright © Bentley Systems, Inc. 1984 - 2012	www.bentley.com
Phone: 1-800-778-4277	
File Name:	NEXT D6-39ft105nonTransform.csl

SHEAR AND MOMENT ENVELOPE : Span : 1, Beam : 2, STRENGTH I
 Shears: kips, Moments: kft

		Bearing	Trans	H/2	0.10L	0.20L	0.30L	0.40L	Midspan
Location,	ft	0.00	2.06	0.88	3.55	7.54	11.53	15.51	19.50
Self wt. :	M	0.0	47.4	20.7	78.3	147.5	197.0	226.6	236.5
(Max)	V	24.3	21.7	23.2	19.8	14.9	9.9	5.0	0.0
Self wt. :	M	0.0	34.1	14.9	56.4	106.2	141.8	163.2	170.3
(Min)	V	17.5	15.6	16.7	14.3	10.7	7.1	3.6	0.0
DL-Prec. :	M	0.0	10.5	4.6	17.4	32.8	43.7	50.3	52.5
DC(Max)	V	5.4	4.8	5.1	4.4	3.3	2.2	1.1	0.0
DL-Prec. :	M	0.0	7.6	3.3	12.5	23.6	31.5	36.2	37.8
DC(Min)	V	3.9	3.5	3.7	3.2	2.4	1.6	0.8	0.0
DL-Prec. :	M	0.0	15.6	6.8	25.8	48.6	64.8	74.6	77.9
DW(Max)	V	8.0	7.1	7.6	6.5	4.9	3.3	1.6	0.0
DL-Prec. :	M	0.0	6.8	3.0	11.2	21.0	28.1	32.3	33.7
DW(Min)	V	3.5	3.1	3.3	2.8	2.1	1.4	0.7	0.0
Deck + :	M	0.0	0.0	0.0	0.0	0.0	0.0	0.0	0.0
Haunch (Max)	V	0.0	0.0	0.0	0.0	0.0	0.0	0.0	0.0
Deck + :	M	0.0	0.0	0.0	0.0	0.0	0.0	0.0	0.0
Haunch (Min)	V	0.0	0.0	0.0	0.0	0.0	0.0	0.0	0.0
Diaphragm :	M	0.0	0.0	0.0	0.0	0.0	0.0	0.0	0.0
(Max)	V	0.0	0.0	0.0	0.0	0.0	0.0	0.0	0.0
Diaphragm :	M	0.0	0.0	0.0	0.0	0.0	0.0	0.0	0.0
(Min)	V	0.0	0.0	0.0	0.0	0.0	0.0	0.0	0.0
DL-Comp :	M	0.0	0.0	0.0	0.0	0.0	0.0	0.0	0.0
DC(Max)	V	0.0	0.0	0.0	0.0	0.0	0.0	0.0	0.0
DL-Comp :	M	0.0	0.0	0.0	0.0	0.0	0.0	0.0	0.0
DC(Min)	V	0.0	0.0	0.0	0.0	0.0	0.0	0.0	0.0
DL-Comp :	M	0.0	0.0	0.0	0.0	0.0	0.0	0.0	0.0
DW(Max)	V	0.0	0.0	0.0	0.0	0.0	0.0	0.0	0.0
DL-Comp :	M	0.0	0.0	0.0	0.0	0.0	0.0	0.0	0.0
DW(Min)	V	0.0	0.0	0.0	0.0	0.0	0.0	0.0	0.0
LL + I :	M+	-0.0	156.5	69.1	255.6	463.7	590.4	660.8	678.8
	V	101.4	93.2	97.9	87.3	72.9	58.7	7.1	35.4
LL + I :	M-	-0.0	-0.0	-0.0	0.0	0.0	0.0	0.0	0.0
	V	0.0	0.0	0.0	0.0	0.0	0.0	0.0	0.0
LL + I :	Vmx	101.4	93.2	97.9	87.3	73.3	59.9	48.7	39.2
	M	-0.0	158.1	70.3	255.6	448.6	560.7	613.4	620.1
Total :	M+	0.0	230.0	101.3	377.0	692.5	896.0	1012.3	1045.7
	V	139.0	126.8	133.8	118.1	96.0	74.1	14.8	35.4
Total :	M-	0.0	0.0	0.0	0.0	0.0	0.0	0.0	0.0
	V	0.0	0.0	0.0	0.0	0.0	0.0	0.0	0.0
Total :	Vmx	139.0	126.8	133.8	118.1	96.4	75.3	56.4	39.2
	M	-0.0	222.7	98.6	362.4	649.9	829.5	922.7	942.9

		0.60L	0.70L	0.80L	0.90L	H/2	Trans	Bearing
Location,	ft	23.49	27.47	31.46	35.45	38.13	36.94	39.00
Self wt. :	M	226.6	197.0	147.5	78.3	20.7	4.87	0.0



Sheet #	10
Job #	
Program:	LEAP® CONSPAN® V8i (SELECTseries 5)
Version:	12.01.00.57
Copyright © Bentley Systems, Inc. 1984 - 2012	www.bentley.com
Phone: 1-800-778-4277	
File Name:	NEXT D6-39ft105nonTransform.csl

Academic Use Only	Designed	HS
Date	Oct/17/2013	
Checked		
Date		

		0.60L	0.70L	0.80L	0.90L	H/2	Trans	Bearing
(Max)	V	5.0	9.9	14.9	19.8	23.2	21.7	24.3
Self wt. :	M	163.2	141.8	106.2	56.4	14.9	34.1	0.0
(Min)	V	3.6	7.1	10.7	14.3	16.7	15.6	17.5
DL-Prec. :	M	50.3	43.7	32.8	17.4	4.6	10.5	-0.0
DC(Max)	V	1.1	2.2	3.3	4.4	5.1	4.8	5.4
DL-Prec. :	M	36.2	31.5	23.6	12.5	3.3	7.6	-0.0
DC(Min)	V	0.8	1.6	2.4	3.2	3.7	3.5	3.9
DL-Prec. :	M	74.6	64.8	48.6	25.8	6.8	15.6	-0.0
DW(Max)	V	1.6	3.3	4.9	6.5	7.6	7.1	8.0
DL-Prec. :	M	32.3	28.1	21.0	11.2	3.0	6.8	-0.0
DW(Min)	V	0.7	1.4	2.1	2.8	3.3	3.1	3.5
Deck + :	M	0.0	0.0	0.0	0.0	0.0	0.0	0.0
Haunch (Max)	V	0.0	0.0	0.0	0.0	0.0	0.0	0.0
Deck + :	M	0.0	0.0	0.0	0.0	0.0	0.0	0.0
Haunch (Min)	V	0.0	0.0	0.0	0.0	0.0	0.0	0.0
Diaphragm :	M	0.0	0.0	0.0	0.0	0.0	0.0	0.0
(Max)	V	0.0	0.0	0.0	0.0	0.0	0.0	0.0
Diaphragm :	M	0.0	0.0	0.0	0.0	0.0	0.0	0.0
(Min)	V	0.0	0.0	0.0	0.0	0.0	0.0	0.0
DL-Comp :	M	0.0	0.0	0.0	0.0	0.0	0.0	0.0
DC(Max)	V	0.0	0.0	0.0	0.0	0.0	0.0	0.0
DL-Comp :	M	0.0	0.0	0.0	0.0	0.0	0.0	0.0
DC(Min)	V	0.0	0.0	0.0	0.0	0.0	0.0	0.0
DL-Comp :	M	0.0	0.0	0.0	0.0	0.0	0.0	0.0
DW(Max)	V	0.0	0.0	0.0	0.0	0.0	0.0	0.0
DL-Comp :	M	0.0	0.0	0.0	0.0	0.0	0.0	0.0
DW(Min)	V	0.0	0.0	0.0	0.0	0.0	0.0	0.0
LL + I :	M+	660.8	590.4	463.7	255.6	69.1	156.5	0.0
	V	7.1	58.7	72.9	87.3	97.9	93.2	101.4
LL + I :	M-	0.0	0.0	0.0	0.0	0.0	0.0	0.0
	V	0.0	0.0	0.0	0.0	0.0	0.0	0.0
LL + I :	Vmx	48.7	59.9	73.3	87.3	97.9	93.2	101.4
	M	613.4	560.7	448.6	255.6	70.3	158.1	0.0
Total :	M+	1012.3	896.0	692.5	377.0	101.3	230.0	0.0
	V	14.8	74.1	96.0	118.1	133.8	126.8	139.0
Total :	M-	0.0	0.0	0.0	0.0	0.0	0.0	0.0
	V	0.0	0.0	0.0	0.0	0.0	0.0	0.0
Total :	Vmx	56.4	75.3	96.4	118.1	133.8	126.8	139.0
	M	922.7	829.5	649.9	362.4	98.6	222.7	0.0

REACTIONS (kips), STRENGTH I

Load Type	Left Support	Right Support
Self Wt.	24.3	24.3
Deck+Haunch	0.0	0.0
Diaphragm	0.0	0.0
DL-Prec.(DC)	5.4	5.4
DL-Prec.(DW)	8.0	8.0



Sheet #	11
Job #	
Program:	LEAP® CONSPAN® V8i (SELECTseries 5)
Version:	12.01.00.57
Copyright © Bentley Systems, Inc. 1984 - 2012	www.bentley.com
Phone: 1-800-778-4277	
File Name:	NEXT D6-39ft105nonTransform.csl

Academic Use Only	Designed	HS
Date	Oct/17/2013	
Checked		
Date		

Load Type	Left Support	Right Support
DL-Comp.(DC)	0.0	0.0
DL-Comp.(DW)	0.0	0.0
Live	117.7	117.7
Pedestrian	0.0	0.0

Upward reactions are positive.
 Live Load reactions are per lane with no distribution factor and no impact.
 Reactions are not multiplied by Load Modifiers (ductility, redundancy and operational importance).
 Non-composite load types are per beam.
 Composite and Pedestrian load types are per total bridge width.

SHEAR AND MOMENT ENVELOPE : Span : 1, Beam : 2, FATIGUE I
 Shears: kips, Moments: kft

		Bearing	Trans	H/2	0.10L	0.20L	0.30L	0.40L	Midspan
Location,	ft	0.00	2.06	0.88	3.55	7.54	11.53	15.51	19.50
Self wt. :	M	0.0	37.9	16.6	62.6	118.0	157.6	181.3	189.2
(Max)	V	19.4	17.4	18.5	15.9	11.9	7.9	4.0	0.0
Self wt. :	M	0.0	0.0	0.0	0.0	0.0	0.0	0.0	0.0
(Min)	V	0.0	0.0	0.0	0.0	0.0	0.0	0.0	0.0
DL-Prec. :	M	0.0	8.4	3.7	13.9	26.2	35.0	40.3	42.0
DC(Max)	V	4.3	3.9	4.1	3.5	2.6	1.8	0.9	0.0
DL-Prec. :	M	0.0	0.0	0.0	0.0	0.0	0.0	0.0	0.0
DC(Min)	V	0.0	0.0	0.0	0.0	0.0	0.0	0.0	0.0
DL-Prec. :	M	0.0	10.4	4.6	17.2	32.4	43.2	49.7	51.9
DW(Max)	V	5.3	4.8	5.1	4.4	3.3	2.2	1.1	0.0
DL-Prec. :	M	0.0	0.0	0.0	0.0	0.0	0.0	0.0	0.0
DW(Min)	V	0.0	0.0	0.0	0.0	0.0	0.0	0.0	0.0
Deck + :	M	0.0	0.0	0.0	0.0	0.0	0.0	0.0	0.0
Haunch (Max)	V	0.0	0.0	0.0	0.0	0.0	0.0	0.0	0.0
Deck + :	M	0.0	0.0	0.0	0.0	0.0	0.0	0.0	0.0
Haunch (Min)	V	0.0	0.0	0.0	0.0	0.0	0.0	0.0	0.0
Diaphragm :	M	0.0	0.0	0.0	0.0	0.0	0.0	0.0	0.0
(Max)	V	0.0	0.0	0.0	0.0	0.0	0.0	0.0	0.0
Diaphragm :	M	0.0	0.0	0.0	0.0	0.0	0.0	0.0	0.0
(Min)	V	0.0	0.0	0.0	0.0	0.0	0.0	0.0	0.0
DL-Comp :	M	0.0	0.0	0.0	0.0	0.0	0.0	0.0	0.0
DC(Max)	V	0.0	0.0	0.0	0.0	0.0	0.0	0.0	0.0
DL-Comp :	M	0.0	0.0	0.0	0.0	0.0	0.0	0.0	0.0
DC(Min)	V	0.0	0.0	0.0	0.0	0.0	0.0	0.0	0.0
DL-Comp :	M	0.0	0.0	0.0	0.0	0.0	0.0	0.0	0.0
DW(Max)	V	0.0	0.0	0.0	0.0	0.0	0.0	0.0	0.0
DL-Comp :	M	0.0	0.0	0.0	0.0	0.0	0.0	0.0	0.0
DW(Min)	V	0.0	0.0	0.0	0.0	0.0	0.0	0.0	0.0
LL + I :	M+	0.0	44.1	19.4	72.7	135.7	179.0	202.6	206.5
	V	34.0	30.9	32.7	28.6	25.1	21.7	18.2	14.8
LL + I :	M-	0.0	0.0	0.0	0.0	0.0	0.0	0.0	0.0



Sheet #	12
Job #	
Program:	LEAP® CONSPAN® V8i (SELECTseries 5)
Version:	12.01.00.57
Copyright © Bentley Systems, Inc. 1984 - 2012	www.bentley.com
Phone: 1-800-778-4277	
File Name:	NEXT D6-39ft105nonTransform.csl

		Bearing	Trans	H/2	0.10L	0.20L	0.30L	0.40L	Midspan
LL + I :	V	0.0	0.0	0.0	0.0	0.0	0.0	0.0	0.0
	Vmx	34.0	30.9	32.7	28.6	25.1	21.7	18.2	14.8
	M	0.0	44.1	19.4	72.7	135.7	179.0	202.6	206.5
Total :	M+	0.0	100.9	44.2	166.4	312.3	414.8	473.9	489.6
	V	63.0	56.8	60.4	52.4	43.0	33.6	24.2	14.8
Total :	M-	0.0	0.0	0.0	0.0	0.0	0.0	0.0	0.0
	V	0.0	0.0	0.0	0.0	0.0	0.0	0.0	0.0
Total :	Vmx	63.0	56.8	60.4	52.4	43.0	33.6	24.2	14.8
	M	0.0	100.9	44.2	166.4	312.3	414.8	473.9	489.6

		0.60L	0.70L	0.80L	0.90L	H/2	Trans	Bearing
Location,	ft	23.49	27.47	31.46	35.45	38.13	36.94	39.00
Self wt. :	M	181.3	157.6	118.0	62.6	16.6	37.9	0.0
(Max)	V	4.0	7.9	11.9	15.9	18.5	17.4	19.4
Self wt. :	M	0.0	0.0	0.0	0.0	0.0	0.0	0.0
(Min)	V	0.0	0.0	0.0	0.0	0.0	0.0	0.0
DL-Prec. :	M	40.3	35.0	26.2	13.9	3.7	8.4	-0.0
DC(Max)	V	0.9	1.8	2.6	3.5	4.1	3.9	4.3
DL-Prec. :	M	0.0	0.0	0.0	0.0	0.0	0.0	-0.0
DC(Min)	V	0.0	0.0	0.0	0.0	0.0	0.0	0.0
DL-Prec. :	M	49.7	43.2	32.4	17.2	4.6	10.4	-0.0
DW(Max)	V	1.1	2.2	3.3	4.4	5.1	4.8	5.3
DL-Prec. :	M	0.0	0.0	0.0	0.0	0.0	0.0	-0.0
DW(Min)	V	0.0	0.0	0.0	0.0	0.0	0.0	0.0
Deck + :	M	0.0	0.0	0.0	0.0	0.0	0.0	0.0
Haunch (Max)	V	0.0	0.0	0.0	0.0	0.0	0.0	0.0
Deck + :	M	0.0	0.0	0.0	0.0	0.0	0.0	0.0
Haunch (Min)	V	0.0	0.0	0.0	0.0	0.0	0.0	0.0
Diaphragm :	M	0.0	0.0	0.0	0.0	0.0	0.0	0.0
(Max)	V	0.0	0.0	0.0	0.0	0.0	0.0	0.0
Diaphragm :	M	0.0	0.0	0.0	0.0	0.0	0.0	0.0
(Min)	V	0.0	0.0	0.0	0.0	0.0	0.0	0.0
DL-Comp :	M	0.0	0.0	0.0	0.0	0.0	0.0	0.0
DC(Max)	V	0.0	0.0	0.0	0.0	0.0	0.0	0.0
DL-Comp :	M	0.0	0.0	0.0	0.0	0.0	0.0	0.0
DC(Min)	V	0.0	0.0	0.0	0.0	0.0	0.0	0.0
DL-Comp :	M	0.0	0.0	0.0	0.0	0.0	0.0	0.0
DW(Max)	V	0.0	0.0	0.0	0.0	0.0	0.0	0.0
DL-Comp :	M	0.0	0.0	0.0	0.0	0.0	0.0	0.0
DW(Min)	V	0.0	0.0	0.0	0.0	0.0	0.0	0.0
LL + I :	M+	202.6	179.0	135.7	72.7	19.4	44.1	0.0
	V	18.2	21.7	25.1	28.6	32.7	30.9	34.0
LL + I :	M-	0.0	0.0	0.0	0.0	0.0	0.0	0.0
	V	0.0	0.0	0.0	0.0	0.0	0.0	0.0
LL + I :	Vmx	18.2	21.7	25.1	28.6	32.7	30.9	34.0
	M	202.6	179.0	135.7	72.7	19.4	44.1	0.0
Total :	M+	473.9	414.8	312.3	166.4	44.2	100.9	0.0
	V	24.2	33.6	43.0	52.4	60.4	56.8	63.0
Total :	M-	0.0	0.0	0.0	0.0	0.0	0.0	0.0
	V	0.0	0.0	0.0	0.0	0.0	0.0	0.0
Total :	Vmx	24.2	33.6	43.0	52.4	60.4	56.8	63.0



		Sheet #	13		
		Job #			
Program:	LEAP® CONSPAN® V8i (SELECTseries 5)	Academic Use Only	Designed	HS	
Version:	12.01.00.57	Copyright © Bentley Systems, Inc. 1984 - 2012	Date	Oct/17/2013	
		www.bentley.com	Phone: 1-800-778-4277	Checked	
File Name:	NEXT D6-39ft105nonTransform.csl			Date	

	M	0.60L	0.70L	0.80L	0.90L	H/2	Trans	Bearing
		473.9	414.8	312.3	166.4	44.2	100.9	0.0



Sheet #	14
Job #	
Program:	LEAP® CONSPAN® V8i (SELECTseries 5)
Version:	12.01.00.57
File Name:	NEXT D6-39ft105nonTransform.csl
Academic Use Only	
Copyright © Bentley Systems, Inc. 1984 - 2012	
www.bentley.com	Phone: 1-800-778-4277
Designed	HS
Date	Oct/17/2013
Checked	
Date	

POSITIVE ENVELOPE STRESSES

Span : 1, Beam : 2, SERVICE I

RELEASE STRESSES, (ksi) (LOSS = 4.00 %)

Location, ft	Trans	0.10L /0.90L	0.20L /0.80L	0.30L /0.70L	0.40L /0.60L	Midspan
2.50	3.99	7.98	11.96	15.95	19.94	
Beam-Self						
Precast-top	0.136	0.188	0.334	0.438	0.501	0.521
Bottom	-0.215	-0.320	-0.568	-0.746	-0.853	-0.888
Prestress						
Precast-top	-0.534	-0.528	-0.528	-0.528	-0.528	-0.528
Bottom	2.607	2.583	2.583	2.583	2.583	2.583
Total						
Precast-top	-0.398	-0.341	-0.195	-0.090	-0.028	-0.007
Bottom	2.392	2.263	2.014	1.836	1.730	1.694

SERVICE I

POSITIVE ENVELOPE STRESSES, (ksi) (LOSS = 9.19 %)

Location, ft	Bearing	Trans	H/2	0.10L /0.90L	0.20L /0.80L	0.30L /0.70L	0.40L /0.60L	Midspan
0.00	2.06	0.88	3.55	7.54	11.53	15.51	19.50	
Prestress								
Precast-top	-0.088	-0.505	-0.265	-0.500	-0.500	-0.500	-0.500	-0.500
Bottom	0.432	2.466	1.295	2.443	2.443	2.443	2.443	2.443
Self wt.								
Precast-top	0.000	0.111	0.049	0.165	0.311	0.415	0.478	0.499
Bottom	-0.000	-0.175	-0.077	-0.281	-0.530	-0.708	-0.814	-0.850
DL-Prec (DC)								
Precast-top	-0.000	0.025	0.011	0.037	0.069	0.092	0.106	0.111
Bottom	0.000	-0.039	-0.017	-0.062	-0.118	-0.157	-0.181	-0.189
DL-Prec (DW)								
Precast-top	-0.000	0.030	0.013	0.045	0.085	0.114	0.131	0.137
Bottom	0.000	-0.048	-0.021	-0.077	-0.145	-0.194	-0.223	-0.233



Sheet #	15
Job #	
Program:	LEAP® CONSPAN® V8i (SELECTseries 5)
Version:	12.01.00.57
Copyright © Bentley Systems, Inc. 1984 - 2012	www.bentley.com
Phone: 1-800-778-4277	
File Name:	NEXT D6-39ft105nonTransform.csl

Academic Use Only	Designed	HS
Date	Oct/17/2013	
Checked		
Date		

	Bearing	Trans	H/2	0.10L /0.90L	0.20L /0.80L	0.30L /0.70L	0.40L /0.60L	Midspan
Diaphragm								
Precast-top	-0.000	-0.000	-0.000	-0.000	-0.000	-0.000	-0.000	-0.000
Bottom	-0.000	-0.000	-0.000	-0.000	-0.000	-0.000	-0.000	-0.000
Deck + Haunch								
Precast-top	-0.000	-0.000	-0.000	-0.000	-0.000	-0.000	-0.000	-0.000
Bottom	-0.000	-0.000	-0.000	-0.000	-0.000	-0.000	-0.000	-0.000
DL-Comp (DC)								
Precast-top	-0.000	-0.000	-0.000	-0.000	-0.000	-0.000	-0.000	-0.000
Bottom	-0.000	-0.000	-0.000	-0.000	-0.000	-0.000	-0.000	-0.000
DL-Comp (DW)								
Precast-top	-0.000	-0.000	-0.000	-0.000	-0.000	-0.000	-0.000	-0.000
Bottom	-0.000	-0.000	-0.000	-0.000	-0.000	-0.000	-0.000	-0.000
LL+I(+)								
Precast-top	0.000	0.262	0.116	0.428	0.777	0.990	1.107	1.138
Bottom	-0.000	-0.414	-0.183	-0.675	-1.225	-1.560	-1.746	-1.794
Final 1 (P/S + DL + LL)								
Precast-top	-0.088	-0.077	-0.077	0.175	0.743	1.111	1.323	1.384
Bottom	0.432	1.790	0.997	1.347	0.425	-0.176	-0.521	-0.622
Final 2 (P/S + DL)								
Precast-top	-0.088	-0.339	-0.192	-0.253	-0.034	0.122	0.215	0.247
Bottom	0.432	2.204	1.180	2.022	1.650	1.384	1.225	1.172

Span : 1, Beam : 2, SERVICE III

RELEASE STRESSES, (ksi) (LOSS = 4.00 %)

Location, ft	Trans	0.10L /0.90L	0.20L /0.80L	0.30L /0.70L	0.40L /0.60L	Midspan
2.50	3.99	7.98	11.96	15.95	19.94	
Beam-Self						
Precast-top	0.136	0.188	0.334	0.438	0.501	0.521
Bottom	-0.215	-0.320	-0.568	-0.746	-0.853	-0.888
Prestress						
Precast-top	-0.534	-0.528	-0.528	-0.528	-0.528	-0.528
Bottom	2.607	2.583	2.583	2.583	2.583	2.583



Sheet #	16
Job #	
Program:	LEAP® CONSPAN® V8i (SELECTseries 5)
Version:	12.01.00.57
Copyright © Bentley Systems, Inc. 1984 - 2012	www.bentley.com
Phone: 1-800-778-4277	
File Name:	NEXT D6-39ft105nonTransform.csl

Academic Use Only	Designed	HS
Date	Oct/17/2013	
Checked		
Date		

	Trans	0.10L /0.90L	0.20L /0.80L	0.30L /0.70L	0.40L /0.60L	Midspan
Total						
Precast-top	-0.398	-0.341	-0.195	-0.090	-0.028	-0.007
Bottom	2.392	2.263	2.014	1.836	1.730	1.694
As_top, in2	1.429	1.123	0.000	0.000	0.000	0.000
Ast_prvd, in2	2.400	2.400	2.400	2.400	2.400	2.400

SERVICE III

POSITIVE ENVELOPE STRESSES, (ksi) (LOSS = 9.19 %)

	Bearing	Trans	H/2	0.10L /0.90L	0.20L /0.80L	0.30L /0.70L	0.40L /0.60L	Midspan
Location, ft	0.00	2.06	0.88	3.55	7.54	11.53	15.51	19.50
Prestress								
Precast-top	-0.088	-0.505	-0.265	-0.500	-0.500	-0.500	-0.500	-0.500
Bottom	0.432	2.466	1.295	2.443	2.443	2.443	2.443	2.443
Self wt.								
Precast-top	0.000	0.111	0.049	0.165	0.311	0.415	0.478	0.499
Bottom	-0.000	-0.175	-0.077	-0.281	-0.530	-0.708	-0.814	-0.850
DL-Prec (DC)								
Precast-top	-0.000	0.025	0.011	0.037	0.069	0.092	0.106	0.111
Bottom	0.000	-0.039	-0.017	-0.062	-0.118	-0.157	-0.181	-0.189
DL-Prec (DW)								
Precast-top	-0.000	0.030	0.013	0.045	0.085	0.114	0.131	0.137
Bottom	0.000	-0.048	-0.021	-0.077	-0.145	-0.194	-0.223	-0.233
Diaphragm								
Precast-top	-0.000	-0.000	-0.000	-0.000	-0.000	-0.000	-0.000	-0.000
Bottom	-0.000	-0.000	-0.000	-0.000	-0.000	-0.000	-0.000	-0.000
Deck + Haunch								
Precast-top	-0.000	-0.000	-0.000	-0.000	-0.000	-0.000	-0.000	-0.000
Bottom	-0.000	-0.000	-0.000	-0.000	-0.000	-0.000	-0.000	-0.000
DL-Comp (DC)								
Precast-top	-0.000	-0.000	-0.000	-0.000	-0.000	-0.000	-0.000	-0.000
Bottom	-0.000	-0.000	-0.000	-0.000	-0.000	-0.000	-0.000	-0.000
DL-Comp (DW)								
Precast-top	-0.000	-0.000	-0.000	-0.000	-0.000	-0.000	-0.000	-0.000



Sheet #	17
Job #	
Program:	LEAP® CONSPAN® V8i (SELECTseries 5)
Version:	12.01.00.57
Copyright © Bentley Systems, Inc. 1984 - 2012	www.bentley.com
Phone: 1-800-778-4277	
File Name:	NEXT D6-39ft105nonTransform.csl

Academic Use Only	Designed	HS
Date	Oct/17/2013	
Checked		
Date		

	Bearing	Trans	H/2	0.10L /0.90L	0.20L /0.80L	0.30L /0.70L	0.40L /0.60L	Midspan
Bottom	-0.000	-0.000	-0.000	-0.000	-0.000	-0.000	-0.000	-0.000
LL+I(+)								
Precast-top	0.000	0.210	0.093	0.343	0.622	0.792	0.886	0.910
Bottom	-0.000	-0.331	-0.146	-0.540	-0.980	-1.248	-1.397	-1.435
Final 1 (P/S + DL + LL)								
Precast-top	-0.088	-0.129	-0.100	0.090	0.587	0.913	1.101	1.157
Bottom	0.432	1.873	1.034	1.482	0.670	0.136	-0.172	-0.263

Span : 1, Beam : 2, FATIGUE I
 POSITIVE ENVELOPE STRESSES, (ksi)

Location, ft	Bearing	Trans	H/2	0.10L /0.90L	0.20L /0.80L	0.30L /0.70L	0.40L /0.60L	Midspan
	0.00	2.06	0.88	3.55	7.54	11.53	15.51	19.50
F_LL+I(+)								
Precast-top	-0.000	0.129	0.057	0.213	0.398	0.525	0.594	0.606
Bottom	-0.000	-0.204	-0.090	-0.336	-0.628	-0.828	-0.937	-0.955
Final 3 (50% P/S + 50% DL + F_LL)								
Precast-top	-0.044	-0.040	-0.039	0.087	0.381	0.586	0.702	0.729
Bottom	0.216	0.898	0.500	0.675	0.197	-0.136	-0.325	-0.369



Sheet #	18
Job #	
Program:	LEAP® CONSPAN® V8i (SELECTseries 5)
Version:	12.01.00.57
File Name:	NEXT D6-39ft105nonTransform.csl
Academic Use Only	Designed HS
Copyright © Bentley Systems, Inc. 1984 - 2012	Date Oct/17/2013
www.bentley.com	Checked
Phone: 1-800-778-4277	Date

VERTICAL/HORIZONTAL SHEAR

VERTICAL SHEAR (Art. 5.8) - Span : 1, Beam : 2, STRENGTH I
 Using General Beta Theta Equation procedure - Art.5.8.3.4.2

Location(ft)	Vu (kips)	bv (in)	de (in)	Aps (in ²)	Vp (kips)	eps_x	Theta	Vs-reqd (kips)	Av/s (in ² /ft)	Av-prvd (in ² /ft)	Al_reqd (in ²)
	Mcor (kft)	a (in)	dv (in)	fpo (ksi)	vu/fc	Vc-com (kips)	Beta	Max.spc. (in)	min.Av/s (in ² /ft)	pVn/Vu	Aps* (in ²)
Bearing :		0.44									
	139.0	29.19	17.61	0.243	0.0	6.00e-3	50.0	118.6	1.618	6.400	0.00
	0.0	0.29	17.47	33.1	0.047	35.9	0.87	13.97	0.470	3.269	0.347
Transfer :		2.50									
	126.8	29.19	17.61	2.754	0.0	-0.10e-3	28.7	0.0	0.470	0.533	0.00
	222.7	1.63	16.80	189.0	0.044	204.6	5.18	13.44	0.470	2.033	1.980
Critical :		1.85									
	130.6	29.19	17.61	2.754	0.0	-0.11e-3	28.6	0.0	0.470	1.600	0.00
	152.1	1.21	17.01	189.0	0.045	208.9	5.22	13.61	0.470	3.156	1.469
0.1L :		3.99									
	118.1	29.19	17.61	2.754	0.0	-0.06e-3	28.8	0.0	0.470	0.533	0.00
	362.4	1.93	16.65	189.0	0.042	196.6	5.02	13.32	0.470	2.114	2.356
0.2L :		7.97									
	96.4	29.19	17.61	2.754	0.0	0.62e-3	31.2	0.0	0.470	0.533	0.00
	649.9	2.25	16.49	189.0	0.034	126.9	3.27	13.19	0.470	1.864	2.754
0.3L :		11.96									
	75.3	29.19	17.61	2.754	0.0	2.02e-3	36.1	9.6	0.470	0.533	0.00
	829.5	2.25	16.49	189.0	0.027	74.0	1.91	13.19	0.470	1.607	2.754
0.4L :		15.95									
	56.4	29.19	17.61	2.754	0.0	2.64e-3	38.3	0.2	0.470	0.533	0.00
	922.7	2.25	16.49	189.0	0.020	62.4	1.61	13.19	0.470	1.887	2.754
0.5L :		19.94									
	39.2	29.19	17.61	2.754	0.0	2.61e-3	38.1	0.0	0.470	0.533	0.00
	942.9	2.25	16.49	189.0	0.014	62.9	1.62	13.19	0.470	2.734	2.754
0.6L :		23.93									
	56.4	29.19	17.61	2.754	0.0	2.64e-3	38.3	0.2	0.470	0.533	0.00
	922.7	2.25	16.49	189.0	0.020	62.4	1.61	13.19	0.470	1.887	2.754
0.7L :		27.91									
	75.3	29.19	17.61	2.754	0.0	2.02e-3	36.1	⁴⁹⁶ 9.6	0.470	0.533	0.00



Sheet #	19
Job #	
Program:	LEAP® CONSPAN® V8i (SELECTseries 5)
Version:	12.01.00.57
Copyright © Bentley Systems, Inc. 1984 - 2012	www.bentley.com
Phone: 1-800-778-4277	
File Name:	NEXT D6-39ft105nonTransform.csl

Location(ft)	Vu (kips)	bv (in)	de (in)	Aps (in2)	Vp (kips)	eps_x	Theta	Vs-reqd (kips)	Av/s (in2/ft)	Av-prvd (in2/ft)	Al_reqd (in2)
Mcor (kft)	a (in)	dv (in)	fpo (ksi)	vu/fc	Vc-com (kips)	Beta	Max.spc. (in)	min.Av/s (in2/ft)	pVn/Vu	Aps* (in2)	
	829.5	2.25	16.49	189.0	0.027	74.0	1.91	13.19	0.470	1.607	2.754
0.8L :		31.90									
	96.4	29.19	17.61	2.754	0.0	0.62e-3	31.2	0.0	0.470	0.533	0.00
	649.9	2.25	16.49	189.0	0.034	126.9	3.27	13.19	0.470	1.864	2.754
0.9L :		35.89									
	118.1	29.19	17.61	2.754	0.0	-0.06e-3	28.8	0.0	0.470	0.533	0.00
	362.4	1.93	16.65	189.0	0.042	196.6	5.02	13.32	0.470	2.114	2.356
Critical :		38.02									
	130.6	29.19	17.61	2.754	0.0	-0.11e-3	28.6	0.0	0.470	1.600	0.00
	152.1	1.21	17.01	189.0	0.045	208.9	5.22	13.61	0.470	3.156	1.469
Transfer :		37.38									
	126.8	29.19	17.61	2.754	0.0	-0.10e-3	28.7	0.0	0.470	0.533	0.00
	222.7	1.63	16.80	189.0	0.044	204.6	5.18	13.44	0.470	2.033	1.980
Bearing :		39.44									
	139.0	29.19	17.61	0.243	0.0	6.00e-3	50.0	118.6	1.618	2.400	0.00
	0.0	0.29	17.47	33.1	0.047	35.9	0.87	13.97	0.470	1.371	0.347

ANCHORAGE ZONE REINFORCEMENT (Art. 5.10.10)
 Span : 1, Beam : 2

Fpi (kips)	fs (ksi)	h/4 (in)	Abrst_rqrd (in2)
681.61	20.00	5.25	1.36



Sheet #	20
Job #	
Program:	LEAP® CONSPAN® V8i (SELECTseries 5)
Version:	12.01.00.57
Copyright © Bentley Systems, Inc. 1984 - 2012	Date
www.bentley.com	Checked
Phone: 1-800-778-4277	Date

Academic Use Only	Designed	HS
Copyright © Bentley Systems, Inc. 1984 - 2012	Date	Oct/17/2013
www.bentley.com	Checked	
Phone: 1-800-778-4277	Date	

File Name: NEXT D6-39ft105nonTransform.csl

CAMBER/DEFLECTION

CAMBER AND DEFLECTIONS: SERVICE I
(Span : 1, Beam : 2; Units: in)

	Release	Mult	Erection	Mult	Final
At 0.1 x L =	3.55 ft				
Prestress	0.347	1.80	0.625	2.45	0.851
Self Wt.	-0.122	1.85	-0.226	2.70	-0.329
Deck + Haunch			0.000	2.30	0.000
DL-Prec. (DC)			-0.020	3.00	-0.061
Diaphragm			0.000	3.00	0.000
DL-Prec. (DW)			-0.025	3.00	-0.075
DL-Comp. (DC)			0.000	3.00	0.000
DL-Comp. (DW)			0.000	3.00	0.000
Live Load					-0.147
Total	0.225		0.355		0.239

	Release	Mult	Erection	Mult	Final
At 0.2 x L =	7.54 ft				
Prestress	0.622	1.80	1.119	2.45	1.523
Self Wt.	-0.231	1.85	-0.427	2.70	-0.623
Deck + Haunch			0.000	2.30	0.000
DL-Prec. (DC)			-0.041	3.00	-0.122
Diaphragm			0.000	3.00	0.000
DL-Prec. (DW)			-0.050	3.00	-0.151
DL-Comp. (DC)			0.000	3.00	0.000
DL-Comp. (DW)			0.000	3.00	0.000
Live Load					-0.297
Total	0.391		0.601		0.330

	Release	Mult	Erection	Mult	Final
At 0.3 x L =	11.52 ft				
Prestress	0.817	1.80	1.471	2.45	2.003
Self Wt.	-0.316	1.85	-0.584	2.70	-0.853
Deck + Haunch			0.000	2.30	0.000
DL-Prec. (DC)			-0.057	3.00	-0.170
Diaphragm			0.000	3.00	0.000
DL-Prec. (DW)			-0.070	3.00	-0.211
DL-Comp. (DC)			0.000	3.00	0.000
DL-Comp. (DW)			0.000	3.00	0.000
Live Load					-0.412
Total	0.502		0.760		0.357

	Release	Mult	Erection	Mult	Final
At 0.4 x L =	15.51 ft				
Prestress	0.935	1.80	1.683	2.45	2.291



Sheet #	21
Job #	
Program:	LEAP® CONSPAN® V8i (SELECTseries 5)
Version:	12.01.00.57
Copyright © Bentley Systems, Inc. 1984 - 2012	Date
www.bentley.com	Phone: 1-800-778-4277
File Name: NEXT D6-39ft105nonTransform.csl	Date

	Release	Mult	Erection	Mult	Final
Self Wt.	-0.370	1.85	-0.684	2.70	-0.998
Deck + Haunch			0.000	2.30	0.000
DL-Prec. (DC)			-0.067	3.00	-0.201
Diaphragm			0.000	3.00	0.000
DL-Prec. (DW)			-0.083	3.00	-0.249
DL-Comp. (DC)			0.000	3.00	0.000
DL-Comp. (DW)			0.000	3.00	0.000
Live Load					-0.485
Total	0.565		0.849		0.357

	Release	Mult	Erection	Mult	Final
At 0.5 x L = 19.50 ft					
Prestress	0.974	1.80	1.753	2.45	2.387
Self Wt.	-0.388	1.85	-0.718	2.70	-1.048
Deck + Haunch			0.000	2.30	0.000
DL-Prec. (DC)			-0.071	3.00	-0.212
Diaphragm			0.000	3.00	0.000
DL-Prec. (DW)			-0.087	3.00	-0.262
DL-Comp. (DC)			0.000	3.00	0.000
DL-Comp. (DW)			0.000	3.00	0.000
Live Load					-0.509
Total	0.586		0.877		0.356

	Release	Mult	Erection	Mult	Final
At 0.6 x L = 23.49 ft					
Prestress	0.935	1.80	1.683	2.45	2.291
Self Wt.	-0.370	1.85	-0.684	2.70	-0.998
Deck + Haunch			0.000	2.30	0.000
DL-Prec. (DC)			-0.067	3.00	-0.201
Diaphragm			0.000	3.00	0.000
DL-Prec. (DW)			-0.083	3.00	-0.249
DL-Comp. (DC)			0.000	3.00	0.000
DL-Comp. (DW)			0.000	3.00	0.000
Live Load					-0.485
Total	0.565		0.849		0.357

	Release	Mult	Erection	Mult	Final
At 0.7 x L = 27.48 ft					
Prestress	0.817	1.80	1.471	2.45	2.003
Self Wt.	-0.316	1.85	-0.584	2.70	-0.853
Deck + Haunch			0.000	2.30	0.000
DL-Prec. (DC)			-0.057	3.00	-0.170
Diaphragm			0.000	3.00	0.000
DL-Prec. (DW)			-0.070	3.00	-0.211
DL-Comp. (DC)			0.000	3.00	0.000
DL-Comp. (DW)			0.000	3.00	0.000
Live Load					-0.412



Sheet #	22
Job #	
Program:	LEAP® CONSPAN® V8i (SELECTseries 5)
Version:	12.01.00.57
Copyright © Bentley Systems, Inc. 1984 - 2012	www.bentley.com
Phone: 1-800-778-4277	
File Name:	NEXT D6-39ft105nonTransform.csl

Academic Use Only	Designed	HS
Date	Oct/17/2013	
Checked		
Date		

	Release	Mult	Erection	Mult	Final
Total	0.502		0.760		0.357

	Release	Mult	Erection	Mult	Final
At 0.8 x L =	31.46 ft				
Prestress	0.622	1.80	1.119	2.45	1.523
Self Wt.	-0.231	1.85	-0.427	2.70	-0.623
Deck + Haunch			0.000	2.30	0.000
DL-Prec. (DC)			-0.041	3.00	-0.122
Diaphragm			0.000	3.00	0.000
DL-Prec. (DW)			-0.050	3.00	-0.151
DL-Comp. (DC)			0.000	3.00	0.000
DL-Comp. (DW)			0.000	3.00	0.000
Live Load					-0.297
Total	0.391		0.601		0.330

	Release	Mult	Erection	Mult	Final
At 0.9 x L =	35.45 ft				
Prestress	0.347	1.80	0.625	2.45	0.851
Self Wt.	-0.122	1.85	-0.226	2.70	-0.329
Deck + Haunch			0.000	2.30	0.000
DL-Prec. (DC)			-0.020	3.00	-0.061
Diaphragm			0.000	3.00	0.000
DL-Prec. (DW)			-0.025	3.00	-0.075
DL-Comp. (DC)			0.000	3.00	0.000
DL-Comp. (DW)			0.000	3.00	0.000
Live Load					-0.147
Total	0.225		0.355		0.239



Sheet #	23
Job #	
Program:	LEAP® CONSPAN® V8i (SELECTseries 5)
Version:	12.01.00.57
Copyright © Bentley Systems, Inc. 1984 - 2012	www.bentley.com
Phone: 1-800-778-4277	
File Name:	NEXT D6-39ft105nonTransform.csl

ULTIMATE MOMENT

ULTIMATE - Span : 1, Beam : 2, STRENGTH I
 (Mr-prvd computed by Strain Compatibility method. Ult. Conc. Strain = 0.00300)

Location (ft)	dp in	Aps in ²	fps ksi	c in	a in	Mr-prvd k.ft	c/dt	Phi	Mcr k.ft	min Mr k.ft	Crkg Ratio	Mu-p/r Ratio
Transfer	2.06											
230.0	15.8	2.420	267.3	2.2	1.6	807.7	0.120T	1.00	-	-	-	-
H/2	0.88											
101.3	15.8	1.271	268.7	1.2	0.9	436.8	0.064T	1.00	-	-	-	-
0.1L	3.55											
377.0	15.8	2.879	266.6	2.6	1.9	949.2	0.143T	1.00	-	-	-	-
0.2L	7.54											
692.5	15.8	3.366	265.8	3.1	2.2	1095.2	0.167T	1.00	797.0	797.0	1.37	-
0.3L	11.53											
896.0	15.8	3.366	265.8	3.1	2.2	1095.2	0.167T	1.00	798.4	798.4	1.37	-
0.4L	15.51											
1012.3	15.8	3.366	265.8	3.1	2.2	1095.2	0.167T	1.00	799.3	799.3	1.37	-
0.5L	19.50											
1045.7	15.8	3.366	265.8	3.1	2.2	1095.2	0.167T	1.00	799.6	799.6	1.37	-
0.6L	23.49											
1012.3	15.8	3.366	265.8	3.1	2.2	1095.2	0.167T	1.00	799.3	799.3	1.37	-
0.7L	27.48											
896.0	15.8	3.366	265.8	3.1	2.2	1095.2	0.167T	1.00	798.4	798.4	1.37	-
0.8L	31.46											
692.5	15.8	3.366	265.8	3.1	2.2	1095.2	0.167T	1.00	797.0	797.0	1.37	-
0.9L	35.45											
377.0	15.8	2.879	266.6	2.6	1.9	949.2	0.143T	1.00	-	-	-	-
H/2	38.13											
101.3	15.8	1.271	268.7	1.2	0.9	436.8	0.064T	1.00	-	-	-	-
Transfer	36.94											
230.0	15.8	2.420	267.3	2.2	1.6	807.7	0.120T	1.00	-	-	-	-

Legend: C = Compression-Controlled (c/dt > 0.600)
 I = In-Transition (0.60 >= c/dt > 0.375)
 T = Tension-Controlled (c/dt <= 0.375)
 Note : fr used for calculating Mcr is computed using AASHTO method (Art.5.4.2.6.)
 Consider Bottom Tension Steel Contribution : NO



Sheet #	24
Job #	
Program:	LEAP® CONSPAN® V8i (SELECTseries 5)
Version:	12.01.00.57
Copyright © Bentley Systems, Inc. 1984 - 2012	www.bentley.com
Phone: 1-800-778-4277	
File Name:	NEXT D6-39ft105nonTransform.csl

Academic Use Only	Designed	HS
Date	Oct/17/2013	Checked
Date		

DETENSIONING

Span : 1, Beam : 2; Groups 1-11; Units: ksi

Grp	Str	Ys,in	2.50ft
1	2	E 2.50	Ft 0.048
		M 2.50	Fb 0.084
2	2	E 13.50	Ft 0.120
		M 13.50	Fb 0.132
3	2	E 13.50	Ft 0.192
		M 13.50	Fb 0.179
4	2	E 4.50	Ft 0.133
		M 4.50	Fb 0.433
5	2	E 4.50	Ft 0.073
		M 4.50	Fb 0.686
6	2	E 4.50	Ft 0.014
		M 4.50	Fb 0.940
7	2	E 4.50	Ft -0.045
		M 4.50	Fb 1.194
8	2	E 2.50	Ft -0.133
		M 2.50	Fb 1.493
9	2	E 2.50	Ft -0.221
		M 2.50	Fb 1.793
10	2	E 2.50	Ft -0.309
		M 2.50	Fb 2.092
11	2	E 2.50	Ft -0.398
		M 2.50	Fb 2.392



		Sheet #	25
		Job #	
Program:	LEAP® CONSPAN® V8i (SELECTseries 5)	Academic Use Only	Designed HS
Version:	12.01.00.57	Copyright © Bentley Systems, Inc. 1984 - 2012	Date Oct/17/2013
		www.bentley.com	Phone: 1-800-778-4277
File Name:	NEXT D6-39ft105nonTransform.csl		Checked
			Date

DESIGN SUMMARY

Span: 1, Beam: 2, Interior beam

Beam type:	Double Tee,	Next D6-21-interior
Precast Length,	ft	39.88
Release Length,	ft	39.88
Strand Pattern:	Straight	
Strand:	1/2-270K-LL	
Strand Es,	ksi:	28500.0
No. of strands:	22	
	Draped:	0
	Straight:	22
Concrete Strength:		
	f'ci:	5.2 ksi
	f'c:	6.5 ksi
	f'ct:	6.5 ksi
Initial losses:	4.00 %	
Final losses:	9.19 %	

Specification	Allowable	Computed	Location	Status
Release Stresses (ksi) (Art. 5.9.4.1)				
Precast Bot (compression)	3.120	2.392	Trans	OK
Precast Top w/ no reinf. (tension)	-0.200	-0.398	Trans	
Precast Top w/ reinf. (tension)	-0.547			
Strength I (Art. 3.4.1, 5.7.3.1.1)	Provided	Required	Location	Status
Ult. Moment (k.ft)	1095.22	1045.72	Midspan	OK
Debonding Limits (Art. 5.11.4.3)	Allowable	Computed		Status
Max. Debond per Row	40.00 %	0.00 %		OK
Max. Debond Total	25.00 %	0.00 %		OK

Positive Moment Envelope Stresses (ksi) (Art. 3.4.1 and 5.9.4.2)



		Sheet # 26	
		Job #	
Program:	LEAP® CONSPAN® V8i (SELECTseries 5)	Academic Use Only	
Version:	12.01.00.57	Copyright © Bentley Systems, Inc. 1984 - 2012	Date Oct/17/2013
		www.bentley.com	Phone: 1-800-778-4277
File Name:	NEXT D6-39ft105nonTransform.csl	Checked	Date

Specification	Allow	Final 1 Comp	Loc.	Allow	Final 2 Comp	Loc.	Allow	Final 3 Comp	Loc.
Service I Limit State - Compressive	Stresses	Only							
Precast Top	3.900	1.384	Midspan	2.925	0.247	Midspan			
Precast Bot	3.900	1.790	Transfer	2.925	2.204	Transfer			
Service III Limit State - Tensile	Stresses	Only							
Precast Top	-0.484	-0.129	Transfer						
Precast Bot	-0.484	-0.263	Midspan						
Fatigue I Limit State - Compressive	Stresses	Only							
Precast Top							2.600	0.729	Midspan
Precast Bot							2.600	0.898	Transfer

CAMBER / DEFLECTION: (PCI Design Handbook - 4th Ed.- Table 4.6.2)

0.5 x L = 19.50 ft

	Release	Mult	Erection	Mult	Final
Prestress	0.974	1.80	1.753	2.45	2.387
Self Wt.	-0.388	1.85	-0.718	2.70	-1.048
Deck + Haunch			0.000	2.30	0.000
DL-Prec. (DC)			-0.071	3.00	-0.212
Diaphragm			0.000	3.00	0.000
DL-Prec. (DW)			-0.087	3.00	-0.262
DL-Comp. (DC)			0.000	3.00	0.000
DL-Comp. (DW)			0.000	3.00	0.000
Live Load					-0.509
Total	0.586		0.877		0.356

Positive values indicate upward deflection.

K.4 NEXT-8 40 ft. - Input



		Sheet #	1		
		Job #			
Program:	LEAP® CONSPAN® V8i (SELECTseries 5)	Academic Use Only	Designed	HS	
Version:	12.01.00.57	Copyright © Bentley Systems, Inc. 1984 - 2012	Date	Oct/17/2013	
		www.bentley.com	Phone: 1-800-778-4277	Checked	
File Name:	NEXT D8-39ft105nonTransform.csl			Date	

PROJECT DATA

Project:	NEXT D8-21-40ft
Designer:	HS
Date:	Oct/17/2013
Checked By:	
Date Checked:	
User job number:	
State:	SC, State Job #:
State	None
Specification:	
Design Code:	AASHTO LRFD - [6th Edition, 2012]
Units:	US
Span Type:	Simple Span
Flared Girder:	No
File Name:	C:\SCDOT\HUAN\SCDOT\CONSPAN BRIDGE\FinalDesign\ModifiedDesign\NEXT D8-39ft105nonTransform.csl



Sheet #	2
Job #	
Program:	LEAP® CONSPAN® V8i (SELECTseries 5)
Version:	12.01.00.57
Copyright © Bentley Systems, Inc. 1984 - 2012	www.bentley.com
Phone: 1-800-778-4277	
File Name:	NEXT D8-39ft105nonTransform.csl

GEOMETRY DATA

BRIDGE LAYOUT

Overall Width (ft)	48.000
Left curb (ft)	1.583
Right curb (ft)	1.583
Curb-to-curb width (ft)	44.833
Number of spans	1
Number of lanes	3
Lane width (ft)	12.000
Eff Deck thick (in)	0.000
Sacrificial thick (in)	0.000
Haunch thickness (in)	0.000
Haunch width (in)	0.000
Bridge c/s,MI(Ixx) (in4)	222720.00

SPAN DATA

Precast length,	ft =	39.875
Bearing-to-bearing,	ft =	39.000
Release span,	ft =	39.875

BEAM DATA

No	ID	Loc-prev ft	Area in2	MI(Ixx) in4	Height in	Yb in	B-topg in	B-trib ft
1	Next D8-21-exterior	4.000	1147.4	37120.0	21.00	13.54	96.00	8.000
2	Next D8-21-interior	8.000	1147.4	37120.0	21.00	13.54	96.00	8.000
3	Next D8-21-interior	8.000	1147.4	37120.0	21.00	13.54	96.00	8.000
4	Next D8-21-interior	8.000	1147.4	37120.0	21.00	13.54	96.00	8.000
5	Next D8-21-interior	8.000	1147.4	37120.0	21.00	13.54	96.00	8.000
6	Next D8-21-exterior	8.000	1147.4	37120.0	21.00	13.54	96.00	8.000

MATERIAL DATA - Project Level

As defined in Material Tab. For beam level properties look at Beam Specific output.

CONCRETE PROPERTIES

	Precast Release	Precast Final	C.I.P
f'c (ksi)	5.200	6.500	6.500
Wc (pcf)	150.000	150.000	150.000
Ec (ksi)	4371.720	4887.730	4887.730
K1	1.000	1.000	1.000
Thermal coeff.(1/°F)	0.00000600		

STRAND AND REBAR PROPERTIES

PRESTRESSED STEEL:



		Sheet #	3		
		Job #			
Program:	LEAP® CONSPAN® V8i (SELECTseries 5)	Academic Use Only	Designed	HS	
Version:	12.01.00.57	Copyright © Bentley Systems, Inc. 1984 - 2012	Date	Oct/17/2013	
		www.bentley.com	Phone: 1-800-778-4277	Checked	
File Name:	NEXT D8-39ft105nonTransform.csl			Date	

1/2-270K-LL, Low relaxation strands
Straight Pattern
Strand Diameter = 0.500 in
Tensile Strength(fpu) = 270.0 ksi
Use transformed strand and rebar: No

REINFORCING STEEL:

Tension/Shear steel: $f_y = 60.0$ ksi $E_s = 29000$ ksi $f_s = 24.0$ ksi



Sheet #	4
Job #	
Program:	LEAP® CONSPAN® V8i (SELECTseries 5)
Version:	12.01.00.57
Copyright © Bentley Systems, Inc. 1984 - 2012	
www.bentley.com	Phone: 1-800-778-4277
File Name:	NEXT D8-39ft105nonTransform.csl
Designed	HS
Date	Oct/17/2013
Checked	
Date	

LOADS DATA

Loads generated using Permanent Load Wizard: NO
DEAD LOADS ON PRECAST
 UNITS: (Point: kips, Location: ft, Line: klf, Trapez: klf)

Span	Beam	DC/DW	Type	Mag.1	Loc.1	Mag.2	Loc.2	Description
1	1	DC	Line	0.221	0.000	0.221	39.000	Barrier Parapet
1	1	DW	Line	0.349	0.000	0.349	39.000	4 in bituminous wearing
1	2	DC	Line	0.221	0.000	0.221	39.000	Barrier Parapet
1	2	DW	Line	0.349	0.000	0.349	39.000	4 in bituminous wearing
1	3	DW	Line	0.349	0.000	0.349	39.000	4 in bituminous wearing
1	4	DW	Line	0.349	0.000	0.349	39.000	4 in bituminous wearing
1	5	DC	Line	0.221	0.000	0.221	39.000	Barrier Parapet
1	5	DW	Line	0.349	0.000	0.349	39.000	4 in bituminous wearing
1	6	DC	Line	0.221	0.000	0.221	39.000	Barrier Parapet
1	6	DW	Line	0.349	0.000	0.349	39.000	4 in bituminous wearing

DIAPHRAGM LOADS - NONE

DEAD LOADS ON COMPOSITE - NONE

TEMPERATURE LOADS - NONE

LIVE LOADS

Live load deflection: included.

ID	Type
Design Lane	Design Lane
Design Tandem	Design Tandem
Design Truck	Design Truck

Pedestrian Load - NONE



Sheet #	5
Job #	
Program:	LEAP® CONSPAN® V8i (SELECTseries 5)
Version:	12.01.00.57
File Name:	NEXT D8-39ft105nonTransform.csl

Academic Use Only	Designed	HS
Copyright © Bentley Systems, Inc. 1984 - 2012	Date	Oct/17/2013
www.bentley.com Phone: 1-800-778-4277	Checked	
	Date	

LIVE LOADS USED

LIVE LOAD LIBRARY: Default.cs3

1 ID: Design Lane

Description:	Design Lane as in AASHTO-LRFD
Type:	Design Lane

Lane Load: Intensity = 0.64 klf, Width = 10.00 ft

2 ID: Design Tandem

Description:	Design Tandem as in AASHTO-LRFD
Type:	Design Tandem

First Axle Magnitude = 25.00 k, Wheel Spacing = 6.00 ft, Truck Width = 10.00 ft

#	Magnitude, k	Max Spacing, ft	Min Spacing, ft	Increment, ft
1	25.00	4.00	4.00	0.00

3 ID: Design Truck

Description:	Design Truck as in AASHTO-LRFD
Type:	Design Truck

First Axle Magnitude = 8.00 k, Wheel Spacing = 6.00 ft, Truck Width = 10.00 ft

#	Magnitude, k	Max Spacing, ft	Min Spacing, ft	Increment, ft
1	32.00	14.00	14.00	0.00
2	32.00	30.00	14.00	2.00


4 ID: Fatigue Truck

Description:	Fatigue Truck as in AASHTO-LRFD
Type:	Fatigue Truck

First Axle Magnitude = 8.00 k, Wheel Spacing = 6.00 ft, Truck Width = 10.00 ft

#	Magnitude, k	Max Spacing, ft	Min Spacing, ft	Increment, ft
1	32.00	14.00	14.00	0.00
2	32.00	30.00	30.00	0.00

RATING LOADS - NONE

		Sheet #	6
		Job #	
Program:	LEAP® CONSPAN® V8i (SELECTseries 5)	Academic Use Only	Designed HS
Version:	12.01.00.57	Copyright © Bentley Systems, Inc. 1984 - 2012	Date Oct/17/2013
		www.bentley.com	Phone: 1-800-778-4277
File Name:	NEXT D8-39ft105nonTransform.csl		Checked
			Date

ANALYSIS DATA

ANALYSIS PARAMETERS DATA

Truck impact:	1.330
Lane impact:	1.000
Strength II impact:	1.330
Fatigue impact:	1.150

DISTRIBUTION FACTORS (Art. 4.6.2.2):

Is Span Post-tensioned:	YES
ADTT (Average Daily Truck Traffic) :	5000
Percent of the specified force effect :	1.00

NOTE: Beam specific dead and live load DFs are printed in beam level reports.

LOAD FACTORS: (Table 3.4.1-1 & 3.4.1-2)

	Live	DC(max)	DC(min)	DW(max)	DW(min)
Service I:	1.00	1.00	-	1.00	-
Service III:	0.80	1.00	-	1.00	-
Strength I:	1.75	1.25	0.90	1.50	0.65
Fatigue I:	1.50	-	-	-	-

Ductility Factor:	1.00
Redundancy Factor:	1.00
Importance Factor:	1.00



Sheet #	7
Job #	
Program:	LEAP® CONSPAN® V8i (SELECTseries 5)
Version:	12.01.00.57
File Name:	NEXT D8-39ft105nonTransform.csl

Academic Use Only	Designed	HS
Copyright © Bentley Systems, Inc. 1984 - 2012	Date	Oct/17/2013
www.bentley.com Phone: 1-800-778-4277	Checked	
	Date	

PROJECT DESIGN PARAMETERS

MULTIPLIERS:

Trans len mult:	Bonded	1.00
	Debonded	1.00
Dev len mult:	Bonded	1.00
	Debonded	2.00

Camber & Deflection Multiplier (PCI ref.)

	Erection	Final
Prestress:	1.80	2.45
Self. Wt:	1.85	2.70
Deck + Haunch:		2.30
Diaphragm:		3.00
DL-Prec.:		3.00
DL-Comp.:		3.00

MOMENT AND SHEAR PROVISIONS:

Ultimate Moment Capacity, Mr-prvd computed:	Strain Compatibility method.
Ultimate Concrete Strain:	0.0030
Horizontal Shear, Beam and Slab effects in Vu:	EXCLUDED

STRESS LIMITS (Art. 5.9.4):

STRESS LIMITS AT RELEASE BEFORE LOSSES:

	PRECAST	
Strength	5.20	ksi
Elasticity	4371.7	ksi
Max comp	3.12	ksi
Max tens	-0.20	ksi
Max tens, w/reinf	-0.55	ksi

STRESS LIMITS AT FINAL AFTER LOSSES:

	PRECAST		DECK	
Strength	6.50	ksi	6.50	ksi
Elasticity	4887.73	ksi	4887.73	ksi

STRESS LIMITS AT FINAL 1 (P/S + DL + LL):

	PRECAST		DECK	
Max comp	3.90	ksi	3.90	ksi

STRESS LIMITS AT FINAL 2 (P/S + DL):

	PRECAST		DECK	
Max comp	2.93	ksi	2.93	ksi



Sheet #	8
Job #	
Program:	LEAP® CONSPAN® V8i (SELECTseries 5)
Version:	12.01.00.57
File Name:	NEXT D8-39ft105nonTransform.csl

Academic Use Only
 Copyright © Bentley Systems, Inc. 1984 - 2012
www.bentley.com Phone: 1-800-778-4277

FATIGUE I STRESS LIMITS AT FINAL 3 (50% P/S + 50% DL + F_LL) (Art. 5.5.3.1):

	PRECAST		DECK	
Max comp	2.60	ksi	-	ksi

SERVICE III (Tension):

	PRECAST		DECK	
Max tens	-0.48	ksi	-0.48	ksi

RESISTANCE FACTORS (Art. 5.5.4.2):

Flexure Reinforced	
Compression controlled sections	0.75
Tension controlled sections	0.90
Flexure Prestressed	
Compression controlled sections	0.75
Tension controlled sections	1.00
Shear	0.90

PRESTRESS LOSSES:

Time Dependent Losses, Approximate Method (Art.5.9.5.3)
Days to release = 0.75
Rel. Humid.(RH) = 75.0 %



		Sheet #	9
		Job #	
Program:	LEAP® CONSPAN® V8i (SELECTseries 5)	Academic Use Only	Designed
Version:	12.01.00.57	Copyright © Bentley Systems, Inc. 1984 - 2012	Date
		www.bentley.com	Phone: 1-800-778-4277
File Name:	NEXT D8-39ft105nonTransform.csl	Checked	Date

RATING PARAMETERS

Rating Factors	References	Values
Condition Factor	Table 6A.4.2.3-1	1.00
System Factor for Flexural Effect	Table 6A.4.2.4-1	1.00
System Factor for Shear Effect	Art. 6A.4.2.4	1.00
ADTT	Section C3.6.1.1.2	5000
Dynamic Load Factor for Design Level	Art. 6A.4.3.3	0.33
Dynamic Load Factor for Legal and Permit Level	Table C6A.4.4.3-1	0.33

For Flexural Effect: Condition Factor * System Factor = 1.00 >= 0.85 (Art. 6A.4.2.1) OK

For Shear Effect: Condition Factor * System Factor = 1.00 >= 0.85 (Art. 6A.4.2.1 and 6A.4.2.4) OK

Dead Load Factors (Table 6A.4.2.2-1)

Limit State	DC	DW
Strength I	1.25	1.50
Strength II	1.25	1.50
Service I	1.00	1.00
Service III	1.00	1.00

Allowable Stresses (ksi)

Rating Level	Concrete Compression	Concrete Tension	Steel
Design Inventory	0.60 x f'c = 3.90	0.19 x sqrt(f'c) = 0.48	0.90 x f'y = 218.70
Design Operating	0.60 x f'c = 3.90	0.19 x sqrt(f'c) = 0.48	0.90 x f'y = 218.70
Legal	0.60 x f'c = 3.90	0.19 x sqrt(f'c) = 0.48	-
Permit	0.60 x f'c = 3.90	0.19 x sqrt(f'c) = 0.48	0.90 x f'y = 218.70

Consider shear reinf. across plane (FDOT alternative): No



Sheet #	10
Job #	
Program:	LEAP® CONSPAN® V8i (SELECTseries 5)
Version:	12.01.00.57
File Name:	NEXT D8-39ft105nonTransform.csl
Academic Use Only	Designed HS
Copyright © Bentley Systems, Inc. 1984 - 2012	Date Oct/17/2013
www.bentley.com Phone: 1-800-778-4277	Checked
	Date

BEAM REINFORCEMENT

BEAM SPECIFIC MATERIAL PROPERTIES:

Span#, Beam#	Tendon-ID	Girder-f'ci ksi	Girder-f'c ksi	Deck-f'c ksi
Span:1, Beam:1	1/2-270K-LL	5.20	6.50	6.50
Span:1, Beam:2	1/2-270K-LL	5.20	6.50	6.50
Span:1, Beam:3	1/2-270K-LL	5.20	6.50	6.50
Span:1, Beam:4	1/2-270K-LL	5.20	6.50	6.50
Span:1, Beam:5	1/2-270K-LL	5.20	6.50	6.50
Span:1, Beam:6	1/2-270K-LL	5.20	6.50	6.50

Span:1, Beam:1

PRESTRESSED STEEL:

30 strands, 1/2-270K-LL, Low relaxation strands
Straight Pattern

END PATTERN (Ycg = 5.43 in):

10 @ 2.500 in	10 @ 4.500 in	6 @ 6.500 in	4 @ 13.500 in
---------------	---------------	--------------	---------------

REINFORCING STEEL:

Tension	steel:	
fy	60.0	ksi
Es	29000	ksi
fs	24.0	ksi

Stirrups:

# legs	Size	fy (ksi)	Area (in2)	Spacing (in)	Start (ft)	End (ft)	Extends into Deck
4	US#4[M13]	60.0	0.80	1.50	0.1900	0.4400	No
2	US#4[M13]	60.0	0.40	2.00	0.4400	0.9400	No
2	US#4[M13]	60.0	0.40	3.00	0.9400	1.9400	No
2	US#4[M13]	60.0	0.40	9.00	1.9400	37.9400	No
2	US#4[M13]	60.0	0.40	3.00	37.9400	38.9400	No
2	US#4[M13]	60.0	0.40	2.00	38.9400	39.4400	No
4	US#4[M13]	60.0	0.80	1.50	39.4400	39.6900	No

Top Steel:

#bars	Size	Dist. from Top (in)	Area (in2)	Start (ft)	End (ft)	Side Cover 515 (in)
-------	------	------------------------	---------------	---------------	-------------	------------------------



Sheet #	11
Job #	
Program:	LEAP® CONSPAN® V8i (SELECTseries 5)
Version:	12.01.00.57
Copyright © Bentley Systems, Inc. 1984 - 2012	www.bentley.com
Phone: 1-800-778-4277	
File Name:	NEXT D8-39ft105nonTransform.csl

Academic Use Only	Designed	HS
Date	Oct/17/2013	
Checked		
Date		

#bars	Size	Dist. from Top (in)	Area (in2)	Start (ft)	End (ft)	Side Cover (in)
12	US#4[M13]	2.25	2.400	0.1667	39.7083	7.50
12	US#4[M13]	6.25	2.400	0.1667	39.7083	7.50

Bottom Steel:

#bars	Size	Dist. from Top (in)	Area (in2)	Start (ft)	End (ft)	Side Cover (in)
-------	------	---------------------	------------	------------	----------	-----------------

Span:1, Beam:2

PRESTRESSED STEEL:

26 strands, 1/2-270K-LL, Low relaxation strands
Straight Pattern

END PATTERN (Ycg = 5.27 in):

10 @ 2.500 in	10 @ 4.500 in	2 @ 6.500 in	4 @ 13.500 in
---------------	---------------	--------------	---------------

REINFORCING STEEL:

Tension	steel:	
fy	60.0	ksi
Es	29000	ksi
fs	24.0	ksi

Stirrups:

# legs	Size	fy (ksi)	Area (in2)	Spacing (in)	Start (ft)	End (ft)	Extends into Deck
4	US#4[M13]	60.0	0.80	1.50	0.1900	0.4400	No
2	US#4[M13]	60.0	0.40	2.00	0.4400	0.9400	No
2	US#4[M13]	60.0	0.40	3.00	0.9400	1.9400	No
2	US#4[M13]	60.0	0.40	9.00	1.9400	37.9400	No
2	US#4[M13]	60.0	0.40	3.00	37.9400	38.9400	No
2	US#4[M13]	60.0	0.40	2.00	38.9400	39.4400	No
4	US#4[M13]	60.0	0.80	1.50	39.4400	39.6900	No

Top Steel:

#bars	Size	Dist. from Top (in)	Area (in2)	Start (ft)	End (ft)	Side Cover (in)
12	US#4[M13]	2.25	2.400	0.1667	39.7083	5.50
12	US#4[M13]	6.25	2.400	0.1667	39.7083	5.50



Sheet #	12
Job #	
Program:	LEAP® CONSPAN® V8i (SELECTseries 5)
Version:	12.01.00.57
Copyright © Bentley Systems, Inc. 1984 - 2012	www.bentley.com
Phone: 1-800-778-4277	
File Name:	NEXT D8-39ft105nonTransform.csl

Academic Use Only	Designed	HS
Date	Oct/17/2013	
Checked		
Date		

Bottom Steel:

#bars	Size	Dist. from Top (in)	Area (in ²)	Start (ft)	End (ft)	Side Cover (in)
-------	------	---------------------	-------------------------	------------	----------	-----------------

Span:1, Beam:3

PRESTRESSED STEEL:

26 strands, 1/2-270K-LL, Low relaxation strands
Straight Pattern

END PATTERN (Ycg = 5.27 in):

10 @ 2.500 in	10 @ 4.500 in	2 @ 6.500 in	4 @ 13.500 in
---------------	---------------	--------------	---------------

REINFORCING STEEL:

Tension	steel:	
fy	60.0	ksi
Es	29000	ksi
fs	24.0	ksi

Stirrups:

# legs	Size	fy (ksi)	Area (in ²)	Spacing (in)	Start (ft)	End (ft)	Extends into Deck
4	US#4[M13]	60.0	0.80	1.50	0.1900	0.4400	No
2	US#4[M13]	60.0	0.40	2.00	0.4400	0.9400	No
2	US#4[M13]	60.0	0.40	3.00	0.9400	1.9400	No
2	US#4[M13]	60.0	0.40	9.00	1.9400	37.9400	No
2	US#4[M13]	60.0	0.40	3.00	37.9400	38.9400	No
2	US#4[M13]	60.0	0.40	2.00	38.9400	39.4400	No
4	US#4[M13]	60.0	0.80	1.50	39.4400	39.6900	No

Top Steel:

#bars	Size	Dist. from Top (in)	Area (in ²)	Start (ft)	End (ft)	Side Cover (in)
12	US#4[M13]	2.25	2.400	0.1667	39.7083	5.50
12	US#4[M13]	6.25	2.400	0.1667	39.7083	5.50

Bottom Steel:

#bars	Size	Dist. from Top (in)	Area (in ²)	Start (ft)	End (ft)	Side Cover (in)
-------	------	---------------------	-------------------------	------------	----------	-----------------

517



		Sheet #	13
		Job #	
Program:	LEAP® CONSPAN® V8i (SELECTseries 5)	Academic Use Only	Designed HS
Version:	12.01.00.57	Copyright © Bentley Systems, Inc. 1984 - 2012	Date Oct/17/2013
		www.bentley.com	Phone: 1-800-778-4277
File Name:	NEXT D8-39ft105nonTransform.csl	Checked	Date

Span:1, Beam:4

PRESTRESSED STEEL:

26 strands, 1/2-270K-LL, Low relaxation strands
Straight Pattern

END PATTERN (Ycg = 5.27 in):

10 @ 2.500 in	10 @ 4.500 in	2 @ 6.500 in	4 @ 13.500 in
---------------	---------------	--------------	---------------

REINFORCING STEEL:

Tension	steel:	
fy	60.0	ksi
Es	29000	ksi
fs	24.0	ksi

Stirrups:

# legs	Size	fy (ksi)	Area (in2)	Spacing (in)	Start (ft)	End (ft)	Extends into Deck
4	US#4[M13]	60.0	0.80	1.50	0.1900	0.4400	No
2	US#4[M13]	60.0	0.40	2.00	0.4400	0.9400	No
2	US#4[M13]	60.0	0.40	3.00	0.9400	1.9400	No
2	US#4[M13]	60.0	0.40	9.00	1.9400	37.9400	No
2	US#4[M13]	60.0	0.40	3.00	37.9400	38.9400	No
2	US#4[M13]	60.0	0.40	2.00	38.9400	39.4400	No
4	US#4[M13]	60.0	0.80	1.50	39.4400	39.6900	No

Top Steel:

#bars	Size	Dist. from Top (in)	Area (in2)	Start (ft)	End (ft)	Side Cover (in)
12	US#4[M13]	2.25	2.400	0.1667	39.7083	5.50
12	US#4[M13]	6.25	2.400	0.1667	39.7083	5.50

Bottom Steel:

#bars	Size	Dist. from Top (in)	Area (in2)	Start (ft)	End (ft)	Side Cover (in)
-------	------	---------------------	------------	------------	----------	-----------------

Span:1, Beam:5



		Sheet #	14
		Job #	
Program:	LEAP® CONSPAN® V8i (SELECTseries 5)	Academic Use Only	Designed HS
Version:	12.01.00.57	Copyright © Bentley Systems, Inc. 1984 - 2012	Date Oct/17/2013
		www.bentley.com	Phone: 1-800-778-4277
File Name:	NEXT D8-39ft105nonTransform.csl		Checked
			Date

PRESTRESSED STEEL:

26 strands, 1/2-270K-LL, Low relaxation strands
Straight Pattern

END PATTERN (Ycg = 5.27 in):

10 @ 2.500 in	10 @ 4.500 in	2 @ 6.500 in	4 @ 13.500 in
---------------	---------------	--------------	---------------

REINFORCING STEEL:

Tension	steel:	
fy	60.0	ksi
Es	29000	ksi
fs	24.0	ksi

Stirrups:

# legs	Size	fy (ksi)	Area (in2)	Spacing (in)	Start (ft)	End (ft)	Extends into Deck
4	US#4[M13]	60.0	0.80	1.50	0.1900	0.4400	No
2	US#4[M13]	60.0	0.40	2.00	0.4400	0.9400	No
2	US#4[M13]	60.0	0.40	3.00	0.9400	1.9400	No
2	US#4[M13]	60.0	0.40	9.00	1.9400	37.9400	No
2	US#4[M13]	60.0	0.40	3.00	37.9400	38.9400	No
2	US#4[M13]	60.0	0.40	2.00	38.9400	39.4400	No
4	US#4[M13]	60.0	0.80	1.50	39.4400	39.6900	No

Top Steel:

#bars	Size	Dist. from Top (in)	Area (in2)	Start (ft)	End (ft)	Side Cover (in)
12	US#4[M13]	2.25	2.400	0.1667	39.7083	5.50
12	US#4[M13]	6.25	2.400	0.1667	39.7083	5.50

Bottom Steel:

#bars	Size	Dist. from Top (in)	Area (in2)	Start (ft)	End (ft)	Side Cover (in)

Span:1, Beam:6

PRESTRESSED STEEL:

30 strands, 1/2-270K-LL, Low relaxation strands
Straight Pattern



		Sheet #	15
		Job #	
Program:	LEAP® CONSPAN® V8i (SELECTseries 5)	Academic Use Only	Designed
Version:	12.01.00.57	Copyright © Bentley Systems, Inc. 1984 - 2012	Date
	www.bentley.com	Phone: 1-800-778-4277	Checked
File Name:	NEXT D8-39ft105nonTransform.csl		Date

END PATTERN (Ycg = 5.43 in):

10 @ 2.500 in	10 @ 4.500 in	6 @ 6.500 in	4 @ 13.500 in
---------------	---------------	--------------	---------------

REINFORCING STEEL:

Tension	steel:	
fy	60.0	ksi
Es	29000	ksi
fs	24.0	ksi

Stirrups:

# legs	Size	fy (ksi)	Area (in2)	Spacing (in)	Start (ft)	End (ft)	Extends into Deck
4	US#4[M13]	60.0	0.80	1.50	0.1900	0.4400	No
2	US#4[M13]	60.0	0.40	2.00	0.4400	0.9400	No
2	US#4[M13]	60.0	0.40	3.00	0.9400	1.9400	No
2	US#4[M13]	60.0	0.40	9.00	1.9400	37.9400	No
2	US#4[M13]	60.0	0.40	3.00	37.9400	38.9400	No
2	US#4[M13]	60.0	0.40	2.00	38.9400	39.4400	No
4	US#4[M13]	60.0	0.80	1.50	39.4400	39.6900	No

Top Steel:

#bars	Size	Dist. from Top (in)	Area (in2)	Start (ft)	End (ft)	Side Cover (in)
12	US#4[M13]	2.25	2.400	0.1667	39.7083	7.50
12	US#4[M13]	6.25	2.400	0.1667	39.7083	7.50

Bottom Steel:

#bars	Size	Dist. from Top (in)	Area (in2)	Start (ft)	End (ft)	Side Cover (in)
-------	------	---------------------	------------	------------	----------	-----------------

K.5 NEXT-8 40 ft. - Exterior Beam Output



Sheet #	1
Job #	
Program:	LEAP® CONSPAN® V8i (SELECTseries 5)
Version:	12.01.00.57
File Name:	NEXT D8-39ft105nonTransform.csl

Academic Use Only	Designed	HS
Copyright © Bentley Systems, Inc. 1984 - 2012	Date	Oct/17/2013
www.bentley.com	Checked	
Phone: 1-800-778-4277	Date	

PROPERTIES

Span:1, Beam:1

PRECAST DATA:

Section Id	Next D8-21-exterior		
Type	Double Tee		
Flng width	Top	96.000	in
thick	Top	8.000	in
Stems	No	2	
	Top	15.000	in
	Bot	14.190	in
Shear width		29.190	in

Minimum Thickness Criteria, Article 5.14.1.2.2 checked: OK.

GENERAL BRIDGE DATA:

Bridge Width	48.00	ft
Curb-to-curb	44.83	ft
Beam Spac. Lt./Rt	4.00/ 8.00	ft
Lane width	12.00	ft
Number of lanes	3	
Interior/Exterior	Exterior	
Start Skew Angle	0.00	degrees
End Skew Angle	0.00	degrees

TOPPING DATA:

Deck	Thickness	0.000	in	
Haunch:	Thickness	0.000	in	
	Width	0.000	in	
Effective	width	96.000	in	(Art. 4.6.2.6.1)

GENERAL LOAD DATA:

DEAD LOADS ON PRECAST

UNITS: (Point: kips, Location: ft, Line: klf, Trapez: klf)

DC/DW	Type	Mag.1	Loc.1	Mag.2	Loc.2	Description
DC	Line	0.221	0.000	0.221	39.000	Barrier Parapet
DW	Line	0.349	0.000	0.349	39.000	4 in bituminous wearing

Dead loads on composite: See Project info for composite loads

GENERAL SPAN DATA:



		Sheet #	2
		Job #	
Program:	LEAP® CONSPAN® V8i (SELECTseries 5)	Academic Use Only	Designed HS
Version:	12.01.00.57	Copyright © Bentley Systems, Inc. 1984 - 2012	Date Oct/17/2013
		www.bentley.com	Phone: 1-800-778-4277
File Name:	NEXT D8-39ft105nonTransform.csl		Date

Overall length	39.875	ft
Release length	39.875	ft
Design length	39.000	ft

KERN POINTS:

Upper	15.93	in
Lower	9.20	in

DISTRIBUTION FACTORS (Art. 4.6.2.2):

Type i, post-tensioned

Live Moment	(2+ lanes loaded)	0.589	(Manual input)
Live Moment	(1 lane loaded)	0.813	(Manual input)
Live Shear	(2+ lanes loaded)	0.572	(Manual input)
Live Shear	(1 lane loaded)	0.813	(Manual input)

Pedestrian	0.167	(Manual input)
Comp. DC	0.167	(Calculated)
Comp. DW	0.167	(Calculated)

Dead Loads distributed equally to all beams

RESISTANCE FACTORS (Art. 5.5.4.2):

Flexure Reinforced	
Compression controlled sections	0.75
Tension controlled sections	0.90
Flexure Prestressed	
Compression controlled sections	0.75
Tension controlled sections	1.00
Shear	0.90

SECTION PROPERTIES:

	PRECAST		COMPOSITE		
Area	1147.4	in ²	1147.4	in ²	#
Total Height	21.00	in	21.00	in	
Mom. of Inertia (I _{xx})	37120	in ⁴	37120	in ⁴	#
Ht. of c.g.	13.54	in	13.54	in	#
Density	150.00	pcf	150.00	pcf	
Self-weight	1195.2	plf	1195.2	plf	
Mom. of Inertia (I _{yy})	719514.1	in ⁴			
Poisson's Ratio	0.2				
Thermal Coeff.	0.000006000	1/°F			



Sheet #	3
Job #	
Program:	LEAP® CONSPAN® V8i (SELECTseries 5)
Version:	12.01.00.57
File Name:	NEXT D8-39ft105nonTransform.csl
Academic Use Only	
Copyright © Bentley Systems, Inc. 1984 - 2012	
www.bentley.com	Phone: 1-800-778-4277
Designed	HS
Date	Oct/17/2013
Checked	
Date	

(#) Of Total Section using Ect/Ec = 1.0000
 Use transformed strand and rebar: No

Span:1, Beam:1

STRESS LIMITS (Art. 5.9.4):

STRESS LIMITS AT RELEASE BEFORE LOSSES:

	PRECAST	
Strength	5.20	ksi
Elasticity	4371.7	ksi
Max comp	3.12	ksi
Max tens	-0.20	ksi
Max tens, w/reinf	-0.55	ksi

STRESS LIMITS AT FINAL AFTER LOSSES:

	PRECAST		DECK	
Strength	6.50	ksi	6.50	ksi
Elasticity	4887.73	ksi	4887.73	ksi

STRESS LIMITS AT FINAL 1 (P/S + DL + LL):

	PRECAST		DECK	
Max comp	3.90	ksi	3.90	ksi

STRESS LIMITS AT FINAL 2 (P/S + DL):

	PRECAST		DECK	
Max comp	2.93	ksi	2.93	ksi

FATIGUE I STRESS LIMITS AT FINAL 3 (50% P/S + 50% DL + F_LL) (Art. 5.5.3.1):

	PRECAST		DECK	
Max comp	2.60	ksi	-	ksi

SERVICE III (Tension):

	PRECAST		DECK	
Max tens	-0.48	ksi	-0.48	ksi

Span:1, Beam:1

PRESTRESSED STEEL:

30 strands, 1/2-270K-LL, Low relaxation strands

Straight Pattern



		Sheet #	4
		Job #	
Program:	LEAP® CONSPAN® V8i (SELECTseries 5)	Academic Use Only	Designed
Version:	12.01.00.57	Copyright © Bentley Systems, Inc. 1984 - 2012	Date
		www.bentley.com	Phone: 1-800-778-4277
File Name:	NEXT D8-39ft105nonTransform.csl	Checked	Date

END PATTERN (Ycg = 5.43 in):

10 @ 2.500 in	10 @ 4.500 in	6 @ 6.500 in	4 @ 13.500 in
---------------	---------------	--------------	---------------

Strand Diameter	0.500	in
Strand Area	0.153	in ²
Total Strand Area	4.590	in ²
Trans. Len, bonded	2.500	ft
Trans. Len, debonded	2.500	ft
Dev. Len, bonded	5.618	ft
Dev. Len, debonded	11.236	ft
Holddown Force	0.000	kips
Tensile Strength(fpu)	270.0	ksi
Initial Prestress = 0.75fpu	202.5	ksi
Initial Pull	929.5	kips
Beam Shrtng (PL/AE)	0.084	in

Span:1, Beam:1

ESTIMATED QUANTITIES

Prestressing (linear ft)	Strands (LB/1000ft)	(LB)	Beam Vol(C.Y.)	Concrete Wt(LB)	Stirrups (LB)	Longitudinal Bars (LB)
1196.250	520	622.050	11.768	47659.035	166.757	645.924

Span:1, Beam:1

REINFORCING STEEL:

Tension	steel:	
fy	60.0	ksi
Es	29000	ksi
fs	24.0	ksi

Stirrups:

# legs	Size	fy (ksi)	Area (in ²)	Spacing (in)	Start (ft)	End (ft)	Extends into Deck
4	US#4[M13]	60.0	0.80	1.50	0.1900	0.4400	No
2	US#4[M13]	60.0	0.40	2.00	0.4400	0.9400	No
2	US#4[M13]	60.0	0.40	3.00	0.9400	1.9400	No
2	US#4[M13]	60.0	0.40	9.00	1.9400	37.9400	No
2	US#4[M13]	60.0	0.40	3.00	37.9400	38.9400	No
2	US#4[M13]	60.0	0.40	2.00	38.9400	39.4400	No
4	US#4[M13]	60.0	0.80	1.50	39.4400	39.6900	No

Top Steel:

#bars	Size	Dist. from Top (in)	Area (in ²)	Start (ft)	End (ft)	Side Cover (in)
12	US#4[M13]	2.25	2.400	0.1667	39.7083	525 7.50
12	US#4[M13]	6.25	2.400	0.1667	39.7083	7.50



		Sheet #	5
		Job #	
Program:	LEAP® CONSPAN® V8i (SELECTseries 5)	Academic Use Only	Designed HS
Version:	12.01.00.57	Copyright © Bentley Systems, Inc. 1984 - 2012	Date Oct/17/2013
		www.bentley.com	Phone: 1-800-778-4277
File Name:	NEXT D8-39ft105nonTransform.csl	Checked	Date

Bottom Steel:

#bars	Size	Dist. from Top (in)	Area (in ²)	Start (ft)	End (ft)	Side Cover (in)
-------	------	---------------------	-------------------------	------------	----------	-----------------

LOSSES

Note: Values are calculated at Midspan

Str. area	4.5900	in ²
Ycg	5.43	in
P_init	929.5	kips
Ecc	8.11	in
Days to release	0.75	
Rel. Humid.(RH)	75.0	%
Es	28500.0	ksi
Eci	4372	ksi

AASHTO LOSSES

Elastic Shortening 11.23 ksi (Eq 5.9.5.2.3a-1), (fcgp= 1.723 ksi)

Elastic Gains		Gains		Adjustment	
due to Precast Loads		-1.66	ksi	0.11	ksi
due to Composite Loads		-0.00	ksi	0.00	ksi
due to Live Loads		-6.99	ksi	0.58	ksi

Time Dependent Losses (Approximate Method (Art.5.9.5.3))

	Initial	Final	
Steel relaxation	0.00 ksi	2.40 ksi	(Eq 5.9.5.3-1)
Concrete shrinkage	0.00 ksi	9.19 ksi	(Eq 5.9.5.3-1)
Concrete creep	0.00 ksi	6.21 ksi	(Eq 5.9.5.3-1)
Sub-total	11.23 ksi	9.84 ksi	(4.86 %)
Total Prestress Losses		21.08 ksi	(10.41 %)

Prestressing Stress Limit Check (Table 5.9.3.1)

initial fpi = 202.5 ksi < 0.75 fpu, OK
 initial fpe = 181.4 ksi < 0.80 fpy, OK



Sheet #	6
Job #	
Program:	LEAP® CONSPAN® V8i (SELECTseries 5)
Version:	12.01.00.57
Copyright © Bentley Systems, Inc. 1984 - 2012	www.bentley.com
Phone: 1-800-778-4277	
File Name:	NEXT D8-39ft105nonTransform.csl

Academic Use Only	Designed	HS
Copyright © Bentley Systems, Inc. 1984 - 2012	Date	Oct/17/2013
www.bentley.com	Checked	
Phone: 1-800-778-4277	Date	

SHEAR/MOMENT ENVELOPE (&REACTIONS)

SHEAR AND MOMENT ENVELOPE : Span : 1, Beam : 1, SERVICE I
 Shears: kips, Moments: kft

		Bearing	Trans	H/2	0.10L	0.20L	0.30L	0.40L	Midspan
Location,	ft	0.00	2.06	0.88	3.55	7.54	11.53	15.51	19.50
Self wt. :	M	0.0	45.5	19.9	75.2	141.7	189.2	217.7	227.2
(Max)	V	23.3	20.8	22.3	19.1	14.3	9.5	4.8	0.0
DL-Prec. :	M	-0.0	8.4	3.7	13.9	26.2	35.0	40.3	42.0
DC(Max)	V	4.3	3.9	4.1	3.5	2.6	1.8	0.9	0.0
DL-Prec. :	M	-0.0	13.3	5.8	22.0	41.4	55.3	63.6	66.4
DW(Max)	V	6.8	6.1	6.5	5.6	4.2	2.8	1.4	0.0
Deck + :	M	0.0	0.0	0.0	0.0	0.0	0.0	0.0	0.0
Haunch (Max)	V	0.0	0.0	0.0	0.0	0.0	0.0	0.0	0.0
Diaphragm :	M	0.0	0.0	0.0	0.0	0.0	0.0	0.0	0.0
(Max)	V	0.0	0.0	0.0	0.0	0.0	0.0	0.0	0.0
DL-Comp :	M	0.0	0.0	0.0	0.0	0.0	0.0	0.0	0.0
DC(Max)	V	0.0	0.0	0.0	0.0	0.0	0.0	0.0	0.0
DL-Comp :	M	0.0	0.0	0.0	0.0	0.0	0.0	0.0	0.0
DW(Max)	V	0.0	0.0	0.0	0.0	0.0	0.0	0.0	0.0
LL + I :	M+	0.0	131.8	58.2	215.2	390.5	497.2	556.5	571.6
	V	69.3	63.7	67.0	59.7	49.8	40.1	4.8	24.2
LL + I :	M-	0.0	0.0	0.0	0.0	0.0	0.0	0.0	0.0
	V	0.0	0.0	0.0	0.0	0.0	0.0	0.0	0.0
LL + I :	Vmx	69.3	63.7	67.0	59.7	50.1	41.0	33.3	26.8
	M	0.0	133.1	59.2	215.2	377.7	472.2	516.5	522.2
Total :	M+	0.0	199.1	87.7	326.3	599.8	776.7	878.0	907.3
	V	103.7	94.5	99.8	87.9	71.0	54.2	11.9	24.2
Total :	M-	0.0	0.0	0.0	0.0	0.0	0.0	0.0	0.0
	V	0.0	0.0	0.0	0.0	0.0	0.0	0.0	0.0
Total :	Vmx	103.7	94.5	99.8	87.9	71.2	55.0	40.3	26.8
	M	0.0	200.4	88.7	326.3	587.0	751.6	838.1	857.8

		0.60L	0.70L	0.80L	0.90L	H/2	Trans	Bearing
Location,	ft	23.49	27.47	31.46	35.45	38.13	36.94	39.00
Self wt. :	M	217.7	189.2	141.7	75.2	19.9	45.5	0.0
(Max)	V	4.8	9.5	14.3	19.1	22.3	20.8	23.3
DL-Prec. :	M	40.3	35.0	26.2	13.9	3.7	8.4	0.0
DC(Max)	V	0.9	1.8	2.6	3.5	4.1	3.9	4.3
DL-Prec. :	M	63.6	55.3	41.4	22.0	5.8	13.3	-0.0
DW(Max)	V	1.4	2.8	4.2	5.6	6.5	6.1	6.8
Deck + :	M	0.0	0.0	0.0	0.0	0.0	0.0	0.0
Haunch (Max)	V	0.0	0.0	0.0	0.0	0.0	0.0	0.0
Diaphragm :	M	0.0	0.0	0.0	0.0	0.0	0.0	0.0
(Max)	V	0.0	0.0	0.0	0.0	0.0	0.0	0.0
DL-Comp :	M	0.0	0.0	0.0	0.0	0.0	0.0	0.0
DC(Max)	V	0.0	0.0	0.0	0.0	0.0	0.0	0.0
DL-Comp :	M	0.0	0.0	0.0	0.0	0.0	0.0	0.0
DW(Max)	V	0.0	0.0	0.0	0.0	0.0	0.0	0.0



Sheet #	7
Job #	
Program:	LEAP® CONSPAN® V8i (SELECTseries 5)
Version:	12.01.00.57
Copyright © Bentley Systems, Inc. 1984 - 2012	www.bentley.com
Phone: 1-800-778-4277	
File Name:	NEXT D8-39ft105nonTransform.csl

Academic Use Only	Designed	HS
Date	Oct/17/2013	
Checked		
Date		

		0.60L	0.70L	0.80L	0.90L	H/2	Trans	Bearing
LL + I :	M+	556.5	497.2	390.5	215.2	58.2	131.8	0.0
	V	4.8	40.1	49.8	59.7	67.0	63.7	69.3
LL + I :	M-	0.0	0.0	0.0	0.0	0.0	0.0	0.0
	V	0.0	0.0	0.0	0.0	0.0	0.0	0.0
LL + I :	Vmx	33.3	41.0	50.1	59.7	67.0	63.7	69.3
	M	516.5	472.2	377.7	215.2	59.2	133.1	0.0
Total :	M+	878.0	776.7	599.8	326.3	87.7	199.1	0.0
	V	11.9	54.2	71.0	87.9	99.8	94.5	103.7
Total :	M-	0.0	0.0	0.0	0.0	0.0	0.0	0.0
	V	0.0	0.0	0.0	0.0	0.0	0.0	0.0
Total :	Vmx	40.3	55.0	71.2	87.9	99.8	94.5	103.7
	M	838.1	751.6	587.0	326.3	88.7	200.4	0.0

REACTIONS (kips), SERVICE I

Load Type	Left Support	Right Support
Self Wt.	23.3	23.3
Deck+Haunch	0.0	0.0
Diaphragm	0.0	0.0
DL-Prec.(DC)	4.3	4.3
DL-Prec.(DW)	6.8	6.8
DL-Comp.(DC)	0.0	0.0
DL-Comp.(DW)	0.0	0.0
Live	67.2	67.2
Pedestrian	0.0	0.0

Upward reactions are positive.

Live Load reactions are per lane with no distribution factor and no impact.

Reactions are not multiplied by Load Modifiers (ductility, redundancy and operational importance).

Non-composite load types are per beam.

Composite and Pedestrian load types are per total bridge width.

SHEAR AND MOMENT ENVELOPE : Span : 1, Beam : 1, SERVICE III

Shears: kips, Moments: kft

Location,	ft	Bearing	Trans	H/2	0.10L	0.20L	0.30L	0.40L	Midspan
Self wt. :	M	0.0	45.5	19.9	75.2	141.7	189.2	217.7	227.2
(Max)	V	23.3	20.8	22.3	19.1	14.3	9.5	4.8	0.0
DL-Prec. :	M	-0.0	8.4	3.7	13.9	26.2	35.0	40.3	42.0
DC(Max)	V	4.3	3.9	4.1	3.5	2.6	1.8	0.9	0.0
DL-Prec. :	M	-0.0	13.3	5.8	22.0	41.4	55.3	63.6	66.4
DW(Max)	V	6.8	6.1	6.5	5.6	4.2	2.8	1.4	0.0
Deck + :	M	0.0	0.0	0.0	0.0	0.0	0.0	0.0	0.0
Haunch (Max)	V	0.0	0.0	0.0	0.0	0.0	0.0	0.0	0.0



Sheet #	8
Job #	
Program:	LEAP® CONSPAN® V8i (SELECTseries 5)
Version:	12.01.00.57
Copyright © Bentley Systems, Inc. 1984 - 2012	www.bentley.com
Phone: 1-800-778-4277	
File Name:	NEXT D8-39ft105nonTransform.csl

		Bearing	Trans	H/2	0.10L	0.20L	0.30L	0.40L	Midspan
Diaphragm :	M	0.0	0.0	0.0	0.0	0.0	0.0	0.0	0.0
(Max)	V	0.0	0.0	0.0	0.0	0.0	0.0	0.0	0.0
DL-Comp :	M	0.0	0.0	0.0	0.0	0.0	0.0	0.0	0.0
DC(Max)	V	0.0	0.0	0.0	0.0	0.0	0.0	0.0	0.0
DL-Comp :	M	0.0	0.0	0.0	0.0	0.0	0.0	0.0	0.0
DW(Max)	V	0.0	0.0	0.0	0.0	0.0	0.0	0.0	0.0
LL + I :	M+	0.0	105.5	46.6	172.2	312.4	397.8	445.2	457.3
	V	55.5	51.0	53.6	47.8	39.9	32.1	3.9	19.4
LL + I :	M-	0.0	0.0	0.0	0.0	0.0	0.0	0.0	0.0
	V	0.0	0.0	0.0	0.0	0.0	0.0	0.0	0.0
LL + I :	Vmx	55.5	51.0	53.6	47.8	40.1	32.8	26.6	21.4
	M	0.0	106.5	47.4	172.2	302.2	377.7	413.2	417.8
Total :	M+	0.0	172.7	76.0	283.2	521.7	677.2	766.7	792.9
	V	89.9	81.8	86.4	75.9	61.0	46.2	10.9	19.4
Total :	M-	0.0	0.0	0.0	0.0	0.0	0.0	0.0	0.0
	V	0.0	0.0	0.0	0.0	0.0	0.0	0.0	0.0
Total :	Vmx	89.9	81.8	86.4	75.9	61.2	46.9	33.7	21.4
	M	0.0	173.7	76.8	283.2	511.5	657.2	734.8	753.4

		0.60L	0.70L	0.80L	0.90L	H/2	Trans	Bearing
Location,	ft	23.49	27.47	31.46	35.45	38.13	36.94	39.00
Self wt. :	M	217.7	189.2	141.7	75.2	19.9	45.5	0.0
(Max)	V	4.8	9.5	14.3	19.1	22.3	20.8	23.3
DL-Prec. :	M	40.3	35.0	26.2	13.9	3.7	8.4	0.0
DC(Max)	V	0.9	1.8	2.6	3.5	4.1	3.9	4.3
DL-Prec. :	M	63.6	55.3	41.4	22.0	5.8	13.3	-0.0
DW(Max)	V	1.4	2.8	4.2	5.6	6.5	6.1	6.8
Deck + :	M	0.0	0.0	0.0	0.0	0.0	0.0	0.0
Haunch (Max)	V	0.0	0.0	0.0	0.0	0.0	0.0	0.0
Diaphragm :	M	0.0	0.0	0.0	0.0	0.0	0.0	0.0
(Max)	V	0.0	0.0	0.0	0.0	0.0	0.0	0.0
DL-Comp :	M	0.0	0.0	0.0	0.0	0.0	0.0	0.0
DC(Max)	V	0.0	0.0	0.0	0.0	0.0	0.0	0.0
DL-Comp :	M	0.0	0.0	0.0	0.0	0.0	0.0	0.0
DW(Max)	V	0.0	0.0	0.0	0.0	0.0	0.0	0.0
LL + I :	M+	445.2	397.8	312.4	172.2	46.6	105.5	0.0
	V	3.9	32.1	39.9	47.8	53.6	51.0	55.5
LL + I :	M-	0.0	0.0	0.0	0.0	0.0	0.0	0.0
	V	0.0	0.0	0.0	0.0	0.0	0.0	0.0
LL + I :	Vmx	26.6	32.8	40.1	47.8	53.6	51.0	55.5
	M	413.2	377.7	302.2	172.2	47.4	106.5	0.0
Total :	M+	766.7	677.2	521.7	283.2	76.0	172.7	0.0
	V	10.9	46.2	61.0	75.9	86.4	81.8	89.9
Total :	M-	0.0	0.0	0.0	0.0	0.0	0.0	0.0
	V	0.0	0.0	0.0	0.0	0.0	0.0	0.0
Total :	Vmx	33.7	46.9	61.2	75.9	86.4	81.8	89.9
	M	734.8	657.2	511.5	283.2	76.8	173.7	0.0



Sheet #	9
Job #	
Program:	LEAP® CONSPAN® V8i (SELECTseries 5)
Version:	12.01.00.57
Copyright © Bentley Systems, Inc. 1984 - 2012	www.bentley.com
Phone: 1-800-778-4277	
File Name:	NEXT D8-39ft105nonTransform.csl

SHEAR AND MOMENT ENVELOPE : Span : 1, Beam : 1, STRENGTH I
 Shears: kips, Moments: kft

		Bearing	Trans	H/2	0.10L	0.20L	0.30L	0.40L	Midspan
Location,	ft	0.00	2.06	0.88	3.55	7.54	11.53	15.51	19.50
Self wt. :	M	0.0	56.9	24.9	94.0	177.2	236.5	272.2	284.0
(Max)	V	29.1	26.1	27.8	23.8	17.9	11.9	6.0	0.0
Self wt. :	M	0.0	41.0	17.9	67.7	127.5	170.3	196.0	204.5
(Min)	V	21.0	18.8	20.0	17.2	12.9	8.6	4.3	0.0
DL-Prec. :	M	-0.0	10.5	4.6	17.4	32.8	43.7	50.3	52.5
DC(Max)	V	5.4	4.8	5.1	4.4	3.3	2.2	1.1	0.0
DL-Prec. :	M	-0.0	7.6	3.3	12.5	23.6	31.5	36.2	37.8
DC(Min)	V	3.9	3.5	3.7	3.2	2.4	1.6	0.8	0.0
DL-Prec. :	M	-0.0	19.9	8.7	32.9	62.1	82.9	95.4	99.5
DW(Max)	V	10.2	9.1	9.8	8.3	6.3	4.2	2.1	0.0
DL-Prec. :	M	-0.0	8.6	3.8	14.3	26.9	35.9	41.3	43.1
DW(Min)	V	4.4	4.0	4.2	3.6	2.7	1.8	0.9	0.0
Deck + :	M	0.0	0.0	0.0	0.0	0.0	0.0	0.0	0.0
Haunch (Max)	V	0.0	0.0	0.0	0.0	0.0	0.0	0.0	0.0
Deck + :	M	0.0	0.0	0.0	0.0	0.0	0.0	0.0	0.0
Haunch (Min)	V	0.0	0.0	0.0	0.0	0.0	0.0	0.0	0.0
Diaphragm :	M	0.0	0.0	0.0	0.0	0.0	0.0	0.0	0.0
(Max)	V	0.0	0.0	0.0	0.0	0.0	0.0	0.0	0.0
Diaphragm :	M	0.0	0.0	0.0	0.0	0.0	0.0	0.0	0.0
(Min)	V	0.0	0.0	0.0	0.0	0.0	0.0	0.0	0.0
DL-Comp :	M	0.0	0.0	0.0	0.0	0.0	0.0	0.0	0.0
DC(Max)	V	0.0	0.0	0.0	0.0	0.0	0.0	0.0	0.0
DL-Comp :	M	0.0	0.0	0.0	0.0	0.0	0.0	0.0	0.0
DC(Min)	V	0.0	0.0	0.0	0.0	0.0	0.0	0.0	0.0
DL-Comp :	M	0.0	0.0	0.0	0.0	0.0	0.0	0.0	0.0
DW(Max)	V	0.0	0.0	0.0	0.0	0.0	0.0	0.0	0.0
DL-Comp :	M	0.0	0.0	0.0	0.0	0.0	0.0	0.0	0.0
DW(Min)	V	0.0	0.0	0.0	0.0	0.0	0.0	0.0	0.0
LL + I :	M+	0.0	230.7	101.9	376.6	683.3	870.1	973.8	1000.4
	V	121.3	111.5	117.2	104.5	87.2	70.3	8.5	42.4
LL + I :	M-	0.0	0.0	0.0	0.0	0.0	0.0	0.0	0.0
	V	0.0	0.0	0.0	0.0	0.0	0.0	0.0	0.0
LL + I :	Vmx	121.3	111.5	117.2	104.5	87.7	71.7	58.3	46.9
	M	0.0	233.0	103.6	376.6	661.0	826.3	904.0	913.9
Total :	M+	0.0	318.1	140.1	520.9	955.3	1233.3	1391.7	1436.5
	V	166.0	151.5	159.9	141.1	114.7	88.5	17.6	42.4
Total :	M-	0.0	0.0	0.0	0.0	0.0	0.0	0.0	0.0
	V	0.0	0.0	0.0	0.0	0.0	0.0	0.0	0.0
Total :	Vmx	166.0	151.5	159.9	141.1	115.1	90.0	67.4	46.9
	M	0.0	309.0	136.9	502.3	897.8	1142.5	1267.8	1293.6

		0.60L	0.70L	0.80L	0.90L	H/2	Trans	Bearing
Location,	ft	23.49	27.47	31.46	35.45	38.13	36.94	39.00
Self wt. :	M	272.2	236.5	177.2	94.0	24.9	56.9	0.0



Sheet #	10
Job #	
Program:	LEAP® CONSPAN® V8i (SELECTseries 5)
Version:	12.01.00.57
Copyright © Bentley Systems, Inc. 1984 - 2012	www.bentley.com
Phone: 1-800-778-4277	
File Name:	NEXT D8-39ft105nonTransform.csl

Academic Use Only	Designed	HS
Date	Oct/17/2013	
Checked		
Date		

		0.60L	0.70L	0.80L	0.90L	H/2	Trans	Bearing
(Max)	V	6.0	11.9	17.9	23.8	27.8	26.1	29.1
Self wt. :	M	196.0	170.3	127.5	67.7	17.9	41.0	0.0
(Min)	V	4.3	8.6	12.9	17.2	20.0	18.8	21.0
DL-Prec. :	M	50.3	43.7	32.8	17.4	4.6	10.5	0.0
DC(Max)	V	1.1	2.2	3.3	4.4	5.1	4.8	5.4
DL-Prec. :	M	36.2	31.5	23.6	12.5	3.3	7.6	0.0
DC(Min)	V	0.8	1.6	2.4	3.2	3.7	3.5	3.9
DL-Prec. :	M	95.4	82.9	62.1	32.9	8.7	19.9	-0.0
DW(Max)	V	2.1	4.2	6.3	8.3	9.8	9.1	10.2
DL-Prec. :	M	41.3	35.9	26.9	14.3	3.8	8.6	-0.0
DW(Min)	V	0.9	1.8	2.7	3.6	4.2	4.0	4.4
Deck + :	M	0.0	0.0	0.0	0.0	0.0	0.0	0.0
Haunch (Max)	V	0.0	0.0	0.0	0.0	0.0	0.0	0.0
Deck + :	M	0.0	0.0	0.0	0.0	0.0	0.0	0.0
Haunch (Min)	V	0.0	0.0	0.0	0.0	0.0	0.0	0.0
Diaphragm :	M	0.0	0.0	0.0	0.0	0.0	0.0	0.0
(Max)	V	0.0	0.0	0.0	0.0	0.0	0.0	0.0
Diaphragm :	M	0.0	0.0	0.0	0.0	0.0	0.0	0.0
(Min)	V	0.0	0.0	0.0	0.0	0.0	0.0	0.0
DL-Comp :	M	0.0	0.0	0.0	0.0	0.0	0.0	0.0
DC(Max)	V	0.0	0.0	0.0	0.0	0.0	0.0	0.0
DL-Comp :	M	0.0	0.0	0.0	0.0	0.0	0.0	0.0
DC(Min)	V	0.0	0.0	0.0	0.0	0.0	0.0	0.0
DL-Comp :	M	0.0	0.0	0.0	0.0	0.0	0.0	0.0
DW(Max)	V	0.0	0.0	0.0	0.0	0.0	0.0	0.0
DL-Comp :	M	0.0	0.0	0.0	0.0	0.0	0.0	0.0
DW(Min)	V	0.0	0.0	0.0	0.0	0.0	0.0	0.0
LL + I :	M+	973.8	870.1	683.3	376.6	101.9	230.7	0.0
	V	8.5	70.3	87.2	104.5	117.2	111.5	121.3
LL + I :	M-	0.0	0.0	0.0	0.0	0.0	0.0	0.0
	V	0.0	0.0	0.0	0.0	0.0	0.0	0.0
LL + I :	Vmx	58.3	71.7	87.7	104.5	117.2	111.5	121.3
	M	904.0	826.3	661.0	376.6	103.6	233.0	0.0
Total :	M+	1391.7	1233.3	955.3	520.9	140.1	318.1	0.0
	V	17.6	88.5	114.7	141.1	159.9	151.5	166.0
Total :	M-	0.0	0.0	0.0	0.0	0.0	0.0	0.0
	V	0.0	0.0	0.0	0.0	0.0	0.0	0.0
Total :	Vmx	67.4	90.0	115.1	141.1	159.9	151.5	166.0
	M	1267.8	1142.5	897.8	502.3	136.9	309.0	0.0

REACTIONS (kips), STRENGTH I

Load Type	Left Support	Right Support
Self Wt.	29.1	29.1
Deck+Haunch	0.0	0.0
Diaphragm	0.0	0.0
DL-Prec.(DC)	5.4	5.4
DL-Prec.(DW)	10.2	10.2



Sheet #	11
Job #	
Program:	LEAP® CONSPAN® V8i (SELECTseries 5)
Version:	12.01.00.57
Copyright © Bentley Systems, Inc. 1984 - 2012	www.bentley.com
Phone: 1-800-778-4277	
File Name:	NEXT D8-39ft105nonTransform.csl

Academic Use Only	Designed	HS
Date	Oct/17/2013	
Checked		
Date		

Load Type	Left Support	Right Support
DL-Comp.(DC)	0.0	0.0
DL-Comp.(DW)	0.0	0.0
Live	117.7	117.7
Pedestrian	0.0	0.0

Upward reactions are positive.
 Live Load reactions are per lane with no distribution factor and no impact.
 Reactions are not multiplied by Load Modifiers (ductility, redundancy and operational importance).
 Non-composite load types are per beam.
 Composite and Pedestrian load types are per total bridge width.

SHEAR AND MOMENT ENVELOPE : Span : 1, Beam : 1, FATIGUE I
 Shears: kips, Moments: kft

		Bearing	Trans	H/2	0.10L	0.20L	0.30L	0.40L	Midspan
Location,	ft	0.00	2.06	0.88	3.55	7.54	11.53	15.51	19.50
Self wt. :	M	0.0	45.5	19.9	75.2	141.7	189.2	217.7	227.2
(Max)	V	23.3	20.8	22.3	19.1	14.3	9.5	4.8	0.0
Self wt. :	M	0.0	0.0	0.0	0.0	0.0	0.0	0.0	0.0
(Min)	V	0.0	0.0	0.0	0.0	0.0	0.0	0.0	0.0
DL-Prec. :	M	-0.0	8.4	3.7	13.9	26.2	35.0	40.3	42.0
DC(Max)	V	4.3	3.9	4.1	3.5	2.6	1.8	0.9	0.0
DL-Prec. :	M	-0.0	0.0	0.0	0.0	0.0	0.0	0.0	0.0
DC(Min)	V	0.0	0.0	0.0	0.0	0.0	0.0	0.0	0.0
DL-Prec. :	M	-0.0	13.3	5.8	22.0	41.4	55.3	63.6	66.4
DW(Max)	V	6.8	6.1	6.5	5.6	4.2	2.8	1.4	0.0
DL-Prec. :	M	-0.0	0.0	0.0	0.0	0.0	0.0	0.0	0.0
DW(Min)	V	0.0	0.0	0.0	0.0	0.0	0.0	0.0	0.0
Deck + :	M	0.0	0.0	0.0	0.0	0.0	0.0	0.0	0.0
Haunch (Max)	V	0.0	0.0	0.0	0.0	0.0	0.0	0.0	0.0
Deck + :	M	0.0	0.0	0.0	0.0	0.0	0.0	0.0	0.0
Haunch (Min)	V	0.0	0.0	0.0	0.0	0.0	0.0	0.0	0.0
Diaphragm :	M	0.0	0.0	0.0	0.0	0.0	0.0	0.0	0.0
(Max)	V	0.0	0.0	0.0	0.0	0.0	0.0	0.0	0.0
Diaphragm :	M	0.0	0.0	0.0	0.0	0.0	0.0	0.0	0.0
(Min)	V	0.0	0.0	0.0	0.0	0.0	0.0	0.0	0.0
DL-Comp :	M	0.0	0.0	0.0	0.0	0.0	0.0	0.0	0.0
DC(Max)	V	0.0	0.0	0.0	0.0	0.0	0.0	0.0	0.0
DL-Comp :	M	0.0	0.0	0.0	0.0	0.0	0.0	0.0	0.0
DC(Min)	V	0.0	0.0	0.0	0.0	0.0	0.0	0.0	0.0
DL-Comp :	M	0.0	0.0	0.0	0.0	0.0	0.0	0.0	0.0
DW(Max)	V	0.0	0.0	0.0	0.0	0.0	0.0	0.0	0.0
DL-Comp :	M	0.0	0.0	0.0	0.0	0.0	0.0	0.0	0.0
DW(Min)	V	0.0	0.0	0.0	0.0	0.0	0.0	0.0	0.0
LL + I :	M+	0.0	100.1	43.9	164.8	307.7	405.9	459.4	468.1
	V	55.2	50.1	53.0	46.4	40.8	35.2	29.6	24.0
LL + I :	M-	0.0	0.0	0.0	0.0	0.0	0.0	0.0	0.0



Sheet #	12
Job #	
Program:	LEAP® CONSPAN® V8i (SELECTseries 5)
Version:	12.01.00.57
Copyright © Bentley Systems, Inc. 1984 - 2012	www.bentley.com
Phone: 1-800-778-4277	
File Name:	NEXT D8-39ft105nonTransform.csl

Academic Use Only	Designed	HS
Date	Oct/17/2013	
Checked		
Date		

		Bearing	Trans	H/2	0.10L	0.20L	0.30L	0.40L	Midspan
LL + I :	V	0.0	0.0	0.0	0.0	0.0	0.0	0.0	0.0
	Vmx	55.2	50.1	53.0	46.4	40.8	35.2	29.6	24.0
	M	0.0	100.1	43.9	164.8	307.7	405.9	459.4	468.1
Total :	M+	0.0	167.3	73.4	275.9	517.0	685.4	780.9	803.7
	V	89.6	80.9	85.9	74.6	61.9	49.3	36.7	24.0
Total :	M-	0.0	0.0	0.0	0.0	0.0	0.0	0.0	0.0
	V	0.0	0.0	0.0	0.0	0.0	0.0	0.0	0.0
Total :	Vmx	89.6	80.9	85.9	74.6	61.9	49.3	36.7	24.0
	M	0.0	167.3	73.4	275.9	517.0	685.4	780.9	803.7

		0.60L	0.70L	0.80L	0.90L	H/2	Trans	Bearing
Location,	ft	23.49	27.47	31.46	35.45	38.13	36.94	39.00
Self wt. :	M	217.7	189.2	141.7	75.2	19.9	45.5	0.0
(Max)	V	4.8	9.5	14.3	19.1	22.3	20.8	23.3
Self wt. :	M	0.0	0.0	0.0	0.0	0.0	0.0	0.0
(Min)	V	0.0	0.0	0.0	0.0	0.0	0.0	0.0
DL-Prec. :	M	40.3	35.0	26.2	13.9	3.7	8.4	0.0
DC(Max)	V	0.9	1.8	2.6	3.5	4.1	3.9	4.3
DL-Prec. :	M	0.0	0.0	0.0	0.0	0.0	0.0	0.0
DC(Min)	V	0.0	0.0	0.0	0.0	0.0	0.0	0.0
DL-Prec. :	M	63.6	55.3	41.4	22.0	5.8	13.3	-0.0
DW(Max)	V	1.4	2.8	4.2	5.6	6.5	6.1	6.8
DL-Prec. :	M	0.0	0.0	0.0	0.0	0.0	0.0	-0.0
DW(Min)	V	0.0	0.0	0.0	0.0	0.0	0.0	0.0
Deck + :	M	0.0	0.0	0.0	0.0	0.0	0.0	0.0
Haunch (Max)	V	0.0	0.0	0.0	0.0	0.0	0.0	0.0
Deck + :	M	0.0	0.0	0.0	0.0	0.0	0.0	0.0
Haunch (Min)	V	0.0	0.0	0.0	0.0	0.0	0.0	0.0
Diaphragm :	M	0.0	0.0	0.0	0.0	0.0	0.0	0.0
(Max)	V	0.0	0.0	0.0	0.0	0.0	0.0	0.0
Diaphragm :	M	0.0	0.0	0.0	0.0	0.0	0.0	0.0
(Min)	V	0.0	0.0	0.0	0.0	0.0	0.0	0.0
DL-Comp :	M	0.0	0.0	0.0	0.0	0.0	0.0	0.0
DC(Max)	V	0.0	0.0	0.0	0.0	0.0	0.0	0.0
DL-Comp :	M	0.0	0.0	0.0	0.0	0.0	0.0	0.0
DC(Min)	V	0.0	0.0	0.0	0.0	0.0	0.0	0.0
DL-Comp :	M	0.0	0.0	0.0	0.0	0.0	0.0	0.0
DW(Max)	V	0.0	0.0	0.0	0.0	0.0	0.0	0.0
DL-Comp :	M	0.0	0.0	0.0	0.0	0.0	0.0	0.0
DW(Min)	V	0.0	0.0	0.0	0.0	0.0	0.0	0.0
LL + I :	M+	459.4	405.9	307.7	164.8	43.9	100.1	0.0
	V	29.6	35.2	40.8	46.4	53.0	50.1	55.2
LL + I :	M-	0.0	0.0	0.0	0.0	0.0	0.0	0.0
	V	0.0	0.0	0.0	0.0	0.0	0.0	0.0
LL + I :	Vmx	29.6	35.2	40.8	46.4	53.0	50.1	55.2
	M	459.4	405.9	307.7	164.8	43.9	100.1	0.0
Total :	M+	780.9	685.4	517.0	275.9	73.4	167.3	0.0
	V	36.7	49.3	61.9	74.6	85.9	80.9	89.6
Total :	M-	0.0	0.0	0.0	0.0	0.0	0.0	0.0
	V	0.0	0.0	0.0	0.0	0.0	0.0	0.0
Total :	Vmx	36.7	49.3	61.9	74.6	85.9	80.9	89.6



		Sheet #	13	
		Job #		
Program:	LEAP® CONSPAN® V8i (SELECTseries 5)	Academic Use Only	Designed	HS
Version:	12.01.00.57	Copyright © Bentley Systems, Inc. 1984 - 2012	Date	Oct/17/2013
		www.bentley.com	Phone: 1-800-778-4277	Checked
File Name:	NEXT D8-39ft105nonTransform.csl			Date

	M	0.60L	0.70L	0.80L	0.90L	H/2	Trans	Bearing
		780.9	685.4	517.0	275.9	73.4	167.3	0.0



Sheet #	14
Job #	
Program:	LEAP® CONSPAN® V8i (SELECTseries 5)
Version:	12.01.00.57
Copyright © Bentley Systems, Inc. 1984 - 2012	www.bentley.com
Phone: 1-800-778-4277	
File Name:	NEXT D8-39ft105nonTransform.csl

Academic Use Only	Designed	HS
Date	Oct/17/2013	
Checked		
Date		

POSITIVE ENVELOPE STRESSES

Span : 1, Beam : 1, SERVICE I

RELEASE STRESSES, (ksi) (LOSS = 5.55 %)

Location, ft	Trans	0.10L /0.90L	0.20L /0.80L	0.30L /0.70L	0.40L /0.60L	Midspan
2.50	3.99	7.98	11.96	15.95	19.94	
Beam-Self						
Precast-top	0.135	0.206	0.367	0.481	0.550	0.573
Bottom	-0.244	-0.374	-0.665	-0.873	-0.998	-1.040
Prestress						
Precast-top	-0.665	-0.665	-0.665	-0.665	-0.665	-0.665
Bottom	3.361	3.361	3.361	3.361	3.361	3.361
Total						
Precast-top	-0.530	-0.459	-0.299	-0.184	-0.115	-0.092
Bottom	3.117	2.987	2.696	2.488	2.363	2.321

SERVICE I

POSITIVE ENVELOPE STRESSES, (ksi) (LOSS = 10.41 %)

Location, ft	Bearing	Trans	H/2	0.10L /0.90L	0.20L /0.80L	0.30L /0.70L	0.40L /0.60L	Midspan
0.00	2.06	0.88	3.55	7.54	11.53	15.51	19.50	
Prestress								
Precast-top	-0.110	-0.631	-0.331	-0.631	-0.631	-0.631	-0.631	-0.631
Bottom	0.558	3.188	1.674	3.188	3.188	3.188	3.188	3.188
Self wt.								
Precast-top	0.000	0.110	0.048	0.181	0.342	0.456	0.525	0.548
Bottom	-0.000	-0.199	-0.087	-0.329	-0.620	-0.828	-0.953	-0.995
DL-Prec (DC)								
Precast-top	-0.000	0.020	0.009	0.034	0.063	0.084	0.097	0.101
Bottom	0.000	-0.037	-0.016	-0.061	-0.115	-0.153	-0.176	-0.184
DL-Prec (DW)								
Precast-top	-0.000	0.032	0.014	0.053	0.100	0.133	0.153	0.160
Bottom	0.000	-0.058	-0.025	-0.096	-0.181	-0.242	-0.278	-0.290



Sheet #	15
Job #	
Program:	LEAP® CONSPAN® V8i (SELECTseries 5)
Version:	12.01.00.57
Copyright © Bentley Systems, Inc. 1984 - 2012	www.bentley.com
Phone: 1-800-778-4277	
File Name:	NEXT D8-39ft105nonTransform.csl

Academic Use Only	Designed	HS
Date	Oct/17/2013	
Checked		
Date		

	Bearing	Trans	H/2	0.10L /0.90L	0.20L /0.80L	0.30L /0.70L	0.40L /0.60L	Midspan
Diaphragm								
Precast-top	-0.000	-0.000	-0.000	-0.000	-0.000	-0.000	-0.000	-0.000
Bottom	-0.000	-0.000	-0.000	-0.000	-0.000	-0.000	-0.000	-0.000
Deck + Haunch								
Precast-top	-0.000	-0.000	-0.000	-0.000	-0.000	-0.000	-0.000	-0.000
Bottom	-0.000	-0.000	-0.000	-0.000	-0.000	-0.000	-0.000	-0.000
DL-Comp (DC)								
Precast-top	-0.000	-0.000	-0.000	-0.000	-0.000	-0.000	-0.000	-0.000
Bottom	-0.000	-0.000	-0.000	-0.000	-0.000	-0.000	-0.000	-0.000
DL-Comp (DW)								
Precast-top	-0.000	-0.000	-0.000	-0.000	-0.000	-0.000	-0.000	-0.000
Bottom	-0.000	-0.000	-0.000	-0.000	-0.000	-0.000	-0.000	-0.000
LL+I(+)								
Precast-top	0.000	0.318	0.140	0.519	0.942	1.199	1.342	1.379
Bottom	-0.000	-0.577	-0.255	-0.942	-1.709	-2.176	-2.436	-2.502
Final 1 (P/S + DL + LL)								
Precast-top	-0.110	-0.151	-0.120	0.156	0.816	1.242	1.487	1.557
Bottom	0.558	2.317	1.290	1.760	0.563	-0.212	-0.655	-0.783
Final 2 (P/S + DL)								
Precast-top	-0.110	-0.469	-0.260	-0.363	-0.126	0.043	0.145	0.178
Bottom	0.558	2.894	1.545	2.702	2.272	1.965	1.781	1.719

Span : 1, Beam : 1, SERVICE III

RELEASE STRESSES, (ksi) (LOSS = 5.55 %)

Location, ft	Trans	0.10L /0.90L	0.20L /0.80L	0.30L /0.70L	0.40L /0.60L	Midspan
2.50	3.99	7.98	11.96	15.95	19.94	
Beam-Self						
Precast-top	0.135	0.206	0.367	0.481	0.550	0.573
Bottom	-0.244	-0.374	-0.665	-0.873	-0.998	-1.040
Prestress						
Precast-top	-0.665	-0.665	-0.665	-0.665	-0.665	-0.665
Bottom	3.361	3.361	3.361	3.361	3.361	3.361



Sheet #	16
Job #	
Program:	LEAP® CONSPAN® V8i (SELECTseries 5)
Version:	12.01.00.57
Copyright © Bentley Systems, Inc. 1984 - 2012	www.bentley.com
Phone: 1-800-778-4277	
File Name:	NEXT D8-39ft105nonTransform.csl

Academic Use Only	Designed	HS
Date	Oct/17/2013	
Checked		
Date		

	Trans	0.10L /0.90L	0.20L /0.80L	0.30L /0.70L	0.40L /0.60L	Midspan
Total						
Precast-top	-0.530	-0.459	-0.299	-0.184	-0.115	-0.092
Bottom	3.117	2.987	2.696	2.488	2.363	2.321
As_top, in2	2.593	2.054	1.000	0.000	0.000	0.000
Ast_prvd, in2	4.800	4.800	4.800	4.800	4.800	4.800

SERVICE III

POSITIVE ENVELOPE STRESSES, (ksi) (LOSS = 10.41 %)

	Bearing	Trans	H/2	0.10L /0.90L	0.20L /0.80L	0.30L /0.70L	0.40L /0.60L	Midspan
Location, ft	0.00	2.06	0.88	3.55	7.54	11.53	15.51	19.50
Prestress								
Precast-top	-0.110	-0.631	-0.331	-0.631	-0.631	-0.631	-0.631	-0.631
Bottom	0.558	3.188	1.674	3.188	3.188	3.188	3.188	3.188
Self wt.								
Precast-top	0.000	0.110	0.048	0.181	0.342	0.456	0.525	0.548
Bottom	-0.000	-0.199	-0.087	-0.329	-0.620	-0.828	-0.953	-0.995
DL-Prec (DC)								
Precast-top	-0.000	0.020	0.009	0.034	0.063	0.084	0.097	0.101
Bottom	0.000	-0.037	-0.016	-0.061	-0.115	-0.153	-0.176	-0.184
DL-Prec (DW)								
Precast-top	-0.000	0.032	0.014	0.053	0.100	0.133	0.153	0.160
Bottom	0.000	-0.058	-0.025	-0.096	-0.181	-0.242	-0.278	-0.290
Diaphragm								
Precast-top	-0.000	-0.000	-0.000	-0.000	-0.000	-0.000	-0.000	-0.000
Bottom	-0.000	-0.000	-0.000	-0.000	-0.000	-0.000	-0.000	-0.000
Deck + Haunch								
Precast-top	-0.000	-0.000	-0.000	-0.000	-0.000	-0.000	-0.000	-0.000
Bottom	-0.000	-0.000	-0.000	-0.000	-0.000	-0.000	-0.000	-0.000
DL-Comp (DC)								
Precast-top	-0.000	-0.000	-0.000	-0.000	-0.000	-0.000	-0.000	-0.000
Bottom	-0.000	-0.000	-0.000	-0.000	-0.000	-0.000	-0.000	-0.000
DL-Comp (DW)								
Precast-top	-0.000	-0.000	-0.000	-0.000	-0.000	-0.000	-0.000	-0.000



Sheet #	17
Job #	
Program:	LEAP® CONSPAN® V8i (SELECTseries 5)
Version:	12.01.00.57
Copyright © Bentley Systems, Inc. 1984 - 2012	www.bentley.com
Phone: 1-800-778-4277	
File Name:	NEXT D8-39ft105nonTransform.csl

	Bearing	Trans	H/2	0.10L /0.90L	0.20L /0.80L	0.30L /0.70L	0.40L /0.60L	Midspan
Bottom	-0.000	-0.000	-0.000	-0.000	-0.000	-0.000	-0.000	-0.000
LL+I(+)								
Precast-top	0.000	0.254	0.112	0.415	0.753	0.959	1.074	1.103
Bottom	-0.000	-0.462	-0.204	-0.754	-1.367	-1.741	-1.949	-2.002
Final 1 (P/S + DL + LL)								
Precast-top	-0.110	-0.214	-0.148	0.052	0.627	1.002	1.218	1.281
Bottom	0.558	2.432	1.341	1.948	0.905	0.224	-0.168	-0.283

Span : 1, Beam : 1, FATIGUE I
 POSITIVE ENVELOPE STRESSES, (ksi)

Location, ft	Bearing	Trans	H/2	0.10L /0.90L	0.20L /0.80L	0.30L /0.70L	0.40L /0.60L	Midspan
	0.00	2.06	0.88	3.55	7.54	11.53	15.51	19.50
F_LL+I(+)								
Precast-top	-0.000	0.241	0.106	0.398	0.742	0.979	1.108	1.129
Bottom	-0.000	-0.438	-0.192	-0.721	-1.347	-1.777	-2.011	-2.049
Final 3 (50% P/S + 50% DL + F_LL)								
Precast-top	-0.055	0.007	-0.024	0.216	0.679	1.000	1.180	1.218
Bottom	0.279	1.009	0.580	0.630	-0.211	-0.794	-1.120	-1.189



Sheet #	18
Job #	
Program:	LEAP® CONSPAN® V8i (SELECTseries 5)
Version:	12.01.00.57
File Name:	NEXT D8-39ft105nonTransform.csl

Academic Use Only	Designed	HS
Copyright © Bentley Systems, Inc. 1984 - 2012	Date	Oct/17/2013
www.bentley.com	Checked	
Phone: 1-800-778-4277	Date	

VERTICAL/HORIZONTAL SHEAR

VERTICAL SHEAR (Art. 5.8) - Span : 1, Beam : 1, STRENGTH I
 Using General Beta Theta Equation procedure - Art.5.8.3.4.2

Location(ft)	Vu (kips)	bv (in)	de (in)	Aps (in ²)	Vp (kips)	eps_x	Theta	Vs-reqd (kips)	Av/s (in ² /ft)	Av-prvd (in ² /ft)	Al_reqd (in ²)
	Mcor (kft)	a (in)	dv (in)	fpo (ksi)	vu/fc	Vc-com (kips)	Beta	Max.spc. (in)	min.Av/s (in ² /ft)	pVn/Vu	Aps* (in ²)
Bearing :		0.44									
166.0	29.19	16.81	0.309	0.0	6.00e-3	50.0	150.3	2.150	6.400	0.00	
0.0	0.29	16.66	33.1	0.058	34.2	0.87	13.33	0.470	2.610	0.495	
Transfer :		2.50									
151.5	29.19	16.81	3.978	0.0	-0.13e-3	28.6	0.0	0.470	0.533	0.00	
309.0	1.64	15.99	189.0	0.056	199.4	5.30	12.79	0.470	1.649	2.827	
Critical :		1.79									
156.5	29.19	16.81	3.978	0.0	-0.15e-3	28.5	0.0	0.470	1.600	0.00	
202.0	1.18	16.22	189.0	0.057	206.4	5.41	12.97	0.470	2.562	2.023	
0.1L :		3.99									
141.1	29.19	16.81	3.978	0.0	-0.08e-3	28.7	0.0	0.470	0.533	0.00	
502.3	1.96	15.83	189.0	0.052	190.0	5.10	12.66	0.470	1.703	3.376	
0.2L :		7.97									
115.1	29.19	16.81	3.978	0.0	0.45e-3	30.6	0.0	0.470	0.533	0.00	
897.8	2.30	15.66	189.0	0.043	131.9	3.58	12.53	0.470	1.583	3.978	
0.3L :		11.96									
90.0	29.19	16.81	3.978	0.0	1.89e-3	35.6	26.7	0.470	0.533	0.00	
1142.5	2.30	15.66	189.0	0.034	73.2	1.99	12.53	0.470	1.316	3.978	
0.4L :		15.95									
67.4	29.19	16.81	3.978	0.0	2.53e-3	37.9	13.9	0.470	0.533	0.00	
1267.8	2.30	15.66	189.0	0.025	61.0	1.66	12.53	0.470	1.531	3.978	
0.5L :		19.94									
46.9	29.19	16.81	3.978	0.0	2.53e-3	37.8	0.0	0.470	0.533	0.00	
1293.6	2.30	15.66	189.0	0.018	61.1	1.66	12.53	0.470	2.205	3.978	
0.6L :		23.93									
67.4	29.19	16.81	3.978	0.0	2.53e-3	37.9	13.9	0.470	0.533	0.00	
1267.8	2.30	15.66	189.0	0.025	61.0	1.66	12.53	0.470	1.531	3.978	
0.7L :		27.91									
90.0	29.19	16.81	3.978	0.0	1.89e-3	35.6	539 26.7	0.470	0.533	0.00	



Sheet #	19
Job #	
Program:	LEAP® CONSPAN® V8i (SELECTseries 5)
Version:	12.01.00.57
Copyright © Bentley Systems, Inc. 1984 - 2012	www.bentley.com
Phone: 1-800-778-4277	
File Name:	NEXT D8-39ft105nonTransform.csl

Location(ft)	Vu (kips)	bv (in)	de (in)	Aps (in2)	Vp (kips)	eps_x	Theta	Vs-reqd (kips)	Av/s (in2/ft)	Av-prvd (in2/ft)	Al_reqd (in2)
Mcor (kft)	a (in)	dv (in)	fpo (ksi)	vu/fc	Vc-com (kips)	Beta	Max.spc. (in)	min.Av/s (in2/ft)	pVn/Vu	Aps* (in2)	
	1142.5	2.30	15.66	189.0	0.034	73.2	1.99	12.53	0.470	1.316	3.978
0.8L :		31.90									
	115.1	29.19	16.81	3.978	0.0	0.45e-3	30.6	0.0	0.470	0.533	0.00
	897.8	2.30	15.66	189.0	0.043	131.9	3.58	12.53	0.470	1.583	3.978
0.9L :		35.89									
	141.1	29.19	16.81	3.978	0.0	-0.08e-3	28.7	0.0	0.470	0.533	0.00
	502.3	1.96	15.83	189.0	0.052	190.0	5.10	12.66	0.470	1.703	3.376
Critical :		38.09									
	156.5	29.19	16.81	3.978	0.0	-0.15e-3	28.5	0.0	0.470	1.600	0.00
	202.0	1.18	16.22	189.0	0.057	206.4	5.41	12.97	0.470	2.562	2.023
Transfer :		37.38									
	151.5	29.19	16.81	3.978	0.0	-0.13e-3	28.6	0.0	0.470	0.533	0.00
	309.0	1.64	15.99	189.0	0.056	199.4	5.30	12.79	0.470	1.649	2.827
Bearing :		39.44									
	166.0	29.19	16.81	0.309	0.0	6.00e-3	50.0	150.3	2.150	2.400	0.00
	0.0	0.29	16.66	33.1	0.058	34.2	0.87	13.33	0.470	1.095	0.495

ANCHORAGE ZONE REINFORCEMENT (Art. 5.10.10)

Span : 1, Beam : 1

Fpi (kips)	fs (ksi)	h/4 (in)	Abrst_rqrd (in2)
929.47	20.00	5.25	1.86



Sheet #	20
Job #	
Program:	LEAP® CONSPAN® V8i (SELECTseries 5)
Version:	12.01.00.57
Copyright © Bentley Systems, Inc. 1984 - 2012	Date
www.bentley.com	Checked
Phone: 1-800-778-4277	Date

Academic Use Only	Designed	HS
File Name: NEXT D8-39ft105nonTransform.csl	Date	

CAMBER/DEFLECTION

CAMBER AND DEFLECTIONS: SERVICE I
(Span : 1, Beam : 1; Units: in)

	Release	Mult	Erection	Mult	Final
At 0.1 x L =	3.55 ft				
Prestress	0.445	1.80	0.802	2.45	1.091
Self Wt.	-0.132	1.85	-0.243	2.70	-0.355
Deck + Haunch			0.000	2.30	0.000
DL-Prec. (DC)			-0.018	3.00	-0.055
Diaphragm			0.000	3.00	0.000
DL-Prec. (DW)			-0.029	3.00	-0.086
DL-Comp. (DC)			0.000	3.00	0.000
DL-Comp. (DW)			0.000	3.00	0.000
Live Load					-0.195
Total	0.314		0.511		0.400

	Release	Mult	Erection	Mult	Final
At 0.2 x L =	7.54 ft				
Prestress	0.797	1.80	1.434	2.45	1.952
Self Wt.	-0.249	1.85	-0.460	2.70	-0.672
Deck + Haunch			0.000	2.30	0.000
DL-Prec. (DC)			-0.037	3.00	-0.110
Diaphragm			0.000	3.00	0.000
DL-Prec. (DW)			-0.058	3.00	-0.173
DL-Comp. (DC)			0.000	3.00	0.000
DL-Comp. (DW)			0.000	3.00	0.000
Live Load					-0.393
Total	0.548		0.879		0.604

	Release	Mult	Erection	Mult	Final
At 0.3 x L =	11.52 ft				
Prestress	1.048	1.80	1.886	2.45	2.567
Self Wt.	-0.341	1.85	-0.630	2.70	-0.920
Deck + Haunch			0.000	2.30	0.000
DL-Prec. (DC)			-0.051	3.00	-0.153
Diaphragm			0.000	3.00	0.000
DL-Prec. (DW)			-0.081	3.00	-0.242
DL-Comp. (DC)			0.000	3.00	0.000
DL-Comp. (DW)			0.000	3.00	0.000
Live Load					-0.546
Total	0.707		1.124		0.706

	Release	Mult	Erection	Mult	Final
At 0.4 x L =	15.51 ft				
Prestress	1.198	1.80	2.157	2.45	2.936



Sheet #	21
Job #	
Program:	LEAP® CONSPAN® V8i (SELECTseries 5)
Version:	12.01.00.57
Copyright © Bentley Systems, Inc. 1984 - 2012	www.bentley.com
Phone: 1-800-778-4277	
File Name:	NEXT D8-39ft105nonTransform.csl

Academic Use Only	Designed	HS
Date	Oct/17/2013	
Checked		
Date		

	Release	Mult	Erection	Mult	Final
Self Wt.	-0.399	1.85	-0.738	2.70	-1.077
Deck + Haunch			0.000	2.30	0.000
DL-Prec. (DC)			-0.060	3.00	-0.181
Diaphragm			0.000	3.00	0.000
DL-Prec. (DW)			-0.095	3.00	-0.285
DL-Comp. (DC)			0.000	3.00	0.000
DL-Comp. (DW)			0.000	3.00	0.000
Live Load					-0.642
Total	0.799		1.264		0.750

	Release	Mult	Erection	Mult	Final
At 0.5 x L = 19.50 ft					
Prestress	1.249	1.80	2.247	2.45	3.059
Self Wt.	-0.419	1.85	-0.775	2.70	-1.131
Deck + Haunch			0.000	2.30	0.000
DL-Prec. (DC)			-0.063	3.00	-0.190
Diaphragm			0.000	3.00	0.000
DL-Prec. (DW)			-0.100	3.00	-0.300
DL-Comp. (DC)			0.000	3.00	0.000
DL-Comp. (DW)			0.000	3.00	0.000
Live Load					-0.674
Total	0.830		1.309		0.763

	Release	Mult	Erection	Mult	Final
At 0.6 x L = 23.49 ft					
Prestress	1.198	1.80	2.157	2.45	2.936
Self Wt.	-0.399	1.85	-0.738	2.70	-1.077
Deck + Haunch			0.000	2.30	0.000
DL-Prec. (DC)			-0.060	3.00	-0.181
Diaphragm			0.000	3.00	0.000
DL-Prec. (DW)			-0.095	3.00	-0.285
DL-Comp. (DC)			0.000	3.00	0.000
DL-Comp. (DW)			0.000	3.00	0.000
Live Load					-0.642
Total	0.799		1.264		0.750

	Release	Mult	Erection	Mult	Final
At 0.7 x L = 27.48 ft					
Prestress	1.048	1.80	1.886	2.45	2.567
Self Wt.	-0.341	1.85	-0.630	2.70	-0.920
Deck + Haunch			0.000	2.30	0.000
DL-Prec. (DC)			-0.051	3.00	-0.153
Diaphragm			0.000	3.00	0.000
DL-Prec. (DW)			-0.081	3.00	-0.242
DL-Comp. (DC)			0.000	3.00	0.000
DL-Comp. (DW)			0.000	3.00	0.000
Live Load					-0.546



Sheet #	22
Job #	
Program:	LEAP® CONSPAN® V8i (SELECTseries 5)
Version:	12.01.00.57
Copyright © Bentley Systems, Inc. 1984 - 2012	www.bentley.com
Phone: 1-800-778-4277	
File Name:	NEXT D8-39ft105nonTransform.csl

Academic Use Only	Designed	HS
Date	Oct/17/2013	
Checked		
Date		

	Release	Mult	Erection	Mult	Final
Total	0.707		1.124		0.706

	Release	Mult	Erection	Mult	Final
At 0.8 x L =	31.46 ft				
Prestress	0.797	1.80	1.434	2.45	1.952
Self Wt.	-0.249	1.85	-0.460	2.70	-0.672
Deck + Haunch			0.000	2.30	0.000
DL-Prec. (DC)			-0.037	3.00	-0.110
Diaphragm			0.000	3.00	0.000
DL-Prec. (DW)			-0.058	3.00	-0.173
DL-Comp. (DC)			0.000	3.00	0.000
DL-Comp. (DW)			0.000	3.00	0.000
Live Load					-0.393
Total	0.548		0.879		0.604

	Release	Mult	Erection	Mult	Final
At 0.9 x L =	35.45 ft				
Prestress	0.445	1.80	0.802	2.45	1.091
Self Wt.	-0.132	1.85	-0.243	2.70	-0.355
Deck + Haunch			0.000	2.30	0.000
DL-Prec. (DC)			-0.018	3.00	-0.055
Diaphragm			0.000	3.00	0.000
DL-Prec. (DW)			-0.029	3.00	-0.086
DL-Comp. (DC)			0.000	3.00	0.000
DL-Comp. (DW)			0.000	3.00	0.000
Live Load					-0.195
Total	0.314		0.511		0.400



Sheet #	23
Job #	
Program:	LEAP® CONSPAN® V8i (SELECTseries 5)
Version:	12.01.00.57
Copyright © Bentley Systems, Inc. 1984 - 2012	www.bentley.com
Phone: 1-800-778-4277	
File Name:	NEXT D8-39ft105nonTransform.csl

ULTIMATE MOMENT

ULTIMATE - Span : 1, Beam : 1, STRENGTH I
 (Mr-prvd computed by Strain Compatibility method. Ult. Conc. Strain = 0.00300)

Location (ft)	dp in	Aps in ²	fps ksi	c in	a in	Mr-prvd k.ft	c/dt	Phi	Mcr k.ft	min Mr k.ft	Crkg Ratio	Mu-p/r Ratio
Transfer	2.06											
318.1	15.6	3.262	267.3	2.3	1.6	1072.7	0.122T	1.00	-	-	-	-
H/2	0.88											
140.1	15.6	1.712	268.8	1.2	0.9	580.6	0.064T	1.00	-	-	-	-
0.1L	3.55											
520.9	15.6	3.895	266.7	2.7	2.0	1264.8	0.145T	1.00	-	-	-	-
0.2L	7.54											
955.3	15.6	4.590	265.8	3.2	2.3	1469.2	0.170T	1.00	1024.9	1024.9	1.43	-
0.3L	11.53											
1233.3	15.6	4.590	265.8	3.2	2.3	1469.2	0.170T	1.00	1024.9	1024.9	1.43	-
0.4L	15.51											
1391.7	15.6	4.590	265.8	3.2	2.3	1469.2	0.170T	1.00	1024.9	1024.9	1.43	-
0.5L	19.50											
1436.5	15.6	4.590	265.8	3.2	2.3	1469.2	0.170T	1.00	1024.9	1024.9	1.43	-
0.6L	23.49											
1391.7	15.6	4.590	265.8	3.2	2.3	1469.2	0.170T	1.00	1024.9	1024.9	1.43	-
0.7L	27.48											
1233.3	15.6	4.590	265.8	3.2	2.3	1469.2	0.170T	1.00	1024.9	1024.9	1.43	-
0.8L	31.46											
955.3	15.6	4.590	265.8	3.2	2.3	1469.2	0.170T	1.00	1024.9	1024.9	1.43	-
0.9L	35.45											
520.9	15.6	3.895	266.7	2.7	2.0	1264.8	0.145T	1.00	-	-	-	-
H/2	38.13											
140.1	15.6	1.712	268.8	1.2	0.9	580.6	0.064T	1.00	-	-	-	-
Transfer	36.94											
318.1	15.6	3.262	267.3	2.3	1.6	1072.7	0.122T	1.00	-	-	-	-

Legend: C = Compression-Controlled (c/dt > 0.600)
 I = In-Transition (0.60 >= c/dt > 0.375)
 T = Tension-Controlled (c/dt <= 0.375)
 Note : fr used for calculating Mcr is computed using AASHTO method (Art.5.4.2.6.)
 Consider Bottom Tension Steel Contribution : NO



Sheet #	24
Job #	
Program:	LEAP® CONSPAN® V8i (SELECTseries 5)
Version:	12.01.00.57
Copyright © Bentley Systems, Inc. 1984 - 2012	www.bentley.com
Phone: 1-800-778-4277	
File Name:	NEXT D8-39ft105nonTransform.csl

Academic Use Only	Designed	HS
Date	Oct/17/2013	Checked
Date		

DETENSIONING

Span : 1, Beam : 1; Groups 1-15; Units: ksi

Grp	Str	Ys,in	2.50ft
1	E	2.50	Ft 0.056
	M	2.50	Fb 0.042
2	E	13.50	Ft 0.107
	M	13.50	Fb 0.094
3	E	13.50	Ft 0.157
	M	13.50	Fb 0.146
4	E	6.50	Ft 0.125
	M	6.50	Fb 0.347
5	E	6.50	Ft 0.093
	M	6.50	Fb 0.548
6	E	6.50	Ft 0.062
	M	6.50	Fb 0.750
7	E	4.50	Ft 0.006
	M	4.50	Fb 0.994
8	E	4.50	Ft -0.049
	M	4.50	Fb 1.238
9	E	4.50	Ft -0.104
	M	4.50	Fb 1.482
10	E	4.50	Ft -0.160
	M	4.50	Fb 1.726
11	E	4.50	Ft -0.215
	M	4.50	Fb 1.970
12	E	2.50	Ft -0.294
	M	2.50	Fb 2.256
13	E	2.50	Ft -0.373
	M	2.50	Fb 2.543
14	E	2.50	Ft -0.451
	M	2.50	Fb 2.830
15	E	2.50	Ft -0.530
	M	2.50	Fb 3.116



		Sheet #	25
		Job #	
Program:	LEAP® CONSPAN® V8i (SELECTseries 5)	Academic Use Only	Designed HS
Version:	12.01.00.57	Copyright © Bentley Systems, Inc. 1984 - 2012	Date Oct/17/2013
		www.bentley.com	Phone: 1-800-778-4277
File Name:	NEXT D8-39ft105nonTransform.csl		Checked
			Date

DESIGN SUMMARY

Span: 1, Beam: 1, Exterior beam

Beam type:	Double Tee,	Next D8-21-exterior
Precast Length,	ft	39.88
Release Length,	ft	39.88
Strand Pattern:	Straight	
Strand:	1/2-270K-LL	
Strand Es,	ksi:	28500.0
No. of strands:	30	
	Draped:	0
	Straight:	30
Concrete Strength:		
	f'ci:	5.2 ksi
	f'c:	6.5 ksi
	f'ct:	6.5 ksi
Initial losses:	5.55 %	
Final losses:	10.41 %	

Specification	Allowable	Computed	Location	Status
Release Stresses (ksi) (Art. 5.9.4.1)				
Precast Bot (compression)	3.120	3.117	Trans	OK
Precast Top w/ no reinf. (tension)	-0.200	-0.530	Trans	
Precast Top w/ reinf. (tension)	-0.547			
Strength I (Art. 3.4.1, 5.7.3.1.1)	Provided	Required	Location	Status
Ult. Moment (k.ft)	1469.15	1436.47	Midspan	OK
Debonding Limits (Art. 5.11.4.3)	Allowable	Computed		Status
Max. Debond per Row	40.00 %	0.00 %		OK
Max. Debond Total	25.00 %	0.00 %		OK

Positive Moment Envelope Stresses (ksi) (Art. 3.4.1 and 5.9.4.2)



Sheet #	26
Job #	
Program:	LEAP® CONSPAN® V8i (SELECTseries 5)
Version:	12.01.00.57
Copyright © Bentley Systems, Inc. 1984 - 2012	www.bentley.com
Phone: 1-800-778-4277	
File Name:	NEXT D8-39ft105nonTransform.csl

Academic Use Only	Designed	HS
Date	Oct/17/2013	
Checked		
Date		

Specification	Allow	Final 1 Comp	Loc.	Allow	Final 2 Comp	Loc.	Allow	Final 3 Comp	Loc.
Service I Limit State - Compressive	Stresses	Only							
Precast Top	3.900	1.557	Midspan	2.925	0.178	Midspan			
Precast Bot	3.900	2.317	Transfer	2.925	2.894	Transfer			
Service III Limit State - Tensile	Stresses	Only							
Precast Top	-0.484	-0.214	Transfer						
Precast Bot	-0.484	-0.283	Midspan						
Fatigue I Limit State - Compressive	Stresses	Only							
Precast Top							2.600	1.218	Midspan
Precast Bot							2.600	1.009	Transfer

CAMBER / DEFLECTION: (PCI Design Handbook - 4th Ed.- Table 4.6.2)
0.5 x L = 19.50 ft

	Release	Mult	Erection	Mult	Final
Prestress	1.249	1.80	2.247	2.45	3.059
Self Wt.	-0.419	1.85	-0.775	2.70	-1.131
Deck + Haunch			0.000	2.30	0.000
DL-Prec. (DC)			-0.063	3.00	-0.190
Diaphragm			0.000	3.00	0.000
DL-Prec. (DW)			-0.100	3.00	-0.300
DL-Comp. (DC)			0.000	3.00	0.000
DL-Comp. (DW)			0.000	3.00	0.000
Live Load					-0.674
Total	0.830		1.309		0.763

Positive values indicate upward deflection.

K.6 NEXT-8 40 ft. - Interior Beam Output



Sheet #	1
Job #	
Program:	LEAP® CONSPAN® V8i (SELECTseries 5)
Version:	12.01.00.57
File Name:	NEXT D8-39ft105nonTransform.csl
Academic Use Only	
Copyright © Bentley Systems, Inc. 1984 - 2012	
www.bentley.com	Phone: 1-800-778-4277
Designed	HS
Date	Oct/17/2013
Checked	
Date	

PROPERTIES

Span:1, Beam:2

PRECAST DATA:

Section Id	Next D8-21-interior		
Type	Double Tee		
Fling width	Top	96.000	in
thick	Top	8.000	in
Stems	No	2	
	Top	15.000	in
	Bot	14.190	in
Shear width		29.190	in

Minimum Thickness Criteria, Article 5.14.1.2.2 checked: OK.

GENERAL BRIDGE DATA:

Bridge Width	48.00	ft
Curb-to-curb	44.83	ft
Beam Spac. Lt./Rt	8.00/ 8.00	ft
Lane width	12.00	ft
Number of lanes	3	
Interior/Exterior	Interior	
Start Skew Angle	0.00	degrees
End Skew Angle	0.00	degrees

TOPPING DATA:

Deck	Thickness	0.000	in	
Haunch:	Thickness	0.000	in	
	Width	0.000	in	
Effective	width	96.000	in	(Art. 4.6.2.6.1)

GENERAL LOAD DATA:

DEAD LOADS ON PRECAST

UNITS: (Point: kips, Location: ft, Line: klf, Trapez: klf)

DC/DW	Type	Mag.1	Loc.1	Mag.2	Loc.2	Description
DC	Line	0.221	0.000	0.221	39.000	Barrier Parapet
DW	Line	0.349	0.000	0.349	39.000	4 in bituminous wearing

Dead loads on composite: See Project info for composite loads

GENERAL SPAN DATA:



Sheet #	2
Job #	
Program:	LEAP® CONSPAN® V8i (SELECTseries 5)
Version:	12.01.00.57
Copyright © Bentley Systems, Inc. 1984 - 2012	www.bentley.com
Phone: 1-800-778-4277	
File Name:	NEXT D8-39ft105nonTransform.csl

Academic Use Only	Designed	HS
Date	Oct/17/2013	Checked
Date		

Overall length	39.875	ft
Release length	39.875	ft
Design length	39.000	ft

KERN POINTS:

Upper	15.93	in
Lower	9.20	in

DISTRIBUTION FACTORS (Art. 4.6.2.2):

Type i, post-tensioned

Live Moment	(2+ lanes loaded)	0.677	(Calculated)
Live Moment	(1 lane loaded)	0.514	(Calculated)
Live Shear	(2+ lanes loaded)	0.825	(Calculated)
Live Shear	(1 lane loaded)	0.681	(Calculated)

Pedestrian	0.167	(Calculated)
Comp. DC	0.167	(Calculated)
Comp. DW	0.167	(Calculated)

Dead Loads and Pedestrian Load distributed equally to all beams (Art. 4.6.2.2.1)

RESISTANCE FACTORS (Art. 5.5.4.2):

Flexure Reinforced	
Compression controlled sections	0.75
Tension controlled sections	0.90
Flexure Prestressed	
Compression controlled sections	0.75
Tension controlled sections	1.00
Shear	0.90

SECTION PROPERTIES:

	PRECAST		COMPOSITE		
Area	1147.4	in ²	1147.4	in ²	#
Total Height	21.00	in	21.00	in	
Mom. of Inertia (I _{xx})	37120	in ⁴	37120	in ⁴	#
Ht. of c.g.	13.54	in	13.54	in	#
Density	150.00	pcf	150.00	pcf	
Self-weight	1195.2	plf	1195.2	plf	
Mom. of Inertia (I _{yy})	719514.1	in ⁴			
Poisson's Ratio	0.2				
Thermal Coeff.	0.000006000	1/°F			



Sheet #	3
Job #	
Program:	LEAP® CONSPAN® V8i (SELECTseries 5)
Version:	12.01.00.57
File Name:	NEXT D8-39ft105nonTransform.csl
Academic Use Only	
Copyright © Bentley Systems, Inc. 1984 - 2012	
www.bentley.com	Phone: 1-800-778-4277
Designed	HS
Date	Oct/17/2013
Checked	
Date	

(#) Of Total Section using Ect/Ec = 1.0000
 Use transformed strand and rebar: No

Span:1, Beam:2

STRESS LIMITS (Art. 5.9.4):

STRESS LIMITS AT RELEASE BEFORE LOSSES:

	PRECAST	
Strength	5.20	ksi
Elasticity	4371.7	ksi
Max comp	3.12	ksi
Max tens	-0.20	ksi
Max tens, w/reinf	-0.55	ksi

STRESS LIMITS AT FINAL AFTER LOSSES:

	PRECAST		DECK	
Strength	6.50	ksi	6.50	ksi
Elasticity	4887.73	ksi	4887.73	ksi

STRESS LIMITS AT FINAL 1 (P/S + DL + LL):

	PRECAST		DECK	
Max comp	3.90	ksi	3.90	ksi

STRESS LIMITS AT FINAL 2 (P/S + DL):

	PRECAST		DECK	
Max comp	2.93	ksi	2.93	ksi

FATIGUE I STRESS LIMITS AT FINAL 3 (50% P/S + 50% DL + F_LL) (Art. 5.5.3.1):

	PRECAST		DECK	
Max comp	2.60	ksi	-	ksi

SERVICE III (Tension):

	PRECAST		DECK	
Max tens	-0.48	ksi	-0.48	ksi

Span:1, Beam:2

PRESTRESSED STEEL:

26 strands, 1/2-270K-LL, Low relaxation strands

Straight Pattern



		Sheet #	4
		Job #	
Program:	LEAP® CONSPAN® V8i (SELECTseries 5)	Academic Use Only	Designed
Version:	12.01.00.57	Copyright © Bentley Systems, Inc. 1984 - 2012	Date
		www.bentley.com	Phone: 1-800-778-4277
File Name:	NEXT D8-39ft105nonTransform.csl	Checked	Date

END PATTERN (Ycg = 5.27 in):

10 @ 2.500 in	10 @ 4.500 in	2 @ 6.500 in	4 @ 13.500 in
---------------	---------------	--------------	---------------

Strand Diameter	0.500	in
Strand Area	0.153	in ²
Total Strand Area	3.978	in ²
Trans. Len, bonded	2.500	ft
Trans. Len, debonded	2.500	ft
Dev. Len, bonded	5.653	ft
Dev. Len, debonded	11.306	ft
Holddown Force	0.000	kips
Tensile Strength(fpu)	270.0	ksi
Initial Prestress = 0.75fpu	202.5	ksi
Initial Pull	805.5	kips
Beam Shrtng (PL/AE)	0.073	in

Span:1, Beam:2

ESTIMATED QUANTITIES

Prestressing (linear ft)	Strands (LB/1000ft)	(LB)	Beam Vol(C.Y.)	Concrete Wt(LB)	Stirrups (LB)	Longitudinal Bars (LB)
1036.750	520	539.110	11.768	47659.035	166.757	645.924

Span:1, Beam:2

REINFORCING STEEL:

Tension	steel:	
fy	60.0	ksi
Es	29000	ksi
fs	24.0	ksi

Stirrups:

# legs	Size	fy (ksi)	Area (in ²)	Spacing (in)	Start (ft)	End (ft)	Extends into Deck
4	US#4[M13]	60.0	0.80	1.50	0.1900	0.4400	No
2	US#4[M13]	60.0	0.40	2.00	0.4400	0.9400	No
2	US#4[M13]	60.0	0.40	3.00	0.9400	1.9400	No
2	US#4[M13]	60.0	0.40	9.00	1.9400	37.9400	No
2	US#4[M13]	60.0	0.40	3.00	37.9400	38.9400	No
2	US#4[M13]	60.0	0.40	2.00	38.9400	39.4400	No
4	US#4[M13]	60.0	0.80	1.50	39.4400	39.6900	No

Top Steel:

#bars	Size	Dist. from Top (in)	Area (in ²)	Start (ft)	End (ft)	Side Cover (in)
12	US#4[M13]	2.25	2.400	0.1667	39.7083	5.50
12	US#4[M13]	6.25	2.400	0.1667	39.7083	5.50



		Sheet #	5	
		Job #		
Program:	LEAP® CONSPAN® V8i (SELECTseries 5)	Academic Use Only	Designed	HS
Version:	12.01.00.57	Copyright © Bentley Systems, Inc. 1984 - 2012	Date	Oct/17/2013
		www.bentley.com	Phone: 1-800-778-4277	Checked
File Name:	NEXT D8-39ft105nonTransform.csl		Date	

Bottom Steel:

#bars	Size	Dist. from Top (in)	Area (in ²)	Start (ft)	End (ft)	Side Cover (in)
-------	------	---------------------	-------------------------	------------	----------	-----------------

LOSSES

Note: Values are calculated at Midspan

Str. area	3.9780	in ²
Ycg	5.27	in
P_init	805.5	kips
Ecc	8.27	in
Days to release	0.75	
Rel. Humid.(RH)	75.0	%
Es	28500.0	ksi
Eci	4372	ksi

AASHTO LOSSES

Elastic Shortening 9.61 ksi (Eq 5.9.5.2.3a-1), (fcgp= 1.474 ksi)

Elastic Gains		Gains		Adjustment	
due to Precast Loads		-1.69	ksi	0.10	ksi
due to Composite Loads		-0.00	ksi	0.00	ksi
due to Live Loads		-5.94	ksi	0.44	ksi

Time Dependent Losses (Approximate Method (Art.5.9.5.3))

	Initial	Final	
Steel relaxation	0.00 ksi	2.40 ksi	(Eq 5.9.5.3-1)
Concrete shrinkage	0.00 ksi	9.19 ksi	(Eq 5.9.5.3-1)
Concrete creep	0.00 ksi	5.38 ksi	(Eq 5.9.5.3-1)
Sub-total	9.61 ksi	9.88 ksi	(4.88 %)
Total Prestress Losses		19.49 ksi	(9.63 %)

Prestressing Stress Limit Check (Table 5.9.3.1)

initial fpi = 202.5 ksi < 0.75 fpu, OK
 initial fpe = 183.0 ksi < 0.80 fpy, OK



Sheet #	6
Job #	
Program:	LEAP® CONSPAN® V8i (SELECTseries 5)
Version:	12.01.00.57
Copyright © Bentley Systems, Inc. 1984 - 2012	Date
www.bentley.com	Phone: 1-800-778-4277
File Name:	NEXT D8-39ft105nonTransform.csl

Academic Use Only	Designed	HS
Oct/17/2013	Checked	
Date	Date	

SHEAR/MOMENT ENVELOPE (&REACTIONS)

SHEAR AND MOMENT ENVELOPE : Span : 1, Beam : 2, SERVICE I
 Shears: kips, Moments: kft

		Bearing	Trans	H/2	0.10L	0.20L	0.30L	0.40L	Midspan
Location,	ft	0.00	2.06	0.88	3.55	7.54	11.53	15.51	19.50
Self wt. :	M	0.0	45.5	19.9	75.2	141.7	189.2	217.7	227.2
(Max)	V	23.3	20.8	22.3	19.1	14.3	9.5	4.8	0.0
DL-Prec. :	M	-0.0	8.4	3.7	13.9	26.2	35.0	40.3	42.0
DC(Max)	V	4.3	3.9	4.1	3.5	2.6	1.8	0.9	0.0
DL-Prec. :	M	-0.0	13.3	5.8	22.0	41.4	55.3	63.6	66.4
DW(Max)	V	6.8	6.1	6.5	5.6	4.2	2.8	1.4	0.0
Deck + :	M	0.0	0.0	0.0	0.0	0.0	0.0	0.0	0.0
Haunch (Max)	V	0.0	0.0	0.0	0.0	0.0	0.0	0.0	0.0
Diaphragm :	M	0.0	0.0	0.0	0.0	0.0	0.0	0.0	0.0
(Max)	V	0.0	0.0	0.0	0.0	0.0	0.0	0.0	0.0
DL-Comp :	M	0.0	0.0	0.0	0.0	0.0	0.0	0.0	0.0
DC(Max)	V	0.0	0.0	0.0	0.0	0.0	0.0	0.0	0.0
DL-Comp :	M	0.0	0.0	0.0	0.0	0.0	0.0	0.0	0.0
DW(Max)	V	0.0	0.0	0.0	0.0	0.0	0.0	0.0	0.0
LL + I :	M+	0.0	109.9	48.5	179.4	325.4	414.4	463.8	476.4
	V	70.4	64.7	68.0	60.6	50.6	40.8	4.9	24.6
LL + I :	M-	0.0	0.0	0.0	0.0	0.0	0.0	0.0	0.0
	V	0.0	0.0	0.0	0.0	0.0	0.0	0.0	0.0
LL + I :	Vmx	70.4	64.7	68.0	60.6	50.9	41.6	33.8	27.2
	M	0.0	110.9	49.3	179.4	314.8	393.5	430.5	435.2
Total :	M+	0.0	177.1	78.0	290.4	534.7	693.9	785.3	812.0
	V	104.8	95.5	100.9	88.8	71.8	54.9	12.0	24.6
Total :	M-	0.0	0.0	0.0	0.0	0.0	0.0	0.0	0.0
	V	0.0	0.0	0.0	0.0	0.0	0.0	0.0	0.0
Total :	Vmx	104.8	95.5	100.9	88.8	72.0	55.7	40.9	27.2
	M	0.0	178.2	78.8	290.4	524.1	673.0	752.1	770.8

		0.60L	0.70L	0.80L	0.90L	H/2	Trans	Bearing
Location,	ft	23.49	27.47	31.46	35.45	38.13	36.94	39.00
Self wt. :	M	217.7	189.2	141.7	75.2	19.9	45.5	0.0
(Max)	V	4.8	9.5	14.3	19.1	22.3	20.8	23.3
DL-Prec. :	M	40.3	35.0	26.2	13.9	3.7	8.4	0.0
DC(Max)	V	0.9	1.8	2.6	3.5	4.1	3.9	4.3
DL-Prec. :	M	63.6	55.3	41.4	22.0	5.8	13.3	-0.0
DW(Max)	V	1.4	2.8	4.2	5.6	6.5	6.1	6.8
Deck + :	M	0.0	0.0	0.0	0.0	0.0	0.0	0.0
Haunch (Max)	V	0.0	0.0	0.0	0.0	0.0	0.0	0.0
Diaphragm :	M	0.0	0.0	0.0	0.0	0.0	0.0	0.0
(Max)	V	0.0	0.0	0.0	0.0	0.0	0.0	0.0
DL-Comp :	M	0.0	0.0	0.0	0.0	0.0	0.0	0.0
DC(Max)	V	0.0	0.0	0.0	0.0	0.0	0.0	0.0
DL-Comp :	M	0.0	0.0	0.0	0.0	0.0	0.0	0.0
DW(Max)	V	0.0	0.0	0.0	0.0	0.0	0.0	0.0



Sheet #	7
Job #	
Program:	LEAP® CONSPAN® V8i (SELECTseries 5)
Version:	12.01.00.57
Copyright © Bentley Systems, Inc. 1984 - 2012	www.bentley.com
Phone: 1-800-778-4277	
File Name:	NEXT D8-39ft105nonTransform.csl

Academic Use Only	Designed	HS
Date	Oct/17/2013	
Checked		
Date		

		0.60L	0.70L	0.80L	0.90L	H/2	Trans	Bearing
LL + I :	M+	463.8	414.4	325.4	179.4	48.5	109.9	0.0
	V	4.9	40.8	50.6	60.6	68.0	64.7	70.4
LL + I :	M-	0.0	0.0	0.0	0.0	0.0	0.0	0.0
	V	0.0	0.0	0.0	0.0	0.0	0.0	0.0
LL + I :	Vmx	33.8	41.6	50.9	60.6	68.0	64.7	70.4
	M	430.5	393.5	314.8	179.4	49.3	110.9	0.0
Total :	M+	785.3	693.9	534.7	290.4	78.0	177.1	0.0
	V	12.0	54.9	71.8	88.8	100.9	95.5	104.8
Total :	M-	0.0	0.0	0.0	0.0	0.0	0.0	0.0
	V	0.0	0.0	0.0	0.0	0.0	0.0	0.0
Total :	Vmx	40.9	55.7	72.0	88.8	100.9	95.5	104.8
	M	752.1	673.0	524.1	290.4	78.8	178.2	0.0

REACTIONS (kips), SERVICE I

Load Type	Left Support	Right Support
Self Wt.	23.3	23.3
Deck+Haunch	0.0	0.0
Diaphragm	0.0	0.0
DL-Prec.(DC)	4.3	4.3
DL-Prec.(DW)	6.8	6.8
DL-Comp.(DC)	0.0	0.0
DL-Comp.(DW)	0.0	0.0
Live	67.2	67.2
Pedestrian	0.0	0.0

Upward reactions are positive.

Live Load reactions are per lane with no distribution factor and no impact.

Reactions are not multiplied by Load Modifiers (ductility, redundancy and operational importance).

Non-composite load types are per beam.

Composite and Pedestrian load types are per total bridge width.

SHEAR AND MOMENT ENVELOPE : Span : 1, Beam : 2, SERVICE III

Shears: kips, Moments: kft

		Bearing	Trans	H/2	0.10L	0.20L	0.30L	0.40L	Midspan
Location,	ft	0.00	2.06	0.88	3.55	7.54	11.53	15.51	19.50
Self wt. :	M	0.0	45.5	19.9	75.2	141.7	189.2	217.7	227.2
(Max)	V	23.3	20.8	22.3	19.1	14.3	9.5	4.8	0.0
DL-Prec. :	M	-0.0	8.4	3.7	13.9	26.2	35.0	40.3	42.0
DC(Max)	V	4.3	3.9	4.1	3.5	2.6	1.8	0.9	0.0
DL-Prec. :	M	-0.0	13.3	5.8	22.0	41.4	55.3	63.6	66.4
DW(Max)	V	6.8	6.1	6.5	5.6	4.2	2.8	1.4	0.0
Deck + :	M	0.0	0.0	0.0	0.0	0.0	0.0	0.0	0.0
Haunch (Max)	V	0.0	0.0	0.0	0.0	0.0	0.0	0.0	0.0



Sheet #	8
Job #	
Program:	LEAP® CONSPAN® V8i (SELECTseries 5)
Version:	12.01.00.57
Copyright © Bentley Systems, Inc. 1984 - 2012	www.bentley.com
Phone: 1-800-778-4277	
File Name:	NEXT D8-39ft105nonTransform.csl

Academic Use Only	Designed	HS
Date	Oct/17/2013	
Checked		
Date		

		Bearing	Trans	H/2	0.10L	0.20L	0.30L	0.40L	Midspan
Diaphragm :	M	0.0	0.0	0.0	0.0	0.0	0.0	0.0	0.0
(Max)	V	0.0	0.0	0.0	0.0	0.0	0.0	0.0	0.0
DL-Comp :	M	0.0	0.0	0.0	0.0	0.0	0.0	0.0	0.0
DC(Max)	V	0.0	0.0	0.0	0.0	0.0	0.0	0.0	0.0
DL-Comp :	M	0.0	0.0	0.0	0.0	0.0	0.0	0.0	0.0
DW(Max)	V	0.0	0.0	0.0	0.0	0.0	0.0	0.0	0.0
LL + I :	M+	0.0	87.9	38.8	143.5	260.3	331.5	371.0	381.1
	V	56.3	51.8	54.4	48.5	40.5	32.6	3.9	19.7
LL + I :	M-	0.0	0.0	0.0	0.0	0.0	0.0	0.0	0.0
	V	0.0	0.0	0.0	0.0	0.0	0.0	0.0	0.0
LL + I :	Vmx	56.3	51.8	54.4	48.5	40.7	33.3	27.1	21.8
	M	0.0	88.8	39.5	143.5	251.8	314.8	344.4	348.2
Total :	M+	0.0	155.1	68.3	254.6	469.6	611.0	692.6	716.7
	V	90.8	82.6	87.3	76.7	61.6	46.7	11.0	19.7
Total :	M-	0.0	0.0	0.0	0.0	0.0	0.0	0.0	0.0
	V	0.0	0.0	0.0	0.0	0.0	0.0	0.0	0.0
Total :	Vmx	90.8	82.6	87.3	76.7	61.8	47.4	34.1	21.8
	M	0.0	156.0	68.9	254.6	461.2	594.3	666.0	683.8

		0.60L	0.70L	0.80L	0.90L	H/2	Trans	Bearing
Location,	ft	23.49	27.47	31.46	35.45	38.13	36.94	39.00
Self wt. :	M	217.7	189.2	141.7	75.2	19.9	45.5	0.0
(Max)	V	4.8	9.5	14.3	19.1	22.3	20.8	23.3
DL-Prec. :	M	40.3	35.0	26.2	13.9	3.7	8.4	0.0
DC(Max)	V	0.9	1.8	2.6	3.5	4.1	3.9	4.3
DL-Prec. :	M	63.6	55.3	41.4	22.0	5.8	13.3	-0.0
DW(Max)	V	1.4	2.8	4.2	5.6	6.5	6.1	6.8
Deck + :	M	0.0	0.0	0.0	0.0	0.0	0.0	0.0
Haunch (Max)	V	0.0	0.0	0.0	0.0	0.0	0.0	0.0
Diaphragm :	M	0.0	0.0	0.0	0.0	0.0	0.0	0.0
(Max)	V	0.0	0.0	0.0	0.0	0.0	0.0	0.0
DL-Comp :	M	0.0	0.0	0.0	0.0	0.0	0.0	0.0
DC(Max)	V	0.0	0.0	0.0	0.0	0.0	0.0	0.0
DL-Comp :	M	0.0	0.0	0.0	0.0	0.0	0.0	0.0
DW(Max)	V	0.0	0.0	0.0	0.0	0.0	0.0	0.0
LL + I :	M+	371.0	331.5	260.3	143.5	38.8	87.9	0.0
	V	3.9	32.6	40.5	48.5	54.4	51.8	56.3
LL + I :	M-	0.0	0.0	0.0	0.0	0.0	0.0	0.0
	V	0.0	0.0	0.0	0.0	0.0	0.0	0.0
LL + I :	Vmx	27.1	33.3	40.7	48.5	54.4	51.8	56.3
	M	344.4	314.8	251.8	143.5	39.5	88.8	0.0
Total :	M+	692.6	611.0	469.6	254.6	68.3	155.1	0.0
	V	11.0	46.7	61.6	76.7	87.3	82.6	90.8
Total :	M-	0.0	0.0	0.0	0.0	0.0	0.0	0.0
	V	0.0	0.0	0.0	0.0	0.0	0.0	0.0
Total :	Vmx	34.1	47.4	61.8	76.7	87.3	82.6	90.8
	M	666.0	594.3	461.2	254.6	68.9	156.0	0.0



Sheet #	9
Job #	
Program:	LEAP® CONSPAN® V8i (SELECTseries 5)
Version:	12.01.00.57
Copyright © Bentley Systems, Inc. 1984 - 2012	www.bentley.com
Phone: 1-800-778-4277	
File Name:	NEXT D8-39ft105nonTransform.csl

SHEAR AND MOMENT ENVELOPE : Span : 1, Beam : 2, STRENGTH I

Shears: kips, Moments: kft

		Bearing	Trans	H/2	0.10L	0.20L	0.30L	0.40L	Midspan
Location,	ft	0.00	2.06	0.88	3.55	7.54	11.53	15.51	19.50
Self wt. :	M	0.0	56.9	24.9	94.0	177.2	236.5	272.2	284.0
(Max)	V	29.1	26.1	27.8	23.8	17.9	11.9	6.0	0.0
Self wt. :	M	0.0	41.0	17.9	67.7	127.5	170.3	196.0	204.5
(Min)	V	21.0	18.8	20.0	17.2	12.9	8.6	4.3	0.0
DL-Prec. :	M	-0.0	10.5	4.6	17.4	32.8	43.7	50.3	52.5
DC(Max)	V	5.4	4.8	5.1	4.4	3.3	2.2	1.1	0.0
DL-Prec. :	M	-0.0	7.6	3.3	12.5	23.6	31.5	36.2	37.8
DC(Min)	V	3.9	3.5	3.7	3.2	2.4	1.6	0.8	0.0
DL-Prec. :	M	-0.0	19.9	8.7	32.9	62.1	82.9	95.4	99.5
DW(Max)	V	10.2	9.1	9.8	8.3	6.3	4.2	2.1	0.0
DL-Prec. :	M	-0.0	8.6	3.8	14.3	26.9	35.9	41.3	43.1
DW(Min)	V	4.4	4.0	4.2	3.6	2.7	1.8	0.9	0.0
Deck + :	M	0.0	0.0	0.0	0.0	0.0	0.0	0.0	0.0
Haunch (Max)	V	0.0	0.0	0.0	0.0	0.0	0.0	0.0	0.0
Deck + :	M	0.0	0.0	0.0	0.0	0.0	0.0	0.0	0.0
Haunch (Min)	V	0.0	0.0	0.0	0.0	0.0	0.0	0.0	0.0
Diaphragm :	M	0.0	0.0	0.0	0.0	0.0	0.0	0.0	0.0
(Max)	V	0.0	0.0	0.0	0.0	0.0	0.0	0.0	0.0
Diaphragm :	M	0.0	0.0	0.0	0.0	0.0	0.0	0.0	0.0
(Min)	V	0.0	0.0	0.0	0.0	0.0	0.0	0.0	0.0
DL-Comp :	M	0.0	0.0	0.0	0.0	0.0	0.0	0.0	0.0
DC(Max)	V	0.0	0.0	0.0	0.0	0.0	0.0	0.0	0.0
DL-Comp :	M	0.0	0.0	0.0	0.0	0.0	0.0	0.0	0.0
DC(Min)	V	0.0	0.0	0.0	0.0	0.0	0.0	0.0	0.0
DL-Comp :	M	0.0	0.0	0.0	0.0	0.0	0.0	0.0	0.0
DW(Max)	V	0.0	0.0	0.0	0.0	0.0	0.0	0.0	0.0
DL-Comp :	M	0.0	0.0	0.0	0.0	0.0	0.0	0.0	0.0
DW(Min)	V	0.0	0.0	0.0	0.0	0.0	0.0	0.0	0.0
LL + I :	M+	0.0	192.2	84.9	313.9	569.5	725.2	811.6	833.7
	V	123.2	113.3	119.0	106.1	88.6	71.4	8.6	43.1
LL + I :	M-	0.0	0.0	0.0	0.0	0.0	0.0	0.0	0.0
	V	0.0	0.0	0.0	0.0	0.0	0.0	0.0	0.0
LL + I :	Vmx	123.2	113.3	119.0	106.1	89.1	72.8	59.2	47.6
	M	0.0	194.1	86.4	313.9	550.9	688.6	753.4	761.6
Total :	M+	0.0	279.6	123.2	458.2	841.5	1088.3	1229.4	1269.8
	V	168.0	153.3	161.7	142.7	116.1	89.7	17.8	43.1
Total :	M-	0.0	0.0	0.0	0.0	0.0	0.0	0.0	0.0
	V	0.0	0.0	0.0	0.0	0.0	0.0	0.0	0.0
Total :	Vmx	168.0	153.3	161.7	142.7	116.5	91.1	68.3	47.6
	M	0.0	270.2	119.7	439.5	787.7	1004.8	1117.2	1141.3

		0.60L	0.70L	0.80L	0.90L	H/2	Trans	Bearing
Location,	ft	23.49	27.47	31.46	35.45	38.13	36.94	39.00
Self wt. :	M	272.2	236.5	177.2	94.0	24.9	56.9	0.0



Sheet #	10
Job #	
Program:	LEAP® CONSPAN® V8i (SELECTseries 5)
Version:	12.01.00.57
Copyright © Bentley Systems, Inc. 1984 - 2012	www.bentley.com
Phone: 1-800-778-4277	
File Name:	NEXT D8-39ft105nonTransform.csl

Academic Use Only	Designed	HS
Date	Oct/17/2013	
Checked		
Date		

		0.60L	0.70L	0.80L	0.90L	H/2	Trans	Bearing
(Max)	V	6.0	11.9	17.9	23.8	27.8	26.1	29.1
Self wt. :	M	196.0	170.3	127.5	67.7	17.9	41.0	0.0
(Min)	V	4.3	8.6	12.9	17.2	20.0	18.8	21.0
DL-Prec. :	M	50.3	43.7	32.8	17.4	4.6	10.5	0.0
DC(Max)	V	1.1	2.2	3.3	4.4	5.1	4.8	5.4
DL-Prec. :	M	36.2	31.5	23.6	12.5	3.3	7.6	0.0
DC(Min)	V	0.8	1.6	2.4	3.2	3.7	3.5	3.9
DL-Prec. :	M	95.4	82.9	62.1	32.9	8.7	19.9	-0.0
DW(Max)	V	2.1	4.2	6.3	8.3	9.8	9.1	10.2
DL-Prec. :	M	41.3	35.9	26.9	14.3	3.8	8.6	-0.0
DW(Min)	V	0.9	1.8	2.7	3.6	4.2	4.0	4.4
Deck + :	M	0.0	0.0	0.0	0.0	0.0	0.0	0.0
Haunch (Max)	V	0.0	0.0	0.0	0.0	0.0	0.0	0.0
Deck + :	M	0.0	0.0	0.0	0.0	0.0	0.0	0.0
Haunch (Min)	V	0.0	0.0	0.0	0.0	0.0	0.0	0.0
Diaphragm :	M	0.0	0.0	0.0	0.0	0.0	0.0	0.0
(Max)	V	0.0	0.0	0.0	0.0	0.0	0.0	0.0
Diaphragm :	M	0.0	0.0	0.0	0.0	0.0	0.0	0.0
(Min)	V	0.0	0.0	0.0	0.0	0.0	0.0	0.0
DL-Comp :	M	0.0	0.0	0.0	0.0	0.0	0.0	0.0
DC(Max)	V	0.0	0.0	0.0	0.0	0.0	0.0	0.0
DL-Comp :	M	0.0	0.0	0.0	0.0	0.0	0.0	0.0
DC(Min)	V	0.0	0.0	0.0	0.0	0.0	0.0	0.0
DL-Comp :	M	0.0	0.0	0.0	0.0	0.0	0.0	0.0
DW(Max)	V	0.0	0.0	0.0	0.0	0.0	0.0	0.0
DL-Comp :	M	0.0	0.0	0.0	0.0	0.0	0.0	0.0
DW(Min)	V	0.0	0.0	0.0	0.0	0.0	0.0	0.0
LL + I :	M+	811.6	725.2	569.5	313.9	84.9	192.2	0.0
	V	8.6	71.4	88.6	106.1	119.0	113.3	123.2
LL + I :	M-	0.0	0.0	0.0	0.0	0.0	0.0	0.0
	V	0.0	0.0	0.0	0.0	0.0	0.0	0.0
LL + I :	Vmx	59.2	72.8	89.1	106.1	119.0	113.3	123.2
	M	753.4	688.6	550.9	313.9	86.4	194.1	0.0
Total :	M+	1229.4	1088.3	841.5	458.2	123.2	279.6	0.0
	V	17.8	89.7	116.1	142.7	161.7	153.3	168.0
Total :	M-	0.0	0.0	0.0	0.0	0.0	0.0	0.0
	V	0.0	0.0	0.0	0.0	0.0	0.0	0.0
Total :	Vmx	68.3	91.1	116.5	142.7	161.7	153.3	168.0
	M	1117.2	1004.8	787.7	439.5	119.7	270.2	0.0

REACTIONS (kips), STRENGTH I

Load Type	Left Support	Right Support
Self Wt.	29.1	29.1
Deck+Haunch	0.0	0.0
Diaphragm	0.0	0.0
DL-Prec.(DC)	5.4	5.4
DL-Prec.(DW)	10.2	10.2



Sheet #	11
Job #	
Program:	LEAP® CONSPAN® V8i (SELECTseries 5)
Version:	12.01.00.57
Copyright © Bentley Systems, Inc. 1984 - 2012	www.bentley.com
Phone: 1-800-778-4277	
File Name:	NEXT D8-39ft105nonTransform.csl

Academic Use Only	Designed	HS
Date	Oct/17/2013	
Checked		
Date		

Load Type	Left Support	Right Support
DL-Comp.(DC)	0.0	0.0
DL-Comp.(DW)	0.0	0.0
Live	117.7	117.7
Pedestrian	0.0	0.0

Upward reactions are positive.
 Live Load reactions are per lane with no distribution factor and no impact.
 Reactions are not multiplied by Load Modifiers (ductility, redundancy and operational importance).
 Non-composite load types are per beam.
 Composite and Pedestrian load types are per total bridge width.

SHEAR AND MOMENT ENVELOPE : Span : 1, Beam : 2, FATIGUE I
 Shears: kips, Moments: kft

		Bearing	Trans	H/2	0.10L	0.20L	0.30L	0.40L	Midspan
Location,	ft	0.00	2.06	0.88	3.55	7.54	11.53	15.51	19.50
Self wt. :	M	0.0	45.5	19.9	75.2	141.7	189.2	217.7	227.2
(Max)	V	23.3	20.8	22.3	19.1	14.3	9.5	4.8	0.0
Self wt. :	M	0.0	0.0	0.0	0.0	0.0	0.0	0.0	0.0
(Min)	V	0.0	0.0	0.0	0.0	0.0	0.0	0.0	0.0
DL-Prec. :	M	-0.0	8.4	3.7	13.9	26.2	35.0	40.3	42.0
DC(Max)	V	4.3	3.9	4.1	3.5	2.6	1.8	0.9	0.0
DL-Prec. :	M	-0.0	0.0	0.0	0.0	0.0	0.0	0.0	0.0
DC(Min)	V	0.0	0.0	0.0	0.0	0.0	0.0	0.0	0.0
DL-Prec. :	M	-0.0	13.3	5.8	22.0	41.4	55.3	63.6	66.4
DW(Max)	V	6.8	6.1	6.5	5.6	4.2	2.8	1.4	0.0
DL-Prec. :	M	-0.0	0.0	0.0	0.0	0.0	0.0	0.0	0.0
DW(Min)	V	0.0	0.0	0.0	0.0	0.0	0.0	0.0	0.0
Deck + :	M	0.0	0.0	0.0	0.0	0.0	0.0	0.0	0.0
Haunch (Max)	V	0.0	0.0	0.0	0.0	0.0	0.0	0.0	0.0
Deck + :	M	0.0	0.0	0.0	0.0	0.0	0.0	0.0	0.0
Haunch (Min)	V	0.0	0.0	0.0	0.0	0.0	0.0	0.0	0.0
Diaphragm :	M	0.0	0.0	0.0	0.0	0.0	0.0	0.0	0.0
(Max)	V	0.0	0.0	0.0	0.0	0.0	0.0	0.0	0.0
Diaphragm :	M	0.0	0.0	0.0	0.0	0.0	0.0	0.0	0.0
(Min)	V	0.0	0.0	0.0	0.0	0.0	0.0	0.0	0.0
DL-Comp :	M	0.0	0.0	0.0	0.0	0.0	0.0	0.0	0.0
DC(Max)	V	0.0	0.0	0.0	0.0	0.0	0.0	0.0	0.0
DL-Comp :	M	0.0	0.0	0.0	0.0	0.0	0.0	0.0	0.0
DC(Min)	V	0.0	0.0	0.0	0.0	0.0	0.0	0.0	0.0
DL-Comp :	M	0.0	0.0	0.0	0.0	0.0	0.0	0.0	0.0
DW(Max)	V	0.0	0.0	0.0	0.0	0.0	0.0	0.0	0.0
DL-Comp :	M	0.0	0.0	0.0	0.0	0.0	0.0	0.0	0.0
DW(Min)	V	0.0	0.0	0.0	0.0	0.0	0.0	0.0	0.0
LL + I :	M+	0.0	52.8	23.2	87.0	162.4	214.2	242.4	247.0
	V	38.5	35.0	37.0	32.4	28.5	24.6	20.7	16.8
LL + I :	M-	0.0	0.0	0.0	0.0	0.0	0.0	0.0	0.0



Sheet #	12
Job #	
Program:	LEAP® CONSPAN® V8i (SELECTseries 5)
Version:	12.01.00.57
Copyright © Bentley Systems, Inc. 1984 - 2012	www.bentley.com
Phone: 1-800-778-4277	
File Name:	NEXT D8-39ft105nonTransform.csl

		Bearing	Trans	H/2	0.10L	0.20L	0.30L	0.40L	Midspan
LL + I :	V	0.0	0.0	0.0	0.0	0.0	0.0	0.0	0.0
	Vmx	38.5	35.0	37.0	32.4	28.5	24.6	20.7	16.8
	M	0.0	52.8	23.2	87.0	162.4	214.2	242.4	247.0
Total :	M+	0.0	120.1	52.6	198.1	371.7	493.7	564.0	582.6
	V	73.0	65.8	69.9	60.6	49.6	38.7	27.7	16.8
Total :	M-	0.0	0.0	0.0	0.0	0.0	0.0	0.0	0.0
	V	0.0	0.0	0.0	0.0	0.0	0.0	0.0	0.0
Total :	Vmx	73.0	65.8	69.9	60.6	49.6	38.7	27.7	16.8
	M	0.0	120.1	52.6	198.1	371.7	493.7	564.0	582.6

		0.60L	0.70L	0.80L	0.90L	H/2	Trans	Bearing
Location,	ft	23.49	27.47	31.46	35.45	38.13	36.94	39.00
Self wt. :	M	217.7	189.2	141.7	75.2	19.9	45.5	0.0
(Max)	V	4.8	9.5	14.3	19.1	22.3	20.8	23.3
Self wt. :	M	0.0	0.0	0.0	0.0	0.0	0.0	0.0
(Min)	V	0.0	0.0	0.0	0.0	0.0	0.0	0.0
DL-Prec. :	M	40.3	35.0	26.2	13.9	3.7	8.4	0.0
DC(Max)	V	0.9	1.8	2.6	3.5	4.1	3.9	4.3
DL-Prec. :	M	0.0	0.0	0.0	0.0	0.0	0.0	0.0
DC(Min)	V	0.0	0.0	0.0	0.0	0.0	0.0	0.0
DL-Prec. :	M	63.6	55.3	41.4	22.0	5.8	13.3	-0.0
DW(Max)	V	1.4	2.8	4.2	5.6	6.5	6.1	6.8
DL-Prec. :	M	0.0	0.0	0.0	0.0	0.0	0.0	-0.0
DW(Min)	V	0.0	0.0	0.0	0.0	0.0	0.0	0.0
Deck + :	M	0.0	0.0	0.0	0.0	0.0	0.0	0.0
Haunch (Max)	V	0.0	0.0	0.0	0.0	0.0	0.0	0.0
Deck + :	M	0.0	0.0	0.0	0.0	0.0	0.0	0.0
Haunch (Min)	V	0.0	0.0	0.0	0.0	0.0	0.0	0.0
Diaphragm :	M	0.0	0.0	0.0	0.0	0.0	0.0	0.0
(Max)	V	0.0	0.0	0.0	0.0	0.0	0.0	0.0
Diaphragm :	M	0.0	0.0	0.0	0.0	0.0	0.0	0.0
(Min)	V	0.0	0.0	0.0	0.0	0.0	0.0	0.0
DL-Comp :	M	0.0	0.0	0.0	0.0	0.0	0.0	0.0
DC(Max)	V	0.0	0.0	0.0	0.0	0.0	0.0	0.0
DL-Comp :	M	0.0	0.0	0.0	0.0	0.0	0.0	0.0
DC(Min)	V	0.0	0.0	0.0	0.0	0.0	0.0	0.0
DL-Comp :	M	0.0	0.0	0.0	0.0	0.0	0.0	0.0
DW(Max)	V	0.0	0.0	0.0	0.0	0.0	0.0	0.0
DL-Comp :	M	0.0	0.0	0.0	0.0	0.0	0.0	0.0
DW(Min)	V	0.0	0.0	0.0	0.0	0.0	0.0	0.0
LL + I :	M+	242.4	214.2	162.4	87.0	23.2	52.8	0.0
	V	20.7	24.6	28.5	32.4	37.0	35.0	38.5
LL + I :	M-	0.0	0.0	0.0	0.0	0.0	0.0	0.0
	V	0.0	0.0	0.0	0.0	0.0	0.0	0.0
LL + I :	Vmx	20.7	24.6	28.5	32.4	37.0	35.0	38.5
	M	242.4	214.2	162.4	87.0	23.2	52.8	0.0
Total :	M+	564.0	493.7	371.7	198.1	52.6	120.1	0.0
	V	27.7	38.7	49.6	60.6	69.9	65.8	73.0
Total :	M-	0.0	0.0	0.0	0.0	0.0	0.0	0.0
	V	0.0	0.0	0.0	0.0	0.0	0.0	0.0
Total :	Vmx	27.7	38.7	49.6	60.6	69.9	65.8	73.0



		Sheet #	13		
		Job #			
Program:	LEAP® CONSPAN® V8i (SELECTseries 5)	Academic Use Only	Designed	HS	
Version:	12.01.00.57	Copyright © Bentley Systems, Inc. 1984 - 2012	Date	Oct/17/2013	
		www.bentley.com	Phone: 1-800-778-4277	Checked	
File Name:	NEXT D8-39ft105nonTransform.csl			Date	

	M	0.60L	0.70L	0.80L	0.90L	H/2	Trans	Bearing
		564.0	493.7	371.7	198.1	52.6	120.1	0.0



Sheet #	14
Job #	
Program:	LEAP® CONSPAN® V8i (SELECTseries 5)
Version:	12.01.00.57
Copyright © Bentley Systems, Inc. 1984 - 2012	www.bentley.com
Phone: 1-800-778-4277	
File Name:	NEXT D8-39ft105nonTransform.csl

Academic Use Only	Designed	HS
Date	Oct/17/2013	
Checked		
Date		

POSITIVE ENVELOPE STRESSES

Span : 1, Beam : 2, SERVICE I

RELEASE STRESSES, (ksi) (LOSS = 4.75 %)

Location, ft	Trans	0.10L /0.90L	0.20L /0.80L	0.30L /0.70L	0.40L /0.60L	Midspan
2.50	3.99	7.98	11.96	15.95	19.94	
Beam-Self						
Precast-top	0.135	0.206	0.367	0.481	0.550	0.573
Bottom	-0.244	-0.374	-0.665	-0.873	-0.998	-1.040
Prestress						
Precast-top	-0.607	-0.607	-0.607	-0.607	-0.607	-0.607
Bottom	2.984	2.984	2.984	2.984	2.984	2.984
Total						
Precast-top	-0.472	-0.400	-0.240	-0.125	-0.057	-0.034
Bottom	2.739	2.609	2.318	2.110	1.985	1.944

SERVICE I

POSITIVE ENVELOPE STRESSES, (ksi) (LOSS = 9.63 %)

Location, ft	Bearing	Trans	H/2	0.10L /0.90L	0.20L /0.80L	0.30L /0.70L	0.40L /0.60L	Midspan
0.00	2.06	0.88	3.55	7.54	11.53	15.51	19.50	
Prestress								
Precast-top	-0.101	-0.576	-0.302	-0.576	-0.576	-0.576	-0.576	-0.576
Bottom	0.495	2.831	1.486	2.831	2.831	2.831	2.831	2.831
Self wt.								
Precast-top	0.000	0.110	0.048	0.181	0.342	0.456	0.525	0.548
Bottom	-0.000	-0.199	-0.087	-0.329	-0.620	-0.828	-0.953	-0.995
DL-Prec (DC)								
Precast-top	-0.000	0.020	0.009	0.034	0.063	0.084	0.097	0.101
Bottom	0.000	-0.037	-0.016	-0.061	-0.115	-0.153	-0.176	-0.184
DL-Prec (DW)								
Precast-top	-0.000	0.032	0.014	0.053	0.100	0.133	0.153	0.160
Bottom	0.000	-0.058	-0.025	-0.096	-0.181	-0.242	-0.278	-0.290



Sheet #	15
Job #	
Program:	LEAP® CONSPAN® V8i (SELECTseries 5)
Version:	12.01.00.57
Copyright © Bentley Systems, Inc. 1984 - 2012	www.bentley.com
Phone: 1-800-778-4277	
File Name:	NEXT D8-39ft105nonTransform.csl

Academic Use Only	Designed	HS
Date	Oct/17/2013	
Checked		
Date		

	Bearing	Trans	H/2	0.10L /0.90L	0.20L /0.80L	0.30L /0.70L	0.40L /0.60L	Midspan
Diaphragm								
Precast-top	-0.000	-0.000	-0.000	-0.000	-0.000	-0.000	-0.000	-0.000
Bottom	-0.000	-0.000	-0.000	-0.000	-0.000	-0.000	-0.000	-0.000
Deck + Haunch								
Precast-top	-0.000	-0.000	-0.000	-0.000	-0.000	-0.000	-0.000	-0.000
Bottom	-0.000	-0.000	-0.000	-0.000	-0.000	-0.000	-0.000	-0.000
DL-Comp (DC)								
Precast-top	-0.000	-0.000	-0.000	-0.000	-0.000	-0.000	-0.000	-0.000
Bottom	-0.000	-0.000	-0.000	-0.000	-0.000	-0.000	-0.000	-0.000
DL-Comp (DW)								
Precast-top	-0.000	-0.000	-0.000	-0.000	-0.000	-0.000	-0.000	-0.000
Bottom	-0.000	-0.000	-0.000	-0.000	-0.000	-0.000	-0.000	-0.000
LL+I(+)								
Precast-top	0.000	0.265	0.117	0.433	0.785	0.999	1.118	1.149
Bottom	-0.000	-0.481	-0.212	-0.785	-1.424	-1.814	-2.030	-2.085
Final 1 (P/S + DL + LL)								
Precast-top	-0.101	-0.148	-0.114	0.125	0.714	1.098	1.318	1.383
Bottom	0.495	2.056	1.145	1.560	0.490	-0.206	-0.607	-0.724
Final 2 (P/S + DL)								
Precast-top	-0.101	-0.413	-0.231	-0.308	-0.071	0.098	0.200	0.234
Bottom	0.495	2.536	1.357	2.345	1.915	1.607	1.423	1.362

Span : 1, Beam : 2, SERVICE III

RELEASE STRESSES, (ksi) (LOSS = 4.75 %)

Location, ft	Trans	0.10L /0.90L	0.20L /0.80L	0.30L /0.70L	0.40L /0.60L	Midspan
2.50	3.99	7.98	11.96	15.95	19.94	
Beam-Self						
Precast-top	0.135	0.206	0.367	0.481	0.550	0.573
Bottom	-0.244	-0.374	-0.665	-0.873	-0.998	-1.040
Prestress						
Precast-top	-0.607	-0.607	-0.607	-0.607	-0.607	-0.607
Bottom	2.984	2.984	2.984	2.984	2.984	2.984



Sheet #	16
Job #	
Program:	LEAP® CONSPAN® V8i (SELECTseries 5)
Version:	12.01.00.57
Copyright © Bentley Systems, Inc. 1984 - 2012	www.bentley.com
Phone: 1-800-778-4277	
File Name:	NEXT D8-39ft105nonTransform.csl

Academic Use Only	Designed	HS
Date	Oct/17/2013	
Checked		
Date		

	Trans	0.10L /0.90L	0.20L /0.80L	0.30L /0.70L	0.40L /0.60L	Midspan
Total						
Precast-top	-0.472	-0.400	-0.240	-0.125	-0.057	-0.034
Bottom	2.739	2.609	2.318	2.110	1.985	1.944
As_top, in2	2.331	1.790	0.757	0.000	0.000	0.000
Ast_prvd, in2	4.800	4.800	4.800	4.800	4.800	4.800

SERVICE III

POSITIVE ENVELOPE STRESSES, (ksi) (LOSS = 9.63 %)

	Bearing	Trans	H/2	0.10L /0.90L	0.20L /0.80L	0.30L /0.70L	0.40L /0.60L	Midspan
Location, ft	0.00	2.06	0.88	3.55	7.54	11.53	15.51	19.50
Prestress								
Precast-top	-0.101	-0.576	-0.302	-0.576	-0.576	-0.576	-0.576	-0.576
Bottom	0.495	2.831	1.486	2.831	2.831	2.831	2.831	2.831
Self wt.								
Precast-top	0.000	0.110	0.048	0.181	0.342	0.456	0.525	0.548
Bottom	-0.000	-0.199	-0.087	-0.329	-0.620	-0.828	-0.953	-0.995
DL-Prec (DC)								
Precast-top	-0.000	0.020	0.009	0.034	0.063	0.084	0.097	0.101
Bottom	0.000	-0.037	-0.016	-0.061	-0.115	-0.153	-0.176	-0.184
DL-Prec (DW)								
Precast-top	-0.000	0.032	0.014	0.053	0.100	0.133	0.153	0.160
Bottom	0.000	-0.058	-0.025	-0.096	-0.181	-0.242	-0.278	-0.290
Diaphragm								
Precast-top	-0.000	-0.000	-0.000	-0.000	-0.000	-0.000	-0.000	-0.000
Bottom	-0.000	-0.000	-0.000	-0.000	-0.000	-0.000	-0.000	-0.000
Deck + Haunch								
Precast-top	-0.000	-0.000	-0.000	-0.000	-0.000	-0.000	-0.000	-0.000
Bottom	-0.000	-0.000	-0.000	-0.000	-0.000	-0.000	-0.000	-0.000
DL-Comp (DC)								
Precast-top	-0.000	-0.000	-0.000	-0.000	-0.000	-0.000	-0.000	-0.000
Bottom	-0.000	-0.000	-0.000	-0.000	-0.000	-0.000	-0.000	-0.000
DL-Comp (DW)								
Precast-top	-0.000	-0.000	-0.000	-0.000	-0.000	-0.000	-0.000	-0.000



Sheet #	17
Job #	
Program:	LEAP® CONSPAN® V8i (SELECTseries 5)
Version:	12.01.00.57
Copyright © Bentley Systems, Inc. 1984 - 2012	www.bentley.com
Phone: 1-800-778-4277	
File Name:	NEXT D8-39ft105nonTransform.csl

Academic Use Only	Designed	HS
Date	Oct/17/2013	
Checked		
Date		

	Bearing	Trans	H/2	0.10L /0.90L	0.20L /0.80L	0.30L /0.70L	0.40L /0.60L	Midspan
Bottom	-0.000	-0.000	-0.000	-0.000	-0.000	-0.000	-0.000	-0.000
LL+I(+)								
Precast-top	0.000	0.212	0.094	0.346	0.628	0.799	0.895	0.919
Bottom	-0.000	-0.385	-0.170	-0.628	-1.140	-1.451	-1.624	-1.668
Final 1 (P/S + DL + LL)								
Precast-top	-0.101	-0.201	-0.138	0.038	0.557	0.898	1.095	1.153
Bottom	0.495	2.152	1.187	1.717	0.775	0.156	-0.201	-0.306

Span : 1, Beam : 2, FATIGUE I
 POSITIVE ENVELOPE STRESSES, (ksi)

Location, ft	Bearing	Trans	H/2	0.10L /0.90L	0.20L /0.80L	0.30L /0.70L	0.40L /0.60L	Midspan
	0.00	2.06	0.88	3.55	7.54	11.53	15.51	19.50
F_LL+I(+)								
Precast-top	-0.000	0.127	0.056	0.210	0.392	0.517	0.585	0.596
Bottom	-0.000	-0.231	-0.101	-0.381	-0.711	-0.938	-1.061	-1.081
Final 3 (50% P/S + 50% DL + F_LL)								
Precast-top	-0.050	-0.079	-0.060	0.056	0.356	0.566	0.685	0.713
Bottom	0.248	1.037	0.577	0.792	0.247	-0.134	-0.349	-0.400



Sheet #	18
Job #	
Program:	LEAP® CONSPAN® V8i (SELECTseries 5)
Version:	12.01.00.57
File Name:	NEXT D8-39ft105nonTransform.csl

Academic Use Only	Designed	HS
Copyright © Bentley Systems, Inc. 1984 - 2012	Date	Oct/17/2013
www.bentley.com	Checked	
Phone: 1-800-778-4277	Date	

VERTICAL/HORIZONTAL SHEAR

VERTICAL SHEAR (Art. 5.8) - Span : 1, Beam : 2, STRENGTH I
 Using General Beta Theta Equation procedure - Art.5.8.3.4.2

Location(ft)	Vu (kips)	bv (in)	de (in)	Aps (in ²)	Vp (kips)	eps_x	Theta	Vs-reqd (kips)	Av/s (in ² /ft)	Av-prvd (in ² /ft)	Al_reqd (in ²)
	Mcor (kft)	a (in)	dv (in)	fpo (ksi)	vu/fc	Vc-com (kips)	Beta	Max.spc. (in)	min.Av/s (in ² /ft)	pVn/Vu	Aps* (in ²)
Bearing :		0.44									
168.0	29.19	17.23	0.277	0.0	6.00e-3	50.0	151.5	2.112	6.400	0.00	
0.0	0.25	17.10	33.1	0.058	35.1	0.87	13.68	0.470	2.648	0.419	
Transfer :		2.50									
153.3	29.19	17.23	3.366	0.0	-0.10e-3	28.7	0.0	0.470	0.533	0.00	
270.2	1.43	16.51	189.0	0.054	201.4	5.18	13.21	0.470	1.655	2.394	
Critical :		1.83									
158.1	29.19	17.23	3.366	0.0	-0.11e-3	28.6	0.0	0.470	1.600	0.00	
181.5	1.05	16.70	189.0	0.055	205.6	5.23	13.36	0.470	2.565	1.752	
0.1L :		3.99									
142.7	29.19	17.23	3.366	0.0	-0.06e-3	28.8	0.0	0.470	0.533	0.00	
439.5	1.70	16.38	189.0	0.051	193.5	5.02	13.10	0.470	1.721	2.853	
0.2L :		7.97									
116.5	29.19	17.23	3.366	0.0	0.66e-3	31.3	6.6	0.470	0.533	0.00	
787.7	2.00	16.23	189.0	0.042	122.9	3.22	12.98	0.470	1.499	3.366	
0.3L :		11.96									
91.1	29.19	17.23	3.366	0.0	2.06e-3	36.2	29.3	0.470	0.533	0.00	
1004.8	2.00	16.23	189.0	0.033	71.9	1.88	12.98	0.470	1.294	3.366	
0.4L :		15.95									
68.3	29.19	17.23	3.366	0.0	2.69e-3	38.4	15.3	0.470	0.533	0.00	
1117.2	2.00	16.23	189.0	0.025	60.7	1.59	12.98	0.470	1.518	3.366	
0.5L :		19.94									
47.6	29.19	17.23	3.366	0.0	2.66e-3	38.3	0.0	0.470	0.533	0.00	
1141.3	2.00	16.23	189.0	0.017	61.1	1.60	12.98	0.470	2.191	3.366	
0.6L :		23.93									
68.3	29.19	17.23	3.366	0.0	2.69e-3	38.4	15.3	0.470	0.533	0.00	
1117.2	2.00	16.23	189.0	0.025	60.7	1.59	12.98	0.470	1.518	3.366	
0.7L :		27.91									
91.1	29.19	17.23	3.366	0.0	2.06e-3	36.2	⁵⁶⁶ 29.3	0.470	0.533	0.00	



Sheet #	19
Job #	
Program:	LEAP® CONSPAN® V8i (SELECTseries 5)
Version:	12.01.00.57
Copyright © Bentley Systems, Inc. 1984 - 2012	www.bentley.com
Phone: 1-800-778-4277	
File Name:	NEXT D8-39ft105nonTransform.csl

Location(ft)	Vu (kips)	bv (in)	de (in)	Aps (in ²)	Vp (kips)	eps_x	Theta	Vs-reqd (kips)	Av/s (in ² /ft)	Av-prvd (in ² /ft)	Al_reqd (in ²)
Mcor (kft)	a (in)	dv (in)	fpo (ksi)	vu/fc	Vc-com (kips)	Beta	Max.spc. (in)	min.Av/s (in ² /ft)	pVn/Vu	Aps* (in ²)	
1004.8	2.00	16.23	189.0	0.033	71.9	1.88	12.98	0.470	1.294	3.366	
0.8L :	31.90										
116.5	29.19	17.23	3.366	0.0	0.66e-3	31.3	6.6	0.470	0.533	0.00	
787.7	2.00	16.23	189.0	0.042	122.9	3.22	12.98	0.470	1.499	3.366	
0.9L :	35.89										
142.7	29.19	17.23	3.366	0.0	-0.06e-3	28.8	0.0	0.470	0.533	0.00	
439.5	1.70	16.38	189.0	0.051	193.5	5.02	13.10	0.470	1.721	2.853	
Critical :	38.05										
158.1	29.19	17.23	3.366	0.0	-0.11e-3	28.6	0.0	0.470	1.600	0.00	
181.5	1.05	16.70	189.0	0.055	205.6	5.23	13.36	0.470	2.565	1.752	
Transfer :	37.38										
153.3	29.19	17.23	3.366	0.0	-0.10e-3	28.7	0.0	0.470	0.533	0.00	
270.2	1.43	16.51	189.0	0.054	201.4	5.18	13.21	0.470	1.655	2.394	
Bearing :	39.44										
168.0	29.19	17.23	0.277	0.0	6.00e-3	50.0	151.5	2.112	2.400	0.00	
0.0	0.25	17.10	33.1	0.058	35.1	0.87	13.68	0.470	1.111	0.419	

ANCHORAGE ZONE REINFORCEMENT (Art. 5.10.10)
 Span : 1, Beam : 2

Fpi (kips)	fs (ksi)	h/4 (in)	Abrst_rqrd (in ²)
805.54	20.00	5.25	1.61



Sheet #	20
Job #	
Program:	LEAP® CONSPAN® V8i (SELECTseries 5)
Version:	12.01.00.57
Copyright © Bentley Systems, Inc. 1984 - 2012	Date
www.bentley.com	Checked
Phone: 1-800-778-4277	Date

Academic Use Only	Designed	HS
Copyright © Bentley Systems, Inc. 1984 - 2012	Date	Oct/17/2013
www.bentley.com	Checked	
Phone: 1-800-778-4277	Date	

File Name: NEXT D8-39ft105nonTransform.csl

CAMBER/DEFLECTION

CAMBER AND DEFLECTIONS: SERVICE I
(Span : 1, Beam : 2; Units: in)

	Release	Mult	Erection	Mult	Final
At 0.1 x L =	3.55 ft				
Prestress	0.397	1.80	0.715	2.45	0.973
Self Wt.	-0.132	1.85	-0.243	2.70	-0.355
Deck + Haunch			0.000	2.30	0.000
DL-Prec. (DC)			-0.018	3.00	-0.055
Diaphragm			0.000	3.00	0.000
DL-Prec. (DW)			-0.029	3.00	-0.086
DL-Comp. (DC)			0.000	3.00	0.000
DL-Comp. (DW)			0.000	3.00	0.000
Live Load					-0.163
Total	0.266		0.425		0.314

	Release	Mult	Erection	Mult	Final
At 0.2 x L =	7.54 ft				
Prestress	0.710	1.80	1.279	2.45	1.741
Self Wt.	-0.249	1.85	-0.460	2.70	-0.672
Deck + Haunch			0.000	2.30	0.000
DL-Prec. (DC)			-0.037	3.00	-0.110
Diaphragm			0.000	3.00	0.000
DL-Prec. (DW)			-0.058	3.00	-0.173
DL-Comp. (DC)			0.000	3.00	0.000
DL-Comp. (DW)			0.000	3.00	0.000
Live Load					-0.327
Total	0.462		0.724		0.458

	Release	Mult	Erection	Mult	Final
At 0.3 x L =	11.52 ft				
Prestress	0.934	1.80	1.682	2.45	2.289
Self Wt.	-0.341	1.85	-0.630	2.70	-0.920
Deck + Haunch			0.000	2.30	0.000
DL-Prec. (DC)			-0.051	3.00	-0.153
Diaphragm			0.000	3.00	0.000
DL-Prec. (DW)			-0.081	3.00	-0.242
DL-Comp. (DC)			0.000	3.00	0.000
DL-Comp. (DW)			0.000	3.00	0.000
Live Load					-0.455
Total	0.594		0.920		0.519

	Release	Mult	Erection	Mult	Final
At 0.4 x L =	15.51 ft				
Prestress	1.069	1.80	1.924	2.45	2.618



Sheet #	21
Job #	
Program:	LEAP® CONSPAN® V8i (SELECTseries 5)
Version:	12.01.00.57
Copyright © Bentley Systems, Inc. 1984 - 2012	Date
www.bentley.com	Phone: 1-800-778-4277
File Name: NEXT D8-39ft105nonTransform.csl	Date

	Release	Mult	Erection	Mult	Final
Self Wt.	-0.399	1.85	-0.738	2.70	-1.077
Deck + Haunch			0.000	2.30	0.000
DL-Prec. (DC)			-0.060	3.00	-0.181
Diaphragm			0.000	3.00	0.000
DL-Prec. (DW)			-0.095	3.00	-0.285
DL-Comp. (DC)			0.000	3.00	0.000
DL-Comp. (DW)			0.000	3.00	0.000
Live Load					-0.535
Total	0.670		1.030		0.539

	Release	Mult	Erection	Mult	Final
At 0.5 x L = 19.50 ft					
Prestress	1.113	1.80	2.004	2.45	2.728
Self Wt.	-0.419	1.85	-0.775	2.70	-1.131
Deck + Haunch			0.000	2.30	0.000
DL-Prec. (DC)			-0.063	3.00	-0.190
Diaphragm			0.000	3.00	0.000
DL-Prec. (DW)			-0.100	3.00	-0.300
DL-Comp. (DC)			0.000	3.00	0.000
DL-Comp. (DW)			0.000	3.00	0.000
Live Load					-0.562
Total	0.694		1.066		0.544

	Release	Mult	Erection	Mult	Final
At 0.6 x L = 23.49 ft					
Prestress	1.069	1.80	1.924	2.45	2.618
Self Wt.	-0.399	1.85	-0.738	2.70	-1.077
Deck + Haunch			0.000	2.30	0.000
DL-Prec. (DC)			-0.060	3.00	-0.181
Diaphragm			0.000	3.00	0.000
DL-Prec. (DW)			-0.095	3.00	-0.285
DL-Comp. (DC)			0.000	3.00	0.000
DL-Comp. (DW)			0.000	3.00	0.000
Live Load					-0.535
Total	0.670		1.030		0.539

	Release	Mult	Erection	Mult	Final
At 0.7 x L = 27.48 ft					
Prestress	0.934	1.80	1.682	2.45	2.289
Self Wt.	-0.341	1.85	-0.630	2.70	-0.920
Deck + Haunch			0.000	2.30	0.000
DL-Prec. (DC)			-0.051	3.00	-0.153
Diaphragm			0.000	3.00	0.000
DL-Prec. (DW)			-0.081	3.00	-0.242
DL-Comp. (DC)			0.000	3.00	0.000
DL-Comp. (DW)			0.000	3.00	0.000
Live Load					-0.455



Sheet #	22
Job #	
Program:	LEAP® CONSPAN® V8i (SELECTseries 5)
Version:	12.01.00.57
Copyright © Bentley Systems, Inc. 1984 - 2012	www.bentley.com
Phone: 1-800-778-4277	
File Name:	NEXT D8-39ft105nonTransform.csl

Academic Use Only	Designed	HS
Date	Oct/17/2013	
Checked		
Date		

	Release	Mult	Erection	Mult	Final
Total	0.594		0.920		0.519

	Release	Mult	Erection	Mult	Final
At 0.8 x L =	31.46 ft				
Prestress	0.710	1.80	1.279	2.45	1.741
Self Wt.	-0.249	1.85	-0.460	2.70	-0.672
Deck + Haunch			0.000	2.30	0.000
DL-Prec. (DC)			-0.037	3.00	-0.110
Diaphragm			0.000	3.00	0.000
DL-Prec. (DW)			-0.058	3.00	-0.173
DL-Comp. (DC)			0.000	3.00	0.000
DL-Comp. (DW)			0.000	3.00	0.000
Live Load					-0.327
Total	0.462		0.724		0.458

	Release	Mult	Erection	Mult	Final
At 0.9 x L =	35.45 ft				
Prestress	0.397	1.80	0.715	2.45	0.973
Self Wt.	-0.132	1.85	-0.243	2.70	-0.355
Deck + Haunch			0.000	2.30	0.000
DL-Prec. (DC)			-0.018	3.00	-0.055
Diaphragm			0.000	3.00	0.000
DL-Prec. (DW)			-0.029	3.00	-0.086
DL-Comp. (DC)			0.000	3.00	0.000
DL-Comp. (DW)			0.000	3.00	0.000
Live Load					-0.163
Total	0.266		0.425		0.314



Sheet #	23
Job #	
Program:	LEAP® CONSPAN® V8i (SELECTseries 5)
Version:	12.01.00.57
Copyright © Bentley Systems, Inc. 1984 - 2012	www.bentley.com
Phone: 1-800-778-4277	
File Name:	NEXT D8-39ft105nonTransform.csl

ULTIMATE MOMENT

ULTIMATE - Span : 1, Beam : 2, STRENGTH I
 (Mr-prvd computed by Strain Compatibility method. Ult. Conc. Strain = 0.00300)

Location (ft)	dp in	Aps in ²	fps ksi	c in	a in	Mr-prvd k.ft	c/dt	Phi	Mcr k.ft	min Mr k.ft	Crkg Ratio	Mu-p/r Ratio
Transfer	2.06											
279.6	15.7	2.829	267.8	2.0	1.4	949.1	0.106T	1.00	-	-	-	-
H/2	0.88											
123.2	15.7	1.485	268.9	1.0	0.8	511.4	0.056T	1.00	-	-	-	-
0.1L	3.55											
458.2	15.8	3.371	267.2	2.3	1.7	1118.8	0.126T	1.00	-	-	-	-
0.2L	7.54											
841.5	15.8	3.978	266.5	2.7	2.0	1304.2	0.148T	1.00	935.1	935.1	1.39	-
0.3L	11.53											
1088.3	15.8	3.978	266.5	2.7	2.0	1304.2	0.148T	1.00	935.1	935.1	1.39	-
0.4L	15.51											
1229.4	15.8	3.978	266.5	2.7	2.0	1304.2	0.148T	1.00	935.1	935.1	1.39	-
0.5L	19.50											
1269.8	15.8	3.978	266.5	2.7	2.0	1304.2	0.148T	1.00	935.1	935.1	1.39	-
0.6L	23.49											
1229.4	15.8	3.978	266.5	2.7	2.0	1304.2	0.148T	1.00	935.1	935.1	1.39	-
0.7L	27.48											
1088.3	15.8	3.978	266.5	2.7	2.0	1304.2	0.148T	1.00	935.1	935.1	1.39	-
0.8L	31.46											
841.5	15.8	3.978	266.5	2.7	2.0	1304.2	0.148T	1.00	935.1	935.1	1.39	-
0.9L	35.45											
458.2	15.8	3.371	267.2	2.3	1.7	1118.8	0.126T	1.00	-	-	-	-
H/2	38.13											
123.2	15.7	1.485	268.9	1.0	0.8	511.4	0.056T	1.00	-	-	-	-
Transfer	36.94											
279.6	15.7	2.829	267.8	2.0	1.4	949.1	0.106T	1.00	-	-	-	-

Legend: C = Compression-Controlled (c/dt > 0.600)
 I = In-Transition (0.60 >= c/dt > 0.375)
 T = Tension-Controlled (c/dt <= 0.375)
 Note : fr used for calculating Mcr is computed using AASHTO method (Art.5.4.2.6.)
 Consider Bottom Tension Steel Contribution : NO



Sheet #	24
Job #	
Program:	LEAP® CONSPAN® V8i (SELECTseries 5)
Version:	12.01.00.57
Copyright © Bentley Systems, Inc. 1984 - 2012	www.bentley.com
Phone: 1-800-778-4277	
File Name:	NEXT D8-39ft105nonTransform.csl

Academic Use Only	Designed	HS
Date	Oct/17/2013	Checked
Date		

DETENSIONING

Span : 1, Beam : 2; Groups 1-13; Units: ksi

Grp	Str	Ys,in	2.50ft
1	2	E 2.50	Ft 0.055
		M 2.50	Fb 0.044
2	2	E 13.50	Ft 0.106
		M 13.50	Fb 0.097
3	2	E 13.50	Ft 0.157
		M 13.50	Fb 0.149
4	2	E 6.50	Ft 0.125
		M 6.50	Fb 0.352
5	2	E 4.50	Ft 0.069
		M 4.50	Fb 0.598
6	2	E 4.50	Ft 0.014
		M 4.50	Fb 0.844
7	2	E 4.50	Ft -0.042
		M 4.50	Fb 1.090
8	2	E 4.50	Ft -0.098
		M 4.50	Fb 1.336
9	2	E 4.50	Ft -0.154
		M 4.50	Fb 1.582
10	2	E 2.50	Ft -0.233
		M 2.50	Fb 1.872
11	2	E 2.50	Ft -0.313
		M 2.50	Fb 2.161
12	2	E 2.50	Ft -0.392
		M 2.50	Fb 2.450
13	2	E 2.50	Ft -0.472
		M 2.50	Fb 2.739



		Sheet #	25
		Job #	
Program:	LEAP® CONSPAN® V8i (SELECTseries 5)	Academic Use Only	Designed HS
Version:	12.01.00.57	Copyright © Bentley Systems, Inc. 1984 - 2012	Date Oct/17/2013
		www.bentley.com	Phone: 1-800-778-4277
File Name:	NEXT D8-39ft105nonTransform.csl		Checked
			Date

DESIGN SUMMARY

Span: 1, Beam: 2, Interior beam

Beam type:	Double Tee,	Next D8-21-interior
Precast Length,	ft	39.88
Release Length,	ft	39.88
Strand Pattern:	Straight	
Strand:	1/2-270K-LL	
Strand Es,	ksi:	28500.0
No. of strands:	26	
	Draped:	0
	Straight:	26
Concrete Strength:		
	f'ci:	5.2 ksi
	f'c:	6.5 ksi
	f'ct:	6.5 ksi
Initial losses:	4.75 %	
Final losses:	9.63 %	

Specification	Allowable	Computed	Location	Status
Release Stresses (ksi) (Art. 5.9.4.1)				
Precast Bot (compression)	3.120	2.739	Trans	OK
Precast Top w/ no reinf. (tension)	-0.200	-0.472	Trans	
Precast Top w/ reinf. (tension)	-0.547			
Strength I (Art. 3.4.1, 5.7.3.1.1)	Provided	Required	Location	Status
Ult. Moment (k.ft)	1304.17	1269.81	Midspan	OK
Debonding Limits (Art. 5.11.4.3)	Allowable	Computed		Status
Max. Debond per Row	40.00 %	0.00 %		OK
Max. Debond Total	25.00 %	0.00 %		OK

Positive Moment Envelope Stresses (ksi) (Art. 3.4.1 and 5.9.4.2)



		Sheet #	26
		Job #	
Program:	LEAP® CONSPAN® V8i (SELECTseries 5)	Academic Use Only	Designed
Version:	12.01.00.57	Copyright © Bentley Systems, Inc. 1984 - 2012	Date
		www.bentley.com	Phone: 1-800-778-4277
File Name:	NEXT D8-39ft105nonTransform.csl		Date

Specification	Allow	Final 1 Comp	Loc.	Allow	Final 2 Comp	Loc.	Allow	Final 3 Comp	Loc.
Service I Limit State - Compressive	Stresses	Only							
Precast Top	3.900	1.383	Midspan	2.925	0.234	Midspan			
Precast Bot	3.900	2.056	Transfer	2.925	2.536	Transfer			
Service III Limit State - Tensile	Stresses	Only							
Precast Top	-0.484	-0.201	Transfer						
Precast Bot	-0.484	-0.306	Midspan						
Fatigue I Limit State - Compressive	Stresses	Only							
Precast Top							2.600	0.713	Midspan
Precast Bot							2.600	1.037	Transfer

CAMBER / DEFLECTION: (PCI Design Handbook - 4th Ed.- Table 4.6.2)
0.5 x L = 19.50 ft

	Release	Mult	Erection	Mult	Final
Prestress	1.113	1.80	2.004	2.45	2.728
Self Wt.	-0.419	1.85	-0.775	2.70	-1.131
Deck + Haunch			0.000	2.30	0.000
DL-Prec. (DC)			-0.063	3.00	-0.190
Diaphragm			0.000	3.00	0.000
DL-Prec. (DW)			-0.100	3.00	-0.300
DL-Comp. (DC)			0.000	3.00	0.000
DL-Comp. (DW)			0.000	3.00	0.000
Live Load					-0.562
Total	0.694		1.066		0.544

Positive values indicate upward deflection.